J. Betten

with CD-ROM

Creep Mechanics

3rd Edition

Springer

Creep Mechanics

Josef Betten

Creep Mechanics

Third Edition

With 95 Figures and 16 Tables

Springer

Univ.-Professor Dr.-Ing. habil. JOSEF BETTEN
Mathematical Models in Materials
Science and Continuum Mechanics
RWTH-Aachen University
Templergraben 55
D-52056 Aachen
Germany
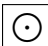betten@mmw.rwth-aachen.de

Preface to the Third Edition

Many developments and clarifications in the theory of creep and its applications to engineering proplems, which have occured since the publication of the second edition in 2005, are reflected in numerous additions and emendations in the present edition. Many improvements have been made throughout, e.g. by elimination and rearrangement as well as necessary additions.

Session 4.1 has been extended to the primary creep behaviour of austenitic steel including own experimental data, where both the strain- and time-hardening-theory have been taken into account in more detail.

Typical creep curves for metals, polymers, and ceramics have been discussed in a new Chapter 14.

Some new publications have been discussed in the text and added to the list of References.

Furthermore, the navigation system on the CD on the inside back cover of the book has been checked and improved.

Again, for users, executing the MAPLE worksheets interactively, the programs are indicated in the text by data names like $\boxed{\odot \; 11\_3.mws}$, for instance. For a better overview, a MAPLE navigation worksheet (*index.mws*) with a direct access to all application examples and algorithms, is also included on the compact disk CD-ROM.

Finally, I would like to express my appreciation to my Assistant, Dipl.-Ing. Uwe NAVRATH, for preparing the camera-ready manuscript in LaTeX. His competence and skill have been indispensable for me.

Thanks are due to Springer-Verlag, in particular to Mrs. Carmen WOLF and Dr. Christoph BAUMANN for their readiness to publish the third edition of this monograph and for their agreeable cooperation.

Aachen, April 2008   *Josef Betten*

Preface to the Second Edition

In the revision of this monograph for a *second edition*, the primary intention and purpose of the *first edition* have been preserved.

The whole text has been reexamined, and many minor improvements have been made throughout by elimination and rearrangement as well as addition.

The major additions reflect developments and extensions of interest and practical applicability that have occurred since the publication of the first edition in 2002.

An essential feature of the new edition is the CD on the inside back cover of the book. All the application examples and algorithms are included and extended in more detail in this compact disk CD-ROM, where the results, when illustrated in Figures, are presented in colour. All the MAPLE programs are saved as *maple work sheets (*.mws)* and for earlier releases in *ascii-format*. For users executing the MAPLE worksheets interactively the programs are indicated in the text by data names like $\boxed{\odot\ 11\_3.mws}$, for instance. For a better overview a MAPLE navigation work sheet (*index.mws*) with a direct access to all the application examples and algorithms, is also included on the compact disk CD-ROM.

Finally, I would like to express my appreciation to my Assistant, Dipl.-Ing. Uwe NAVRATH, for preparing the camera-ready manuscript in LaTeX. His competence and skill have been indispensable for me.

Thanks are due to Springer-Verlag, in particular to Dr. Dieter MERKLE and Dr. Hubertus v. RIEDESEL for their readiness to publish the second edition of this monograph and for their agreeable cooperation.

Aachen, July 2004   *Josef Betten*

Preface to the First Edition

This book is based upon lectures on *Mathematical Models in Materials Science* held at the University of Aachen, Germany, since 1969. Guest-lectures at several Universities in Germany and abroad or representations at International Conferences have also been included. Furthermore, I represent some parts of this book on ANSYS-Seminars about *viscoelasticity* and *viscoplasticity* in Munich, Stuttgart, and Hannover. Some results of research projects, which I have carried out in recent years, are also discussed in this exposition.

Over the last two or three decades much effort has been devoted to the elaboration of phenomenological theories describing the relations between force and deformation in bodies of materials, which obey neither the linear laws of the classical theories of elasticity nor the hydrodynamics of viscous fluids.

Material laws and constitutive theories are the fundamental bases for describing the mechanical behavior of materials under multi-axial states of stress involving *creep* and *creep rupture*. The tensor function theory has become a powerful tool for solving such complex problems.

The present book will provide a survey of some recent advances in the mathematical modelling of materials behavior under creep conditions. The mechanical behavior of anisotropic solids requires a suitable mathematical modelling. The properties of *tensor functions* with several argumenttensors constitute a rational basis for a consistent mathematical modelling of complex material behavior.

This monograph presents certain principles, methods, and recent successful applications of tensor functions in creep mechanics. Thus, a proper understanding of the subject matter requires fundamental knowledge of *tensor algebra* and *tensor analysis*. Therefore, Chapter 2 is devoted to tensor notation, where both symbolic and index notation have been discussed. For higher-order tensors and for final results in most of the derivations the index notation provides the reader with more insight.

The simplest way to formulate the basic equations of continuum mechanics and the constitutive or evolutional equations of various materials is to restrict ourselves to rectangular cartesian coordinates. However, solving particular problems, for instance in Chapter 5, it may be preferable to work in terms of more suitable coordinate systems and their associated bases. Therefore, Chapter 2 is also concerned with the standard techniques of tensor analysis in general coordinate systems.

Creep mechanics is a part of continuum mechanics, like elasticity or plasticity. Therefore, some basic equations of *continuum mechanics* are put together in Chapter 3. These equations can apply equally to all materials and they are insufficient to describe the mechanical behavior of any particular material. Thus, we need additional equations characterizing the individual material and its reaction under creep condition according to Chapter 4, which is subdivided into three parts: the *primary*, the *secondary*, and the *tertiary creep* behavior of *isotropic* and *anisotropic* materials.

The creep behavior of a *thick-walled tube* subjected to internal pressure is discussed in Chapter 5. The tube is partly plastic and partly elastic at time zero. The investigation is based upon the usual assumptions of incompressibility and zero axial creep. The creep deformations are considered to be of such magnitude that the use of *finite-strain theory* is necessary. The inner and outer radius, the stress distributions as functions of time, and the creep-failure time are calculated.

In Chapter 6 the *creep potentials hypothesis* is compared with the *tensor function theory*. It has been shown that the former theory is compatible with the latter, if the material is isotropic, and if additional conditions are fulfilled.

However, for anisotropic materials the creep potential hypothesis only furnishes restricted forms of constitutive equations, even if a general creep potential has been assumed. Consequently, the classical normality rule is modified for anisotropic solids based upon the representation theory of tensor functions.

The existance of a creep potential in the tertiary creep phase is not justified. This phase is accompanied by the formation of microscopic cracks on the grain boundaries, so that *damage accumulation* occurs. In some cases voids are caused by a given stress history and, therefore, they are distributed *anisotropically* among the grain boundaries.

Because of this microscopic nature, *damage* has an *anisotropic* character even if the material was originally isotropic. The fissure orientation and length cause anisotropic macroscopic behavior. Therefore, damage in an

isotropic or anisotropic material that is in a state of multiaxial stress can only be described in a tensorial form.

Thus, the mechanical behavior will be *anisotropic*, and it is therefore necessary to investigate this kind of anisotropy by introducing appropiately defined *anisotropic damage tensors* into *constitutive equations*.

In Sections 4.3.2 and 6.4 *constitutive equations* involving *damage* and *initial ansisotropy* have been formulated in detail. Chapter 7 is concerned with the construction of *damage tensors* or *tensors of continuity* (Section 7.1). Then, the multiaxial state of stress in a damaged continuum is analized in more detail (Section 7.2). Finally, some damage effective stress concepts are also discussed (Section 7.3).

For engineering applications it is very important to generalize uniaxial constitutive laws to multiaxial states of stress. This can be achieved by applying *interpolation methods for tensor functions* developed in Chapter 8.

In foregoing Chapters, the creep behavior of *solids* has been described. Chapters 9 and 10 are devoted to *fluids*, where linear and nonlinear fluids and *memory fluids* are taken into consideration.

Many materials exihibt both features of elastic solids and characteristics of viscous fluids. Such materials are called *viscoelastic*, to which the extended Chapter 11 has been devoted. Several rheological models (both linear and nonlinear) are discussed in more detail, and their *creep* or *relaxation* behavior has been compared with experimental data.

In contrast to fluids (Chapter 9) *viscoplastic* materials can sustain a shear stress even at rest. They begin to flow with viscous stress after a *yield condition* has been satisfied. Chapter 12 is subdivided in linear and nonlinear theory of viscoplasticity. As an example, viscoplastic behavior of metals in comparison with experimental results is discussed.

Together with my coworkers I have carried out own experiments to examine the validity of the mathematical modelling. Furthermore, an overview of some important experimental investigations in creep mechanics of other scientists has been provided in Chapter 13.

The mathematical backround required has been kept to a minimum and supplemented by explanations where it has been necessary to introduce special topics, for instance, concerning tensor algebra and tensor analysis or representation of tensor functions. Furthermore, two appendices have been included to provide sufficient foundations of DIRAC and HEVISIDE *functions* or of LAPLACE *transformations*, since these special techniques play a fundamental role in creep mechanics.

In many examples or for many graphically representations the MAPLE software has been utilized. MAPLE or MATHEMATICA and many other symbolic manipulation codes are interactive computer programs, which are called *computer algebra systems*. They allow their users to compute not only with numbers, but also with symbols, formulae, equations, and so on. Many mathematical operations such as differentiation, integration, LAPLACE transformations, inversion of matrices with symbolic entries, etc. etc. can be carried out with great speed and exactness of the results. Computer algebra systems are powerful tools for mathematicians, physicists, engineers, etc., and are indispensable in scientific research and education.

I would like to express my appreciation to my Assistant, Dipl.-Ing. Uwe NAVRATH, for preparing the camera-ready manuscript in LaTeX. His competence and skill have been indispensable for me.

Thanks are due to Springer-Verlag, in particular to Dr. Dieter MERKLE and Dr. Hubertus v. RIEDESEL for their readiness to publish this monograph and for their agreeable cooperation.

Aachen, May 2002   *Josef Betten*

Contents

1 Introduction

The increasing technical importance of high-temperature equipment, i.e., the urgent needs of designers and computing engineers dealing with high-temperature machinery, jet engines, and high-velocity aeronautics have resulted in a huge and rapidly growing literature in *creep mechanics* .

There is a tradition to organize IUTAM-Symposia on *Creep in Structures* every ten years: the first one was organized by N.J. HOFF in Stanford (1960), the second one by J. HULT in Göteburg (1970), the third one by A.R.S. PONTER and D.R. HAYHURST in Leicester (1980), the fourth Symposium by M. ŻYCZKOWSKI in Cracow (1990) and, finally, the fifth Symposium was organized by S. MURAKAMI and N. OHNO in Nagoya (2000).

Other events are, for instance, the traditional Conferences on *Creep and Fracture of Engineering Materials and Structures* organized by B. WILSHIRE and D.R.J. OWEN in Swansea (1981, 1984 etc. every three years).

The aim of such conferences is to bring together experimentalists, theoreticians, and engineers interested in various features of creep mechanics, in order to permit an interdisciplinary exchange of understanding, experience, and methods. Therefore, such conferences essentially contribute to the progress in *creep mechanics* . The advances have been reviewed in the Conference Proceedings from several points of view: *mathematical*, *mechanical*, *metallurgical*, etc..

Over the last two decades much effort has been devoted to the elaboration of phenomenological theories describing the relation between force and deformation in bodies of materials which obey neither the linear laws of the classical theories of elasticity nor the hydrodynamics of viscous fluids. Such problems will play a central role for mathematticans, physicits, and engineers in the future (ASTRARITA, 1979).

Material laws and constitutive theories are the fundamental bases for describing the mechanical behavior of materials under multiaxial states of stress involving creep and creep rupture. The tensor function theory has be-

come a powerful tool (BETTEN, 1987b; 1987c) for solving such complex problems.

The mechanical behavior of anisotropic solids (which are materials with oriented internal structures produced by forming processes and manufacturing procedures or induced by permanent deformation) requires a suitable mathematical modelling. The properties of tensor functions with several argumenttensors constitute a rational basis for a consistent mathematical modelling of complex material behavior (BETTEN, 2001a; BOEHLER, 1987; RIVLIN, 1955, 1970; SPENCER, 1971; TRUESDELL and NOLL, 1965; WANG, 1971).

In creep mechanics one can differentiate between three stages: the *primary*, *secondary*, and *tertiary* creep stage (Chapter 4). These terms correspond to a decreasing, constant, and increasing creep strain rate, respectively, and were introduced by ANDRADE (1910).

In order to describe the creep behavior of metals in the primary stage *tensorial nonlinear constitutive equations involving the strain hardening hypothesis* are proposed by BETTEN et al.(1989). Based upon these general relations, the primary creep behavior of a thinwalled circular cylindrical shell subjected to internal pressure is also analysed by BETTEN et al. (1989). The *creep buckling* of cylindrical shells subjected to internal pressure and axial compression was investigated by BETTEN and BUTTERS (1990) by considering *tensorial nonlinearities* and *anisotropic primary creep* . The problem of *creep buckling* of cylindrical shells have earlier been discussed, for instance, by MURAKAMI and TANAKA (1976), OBRECHT (1977) or HAYMAN (1980).

Based upon a *creep velocity potential* JAKOWLUK and MIELESZKO (1983) formulate constitutive equations of the *primary* creep stage in comparison with experimental data on FeMnAl steel.

In Chapter 4, the secondary creep stage of isotropic and anisotropic solids in a state of multiaxial stress will be discussed. Creep deformations of metals usually remain unaffected if hydrostatic pressure is superimposed. In order to describe the secondary creep behavior of isotropic materials some authors use a *creep potential* (BETTEN, 1981a; JAKOWLUK and MIELESZKO, 1985; RABOTNOV, 1969), which is a scalar-valued function of CAUCHY's *stress tensor* . One can show that the *creep potential theory* is compatible with the *tensor function theory* provided the material is *isotropic* and additional conditions are fulfilled (BETTEN, 1985). However, the creep potential hypothesis only furnishes restricted forms of constitutive equations

and, therefore, has only limited justification if the material is *anisotropic* , as has been discussed in Chapter 6.

The tertiary creep phase is also considered in Chapter 4. In this phase, the creep process is accompanied by the formation of microscopic cracks on the grain boundaries, so that damage accumulation occurs. In some cases voids are caused by a given stress history and, therefore, they are distributed anisotropically amongst the grain boundaries. Thus, the mechanical behavior will be *anisotropic* and it is therefore necessary to investigate this kind of anisotropy by introducing appropiately defined *anisotropic damage tensors* into constitutive equations. *Damage tensors* have been constructed, for instance, by BETTEN (1981b; 1983b) or by MURAKAMI and OHNO (1981). A detailed survey of several damage variables is carried out in Chapter 7.

Problems of *creep damage* have been investigated by many authors. Very extensive surveys into recent advances in *damage mechanics* are given by BODNER and HASHIN (1986), KRAJCINOVIC (1996) and KRAJCINOVIC and LEMAITRE (1987), for instance. Further contributions to the theory of *Continuum Damage Mechanics* should be mentioned in the literature, for example, AL-GADHIB et al (2000), BETTEN (1983b; 1986a; 1992), CHABOCHE (1984; 1999), CHRZANOWSKI (1976), HAYAKAWA and MURAKAMI (1998), JAKOWLUK (1993), KRAJCINOVIC (1983), LEMAITRE (1992; 1996), LEMAITRE and CHABOCHE (1990), LITEWKA and HULT (1989), LITEWKA and MORZÝNSKA (1989), MURAKAMI (1983; 1987), MURAKAMI and KAMIYA (1997), MURAKAMI and OHNO (1981), MURAKAMI and SAWCZUK (1981), MURAKAMI, SANOMURA and SAITOH (1986), MURAKAMI, HAYAKAWA and LIU (1998), ONAT (1986), and SKRZYPEK (1999).

In the past two decades there has been considerable progress and significant advances made in the development of fundamental concepts of damage mechanics and their application to solve practical engineering problems. For instance, new concepts have been effectively applied to characterize creep damage, low and high cycle fatigue damage, creep-fatigue interaction, brittle/elastic damage, ductile/plastic damage, strain softening, strain-rate-sensitivity damage, impact damage, and other physical phenomena. The materials include rubbers, concretes, rocks, polymers, composites, ceramics, and metals. This area has attracted the interest of a broad spectrum of international research scientists in micromechanics, continuum mechanics, mathematics, materials science, physics, chemistry and numerical analysis. However, sustained rapid growth in the development of damage mechanics requires the prompt dissemination of original research results, not only for

the benefit of the researchers themselves, but also for the practising engineers who are under continued pressure to incorporate the latest research results in their design procedures and processing techniques with newly developed materials.

In this context an excellent book, recently published by SKRZYPEK and GANCZARSKI (1999), should be recommended. This book is an extensive and comprehensive survey of one- and three- dimensional damage models for elastic and inelastic solids. The state–of-the-art is reported by more than 200 references. The book not only provides a rich current source of knowledge, but also describes examples of practical applications, numerical procedures and computer codes. The style of the presentation is systematic, clear, and concise, and is supported by illustrative diagrams.

Because of the broad applicability and versatility of the concept of damage mechanics, the research results have been published in over thirty English and non-English technical journals. This multiplicity has imposed an unnecessary burden on scientists and engineers alike to keep abreast with the latest development in the subject area. The new *International Journal of Damage Mechanics* has been inaugurated to provide an effective mechanism hitherto unavailable to them, which will accelerate the dissemination of information on damage mechanics not only within the research community but also between the research laboratory and industrial design department, and it should promote and contribute to future development of the concept of damage mechanics.

Furthermore, one should emphasize that special *Conferences on Damage Mechanics* has contributed significantly to the development of theories and experiments in Damage Mechanics, for instance, the Conference on *Damage Mechanics* held in Cachan (1981) or the IUTAM-Symposium on *Mechanics of Damage and Fatigue* held in Haifa and Tel Aviv (1985), CEEPUS Summer School on *Analysis of Elastomers and Creep and Flow of Glas and Metals* held in Zilina,Slovakia (1996), CISM Advanced School on *Applications of Tensor Functions in Solid Mechanics* held in Udine (1984) and in Bad Honnef (1986), CISM Advanced School on *Modelling of Creep and Damage Processes in Materials and Structures* held in Udine (1998), Workshop on Modelling of *Damage Localisation and Fracture Processes in Engineering Materials* held in Kazimierz Dolny, Poland(1998), Symposium on *Anisotropic Behaviour of Damaged Materials*, held in Kraków-Przegorzaly, Poland (2002), to name just a few, gave many impulses. The keynote lectures delivered during the last Symposium in Kraków have been printed in a new book, edited by SKRZYPEK and GANCZARSKI (2003).

This book provides a survey of various damage models focusing on the damage response in anisotropic materials as well as damage-induced anisotropy. There was a lack of such a book that would deal with the anisotropic damage mechanics with micro-mechanical aspects and thermo-mechanical coupling involved.

The book is divided into three parts. Part I *General description of anisotropically damaged materials* contains the Chapters 1-4 on: the mathematical bases of tensor functions application to damage anisotropy (J. BETTEN, *Technical University of Aachen*); the multi-scale damage mechanics (J.-L. CHABOCHE, *ONERA*, Chatillon, co-author N. CARRÈRE); an alternative approach to anisotropic damage via critical plane concept (Z. MRÓZ, *IPPT PAN*, Warsaw, co-author J. MACIEJEWSKI) and a formal description of damage induced anisotropy (J. GRABACKI, *Cracow University of Technology*, Kraków)

Part II *Phenomenological- and micro-mechanical-based approaches to anisotropic damage and fracture in brittle materials* includes Chapters 5-7 on: anisotropic elastic-brittle damage and fracture description based on irreversible thermodynamics (J. J. SKRZYPEK, *Cracow University of Technology*, Kraków, co-author H. KUNU-CISKAL); experimental nnd theoretical investigations of anisotropic damage in concrete and fiber reinforced concrete (A. LITEWKA et al., *Universidade da Beira Interior*, Covilha) and micro-mechanical damage model in rock-like solids (M. BASISTA, *IPPT PAN*, Warsaw).

Part III *Damage induced creep anisotropy of metallic materials under thermo- mechanical loadings* consists of Chapters 8-10 on: an extension of isotropic creep damage theories to anisotropic materials (H. ALTENBACH, *Martin-Luther-University*, Halle-Wittenberg); experimental investigations of creep fracture anisotropy in weld metal at elevated temperature (T. H. HYDE et al.,*University of Nottingham*) and non-classical problems of coupled thermo-damage fields (A. GANCZARSKI, *Cracow University of Technology*, Kraków),

To summarize the scope of this book as well as to briefly present other directions of research and future trends the Editors decided to include to the book additional concluding remarks (M. ZYCZKOWSKI, *Cracow University of Technology*, Kraków).

The best way to give a quick overview of some important works in damage mechanics may be in form of a table as has proposed by MURAKAMI (1987). The following Table 1.1 based upon MURAKAMI's scheme (1987)

has been modified by SKRZYPEK and GANCZARSKI (1999) and by BETTEN (2001b).

Table 1.1: Classification of material damage, microscopic mechanisms and chararacteristic features

References	Microscopic mechanisms and characteristic features
Elastic-brittle damage	
GRABACKI (1994) KRAJCINOVIC and FONSEKA (1981) KRAJCINOVIC (1984; 1996) LEMAITRE and CHABOCHE (1990) LITEWKA (1985; 1989) LITEWKA and HULT (1989) MARIGO (1985) MURAKAMI and KAMIYA (1997) NAJAR (1994)	Nucleation and growth of microscopic cracks caused by elastic deformations. Change of effective stiffness and compliance due to the strength reduction and elastic modulus drop with damage evolution. (Metals, rocks, concrete, composites).
Elastic-plastic damage	
TVERGAARD (1988) CHOW and LU (1992) DRAGON (1985) LEMAITRE (1985) MURZEWSKI (1992) MOU and HAN (1996) SAANOUNI (1994) VOYIADJIS and KATTAN (1992)	Nucleation, growth, and coalescence of microscopic voids caused by the (large) elastic-plastic deformation. Intersection of slipbands, decohesion of particles from the matrix material, cracking of particles. Void coalescence of shear bands formation. (Metals, composite, polymers).
Spall damage	
DAVISON et al. (1977; 1978) GRADY (1982) JOHNSON (1981) NEMES (1990) PERZYNA (1986)	Elastic and elastic-plastic damage due to impulsive loads. Propagation of shock plastic waves. Coupling between nucleation and growth of voids and stress waves. Coalescence of microcrack prior to the fragmentation process. Full separation resulting from macrocrack propagation through heavily damaged material.
Fatigue damage	
COFFIN (1954) CHABOCHE (1974) DUFAILLY and LEMAITRE (1995) KRAJCINOVIC (1996) LEMAITRE (1992) LEMAITRE and CHABOCHE (1990) MANSON (1979) NAJAR (1994) SKOCZEN (1996)	Nucleation and growth of microscopic transgranular cracks in the vicinity of surface. High cycle fatigue (number of cycles to failure larger than 10^5): effect of macroscopic plastic strain is negligible. Very low cycle fatigue (number of cycles below 10): crack initiation in the vicinity of surface in the slip bands in grains prior to the rapid transgranular mode in the slip planes.

Table 1.1: Classification of material damage, microscopic mechanisms and chararacteristic features

References	Microscopic mechanisms and characteristic features
Creep damage	
BETTEN (1983b; 1992) BETTEN et al. (1999) CHABOCHE (1981; 1988) H.ALTENBACH et al. (1990; 1997) HAYHURST and LECKIE (1973) HAYHURST et al.(1984) J.ALTENBACH et al. (1997) KACHANOV (1958) KOWALESKI (1996a,b,c) KRAJCINOVIC (1983; 1996) LECKIE and HAYHURST (1974) MURAKAMI (1983) NAUMENKO (1996) NEEDLEMAN et al. (1995) QI (1998) QI and BERTRAM (1997) RABOTNOV (1969) STIGH (1985) TRAMPCZYNSKI et al. (1981) ZHENG and BETTEN (1996)	Nucleation and growth of microscopic voids and cracks in metal grains (ductile transgranular creep damage at low temperatures), or on intergranular boundaries (brittle intergranular damage at high temperatures) mainly due to grain boundaries sliding and diffusion.
Creep-fatigue damage	
CHRZANOWSKI (1976) DUNNE and HAYHURST (1994) HELLE and TVERGAARD (1998) JAKOWLUK (1993) LEMAITRE and CHABOCHE (1975; 1990) WANG (1992)	Damage induced by repeated mechanical and thermal loadings at high temperature. Coupled creep-cyclic plasticity damage. Nonlinear interaction between intergranular voids and transgranular cracks. Slip bands formation due to plasticity (low temperature) combined with microcrack development due to creep (high temperature). (Metals, alloy steels, aluminum alloy, copper).
Irradiation damage	
GITTUS (1978) MURAKAMI and MIZUNO (1992) TETELMAN and MCEVILY (1970)	Damage caused by irradiation of neutron particles and α rays. Knock-on of atoms, nucleation of voids and bubbles, swelling. Ductile behavior of creep under irradiation and brittle behavior on post-irradiation creep.

Table 1.1: Classification of material damage, microscopic mechanisms and
chararacteristic features

References	Microscopic mechanisms and characteristic features
Anisotropic damage	
BETTEN (1992) CHABOCHE (1993) CHABOCHE et al. (1995) CHEN and CHOW (1995) CHOW and WANG (1987a,b) LADEVEZE (1990) LIS (1992) LITEWKA (1985) MATZENMILLER and SACKMANN (1994) MURAKAMI and KAMIYA (1997) SIDOROFF (1981) VOYIADJIS and VENSON (1995) ZHENG and BETTEN (1996)	Damage induced anisotropy of solids or damage anisotropic materials (composites). Unilateral damage (opening/closure effect). Anisotropic elastic-brittle damage. Nonproportional and cyclic loadings. Effective state variables and damage effect tensor. (Concrete, anisotropic ceramic composites).
Thermo-creep damage	
GANCZARSKI and SKRZYPEK (1995; 1997) KAVIANY (1995) SAANOUNI et al. (1994) SKRZYPEK and GANCZARSKI (1998)	Thermo-elastic-viscoplastic damage (fully coupled approach). Damage effect on heat flux in solids. Change of temperature gradient due to damage evolution.

Further reviews should be mentioned, for instance, the extended reports by ZHENG (1994), KRAJCINOVIC (1984), MURAKAMI (1987), ZYCZKOWSKI (1988; 1996) or the comprehensive surveys in the monographs and textbooks published by KRAJCINOVIC and LEMAITRE (1987), KACHANOV (1986), KRAJCINOVIC (1996), LEMAITRE and CHABOCHE (1990), LEMAITRE (1992), SKRZYPEK and GANCZARSKI (1999), to name but a few.

The different types of material damage listed in Table 1.1 have (more or less) a significant influence on the mechanical properties of the material, e.g., on the elasticity modulus, the elastic stiffness, the velocities of elastic waves, the plastic properties, the strength of materials, the fatigue strength, the creep rupture time, etc.. Thus, damage mechanics and their application play a central role in solving practical engineering problems.

Before formulating some basic equations of continuum mechanics and constitutive equations for materials under multi-axial states of stress and creep conditions, a short outline of tensor algebra should be given in the next chapter.

2 Tensor Notation

It will be convenient in this monograph to use the compact notation often referred to as *indicial* or *index notation* . It allows a strong reduction in the number of terms in an equation and is commonly used in the current literature when stress, strain, and constitutive equations are discussed. Therefore, a basic knowledge of the index notation is helpful in studying continuum mechanics, especially constitutive modelling of materials. With such a notation, the various stress-strain relationships for materials under multi-axial states of stress can be expressed in a compact form. Thus, greater attention can be paid to physical principles rather than to the equations themselves. A short outline of this notation should therefore be given in the following. In comparison, some expressions or equations shall also be written in *symbolic* or *matrix notation* , employing whichever is more convenient for the derivation or analysis at hand, but taking care to establish the interrelationship between the two distinct notations.

2.1 Cartesian Tensors

We consider vectors and tensors in three-dimensional EUCLIDean space. For simplicity, rectangular Cartesian coordinates x_i, $i = 1, 2, 3$, are used throughout. Results may, if desired, be expressed in terms of curvlinear coordinate systems by standard techniques of tensor analysis (BETTEN, 1987c), as has been pointed out in Section 2.2 and used in Chapter 5.

In a rectangular Cartesian coordinate system, a *vector V* can be decomposed in the following three components

$$\boldsymbol{V} = (V_1, V_2, V_3) = V_1 \boldsymbol{e}_1 + V_2 \boldsymbol{e}_2 + V_3 \boldsymbol{e}_3 \, , \qquad (2.1)$$

where $\boldsymbol{e}_1, \boldsymbol{e}_2, \boldsymbol{e}_3$ are unit base vectors:

$$\boldsymbol{e}_i \cdot \boldsymbol{e}_j = \delta_{ij} \, . \qquad (2.2)$$

In 2.2 the Symbol δ_{ij} is known as KRONECKER's delta. Thus, the set of unit vectors, $\{e_i\}$, constitutes an *orthonormal basis* .

A very useful notational device in the manipulation of matrix, vector, and tensor expressions is the *summation convention* introduced by EINSTEIN (1916):

> Whenever an index occurs twice in the same term, summation over the values 1, 2, and 3 of that index is automatically assumed, and the summation sign is omitted.

Thus, the decomposition (2.1) can be written in the more compact form

$$V = V_i e_i \equiv V_k e_k \ . \tag{2.1*}$$

The repeated index i or k in (2.1*) is often called *summation index* or *dummy index* because the choice of the letter for this index is immaterial. However, we have to notice that an index must not appear more than twice in the same term of an expression or equation. Otherwise, there is a mistake. An expression such as $A_{ijk}B_{kk}$ would be meaningless.

Consider a sum in which one of the repeated indices is on the KRO-NECKER delta, for example,

$$\delta_{ik}A_{ij} = \delta_{1k}A_{1j} + \delta_{2k}A_{2j} + \delta_{3k}A_{3j} \ .$$

Only one term in this sum does not vanish, namely the term in which $i = k = 1, 2, 3$. Consequently, the sum reduces to

$$\delta_{ik}A_{ij} = A_{kj} \ .$$

A similar example is: $\delta_{ij}V_j = V_i$. Notice that the summation, involving one index of the KRONECKER delta and one of another factor, has the effect of *substituting* the free index of the delta for the repeated index of the other factor. For this reason the KRONECKER delta could be called *substitution tensor* (BETTEN, 1987c).

Another example of the summation convention is the scalar product (dot product, inner product) of two vectors U and V. It can be written as

$$U \cdot V = U_1 V_1 + U_2 V_2 + U_3 V_3 \equiv U_k V_k \ . \tag{2.3}$$

Note that the expression

$$(A_{ii})^2 \equiv (A_{11} + A_{22} + A_{33})^2$$

is different from the sum

$$A_{ii}^2 \equiv A_{11}^2 + A_{22}^2 + A_{33}^2 \, ,$$

where the first one is the square of the sum A_{ii}, while the second one is the sum of the squares.

The vector product (cross product) has the following form:

$$\boldsymbol{C} = \boldsymbol{A} \times \boldsymbol{B} = \begin{vmatrix} \boldsymbol{e}_1 & \boldsymbol{e}_2 & \boldsymbol{e}_3 \\ A_1 & A_2 & A_3 \\ B_1 & B_2 & B_3 \end{vmatrix} \equiv \varepsilon_{ijk} \boldsymbol{e}_i A_j B_k \, . \qquad (2.4a)$$

Its components are given by

$$C_i = \varepsilon_{ijk} A_j B_k \, . \qquad (2.4b)$$

In (2.4a,b) the *alternating symbol* ε_{ijk} (also known as permutation symbol or third-order alternating tensor) is used. It is defined as:

$$\varepsilon_{ijk} \begin{cases} = +1 & \text{if } ijk \text{ represents an even permutation of } 123 \text{ ;} \\ = 0 & \text{if any two of } ijk \text{ indices are equal ;} \\ = -1 & \text{if } ijk \text{ represents an odd permutation of } 123 \text{ .} \end{cases} \qquad (2.5)$$

It follows from this definition that ε_{ijk} has the symmetry properties

$$\varepsilon_{ijk} = \varepsilon_{jki} = \varepsilon_{kij} = -\varepsilon_{ikj} = -\varepsilon_{jik} = -\varepsilon_{kji} \, . \qquad (2.6)$$

The triple scalar product can also be calculated by using the alternating symbol:

$$(\boldsymbol{A} \times \boldsymbol{B}) \cdot \boldsymbol{C} = \begin{vmatrix} A_1 & A_2 & A_3 \\ B_1 & B_2 & B_3 \\ C_1 & C_2 & C_3 \end{vmatrix} = \varepsilon_{ijk} A_i B_j C_k \, . \qquad (2.7)$$

The following relation between the KRONECKER delta and the alternating tensor is very important and useful (BETTEN, 1987c):

$$\varepsilon_{ijk} \varepsilon_{pqr} = \begin{vmatrix} \delta_{ip} & \delta_{iq} & \delta_{ir} \\ \delta_{jp} & \delta_{jq} & \delta_{jr} \\ \delta_{kp} & \delta_{kq} & \delta_{kr} \end{vmatrix} \equiv 3! \, \delta_{i[p]} \delta_{j[q]} \delta_{k[r]} \, , \qquad (2.8)$$

where on the right-hand side the operation of alternation is used. This process is indicated by placing square brackets around those indices to which it applies, that is, the three indices pqr are permutated in all possible ways. Thus, we obtain 3! terms. The terms corresponding to even permutations are given a plus sign, those which correspond to odd permutations a minus sign, and they are then added and divided by 3!.

From (2.8) we immediately obtain the *contraction*

$$\varepsilon_{ijk}\varepsilon_{pqk} = \delta_{ip}\delta_{jq} - \delta_{iq}\delta_{jp} , \qquad (2.9a)$$

for instance, i.e., the tensor of rank six in (2.8) is reduced to the fourth-order tensor (2.9a). Other *contractions* are

$$\varepsilon_{pqi}\varepsilon_{pqj} = 2\delta_{ij} \quad \text{and} \quad \varepsilon_{pqr}\varepsilon_{pqr} = 6 , \qquad (2.9b,c)$$

for instance.

Now let us consider a coordinate transformation, i.e., we introduce a new rectangular right-handed Cartesian coordinate system and new base vectors e_i^*, $i = 1, 2, 3$. The new system may be regarded as having been derived from the old by a rigid rotation of the triad of coordinate axes about the same origin. Let a vector V have components V_i in the original coordinate system and components V_i^* in the new system. Thus, one can write:

$$V = V_i e_i = V_i^* e_i^* . \qquad (2.10)$$

We denote by a_{ij} the cosine of the angle between e_i^* and e_j, so that

$$a_{ij} \equiv \cos(e_i^*, e_j) = e_i^* \cdot e_j , \qquad (2.11)$$

i.e., a_{ij} are the direction cosines of e_i^* relative to the first coordinate system, or, equivalently, a_{ij} are the components of the new base vectors e_i^*, in the first system. Thus

$$e_i^* = a_{ij}e_j . \qquad (2.12)$$

It is geometrically evident that the nine quantities a_{ij} are not independent. Since e_i^* are mutually perpendicular unit vectors,

$$e_i^* \cdot e_j^* = \delta_{ij} , \qquad (2.13)$$

we arrive at

$$e_i^* \cdot e_j^* = a_{ip}e_p \cdot a_{jr}e_r = a_{ip}a_{jr}e_p \cdot e_r = a_{ip}a_{jr}\delta_{pr} = a_{ip}a_{jp}$$

by considering (2.2) and (2.12). Hence

$$a_{ip}a_{jp} = \delta_{ij} \quad \text{or in matrix notation} \quad \boldsymbol{a}\boldsymbol{a}^t = \boldsymbol{\delta} \; , \tag{2.14a}$$

where $\boldsymbol{a}^t$ is the transpose of the matrix $\boldsymbol{a}$. Because of the symmetry $\delta_{ij} = \delta_{ji}$, the result (2.14a) represents a set of six relations between the nine quantities a_{ij}. Similarly to (2.14a), we find:

$$a_{pi}a_{pj} = \delta_{ij} \quad \text{or in matrix notation} \quad \boldsymbol{a}^t\boldsymbol{a} = \boldsymbol{\delta} \; . \tag{2.14b}$$

It follows immediately from (2.14a,b) that $|a_{ij}| = \pm 1$ and, furthermore, that the transpose $\boldsymbol{a}^t$ is identical to the inverse $\boldsymbol{a}^{-1}$. Thus, the matrix $\boldsymbol{a}$ is *orthogonal*, and the reciprocal relation to (2.12) is

$$\boldsymbol{e}_i = a_{ji}\boldsymbol{e}_j^* \; . \tag{2.15}$$

Inserting (2.15) or (2.12) into (2.10), we arrive at

$$V_i^* = a_{ij}V_j \quad \text{or} \quad V_i = a_{ji}V_j^* \; , \tag{2.16a,b}$$

respectively. In particular, if $\boldsymbol{V}$ is the position vector $\boldsymbol{x}$ of the point P relative to the origin, then

$$x_i^* = a_{ij}x_j \quad \text{and} \quad x_i = a_{ji}x_j^* \; , \tag{2.17a,b}$$

where x_i^* and x_i are the coordinates of the point P in the new and original coordinate systerns, respectively.

Now, let us consider a vector function

$$\boldsymbol{Y} = \boldsymbol{f}(\boldsymbol{X}) \quad \text{or in index notation:} \quad Y_i = f_i(X_p) \; , \tag{2.18a,b}$$

where $\boldsymbol{X}$ is the argument vector which is transformed to another vector $\boldsymbol{Y}$. The simplest form is a *linear transformation*

$$Y_i = T_{ij}X_j \; , \tag{2.19}$$

where T_{ij} are the cartesian components of a *second-order tensor* $\boldsymbol{T}$, also called *second-rank tensor* , i.e., a second-order tensor can be interpreted as a linear operator which transforms a vector $\boldsymbol{X}$ into an image vector $\boldsymbol{Y}$.

In extension of the law (2.16a,b), the components of a second-order tensor $\boldsymbol{T}$ transform according to the rule

$$T_{ij}^* = a_{ip}a_{jq}T_{pq} \quad \text{or} \quad T_{ij} = a_{pi}a_{qj}T_{pq}^* \; , \tag{2.20a,b}$$

which can be expressed in matrix notation:

$$\boldsymbol{T}^* = \boldsymbol{a}\boldsymbol{T}\boldsymbol{a}^t \quad \text{or} \quad \boldsymbol{T} = \boldsymbol{a}^t\boldsymbol{T}^*\boldsymbol{a} \ . \qquad (2.21\text{a,b})$$

Second-rank tensors play a central role in continuum mechanics, for instance, strain and stress tensors are second-order tensors. It is sometimes useful in continuum mechanics, especially in the theory of plasticity or in creep mechanics, to decompose a tensor into the sum of its *deviator* and a *spherical tensor* as follows:

$$T_{ij} = T'_{ij} + T_{kk}\delta_{ij}/3 \ . \qquad (2.22)$$

For instance, the stress deviator

$$\sigma'_{ij} := \sigma_{ij} - \sigma_{kk}\delta_{ij}/3 \qquad (2.23)$$

is responsible for the change of shape (*distortion*), while the hydrostatic stress $\sigma_{kk}\delta_{ij}/3$ produces volume change without change of shape in an *isotropic* continuum, i.e., in a material with the same material properties in all directions. Clearly, a uniform all-around pressure should merely decrease the volume of a sphere of material with the same strength in all directions. However, if the sphere were weaker in one direction, that diameter would be changed more than others. Thus, hydrostatic pressure can produce a change of shape in *anisotropic* materials.

The deviator (2.23) is often called a *traceless tensor* , since its trace $\operatorname{tr}\boldsymbol{\sigma}' \equiv \sigma'_{kk}$ is identical to zero.

A second-order tensor has three *irreducible invariants*

$$J_1 \equiv \delta_{ij}T_{ji} = T_{jj} \equiv T_{kk} \ , \qquad (2.24\text{a})$$
$$J_2 \equiv -T_{i[i]}T_{j[j]} = (T_{ij}T_{ji} - T_{ii}T_{jj})/2 \ , \qquad (2.24\text{b})$$
$$J_3 \equiv T_{i[i]}T_{j[j]}T_{k[k]} = \det(T_{ij}) \equiv |T_{ij}| \ , \qquad (2.24\text{c})$$

which are scalar quantities appearing in the *characteristic equation*

$$\det(\lambda\delta_{ij} - T_{ij}) = \lambda^3 - J_1\lambda^2 - J_2\lambda - J_3 = 0 \ . \qquad (2.25)$$

In (2.24b,c) the operation of alternation is used and indicated by placing square brackets around those indices to which it applies. This process is already illustrated in the context with (2.8).

We read from (2.24a,b,c): The first (linear) invariant J_1 is the trace of $\boldsymbol{T}$, the second (quadratic) invariant J_2 is defined as the *negative* sum of the three

principal minors of order 2, while the third (cubic) invariant is given by the determinant of the tensor. A deviator has only two non-vanishing invariants:

$$J_2' = T_{ij}'T_{ji}'/2 \ , \qquad\qquad J_3' = \det(T_{ij}') \ . \qquad\qquad (2.26\text{a,b})$$

Remark: Because of the definition (2.24b) the second invariant (2.26a) of the deviator is always *positive*. Therefore, J_2 is defined as the *negative* sum of the principal minors in this text.

The invariants (2.24a,b,c) can be expressed through the principal values T_I, T_{II}, T_{III} of the Tensor $\boldsymbol{T}$, i.e., the *elementary symmetric functions* of the three arguments $T_I, \ldots, T_{III}$ are related to the *irreducible invariants* (2.24a,b,c) as follows:

$$T_I + T_{II} + T_{III} = J_1 \ , \qquad\qquad (2.27\text{a})$$
$$T_IT_{II} + T_{II}T_{III} + T_{III}T_I = -J_2 \ , \qquad\qquad (2.27\text{b})$$
$$T_IT_{II}T_{III} = J_3 \ . \qquad\qquad (2.27\text{c})$$

After some manipulation one can arrive from (2.22), (2.24), and (2.26) at the relations

$$J_2' = J_2 + \frac{1}{3}J_1^2 \ , \qquad J_3' = J_3 + \frac{1}{3}J_1J_2 + \frac{2}{27}J_1^3 \ . \qquad (2.28\text{a,b})$$

In the theory of invariants the HAMILTON-CAYLEY *theorem* plays an important role. It states that

$$T_{ij}^{(3)} - J_1 T_{ij}^{(2)} - J_2 T_{ij} - J_3 \delta_{ij} = 0_{ij} \ , \qquad\qquad (2.29)$$

where $T_{ij}^{(3)} \equiv T_{ip}T_{pr}T_{rj}$ and $T_{ij}^{(2)} \equiv T_{ip}T_{pj}$ are, respectively, the third and the second power of the tensor $\boldsymbol{T}$. Thus, every second-order tensor (*linear operator*) satisfies its own *characteristic equation* (2.25). BETTEN (1987c; 2001c) has proposed extended characteristic polynomials in order to find irreducible invariants for *fourth-order tensors* (Section 4.3.2).

By analogy with (2.19), a *fourth-order tensor* $\boldsymbol{A}$, having 81 components A_{ijkl}, can be interpreted as a linear operator:

$$Y_{ij} = A_{ijkl}X_{kl} \qquad\qquad (2.30)$$

where X_{kl} and Y_{ij} are the cartesian components of the second-rank tensors $\boldsymbol{X}$ and $\boldsymbol{Y}$. For example, the constitutive equation

$$\sigma_{ij} = E_{ijkl}\varepsilon_{kl} \qquad\qquad (2.31)$$

describes the mechanical behavior of an anisotropic linear-elastic material, where σ_{ij} are the components of CAUCHY's stress tensor, ε_{ij} are the components of the infinitesimal strain tensor, and E_{ijkl} are the components (elatic constants) of the fourth-order material tensor characterising the *anisotropy* of the material.

2.2 General Bases

In the foregoing Section we have introduced an *orthonormal basis* $\{\boldsymbol{e}_i\}$ characterized by (2.2), i.e., we have restricted ourselves to rectangular cartesian coordinates. This is the simplest way to formulate the basic equations of continuum mechanics and the constitutive or evolutional equations of various materials. However, solving particular problems, it may be preferable to work in terms of more suitable coordinate systems and their associated bases.

In particular, cylindrical polar coordinates are useful for configurations which are symmetric about an axis, e.g., thick-walled tubes in Chapter 5. Another example is the system of spherical polar coordinates, which should be preferred when there is some symmetry about a point. Thus, it is useful to express the basic equations of continuum mechanics and the constitutive laws of several materials in terms of general (most curvlinear) coordinates. Thus, in the following some fundamentals of curvlinear tensor calculus should be discussed.

Let

$$x_i = x_i(\xi^p) \quad \Leftrightarrow \quad \xi^i = \xi^i(x_p) \tag{2.32}$$

be an admissible transformation of coordinates with JACOBIans

$$J \equiv |\partial x_i / \partial \xi^j| \quad \text{and} \quad K \equiv |\partial \xi^i / \partial x_j| \,,$$

which does not vanish at any point of the considered region, then $JK = 1$. Further important properties of admissible coordinate transformations are discussed, for instance, by SOKOLNIKOFF (1964) and BETTEN (1974) in more detail.

The coordinates x_i in (2.32) referred to a right-handed orthogonal cartesian system of axes define a three-dimensional EUCLIDean *space* , while the ξ^i are *curvlinear coordinates* . Because of the admissible transformation (2.32), each set of values of x_i corresponds a unique set of values of ξ^i, and vice versa. The values ξ^i therefore determine points in the defined three-dimensional EUCLIDean space. Hence we may represent our space by

the variables ξ^i instead by the cartesian system x_i, but the space remains, of course, EUCLIDean.

In this Section, we consider symbols characterized by one or several indices which may be either *subscripts* or *superscripts*, such as A_i, A^i, B_{ij}, B^{ij}, B^i_j, etc., where indices as superscripts are not taken as powers. Sometimes it is necessary to indicate the order of the indices when subscripts and superscripts occur together. In that case, for example, we write $A^i_{\bullet j}$ where the dot before j indicates that j is the second index while i is the first one.

As explained later, the values A_i and A^i can be considered as the *covariant* and the *contravariant components* , respectively, of the vector $\boldsymbol{A}$. However, the position of the indices on the "kernel" letters x and ξ in the *transformation of coordinates* (2.32) has nothing to do with *covariance* or *contravariance* and is therefore immaterial. In this context we refer to the following remarks of other authors:

- ❐ FUNG (1965, p38): The differential $d\theta^i$ is a contravariant vector, the set of variables θ^i itself does not transform like a vector. Hence, in this instance, the position of the index of θ^i must be regarded as without significance.
- ❐ GREEN/ZERNA (1968, pp5/6): The differentials $d\theta^i$ transform according to the law for contravariant tensors, so that the position of the upper index is justified. The variables θ^i themselves are in general neither contravariant nor covariant and the position of their index must be recognized as an exception. In future the index in non-tensors will be placed either above or below according to convenience. For example, we shall use either θ^i or θ_i.
- ❐ GREEN/ADKINS (1970, p1): The position of the index on coordinates x_i, y_i and θ^i is immaterial and it is convenient to use either upper or lower indices. The differential involving general curvilinear coordinates will always be denoted by $d\theta^i$ since $d\theta_i$ has a different meaning and is not a differential. For rectangular coordinates, however, we use either dx_i, dx^i for differentials, since $dx_i = dx^i$.
- ❐ MALVERN (1969, p603): **Warning**: Although the differentials dx^m are tensor components, the curvilinear coordinates x^m are not, since the coordinate transformations are general functional transformations and not the linear homogeneous transformations required for tensor components.

According to the above remarks, it is immaterial, if we write ξ^i or ξ_i. Since the differentials $d\xi^i$ transform corresponding to the law for con-

travariant tensors, the position of the upper index, ξ^i, is justified. Thus, the differential dT of a stationary scalar field $T = T(\xi^i)$ should be written as $dT = (\partial T / \partial \xi^i) d\xi^i$.

The position of a point P can be determined by x_i or, alternatively, by ξ^i as illustrated in Fig.2.1.
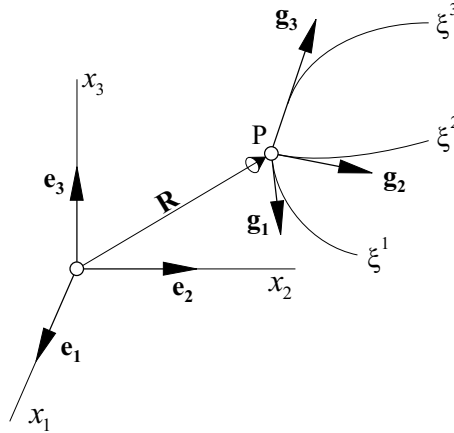
Fig. 2.1 Orthonormal and covariant base vectors

The position vector $\boldsymbol{R}$ of any point $P(x_i)$ can be decomposed in the form

$$\boldsymbol{R} = x_k \boldsymbol{e}_k \; . \tag{2.33}$$

Since the orthonormal base vectors $\boldsymbol{e}_i$ are independent of the position of the point $P(x_i)$, we deduce from (2.33) that

$$\partial \boldsymbol{R} / \partial x_i = \boldsymbol{e}_k (\partial x_k / \partial x_i) = \boldsymbol{e}_k \delta_{ki} = \boldsymbol{e}_i \; , \tag{2.34}$$

i.e., the orthonormal base vectors can be expressed by partial derivatives of the position vector $\boldsymbol{R}$ with respect to the rectangular cartesian coordinates x_i.

Analogous to (2.34), we find

$$\partial \boldsymbol{R} / \partial \xi^i = (\partial \boldsymbol{R} / \partial x_p)(\partial x_p / \partial \xi^i) = \boldsymbol{e}_p (\partial x_p / \partial \xi^i) = \boldsymbol{g}_i \; , \tag{2.35}$$

i.e., the geometrical meaning of the vector $\partial \boldsymbol{R} / \partial \xi^i$ is simple: it is a base vector directed tangentially to the ξ^i-coordinate curve. From (2.35) we observe

that the *covariant base vectors* $\boldsymbol{g}_i$ are no longer independent of the coordinates ξ^i, in contrast to the orthonormal base vectors. Furthermore, they need not be mutually perpendicular or of unit length.

The inverse form to (2.35) is given by

$$\boldsymbol{e}_i \equiv \partial \boldsymbol{R}/\partial x_i = (\partial \boldsymbol{R}/\partial \xi^p)(\partial \xi^p/\partial x_i) = \boldsymbol{g}_p(\partial \xi^p/\partial x_i) \ . \qquad (2.36)$$

Besides the *covariant base vectors* defined in (2.35), (2.36), a set of *contravariant base vectors* $\boldsymbol{g}^i$ is obtained from the constant unit vectors $\boldsymbol{e}_i \equiv \boldsymbol{e}^i$ as follows

$$\boldsymbol{g}^i = (\partial \xi^i/\partial x_p) \boldsymbol{e}^p \quad \Leftrightarrow \quad \boldsymbol{e}^i = (\partial x_i/\partial \xi^p) \boldsymbol{g}^p \ . \qquad (2.37)$$

This set of contravariant base vectors, $\boldsymbol{g}^i$, are often called the *dual* or *reciprocal basis* of the *covariant basis* $\boldsymbol{g}_i$, and they are denoted by superscripts. In the special case of rectangular cartesian coordinates, the covariant and contravariant base vectors are identical ($\boldsymbol{e}_i \equiv \boldsymbol{e}^i$).

From (2.35), (2.37) and considering the orthonormal condition we arrive at the relation

$$\boxed{\boldsymbol{g}_i \cdot \boldsymbol{g}^j = \delta_{ij} \equiv \delta_i^j} \ . \qquad (2.38)$$

between the two bases. For example, the contravariant base vector $\boldsymbol{g}^1$ is orthogonal to the two covariant vectors $\boldsymbol{g}_2$ and $\boldsymbol{g}_3$. Since these vectors directed tangentially to the ξ^2- and ξ^3-curves, the contravariant base vector $\boldsymbol{g}^1$ is perpendicular to the ξ^1-surface (Fig.2.2).
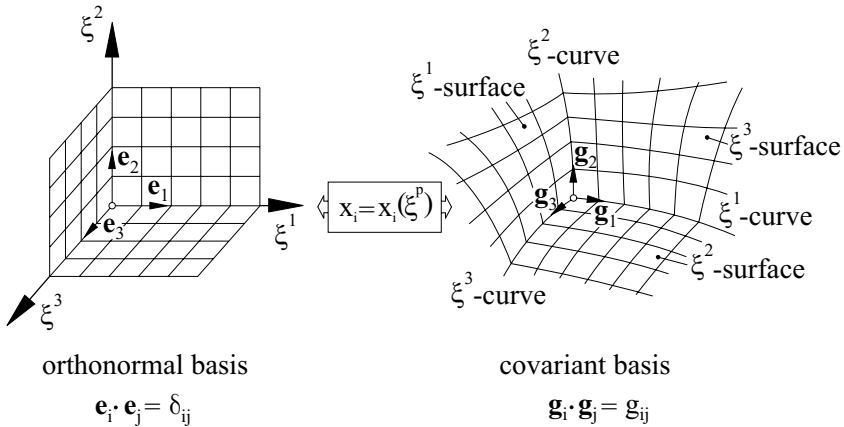

Fig. 2.2 Coordinate surfaces and base vectors

In addition to the relation (2.38) one can form the following scalar products:

$$\boxed{\boldsymbol{g}_i \cdot \boldsymbol{g}_j \equiv g_{ij}} \;, \qquad\qquad \boxed{\boldsymbol{g}^i \cdot \boldsymbol{g}^j \equiv g^{ij}} \;. \qquad\qquad (2.39\text{a,b})$$

These quantities, g_{ij} and g^{ij}, are called the *covariant* and *contravariant metric tensors* , respectively, and, because of (2.38), the KRONECKER *tensor* δ^i_j can be interpreted as a *mixed metric tensor* . The metric tensors (2.38), (2.39a,b) are symmetric since the scalar products of two vectors are commutative.

Inserting the base vectors (2.35) or (2.37) into (2.39a,b), respectively, we can express the *covariant* or *contravariant metric tensors* as

$$\boxed{g_{ij} = \left(\partial x_k / \partial \xi^i\right)\left(\partial x_k / \partial \xi^j\right)} \; \boxed{g^{ij} = \left(\partial \xi^i / \partial x_k\right)\left(\partial \xi^j / \partial x_k\right)} \;,$$
$$(2.40\text{a,b})$$

from which we immediately arrive at the reciprocal relation

$$\boxed{g_{ik} g^{jk} = \delta^j_i} \;. \qquad\qquad (2.41)$$

This result represents a system of linear equations from which the contravariant metric tensor can be calculated accordingly

$$g^{ij} = G^{ij}/g \quad \text{with} \quad G^{ij} \equiv (-1)^{i+j} U(g_{ij}) \;, \qquad (2.42)$$

when the covariant metric tensor is given, where G^{ij} is the *cofactor* of the element g_{ij} in the determinant $g \equiv |g_{ij}|$. From the reciprocal relation (2.41) we deduce the determinant of the contravariant metric tensor as $|g^{ij}| = 1/g$.

The magnitudes of the covariant and contravariant base vectors follow directly from (2.39a,b):

$$|\boldsymbol{g}_i| = \sqrt{\boldsymbol{g}_i \cdot \boldsymbol{g}_{(i)}} = \sqrt{g_{i(i)}} \;, \quad |\boldsymbol{g}^i| = \sqrt{\boldsymbol{g}^i \cdot \boldsymbol{g}^{(i)}} = \sqrt{g^{i(i)}} \;, \qquad (2.43\text{a,b})$$

where the index is not summed, as indicated by parentheses.

An increment $d\boldsymbol{R}$ of the position vector $\boldsymbol{R}$ in Fig.2.1 can be decomposed in the following ways

$$d\boldsymbol{R} = \boldsymbol{e}_i \, dx_i = \boldsymbol{g}_i \, d\xi^i = \boldsymbol{g}^i \, d\xi_i \;. \qquad (2.44)$$

Forming the scalar product

$$\boldsymbol{g}^j \cdot \boldsymbol{e}_i \, dx_i = \boldsymbol{g}^j \cdot \boldsymbol{g}_i \, d\xi^i = \delta_i^j \, d\xi^i = d\xi^j \, ,$$

and then inserting (2.37), we find the transformation

$$d\xi^j = \left(\partial \xi^j / \partial x_p\right) \boldsymbol{e}^p \cdot \boldsymbol{e}_i \, dx_i = \left(\partial \xi^j / \partial x_p\right) dx_p$$

or

$$d\xi^i = \left(\partial \xi^i / \partial x_p\right) dx_p \, , \tag{2.45a}$$

i.e., the $d\xi^i$ in (2.44) transforms *contravariant* (matrix $\partial \xi^i / \partial x_p$) and can be identified with the usual total differential of the variable ξ^i, so that the use of upper index is justified.

In a similar way one can find the *covariant* transformation

$$d\xi_i = \left(\partial x_p / \partial \xi^i\right) dx_p \, , \tag{2.45b}$$

which essentially differs from (2.45a) and cannot be interpreted as the total differential.

Using (2.44) with (2.39a,b) the square of the line element ds can be written in the form

$$ds^2 = d\boldsymbol{R} \cdot d\boldsymbol{R} = dx_k \, dx_k = g_{ij} \, d\xi^i \, d\xi^j = g^{ij} \, d\xi_i \, d\xi_j \, . \tag{2.46}$$

Hence, the reason for the term *metric tensor* g_{ij} is account for. In addition to (2.46), the mixed form $ds^2 = d\xi_k d\xi^k$ is also possible. This form follows immediately from (2.46) because of the *rule* of *raising* $(g^{ij} A_j = A^i)$ and *lowering* $(g_{ij} A^j = A_i)$ the indices.

Considering the decompositions of two vectors

$$\boldsymbol{A} = A^k \boldsymbol{g}_k = A_k \boldsymbol{g}^k \, , \qquad \boldsymbol{B} = B^k \boldsymbol{g}_k = B_k \boldsymbol{g}^k \, , \tag{2.47a,b}$$

we then can represent the scalar product in the following forms

$$\boldsymbol{A} \cdot \boldsymbol{B} = g_{ij} A^i B^j = A^k B_k = A_k B^k = g^{ij} A_i B_j \, , \tag{2.48}$$

from which we can determine the length of a vector $\boldsymbol{B} \equiv \boldsymbol{A}$ as

$$|\boldsymbol{A}| \equiv A = \sqrt{g_{ij} A^i A^j} = \sqrt{A^k A_k} = \sqrt{A_k A^k} = \sqrt{g^{ij} A_i A_j} \, . \tag{2.49}$$

Alternatively, the scalar product (2.48) can be expressed by $AB \cos \alpha$, so that the angle between two vectors can be calculated from the following formula:

$$\cos \alpha = g_{ij} A^i B^j / (AB) \, . \tag{2.50}$$

In particular, the angle α_{12} between the ξ^1-curve and ξ^2-curve, i.e., between the covariant base vectors $\boldsymbol{g}_1$ and $\boldsymbol{g}_2$ in Fig.2.2 can be determined in the following way

$$\left.\begin{array}{c} \underbrace{\boldsymbol{g}_1 \cdot \boldsymbol{g}_2}_{} \equiv g_{12} \\ |\boldsymbol{g_1}||\boldsymbol{g_2}| \cos\alpha_{12} \end{array}\right\} \quad \Rightarrow \quad \cos\alpha_{12} = \frac{g_{12}}{\sqrt{g_{11}g_{12}}} \, , \tag{2.51a}$$

where the relations (2.39a) and (2.43a) have been used. Cyclic permutations yield

$$\cos\alpha_{23} = \frac{g_{23}}{\sqrt{g_{22}g_{33}}} \quad \text{and} \quad \cos\alpha_{31} = \frac{g_{31}}{\sqrt{g_{33}g_{11}}} \, . \tag{2.51b,c}$$

From the result (2.51a,b,c) we deduce the following theorem:

> **A necessary and sufficient condition that a given curvlinear co-ordinate system be *orthogonal* is that the g_{ij} vanish for $i \neq j$ at every point in a region considered, i.e., the matrix (g_{ij}) has the diagonal form.**

According to (2.47a), there are two decompositions of a vector $\boldsymbol{A}$: The *contravariant components* A^k are the components of $\boldsymbol{A}$ in the directions of the *covariant base vectors* $\boldsymbol{g}_k$, while the *covariant components* A_k are the components of $\boldsymbol{A}$ corresponding with the *contravariant base* vectors $\boldsymbol{g}^k$, as illustrated in Fig.2.3.
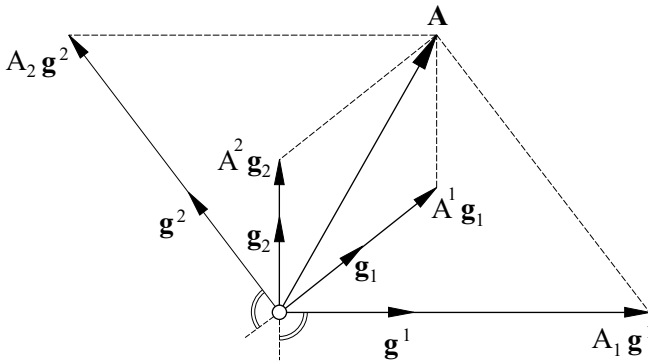

Fig. 2.3 Decomposition of a vector in covariant and contravariant components

A relation between the covariant and contravariant components, A_i and A^i, can be achieved by forming the scalar products of (2.47a), respectively, with the base vectors $\boldsymbol{g}_i$ and $\boldsymbol{g}^i$ according to

$$\boxed{A_i = g_{ik}A^k} \quad \text{and} \quad \boxed{A^i = g^{ik}A_k} . \tag{2.52a,b}$$

These results express the *rule of lowering and raising the indices* , respectively. This operation can also be applied to the base vectors in order to find relations between the *covariant* and *contravariant bases* :

$$\boxed{\boldsymbol{g}_i = g_{ik}\boldsymbol{g}^k} \quad \text{and} \quad \boxed{\boldsymbol{g}^i = g^{ik}\boldsymbol{g}_k} . \tag{2.53a,b}$$

Comparing the decompositions (2.47a) with the decompositions

$$\boldsymbol{A} = \bar{A}_k\boldsymbol{e}^k \equiv \bar{A}^k\boldsymbol{e}_k \tag{2.54}$$

with respect to the orthonormal basis $\boldsymbol{e}_k \equiv \boldsymbol{e}^k$, and considering (2.36), (2.37), one arrives at the folllowing relations between the covariant or contravariant components, A_i or A^i, and the cartesian components $\bar{A}_k \equiv \bar{A}^k$ of the vector $\boldsymbol{A}$:

$$\boxed{A_i = \left(\partial x_p / \partial \xi^i\right)\bar{A}_p} , \qquad \boxed{A^i = \left(\partial \xi^i / \partial x_p\right)\bar{A}^p} . \tag{2.55a,b}$$

We see in (2.55a,b) the same transformation matrices $(\partial x_p/\partial \xi^i)$ and $(\partial \xi^i/\partial x_p)$, respectively, as in (2.35) and (2.37).

In the *tensor analysis* the *Nabla operator* ∇, sometimes called *del operator* , plays a fundamental role. It is a differential operator, and can be decomposed with respect to the orthonormal basis:

$$\nabla = \boldsymbol{e}_i\nabla_i \equiv \boldsymbol{e}_i\frac{\partial}{\partial x_i} . \tag{2.56a}$$

Substituting $\boldsymbol{e}_i \equiv \boldsymbol{e}^i$ in (2.56a) by (2.37), and utilizing the chain rule

$$\frac{\partial}{\partial x_i} = \frac{\partial \xi^p}{\partial x_i}\frac{\partial}{\partial \xi^p} ,$$

we find the decomposition of the *Nabla operator* with respect to the contravariant basis:

$$\boxed{\nabla = \boldsymbol{g}^k\frac{\partial}{\partial \xi^k}} . \tag{2.56b}$$

The *divergence* of a vector field $\boldsymbol{A}$ is defined as the scalar product of the Nabla operator (2.56b) and the vector (2.47a):

$$\text{div } \boldsymbol{A} = \nabla \cdot \boldsymbol{A} = \partial A^i / \partial \xi^i + A^i \Gamma_{\cdot ij}^j \equiv A^i|_i \quad . \qquad (2.57)$$

The functions $T_{\cdot ij}^k$ in (2.57) are called the CHRISTOFFEL *symbols of the second kind* . They are the coefficients in the following decompositions

$$\partial \boldsymbol{g}_i / \partial \xi^j \equiv \Gamma_{\cdot ij}^k \boldsymbol{g}_k \equiv \left\{ \begin{matrix} k \\ ij \end{matrix} \right\} \boldsymbol{g}_k = \Gamma_{ijk} \boldsymbol{g}^k \ , \qquad (2.58a)$$

$$\partial \boldsymbol{g}^i / \partial \xi^j \equiv -\Gamma_{\cdot kj}^i \boldsymbol{g}^k \equiv -\left\{ \begin{matrix} i \\ kj \end{matrix} \right\} \boldsymbol{g}^k \ . \qquad (2.58b)$$

Because of the definition (2.58a), and considering (2.35), (2.36), the CHRISTOFFEL *symbols of the second kind* can be expressed in the form

$$\Gamma_{\cdot ij}^k = \frac{\partial \xi^k}{\partial x_p} \frac{\partial^2 x_p}{\partial \xi^i \partial \xi^j} \ . \qquad (2.59a)$$

They are symmetric with respect to the lower indices (i, j) and can be related to the metric tensors in the following way

$$\Gamma_{\cdot ij}^k \equiv \left\{ \begin{matrix} k \\ ij \end{matrix} \right\} = \frac{1}{2} g^{kl} \left(\partial g_{il} / \partial \xi^j + \partial g_{jl} / \partial \xi^i - \partial g_{ij} / \partial \xi^l \right) \ . \quad (2.59b)$$

In addition, the CHRISTOFFEL *symbols of the first kind* are given by

$$\Gamma_{kij} \equiv [ij, k] = [ji, k] = \frac{1}{2} \left(\partial g_{ik} / \partial \xi^j + \partial g_{jk} / \partial \xi^i - \partial g_{ij} / \partial \xi^k \right) \ . \qquad (2.60)$$

Comparing the two sets (2.59b) and (2.60), we read $g^{kl} \Gamma_{lij} \equiv \Gamma_{\cdot ij}^k$ in agreement with the rule of raising the indices.

Evidently there are $n = 3$ distinct CHRISTOFFEL symbols of each kind for each independent g_{ij}, and, since the number of independent g_{ij}'s is

$$n(n+1)/2 \, ,$$

the number of independent CHRISTOFFEL symbols is

$$n^2(n+1)/2 \, .$$

Note that the CHRISTOFFEL symbols, in general, are not tensors. This is valid also for the partial derivatives $\partial A^i / \partial \xi^j$ and $\partial A_i / \partial \xi^j$ with respect to curvlinear coordinates.

However, the derivative

$$\partial \boldsymbol{A}/\partial \xi^j = A^i|_j \boldsymbol{g}_i = A_i|_j \boldsymbol{g}^i \tag{2.61}$$

is a tensor, where the expressions

$$A^i|_j \equiv \partial A^i/\partial \xi^j + A^k \Gamma^i_{.kj} \quad \text{and} \quad A_i|_j \equiv \partial A_i/\partial \xi^j - A_k \Gamma^k_{.ij} \tag{2.62a,b}$$

are the *covariant derivatives* of the contravariant and covariant vector components, respectively. These derivatives transform like the components of a second-rank-tensor. The trace of (2.62a) immediately yields the divergence (2.57).

Let the vector $\boldsymbol{A}$ in (2.61) be the gradient of a scalar field. We then have

$$\partial \boldsymbol{A}\big/\partial \xi^j = \partial(\nabla \Phi)\big/\partial \xi^j = T_{ij} \boldsymbol{g}^i \ , \tag{2.63}$$

where

$$T_{ij} = T_{ji} = \frac{\partial^2 \Phi}{\partial \xi^i \partial \xi^j} - \Gamma^k_{.ij} \frac{\partial \Phi}{\partial \xi^k} \equiv \Phi_{,i}|_j \tag{2.64}$$

is a symmetric second-rank covariant tensor.

The LAPLACE *operator* Δ is defined as $\Delta \Phi = \mathrm{div\ grad}\,\Phi$. Using (2.56b), (2.57), (2.58), (2.39b), and the abbreviation (2.64), the following relation is obtained:

$$\Delta \Phi = \nabla \cdot \nabla \Phi = \left(\boldsymbol{g}^i \frac{\partial}{\partial \xi^i}\right) \cdot \left(\boldsymbol{g}^k \frac{\partial \Phi}{\partial \xi^k}\right) = g^{ij} T_{ij} \equiv g^{ij}\, \Phi_{,i}|_j \ . \tag{2.65}$$

The *gradient of a vector* $\boldsymbol{A}$ is formed by the *dyadic product* of the Nabla operator (2.56b) and the field vector (2.47a) in connection with (2.62a,b):

$$\boldsymbol{T} \equiv \nabla \otimes \boldsymbol{A} = \left(\boldsymbol{g}^j \frac{\partial}{\partial \xi^j}\right) \otimes (A^i \boldsymbol{g}_i) = A^i\big|_j \boldsymbol{g}^j \otimes \boldsymbol{g}_i \equiv T^i_j \boldsymbol{g}^j \otimes \boldsymbol{g}_i \tag{2.66a}$$

$$\boldsymbol{T} \equiv \nabla \otimes \boldsymbol{A} = \left(\boldsymbol{g}^j \frac{\partial}{\partial \xi^j}\right) \otimes (A_i \boldsymbol{g}^i) = A_i\big|_j \boldsymbol{g}^j \otimes \boldsymbol{g}^i \equiv T_{ij} \boldsymbol{g}^j \otimes \boldsymbol{g}^i \ . \tag{2.66b}$$

In contrast to (2.64), the tensor $T_{ij} \equiv A_i|_j$ in (2.66b) is **not** symmetric. From the representations (2.66a,b) we read that the mixed components T^i_j and the covariant components T_{ij} of *dyadic* $\boldsymbol{T} \equiv \nabla \otimes \boldsymbol{A}$ are identical with the covariant derivatives (2.62a,b), respectively.

In curvlinear coordinates, the constitutive equation (2.31) of the linear theory of elasticity should be expressed in the form

$$\tau^{ij} = E^{ijkl}\gamma_{kl} \, , \tag{2.67}$$

where the infinitesimal strain tensor γ is formed by covariant derivatives from the displacement vector w according to

$$\gamma_{ij} = \left(w_i|_{\,j} + w_j|_{\,i} \right) /2 \ . \tag{2.68}$$

In the absence of body forces the divergence of the stress tensor must be equal to zero. Thus, the *equations of equilibrium* are then given by

$$\tau^{ij}\,|_i = 0^j \ . \tag{2.69}$$

Note that for applications in solid mechanics the *physical components* of the tensors τ_{ij}, γ_{ij} and w_i, used in (2.67), (2.68), (2.69), have to be calculated accordingly to

$$\sigma^{ij} = \tau^{ij}\sqrt{g_{(ii)}g_{(jj)}} \, , \ \ \varepsilon_{ij} = \gamma_{ij}\sqrt{g^{(ii)}g^{(jj)}} \, , \ \ u_i = w_i\sqrt{g^{(ii)}} \, , \ \ (2.70\text{a,b,c})$$

where the bracketed indices should not be summed.

Considering a vector (2.47a) the components of which, $A^1 g_1$, $A^2 g_2$, $A^3 g_3$, form the edges of the parallelepiped whose diagonal is A. Since the g_i are **not** unit vectors in general, we see that the lengths of edges of this parallelepiped, or the *physical components* of A, are determined by the expressions

$$A^1\sqrt{g_{11}} \, , \qquad\qquad A^2\sqrt{g_{22}} \, , \qquad\qquad A^3\sqrt{g_{33}} \, ,$$

since $g_{11} = g_1 \cdot g_1, \ldots, g_{33} = g_3 \cdot g_3$.

As an example, let us introduce cylindrical coordinates

$$x_1 = \xi^1 \cos \xi^2 \, , \qquad x_2 = \xi^1 \sin \xi^2 \, , \qquad x_3 = \xi^3 \, , \tag{2.71}$$

where $\xi^1 \equiv r$, $\xi^2 \equiv \varphi$ and $\xi^3 \equiv z$. The covariant base vectors (2.35) are then given by

$$\left.\begin{aligned}
g_1 &= e_1 \cos \varphi + e_2 \sin \varphi \, , \\
g_2 &= -e_1 r \sin \varphi + e_2 r \cos \varphi \, , \\
g_3 &= e_3 \, ,
\end{aligned}\right\} \tag{2.72a}$$

while the contravariant base vectors (2.37) are immediately found according to

$$\boldsymbol{g}^1 = \boldsymbol{g}_1 \ , \qquad \boldsymbol{g}^2 = \boldsymbol{g}_2 \big/ r^2 \ , \qquad \boldsymbol{g}^3 = \boldsymbol{g}_3 \ . \qquad (2.72\text{b})$$

Since the cylindrical coordinates (2.71) are orthogonal, the metric tensors (2.39a,b), (2.40a,b) have the diagonal forms

$$g_{ij} = \begin{pmatrix} 1 & 0 & 0 \\ 0 & r^2 & 0 \\ 0 & 0 & 1 \end{pmatrix} , \qquad g^{ij} = \begin{pmatrix} 1 & 0 & 0 \\ 0 & 1/r^2 & 0 \\ 0 & 0 & 1 \end{pmatrix} , \qquad (2.73\text{a,b})$$

while the nonvanishing CHRISTOFFEL *symbols* (2.59a,b), (2.60) are given by

$$\Gamma_{122} \equiv -[12,2] = \Gamma^1_{.22} = -r, \quad \Gamma_{221} \equiv [21,2] = [12,2] = r, \quad \Gamma^2_{.12} = 1/r. \qquad (2.74)$$

Taking the covariant derivative (2.62b) into account, the tensor (2.68) can also be represented in the following way

$$\gamma_{ij} = \left(\partial w_i \big/ \partial \xi^j + \partial w_j \big/ \partial \xi^i \right) \big/ 2 - w_k \Gamma^k_{.ij} \ . \qquad (2.75)$$

The physical components (2.70c) of the displacement vector are in cylindrical coordinates because of (2.42b) very simple:

$$u_r = w_1 \ , \qquad u_\varphi = w_2/r \ , \qquad u_z = w_3 \ , \qquad (2.76)$$

and, likewise, we calculate from (2.70b) the physical components

$$\left. \begin{array}{ll} \varepsilon_r = \gamma_{11} \ , \qquad \varepsilon_\varphi = \gamma_{22}/r^2 \ , \qquad \varepsilon_z = \gamma_{33} \ , \\ \varepsilon_{r\varphi} = \gamma_{12}/r \ , \quad \varepsilon_{rz} = \gamma_{13} \ , \qquad \varepsilon_{z\varphi} = \gamma_{32}/r \ , \end{array} \right\} \qquad (2.77)$$

of the infinitesimal strain tensor, so that we finally arrive at the following components

$$\left. \begin{array}{l} \varepsilon_r = \partial u_r \big/ \partial r \ , \quad \varepsilon_\varphi = \left(\partial u_\varphi \big/ \partial \varphi + u_r \right) \big/ r \ , \quad \varepsilon_z = \partial u_z \big/ \partial z \ , \\ \varepsilon_{r\varphi} = \left[\left(\partial u_r \big/ \partial \varphi \right) \big/ r + \partial u_\varphi \big/ \partial r - u_\varphi \big/ r \right] \big/ 2 \ , \\ \varepsilon_{rz} = \left(\partial u_r/\partial z + \partial u_z/\partial r \right)/2 \ , \\ \varepsilon_{z\varphi} = \left[\left(\partial u_z \big/ \partial \varphi \right) \big/ r + \partial u_\varphi \big/ \partial z \right] \big/ 2 \ , \end{array} \right\} \qquad (2.78)$$

by considering (2.74), (2.75), and (2.76).

Finally, the physical components of the stress tensor are deduced from (2.70a):

$$\left.\begin{array}{lll} \sigma_r = \tau^{11} , & \sigma_\varphi = r^2\tau^{22} , & \sigma_z = \tau^{33} , \\ \sigma_{r\varphi} = r\tau^{12} , & \sigma_{\varphi z} = r\tau^{23} , & \sigma_{zr} = \tau^{31} , \end{array}\right\} \qquad (2.79)$$

so that we arrive from (2.69) by considering

$$A^{ij}|_k = \partial A^{ij} \big/ \partial\xi^k + \Gamma^i_{.kp} A^{pj} + \Gamma^j_{.kp} A^{ip} \qquad (2.80)$$

and (2.74) at the *equations of equilibrium*

$$\left.\begin{array}{l} \partial\sigma_r /\partial r + (\partial\sigma_{r\varphi}/\partial\varphi)/r + \partial\sigma_{zr}/\partial z + (\sigma_r - \sigma_\varphi)/r = 0 , \\ \partial\sigma_{r\varphi}/\partial r + (\partial\sigma_\varphi/\partial\varphi)/r + \partial\sigma_{\varphi z}/\partial z + 2\sigma_{r\varphi}/r = 0 , \\ \partial\sigma_{zr}/\partial r + (\partial\sigma_{\varphi z}/\partial\varphi)/r + \partial\sigma_z/\partial z + \sigma_{zr}/r = 0 . \end{array}\right\} \quad (2.81)$$

For *isotropic* materials the fourth-order elasticity tensor in (2.31) has the form

$$E_{ijkl} = \lambda\delta_{ij}\delta_{kl} + \mu(\delta_{ik}\delta_{jl} + \delta_{il}\delta_{jk}) , \qquad (2.82a)$$

while the material tensor in (2.67) is represented by

$$E^{ijkl} = \lambda g^{ij}g^{kl} + \mu\left(g^{ik}g^{jl} + g^{il}g^{jk}\right) , \qquad (2.82b)$$

so that we find from (2.67) in connection with (2.77) and (2.79) the following constitutive equations:

$$\left.\begin{array}{l} \sigma_r = 2\mu\varepsilon_r + \lambda(\varepsilon_r + \varepsilon_\varphi + \varepsilon_z) , \\ \sigma_\varphi = 2\mu\varepsilon_\varphi + \lambda(\varepsilon_r + \varepsilon_\varphi + \varepsilon_z) , \\ \sigma_z = 2\mu\varepsilon_z + \lambda(\varepsilon_r + \varepsilon_\varphi + \varepsilon_z) , \\ \sigma_{r\varphi} = 2\mu\varepsilon_{r\varphi} , \quad \sigma_{\varphi z} = 2\mu\varepsilon_{\varphi z} , \quad \sigma_{zr} = 2\mu\varepsilon_{zr} . \end{array}\right\} \qquad (2.83)$$

According (2.65) together with (2.64), the LAPLACE *operator* is defined in general. In the special case of cylindrical coordinates with (2.73a,b), (2.74) this operator takes the form

$$\Delta = \frac{\partial^2}{\partial r^2} + \frac{1}{r^2}\frac{\partial^2}{\partial\varphi^2} + \frac{1}{r}\frac{\partial}{\partial r} + \frac{\partial^2}{\partial z^2} , \qquad (2.84)$$

which occurs as a differential, for example, in the LAPLACE or POISSON equation. These partial differential equations are fundamental for many applications in continuum mechanic.

In the representation theory of tensor functions the *irreducible basic invariants*

$$S_1 = \delta_{ij}\bar{A}_{ji}\,, \qquad S_2 = \bar{A}_{ij}\bar{A}_{ji}\,, \qquad S_3 = \bar{A}_{ij}\bar{A}_{jk}\bar{A}_{ki} \qquad \text{(2,85a,b,c)}$$

or, alternatively, the *irreducible main invariants*

$$J_1 \equiv S_1\,, \quad J_2 = \left(S_2 - S_1^2\right)/2\,, \qquad \text{(2.86a,b)}$$

$$J_3 = \frac{2S_3 - 3S_2 S_1 + S_1^3}{6} \qquad \text{(2.86c)}$$

play a central role, since they form an *integrity basis* . In (2,85a,b,c) the $\bar{A}_{ij}$ are the components of the tensor $\boldsymbol{A}$ with respect to the orthonormal basis $\boldsymbol{e}_i$. The invariants (2,85a,b,c), e.g., can be expressed in terms of covariant or contravariant components of the tensor $\boldsymbol{A}$. To do this we need the following transformations

$$A_{ij} = \frac{\partial x_p}{\partial \xi^i}\frac{\partial x_q}{\partial \xi^j}\bar{A}_{pq} \quad \Leftrightarrow \quad \bar{A}_{ij} = \frac{\partial \xi^p}{\partial x_i}\frac{\partial \xi^q}{\partial x_j}A_{pq}\,, \qquad \text{(2.87)}$$

and

$$A^{ij} = \frac{\partial \xi^i}{\partial x_p}\frac{\partial \xi^j}{\partial x_q}\bar{A}_{pq} \quad \Leftrightarrow \quad \bar{A}^{ij} = \frac{\partial x_i}{\partial \xi^p}\frac{\partial x_j}{\partial \xi^q}A_{pq}\,, \qquad \text{(2.88)}$$

which are extended forms of (2.35), (2.36), and (2.37). Inserting the transformation (2.87) in (2,85a,b,c) and considering (2.40a,b), we finally find the *irreducible basic invariants* in the following forms:

$$S_1 = g^{pq}A_{pq} = g_{pq}A^{pq} = A_k^k\,, \qquad \text{(2.89a)}$$

$$S_2 = g^{ip}g^{jq}A_{ji}A_{pq} = g_{ip}g_{jq}A^{ji}A^{pq} = A_k^i A_i^k\,, \qquad \text{(2.89b)}$$

$$S_3 = g^{ip}g^{jq}g^{kr}A_{ij}A_{qk}A_{rp} = \cdots = A_j^i A_k^j A_i^k\,, \qquad \text{(2.89c)}$$

and then the *main invariants* (2.86a,b,c) also in terms of *covariant*, *contravariant* or *mixed tensor components*.

A lot of tensor operations are included in the **MAPLE tensor package**. Examples are illustrated in the following MAPLE program, where the metric tensors and the CHRISTOFFEL *symbols* have been calculated for *cylindrical* and *spherical* coordinates

$$\odot\ 2\_1.mws$$

```
>   with(tensor):
>   cylindrical_coord:=[r,phi,z]:
covariant metric tensor:
>   g_compts:=array(symmetric,sparse,1..3,1..3):
```

```
>   g_compts[1,1]:=1:  g_compts[2,2]:=r^2:
>   g_compts[3,3]:=1:
>   g:=create([-1,-1], eval(g_compts));
```

$$g := \text{table}([compts = \begin{bmatrix} 1 & 0 & 0 \\ 0 & r^2 & 0 \\ 0 & 0 & 1 \end{bmatrix} , \ index\_char = [-1, -1]])$$

```
>   D1g:=d1metric(g,cylindrical_coord):
>   Gamma[kij]:=[ijk];
```

```
>       CHRISTOFFEL[first_kind][cylindrical]:=
```

```
>       Gamma[kij]=Christoffel1(D1g):
```

$$\Gamma_{kij} := [ijk]$$

The results are printed as a list on the CD-ROM. They are identical
to those values in (2.74).

```
>   spherical_coord:=[r,phi,theta]:
```
covariant metric tensor:
```
>   g_compts:=array(symmetric,sparse,1..3,1..3):
>   g_compts[1,1]:=1:  g_compts[2,2]:=r^2:
>   g_compts[3,3]:=(r*sin(phi))^2:
>   g:=create([-1,-1], eval(g_compts));
```

$$g := \text{table}([compts = \begin{bmatrix} 1 & 0 & 0 \\ 0 & r^2 & 0 \\ 0 & 0 & r^2\sin(\phi)^2 \end{bmatrix} , \ index\_char = [-1, -1]])$$

```
>   D1g:=d1metric(g,spherical_coord):
>   Gamma[kij]:=[ijk];
```

```
>       CHRISTOFFEL[first_kind][spherical]:=
```

```
>       Gamma[kij]=Christoffel1(D1g):
```

$$\Gamma_{kij} := [ijk]$$

The results are printed as a list on the CD-ROM. In a similar way one can
find the CHRISTOFFEL *symbols* of the second kind.

3 Some Basic Equations of Continuum Mechanics

Creep mechanics is a part of continuum mechanics, like elasticity, plasticity, viscoelasticity, and viscoplasticity.

Continuum Mechanics is concerned with the mechanical behavior of *solids* and *fluids* on the macroscopic scale. It ignores the discrete nature of matter, and treats material as uniformly distributed throughout regions of space. It is then possible to define quantities such as density, displacement, velocity, etc., as continous (or at least piecewise continous) functions of position. This procedure is found to be satisfactory provided that we deal with bodies whose dimensions are large in comparison with the characteristic lengths (e.g.: interatomic spacings in a crystal, or mean free paths in a gas) on the microscopic scale.

Continuum mechanics can also be applied to a granular material such as sand, concrete or soil, provided that the dimensions of the regions considered are large compared with those of an individual grain.

The equations of continuum mechanics are of two main kinds. First, there are equations which apply equally to all materials. They describe universal physical laws, such as conservation of mass and energy. Second, there are equations characterizing the individual material and its reaction to applied loads; such equations are called *constitutive equations* (Chapter 4), since they describe the macroscopic behavior resulting from internal constitution of the particular materials.

In this Chapter, however, only the *kinematics* and the *concept of stress* should briefly be discussed.

3.1 Analysis of Deformation and Strain

This section is concerned with the kinematics of a continuous medium. Kinematics is the study of *motion* without regard to the forces which produce it. To describe the motion of a body, i.e., to specify the position of each particle at each instant we select a particular configuration of the body, for instance

the configuration of the body in its unloaded or undeformed state, and call this the *reference configuration* at the *reference time* $t = 0$. The set of co-ordinates a_i, referred to fixed cartesian axes, uniquely determines a particle of the body and may be regarded as a label by which the particle can be identified for all time (Fig. 3.1).
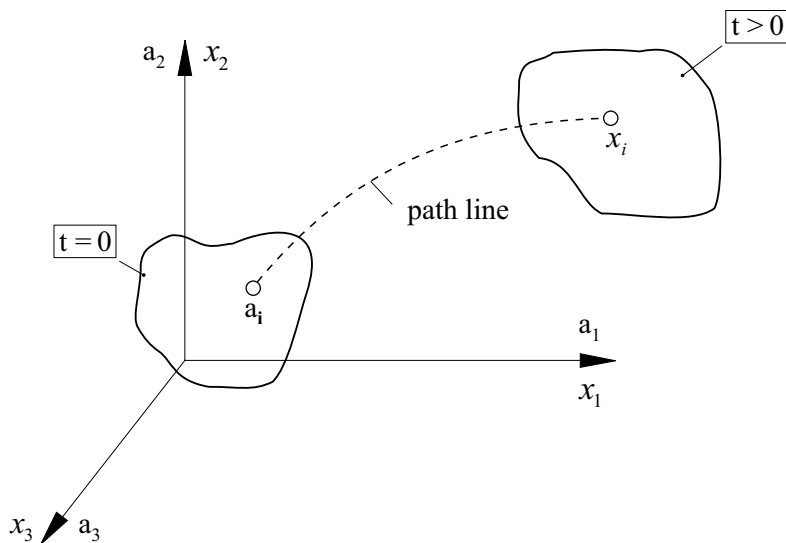

Fig. 3.1 Motion of a particle; reference ($t = 0$) and current ($t > 0$) configurations

The motion of the body may now be described by specifying the position x_i of the particle a_i at time $t > 0$ in the form

$$x_i = x_i(a_p, t) , \quad i, p = 1, 2, 3 . \tag{3.1a}$$

In other words: The place x_i is *occupied* by the body-point a_p at time t. We assume that this function is differentiable with respect to a_p and t as many times as required.

Sometimes we desire to consider only two configurations of the body, an initial and a final configuration. We refer to the mapping from the initial to the final configuration as a *deformation* of the body. The *motion* of the body may be regarded as a one-parameter sequence of deformations.

The mapping (3.1a) has the unique inverse

$$a_i = a_i(x_p, t) , \quad i, p = 1, 2, 3 \tag{3.1b}$$

provided that the JACOBIan determinant

$$J := \det(\partial x_i / \partial a_j) \tag{3.2}$$

exists and that it is always positiv ($J > 0$) at each point. The physical signif-
icance of these assumptions is that the material of the body cannot penetrate
itself, and that material occupying a finite non-zero volume at time $t = 0$
cannot be compressed to a point or expanded to infinite volume during the
motion; remark: $dV = J\, dV_0$.

   The inverse form (3.1b) may be viewed as a description which provides
a tracing to its original position of the particle a_i that *now* (at current time
$t > 0$) occupies the location x_i. In other words: An observer placed on x_i
registers a particle a_i at time t.

   The coordinates a_i are known as *material* (or LAGRANG*ian*) *coordinates*
since distinct sets of these coordinates refer to distinct material particles.
The coordinates x_i are known as *spatial* (or EULER*ian*) *coordinates* since
distinct sets refer to distinct points of space. Problems in continuum mechan-
ics may be formulated either with the material coordinates a_i as independent
variables, in which case we employ the *material description* of the prob-
lem, or with the spatial coordinates x_i as independent variables, in which we
employ the *spatial description* . In the material (LAGRANG*ian*) description
attention is focused on what is happening at (or in the neighbourhood of) a
particular material particle. In the spatial (EULER*ian*) description we concen-
trate on events at (or near to) a particular point in space. The mathematical
formulation of general physical laws and the description of the properties of
particular materials is often most easily accomplished in the material descrip-
tion, but for the solution of special problems it is frequently preferable to use
the spatial description. It is therefore necessary to employ both descriptions
and to relate them to each other. In principle it is possible to transform a
problem from the material to the spatial description or vice versa by using
(3.1a) or (3.1b). In practice the transition is not always accomplished easily.

   The time rate of change of any property of a continuum with respect
to specific particles of the moving continuum is called the *material time
derivative* (or *substantial derivative*) of that property. This derivative may be
thought of as the time rate of change that would be measured by an observer
traveling with a specific particle a_i. For instance, consider the temperature
field in a body

$$T = T(a_i, t) \quad \text{or} \quad T = T(x_i, t) \ . \tag{3.3a,b}$$

Its material time derivative is expressed by

$$\dot{T} = dT/dt = \partial T(a_i, t)/\partial t \; . \tag{3.4a}$$

The right-hand side of (3.4a) is sometimes written as $[\partial T(a_i, t)/\partial t]_{a_i}$ to emphasize that the coordinates a_i are held constant, i.e., a given particle is involved when calculating the partial derivative.

If the temperature field is expressed by the spatial description in the form (3.3b) we arrive, by using the chain rule of partial differentiation, at the following result

$$dT/dt = \partial T(x_i, t)/\partial t + \dot{x}_k \, \partial T(x_i, t)/\partial x_k \; , \tag{3.4b}$$

where $\dot{x}_i = v_i$ is the velocity vector. From (3.4b) we read the operator

$$\frac{d}{dt} = \frac{\partial}{\partial t} + v_k \frac{\partial}{\partial x_k} \quad \text{or} \quad \frac{d}{dt} = \frac{\partial}{\partial t} + \boldsymbol{v} \cdot \text{grad} \; , \tag{3.5}$$

which can be applied to tensor fields of any order, $T_{ij\ldots} = T_{ij\ldots}(x_p, t)$, expressed in spatial coordinates.

The first term on the right-hand side of (3.4b) gives the rate of change at a particular position and is accordingly called the *local rate of change* . This term is sometimes written as $[\partial T(x_i, t)/\partial t]_{x_i}$ to emphasize that x_i is held constant in this differentiation. The second term on the right-hand side of (3.4b) arises because the specific particles are changing their positions in space. This term expresses the contribution due to the motion of the particles in the variable field, and it is therefore called the *convection rate of change* .

The *displacement vector* $\boldsymbol{u} = \boldsymbol{x} - \boldsymbol{a}$ of a typical particle from its position $\boldsymbol{a}$ in the reference configuration to its position $\boldsymbol{x}$ at current time t can be represented as a function of LAGRANGian or EULERian coordinates,

$$u_i = u_i(a_p, t) = x_i(a_p, t) - a_i \; , \tag{3.6a}$$
$$u_i = u_i(x_p, t) = x_i - a_i(x_p, t) \; , \tag{3.6b}$$

by taking (3.1a,b) into account. Partial differentiation of the displacement vector (3.6a,b) with respect to the coordinates produces either the *material displacement gradient*

$$\partial u_i/\partial a_j = \partial x_i/\partial a_j - \delta_{ij} \tag{3.7a}$$

or the *spatial displacement gradient*

$$\partial u_i/\partial x_j = \delta_{ij} - \partial a_i/\partial x_j \; . \tag{3.7b}$$

In a similar way we define the *material* and *spatial deformation gradient*

$$F_{ij} := \partial x_i/\partial a_j \quad \text{and} \quad F_{ij}^{(-1)} := \partial a_i/\partial x_j \;, \qquad (3.8\text{a,b})$$

respectively. The deformation gradient (3.8a) can geometrically be interpreted in the following way. Two neighbouring particles which occupy points P_0 and Q_0 before deformation, move to points P and Q, respectively, in the deformed configuration (Fig. 3.2).
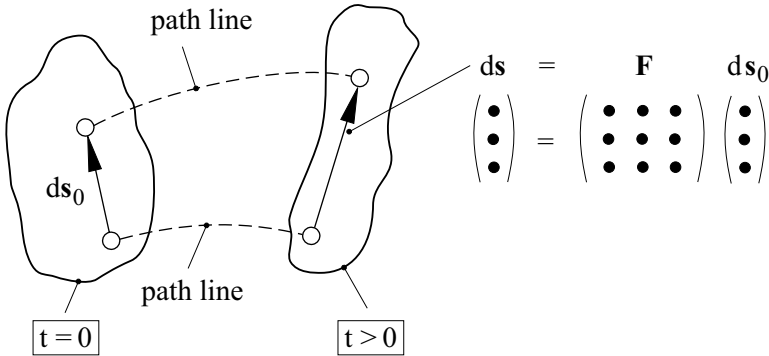

Fig. 3.2 Geometrical interpretation of the deformation gradient (BETTEN, 2001a)

From (3.1a) and (3.8a) the distance differential dx_i (*line element vector* $d\mathbf{s}$) can be expressed as follows:

$$dx_i = (\partial x_i/\partial a_j)\, da_j = F_{ij}\, da_j \quad \text{or} \quad d\mathbf{s} = \mathbf{F}\, d\mathbf{s}_0 \;. \qquad (3.9)$$

Thus, the deformation gradient $\mathbf{F}$ can be interpreted as a linear transformation or a second-rank tensor: the initial line element vector $d\mathbf{s}_0$ is mapped onto the corresponding vector $d\mathbf{s}$ at time t, where a *translation*, a *rigid rotation* , and a *stretching* of the line element is produced. This decomposition of the total *deformation* corresponds with the *polar decomposition theorem* which states that the non-singular deformation gradient (3.8) can be decomposed, uniquely, in either of the products

$$F_{ij} = R_{ik}U_{kj} \;, \qquad\qquad F_{ij} = V_{ik}R_{kj} \;, \qquad (3.10\text{a,b})$$

i.e., in matrix notation: $\mathbf{F} = \mathbf{R}\mathbf{U}$ and $\mathbf{F} = \mathbf{V}\mathbf{R}$, where $\mathbf{R}$ is an orthogonal rotation tensor, and $\mathbf{U}$, $\mathbf{V}$ are positive definite symmetric tensors which are called *right* ($\mathbf{U}$) and *left* ($\mathbf{V}$) *tensors* (BETTEN, 2001a) . However, the "translation part" of the total deformation is not involved in (3.10a,b) since a parallel transport does not change the cartesian components of a vector, here

the line element vector (3.9). The *shifter*, which shifts a vector from one coordinate system to another, is here merely δ_{ij}. But in curvlinear coordinates, parallel transport does change the *covariant* and *contravariant* components of a vector (BETTEN, 1987c) .

Although the deformation gradient tensor $\boldsymbol{F}$ plays a central role in the analysis of deformation, it is not itself a suitable (direct) *measure of strain* , since a measure of strain must be unchanged in a *rigid-body motion*

$$x_i = R_{ij}a_j + c_i \ , \tag{3.11}$$

where R_{ij} is any orthogonal (rotation) tensor ($R_{ik}R_{jk} = \delta_{ij}$). The vector c_i is independent of position and depends only on time t. Thus, the material deformation gradient (3.8a) of the rigid-body motion (3.11) is identical to the rotation tensor: $F_{ij} = R_{ij}$.

The difference $(ds)^2 - (ds_0)^2$ for two neighbouring particles of a continuum can be taken for a suitable measure of strain which occurs in the neighbourhood of the particles between the initial and current configurations. If this difference is identical to zero for all neighbouring particles of a material, a rigid-body motion (3.11) with $R_{ij}R_{ik} = \delta_{jk}$ results in:

$$(ds)^2 - (ds_0)^2 \equiv dx_i \, dx_i - da_i \, da_i = (R_{ij}R_{ik} - \delta_{jk})da_j \, da_k = 0 \, . \tag{3.12}$$

In general, we arrive from (3.9) with (3.8a) at the relation

$$(ds)^2 - (ds_0)^2 = (F_{ij}F_{ik} - \delta_{jk})da_j \, da_k \equiv 2\lambda_{jk} \, da_j \, da_k \tag{3.13}$$

in which the second-order tensor

$$\lambda_{ij} := (F_{ki}F_{kj} - \delta_{ij}) \, /2 \equiv (g_{ij} - \delta_{ij}) \, /2 \tag{3.14}$$

is known as the LAGRANGE *finite strain tensor* , and the tensor

$$C_{ij} \equiv g_{ij} = F_{ki}F_{kj} \quad \text{or} \quad \boldsymbol{C} = \boldsymbol{F}^t \boldsymbol{F} \tag{3.15a,b}$$

is called the *right* CAUCHY-GREEN *tensor* . This tensor and KRONECKER's tensor may be interpreted as metric tensors (BETTEN, 2001a), since the squared lengths of the current and initial line-elements can be written as

$$(ds)^2 = dx_i \, dx_i = g_{jk} \, da_j \, da_k \tag{3.16}$$

and

$$(ds_0)^2 = da_i \, da_i = \delta_{jk} \, da_j \, da_k \ , \tag{3.17}$$

respectively.

In terms of the displacements (3.6a), the LAGRANGE *strain tensor* (3.14) takes the following form

$$\lambda_{ij} = \frac{1}{2}\left(\frac{\partial u_i}{\partial a_j} + \frac{\partial u_j}{\partial a_i} + \frac{\partial u_k}{\partial a_i}\frac{\partial u_k}{\partial a_j}\right) , \qquad (3.18)$$

if F_{ij} from (3.8a) with (3.7a) is substituted into (3.14).

In contrast to the *material description* (3.13), the "strain measure" can be formulated with the spatial coordinates x_i as independent variables (*spatial description*) :

$$(ds)^2 - (ds_0)^2 = \left(\delta_{jk} - F_{ij}^{(-1)}F_{ik}^{(-1)}\right) dx_j\, dx_k \equiv 2\eta_{jk}\, dx_j\, dx_k , \quad (3.19)$$

where η_{jk} is known as the EULER*ian finite strain tensor* . Contrary to (3.18), this tensor takes the form

$$\eta_{ij} = \frac{1}{2}\left(\frac{\partial u_i}{\partial x_j} + \frac{\partial u_j}{\partial x_i} - \frac{\partial u_k}{\partial x_i}\frac{\partial u_k}{\partial x_j}\right) \qquad (3.20)$$

in terms of the displacements (3.6b). The LAGRANGE and EULER strain tensors and the corresponding metric tensors are listed in Table 3.1.

Table 3.1 Finite strain and metric tensors

		LAGRANGE	EULER
metric	deformed continuum	$ds^2 = g_{ij}\, da_i\, da_j$	$ds^2 = \delta_{ij}\, dx_i\, dx_j$
metric	undeformed continuum	$ds_0^2 = \delta_{ij}\, da_i\, da_j$	$ds_0^2 = h_{ij}\, dx_i\, dx_j$
metric tensor	deformed continuum	$g_{ij} \equiv C_{ij} = F_{ki}F_{kj}$ $\boldsymbol{C} = \boldsymbol{F}^t\boldsymbol{F}$	δ_{ij}
metric tensor	undeformed continuum	δ_{ij}	$h_{ij} \equiv B_{ij}^{(-1)} = F_{ki}^{(-1)}F_{kj}^{(-1)}$ $\boldsymbol{B} = \boldsymbol{F}\boldsymbol{F}^t$
strain tensor		$\lambda_{ij} = \frac{1}{2}(g_{ij} - \delta_{ij})$ $\boldsymbol{\lambda} = \frac{1}{2}(\boldsymbol{C} - \boldsymbol{\delta})$	$\eta_{ij} = \frac{1}{2}(\delta_{ij} - h_{ij})$ $\boldsymbol{\eta} = \frac{1}{2}(\boldsymbol{\delta} - \boldsymbol{B}^{-1})$

The *logarithmic strain tensor* is not listed in Table 3.1 although it plays also a central role in the theory of finite deformation because it can be

decomposed into a sum of an *isochoric distortion* and a *volume change* (BETTEN, 2001a). This advantage is uilized, e.g., to describe the creep deformations of thick walled tubes subjected to internal pressure (Chapter 5).

The problem to represent *logarithmic strain tensors* as isotropic tensor functions can be solved by using the interpolation method developed by BETTEN(1984; 1989; 2001a).

In (3.18), if the displacement gradient components $\partial u_i/\partial a_j$ are each small compared to δ_{ij}, the squares and products of these derivatives may be neglected in comparison to the linear terms. The resulting tensor is the LAGRANGE *infinitesimal strain tensor* :

$$\ell_{ij} = (\partial u_i/\partial a_j + \partial u_j/\partial a_i)/2 = (F_{ij} + F_{ji})/2 - \delta_{ij} . \qquad (3.21a)$$

Likewise for $\partial u_i/\partial x_j \ll \delta_{ij}$ in (3.20), the product terms may be dropped to yield the EULER*ian infinitesimal strain tensor* :

$$\boxed{\varepsilon_{ij} = (\partial u_i/\partial x_j + \partial u_j/\partial x_i)/2 \equiv (u_{i,j} + u_{j,i})/2} . \qquad (3.21b)$$

This tensor is sometimes called the *classical strain tensor* . In (3.21b) the notation $u_{i,j}$ is adopted for the partial derivative $\partial u_i/\partial x_j$. Such abbreviations are often used in tensor analysis (BETTEN, 1987c).

If both the displacement gradients (3.7a,b) and the displacements (3.6a,b) themselves are small, there is very little difference in the material (a_i) and spatial (x_i) coordinates of a material particle. Accordingly, the material displacement gradient (3.7a) and spatial displacement gradient (3.7b) are very nearly equal, so that the infinitesimal tensors (3.21a,b) may be taken as equal:

$$\lambda_{ij} \approx \eta_{ij} \approx \ell_{ij} \approx \varepsilon_{ij} .$$

In the elastic deformation of metals the *small-strain theory* is quite adequate, whereas in rubber-like materials and some other synthetic plastics, for instance, elastic deformation may be of much larger magnitude, requiring the use of the *finite-strain theory* . In this theory, *geometrical non-linearities* are considered expressed by the product terms in (3.18) and (3.20). The plastic deformation of metals after yielding may also lead to large strains, but there is usually a considerable range of deformation beyond yield in which small-strain theories may still be used; in metal forming, where large deformations occur, the small-strain components are of doubtful physical significance. Incremental theories of plasticity in effect and also creep theories (Chapter 4) analyze these operations in terms of rate of deformation rather than strain.

The *rate-of-deformation tensor*

$$d_{ij} = (v_{i,j} + v_{j,i})/2 ,\qquad (3.22)$$

sometimes called "rate-of-strain" or "strain-rate tensor", is linear in the velocity gradients $\partial v_i/\partial x_j \equiv v_{i,j}$. This linearity is exact and no approximation has been made in deriving it (BETTEN, 2001a). Furthermore, the tensor (3.22) is not to be confused with the *material time derivative* $\dot{\varepsilon}_{ij} \equiv d\varepsilon_{ij}/dt$ of the infinitesimal tensor (3.21b), because we have:

$$\dot{\varepsilon}_{ij} = d_{ij} - (u_{i,p}v_{p,j} + u_{j,p}v_{p,i})/2 .\qquad (3.23)$$

Only in the case of small displacement gradients ($u_{i,j} \equiv \partial u_i/\partial x_j$) and small velocity gradient tensors ($v_{i,j} \equiv \partial v_i/\partial x_j$), we have: $\dot{\varepsilon}_{ij} \approx d_{ij}$.

If the displacements u_i are given, the six components $\varepsilon_{ij} = \varepsilon_{ji}$ can be easily calculated from (3.21b), provided that the displacements are differentiable functions of the coordinates x_i. However, if the strain components ε_{ij} are given explicitly as functions of the coordinates x_i, the six independent equations (3.21b) may be viewed as a system of six partial differential equations for determining the three displacement components u_i. The system is over-determined and will not, in general, possess a solution for an arbitrary choice of the strain components ε_{ij}. Therefore, if the displacement components u_i are single-valued and continuous, some conditions must be imposed upon the strain components. The necessary and sufficient conditions for integrability can be found by eliminating the displacements u_i in (3.21b):

$$\varepsilon_{ij,k\ell} + \varepsilon_{k\ell,ij} - \varepsilon_{ik,j\ell} - \varepsilon_{j\ell,ik} = 0_{ijk\ell} .\qquad (3.24)$$

Again the partial derivatives are denoted with a comma followed by the indices of the independent variables (spatial coordinates x_i), for example: $\varepsilon_{ij,k\ell} \equiv \partial \varepsilon_{ij}/\partial x_k \partial x_\ell$. The conditions (3.24) are called *compatibility equations* of the infinitesimal strain tensor. There are 81 equations in all in (3.24), but only six are distinct. These six conditions can be written in the compact form

$$R_{ij} := \varepsilon_{ipr}\varepsilon_{jqs}\varepsilon_{pq,rs} \overset{!}{=} 0_{ij}\qquad (3.25)$$

where $R_{ij} = R_{ji}$ is called the *incompatibility tensor* (BETTEN, 2001a), the divergence of which is equal to the zero vector:

$$R_{ij,j} = 0_i .\qquad (3.26)$$

This condition is known as BIANCHI's identity (BETTEN, 2001a).

Caution: **The permutation tensor ε_{ijk} in (3.25) is not to be confused with the strain tensor ε_{ij} and its partial derivatives $\varepsilon_{ij,k\ell}$.**

For plane strain in the x_1-x_2-plane, x_2-x_3-plane, or x_3-x_1-plane the six unique equations (3.26) reduce, respectivelely, to the following single equtions

$$\varepsilon_{11,22} + \varepsilon_{22,11} = 2\varepsilon_{12,12}, ..., \varepsilon_{33,11} + \varepsilon_{11,33} = 2\varepsilon_{31,31}$$

which can easily deduced from (3.21b) by eliminating the displacements u_i as has been pointed out by BETTEN (2001a).

3.2 Analysis of Stress

In this section the definitions of *stress vector* and *stress tensor* will be given and the equations of equilibrium will be derived. We will then show how the stress components change when the frames of reference are changed from one rectangular cartesian frame of reference to another. We will see that the stress components transform according to the tensor transformation rules. The symmetry of the stress tensor and its consequences will then be discussed.

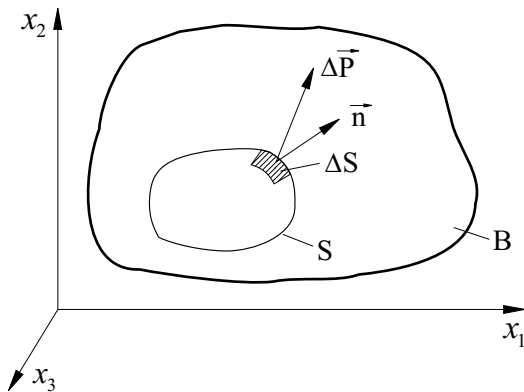Consider a configuration occupied by a loaded body B (Fig 3.3) at some time.

Fig. 3.3 Stress principle

Imagine a closed surface S within B. We would like to know the interaction between the material exterior to this surface and that in the interior.

Let us consider a small surface element of area ΔS on our imaged surface S. The unit vector $\boldsymbol{n}$ is normal to S with its direction outward from the interior of S. Then we can distinguish the two sides of ΔS according to the direction of $\boldsymbol{n}$. Consider the part of material lying on the positive side of the normal. This part exerts a force $\Delta \boldsymbol{P}$ on the other part, which is situated on the negative side of the normal. The force $\Delta \boldsymbol{P}$ is a function of the area and the orientation of the surface. We assume that the ratio $\Delta \boldsymbol{P}/\Delta S$ tends to a definite limit as ΔS tends to zero:

$$\boldsymbol{p} := \lim_{\Delta S \to 0} (\Delta \boldsymbol{P}/\Delta S) = d\boldsymbol{P}/dS \ .$$

This limiting vector is called the *stress vector* , or also known as the *traction vector* . We also assume that the moment of the forces acting on the small surface ΔS about any point within the area vanishes in the limit, i.e., a *couple-stress vector* is not taken into account. Such couple stresses have in fact been included in continuum mechanics, for instance by E. and F. COSSERAT in 1907. Materials in which there may be couple stresses are called *polar* ($\to$ COSSERAT *continuum*) .

Now let us consider three surfaces parallel to the coordinate planes. The normals of these surfaces are in the positive directions of the coordinate axes as drawn in Fig. 3.4.
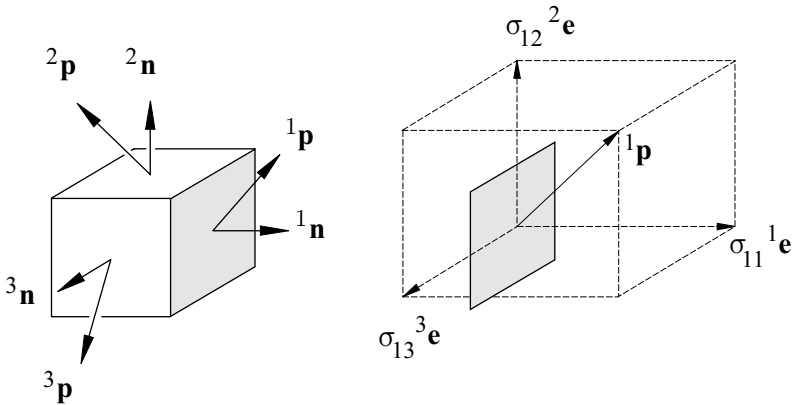

Fig. 3.4 Traction vectors on three planes perpendicular to coordinate axes and notations of stress components

Each of the three traction vectors in Fig. 3.4 can be decomposed in its components parallel to the coordinate axes:

$$^1\boldsymbol{p} = \sigma_{11}\,{}^1\boldsymbol{e} + \sigma_{12}\,{}^2\boldsymbol{e} + \sigma_{13}\,{}^3\boldsymbol{e} \tag{3.27a}$$

$$^2\boldsymbol{p} = \sigma_{21}\,{}^1\boldsymbol{e} + \sigma_{22}\,{}^2\boldsymbol{e} + \sigma_{23}\,{}^3\boldsymbol{e} \tag{3.27b}$$

$$^3\boldsymbol{p} = \sigma_{31}\,{}^1\boldsymbol{e} + \sigma_{32}\,{}^2\boldsymbol{e} + \sigma_{33}\,{}^3\boldsymbol{e} \;. \tag{3.27c}$$

These equations can be written in the following compact form

$$^i\boldsymbol{p} = \sigma_{ij}\,{}^j\boldsymbol{e} \;, \quad i = 1, 2, 3 \;, \tag{3.27*}$$

where σ_{ij} are the cartesian components of the *stress tensor* $\boldsymbol{\sigma}$. As a rule the first subscript on σ_{ij} identifies the plane on which a stress vector is acting, while the second index indicates the direction of the traction component:

$$\sigma_{ik} = {}^i\boldsymbol{p} \cdot {}^k\boldsymbol{e} \;. \tag{3.28}$$

This relation immediately follows from (3.27*) since the unit base vectors are mutually orthogonal: ${}^j\boldsymbol{e} \cdot {}^k\boldsymbol{e} = \delta_{jk}$. The components perpendicular to the planes (σ_{11}, σ_{22}, σ_{33}) are called *normal stresses* . Those acting in (tangentially to) the plane (σ_{12}, σ_{13}, ..., σ_{32}) are called *shear stresses* . A stress component is *positive*, if it is acting on a positive plane in the positive direction of a coordinate axis. Likewise, a stress component is *positive*, if it is acting on a negative plane in the negative direction. Otherwise, the stress components are negative. A plane in Fig. 3.4 is said to be positive if its outer normal points in one of the positive coordinate directions. Otherwise it is said to be negative. In accordance with the above determination of signs, the stress components indicated in Fig. 3.5 are all positive. Thus, a normal stress is considered to be positive for tension and negative for compression.
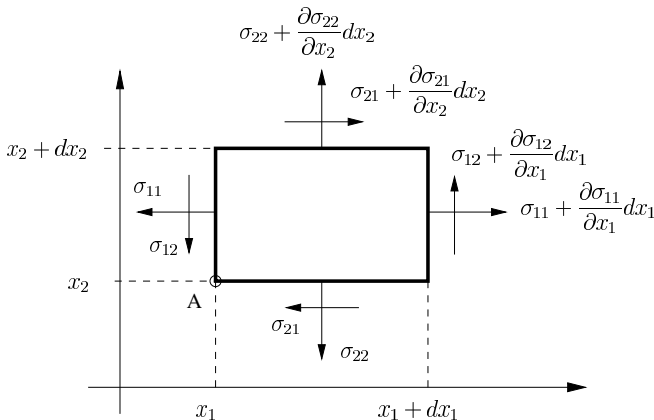

Fig. 3.5 Positive stress components

The relationship between the stress tensor $\boldsymbol{\sigma}$ at some point and the stress vector $\boldsymbol{p}$ on a plane of arbitrary orientation $\boldsymbol{n}$ at that point may be established through the force equilibrium of an infinitesimal tetrahedron of the continuum, having its vertex at the considered point. The base of this tetrahedron is taken perpendicular to $\boldsymbol{n}$, while the three faces are taken perpendicular to the coordinate axes as illustrated in Fig. 3.6.
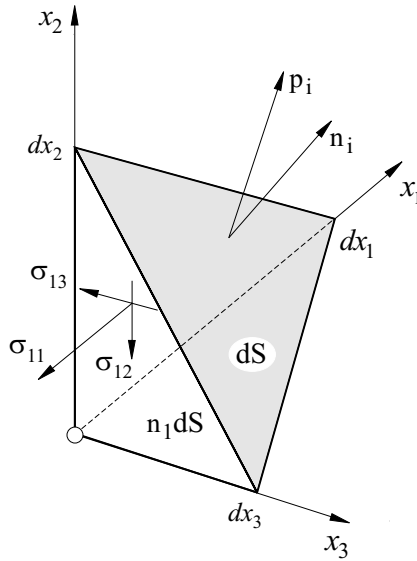

Fig. 3.6 Infinitesimal tetrahedron

Designating the area of the base as dS, the areas of the faces are the projected areas $n_1\,dS$, $n_2\,dS$, and $n_3\,dS$. The force equilibrium in x_1-direction can then be expressed as follows:

$$p_1\,dS = \sigma_{11}n_1\,dS + \sigma_{21}n_2\,dS + \sigma_{31}n_3\,dS\ ,$$

so that, by way of cyclic permutations, we arrive at CAUCHY's formula:

$$\left.\begin{aligned} p_1 &= \sigma_{11}n_1 + \sigma_{21}n_2 + \sigma_{31}n_3 \\ p_2 &= \sigma_{12}n_1 + \sigma_{22}n_2 + \sigma_{32}n_3 \\ p_3 &= \sigma_{13}n_1 + \sigma_{23}n_2 + \sigma_{33}n_3 \end{aligned}\right\} \qquad \boxed{p_i = \sigma_{ji}n_j}\ . \qquad (3.29)$$

This formula expresses the components of the stress vector $\boldsymbol{p}$ acting on an arbitrarily oriented infinitesimal area $\boldsymbol{n}\,dS$ at a considered point in terms of

the components of the stress tensor, $\boldsymbol{\sigma}$, at the point. Thus, the traction $\boldsymbol{p}$ for any $\boldsymbol{n}$ may be calculated from a knowledge of nine basic quantities σ_{ij}.

The result (3.29) can be interpreted as follows: The quantity σ_{ij} serves as a *linear operator* which operates on the *argument* vector n_i to produce the image vector p_i. Hence, σ_{ij} are the cartesian components of a second-order tensor $\boldsymbol{\sigma}$, known as CAUCHY's *stress tensor*. Its components transform according to the rule (2.20a,b).

It can easily be shown (BETTEN, 2001a) that CAUCHY's stress tensor is symmetric, $\sigma_{ij} = \sigma_{ji}$, so that only six of the nine components are specified independently in order to define completely the state of stress at any point. The symmetry of the stress tensor implies what is sometimes called the *theorem of conjugate shear stresses*, also known as BOLTZMANN's *axiom*, which states that the shear stresses on perpendicular planes (having directions such that both stresses point either toward or away from the line of intersection of the planes) are always equal in magnitude. This is not true in the COSSERAT *continuum* or in *damaged materials* BETTEN (1982b; 2001a).

Furthermore, if we would like to study the influence of a strong electromagnetic field on the propagation of elastic waves, or such influence on some high-frequency phenomenon in the material, then the stress level may be very low and the body moment may be significant. In such problems the stress tensor may not be assumed symmetric. Couple stresses and body couples are useful concepts in dealing with materials whose molecules have internal structures, and in the dislocation theory of metals.

The symmetry property of CAUCHY's stress tensor is an advantage in view of several aspects, for instance in view of the principle stresses and principal stress directions or with regard to the formulation of constitutive equations.

Firstly, let us discuss the determination of the principle values and the principal directions for the stress tensor. For that purpose, let us consider Fig. 3.6, where, on the surface element dS, shear stresses are produced. On those surface elements for which the vectors $\boldsymbol{p}$ and $\boldsymbol{n}$ are *collinear*, no shear stresses can be produced. These surfaces are called *principal planes*; their normal directions and the normal stresses are known as *principal directions* and *principal stresses*. If the vectors $\boldsymbol{p}$ and $\boldsymbol{n}$ are collinear, they differ only in length. Thus, together with (3.29) and $\sigma_{ij} = \sigma_{ji}$, we find:

$$\left.\begin{aligned} p_i &\overset{!}{=} \sigma n_i \equiv \sigma \delta_{ij} n_j \\ p_i &= \sigma_{ij} n_j \end{aligned}\right\} \quad \Rightarrow \quad \boxed{(\sigma_{ij} - \sigma \delta_{ij}) n_j = 0_i}. \tag{3.30}$$

The condition for (3.30) to have non-trivial solutions for $\boldsymbol{n}$ is:

$$\det(\sigma_{ij} - \sigma\delta_{ij}) = 0 \quad \Rightarrow \quad \boxed{\sigma^3 - J_1\sigma^2 - J_2\sigma - J_3 = 0} \;. \qquad (3.31)$$

This is the *characteristic equation* (2.25) for the stress tensor, in which J_1, J_2, J_3 are the three *irreducible invariants* (2.24a,b,c) of the stress tensor.

The three roots of (3.31) are the three principal stress values $\sigma_I, \sigma_{II}, \sigma_{III}$. Associated with each principal stress σ_α, $\alpha = I, II, III$, there is a principal stress direction for which the direction cosines n_i^α are solutions of the equations (3.30), where the *eigenvectors* $\boldsymbol{n}^\alpha$, $\alpha = I, II, III$, are normalized without loss of generality; hence

$$\boxed{\left(\sigma_{ij} - \sigma_{(\alpha)}\delta_{ij}\right) n_j^{(\alpha)} = 0_i \;; \quad n_k^{(\alpha)}n_k^{(\alpha)} = 1 \;, \quad \alpha = I, II, III \;.} \quad (3.32)$$

> *Caution*: **There is no sum on the repeated label α, which is therefore enclosed by parentheses.**

From the symmetry property the following statements can be easily deduced:

1. The *eigenvalues* of a real symmetric second-order tensor are all real.
2. The *eigenvectors* associated with two distinct eigenvalues of a symmetric second-order tensor are orthogonal:

$$\sigma_\alpha \neq \sigma_\beta \quad \Rightarrow \quad n_k^\alpha n_k^\beta = 0 \;, \quad \alpha \neq \beta \;.$$

Eigenvalue problems of tensors of order higher than two are discussed by BETTEN (1982a; 1998; 2001c), for instance.

In the following the equilibrium equations should be derived. Furthermore, the symmetry of CAUCHY*'s stress tensor* will be proved. We therefore consider a material body (volume V, bounded by surface S) in equilibrium. It may be subjected to a system of external (surface) forces $\boldsymbol{p}$ per unit area and body forces $\boldsymbol{b}$ per unit mass (including inertia forces, if present) or volume forces $\boldsymbol{f} = \rho\boldsymbol{b}$ per unit volume as shown in Fig. 3.7.

Equilibrium of an arbitrary volume V of a continuum (Fig. 3.7) requires that the resultant force and moment acting on the volume be zero. Summation of surface and body forces results in the integral relation

$$\iint_S p_i \, dS + \iiint_V f_i \, dV = 0_i \;. \qquad (3.33)$$

Replacing p_i by (3.29) and converting the resulting surface integral to a volume integral by using the *divergence theorem of* GAUSS ,
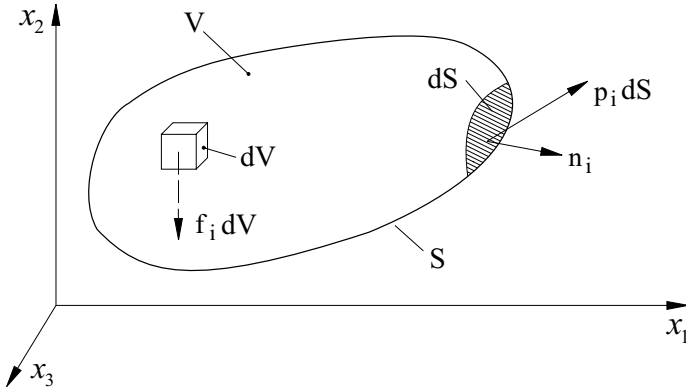
Fig. 3.7 Volume and surface forces

$$\iint_S \sigma_{ji} n_j \, dS = \iiint_V \sigma_{ji,j} \, dV \ , \tag{3.34}$$

equation (3.33) becomes:

$$\iiint_V (\sigma_{ji,j} + f_i) \, dV = 0_i \ . \tag{3.35}$$

Since the volume V is arbitrary, the integrand in (3.35) must vanish, so that we arrive at the *equilibrium equations*

$$\boxed{\sigma_{ji,j} + f_i = 0_i} \ , \tag{3.36}$$

where $\sigma_{ji,j} \equiv \partial \sigma_{ji}/\partial x_j$ is the divergence of the stress tensor. The partial differentiation is denoted with a comma followed by the index of the independent variable.

For a *moving* continuum (mass density ρ; velocity field $v_i \equiv \dot{x}_i$) we have to take *inertial forces* ,

$$dT_i = -\dot{x}_i \, dm \quad \Rightarrow \quad T_i = -\iiint_V \rho \ddot{x}_i \, dV \ , \tag{3.37}$$

into account (D'ALEMBERT*'s principle*) , so that the right-hand side in (3.36) is not equal to zero:

$$\boxed{\sigma_{ji,j} + f_i = \rho \ddot{x}_i} \ . \tag{3.38}$$

These equations are known as CAUCHY's *equations of motion* .

In the absence of *couple stresses* , the equilibrium of moments about the origin (Fig. 3.7) requires that

$$\iint\limits_{S} \varepsilon_{ijk} x_j p_k \, dS + \iiint\limits_{V} \varepsilon_{ijk} x_j f_k \, dV = 0_i \,, \qquad (3.39)$$

where ε_{ijk} is the permutation tensor defined in (2.5) and x_i is the position vector of the surface and volume elements. Again, replacing p_i by (3.29), applying the divergence theorem of GAUSS, and using the equilibrium equations (3.36), the integrals in (3.39) are combined and reduced to

$$\iiint\limits_{V} \varepsilon_{ijk} \sigma_{jk} \, dV = 0_i \,. \qquad (3.40)$$

Since the volume V is arbitrary, the integrand in (3.40) must vanish at any point in the continuum:

$$\varepsilon_{ijk} \sigma_{jk} = 0_i \quad \Rightarrow \quad \boxed{\sigma_{ij} = \sigma_{ji}} \,. \qquad (3.41)$$

This result shows that CAUCHY's *stress tensor is symmetric* .

The CAUCHY stress tensor field is defined as a function of the spatial coordinates, $\sigma_{ij} = \sigma_{ij}(x_p, t)$, and the CAUCHY equations of motion (3.38) apply to the current deformed configuration. A suitable strain measure to use with the CAUCHY stress tensor would therefore be one of the strain or deformation tensors of the EULERian formulation in terms of the spatial position in the deformed configuration. However, the LAGRANGE or material formulation is often preferred in the *finite theory of elasticity* , where a natural state exists to which the body will return when it is unloaded. If we formulate a strain tensor in material coordinates, we need also to express the stresses as functions of material coordinates and derive constitutive equations in the reference state. The two PIOLA-KIRCHHOFF *stress tensors* discussed by BETTEN (2001a) are two alternative definitions of stress in the reference state. The *first* PIOLA-KIRCHHOFF *stress tensor* (sometimes called the LAGRANGE stress tensor) has the disadvantage of being nonsymmetric. It is therefore awkward to use it in constitutive equations with a symmetric strain tensor. Furthermore, this tensor is **not** *objective* (BETTEN, 2001a). The *second* PIOLA-KIRCHHOFF *tensor* $\tilde{T}_{ij}$ is symmetric whenever the CAUCHY stress tensor σ_{ij} is symmetric (*nonpolar case*) and *objective*. Thus, this tensor is preferred in the finite theory of elasticity (BETTEN, 2001a). The relation between these two stress tensors can be expressed as follows:

$$\tilde{T}_{ij} = \frac{\rho_0}{\rho} F_{ijpq}^{(-1)} \sigma_{pq} \qquad \Leftrightarrow \qquad \sigma_{ij} = \frac{\rho}{\rho_0} F_{ijpq} \tilde{T}_{pq} \tag{3.42}$$

where ρ and ρ_0 are the mass densities of the current and reference configurations, respectively. The fourth-order tensor in (3.42) is defined as:

$$F_{ijpq} := \left(F_{ip} F_{jq} + F_{iq} F_{jp} \right)/2 \tag{3.43}$$

and has the following symmetry properties:

$$F_{ijpq} = F_{jipq} = F_{ijqp} . \tag{3.44}$$

Its components can be determined by inserting the given components (3.8a) of the material deformation gradient. It can be shown that the inverse form of (3.43), used in (3.42), can be represented as

$$F_{ijpq}^{(-1)} = \left(F_{ip}^{(-1)} F_{jq}^{(-1)} + F_{iq}^{(-1)} F_{jp}^{(-1)} \right)\Big/ 2 , \tag{3.45}$$

where $F_{ij}^{(-1)}$ are the given components (3.8b) of the spatial deformation gradient (BETTEN, 2001a).

In the foregoing Sections 3.1 and 3.2 we have discussed strain and stress tensors, respectively. Fomulating *constitutive equations* we have to select appropiate pairs of strain and stress tensors. Admissible pairs are called *conjugate variables*. For instance, in the linear constitutive equation of the finite theory of elasticity,

$$\tilde{T}_{ij} = E_{ijk\ell} \lambda_{k\ell} , \tag{3.46}$$

the LAGRANGE *finite strain tensor* (3.14), (3.18) and the *second* PIOLA-KIRCHHOFF *tensor* (3.42) are *conjugate variables* in the reference configuration. Another pair of conjugate variables are the *rate-of-deformation tensor* (3.22) and CAUCHY's *stress tensor* (3.29) in the deformed configuration.

The stress power in a volume V of the current deformed configuration can be expressed by the *conjugate variables* $\dot{\lambda}$ and $\tilde{T}$ in the volume V_0 occupied by the same material in the reference configuration according to

$$\iiint\limits_{V} d_{ij} \sigma_{ji} dV = \iiint\limits_{V_0} F_{jp} F_{iq} d_{ij} \tilde{T}_{pq} dV_0 = \iiint\limits_{V_0} \dot{\lambda}_{ij} \tilde{T}_{ji} dV_0 . \tag{3.47}$$

Further *conjugate variables* are derived by BERTRAM (2005), BETTEN (2001a), HAUPT (2000), SKRZYPEK (1993), for instance.

4 Creep Behavior of Isotropic and Anisotropic Materials; Constitutive Equations

The previous chapters are concerned with tensor notations and some basic equations applicable to all continuous materials. However, these results are insufficient to describe the mechanical behavior of any particular material.

Thus, we need additional equations characterizing the individual material and its reaction to applied loads; such equations are called *constitutive equations*, since they describe the macroscopic behavior resulting from internal constitution of the particular materials. But materials, especially in the solid state, behave in such complex ways when the entire range of possible temperatures and deformations is considered that it is not feasible to write down one equation or set of equations to describe accurately a real material over its entire range of behavior. Instead, we formulate separate equations describing various kinds of *ideal material response*, each of which is a mathematical formulation designed to approximate physical observations of a real material's response over a suitably restricted range.

Physical laws should be independent of the position and orientation of the observer, i.e., if two scientists using different coordinate systems observe the same physical event, it should be possible to state a physical law governing the event in such a way that if the law is true for one observer, it is also true for the other. For this reason, the equations of physical laws are *vector functions* or *tensor functions*, since vectors and tensors transform from one coordinate system to another in such a way that if the vector or tensor equations holds in one coordinate system, it holds in any other coordinate system not moving relative to the first one, i.e., in any other coordinate system in the same reference frame. Invariance of the form of the physical law referred to two frames of references in accelerated motion relative to each other is more difficult and requires the apparatus of general relativity theory, tensors in four-dimensional space-time. For simplicity, we limit ourselves in this book to tensors in three-dimensional EUCLID*ean space*. Furthermore, we use, with the exception of chapter 5, rectangular cartesian coordinates for the components of vectors and tensors.

Constitutive equations must be invariant under changes of frame of reference, i.e., two observers, even if in relative motion with respect to each other, observe the same stress in a loaded material. The *principle of material frame-indifference* is also called the *principle of material objectivity* (BETTEN, 2001a; BASAR and WEICHERT, 2000).

The formulation of constitutive equations is essentially a matter of experimental determination, but a theoretical framework is needed in order to devise suitable experiments and to interpret experimental results. As has been pointed out in more detail by AVULA (1987):

> The validity of a model should not be judged by mathematical rationality alone; nor should it be judged purely by empirical validation at the cost of mathematical and scientific principles. A combination of rationality and empiricism (logic and pragmatism) should be used in the validation.
>
> Experimental observations and measurements are generally accepted to constitute the backbone of physical sciences and engineering because of the physical insight they offer to the scientist for formulating the theory. The concepts that are developed from observations are used as guides for the design of new experiments, which in turn are used for validation of the theory. Thus, experiments and theory have a hand-in-hand relationship.

However, it must be noted, that experimental results can differ greatly from reality just like a bad mathematical model (BETTEN, 1973).

Creep tests are carried out on a specimen loaded, e.g., in tension or compression, usually at constant load, inside a furnace which is maintained at a constant temperature T. The extension of the specimen is measured as a function of time. A typical *creep curve* for metals, polymers, and ceramics is represented in Fig 4.1 and Chapter 14. The temperature at which materials begin to creep depends on their melting point T_M, for instance, $T > 0, 4T_M$ for metals and $T > 0, 5T_M$ for ceramics.

The response of the specimen loaded by σ_0 at time $t = 0$ can be divided into an *elastic* and a *plastic* part as

$$\varepsilon_0 = \sigma_0/E(T) + \varepsilon_p(\sigma_0, T) \ , \tag{4.1}$$

where $E(T)$ is the modulus of Elasticity. The creep strain in Fig. 4.1 can then be expressed according to

$$\varepsilon_c = \varepsilon(t) - \varepsilon_0 \propto t^\kappa \ , \tag{4.2}$$

where $\kappa < 1$ in the *primary*, $\kappa = 1$ in the *secondary*, and $\kappa > 1$ in the *tertiary* creep stage. These terms correspond to a decreasing, constant, and increasing strainrate, respectively, and were introduced by ANDRADE (1910). These three creep stages are often called *transient creep, steady creep* , and *accelerating creep* ; respectively.
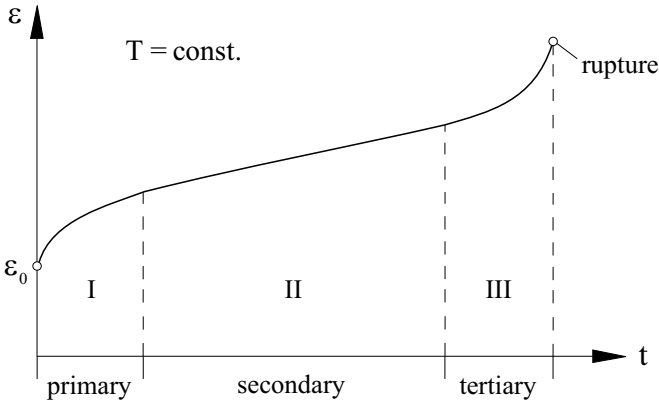

Fig. 4.1 Typical creep curve

The results (4.1) and (4.2) from the creep test justify a classification of material behavior in **three** disciplines: *elasticity, plasticity*, and *creep mechanics* .

Due to a proposal of HAUPT (2000) one can also distinguish four theories of material behavior as follows:

- ❏ The theory of *elasticity* is concerned with the *rate-independent* behavior *without hysteresis*.
- ❏ The theory of *plasticity* specifies the *rate-independent* behavior *with hysteresis*.
- ❏ The theory of *viscoelasticity* describes the *rate-dependent* behavior *without equilibrium hysteresis*.
- ❏ The theory of *viscoplasticity* is devoted to the *rate-dependent* behavior *with equilibrium hysteresis*.

The creep behavior exists in two of the above listed categories, namely in the theories of *viscoelasticity* (Chapter 11) and *viscoplasticity* (Chapter 12).

In the following sections of this chapter let us discuss the *primary, secondary*, and *tertiary* creep behavior of *isotropic* and *anisotropic materials*.

4.1 Primary Creep

The *primary* or *transient creep* is characterized by a monotonic decrease in the rate of creep (Fig. 4.1), and the creep strain (4.2) can be described by the simple formula

$$\varepsilon_c = A\,\sigma^n\,t^m \ ,\tag{4.3}$$

where the parameters A, n, m depend on the temperature. They can be determined in a uniaxial creep test. For instance, PANTELAKIS (1983) found in experiments on the *austenitic steel* X 8 Cr Ni Mo Nb 16 16 at 973 K the values $A = 3.85 \cdot 10^{-15}(\text{N/mm}^2)^{-n}\text{h}^{-m}$, $n = 5.35$, and $m = 0.22$. Based upon a *mechanical equation of state* the *time-hardening* relation (4.3) can be deduced as has been pointed out in more detail by BETTEN (2001a). Further applications of mechanical equations of state were discussed by LUDWIK (1909), LUBAHN and FELGAR (1961), TROOST et al.(1973), to name just a few.

If the stress σ in (4.3) is assumed to be constant the creep rate $d \approx \dot{\varepsilon}_c$ is given by

$$\boxed{\dot{\varepsilon}_c = A\,m\,\sigma^n\,t^{m-1}}\ .\tag{4.4}$$

This relation may be generalized to multiaxial states of stress according to the following tensorial linear constitutive equation

$$d_{ij} = \frac{3}{2}K(J_2')^{(n-1)/2}\,\sigma_{ij}'\,t^{m-1}\tag{4.5}$$

(ODQUIST and HULT, 1962), where d_{ij} are the cartesian components of the rate-of-deformation tensor (3.22), (3.23), and J_2' is the quadratic invariant of the stress deviator (σ_{ij}') according to (2.26a).

Inserting the time t from (4.3) into (4.4), we arrive at the relation

$$\boxed{\dot{\varepsilon}_c = m\,A^{1/m}\,\sigma^{n/m}\varepsilon_c^{(m-1)/m}}\ ,\tag{4.6}$$

which characterizes the *strain-hardening-theory* , i.e., this strain rate equation (4.6) includes *stress* and *strain* as variables. In contrast to (4.6), the strain rate equation (4.4) contains *stress* and *time* as variables and is therefore called the *time-hardening-law* .

4.1.1 Primary Creep for Austenitic Steel

In the following MAPLE worksheet *primary creep curves* for *austenitic steel* are represented.

```
>   restart:
>   epsilon[c]:=A*sigma^n*t^m;   # (4.3)
```

$$\varepsilon_c := A\,\sigma^n\,t^m$$

Inserting the experimental data for *austenitic steel* X 8 Cr Ni Mo Nb 16 16 at 973 K,

```
>   Digits:=4:
>   A:=3.85*10^(-15)*(N/mm^2)^(-n)*h^(-m);
```

$$A := 0.3850\,10^{-14}\,(\frac{N}{mm^2})^{(-n)}\,h^{(-m)}$$

```
>   n:=5.35;    m:=0.22;
```

$$n := 5.35$$
$$m := 0.22$$

we find the following creep curve for austenitic steel:

```
>   epsilon[creep](t,sigma):=subs({A=%%%,n=%%,m=%},
>   epsilon[c]);
```

$$\varepsilon_{creep}(t,\,\sigma) := \frac{0.3850\,10^{-14}\,\sigma^{5.35}\,t^{0.22}}{(\frac{N}{mm^2})^{5.35}\,h^{0.22}}$$

```
>   stress_parameter:=sigma=[150,175,200]*N/mm^2;
```

$$stress\_parameter := \sigma = \frac{[150,\,175,\,200]\,N}{mm^2}$$

```
>   for i in [150,175,200] do
>   EPSILON[i]:=3.85*10^(-15)*i^5.35*t^0.22 od;
```

$$EPSILON_{150} := 0.001689\,t^{0.22}$$
$$EPSILON_{175} := 0.003854\,t^{0.22}$$
$$EPSILON_{200} := 0.007869\,t^{0.22}$$

```
>   alias(H=Heaviside,th=thickness,co=color):
>   plot1:=plot({EPSILON[150],EPSILON[175],
>   EPSILON[200]}, t=0..1, co=black, th=2):
>   plot2:=plot({0.008,0.008*H(t-1)},t=0..1.001):
>   plots[display](plot1,plot2);
```
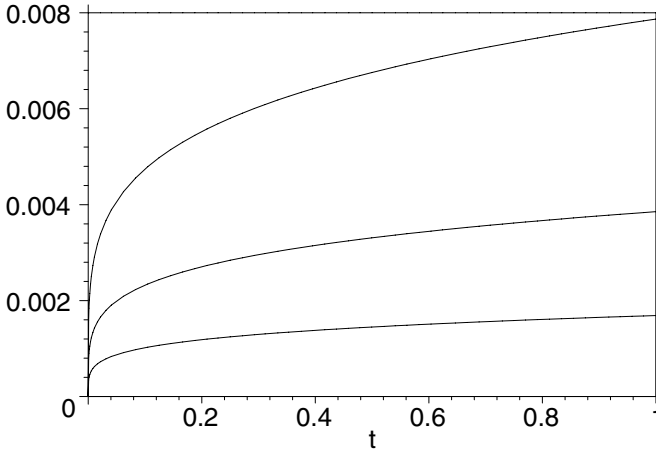
Fig. 4.2 Primary Creep Curves

The creep curves in Fig. 4.2. are valid for serval stress parameters [150, 175, 200] with values [0.0017, 0.0039, 0.0079] at $t = 1$, respectively.

4.1.2 Strain-Hardening-Theory

The *strain-hardening-theory* is characterized by the relation (4.6), which is applied to *austenitic steel* in the following MAPLE worksheet.

```
>   restart: Digits:=4:
>   strain_rate:=
>   m*A^(1/m)*sigma^(n/m)*epsilon[c]^((m-1)/m);
```

$$strain\_rate := m\, A^{\left(\frac{1}{m}\right)} \sigma^{\left(\frac{n}{m}\right)} \varepsilon_c^{\left(\frac{m-1}{m}\right)}$$

Inserting the above experimental data for *austenitic steel* we arrive at the relation:

```
>   strain_rate:=subs({A=3.85*10^(-15),
>   n=5.35,m=0.22},%%);
```

$$strain\_rate := \frac{0.6736\, 10^{-66}\, \sigma^{24.32}}{\varepsilon_c^{3.545}}$$

```
>   stress_parameter:=sigma=[150,175,200]*N/mm^2;
```

$$stress\_parameter := \sigma = \frac{[150,\ 175,\ 200]\, N}{mm^2}$$

```
>   for i in [150,175,200]do STRAIN_RATE[i]:=
>   0.6736*10^(-66)*i^24.32/epsilon[c]^3.545 od;
```

$$STRAIN\_RATE_{150} := \frac{0.5635\, 10^{-13}}{\varepsilon_c^{3.545}}$$

$$STRAIN\_RATE_{175} := \frac{0.2394 \, 10^{-11}}{\varepsilon_c{}^{3.545}}$$

$$STRAIN\_RATE_{200} := \frac{0.6158 \, 10^{-10}}{\varepsilon_c{}^{3.545}}$$

```
>  alias(H=Heaviside,th=thickness,co=color):
>  plot1:=plot({STRAIN_RATE[150],
>  STRAIN_RATE[175],STRAIN_RATE[200]},
>  epsilon[c]=0..0.008,0..0.005):
>  plot2:=plot({0.005,0.005*H(epsilon[c]-0.008)},
>  epsilon[c]=0..0.008001,co=black):
>  plots[display](plot1,plot2);
```
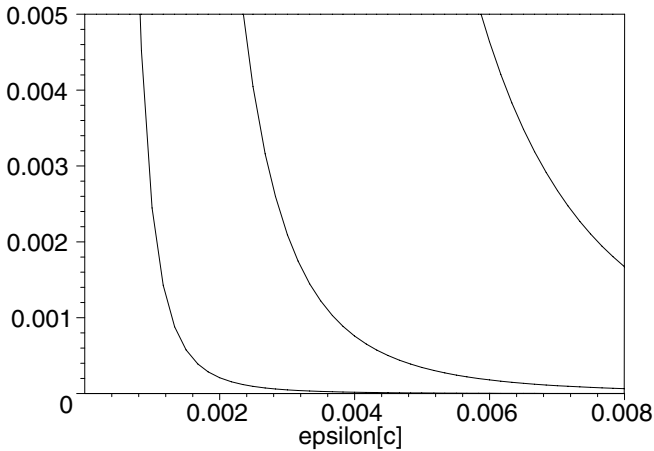

Fig. 4.3 Strain-Hardening

The three curves in this Figure are valid for several stress parameters [150, 175, 200] running from left to right, respectively.

4.1.3 Time-Hardening-Theory

The *time-hardening-theory* is characterized by the relation (4.3), which is applied to *austenitic steel* in the following MAPLE worksheet.

```
>  restart: Digits:=4:
>  epsilon[dot](t,sigma):=A*m*sigma^n*t^(m-1);
```

$$\varepsilon_{dot}(t, \sigma) := A \, m \, \sigma^n \, t^{(m-1)}$$

Inserting the above experimental data for *austenitic steel* we arrive at the relation:

```
>   epsilon[dot](t,sigma):=
>   subs({A=3.85*10^(-15),n=5.35,m=0.22},%%);
```

$$\varepsilon_{dot}(t,\,\sigma) := \frac{0.8470\,10^{-15}\,\sigma^{5.35}}{t^{0.78}}$$

```
>   stress_parameter:=sigma=[150, 175, 200]*N/mm^2;
```

$$stress\_parameter := \sigma = \frac{[150,\,175,\,200]\,N}{mm^2}$$

```
>   for i in [150,175,200] do EPSILON[dot](t,i):=
>   0.847*10^(-15)*i^5.35/t^0.78 od;
```

$$EPSILON_{dot}(t,\,150) := \frac{0.0003715}{t^{0.78}}$$

$$EPSILON_{dot}(t,\,175) := \frac{0.0008478}{t^{0.78}}$$

$$EPSILON_{dot}(t,\,200) := \frac{0.001731}{t^{0.78}}$$

```
>   alias(H=Heaviside,th=thickness,co=color):
>   plot1:=plot({EPSILON[dot](t,150),
>   EPSILON[dot](t,175), EPSILON[dot](t,200)},
>   t=0..1,0..0.005,th=2,co=black):
>   plot2:=plot({0.005,0.005*H(t-1)},
>   t=0..1.001,co=black:
>   plots[display](plot1,plot2);
```
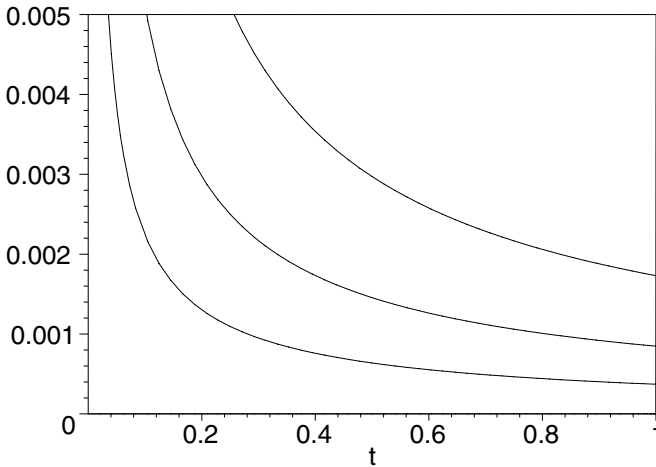

Fig. 4.4 Time-Hardening

The three curves in this Figure are valid for several stress parameters [150, 175, 200] with values [0.00037, 0.00085, 0.0017] at $t = 1$, respectively.

Note that for $m = 1$ both theories, the *time-hardening* (4.4) and the *strain-hardening* (4.6), degenerate to NORTON-BAILEY's power law (4.15) often used for describing the *secondary creep* behavior, for instance, for metals, as has been pointed out in section 4.2 in more detail.

4.1.4 Comparison of Strain- and Time-Hardening

In this Section the reaction of austenitic steel in its primary phase on a stress jump should be illustrated. As an example let us consider a stress step from 190 to 200 at t = 0.003.

```
>   restart:
>   alias(H=Heaviside,th=thickness,l=linestyle):
>   H(t):=190+10*H(t-0.003);
```
$$H(t) := 190 + 10\,H(t - 0.003)$$
```
>   p[1]:=plot(H(t),t=0..0.01,180..210,th=3):
>   p[2]:=plot({190,200,200*H(t-0.003)},
>   t=0..0.01,xtickmarks=[0.001,0.003,0.007,
>   0.01],ytickmarks=[180,190,200,210],l=2):
>   p[3]:=plot(200*H(t-0.003),t=0..0.00301,l=4):
>   plots[display]({seq(p[k],k=1..3)});
```
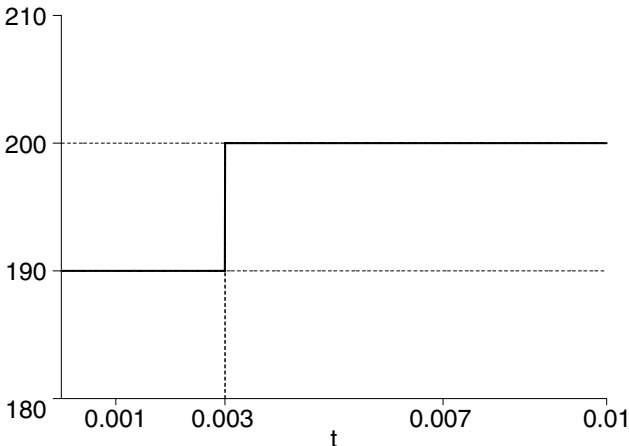

Fig. 4.5 Stress jump from 190 to 200

The primary creep curves for the two stress parameters 190 and 200 for austenitic steel according to Section 4.1.1 are given by:

```
>    EPSILON[190]:=0.005983*t^0.22;
>    EPSILON[200]:=0.007869*t^0.22;
```

$$EPSILON_{190} := 0.005983\, t^{0.22}$$

$$EPSILON_{200} := 0.007869\, t^{0.22}$$

```
>    p[4]:=plot({EPSILON[190],EPSILON[200]},
>    t=0..0.005,co=black, th=3
>    xtickmarks=[0.0008636,0.003,0.005],
>    ytickmarks=[0.001,0.001667,0.002192,0.0025]):
>    p[5]:=plot({0.0025,0.0025*H(t-0.005)},
>    t=0..0.00501,co=black):
>    p[6]:=plot({0.001667,0.002192,
>    0.002192*H(t-0.003)},t=0..0.00301,co=black):
>    p[7]:=plot({0.001667,0.001667*H(t-0.0008636)},
>    t=0..0.000863601,co=black):
>    plots[display]({seq(p[k],k=4..7)});
```
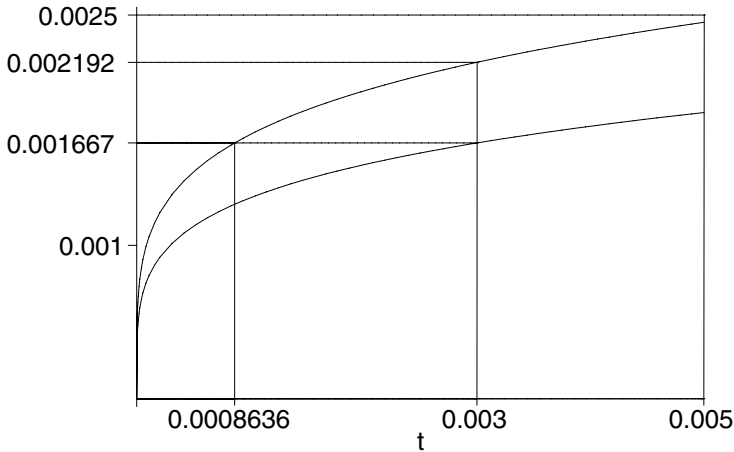

Fig. 4.6 Primary creep curves for 190 and 200

From this Figure we read:

```
>    sigma[1]:=190;    sigma[2]:=200;
```

$$\sigma_1 := 190$$

$$\sigma_2 := 200$$

```
>  t[1]:=0.0008636;  t[2]:=0.003;
```
$$t_1 := 0.0008636$$
$$t_2 := 0.003$$

```
>  Delta[t]:=t[2]-t[1];
```
$$\Delta_t := 0.0021364$$

```
>  epsilon[1]:=0.001667;  epsilon[2]:=0.002192;
```
$$\varepsilon_1 := 0.001667$$
$$\varepsilon_2 := 0.002192$$

```
>  Delta[epsilon]:=epsilon[2]-epsilon[1];
```
$$\Delta_\varepsilon := 0.000525$$

At time $t > t[2] = 0.003$ with the stress $sigma[2] = 200$ we arrive by integration the strain-hardening-relation (4.6) at the following formula:

```
>  restart:
>  Digits:=4:
>  epsilon[s-h](t):=A*(sigma[2])^n*(t-Delta*t)^m;
```
$$\varepsilon_{s-h}(t) := A\,\sigma_2{}^n\,(t - \Delta t)^m$$

In a similar way we arrive by integration the time-hardening-relation (4.4) at the following formula (**?**):

```
>  epsilon[t-h](t):=A*(sigma[2])^n*
>  t^m-Delta*epsilon;
```
$$\varepsilon_{t-h}(t) := A\,\sigma_2{}^n\,t^m - \Delta\varepsilon$$

```
>  epsilon[s-h](t):=subs({A=3.85*10^(-15),n=5.35,
>  m=0.22,Delta*t=0.0021364,sigma[2]=200},%%);
```
$$\varepsilon_{s-h}(t) := 0.007869\,(t - 0.0021364)^{0.22}$$

```
>  epsilon[t-h](t):=subs({A=3.85*10^(-15),n=5.35,
>  m=0.22,Delta*epsilon=0.0005254,
>  sigma[2]=200},%%);
```
$$\varepsilon_{t-h}(t) := 0.007869\,t^{0.22} - 0.0005254$$

```
>  EPSILON[190]:=0.005983*t^0.22;
```
$$EPSILON_{190} := 0.005983\,t^{0.22}$$

```
>  EPSILON[200]:=0.007869*t^0.22;
```
$$EPSILON_{200} := 0.007869\,t^{0.22}$$

```
>  alias(H=Heaviside,th=thickness,co=color):
>  p[1]:=plot(epsilon[s-h](t),t=0.003..0.01,
>  th=3,co=black):
```

```
>    p[2]:=plot(epsilon[t-h](t),t=0.003..0.01,
>    th=3,co=black,style=point,symbol=circle,
>    symbolsize=15):
>    p[3]:=plot({EPSILON[190],EPSILON[200]},
>    t=0..0.01,co=black):
>    p[4]:=plot({0.003,0.003*H(t-0.01)},
>    t=0..0.0101,co=black):
>    p[5]:=plot({0.001667,0.002192*H(t-0.003)},
>    t=0..0.00301,co=black,
>    xtickmarks=[0.003,0.007,0.01],
>    ytickmarks=[0.001,0.001667,0.0025,0.003]):
>    plots[display]({seq(p[k],k=1..5)});
```
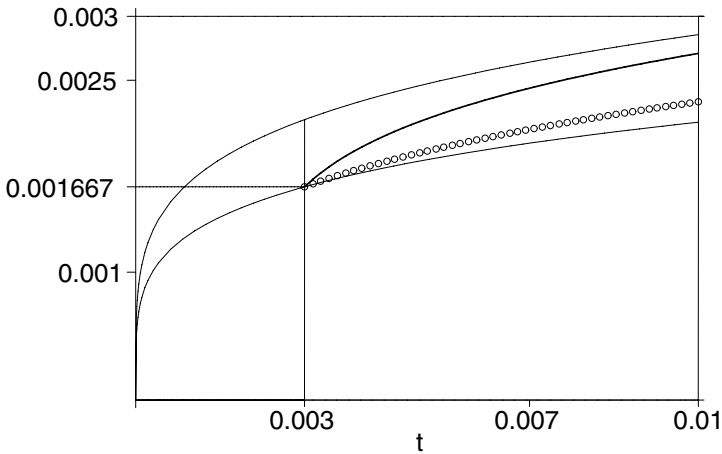

Fig. 4.7 Strain- and time-hardening

In this Figure the thick solid line, starting at $t = 0.003$, characterizes the *strain-hardening-theory:*

$$\varepsilon_{s-h}(t) = A\,\sigma_2{}^n\,(t - \Delta t)^m$$

The *time-hardening-theory*

$$\varepsilon_{t-h}(t) = A\,\sigma_2{}^n\,t^m - \Delta\varepsilon$$

is symbolized by a sequence of small circles.

Both the strain- and time-hardening-curve are parts of the upper creep curve with the stress parameter sigma[2] = 200 , i.e., by shifting this creep

curve from $t = 0.0008636$ to $t = 0.003$ or from epsilon = 0.002192 to epsilon = 0.001667 we arrive at the strain- or time-hardening-curve, respectively.

Many scientists have observed in experiments that the *strain-hardening-theory* predicts better the creep behavior of metals or polymers, for instance, than the *time-hardening-theory.*

Based upon the *creep potential hypothesis* , BETTEN et al. (1989) generalized (4.6) to a *tensorial nonlinear constitutive equation* , and they analysed the primary creep behavior of *thin-walled shells* subjected to internal pressure.

The *creep buckling* of cylindrical shells subjected to internal pressure and axial compression was investigated by BETTEN and BUTTERS (1990) by considering *tensorial nonlinearities* **and** *anisotropic primary creep*.

Further investigations based upon the *creep potential hypothesis* have been carried out by JAKOWLUK (1993), KOLUPAEV (2006), NAUMENKO and ALTENBACH (2007), to name but a few.

The *creep potential hypothesis* mentioned above, can also be applied in the secondary creep stage, as pointed out in detail in the next section.

4.2 Secondary Creep

Creep deformations of the "secondary" stage are large and of a similar character to "pure" plastic deformations. For instance, creep deformations of metals will usually be uninfluenced if a hydrostatic pressure is superimposed. Therefore, such creep behavior can be treated with methods of the "mathematical theory of plasticity," e.g. the theory of the *plastic potential* (MISES, 1928; HILL, 1950) can be used in the mechanics of creep.

BETTEN (1975d) has based a generalized theory of invariants in creep mechanics on the following hypotheses: an *incompressible* and *isotropic* material, a creep rate independent of superimposed hydrostatic pressure, the existence of a *flow potential*, and that NORTON-BAILEY*'s power law* (NORTON, 1929; BAILEY, 1935) is valid for the special case of uniaxial stress. Therefore, the flow potential is expressed in a general form of the second- and third-order invariant of the deviatoric, or reduced, stress tensor. It is also assumed that the *equivalent stress* is a function of *dissipation*. In the special case of the MISES potential the generalized theory leads to ODQUIST's theory.

In the following a creep potential theory of *anisotropic* solids is investigated. For this purpose the mentioned *isotropic concept* (BETTEN, 1975d) will be used by substituting a mapped stress tensor.

4.2.1 Creep Potential Hypothesis

Certain considerations that favor the creep potential hypothesis are presented, for instance, by RABOTNOV (1969). The strain rate-stress relations for creep given below (section 4.2.2) are based on the assumption of the existence of a *creep potential*.

To describe the isotropic creep behavior (BETTEN, 1975d) we can start from a *creep potential* $F = F(\boldsymbol{\sigma})$, which is a scalar-valued tensor function of CAUCHY's stress tensor $\boldsymbol{\sigma}$. This function is said to be *isotropic* if the invariance condition $F(a_{ip}a_{jq}\sigma_{pq}) = F(\sigma_{ij})$ is fulfilled under any orthogonal transformation $\boldsymbol{a}$. It is evident from the theory of isotropic tensor functions that in an isotropic medium the *creep potential*

$$F = F[J_1(\boldsymbol{\sigma}),\ J_2(\boldsymbol{\sigma}),\ J_3(\boldsymbol{\sigma})] \tag{4.7}$$

or, assuming incompressibility,

$$F = F[J_2(\boldsymbol{\sigma}'),\ J_3(\boldsymbol{\sigma}')] \tag{4.8}$$

can depend only on the invariants

$$J_1(\boldsymbol{\sigma}) \equiv \delta_{ij}\sigma_{ji}\ , \tag{4.9a}$$
$$J_2(\boldsymbol{\sigma}) \equiv (\sigma_{ij}\sigma_{ji} - \sigma_{ii}\sigma_{jj})/2\ , \tag{4.9b}$$
$$J_3(\boldsymbol{\sigma}) \equiv (2\sigma_{ij}\sigma_{jk}\sigma_{ki} - 3\sigma_{ij}\sigma_{ji}\sigma_{kk} + \sigma_{ii}\sigma_{jj}\sigma_{kk})/6 \tag{4.9c}$$

of the stress tensor $\boldsymbol{\sigma}$ or on the invariants

$$J_2(\boldsymbol{\sigma}') \equiv \sigma'_{ij}\sigma'_{ji}/2\ , \tag{4.10a}$$
$$J_3(\boldsymbol{\sigma}') \equiv \sigma'_{ij}\sigma'_{jk}\sigma'_{ki}/3 \tag{4.10b}$$

of the stress deviator $\boldsymbol{\sigma}'$, respectively, with the components

$$\sigma'_{ij} = \sigma_{ij} - \sigma_{kk}\delta_{ij}/3\ .$$

The summation convention is utilized, and δ_{ij} represents KRONECKER's tensor (Section 2.1).

The *anisotropic* behavior is described by the *linear transformation*

$$\boxed{\tau_{ij} = \beta_{ijkl}\sigma_{kl}} \, , \tag{4.11}$$

which is used in the creep theory of anisotropic solids (BETTEN, 1981a). By analogy of (4.9), the principal invariants of the *image* tensor (4.11) are given by:

$$J_1(\boldsymbol{\tau}) = A_{pq}\sigma_{pq} \, , \tag{4.12a}$$

$$J_2(\boldsymbol{\tau}) = A_{pqrs}\sigma_{pq}\sigma_{rs}/2 \, , \tag{4.12b}$$

$$J_3(\boldsymbol{\tau}) = A_{pqrstu}\sigma_{pq}\sigma_{rs}\sigma_{tu}/3 \, , \tag{4.12c}$$

if we define:

$$A_{pq} \equiv \beta_{iipq} \, , \tag{4.13a}$$

$$A_{pqrs} \equiv \beta_{ijpq}\beta_{jirs} - \beta_{iipq}\beta_{jjrs} \, , \tag{4.13b}$$

$$A_{pqrstu} \equiv \beta_{ijpq}\beta_{jkrs}\beta_{kitu} - 3\beta_{ijpq}\beta_{jirs}\beta_{kktu}/2$$
$$+ \beta_{iipq}\beta_{jjrs}\beta_{kktu}/2 \, . \tag{4.13c}$$

Under the assumption that the anisotropy of the material is entirely involved in a fourth-rank tensor $\boldsymbol{\beta}$, the *creep potential* is a function $F = F(\boldsymbol{\sigma}, \boldsymbol{\beta})$, and the central problem is to construct an integrity basis the elements of which are the irreducible invariants of the single argument tensors $\boldsymbol{\sigma}$, $\boldsymbol{\beta}$, and the simultaneous or joint invariants.

The invariants (4.12) are elements of the system of joint invariants, which are only considered. Therefore the theory discussed is a simplified theory but very useful in solving practical problems. With (4.12) the function (4.7) takes a form which is often used as *plastic potential* of anisotropic materials (SAYIR, 1970; DUBEY and HILLER, 1972; BETTEN, 1976b; 1977). The idea of substituting the invariants (4.12) of the *mapped stress tensor* (4.11) for the corresponding invariants (4.9) in the *isotropic creep potential* (4.7) is schematically shown in Fig. 4.8.

The actual creep state of an anisotropic solid is mapped on to a fictitious isotropic state with equivalent creep rate $d = \dot{\gamma}$ by a suitable transformation $\tau_{ij} = \tau_{ij}(\sigma_{kl})$. The limiting creep stresses σ_{cx}, σ_{cy}, etc. in Fig. 4.8 for specimens cut along the x direction, y direction, etc., and the transformed fictitious isotropic limiting creep stress τ_c cause defined creep strain ε_c in a defined time, e.g., 1% creep strain in 10^5 h. Therefore, d_c and σ_c are material constants (ODQUIST, 1966).

The theory of *creep potential*, like the theory of the *plastic potential*, is based upon the *principle of maximum dissipation rate*, from which, following LAGRANGE's method in connection with a *creep condition* $F(\sigma_{ij}) =$ const. as a subsidiary condition, we obtain the *flow rule*:
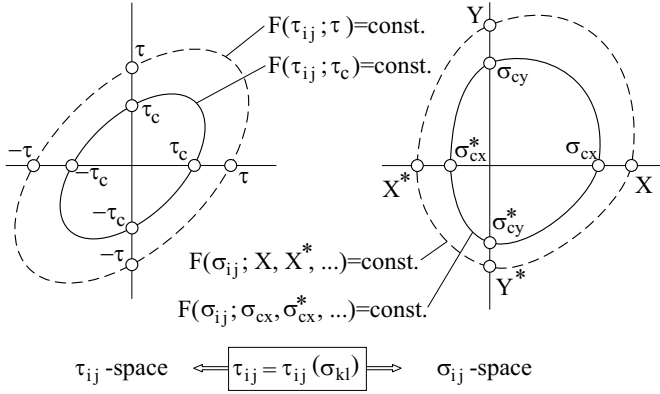
Fig. 4.8 Creep potentials in τ_{ij} and σ_{ij} space: - - -, $|d|$ constant; —, $|d_c|$ constant.

$$d_{ij} = \dot{\Lambda}[\partial F(\boldsymbol{\sigma})/\partial\sigma_{ij}]\,, \tag{4.14a}$$

or

$$d_{ij} = \dot{\Lambda}[\partial F(\boldsymbol{\tau})/\partial\tau_{pq}](\partial\tau_{pq}/\partial\sigma_{ij}) \equiv (\partial\tau_{pq}/\partial\sigma_{ij})\dot{\gamma}_{pq}\,. \tag{4.14b}$$

In (4.14) the factor $\dot{\Lambda}$ is LAGRANGE's *multiplier*. As known, the surfaces $F(\sigma_{ij}) = $ const. or $F(\tau_{ij}) = $ const. must be *convex* in the σ_{ij}-space or $\tau_{ij} - space$, respectively. Inserting (4.11) in (4.14b), we find the *flow rule:*

$$d_{ij} = \beta_{pqij}[\partial F(\boldsymbol{\tau})/\partial\tau_{pq}]\dot{\Lambda} \equiv \beta_{pqij}\dot{\gamma}_{pq}\,. \tag{4.14c}$$

To determine the proportionality factor $\dot{\Lambda}$ NORTON-BAILEY's *power law* (NORTON, 1929; BAILEY, 1935),

$$d = K\,\sigma^n \equiv d_c(\sigma/\sigma_c)^n\,, \tag{4.15}$$

is assumed and is used in different directions with its corresponding limiting creep stresses σ_{cx}, σ_{cy}, etc.

Note that both theories, the *time-hardening* (4.4) and the *strain-hardening* (4.6) degenerate to NORTON-BAILEY's power law (4.15) by taking $m = 1$.

In a fictitious creep state, defined by

$$\dot{\gamma}_c \overset{!}{=} d_c \qquad \text{or} \qquad \dot{\gamma} \overset{!}{=} d\,, \tag{4.16a,b}$$

we have by analogy of (4.15):

$$\dot{\gamma} = L\,\tau^m \equiv \dot{\gamma}_c(\tau/\tau_c)^m = d(\tau/\tau_c)^m = d \,, \qquad (4.17)$$

so that, because of $d_{11} \equiv d$, we have from (4.14c):

$$\dot{\Lambda} = d/(\partial F/\partial \tau_{ij})_{i=j=1} \quad \text{with} \quad \tau_{11} \equiv \tau \,. \qquad (4.18)$$

In (4.18) the fictitious "isotropic" creep stress τ appears, which can be determined by the *hypothesis of the equivalent dissipation rate* . Thus, in connection with (4.16a,b) we require:

$$\tau d \stackrel{!}{=} \sigma_{ij}d_{ij} \equiv \dot{D} \,, \qquad (4.19)$$

so that, using (4.14c), (4.18), and the inverse transformation $\sigma_{ij} = \beta_{ijkl}^{(-1)}\tau_{kl}$ of (4.11) the relation

$$\tau(\partial F/\partial \tau_{ij})_{i=j=1} = \tau_{ij}(\partial F/\partial \tau_{ij}) \qquad (4.20)$$

results, from which we can determine the fictitious stress τ. The *rate of dissipation of creep energy* is obtained from (4.19), combined with (4.11), (4.14c), and (4.18):

$$\dot{D} = \dot{\Lambda}\tau_{pq}[\partial F(\boldsymbol{\tau})/\partial \tau_{pq}] \,. \qquad (4.21)$$

Considering homogeneous creep potentials $F(\tau_{ij})$ of degree r, we use EU-LER*'s theorem on homogeneous functions*,

$$F(S\tau_{ij}) = S^r F(\tau_{ij}) \quad \Rightarrow \quad \tau_{ij}[\partial F(\boldsymbol{\tau})/\partial \tau_{ij}] = rF(\tau_{ij}) \,, \qquad (4.22)$$

and find from (4.21) the dissipation rate $\dot{D} = \varphi r\tau^r\dot{\Lambda}$, if we assume a creep condition $F(\tau_{ij}) = \varphi\tau^r$ of degree r. For instance, the square creep condition $F = \tau_{ij}\tau_{ji}/2 = \tau^2/2$ with $r = 2$ and $\varphi = 1/2$ leads to the dissipation rate $\dot{D} = \dot{\Lambda}\tau^2$ which, because of (4.18), i.e. $\dot{\Lambda} = d/\tau$, agrees with (4.19).

4.2.2 Isochoric Creep Behavior

The assumption of isochoric creep behavior is very important; for instance, metal creep of the "secondary" stage will usually be uninfluenced by a superimposed hydrostatic pressure and takes place without volume change. Therefore, in this section *incompressibility* is adopted, and, using the creep potential hypothesis described in section 4.2.1, the constitutive equations are formulated, i.e., by analogy of (4.8) a *creep potential* of the form

$$F = F[J_2(\boldsymbol{\tau}'), \, J_3(\boldsymbol{\tau}')] \qquad (4.23)$$

is based in the anisotropic case. In (4.23) τ' is the deviator

$$\tau'_{ij} = \beta'_{\{ij\}pq}\sigma'_{pq} \tag{4.24}$$

where the tensor (BETTEN, 1976a)

$$\beta'_{\{ij\}} \equiv \beta_{ijpq} - \beta_{kkpq}\delta_{ij}/3 \tag{4.25}$$

is deviatoric corresponding to the free index pair $\{ij\}$. The invariants of the deviator (4.24) in (4.23) are given, as in (4.10), by

$$J_2(\tau') \equiv \frac{1}{2}\tau'_{ij}\tau'_{ji} = \frac{1}{2}\beta'_{\{ij\}pq}\beta'_{\{ji\}rs}\sigma'_{pq}\sigma'_{rs} \tag{4.26a}$$

$$J_3(\tau') \equiv \frac{1}{3}\tau'_{ij}\tau'_{jk}\tau'_{ki} = \frac{1}{3}\beta'_{\{ij\}pq}\beta'_{\{jk\}rs}\beta'_{\{ki\}tu}\sigma'_{pq}\sigma'_{rs}\sigma'_{tu} \ . \tag{4.26b}$$

From the flow rule (4.14c), combined with the relations (4.17), (4.18), and (4.20), we finally obtain the constitutive equations

$$d_{ij} = \Phi\beta'_{pq\{ij\}}\left(\frac{\partial F}{\partial J_2}\tau'_{qp} + \frac{\partial F}{\partial J_3}\tau''_{qp}\right) \ , \tag{4.27}$$

in which the function Φ is defined by

$$\Phi \equiv \frac{1}{2}L\left\{3\left/\left[\left(\frac{\partial F}{\partial J_2}\right)_V + \frac{1}{3}\tau\left(\frac{\partial F}{\partial J_3}\right)_V\right]\right\}^{(m+1)/2}\right.$$
$$\times\left[\frac{\partial F}{\partial J_2}J_2(\tau') + \frac{3}{2}\frac{\partial F}{\partial J_3}J_3(\tau')\right]^{(m-1)/2} \ . \tag{4.28}$$

The Index V, appended to the round brackets in (4.28), indicates the uniaxial equivalent fictitious stress state $(\tau_{ij})_V \equiv \text{diag}\{\tau_{11} \equiv \tau, 0, 0\}$. Contrary to (4.25), the tensor

$$\beta'_{pq\{ij\}} \equiv \beta_{pqij} - \beta_{pqkk}\delta_{ij}/3 \tag{4.29}$$

in (4.27) is deviatoric corresponding to the second index pair. The symbol

$$\tau''_{qp} \equiv (\tau'_{qp}{}^{(2)})' = \tau'_{qr}\tau'_{rp} - \frac{2}{3}J_2(\tau')\delta_{qp} = \frac{\partial J_3(\tau')}{\partial \tau_{ij}} \tag{4.30}$$

is the deviator of the square of the reduced tensor (4.24).

   Inserting (4.27), together with (4.28), in (4.19), we obtain the rate of *dissipation* of creep energy:

$$\dot{D} = [2(\partial F/\partial J_2)J_2(\boldsymbol{\tau}') + 3(\partial F/\partial J_3)J_3(\boldsymbol{\tau}')]\Phi \, , \tag{4.31a}$$

$$\dot{D} = L \left[3 \frac{\dfrac{\partial F}{\partial J_2}J_2(\boldsymbol{\tau}') + \dfrac{3}{2}\dfrac{\partial F}{\partial J_3}J_3(\boldsymbol{\tau}')}{\left(\dfrac{\partial F}{\partial J_2}\right)_V + \dfrac{1}{3}\tau\left(\dfrac{\partial F}{\partial J_3}\right)_V} \right]^{(m+1)/2} \tag{4.31b}$$

in considering the following transvections:

$$\beta'_{pq\{ij\}}\sigma_{ij} = \tau_{pq}, \quad \tau_{pq}\tau'_{qp} = 2J_2(\boldsymbol{\tau}'), \quad \text{and} \quad \tau_{pq}\tau''_{qp} = 3J_3(\boldsymbol{\tau}') \, .$$

In the isotropic special case, given by $\beta_{pqij} = \delta_{pi}\delta_{qj}$, $L \to K$, $m \to n$, $\tau'_{ij} \to \sigma'_{ij}$, and $\tau''_{ij} \to \sigma''_{ij}$, the constitutive equations (4.27), together with (4.28), immediately lead to the corresponding relations derived by BETTEN (1981a).

4.2.3 Creep Parameters

The essential creep parameters L, m involved in the creep law (4.17) and in the constitutive equations (4.27), (4.28) are related to experimental data. In this section a determination of such parameters is described.

For instance, we consider an *orthotropic material* and use the creep law (4.15) in tests on specimens cut along the mutually perpendicular directions x, y, z. Then, with the notations from Fig. 4.8, we have:

$$d = K_x X^{n_x} \, , \tag{4.32a}$$

$$d = K_y Y^{n_y} \, , \tag{4.32b}$$

$$d = K_z Z^{n_z} \, , \tag{4.32c}$$

from which we find in the "limiting creep stress" state:

$$d_c = (K_x K_y K_z)^{1/3}(\sigma_{cx}^{n_x}\sigma_{cy}^{n_y}\sigma_{cz}^{n_z})^{1/3} \, . \tag{4.33}$$

According to the idea in Fig. 4.8 and using the mapping (4.11), the "limiting creep stresses" can be expressed by the fictitious isotropic "limiting creep stress" τ_c:

$$\tau_c \equiv \tau_{xx} = \beta_{xxxx}\sigma_{cx} \equiv \ell_x\sigma_{cx} \, , \quad \tau_c \equiv \tau_{yy} \, , \quad \text{etc.,} \tag{4.34}$$

so that then the relation (4.33) according to (4.17) takes the form

$$d_c = L\,\tau_c^m \, ,$$

if the fictitious creep factor L is the geometrical mean value

$$L \equiv \left[(K_x/\ell_x^{n_x})(K_y/\ell_y^{n_y})(K_z/\ell_z^{n_z})\right]^{1/3} \tag{4.35}$$

and the fictitious creep exponent m is the arithmetical mean value

$$m \equiv (n_x + n_y + n_z)/3 \tag{4.36}$$

from corresponding experimental data. In the case of an existing BAUSCHINGER *effect*, the compression test data σ_{cx}^*, σ_{cy}^*, etc. appear in the equations (4.34), (4.35), and (4.36), too.

In the *orthotropic* case, the transformation (4.11) can be specified according to (BETTEN, 1976b):

$$\beta_{ijpq} \equiv \omega_{ip}\omega_{jq} \quad \Rightarrow \quad \tau_{ij} = \omega_{ip}\omega_{jq}\sigma_{pq} \ . \tag{4.37}$$

If the second order tensor ω_{ij} is symmetric, then its principal values ω_I, ω_{II}, ω_{III} are all real. For isotropic materials the tensor is identical to KRONECKER's tensor δ_{ij}. Using the notations from Fig. 4.8 and considering (4.37), the diagonal form of the "orthotropic tensor" ω_{ij} is given by

$$\omega_{ij} = \mathrm{diag}\{\sqrt{\tau/X}, \ \sqrt{\tau/Y}, \ \sqrt{\tau/Z}\} \ . \tag{4.38}$$

If ω_{ij} has the diagonal form, then, in accordance with (4.37), the tensors τ_{ij} and σ_{ij} are coaxial. For example, the assumptions of incompressibility (4.24) and orthotropic material (4.37) with

$$\beta'_{\{ij\}pq} = \omega_{ip}\omega_{jq} - \omega_{pq}^{(2)}\delta_{ij}/3 \tag{4.39}$$

immediately lead from the quadratic creep condition

$$J_2(\boldsymbol{\tau}') = \tau^2/3 \tag{4.40}$$

to the HILL-*condition* (HILL, 1950).

4.2.4 Second-Order Effects

If a function $y = f(x)$ can be approximated by a polynomial

$$y = \sum_{\nu=0}^{N} a_\nu x^\nu \tag{4.41}$$

of $N + 1$ terms of order ν, we say that the terms $a_1 x$ and $a_2 x^2$ are the contributions of first and second orders, respectively, in the variable x. Thus, the meaning of "order" is mathematical, not physical (TRUESDELL, 1964).

If the anisotropic behavior can be approximated by a tensor power series in one variable,

$$\dot{\gamma}_{ij} = \dot{\gamma}_{ij}(\tau_{pq}) = \sum_{\nu=0}^{N} B_\nu \tau_{ij}^{(\nu)} \quad \text{where} \quad \tau_{ij} = \beta_{ijkl}\sigma_{kl} , \qquad (4.42)$$

then, by using HAMILTON-CAYLEY's theorem,

$$\tau_{ij}^{(\nu)} = P_{\nu-2}\tau_{ij}^{(2)} + Q_{\nu-1}\tau_{ij} + R_\nu\delta_{ij} , \qquad (4.43)$$

where $P_{\nu-2}$, $Q_{\nu-1}$, and R_ν are scalar-valued functions of the principal invariants (4.12a,b,c), and of the orders $\nu - 2$, $\nu - 1$, ν, respectively, in the tensor τ_{ij} (BETTEN, 1987c), and because of (4.14c), we find the representation (BETTEN, 1979a):

$$d_{ij} = \beta_{pqij}(\varphi_0\delta_{qp} + \varphi_1\tau_{qp} + \varphi_2\tau_{qr}\tau_{rp}) . \qquad (4.44)$$

Assuming *incompressibility* (4.8), we have, instead of (4.44), the *anisotropic representation*

$$d_{ij} = \beta'_{pq\{ij\}}(\psi_0\delta_{qp} + \psi_1\tau'_{qp} + \psi_2\tau'_{qr}\tau'_{rp}) , \qquad (4.45)$$

in which, by comparing (4.45) with the constitutive equations (4.27), (4.28), and considering (4.30), the scalar-valued functions ψ_0, ψ_1, ψ_2 are:

$$\psi_0 \equiv -\frac{2}{3}J_2(\boldsymbol{\tau}')\psi_2 , \qquad (4.46a)$$

$$\psi_1 \equiv \Phi\frac{\partial F}{\partial J_2(\boldsymbol{\tau}')} , \qquad (4.46b)$$

$$\psi_2 \equiv \Phi\frac{\partial F}{\partial J_3(\boldsymbol{\tau}')} . \qquad (4.46c)$$

Because of the incompressibility, not all the values ψ_0, ψ_1, ψ_2 are independent, as we see from (4.46a). The terms $\varphi_1\tau_{qp}\beta_{pqij}$ and $\varphi_2\tau_{qp}^{(2)}\beta_{pqij}$ in (4.44) or $\psi_1\tau'_{qp}\beta'_{pq\{ij\}}$ and $\psi_2\tau'_{qp}{}^{(2)}\beta'_{pq\{ij\}}$ in (4.45) are the contributions of first and second orders, respectively, in the tensor $\boldsymbol{\tau}$ or the deviator $\boldsymbol{\tau}'$.

Similarly, the terms containing τ'_{qp} and τ''_{qp} in (4.27) are the contributions of first and second orders, respectively, in the mapped deviator $\boldsymbol{\tau}'$.

The following considerations are based upon the *creep potential*

$$F = J_2(\boldsymbol{\tau}') + \alpha J_3(\boldsymbol{\tau}')/\tau \quad \text{where} \quad -3 \leq \alpha \leq 3/2 , \tag{4.47}$$

which is suitable to describe *second-order effects*, as shown by BETTEN (1975d; 1976b) for the isotropic case, for instance. The range $-3 \leq \alpha \leq 3/2$ in (4.47) results from the *convexity* of the potential surface $F = \text{const.}$ Using (4.47), the constitutive equations (4.27) together with (4.28) become

$$d_{ij} = \frac{1}{2} L \left(\frac{3}{1 + \alpha/3} \right)^{(m+1)/2} \left[J_2(\boldsymbol{\tau}') + \frac{3}{2}\alpha \frac{J_3(\boldsymbol{\tau}')}{\tau} \right]^{(m-1)/2}$$
$$\times \beta'_{pq\{ij\}} \left(\tau'_{qp} + \frac{\alpha \tau''_{qp}}{\tau} \right) . \tag{4.48}$$

Comparing (4.48) with the representation (4.45) and considering (4.30), we can express the scalar-valued functions (4.46b,c) as:

$$\psi_1 = \frac{1}{2} L \left(\frac{3}{1 + \alpha/3} \right)^{(m+1)/2} \left[J_2(\boldsymbol{\tau}') + \frac{3}{2}\alpha \frac{J_3(\boldsymbol{\tau}')}{\tau} \right]^{(m-1)/2} \tag{4.49a}$$
$$\psi_2 = \alpha(\psi_1/\tau) . \tag{4.49b}$$

From (4.45) and (4.49b) we see that the parameter α in (4.47) is determined by a *second-order effect*.

As mentioned before, the idea of "order" is mathematical and has nothing to do with the phenomenon occuring, since it results only from the mathematical framework we choose in describing the phenomenon.

In the following we show that the POYNTING *effect* can be described by the second-order contribution in the constitutive equation (4.48). The phenomena observed by POYNTING in 1909 can be illustrated by considering the effect of a pure shear stress state

$$\sigma_{ij} = \sigma'_{ij} = \sigma_{12} \begin{pmatrix} 0 & 1 & 0 \\ 1 & 0 & 0 \\ 0 & 0 & 0 \end{pmatrix} . \tag{4.50}$$

Then, the deviator (4.24) and the deviator of its square (4.30) are given by

$$\tau'_{ij} = \omega_I \omega_{II} \sigma'_{ij} \tag{4.51a}$$

and

$$\tau''_{ij} = \frac{1}{3}\omega_I^2\omega_{II}^2\sigma_{12}^2 \operatorname{diag}\{1, 1, -2\} \,, \tag{4.51b}$$

if the stress tensor σ_{ij} and its image τ_{ij} are coaxial. This coaxiality exists if the orthotropic tensor ω_{ij} has the diagonal form (4.38). Because of (4.50), the invariants of the deviator (4.51a) are given by $J_2(\tau') = \omega_I^2\omega_{II}^2\sigma_{12}^2$ and $J_3(\tau') = 0$, so that the constitutive equation (4.48) is reduced to

$$d_{ij} = \frac{1}{6}L\left(\frac{3\omega_I^2\omega_{II}^2}{1 + \alpha/3}\right)^{m/2}\sigma_{12}^m \begin{pmatrix} \alpha\zeta_I & 3\dfrac{\tau}{\sigma_{12}} & 0 \\ 3\dfrac{\tau}{\sigma_{12}} & \alpha\zeta_{II} & 0 \\ 0 & 0 & -2\alpha\zeta_{III} \end{pmatrix} \tag{4.52}$$

in using (4.29), (4.37), (4.50), and (4.51). In the matrix (4.52) the abbreviations

$$\zeta_I \equiv (2\omega_I^2 - \omega_{II}^2 + 2\omega_{III}^2)/3 \,, \tag{4.53a}$$

$$\zeta_{II} \equiv (-\omega_I^2 + 2\omega_{II}^2 + 2\omega_{III}^2)/3 \,, \tag{4.53b}$$

$$\zeta_{III} \equiv (\omega_I^2 + \omega_{II}^2 + 4\omega_{III}^2)/6 \tag{4.53c}$$

are used, while the quotient

$$\tau/\sigma_{12} = \omega_I\omega_{II}\left[\frac{3}{1 + \alpha/3}\right]^{1/2} \tag{4.54}$$

is determined from (4.20), considering (4.47), (4.50), and (4.51a).

From (4.52), (4.53c), and (4.54) we obtain the quotient of the longitudinal strain rate d_{33} and the shearing strain rate d_{12},

$$\frac{d_{33}}{d_{12}} = -\frac{\omega_I^2 + \omega_{II}^2 + 4\omega_{III}^2}{6\omega_I\omega_{II}} \cdot \frac{2\alpha}{3\sqrt{3}}\left(1 + \frac{\alpha}{3}\right)^{1/2} \,, \tag{4.55}$$

which can be considered as a suitable measure of the POYNTING *effect* (Fig. 4.9a).

Regarding experimental investigations (FOUX, 1964; HECKER, 1967; SWIFT, 1947) the α-values are not so large. The limits $\alpha = -3$ and $\alpha = 3/2$ are given by the *convexity* of the *creep potential* (4.47) and are compatible with (4.55), in which the square root must be real. In the isotropic case, $\omega_I = \omega_{II} = \omega_{III} = 1$, the results from Fig. 4.9a are identical with those calculated by BETTEN (1981a).

The anisotropic influence is contained in the factor

$$\frac{\omega_I^2 + \omega_{II}^2 + 4\omega_{III}^2}{6\omega_I\omega_{II}} \,,$$

which is equal to one for isotropic materials, while the function

$$-(2\sqrt{3}\,\alpha/9)\,(1+\alpha/3)^{1/2}$$

of equation (4.55) expresses the *second-order effect*. This possibility of a
"polar" decomposition is based on the fact that, because of (4.38), the tensors σ_{ij} and τ_{ij} are *coaxial*. Similarly, the quotient d_{22}/d_{12} is numerically
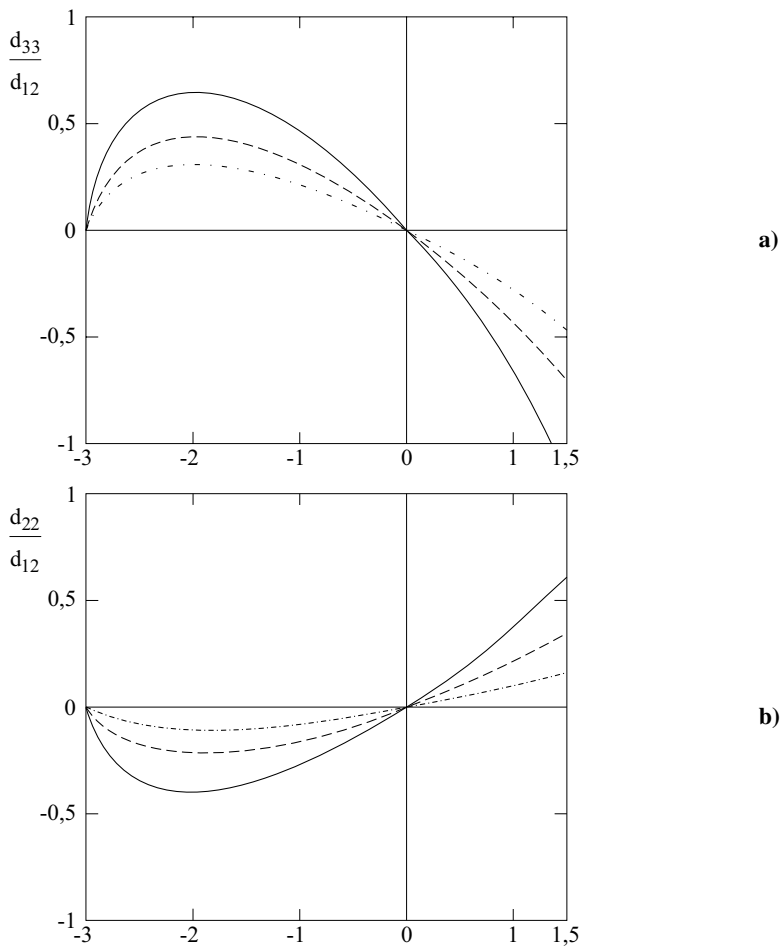evaluated (Fig. 4.9b).

Fig. 4.9 POYNTING effect. ——, $\omega_I = 0.8$, $\omega_{II} = 1.05$, $\omega_{III} = 1.2$;
$---$, isotropy($\omega_I = \omega_{II} = \omega_{III} = 1$; $-\cdot-$, $\omega_I = 1.2$, $\omega_{II} = 1.05$, $\omega_{III} = 0.8$.

As another example, let us consider a *thin-walled circular cylindrical tube* (thickness s, mean radius r) subjected to internal pressure p. Its stress state is given by the components

$$\sigma_{11} \equiv \sigma_r \approx 0, \quad \sigma_{22} \equiv \sigma_u = \frac{r\,p}{s}, \quad \text{and} \quad \sigma_{33} \equiv \sigma_z = \frac{r\,p}{2s}.$$

Then, the invariants (4.26a,b) of the deviator (4.24) become

$$J_2(\boldsymbol{\tau}') = \frac{1}{3}\left(\omega_I^4 + \omega_I^2\omega_{II}^2 + \omega_{II}^4\right)\left(\frac{r}{2s}p\right)^2 \tag{4.56a}$$

$$J_3(\boldsymbol{\tau}') = \frac{1}{27}\left(2\omega_{II}^6 - 3\omega_I^4\omega_{II}^2 + 3\omega_I^2\omega_{II}^4 - 2\omega_I^6\right)\left(\frac{r}{2s}p\right)^3 \tag{4.56b}$$

in the *orthotropic* case (4.37), (4.38). The cubic invariant (4.56b) is zero, if the material reponse is isotropic in planes perpendicular to the tube axis ($\omega_I = \omega_{II}$).

From (4.20), together with (4.47), we find the cubic equation

$$(1 + \alpha/3)\tau^3 - 3J_2(\boldsymbol{\tau}')\tau - 9\alpha J_3(\boldsymbol{\tau}')/2 = 0 , \tag{4.57}$$

which contains the solution (4.54) for the example (4.50).

Since all solutions for τ are real, the discriminant of (4.57),

$$\Delta \equiv \frac{81}{16}\left[\frac{\alpha J_3(\boldsymbol{\tau}')}{1 + \alpha/3}\right]^2 - \left[\frac{J_2(\boldsymbol{\tau}')}{1 + \alpha/3}\right]^3 \tag{4.58}$$

must not be positive:

$$J_2^3 \geq \frac{81}{16}\left(1 + \frac{\alpha}{3}\right)\alpha^2 J_3^2 . \tag{4.59}$$

The right-hand side in (4.59) has a maximum for $\alpha = -2$. Then, we have $J_2^3/27 \geq J_3^2/4$ in accordance with BETTEN (1987c). Therefore, the requirement (4.59) is fulfilled in the whole range $-3 \leq \alpha \leq 0$ considered here. In the following, we use an approximation of (4.57),

$$\tau \approx \left(\frac{3J_2(\boldsymbol{\tau}')}{1 + \alpha/3}\right)^{1/2} , \tag{4.60a}$$

or, inserting (4.56a),

$$\tau \approx \left(\frac{\omega_I^4 + \omega_I^2\omega_{II}^2 + \omega_{II}^4}{1 + \alpha/3}\right)^{1/2}\frac{r\,p}{2s} , \tag{4.60b}$$

which is true for $\omega_I = \omega_{II}$ or $\alpha = 0$.

From (4.48), together with (4.29), (4.37), (4.56), and (4.60b), we find the constitutive equation of a *thin-walled tube* subjected to internal pressure:

$$
d_{ij} = \frac{1}{2} L \left(\frac{3}{1+\alpha/3} \right)^{(m+1)/2} \left(\frac{N}{3} \right)^{(m-1)/2} \left(\frac{r\,p}{2s} \right)^m \begin{pmatrix} M_I & 0 & 0 \\ 0 & M_{II} & 0 \\ 0 & 0 & M_{III} \end{pmatrix} ,
$$

(4.61)

using the following abbreviations:

$$
N \equiv \omega_I^4 + \omega_I^2 \omega_{II}^2 + \omega_{II}^4 ,
$$
(4.62a)

$$
Q \equiv N + 3\omega_I^2 \omega_{II}^2 ,
$$
(4.62b)

$$
M_I \equiv -\frac{1}{9} \left[4\omega_I^4 + 3\omega_I^2 \omega_{II}^2 + 2\omega_{II}^4 + \left(\omega_I^2 - \omega_{II}^2 \right) \omega_{III}^2 \right] + \chi_I ,
$$
(4.63a)

$$
M_{II} \equiv \frac{1}{9} \left[2\omega_I^4 + 3\omega_I^2 \omega_{II}^2 + 4\omega_{II}^4 - \left(\omega_I^2 - \omega_{II}^2 \right) \omega_{III}^2 \right] + \chi_{II} ,
$$
(4.63b)

$$
M_{III} \equiv 2 \left(\omega_I - \omega_{II} \right) \left(\omega_I^2 + \omega_{II}^2 + \omega_{III}^2 \right) / 9 - 2\chi_{III} ,
$$
(4.63c)

$$
\chi_I \equiv \frac{\alpha}{27} \left(\frac{3+\alpha}{3N} \right)^{1/2} \left(4\omega_I^6 - 4\omega_I^2 \omega_{II}^4 + 5\omega_I^4 \omega_{II}^2 - 2\omega_{II}^6 + Q\omega_{III}^2 \right) ,
$$
(4.64a)

$$
\chi_{II} \equiv \frac{\alpha}{27} \left(\frac{3+\alpha}{3N} \right)^{1/2} \left(4\omega_{II}^6 - 4\omega_{II}^2 \omega_I^4 + 5\omega_{II}^4 \omega_I^2 - 2\omega_I^6 + Q\omega_{III}^2 \right) ,
$$
(4.64b)

$$
\chi_{III} \equiv \frac{\alpha}{54} \left(\frac{3+\alpha}{3N} \right)^{1/2} \left(2\omega_I^6 + \omega_I^2 \omega_{II}^4 + \omega_I^4 \omega_{II}^2 + 2\omega_{II}^6 + 2Q\omega_{III}^2 \right) .
$$
(4.64c)

Because of the incompressibility, the trace of the strain-rate tensor (4.61), $M_I + M_{II} + M_{III}$, must be zero. This can easily be checked. In the isotropic special case,

$$
\omega_I = \omega_{II} = \omega_{III} = 1 ,
$$

we have

$$
M_I = -1 + \chi ,
$$
$$
M_{II} = 1 + \chi ,
$$
$$
M_{III} = -2\chi ,
$$

$$
\chi_I = \chi_{II} = \chi_{III} \equiv \chi = \alpha \left(1 + \alpha/3 \right)^{1/2} \left(3\sqrt{3} \right) ,
$$

in accordance with BETTEN (1981a).

To investigate the *second-order effects*, the quotient

$$\frac{(d_{11})_{\alpha\neq0}}{(d_{11})_{\alpha=0}} = \frac{M_I(\alpha)/M_I(\alpha=0)}{(1+\alpha/3)^{(m+1)/2}} \tag{4.65}$$

of the radial strain-rates, obtained from (4.61) together with (4.62)-(4.64), is numerically evaluated. The results are represented in Fig. 4.10.
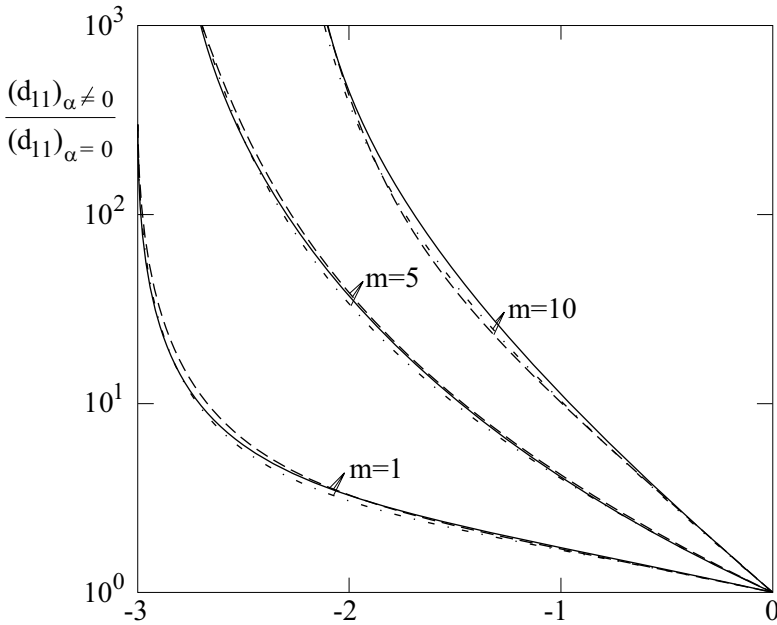

Fig. 4.10 Influence of the *second-order effect* on the radial creep strain rate.
————, isotropy ($\omega_I = \omega_{II} = \omega_{III} = 1$);   − − −, $\omega_I = 1.1, \omega_{II} = 0.9, \omega_{III} = 1$;
− · −, $\omega_I = 0.9, \omega_{II} = 1.1, \omega_{III} = 1$.

Similarly, the influence of the second-order effect on the circumferential strain-rate d_{22} can be expressed by the formula

$$\frac{(d_{22})_{\alpha\neq0}}{(d_{22})_{\alpha=0}} = \frac{M_{II}(\alpha)/M_{II}(\alpha=0)}{(1+\alpha/3)^{(m+1)/2}} , \tag{4.66}$$

the numerical calculation of which is shown in Fig. 4.11.
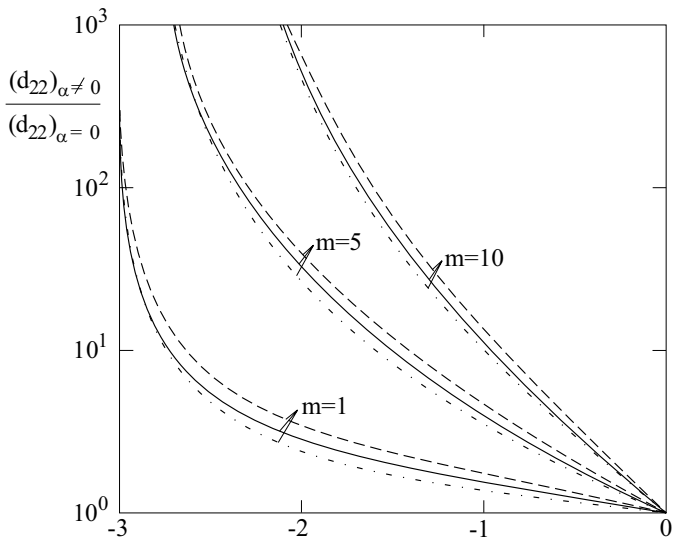
Fig. 4.11 Influence of the *second-order effect* on the circumferential creep strain rate.
————-, isotropy($\omega_I = \omega_{II} = \omega_{III} = 1$); $---$, $\omega_I = 1.1, \omega_{II} = 0.9, \omega_{III} = 1$;
$-\cdot-$, $\omega_I = 0.9, \omega_{II} = 1.1, \omega_{III} = 1$.
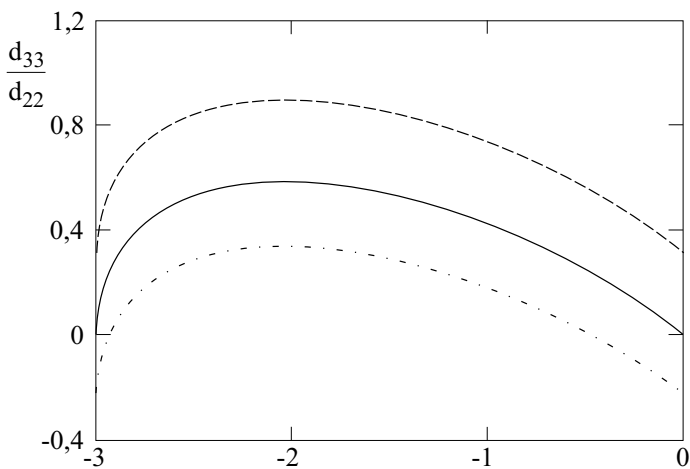
Fig. 4.12 Changes in length of a thin-walled tube as a result from "second order" effect and
anisotropy. ————-, isotropy($\omega_I = \omega_{II} = \omega_{III} = 1$); $---$, $\omega_I = 1.1, \omega_{II} = 0.9$,
$\omega_{III} = 1$; $-\cdot-$, $\omega_I = 0.9, \omega_{II} = 1.1, \omega_{III} = 1$.

Finally, the quotient

$$\frac{d_{33}}{d_{22}} = \frac{M_{III}(\alpha)}{M_{II}(\alpha)} \tag{4.67}$$

of the creep strain-rates in axial (d_{33}) and circumferential (d_{22}) directions is illustrated in Fig. 4.12.

The maximal errors of the approximation (4.60b) are 6% and 8% for the parameter sets $\{\omega_I = 1.1; \omega_{II} = 0.9; \omega_{III} = 1\}$ and $\{\omega_I = 0.9; \omega_{II} = 1.1; \omega_{III} = 1\}$, respectively, which are used in Figs. 4.4, 4.5, and 4.6.

4.3 Tertiary Creep

The *tertiary creep phase* is accompanied by the formation of microscopic cracks on the grain boundaries, so that damage-accumulation occurs. In some cases voids are caused by a given stress history and, therefore, they are distributed anisotropically among the grain boundaries. Thus, the mechanical behavior will be *anisotropic* and it is therefore necessary to investigate this kind of anisotropy by introducing appropiately defined *anisotropic damage tensors* (Chapter 7) into constitutive equations (BETTEN, 1982b; 1983b).

Problems of *creep damage* have been investigated by many authors, some of them are listed in the introduction to this monograph.

In the following sections the uniaxial and multiaxial tertiary creep behavior will be discussed in detail.

4.3.1 Uniaxial Tertiary Creep

In a uniaxial tension specimen, material deterioration can be described by introducing an additional variable ω or, alternatively, $\psi \equiv 1 - \omega$ into constitutive equations, i.e. the strain rate d can be expressed as $d = f(\sigma, \omega)$, or $d = f(\sigma, \psi)$, where σ is the uniaxial stress (Kachanov, 1958; 1986; RABOTNOV, 1969). The material parameters ω and ψ describe the current *damage* state and the *continuity* of the material, respectively. The parameter of *continuity*, ψ, represents that fraction of the cross-sectional area that is not occupied by either voids or internal fissures. The *net-stress* acting over the cross-section of the uniaxial specimen is then $\hat{\sigma} = \sigma / \psi$. When $\psi = 1$ the material is in its virgin undamaged state, and when $\psi = 0$, the material can no longer sustain any load. In the latter case the constitutive equation would be required in order to approach an infinite strain rate. Furthermore,

it is assumed that the damage rate $\dot{\omega}$, or alternatively the rate of continuity change $\dot{\psi}$, is also governed by the uniaxial stress and by the current state of continuity, i.e., $\dot{\omega} = g(\sigma, \omega)$ or $\dot{\psi} = -g(\sigma, \psi)$.

The forms of the functions f and g have been discussed in detail by many scientists, for instance by RABOTNOV (1969), CHRZANOWSKI (1973), LECKIE and PONTER (1974), LECKIE and HAYHURST (1977), GOEL (1975), HAYHURST, TRAMPCZYNSKI and LECKIE (1980), NAUMENKO and AL-TENBACH (2007). Often the forms

$$\frac{d}{d_0} = \frac{(\sigma/\sigma_0)^n}{(1-\omega)^m} \, , \qquad\qquad \frac{\dot{\omega}}{\dot{\omega}_0} = \frac{(\sigma/\sigma_0)^\nu}{(1-\omega)^\mu} \qquad (4.68a,b)$$

are used, where $n \geq \nu, m, \mu, d_0, \dot{\omega}_0$ and σ_0 are constants. The undamaged case ($\omega = 0$) hereby leads to NORTON-BAILEY's *power law* (4.15), which is assumed to be valid for the secondary creep stage, while the creep rate d approaches infinity as ω approaches 1.

Integrating the *kinetic equation* (4.68b) by considering the initial condition $\omega(t = 0) = 0$ and inserting the result into (4.68a), one arrives at the following relation (BETTEN, 1992):

$$\frac{d}{d_0} = \left(\frac{\sigma}{\sigma_0}\right)^n \left[1 - k\left(\frac{\sigma}{\sigma_0}\right)^\nu \dot{\omega}_0 t\right]^{-m/k} \qquad \text{with } k = 1 + \mu \, . \qquad (4.69)$$

A further integration leads to the tertiary creep strain

$$\varepsilon_t = \frac{a}{b(1-c)} \left[1 - (1 - bt)^{1-c}\right] \, , \qquad\qquad (4.70)$$

if we take the initial condition $\varepsilon_t(0) = 0$ into account. The abbreviations

$$a \equiv d_0 \left(\frac{\sigma}{\sigma_0}\right)^n \, , \qquad b \equiv k \left(\frac{\sigma}{\sigma_0}\right)^\nu \dot{\omega}_0 \, , \qquad c \equiv \frac{m}{k} \qquad (4.71a,b,c)$$

have been introduced in (4.70).

Because creep rupture is characterized by $\omega = 1$ or $d \to \infty$ we can immediately find the time to rupture from (4.69):

$$t_r = [k \, (\sigma/\sigma_0)^\nu \dot{\omega}_0]^{-1} \, . \qquad\qquad (4.72)$$

If, for the sake of convenience, the constants m and μ are taken to be equal to the parameters n and ν, respectively, the relations (4.68a,b) can then be simplified to

$$d = K\hat{\sigma}^n \; , \qquad\qquad \dot{\omega} = L\hat{\sigma}^\nu \; , \qquad\qquad (4.73\mathrm{a,b})$$

where $\hat{\sigma} = \sigma/(1 - \omega)$ is interpreted as the *net-stress* acting over the current cross-sectional area of a uniaxial specimen. Thus, the simplification (4.73a,b) can be called the *net-stress concept*. From (4.68a,b) and (4.73a,b) we read:

$$K \equiv d_0/\sigma_0^n \quad \text{and} \quad L \equiv \dot{\omega}_0/\sigma_0^\nu \; . \qquad\qquad (4.74\mathrm{a,b})$$

One immediately arrives at the first relation (4.73a) from NORTON-BAILEY*'s law* (4.15) if we replace the nominal stress σ by the net-stress $\hat{\sigma}$. Furthermore, a *tensorial generalization* of (4.73a,b) can be achieved in a very similar manner to that described in section 4.3.2, where the NORTON-BAILEY *creep law* is generalized. This generalization has been illustrated by BETTEN (1991a).

Because of the simplifications $m = n$ and $\mu = \nu$, which lead to (4.73a,b), the creep rupture time (4.72) takes the form

$$t_r = [(1 + \nu)L\sigma^\nu]^{-1} \; , \qquad\qquad (4.75)$$

where the nominal stress σ can be interpreted as the actual stress at the beginning of the tertiary creep stage ($\omega = 0$), i.e., considering NORTON-BAILEY*'s law* (4.15) and starting from (4.75) we arrive at the formula

$$d_{\min}^{\nu/n} t_r = K^{\nu/n}/L(1 + \nu) \; . \qquad\qquad (4.76\mathrm{a})$$

The quantity $d_{\min}$ in (4.76) is the steady-state or minimum creep-rate. Assuming $\nu = n$, one arrives at the relationship

$$d_{\min} t_r = K/L(1 + n) = \text{const.} \qquad\qquad (4.76\mathrm{b})$$

due to MONKMAN and GRANT (1956). Thus, the *net-stress concept* (4.73a,b) with identical exponents, $\nu \equiv n$, is compatible with the *model of* MONKMAN *and* GRANT . The justification of this model has, for example, been analyzed by ILSCHNER (1973), EDWARD and ASHBY (1979), EVANS (1984) and RIEDEL (1987).

Under certain conditions, the grain boundaries in polycrystals slide during creep deformation. EDWARD and ASHBY (1979) illustrate that this sliding can be accommodated in various ways: elastically, by diffusion, or by non-uniform creep or plastic flow of the grains themselves. In other cases, holes or cracks appear at the grain boundaries and grow until they link, leading to an *intergranular creep fracture*. When fracture is of this sort,

the MONKMAN and GRANT *rule* can be approximatively confirmed. Often, however, the MONKMAN-GRANT *product* , $d_{\min}t_r$, is proportional to the *strain-to-rupture*, ε_r, as has been observed by ILSCHNER (1973) and RIEDEL (1987) or in our own experiments.

Because of its microscopic nature, *damage* generally has an *anisotropic* character even if the material was originally isotropic. The fissure orientation and length cause anisotropic macroscopic behavior. Therefore, damage in an isotropic or anisotropic material which is in a state of multiaxial stress can only be described in a tensorial form.

4.3.2 Multiaxial Tertiary Creep

It must be noted that, from the physical point of view (RICE, 1970), the assumption of a *creep potential* has only limited justifications, especially in the *anisotropic* case (chapter 6) and in the *tertiary creep stage*. Fortunately, constitutive equations can be represented in full as *tensor-valued functions*, as is pointed out in detail in the following.

When generalizing the uniaxial concept (4.68a,b) or (4.73a,b), constitutive equations and anisotropic growth equations are expressed as the *tensor-valued functions*

$$d_{ij} = f_{ij}(\boldsymbol{\sigma}, \boldsymbol{\omega}) , \qquad\qquad \overset{\circ}{\omega}_{ij} = g_{ij}(\boldsymbol{\sigma}, \boldsymbol{\omega}) , \qquad\qquad (4.77\text{a,b})$$

respectively, where $^\circ$ denotes the JAUMANN *derivative*, $\boldsymbol{\sigma}$ is the CAUCHY *stress tensor*, and $\boldsymbol{\omega}$ represents an appropriately defined *damage tensor*.

Damage tensors are constructed, for instance, by BETTEN (1981b; 1983a; 1983b). Furthermore, we also refer to the work of MURAKAMI and OHNO (1981). They assumed that damage accumulating in the process of creep can be expressed through a symmetric tensor of rank two.

Some details about *damage tensors* and *tensors of continuity* are discussed in section 7.1. Furthermore, the influence of material deterioration on the stresses in a continuum is studied in section 7.2.

RABOTNOV (1968) has also introduced a symmetric second-order tensor of damage and defined a symmetric *net-stress tensor* $\hat{\boldsymbol{\sigma}}$ by way of a linear transformation

$$\sigma_{ij} = \Omega_{ijk\ell}\, \hat{\sigma}_{k\ell} , \qquad\qquad (4.78)$$

where the fourth-order tensor $\boldsymbol{\Omega}$ is assumed to be symmetric.

However, it has been pointed out in more detail by BETTEN (1982b) that the fourth-order tensor in (4.78) is only symmetric with reference to the first index pair ij, but not to the second, $k\ell$. Thus, the net-stress tensor is *not*

symmetric in a case of anisotropic damage. The net-stress tensor can be decomposed into a symmetric part and into an antisymmetric one, where only the symmetric part is equal to the *net-stress tensor* introduced by RABOTNOV (1968), as shown by BETTEN (1982b) in Section 7.2.

Starting from a third-order skew-symmetric tensor of continuity to represent area vectors (*bivectors*) of CAUCHY's *tetrahedron* in a damaged state, one finally arrives at a second-order damage tensor which has the *diagonal form* with respect to the rectangular cartesian coordinate system under consideration, as has been pointed out in detail by BETTEN (1983b).

The symmetric tensor-valued functions (4.77a,b) are valid for an *isotropic material* in an *anisotropic damage state*. Furthermore, one must differentiate between *anisotropic damage growth* and the *initial anisotropy* resulting from a forming process, for instance, rolling. Constitutive equations and anisotropic damage growth equations are then represented by expressions such as

$$d_{ij} = f_{ij}(\boldsymbol{\sigma}, \boldsymbol{\omega}, \boldsymbol{A}) \quad \text{and} \quad \overset{\circ}{\omega}_{ij} = g_{ij}(\boldsymbol{\sigma}, \boldsymbol{\omega}, \boldsymbol{A}) \;, \qquad (4.79\text{a,b})$$

respectively, where $\boldsymbol{A}$ is *a fourth-order constitutive tensor* with components A_{pqrs} characterizing the anisotropy from, for example rolling, i.e. the anisotropy of the material in its undamaged state.

A general representation of (4.79a), and similarly (4.79b) is given through a linear combination

$$\boldsymbol{d} = \sum_\alpha \varphi_\alpha \,^\alpha\boldsymbol{G} \quad \text{or} \quad d_{ij} = \sum_\alpha \varphi_\alpha \,^\alpha G_{ij} \;, \qquad (4.80)$$

where the $\boldsymbol{G}$'s are symmetric *tensor generators* of rank two involving the argument tensors $\boldsymbol{\sigma}, \boldsymbol{\omega}, \boldsymbol{A}$. Some possible methods in arriving at such tensor generators have been discussed by BETTEN (1982b; 1983b; 1987c; 1998), for instance. The coefficients φ_α in (4.80) are scalar-valued functions of the integrity basis associated with the representation (4.80). They must also contain experimental data measured in uniaxial creep tests. The main problems are to construct an irreducible set of tensor generators and to determine the scalar coefficients involving the integrity basis and experimental data.

A further aim is to represent the constitutive equation (4.80) in the *canonical form*

$$\boxed{d_{ij} = {}^0H_{ijk\ell}\delta_{k\ell} + {}^1H_{ijk\ell}\sigma_{k\ell} + {}^2H_{ijk\ell}\sigma_{k\ell}^{(2)}} \;, \qquad (4.81)$$

where ${}^0H_{ijk\ell}, \ldots, {}^2H_{ijk\ell}$ are the cartesian components of fourth-order tensor-

valued functions $^0\boldsymbol{H}, \ldots, {}^2\boldsymbol{H}$ depending on the *damage tensor* $\boldsymbol{\omega}$ and the *anisotropy tensor* $\boldsymbol{A}$. The canonical form (4.81) is a representation in three terms, which are the contributions of zero, first, and second orders in the stress tensor $\boldsymbol{\sigma}$ influenced by the functions $^0\boldsymbol{H}$, $^1\boldsymbol{H}$, and $^2\boldsymbol{H}$, respectively. In the isotropic special case the coefficient tensors $^0\boldsymbol{H}, \ldots, {}^2\boldsymbol{H}$ can be expressed as fourth-order spherical tensors:

$$H_{ijk\ell} = \frac{1}{2} \left(\delta_{ik}\delta_{j\ell} + \delta_{i\ell}\delta_{jk} \right) \varphi_\lambda , \quad \lambda = 0, 1, 2 . \tag{4.82}$$

In that case, the *canonical form* (4.81) simplifies to the *standard form*

$$\boxed{d_{ij} = f_{ij}(\boldsymbol{\sigma}) = \varphi_0\delta_{ij} + \varphi_1\sigma_{ij} + \varphi_2\sigma_{ij}^{(2)}} , \tag{4.83}$$

from which we obtain by *transvection*,

$$d_{ij}\sigma_{ji} = \varphi_0\delta_{ij}\sigma_{ji} + \varphi_1\sigma_{ij}\sigma_{ji} + \varphi_2\sigma_{ik}\sigma_{kj}\sigma_{ji} ,$$

a set of three *irreducible invariants*

$$S_\lambda = \mathrm{tr}\,\boldsymbol{\sigma}^\lambda, \quad \lambda = 1, 2, 3, \tag{2.85}$$

alternatively to the *integrity basis* (2.24):

$$J_1 \equiv S_1, \quad J_2 \equiv \frac{1}{2} \left(S_2 - S_1^2 \right), \quad J_3 \equiv \frac{1}{6} \left(2S_3 - 3S_2S_1 + S_1^3 \right) .$$
$$\tag{2.86a,b,c}$$

It may be impossible to find a canonical form (4.81) for all types of anisotropy. However, for the most important kinds of anisotropy, namely *transversely isotropic* and *orthotropic behavior*, the constitutive equation (4.80) can be expressed in the *canonical form* (4.81) as has been illustrated by BETTEN (1982b; 1983b; 1987c; 1998), for instance.

When formulating constitutive equations such as (4.79a) one has to take the following into account: The undamaged case ($\boldsymbol{\omega} \rightarrow \boldsymbol{0}$) immediately leads to the secondary creep stage, while the *rate-of-deformation tensor* $\boldsymbol{d}$ approaches infinity as $\boldsymbol{\omega}$ approaches the unit tensor $\boldsymbol{\delta}$. In view of polynomial representations of constitutive equations it is convenient to use the tensor

$$D_{ij} := (\delta_{ij} - \omega_{ij})^{(-1)} \equiv \psi_{ij}^{(-1)} \tag{4.84}$$

as an argument tensor instead of the tensorial damage variable $\boldsymbol{\omega}$. Thus, similar to (4.79a,b), expressions such as

$$d_{ij} = f_{ij}(\boldsymbol{\sigma}, \boldsymbol{D}, \boldsymbol{A}) \quad \text{and} \quad \overset{\circ}{D}_{ij} = g_{ij}(\boldsymbol{\sigma}, \boldsymbol{D}, \boldsymbol{A}) \qquad (4.85\text{a,b})$$

must be taken into consideration, i.e., an irreducible set of *invariants* and *tensor generators* of the representation (4.80) involving the argument tensors $\boldsymbol{\sigma}$, $\boldsymbol{D}$, $\boldsymbol{A}$ should be constructed. Some possible representations of such functions are discussed in the following.

In order to find irreducible sets of invariants for tensors of order higher than two, BETTEN (1987c; 2001a; 2001c) proposed three methods:

- ☐ **by way of an extended characteristic polynomial**
  (Section 6.4.4),
- ☐ **application of a modified LAGRANGE-multiplier method**
  (Section 6.4.5),
- ☐ **combinatorial method**
  (Section 6.4.6),

where the third one is most effective and not restricted to produce *irreducible invariants*, but also leads to results on tensor-valued terms called *tensor generators*. For instance, the expressions

$$\delta_{ij}\delta_{k\ell}A_{k\ell} \equiv A_{kk}\delta_{ij}, \quad \delta_{ik}\delta_{j\ell}A_{k\ell} \equiv A_{ij}, \qquad (4.86\text{a,b})$$

$$\delta_{ip}\delta_{qr}\delta_{sj}A_{pq}A_{rs} \equiv A_{ir}A_{rj} \equiv A_{ij}^{(2)}, \qquad (4.86\text{c})$$

are the three *irreducible tensor generators* of a second-order tensor A_{ij} or σ_{ij} in (4.83). Forming the traces $(i = j)$ in (4.86a,b,c) we immediately arrive at the three *irreducible invariants* (2.85). Note that $\text{tr}\boldsymbol{\delta} \equiv \delta_{jj} = 3$.

Other examples are the *transvections*

$$\delta_{ip}\delta_{qr}\delta_{sj}A_{pq}B_{rs} \equiv A_{ir}B_{rj}, \qquad (4.87\text{a})$$

$$\delta_{ip}\delta_{qr}\delta_{st}\delta_{uv}\delta_{wj}A_{pqrs}A_{tuvw} \equiv A_{irrs}A_{suuj}, \qquad (4.87\text{b})$$

which are index-combinations with the two free indices ij, that is, second-order tensor-valued terms, the *traces* of which are *invariants*.

Our special developed computer programm forms all possible index-combinations, such as (4.87a,b), and selects all redundant elements by considering index-symmetries. Thus, we find sets of *irreducible tensor-generators*, which are **complete**, too. Some results are listed in Table 6.5 of Section 6.4.6.

5 Creep Behavior of Thick-Walled Tubes

The expansion of a long cylindrical tube by uniform internal pressure is an eternal problem because of its connection with the autofrettage of pressure vessels; the process has also been used to determine the influence of a stress gradient on the criterion of yielding. Therefore, many scientists have examined the problem. Very detailed statements are given e.g. by HILL (1950), SZABÓ (1964) and BUCHTER (1967).

The solution of the stress and deformation problem of thick-walled tubes under axially symmetric loading in the elastic range is given by the familiar LAMÉ equations (LAMÉ, 1852). The elastic-plastic state in a thick-walled tube was first investigated by TURNER (1909).

The afore-mentioned publications are not concerned with problems of creep in thick-walled tubes. The creep-behavior is treated for example by BAILEY (1935), DAVIS (1960), RIMROTT (1959), RIMROTT, MILLS and MARIN (1960), BESSELING (1962), ODQUIST and HULT (1962), ODQUIST (1966), MARIOTT (1972), FAIRBAIRN and MACKIE (1972), ZYCZKOWSKI and SKRZYPEK (1972), PENNY and MARIOTT (1971), SETH (1972), BHATNAGAR and ARYA (1974), and HULT (1974).

In this chapter the creep-behavior of an elastic-plastic thick-walled cylinder subjected to a constant internal pressure is investigated. The tube may be partly plastic (region I) and partly elastic (region II) at time zero. Then creep will occur in the regions I and II, while the internal pressure is kept constant.

5.1 Method to discribe the Kinematics

Let the current internal and external radii of the tube be denoted by a and b, and their initial values by a_0 and b_0 (Fig. 5.1). The thick-walled cylinder is subjected by uniformly distributed pressure p_0 at time $t = 0$, so that there is a plastic region (I) and an elastic (II) one. Generally we can say that the tube is double-walled and that the material-behavior is different in the regions I

and II. The radius of the boundary between the two regions is denoted by c (initial value c_0).
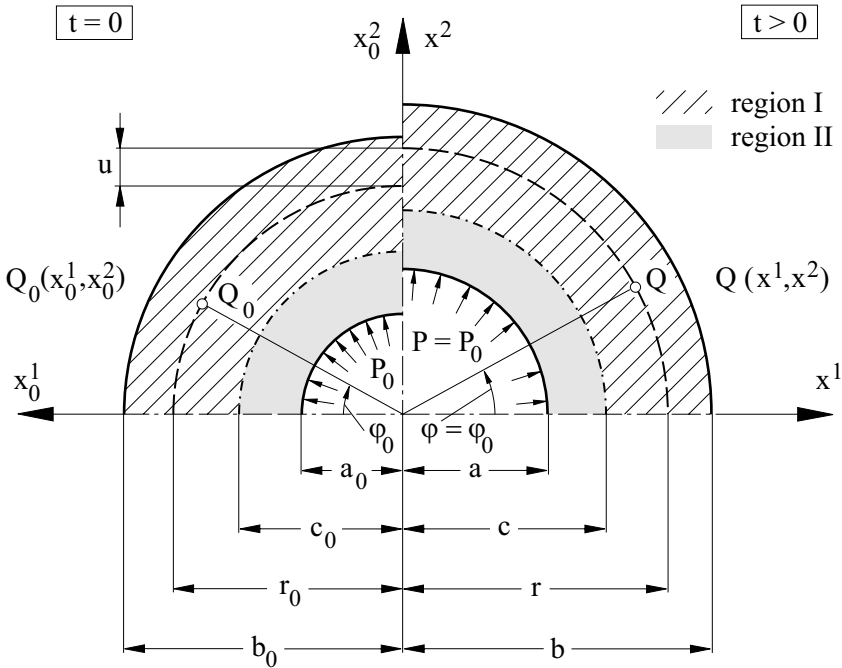
Fig. 5.1 Thick-walled cylindrical tube subjected to internal pressure

If region I is plastic-rigid and region II is elastic at time $t = 0$, the initial value c_0 can be calculated by TURNER's well-known equation (HILL, 1950; TURNER, 1909). Another possibility will be found in this chapter.

As a result of creep by constant internal pressure $p = p_0$, an arbitrary point Q_0 is carried into Q, while the internal radius a_0, the external radius b_0, and the boundary c_0 increase to $a = a(t)$, $b = b(t)$ and $c = c(t)$, respectively. This motion can be described in *body-fixed* or *space-fixed* coordinate systems, e.g. in rectangular cartesian coordinate systems:

$$x^\alpha = x^\alpha(x_0^i, t) \quad \Leftrightarrow \quad x_0^i = x_0^i(x^\alpha, t) \equiv x_0^\alpha \,, \tag{5.1a,b}$$

in which the *material coordinates* are denoted by the kernel letter x_0 and Latin indexes, whereas the *spatial coordinates* are denoted by the kernel letter x and Greek indexes.

The description (5.1b) is a dual form of (5.1a), or vice versa, i.e.: *one form is carried into the other by interchanging the kernel letters and the indexes*. This *principle of duality* (TRUESDELL and TOUPIN, 1960) is often used in this book [1].

To describe the kinematics of circular cylinders it is expedient to use cylindrical polar coordinates instead of (5.1a,b):

$$y^\alpha = y^\alpha(y_0^i, t) \quad \Leftrightarrow \quad y_0^i = y_0^i(y^\alpha, t) \equiv y_0^\alpha \qquad (5.2\text{a,b})$$

with

$$y^\alpha = \{y^1, y^2, y^3\} \equiv \{r, \varphi, z\}, \qquad (5.3\text{a})$$
$$y_0^i = \{y_0^1, y_0^2, y_0^3\} \equiv \{r_0, \varphi_0, z_0\}. \qquad (5.3\text{b})$$

In connection with (5.3a,b), the relation between (5.1a,b) and (5.2a,b) is given by:

$$\left\{ \begin{array}{l} x^1 = y^1 \cos y^2 \equiv r \cos \varphi \\ x^2 = y^1 \sin y^2 \equiv r \sin \varphi \\ x^3 = y^3 \equiv z \end{array} \right\} \Leftrightarrow \left\{ \begin{array}{l} x_0^1 = y_0^1 \cos y_0^2 \equiv r_0 \cos \varphi_0 \\ x_0^2 = y_0^1 \sin y_0^2 \equiv r_0 \sin \varphi_0 \\ x_0^3 = y_0^3 \equiv z_0 \end{array} \right\},$$
$$(5.4\text{a,b})$$

so that the *metric tensors* are:

$$g_{\alpha\beta} = \frac{\partial x^\gamma}{\partial y^\alpha} \frac{\partial x^\gamma}{\partial y^\beta} = \begin{pmatrix} 1 & 0 & 0 \\ 0 & r^2 & 0 \\ 0 & 0 & 1 \end{pmatrix} \Leftrightarrow g_{ij}^0 = \frac{\partial x_0^k}{\partial y_0^i} \frac{\partial x_0^k}{\partial y_0^j} = \begin{pmatrix} 1 & 0 & 0 \\ 0 & r_0^2 & 0 \\ 0 & 0 & 1 \end{pmatrix}.$$
$$(5.5\text{a,b})$$

The fundamental quantities for the analysis of local properties of the deformation are the two sets of the *material deformation gradient* and *spatial deformation gradient* :

$$F_i^\alpha = \frac{\partial x^\alpha}{\partial x_0^i} = \sqrt{\frac{g_{(\alpha\alpha)}}{g_{(ii)}^0}} \frac{\partial y^\alpha}{\partial y_0^i} \quad \Leftrightarrow \quad G_\alpha^i = \frac{\partial x_0^i}{\partial x^\alpha} = \sqrt{\frac{g_{(ii)}^0}{g_{(\alpha\alpha)}}} \frac{\partial y_0^i}{\partial y^\alpha},$$
$$(5.6\text{a,b})$$

where no sum on i and α is carried out. The deformation gradient is a *double tensor* (MICHAL 1927; 1947) of rank two, which maps a line element vector

---

[1] This is similar to the principle of dualtity of the projective geometry and of the determinants theory (REICHARDT, 1968).

ds_0^i of the reference configuration $(t = 0)$ onto the corresponding infinitesimal vector ds^α of the actual or current configuration $(t > 0)$:

$$ds^\alpha = F_i^\alpha \, ds_0^i \quad \Leftrightarrow \quad ds_0^i = G_\alpha^i \, ds^\alpha \, , \tag{5.7a,b}$$

i.e. the deformation gradient maps the neighbourhood of a point x_0 onto the neighbourhood of its image x .

For plane strain deformation

$$\left\{ \begin{array}{l} y^1 \equiv r = r(r_0, \varphi_0) \\ y^2 \equiv \varphi = \varphi(r_0, \varphi_0) \\ y^3 \equiv z = z_0 \end{array} \right\} \quad \Leftrightarrow \quad \left\{ \begin{array}{l} y_0^1 \equiv r_0 = r_0(r, \varphi) \\ y_0^2 \equiv \varphi_0 = \varphi_0(r, \varphi) \\ y_0^3 \equiv z_0 = z \end{array} \right\} \tag{5.8a,b}$$

the matrices of the deformation gradient (5.6a,b) together with (5.5a,b) are given by:

$$F_i^\alpha = \begin{pmatrix} \dfrac{\partial r}{\partial r_0} & \dfrac{1}{r_0}\dfrac{\partial r}{\partial \varphi_0} & 0 \\[2ex] r\dfrac{\partial \varphi}{\partial r_0} & \dfrac{r}{r_0}\dfrac{\partial \varphi}{\partial \varphi_0} & 0 \\[2ex] 0 & 0 & 1 \end{pmatrix} \quad \Leftrightarrow \quad G_\alpha^i = \begin{pmatrix} \dfrac{\partial r_0}{\partial r} & \dfrac{1}{r}\dfrac{\partial r_0}{\partial \varphi} & 0 \\[2ex] r_0\dfrac{\partial \varphi_0}{\partial r} & \dfrac{r_0}{r}\dfrac{\partial \varphi_0}{\partial \varphi} & 0 \\[2ex] 0 & 0 & 1 \end{pmatrix} . \tag{5.9a,b}$$

The special case of cylindrical expansion

$$\left\{ \begin{array}{l} r = r_0 + u(r_0) \\ \varphi = \varphi_0 \, ; \quad z = z_0 \end{array} \right\} \quad \Leftrightarrow \quad \left\{ \begin{array}{l} r_0 = r - u(r) \\ \varphi_0 = \varphi \, ; \quad z_0 = z \end{array} \right\} \tag{5.10a,b}$$

leads to:

$$F_i^\alpha = \begin{pmatrix} 1 + \dfrac{\partial u}{\partial r_0} & 0 & 0 \\[2ex] 0 & 1 + \dfrac{u}{r_0} & 0 \\[2ex] 0 & 0 & 1 \end{pmatrix} \quad \Leftrightarrow \quad G_\alpha^i = \begin{pmatrix} 1 - \dfrac{\partial u}{\partial r} & 0 & 0 \\[2ex] 0 & 1 - \dfrac{u}{r} & 0 \\[2ex] 0 & 0 & 1 \end{pmatrix} . \tag{5.11a,b}$$

In (5.10a,b) and (5.11a,b) u is the displacement in radial direction. As seen in (5.10a,b), if we use the principle of duality, we must notice that

$$\text{dual}\,[u(r_0)] = -u(r) \quad \text{vice versa:} \quad \text{dual}\,[u(r)] = -u(r_0) \, . \tag{5.12a,b}$$

As a suitable measure of deformation the mixed-variant logarithmical tensor [HENCKY*'s strain tensor* (HENCKY, 1925), LUDWIK-*deformations* (LUDWIK, 1909)] is used:

$$\varepsilon^i_j \underset{\text{def}}{=} \frac{1}{2} \ln \left(F^i_\alpha F^\alpha_j \right) \quad \Leftrightarrow \quad \varepsilon^\alpha_\beta \underset{\text{def}}{=} -\frac{1}{2} \ln \left(G^\alpha_i G^i_\beta \right) , \tag{5.13a,b}$$

which can be decomposed into a sum of an isochoric distortion part and a part of volume change (RICHTER, 1949). The definitions (5.13a,b) combined with (5.11a,b) lead to:

$$\varepsilon^i_j = \begin{pmatrix} \ln\left(1 + \dfrac{\partial u}{\partial r_0}\right) & 0 & 0 \\ 0 & \ln\left(1 + \dfrac{u}{r_0}\right) & 0 \\ 0 & 0 & 0 \end{pmatrix}$$

$$\Updownarrow \tag{5.14a,b}$$

$$\varepsilon^\alpha_\beta = - \begin{pmatrix} \ln\left(1 - \dfrac{\partial u}{\partial r}\right) & 0 & 0 \\ 0 & \ln\left(1 - \dfrac{u}{r}\right) & 0 \\ 0 & 0 & 0 \end{pmatrix} \cdot$$

The argument of the logarithmic function in (5.13a) is called the CAUCHY strain tensor (MACVEAN, 1968) or sometimes also the *right* CAUCHY-GREEN *tensor* (BECKER and BÜRGER, 1975; LEIGH, 1968; TRUESDELL, 1977), and the square root of the argument is known as "rechte Streckung" (MACVEAN, 1968), as "Rechts-Streck-Tensor" (BECKER and BÜRGER, 1975) or as *right stretch tensor* (LEIGH, 1968; TRUESDELL, 1977). Often the HENCKY strain tensor (5.13a) is expressed in the form [2]

$$\varepsilon^i_j = \frac{1}{2} \ln \left(g^{ik}_0 g_{kj} \right) , \tag{5.15}$$

in which the *material contravariant metric tensor* g^{ij}_0 at time $t = 0$ is calculated from (5.5b) or given by

$$g^{ij}_0 = \frac{\partial y^i_0}{\partial x^k_0} \frac{\partial y^j_o}{\partial x^k_o} = \begin{pmatrix} 1 & 0 & 0 \\ 0 & 1/r^2_0 & 0 \\ 0 & 0 & 1 \end{pmatrix} \tag{5.16}$$

---

[2] This form is used by LEHMANN (1960; 1962; 1972).

and the *spatial covariant metric tensor* g_{ij} at time $t > 0$ can be determined in connection with (5.5a) by the formula

$$g_{ij} = \frac{\partial y^\alpha}{\partial y_0^i} \frac{\partial y^\beta}{\partial y_0^j} g_{\alpha\beta} = \frac{\partial x^\gamma}{\partial y_0^i} \frac{\partial x^\gamma}{\partial y_0^j} \qquad (5.17a)$$

or combined with (5.4a) and (5.l0a):

$$g_{ij} = \begin{pmatrix} \left(\dfrac{\partial r}{\partial r_0}\right)^2 & 0 & 0 \\ 0 & r^2 & 0 \\ 0 & 0 & 1 \end{pmatrix} = \begin{pmatrix} \left(1 + \dfrac{\partial u}{\partial r_0}\right)^2 & 0 & 0 \\ 0 & (r_0 + u)^2 & 0 \\ 0 & 0 & 1 \end{pmatrix}. \qquad (5.17b)$$

Formula (5.15), combined with the metric tensors (5.16) and (5.17b), results in (5.14a).

5.2 Isochoric Creep Behavior

Creep deformations of metals are from a similar character as pure plastic deformations, i.e. they will usually [3] be uninfluenced if a hydrostatic pressure is superimposed. Therefore, such creep behavior can be treated with methods of the "mathematical theory of plasticity", e.g. the "theory of the *plastic potential*" (HILL, 1950; MISES, 1928) can be used in the mechanics of creep (ODQUIST and HULT, 1962; BETTEN, 1975a).

The *isochoric* deformation is defined by the condition that volumes are unaltered. The change in volume can be expressed by the trace of the *logarithmical strain tensor* (RICHTER, 1949; BETTEN, 2001a). From (5.13a,b) we therefore have the necessary and sufficient local conditions for an isochoric deformation

$$\varepsilon_i^i = \text{tr}\left[\frac{1}{2}\ln\left(F_\alpha^i F_j^\alpha\right)\right] = \ln\left[\det\left(F_i^\alpha\right)\right] \overset{!}{=} 0, \qquad (5.18a)$$

$$\varepsilon_\alpha^\alpha = -\text{tr}\left[\frac{1}{2}\ln\left(G_i^\alpha G_\beta^i\right)\right] = -\ln\left[\det\left(G_\alpha^i\right)\right] \overset{!}{=} 0. \qquad (5.18b)$$

As an alternative to (5.18a), we get from (5.15) combining with the familiar rule for the multiplication of two determinants the incompressibility condition

---

[3] The usual assumption of plastic incompressibility can be considered as a special case (BETTEN, 1975a; 1977).

$$\varepsilon_i^i = \text{tr}\left[\frac{1}{2}\ln\left(g_0^{ik}g_{kj}\right)\right] = \frac{1}{2}\ln\left[\det\left(g_0^{ik}g_{kj}\right)\right] = \frac{1}{2}\ln\left(\frac{g}{g_0}\right) \overset{!}{=} 0 ,$$
(5.19)

in which g represents the determinant of the covariant metric tensor (5.17b), whereas g_0 is the same determinant at time $t = 0$, i.e. we obtain g_0 from (5.17b) or g for $u = 0$.

The conditions (5.18a,b) are equivalent to requiring that the JACOBIan determinants of the transformations (5.1a,b) must have the value one. Hence, combining this with (5.6a,b), the incompressibility can be expressed by:

$$J \equiv \left|\frac{\partial x^\alpha}{\partial x_0^i}\right| = \det\left(F_i^\alpha\right) \overset{!}{=} 1 \quad \Leftrightarrow \quad J^{(-1)} \equiv \left|\frac{\partial x_0^i}{\partial x^\alpha}\right| = \det\left(G_\alpha^i\right) \overset{!}{=} 1 .$$
(5.20a,b)

These requirements, together with (5.11a,b) and (5.12a,b), lead to a differential equation and its dual, respectively, for the displacements $u = u(r_0)$ and $u = u(r)$:

$$\frac{\partial u}{\partial r_0} + \frac{u}{r_0} + \frac{u}{r_0}\frac{\partial u}{\partial r_0} = 0 \quad \Leftrightarrow \quad \frac{\partial u}{\partial r} + \frac{u}{r} - \frac{u}{r}\frac{\partial u}{\partial r} = 0 , \qquad (5.21\text{a,b})$$

which are from the separable type and which are solved by

$$u = u(r_0; t) = \sqrt{r_0^2 + \lambda^2} - r_0 \quad \Leftrightarrow \quad u = u(r; t) = r - \sqrt{r^2 - \kappa^2} .$$
(5.22a,b)

Therefore,

$$r = r_0\sqrt{1 + (\lambda/r_0)^2} \quad \Leftrightarrow \quad r_0 = r\sqrt{1 - (\kappa/r)^2} , \qquad (5.23\text{a,b})$$

after using (5.10a,b).

In (5.22a,b) and (5.23a,b) the time functions $\lambda = \lambda(t)$ and $\kappa = \kappa(t)$ are constants of integration relative to r_0 and r. From (5.22a,b) and (5.23a,b) we see:

$$\lambda(t) \equiv \kappa(t) , \quad \text{dual}\left[\lambda^2(t)\right] = -\lambda^2(t) . \qquad (5.24\text{a,b})$$

From (5.14a,b), combined with (5.22a,b) and (5.24a,b), we find the components of the strain tensor in engineering notation ($\varepsilon_1^1 \equiv \varepsilon_r$; $\varepsilon_2^2 \equiv \varepsilon_\varphi$; $\varepsilon_3^3 \equiv \varepsilon_z = 0$):

$$\varepsilon_\varphi = -\varepsilon_r = \frac{1}{2}\ln\left[1 + (\kappa/r_0)^2\right] \quad \Leftrightarrow \quad \varepsilon_\varphi = -\varepsilon_r = \frac{1}{2}\ln\frac{1}{1 - (\kappa/r)^2} .$$
(5.25a,b)

With these components the *equivalent creep strain*

$$\varepsilon = \sqrt{2\varepsilon_j^i \varepsilon_i^j / 3} \tag{5.26}$$

is determined by

$$\varepsilon = \frac{2}{\sqrt{3}}\varepsilon_\varphi = \frac{1}{\sqrt{3}} \ln\left[1 + \left(\frac{\kappa}{r_0}\right)^2\right] = \frac{1}{\sqrt{3}} \ln \frac{1}{1 - \left(\frac{\kappa}{r}\right)^2} , \tag{5.27}$$

and, using (5.23b), the creep strain-rate $\dot\varepsilon$ is given by

$$\dot\varepsilon = \frac{2}{\sqrt{3}} \frac{\dot\kappa \kappa}{r_0^2 + \kappa^2} = \frac{2}{\sqrt{3}} \frac{\dot\kappa \kappa}{r^2} = \frac{2}{\sqrt{3}} \frac{\dot r}{r} . \tag{5.28}$$

These equations and a creep law $\dot\varepsilon = \dot\varepsilon(\sigma)$ lead to the time functions $a = a(t)$ and $b = b(t)$ for the cylindrical expansion and to the boundary function $c = c(t)$ between regions I and II (Fig. 5.1).

In the following, the power law of NORTON-BAILEY (BAILEY, 1935; NORTON, 1929),

$$\dot\varepsilon = K\sigma^n , \tag{5.29}$$

is assumed, and is used for the regions I and II in Fig. 5.1 with different material constants K_I, n_I and K_{II}, n_{II}, respectively. By considering (5.28) and substituting $r = c$ we thus get:

$$\frac{2}{\sqrt{3}}\frac{\dot c}{c} = \begin{cases} K_I \left[\sigma(c;t)\right]^{n_I} \\ K_{II} \left[\sigma(c;t)\right]^{n_{II}} \end{cases} \tag{5.30}$$

and because of *compatibility*:

$$\frac{2}{\sqrt{3}}\frac{\dot c}{c} = \sqrt{K_I K_{II}} \left[\sigma(c;t)\right]^{(n_I + n_{II})/2} . \tag{5.31}$$

In (5.29) or (5.30) and (5.31), σ or $\sigma(c;t)$ is the equivalent stress, which can be calculated by VON MISES' criteria (MISES, 1928):

$$\sigma = \sqrt{3\sigma_j'^i \sigma_i'^j / 2} , \tag{5.32}$$

where $\sigma_j'^i = \sigma_j^i - \sigma_k^k \delta_j^i / 3$ is the deviatoric, or reduced, stress tensor.

In the case of multi-axial stress, the law (5.29) can be generalized according to the theory of invariants (ODQUIST and HULT, 1962; BETTEN, 1975d) combined with the quadratic *plastic potential* of MISES (1928), which agrees with the second deviatoric invariant J_2':

$$\dot{\varepsilon}^i_j = \frac{3}{2} K (3 J'_2)^{(n-1)/2} \, \sigma'^i_j \; . \tag{5.33}$$

The hypotheses of incompressibility, isotropy, coaxiality, and independence of superimposed hydrostatic pressure is applied in this case, too.

From (5.33) we find that for plane strain ($\dot{\varepsilon}^3_3 \equiv \dot{\varepsilon}_z = 0$) the deviatoric stress component $\sigma'^3_3 \equiv \sigma'_z$ vanishes. Hence

$$\sigma_z = (\sigma_r + \sigma_\varphi) \, / 2 \; , \tag{5.34}$$

and the equivalent stress (5.32) becomes:

$$\sigma = \sqrt{3} \, (\sigma_\varphi - \sigma_r) \, / 2 \; . \tag{5.35}$$

After calculating the circumferential and radial stresses, σ_φ and σ_r, and substituting these expressions in (5.35), we obtain from the differential equation (5.31) by separating the variables c, t and by integrating the boundary $r = c$ between regions I, II as a function of time, $c = c(t)$,

$$\sqrt{K_I K_{II}} \, \sigma_F^{(n_I + n_{II})/2} t = \frac{2}{\sqrt{3}} \int\limits_{c_o}^{c} \left[\frac{\sigma_F}{\sigma(c^*)} \right]^{\frac{n_I + n_{II}}{2}} \frac{dc^*}{c^*} \; . \tag{5.36}$$

The left side in (5.36) is a dimensionless time, in which all material constants are contained. The tensile yield stress σ_F can be considered as an initial value, which is reached at time $t = 0$ on the elastic-plastic boundary $r_0 = c_0$, i.e.: $\sigma_F \equiv \sigma_0(c_0)$.

The calculation of the circumferential and the radial stresses, σ_φ and σ_r in (5.35) is dealt with in the next section.

5.3 Stress Field

For the *thick-walled tube* , loaded as in Fig. 5.1, the derivatives of stresses with respect to the variables z and φ are equal to zero. Thus, the equation of internal equilibrium take the simple form:

$$\sigma_\varphi - \sigma_r = r \, \partial \sigma_r / \partial r \; . \tag{5.37}$$

The left side in (5.37) can be expressed by

$$\sigma_\varphi - \sigma_r = \left(\frac{2}{\sqrt{3}} \right)^{\frac{1+n}{n}} K^{-\frac{1}{n}} \, (\dot{\kappa} \kappa)^{\frac{1}{n}} \, r^{-\frac{2}{n}} \; , \tag{5.38}$$

if the relations (5.28), (5.29) and (5.35) are used. Thus the integration of (5.37) leads to

$$\sigma_r = A(c/r)^{2/n} + B \tag{5.39}$$

with

$$A = A(t) \equiv -\frac{n}{2}\left(\frac{2}{\sqrt{3}}\right)^{\frac{1+n}{2}}\left(\frac{\dot{\kappa}\kappa}{Kc^2}\right)^{\frac{1}{n}} = -\frac{n}{2}\left(\frac{2}{\sqrt{3}}\right)^{\frac{1+n}{2}}\left(\frac{\dot{c}}{Kc}\right)^{\frac{1}{n}} , \tag{5.40}$$

where the relation $\dot{\kappa}\kappa = \dot{c}c$, resulting from (5.23b), is used. On the other hand $A = A(t)$ and also $B = B(t)$ are, in respect of the variable r, constants of integration, which are determined from the boundary conditions. For that purpose we formulate equation (5.39) for the two regions I and II in Fig. 5.1, i.e.

$$\text{region } I: \quad a \le r \le c \quad \text{with} \quad n = n_I ; \quad K = K_I \tag{5.41a}$$
$$\text{region } II: \quad c \le r \le b \quad \text{with} \quad n = n_{II} ; \quad K = K_{II} . \tag{5.41b}$$

Hence,

$$^I\sigma_r = {}^IA(c/r)^{2/n_I} + {}^IB \quad \text{for} \quad r = \langle a, c \rangle , \tag{5.42a}$$
$$^{II}\sigma_r = {}^{II}A(c/r)^{2/n_{II}} + {}^{II}B \quad \text{for} \quad r = \langle c, b \rangle . \tag{5.42b}$$

Therefore, we have to determine four constants of integration. To do this, we can use the two boundary conditions

$$^I\sigma_r(a,t) = -p \equiv -p_0 H(t) , \quad {}^{II}\sigma_r(b,t) = 0 \tag{5.43a,b}$$

(p internal pressure, $H(t)$ HEAVISIDE-*function*) and the two conditions of continuity

$$^I\sigma_r(c,t) = {}^{II}\sigma_r(c,t) , \quad \left[\frac{\partial^I\sigma_r}{\partial r}\right]_{r=c} = \left[\frac{\partial^{II}\sigma_r}{\partial r}\right]_{r=c} . \tag{5.44a,b}$$

Thus

$$^IA = -p\,\frac{n_I}{n_I\left[\left(\frac{c}{a}\right)^{2/n_I} - 1\right] + n_{II}\left[1 - \left(\frac{c}{b}\right)^{2/n_{II}}\right]} , \tag{5.45a}$$

$$^{II}A = (n_{II}/n_I)\,{}^IA , \tag{5.45b}$$

$$^IB = -p - {}^IA(c/a)^{2/n_I} , \quad {}^{II}B = -{}^IA(c/b)^{2/n_{II}} . \tag{5.46a,b}$$

From the equations (5.40) and (5.45a,b), the boundary between regions I and II can be immediately determined as a function of time, $c = c(t)$. For this it is not necessary to calculate the equivalent stress (5.35) from the stress field as formula (5.36) requires.

Inserting the constants of integration (45a,b) and (5.46a,b) into equations (5.42a,b), the final expressions for the radial stresses are then:

$$a \leq r \leq c:$$

$$\frac{{}^I\sigma_r}{p} = -\frac{n_I\left[\left(\frac{c}{r}\right)^{2/n_I} - 1\right] + n_{II}\left[1 - \left(\frac{c}{b}\right)^{2/n_{II}}\right]}{n_I\left[\left(\frac{c}{a}\right)^{2/n_I} - 1\right] + n_{II}\left[1 - \left(\frac{c}{b}\right)^{2/n_{II}}\right]}, \qquad (5.47a)$$

$$c \leq r \leq b:$$

$$\frac{{}^{II}\sigma_r}{p} = -\frac{n_{II}\left[\left(\frac{c}{r}\right)^{2/n_{II}} - \left(\frac{c}{b}\right)^{2/n_{II}}\right]}{n_I\left[\left(\frac{c}{a}\right)^{2/n_I} - 1\right] + n_{II}\left[1 - \left(\frac{c}{b}\right)^{2/n_{II}}\right]}. \qquad (5.47b)$$

With these solutions we immediately obtain the *circumferential stresses* from the equilibrium equation (5.37):

$$a \leq r \leq c:$$

$$\frac{{}^I\sigma_\varphi}{p} = \frac{2\left(\frac{c}{r}\right)^{2/n_I} - n_I\left[\left(\frac{c}{r}\right)^{2/n_I} - 1\right] - n_{II}\left[1 - \left(\frac{c}{b}\right)^{2/n_{II}}\right]}{n_I\left[\left(\frac{c}{a}\right)^{2/n_I} - 1\right] + n_{II}\left[1 - \left(\frac{c}{b}\right)^{2/n_{II}}\right]}, $$

$$(5.48a)$$

$$c \leq r \leq b:$$

$$\frac{{}^{II}\sigma_\varphi}{p} = \frac{2\left(\frac{c}{r}\right)^{2/n_{II}} - n_{II}\left[\left(\frac{c}{r}\right)^{2/n_{II}} - \left(\frac{c}{b}\right)^{2/n_{II}}\right]}{n_I\left[\left(\frac{c}{a}\right)^{2/n_I} - 1\right] + n_{II}\left[1 - \left(\frac{c}{b}\right)^{2/n_{II}}\right]}. \qquad (5.48b)$$

Finally, the *longitudinal stresses* ${}^I\sigma_z$ and ${}^{II}\sigma_z$ can be calculated by placing the solutions (5.47a,b) and (5.48a,b) into equation (5.34).

The radial stresses (5.47a,b) are continuous and have a continuous first derivative in the whole range $r = \langle a, b \rangle$, especially on the boundary $r = c$, whereas the circumferential stresses (5.48a,b) and the longitudinal stresses are indeed continuous everywhere in the tube, but they have not a continuous first derivative at $r = c$. For linear viscoelastic material in region I with $n_I = 1$ or in region II with $n_{II} = 1$ the longitudinal stress $^I\sigma_z$ or $^{II}\sigma_z$ respectively, is independent of the variable radius r in region I or region II.

The fact that the plane strain axial load L agrees with the closed-end force may be shown as follows: using the plane strain condition (5.34), together with the solutions (5.47a,b) and (5.48a,b), we see

$$L = 2\pi \int_a^c {}^I\sigma_z\, r\, dr + 2\pi \int_c^b {}^{II}\sigma_z\, r\, dr = \pi p^2 a^2 \,, \tag{5.49}$$

which is just the closed-end condition. Without needing to use the solutions (5.47a,b) and (5.48a,b), we immediately have the result (5.49) from (5.34) employing the equilibrium equation (5.37):

$$L = 2\pi \int_a^b \sigma_z\, r\, dr = \pi \int_a^b \frac{\partial\left(r^2\sigma_r\right)}{\partial r}\, dr = \pi \left[r^2\sigma_r\right]_a^b \tag{5.50}$$

and the boundary conditions (5.43a,b).

The solutions (5.47a,b) and (5.48a,b) consist of terms like $\pm n \left[x^{2/n} - 1\right]$, which approach $\pm 2 \ln x$ as n approaches infinity:

$$\lim_{n\to\infty} n \left[x^{2/n} - 1\right] = 2 \ln x \,. \tag{5.51}$$

Considering this limit, we find in (5.47a,b) and (5.48a,b) some special cases, which are listed in Table 5.1.

The equivalent stress (5.35) in regions I and II follows from the stress field (5.47a,b)/(5.48a,b):

$$\frac{{}^I\sigma(r,t)}{\sigma(c,t)} = \left(\frac{c}{r}\right)^{2/n_I} \,, \qquad \frac{{}^{II}\sigma(r,t)}{\sigma(c,t)} = \left(\frac{c}{r}\right)^{2/n_{II}} \,. \tag{5.52a,b}$$

In these relations, $\sigma(c,t)$ is the equivalent stress on the boundary $r = c$:

$$\sigma(c,t) = \frac{\sqrt{3}p}{n_I \left[\left(\frac{c}{a}\right)^{2/n_I} - 1\right] + n_{II} \left[1 - \left(\frac{c}{b}\right)^{2/n_{II}}\right]} \,. \tag{5.53}$$

Table 5.1 Some special cases of stress field (5.47a,b)/(5.48a,b)

Special cases	*Behavior*	*Authors*
$c \to a$ or $c \to b$ $n_I = n_{II} = n$	creep with $n_I = n_{II} = n$ creep with $c = a$ or $c = b$	(BAILEY, 1935), (ODQUIST and HULT, 1962)
$n_I = n_{II} = 1$	elastic	(LAMÉ, 1852), (TIMOSHENKO, 1934)
$n_I = n_{II} = n \to \infty$ $n_I \to \infty$ $n_{II} = 1$	plastic-rigid plastic-rigid in region I elastic in region II	(TURNER, 1909), (HILL, 1950), (SZABÓ, 1964)

Considering (5.51), we find the following limits:

$$\lim_{\left\{ {n_I \atop n_{II}} \right\} \to \infty} {}^I\sigma(r,t) = \lim_{\left\{ {n_I \atop n_{II}} \right\} \to \infty} {}^{II}\sigma(r,t) \equiv \sigma_F = \frac{\sqrt{3}\,p_T}{2\ln\dfrac{b}{a}} \tag{5.54}$$

from (5.52a,b) and (5.53) with p_T as the pressure for the fully-plastic tube (*limit pressure*) and

$$\lim_{\left\{ {n_I \atop n_{II}} \right\} \to 1} {}^I\sigma(r,t) = \lim_{\left\{ {n_I \atop n_{II}} \right\} \to 1} {}^{II}\sigma(r,t) \equiv {}^e\sigma = \frac{\sqrt{3}\,p(a/r)^2}{1-(a/b)^2} . \tag{5.55}$$

This equation is true until the elastic equivalent stress ${}^e\sigma$ on the internal radius $r = a$ approaches the yield stress σ_F. The corresponding *yield pressure* p_F is then given by:

$$p_F = \sigma_F \left[1 - (a/b)^2\right]/\sqrt{3} . \tag{5.56}$$

Eventually, the *residual stresses* are obtained (if a possible BAUSCHINGER *effect* is neglected) by subtracting the corresponding elastic stress distribution ($n_I = n_{II} = 1$) from (5.47a,b), (5.48a,b) and (5.34), i.e.:

$$ {}^E\sigma_{r;\varphi;z} \underset{\text{def}}{=} \sigma_{r;\varphi;z}\,(r,t;n_I,n_{II}) - \sigma_{r;\varphi;z}(r,t;1,1) . \tag{5.57}$$

5.4 Expansion and Failure Time

To describe the expansion $a = a(t)$ and $b = b(t)$ of the thick-walled tube as result of creep, we use the solution (5.36) and the equivalent stress (5.53):

$$\tau = \frac{2}{\sqrt{3}} \int\limits_{c_o}^{c} \left\{ n_I \left[\left(\frac{c^*}{a^*}\right)^{2/n_I} - 1 \right] + n_{II} \left[1 - \left(\frac{c^*}{b^*}\right)^{2/n_{II}} \right] \right\}^{\frac{n_I+n_{II}}{2}} \frac{dc^*}{c^*} .$$

$$(5.58)$$

The variables a^* and b^* must be expressed by the integration variable c^* when considering (5.23a,b) as shown later. The integration (5.58) leads to a dimensionless time

$$\tau \underset{\text{def}}{=} \sqrt{K_I K_{II}} \left(\sqrt{3}\, p\right)^{(n_I+n_{II})/2} t , \qquad (5.59)$$

containing the material constants $K_{I;II}$, $n_{I,II}$ and the internal pressure p.

   From the creep law (5.29), which is used in regions I and II (Fig. 5.1) with different material constants K_I, n_I and K_{II}, n_{II} (5.41a,b), respectively, we get the initial creep rate of the boundary c_0 at time $t = 0^+$:

$$\dot\varepsilon_0(c_0) = \frac{\sqrt{K_I K_{II}} \left(\sqrt{3}\, p\right)^{(n_I+n_{II})/2}}{\left\{ n_I \left[\left(\dfrac{c_0}{a_0}\right)^{2/n_I} - 1 \right] + n_{II} \left[1 - \left(\dfrac{c_0}{b_0}\right)^{2/n_{II}} \right] \right\}^{\frac{n_I+n_{II}}{2}}} ,$$

$$(5.60)$$

after using (5.53). Immediately before creep beginning, $t = 0^-$, the relationship between the internal pressure p_0 and the boundary c_0 is thus given by

$$n_{I0} \left[\left(\frac{c_0}{a_0}\right)^{2/n_{I0}} - 1 \right] + n_{II0} \left[1 - \left(\frac{c_0}{b_0}\right)^{2/n_{II0}} \right] = \frac{\sqrt{3}\, p_0}{\sigma_0(c_0)} . \qquad (5.61)$$

For example, from (5.61) we find TURNER's formula (TURNER, 1909) for a cylindrical tube, which is stressed elastic-plastic immediately before the beginning of creep ($n_{I0} \to \infty$, $n_{II0} = 1$)

$$1 - (c_0/b_0)^2 + 2 \ln (c_0/a_0) = \sqrt{3}\, p_0/\sigma_F \qquad (5.62)$$

in using the limits (5.51) and $\sigma_0(c_0) \to \sigma_F$. The relation (5.61) or its special case (5.62) characterizes the initial state of the cylinder (loading state before time-point at which creep begins). Because of (5.51), the relation (5.61) immediately leads to the limit pressure (5.54) for $n_{I0} = n_{II0} \to \infty$ or for $c_0 \to b_0$; $n_{I0} \to \infty$, whereas the yield pressure (5.56) follows from (5.61) when $c = a_0$, $n_{II0} = 1$ is inserted. If $r = a$, $r = b$, $r = c$ successively in (5.23a) or (5.23b) we have the relations

$$a^2 - a_0^2 = c^2 - c_0^2 = b^2 - b_0^2 , \qquad (5.63\text{a,b})$$

which express the *incompressibility*. Then the integral (5.58) combined with (5.59) and (5.60) takes the form

$$\dot{\varepsilon}_0(c_0)t = \frac{2/\sqrt{3}}{[f(\zeta = 1)]^{\frac{n_I + n_{II}}{2}}} \int_\zeta^1 [f(\zeta^*)]^{\frac{n_I + n_{II}}{2}} \frac{d\zeta^*}{\zeta^*} \qquad (5.64)$$

in which

$$\zeta = \zeta(t) \equiv c_0/c \quad \text{with} \quad 0 \leq \zeta \leq 1 \qquad (5.65)$$

is introduced as a dimensionless function of time to describe the expansion of the boundary $c = c(t)$ between regions I and II. Thus, the beginning of creep is characterized by $\zeta = 1$, whereas the failure state is approached as ζ approaches zero, i.e. the creep-failure time is then defined as the time at which the strains reach infinity. The function $f(\zeta)$ in (5.64) is defined as:

$$f(\zeta) = n_I \left\{ \left[\frac{1}{1 - \left[1 - \left(\frac{a_0}{c_0} \right)^2 \right] \zeta^2} \right]^{1/n_I} - 1 \right\}$$
$$+ n_{II} \left\{ 1 - \left[\frac{1}{1 + \left[\left(\frac{b_0}{c_0} \right)^2 - 1 \right] \zeta^2} \right]^{1/n_{II}} \right\} . \qquad (5.66)$$

The solution (5.64) formally agrees e.g. with the analogous solutions of compression creep, of elastic-plastic bending creep and of elastic-plastic torsion creep. The differents are seen in the definition of the variable ζ and in the function $f(\zeta)$, which correspond to the special problem (BETTEN, 1971).

The general solution (5.64) contains RIMROTT's classical solution as a special case for $n_I = n_{II}$ (RIMROTT, 1959). To show this informal transition, the variable $\zeta \equiv c_0/c$ in (5.64) is first expressed by the new introduced variable $\omega \equiv a_0/a$. Hence, from (5.63a),

$$\zeta = (c_0/a_0)\,\omega \left/ \sqrt{1 + \left[(c_0/a_0)^2 - 1 \right] \omega^2} \right. . \qquad (5.67)$$

Therefore, equation (5.64) combined with (5.60) leads to the simplification

$$K\left(\sqrt{3}\,p\right)^n t = \frac{2n^n}{\sqrt{3}} \int\limits_{\omega}^{1} \left[1 - \left(\frac{1}{1 + \left[\left(\frac{b_0}{c_0}\right)^2 - 1\right]\omega^{*2}} \right)^{1/n} \right]^n \frac{d\omega^*}{\omega^*}$$

(5.68)

after inserting $n_I = n_{II} \equiv n$ and $K_I = K_{II} \equiv K$. Substituting

$$x \equiv \left\{ 1 + \left[(b_0/a_0)^2 - 1 \right] \omega^2 \right\}^{-1/n} ,$$

(5.69)

equation (5.68) can be written in the form:

$$\frac{K\left(\sqrt{3}\,p\right)^n}{n^n} t = \frac{n}{\sqrt{3}} \int\limits_{x_1}^{x_2} \frac{(1-x)^n}{1-x^n} \frac{dx}{x} ,$$

(5.70)

where the lower and upper limit of integration are respectively given by

$$x_1 = (a_0/b_0)^{2/n} \quad \text{and} \quad x_2 = \left\{ 1 + \left[(b_0/a_0)^2 - 1 \right] \omega^2 \right\}^{-1/n} .$$

(5.71a,b)

The theoretical failure state is characterized by an infinite expansion $a \to \infty$ i.e. by $\omega \to 0$ or because of (5.71b) by $x_2 \to 1$. From (5.27) and (5.23a,b) we have the equivalent strain $\varepsilon = 2[\ln(r/r_0)]/\sqrt{3}$, which takes the value

$$\varepsilon_a = 2\left[\ln\left(1/\omega\right)\right]/\sqrt{3}$$

(5.72)

on the internal radius $r = a$. Thus, the upper limit of integration (5.71b) becomes:

$$x_2 = \left\{ \frac{(a_0/b_0)^2 \exp\left(\sqrt{3}\,\varepsilon_a\right)}{1 + (a_0/b_0)^2 \left[\exp\left(\sqrt{3}\,\varepsilon_a\right) - 1\right]} \right\}^{1/n}$$

(5.73)

and has the limit one as ε_a approaches infinity at the failure time. The integral (5.70) with the limits of integration (5.71a) and (5.73) is known as RIMROTT's *solution* (RIMROTT, 1959).

5.5 Numerical Computation and Examples

For numerical computation it is expedient to introduce the dimensionless variables

$$\xi \equiv (r-a)/(b-a) , \qquad \eta \equiv (c-a)/(b-a)$$

(5.74a,b)

with:

$$\xi = \begin{cases} \langle 0, \eta \rangle & \stackrel{\wedge}{=} \text{ region } I \ , \\ \langle \eta, 1 \rangle & \stackrel{\wedge}{=} \text{ region } II \ . \end{cases} \tag{5.75}$$

Thus, at every time-point the inner and outer surface of the cylinder are characterized by $\xi = 0$ and $\xi = 1$, respectively, whereas the time function $\eta = \eta(t)$ characterizes the position of the boundary between regions I and II in the range $\xi = \langle 0, 1 \rangle$ at time t.

In all solutions which are numerically represented below, the time dependent quotients c/a, c/b and c/r can be expressed by the variables (5.74a,b):

$$c/a = 1 + (b/a - 1)\eta \ , \tag{5.76a}$$

$$c/b = a/b + (1 - a/b)\eta \ , \tag{5.76b}$$

$$c/r = [1 + (b/a - 1)\eta] \, / \, [1 + (b/a - 1)\xi] \ . \tag{5.76c}$$

The corresponding initial values are given by:

$$c_0/a_0 = 1 + (b_0/a_0 - 1)\eta_0 \ , \tag{5.77a}$$

$$c_0/b_0 = a_0/b_0 + (1 - a_0/b_0)\eta_0 \ . \tag{5.77b}$$

In these the parameter b_0/a_0 characterizes the initial geometry of the cylinder and, combining (5.77a,b) with (5.62), the value $\eta_0 \equiv (c_0 - a_0)/(b_0 - a_0)$ can be interpreted as a measure of the loading state immediately before the onset of creep (Fig. 5.2).
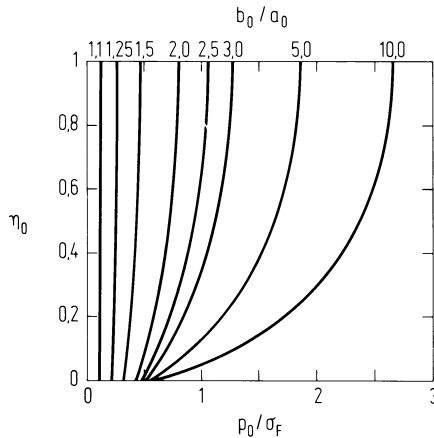
Fig. 5.2 The loading state immediately before creep beginning using (5.62) and 5.77a,b)

In (5.76a,b,c) we must insert the quotient b/a as a function of time. To do this we first express the time functions $a = a(t)$ and $b = b(t)$ as functions of $\zeta \equiv c_0/c$

$$a_0/a = (a_0/c_0)\zeta \Big/ \{1 - [1 - (a_0/c_0)^2]\,\zeta^2\}^{1/2} \ , \tag{5.78a}$$

$$b_0/b = (b_0/c_0)\zeta \Big/ \{1 + [(b_0/c_0)^2 - 1]\,\zeta^2\}^{1/2} \ , \tag{5.78b}$$

in using (5.63a,b) and find:

$$b/a = \{1 + [(b_0/c_0)^2 - 1]\,\zeta^2\}^{1/2} \Big/ \{1 - [1 - (a_0/c_0)^2]\,\zeta^2\}^{1/2} \ . \tag{5.79}$$

Inserting (5.79) and (5.78a) in (5.74b), we have a relation between η and ζ:

$$\eta = \frac{1 - \left\{1 - \left[1 - \left(\dfrac{a_0}{c_0}\right)^2\right]\zeta^2\right\}^{1/2}}{\left\{1 + \left[\left(\dfrac{b_0}{c_0}\right)^2 - 1\right]\zeta^2\right\}^{1/2} - \left\{1 - \left[1 - \left(\dfrac{a_0}{c_0}\right)^2\right]\zeta^2\right\}^{1/2}} \tag{5.80}$$

with the limits

$$\lim_{\zeta \to 1} \eta = \frac{c_0 - a_0}{b_0 - a_0} \equiv \eta_0 \tag{5.81a}$$

and

$$\lim_{\zeta \to 0} \eta = \frac{c_0^2 - a_0^2}{b_0^2 - a_0^2} = \frac{2 + (b_0/a_0 - 1)\eta_0}{1 + b_0/a_0}\eta_0 \ , \tag{5.81b}$$

which are approached at the beginning of creep and in the state of failure, respectively (Fig. 5.3).

Because of (5.79) and (5.80), the quotients (5.76a,b,c) can be expressed by ζ, too. Therefore, the time influence, e.g. on the stress field (5.47a,b), (5.48a,b), can be measured by the time function $\zeta = \zeta(t)$. This function is obtained from (5.64) by numerical integration. If the cylinder is elastic-plastic stressed at time zero, the function $\zeta = \zeta(t)$ is calculated from (5.64) together with (5.60), (5.62) and (5.66), i.e. from:

$$\kappa\,\sigma_F^\nu\,t = \frac{2/\sqrt{3}}{\left[1 - \left(\dfrac{c_0}{b_0}\right)^2 + 2\ln\dfrac{c_0}{a_0}\right]^\nu} \int_\zeta^1 [f(\zeta^*)]^\nu \frac{d\zeta^*}{\zeta^*} \ . \tag{5.82}$$
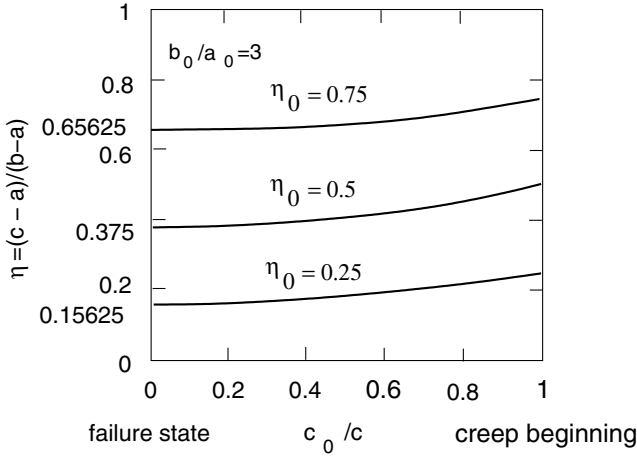
Fig. 5.3 The position of the boundary between regions I and II using equation (5.80)

In equation (5.82) the parameter $\kappa \equiv \sqrt{K_I\,K_{II}}$ is the *geometrical mean value* from the material constants K_I, K_{II}, while $\nu \equiv (n_I + n_{II})/2$ represents the *arithmetical mean value* from the exponents n_I, n_{II}.

The integral in (5.82) is numerically evaluated for a sufficient number of ζ-values in the range $\zeta = \langle 0, 1 \rangle$ by the subroutine ROMINT, which uses ROMBERG's method of numerical integration (ENGELN-MÜLLGES and REUTER, 1993). The integration with $\zeta = 0$ immediately leads to the value t_{cr}, which is called the *failure time*.

ROMBERG's *integration method* is a very suitable one, if digital computers are used (ENGELN-MÜLLGES and REUTER, 1993).

Some results of the mentioned numerical evaluation of the integral in (5.82) are represented in Fig. 5.4.

In addition to Fig. 5.4, the cylindrical expansion $a = a(t)$, $b = b(t)$ is shown in Fig. 5.5.

We clearly see the influence of the initial loading state expressed by the parameter η_0 taken from Fig. 5.2. As expected, greater η_0-values lead to shorter failure times t_{cr}, which can be seen from Fig. 5.4 on the time axis. In Table 5.2 more parameter sets are listed.

From (5.82), the numerical evaluation of the stress distributions (5.47a,b), (5.48a,b) and of the equivalent stresses (5.52a,b), combined with (5.76a,b,c), (5.79), and (5.80), is based on the time function $\zeta = \zeta(t)$, i.e., the time influence can be considered by the time parameter $\zeta = \langle 0, 1 \rangle$, which can be taken from Fig. 5.4.

Table 5.2 Creep-failure time $t_{cr} = \lim t(\zeta)$ calculated from (5.82)

n	$\{n_I, n_{II}\}$	$\sqrt{K_1 K_{11}}\sigma_F^{(n_1 + n_{11}/2)} t_{cr}$				
		$\eta_0 = 0$	$\eta_0 = 0.25$	$\eta_0 = 0.5$	$\eta_0 = 0.75$	$\eta_0 = 1$
$n_I > n_{II} = 1$	$\{2,1\}$	1.150	0.546	0.404	0.342	0.313
	$\{4,1\}$	0.837	0.326	0.225	0.182	0.156
	$\{6,1\}$	0.684	0.229	0.154	0.122	0.104
	$\{8,1\}$	0.571	0.172	0.116	0.091	0.077
	$\{10,1\}$	0.058	0.142	0.093	0.072	0.061
$n_I > n_{II} > 1$	$\{4,3\}$	3.140	0.467	0.219	0.153	0.135
	$\{6,3\}$	4.520	0.439	0.173	0.110	0.091
	$\{8,3\}$	6.717	0.437	0.148	0.087	0.069
	$\{10,3\}$	10.230	0.451	0.132	0.072	0.056
	$\{6,4\}$	7.725	0.512	0.175	0.105	0.088
	$\{8,4\}$	12.578	0.535	0.153	0.084	0.067
	$\{10,4\}$	21.012	0.577	0.139	0.070	0.054
	$\{8,6\}$	35.130	0.734	0.161	0.080	0.064
	$\{10,6\}$	64.560	0.830	0.150	0.067	0.051
	$\{10,8\}$	170.600	1.136	0.160	0.066	0.050
$n_I = n_{II}$	$\{2,2\}$	1.680	0.546	0.352	0.292	0.275
	$\{4,4\}$	4.895	0.516	0.215	0.146	0.131
	$\{6,6\}$	19.450	0.664	0.179	0.100	0.085
	$\{8,8\}$	87.868	0.973	0.170	0.078	0.063
	$\{10,10\}$	425.292	1.525	0.172	0.066	0.050
$n_I = 1 < n_{II}$	$\{1,2\}$	1.674	0.697	0.536	0.520	0.567
	$\{1,4\}$	2.721	0.674	0.534	0.649	0.960
	$\{1,6\}$	5.002	0.781	0.677	1.084	2.227
	$\{1,8\}$	9.846	0.995	0.974	2.077	5.904
	$\{1,10\}$	20.222	1.344	1.500	4.277	16.905
$1 < n_I < n_{II}$	$\{3,4\}$	3.940	0.532	0.250	0.185	0.176
	$\{3,6\}$	8.370	0.625	0.249	0.184	0.189
	$\{3,8\}$	17.870	0.762	0.264	0.195	0.217
	$\{3,10\}$	38.690	0.958	0.290	0.217	0.262
	$\{4,6\}$	11.010	0.625	0.214	0.151	0.132
	$\{4,8\}$	24.400	0.776	0.224	0.144	0.141
	$\{4,10\}$	53.740	0.980	0.240	0.150	0.156
	$\{6,8\}$	45.750	0.851	0.187	0.099	0.086
	$\{6,10\}$	106.010	1.099	0.190	0.0996	0.089
	$\{8,10\}$	211.221	1.270	0.180	0.078	0.063
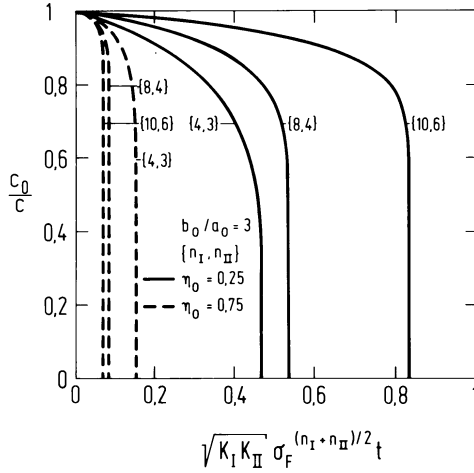
Fig. 5.4 The boundary between regions I and II as function of time
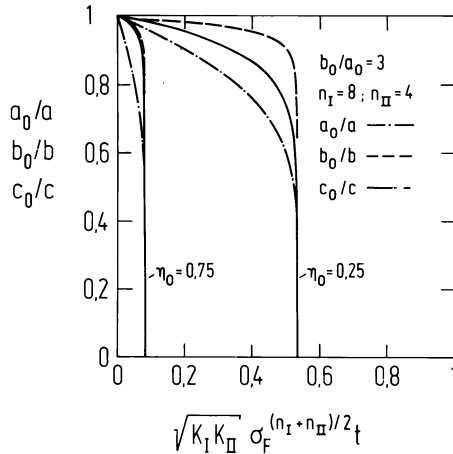
Fig. 5.5 Cylindrical expansion

In the equations (5.47a,b), (5.48a,b) the internal pressure $p \equiv p_0$ is chosen as a reference value. Because of its relation to η_0, according to (5.62) and (5.77a,b) or Fig. 5.2, it is more advisable to choose a material constant, e.g. the yield stress σ_F, as reference value. Thus, from (5.62), we have the conversion relation:

$$\frac{^{I;II}\sigma_{r;\varphi}}{\sigma_F} = \frac{Z}{\sqrt{3}} \frac{^{I;II}\sigma_{r;\varphi}}{p} \quad \text{with} \quad Z \underset{\text{def}}{=} 1 - \left(\frac{c_0}{b_0}\right)^2 + 2\ln\frac{c_0}{a_0} , \qquad (5.83)$$

which is used to represent the stress distribution (Fig. 5.6).
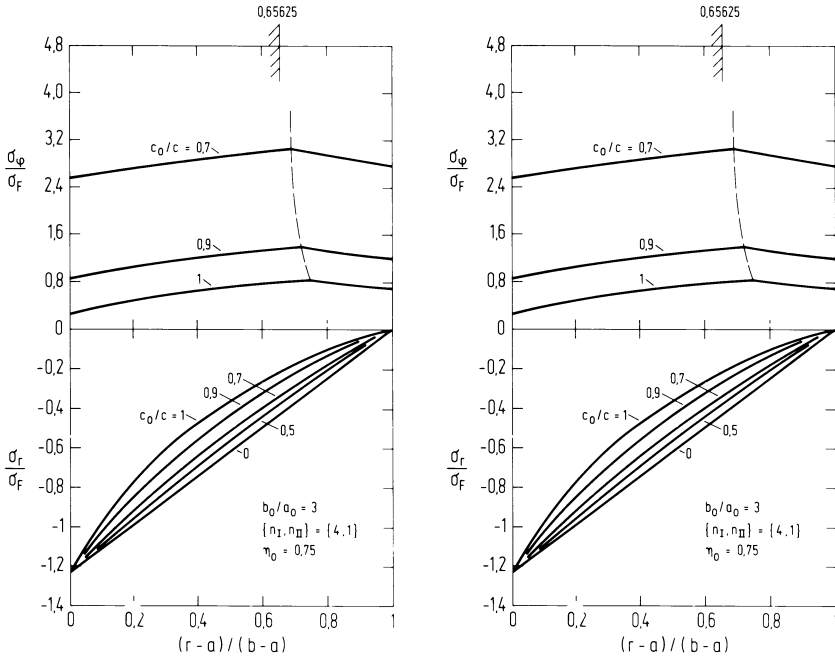
Fig. 5.6 Stress distributions from (5.83) combined with (5.47a,b), (5.48a,b), (5.74a,b), (5.74a,b), (5.77a,b) and (5.79) with $\{n_I, n_{II}\} = \{4, 1\}$

The absolute stress values increase if the time parameter $\zeta \equiv c_0/c$ decreases, i.e. because of Fig. 5.4, if the time t increases, while the boundary $\xi = \eta$ takes the position which is characterized by $\eta < \eta_0$ (Fig. 5.3) and which approaches the limit position (5.81) at the *failure time* ($\zeta \to 0$), e.g. the limit 0,65625 if $\eta_0 = 0,75$. This fact is indicated in Fig. 5.6 by a broken curve.

Similarly to the numerical evaluation of the *stress distributions* (5.83), the *equivalent stresses* $^I\sigma$ and $^{II}\sigma$ may be calculated, i.e., from (5.52a,b) together with (5.53) and (5.62), we find the formulae:

$$^I\sigma/\sigma_F = (Z/N)(c/r)^{2/n_I} , \qquad ^{II}\sigma/\sigma_F = (Z/N)(c/r)^{2/n_{II}} , \qquad (5.84a,b)$$

in which the numerator Z is defined in (5.83) while the denominator N is given by:

$$N \underset{\text{def}}{=} n_I \left[(c/a)^{2/n_I} - 1 \right] + n_{II} \left[1 - (c/b)^{2/n_{II}} \right] \ .$$ (5.85)

Some numerical examples to equations (5.84a,b) are shown in Fig. 5.7.
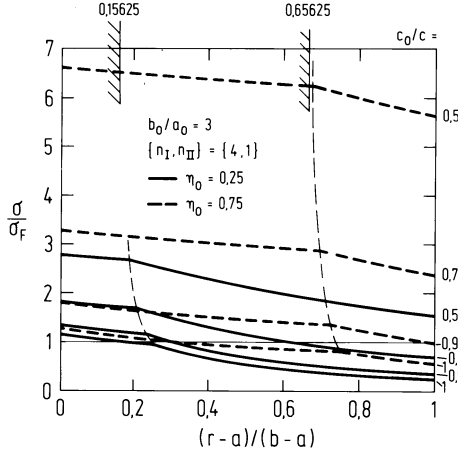
Fig. 5.7 Equivalent stresses from (5.84a,b) with $\{n_I, n_{II}\} = \{4, 1\}$

If the set $\{n_I, n_{II}\}$ approaches $\{\infty, 1\}$ at time zero ($\zeta = 1$), the denominator (5.85) in (5.84a,b) approaches the numerator Z, so that the equivalent stresses (5.84a,b) agree with the yield stress σ_F on the boundary $r = c$.

Finally, the equivalent strain-rate $\dot{\varepsilon}$ is obtained from (5.29), (5.41a,b), (5.52a,b), (5.53) and (5.60),

$$\frac{\dot{\varepsilon}(r,t)}{\dot{\varepsilon}_0(c_0)} = \left\{ \frac{n_I \left[\left(\dfrac{c_0}{a_o} \right)^{2/n_I} - 1 \right] + n_{II} \left[1 - \left(\dfrac{c_0}{b_o} \right)^{2/n_{II}} \right]}{n_I \left[\left(\dfrac{c}{a} \right)^{2/n_I} - 1 \right] + n_{II} \left[1 - \left(\dfrac{c}{b} \right)^{2/n_{II}} \right]} \right\}^{\frac{n_I + n_{II}}{2}} \left(\frac{c}{r} \right)^2 ,$$

(5.86)

which is continuous and continuously differentiable. For numerical evaluation of equation (5.86), the formulae (5.76a,b,c), (5.77a,b), (5.79) and (5.80) are used. The results are represented in Fig. 5.8.
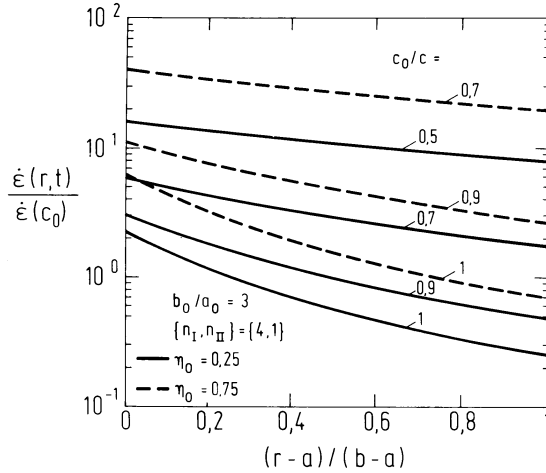
Fig. 5.8 Equivalent strain-rates from (5.86) with $\{n_I, n_{II}\} = \{4, 1\}$

Similarly, the strain-rates $\dot{\varepsilon}_r$ and $\dot{\varepsilon}_\varphi$ can be numerically evaluated:

$$\dot{\varepsilon}_r/\dot{\varepsilon}_r(c_0, 0) = \dot{\varepsilon}_\varphi/\dot{\varepsilon}_\varphi(c_0, 0) = \dot{\varepsilon}(r, t)/\dot{\varepsilon}_0(c_0) . \qquad (5.87)$$

In this chapter a long thick-walled circular cylindrical tube subjected to internal pressure is considered. The tube is partly plastic (region I) and partly elastic (region II) at time zero. Then creep occurs in both regions while the internal pressure is constant.

To describe the creep behavior, NORTON-BAILEY's power law is adopted, and is used in the regions I and II with different creep exponents n_I and n_{II}, respectively.

The investigation is based upon the usual assumptions of incompressibility and zero axial creep. The creep deformations are considered to be of such magnitude that the use of *finite-strain theory* is necessary. Therefore, we use HENCKY's *strain tensor* .

The inner and outer radius, the position of the boundary between regions I and II, the stress distributions as functions of time and the *creep-failure* time are calculated.

In addition to the numerical computation and examples discussed in this chapter, a lot of further numerical calculations have been carried out by BETTEN (1980; 1982c).

6 The Creep Potential Hypothesis in Comparison with the Tensor Function Theory

In this chapter the *creep potential hypothesis* is compared with the *tensor function theory* . It will be shown that the former theory is compatible with the latter, if the material is isotropic, and if additional conditions are fulfilled.

However, for *anisotropic materials* the creep potential hypothesis only furnishes restricted forms of constitutive equations, even if a general plastic potential has been assumed (BETTEN, 1985). Consequently, the *classical normality rule* $d_{ij} = \dot{\Lambda}\, \partial F / \partial \sigma_{ij}$ according to (4.14a) must be modified for anisotropic solids. In the following, appropiate modifications are discussed and resulting conditions of "*compatibility*" are derived.

6.1 Isotropy

For isotropic materials the *creep potential* $F = F(\sigma_{ij})$ can be expressed as a single-valued function $F = F[S_\nu(\boldsymbol{\sigma})]$ of the irreducible invariants $S_\nu \equiv \operatorname{tr}\boldsymbol{\sigma}^\nu$, $\nu = 1, 2, 3$, of the stress tensor. Thus, considering the form $F = F(S_1, S_2, S_3)$ and using the classical flow rule (4.14a), one immediately obtains the constitutive equation

$$d_{ij} = \dot{\Lambda} \left[\left(\frac{\partial F}{\partial S_1} \right) \delta_{ij} + 2 \left(\frac{\partial F}{\partial S_2} \right) \sigma_{ij} + 3 \left(\frac{\partial F}{\partial S_3} \right) \sigma_{ij}^{(2)} \right] . \qquad (6.1)$$

Instead of (6.1), one can represent the *rate of deformation tensor* d_{ij} as a symmetric tensor-valued function of one second-order argument tensor:

$$d_{ij} = f_{ij}(\boldsymbol{\sigma}) = \varphi_0 \delta_{ij} + \varphi_1 \sigma_{ij} + \varphi_2 \sigma_{ij}^{(2)} , \qquad (6.2)$$

where φ_0, φ_1, φ_2 are scalar-valued functions of the *integrity basis*, the elements of which are the irreducible invariants S_1, S_2, S_3.

Comparing the "*minimum polynomial representation*" (6.2) with the result (6.1) based upon the creep potential hypothesis, one can find the following identities:

$$\varphi_0 \equiv \dot{\Lambda}\frac{\partial F}{\partial S_1} \,, \qquad \varphi_1 \equiv 2\dot{\Lambda}\frac{\partial F}{\partial S_2} \,, \qquad \varphi_2 \equiv 3\dot{\Lambda}\frac{\partial F}{\partial S_3} \,. \qquad (6.3)$$

By eliminating the creep potential F in (6.3) we can find additional restrictions imposed on the scalar functions φ_0, φ_1, φ_2, if the existence of a creep potential is assumed:

$$2\frac{\partial \varphi_0}{\partial S_2} = \frac{\partial \varphi_1}{\partial S_1} \,, \qquad 3\frac{\partial \varphi_0}{\partial S_3} = \frac{\partial \varphi_2}{\partial S_1} \,, \qquad 3\frac{\partial \varphi_1}{\partial S_3} = 2\frac{\partial \varphi_2}{\partial S_2} \,. \qquad (6.4)$$

Thus, in the isotropic special case the creep potential hypothesis is compatible with the tensor function theory, if the conditions of "*compatibility*" in (6.4) have been fulfilled.

For example, the requirements in (6.4) can be satisfied, if one assumes:

$$\varphi_0 = \varphi_0(S_1) \,, \qquad \varphi_1 = \varphi_1(S_2) \,, \qquad \varphi_2 = \varphi_2(S_3) \,. \qquad (6.5)$$

Then, because of (6.3), the *creep potential* can be represented as

$$F = F(S_1, S_2, S_3) = g_1(S_1) + g_2(S_2) + g_3(S_3) \,, \qquad (6.6)$$

where g_1, g_2 and g_3 are arbitrary functions of the invariants S_1, S_2, and S_3, respectively.

The conditions of "*compatibility*" in (6.4) can be found in the following way. The identities (6.3) can be written in the form

$$\frac{\partial F}{\partial S_1} \equiv \varphi_0 L \,, \qquad \frac{\partial F}{\partial S_2} \equiv \varphi_1 L/2 \,, \qquad \frac{\partial F}{\partial S_3} \equiv \varphi_2 L/3 \,, \qquad (6.7)$$

where

$$L \equiv 1/d\Lambda = L(S_1, S_2, S_3) \qquad (6.8)$$

is normally a scalar-valued function of the integrity basis. The creep potential F in (6.7) can be eliminated, if we consider the $\binom{3}{2}$ equalities

$$\frac{\partial^2 F}{\partial S_1\,\partial S_2} = \frac{\partial^2 F}{\partial S_2\,\partial S_1} \,, \quad \frac{\partial^2 F}{\partial S_1\,\partial S_3} = \frac{\partial^2 F}{\partial S_3\,\partial S_1} \,, \quad \frac{\partial^2 F}{\partial S_2\,\partial S_3} = \frac{\partial^2 F}{\partial S_3\,\partial S_2} \,,$$
$$(6.9)$$

i.e., assuming the second partial derivatives of the creep potential to be continuous. Hence, from (6.7) and (6.9) we find a system of linear equations in the partial derivatives $\partial L/\partial S_\lambda \equiv L_{,\lambda}$ with $\lambda = 1, 2, 3$:

$$\left.\begin{aligned} \varphi_1 L_{,1} - 2\varphi_0 L_{,2} + 0 &= [2(\varphi_0)_{,2} - (\varphi_1)_{,1}]\,L \\ \varphi_2 L_{,1} + 0 \quad - 3\varphi_0 L_{,3} &= [3(\varphi_0)_{,3} - (\varphi_2)_{,1}]\,L \\ 0 + 2\varphi_2 L_{,2} - 3\varphi_1 L_{,3} &= [3(\varphi_1)_{,3} - 2(\varphi_2)_{,2}]\,L \,. \end{aligned}\right\} \qquad (6.10)$$

On the right hand side in (6.10) the abbreviations $(\varphi_0)_{,2} \equiv \partial\varphi_0/\partial S_2, \ldots,$ $(\varphi_2)_{,2} \equiv \partial\varphi_2/\partial S_2$ are used. Because the coefficient determinant in (6.10) vanishes,

$$
\begin{vmatrix}
\varphi_1 & -2\varphi_0 & 0 \\
\varphi_2 & 0 & -3\varphi_0 \\
0 & 2\varphi_2 & -3\varphi_1
\end{vmatrix} = 0 ,
\tag{6.11}
$$

one can assume that the right hand side of the system (6.10) is also equal to zero. It is possible to find the three conditions of "*compatibility*" in (6.4) . Note that these conditions are only sufficient. But if we use CRAMER*'s rule*, we find the following sufficient and necessary condition

$$
\boxed{\left(3\frac{\partial\varphi_1}{\partial S_3} - 2\frac{\partial\varphi_2}{\partial S_2}\right)\varphi_0 + \left(\frac{\partial\varphi_2}{\partial S_1} - 3\frac{\partial\varphi_0}{\partial S_3}\right)\varphi_1 + \left(2\frac{\partial\varphi_0}{\partial S_2} - 2\frac{\partial\varphi_1}{\partial S_1}\right)\varphi_2 = 0} ,
$$
$$\tag{6.12}$$

which contains (6.4) as a special case. As has already been mentioned before, the conditions in (6.4) are only sufficient, whereas similar conditions in elasticity are both sufficient and necessary (BETTEN, 2001c).

For more complicated examples than the above mentioned the creep potential hypothesis is not compatible with the tensor function theory. For instance, MURAKAMI and SAWCZUK (1979) found that for the model of prestrained plastic solids the flow theory of classical plasticity only furnishes restricted forms of constitutive equations. LEHMANN (1972) proposed an extended form of the classical flow rule (4.14a) with respect to experimental results and based upon thermodynamical considerations. BETTEN (1985) considered oriented solids and discussed an appropiate modification of the *classical flow rule*.

6.2 Oriented Solids

In order to describe yielding and failure of oriented solids BOEHLER and SAWCZUK (1976; 1977) use the tensor generator $\boldsymbol{A} = \boldsymbol{v} \otimes \boldsymbol{v}$, where the vector $\boldsymbol{v}$ specifies a *privileged direction*. The constitutive equation can then be represented by the *minimum polynomial*

$$
d_{ij} = f_{ij}(\sigma_{pq}, A_{pq}) = \frac{1}{2}\sum_{\lambda,\nu=0}^{2} \varphi_{[\lambda,\nu]}\left(M_{ij}^{[\lambda,\nu]} + M_{ji}^{[\lambda,\nu]}\right) ,
\tag{6.13}
$$

where $[\lambda, \nu]$ several symmetric *tensor generators* are formed by matrix products of the forms

$$M_{ij}^{[\lambda,\nu]} \equiv \sigma_{ik}^{(\lambda)} A_{kj}^{(\nu)}, \quad \lambda, \nu = 0, 1, 2 . \tag{6.14}$$

The $\varphi_{[\lambda,\nu]}$'s in (6.13) are nine scalar functions of the *integrity basis*, the elements of which can be found by forming all the irreducible traces of the matrix products (6.14) according to:

$$M_{rr}^{[\lambda,\nu]} \equiv \sigma_{pq}^{(\lambda)} A_{qp}^{(\nu)}, \quad \text{with} \quad \left\{ \begin{array}{l} \lambda, \nu = 1, 2 \\ \lambda = 0 \Rightarrow \nu = 1, 2, 3 \\ \nu = 0 \Rightarrow \lambda = 1, 2, 3, \end{array} \right\} \tag{6.15a}$$

which can be written as:

$$\begin{array}{l} S_\lambda \equiv \operatorname{tr} \boldsymbol{\sigma}^\lambda , \quad T_\nu \equiv \operatorname{tr} \boldsymbol{A}^\nu ; \quad \lambda, \nu = 1, 2, 3 ; \\ \Omega_1 \equiv \operatorname{tr} \boldsymbol{\sigma} \boldsymbol{A} , \quad \Omega_2 \equiv \operatorname{tr} \boldsymbol{\sigma} \boldsymbol{A}^2 , \quad \Omega_3 \equiv \operatorname{tr} \boldsymbol{A} \boldsymbol{\sigma}^2 , \quad \Omega_4 \equiv \operatorname{tr} \boldsymbol{\sigma}^2 \boldsymbol{A}^2 . \end{array} \tag{6.15b}$$

¿From the ten invariants in (6.15a,b) only the seven stress-dependent invariants are essential for the creep potential:

$$F = F\left(M_{rr}^{[\lambda,\nu]}\right) , \quad \text{with} \quad \left\{ \begin{array}{l} \lambda, \nu = 1, 2 \\ \nu = 0 \Rightarrow \lambda = 1, 2, 3 . \end{array} \right\} \tag{6.16}$$

Thus, by using the *normality rule* (4.14a), one can find the constitutive equation

$$\begin{array}{l} d_{ij} = \dot{\Lambda} \sum_{\lambda,\nu} \left(\partial F \big/ \partial M_{rr}^{[\lambda,\nu]}\right) Q_{ijpq}^{[\lambda]} A_{qp}^{[\nu]} \\ \text{with} \quad \left\{ \begin{array}{l} \lambda, \nu = 1, 2 \\ \nu = 0 \Rightarrow \lambda = 1, 2, 3 . \end{array} \right\} \end{array} \tag{6.17}$$

In (6.17) the λ several fourth-rank tensors $\boldsymbol{Q}^{[\lambda]}$ are defined as

$$Q_{pqij}^{[\lambda]} \equiv \partial \sigma_{pq}^{(\lambda)} \big/ \partial \sigma_{ij} = \frac{1}{2} \sum_{\alpha=0}^{\lambda-1} \left[\sigma_{pi}^{(\alpha)} \sigma_{qj}^{(\lambda-1-\alpha)} + \sigma_{pj}^{(\alpha)} \sigma_{qi}^{(\lambda-1-\alpha)} \right] \tag{6.18}$$

and have the following properties of symmetry:

$$Q_{pqij}^{[\lambda]} = Q_{qpij}^{[\lambda]} = Q_{pqji}^{[\lambda]} = Q_{ijpq}^{[\lambda]} . \tag{6.19}$$

One can see that, because of (6.18), the value λ cannot be equal to zero. Therefore, only the seven stress-dependent invariants of the integrity basis

(6.15a,b) are relevant for the creep potential (6.16). Furthermore, by comparing the constitutive equations (6.13) and (6.17), one can see that the *minimum polynomial* (6.13) consists of nine *tensor generators*, whereas (6.17) has only seven terms, i.e., *the creep potential theory* furnishes only restricted forms of constitutive equations, even if a general creep potential is assumed in an *anisotropic* case.

It may be more useful for practical applications to represent the constitutive equation (6.13) in a *canonical form*

$$
d_{ij} = {}^{0}H_{ijkl}\delta_{kl} + {}^{1}H_{ijkl}\sigma_{kl} + {}^{2}H_{ijkl}\sigma_{kl}^{(2)} \, , \tag{6.20}
$$

where the fourth-order tensor-valued functions ${}^{0}\boldsymbol{H}$, ${}^{1}\boldsymbol{H}$, and ${}^{2}\boldsymbol{H}$ are defined in the following way:

$$
{}^{0}H_{ijkl} \equiv \varphi_{[0,0]}m_{ijkl}^{(0)} + \varphi_{[0,1]}m_{ijkl} + \varphi_{[0,2]}m_{ijkl}^{[2]} \tag{6.21a}
$$

$$
{}^{1}H_{ijkl} \equiv \varphi_{[1,0]}m_{ijkl}^{(0)} + \varphi_{[1,1]}m_{ijkl} + \varphi_{[1,2]}m_{ijkl}^{[2]} \tag{6.21b}
$$

$$
{}^{2}H_{ijkl} \equiv \varphi_{[2,0]}m_{ijkl}^{(0)} + \varphi_{[2,1]}m_{ijkl} + \varphi_{[2,2]}m_{ijkl}^{[2]} \tag{6.21c}
$$

having the symmetric tensors $\boldsymbol{m}^{[\nu]}$, $\nu = 0, 1, 2$, of rank four:

$$
m_{ijkl}^{[\nu]} \equiv \frac{1}{4}\left(A_{ik}^{(\nu)}\delta_{jl} + A_{il}^{(\nu)}\delta_{jk} + \delta_{ik}A_{jl}^{(\nu)} + \delta_{il}A_{jk}^{(\nu)}\right) \, . \tag{6.22}
$$

Especially, for $\nu = 0$ one finds in (6.22) the zero power tensor of rank four:

$$
m_{ijkl}^{[0]} \equiv m_{ijkl}^{(0)} \equiv m_{ijpq}m_{pqkl}^{(-1)} = \frac{1}{2}\left(\delta_{ik}\delta_{jl} + \delta_{il}\delta_{jk}\right) = m_{ijpq}^{(-1)}m_{pqkl} \, . \tag{6.23}
$$

The representation found in the *canonical form* (6.20) consists of three terms, which are the contributions of zero, first, and second-orders in the stress tensor $\boldsymbol{\sigma}$, influenced by the functions ${}^{0}\boldsymbol{H}$, ${}^{1}\boldsymbol{H}$, and ${}^{2}\boldsymbol{H}$, respectively. In finding these fourth-order tensor-valued functions, the identities

$$
\left\{\frac{1}{2}\left(\boldsymbol{X}^{\lambda}\boldsymbol{Y}^{\nu} + \boldsymbol{Y}^{\nu}\boldsymbol{X}^{\lambda}\right)\right\}_{ij} \equiv \eta_{ijkl}^{[\nu]}X_{kl}^{(\lambda)} \equiv \xi_{ijkl}^{[\lambda]}Y_{kl}^{(\nu)} \, ,
$$

$$
\xi_{ijkl}^{[\lambda]} \equiv \frac{1}{4}\left(X_{ik}^{(\lambda)}\delta_{jl} + X_{il}^{(\lambda)}\delta_{jk} + \delta_{ik}X_{jl}^{(\lambda)} + \delta_{il}X_{jk}^{(\lambda)}\right) \, ,
$$

$$
\eta_{ijkl}^{[\nu]} \equiv \frac{1}{4}\left(Y_{ik}^{(\nu)}\delta_{jl} + Y_{il}^{(\nu)}\delta_{jk} + \delta_{ik}Y_{jl}^{(\nu)} + \delta_{il}Y_{jk}^{(\nu)}\right)
$$

have been used (BETTEN, 1982b; 1985) where $\boldsymbol{X}$ and $\boldsymbol{Y}$ are two symmetric second-order tensors. Similar identities for non-symmetric tensors were introduced by BETTEN (1982b).

In the *isotropic* special case the coefficient tensors ${}^0\boldsymbol{H}, \ldots, {}^2\boldsymbol{H}$ in (6.20) can be expressed as fourth-order spherical tensors:

$$ {}^\lambda H_{ijkl} = \frac{1}{2} \left(\delta_{ik}\delta_{jl} + \delta_{il}\delta_{jk} \right) \varphi_\lambda , \quad \lambda = 0, 1, 2 . $$

In that case, the *canonical form* (6.20) simplifies to the *standard form* (6.2).
Remark: It may be impossible to find a canonical form (6.20) for all types of anisotropy. However, for the most important kinds of anisotropy, namely, *transversely isotropic* and *orthotropic behavior*, the constitutive equation can be expressed in the *canonical form* (6.20) as has been illustrated by BETTEN (1982b; 1983b; 1998), for instance.

Similarly to (6.20), one can represent the constitutive equation (6.17), derived from the *creep potential hypothesis*, in a *canonical form*:

$$ d_{ij} = {}^0h_{ijkl}\delta_{kl} + {}^1h_{ijkl}\sigma_{kl} + {}^2h_{ijkl}\sigma_{kl}^{(2)} , \tag{6.24} $$

where the fourth-order tensor-valued functions ${}^0\boldsymbol{h}$, ${}^1\boldsymbol{h}$ and ${}^2\boldsymbol{h}$ are defined by using (6.22) in the following way:

$$ {}^0h_{ijkl} \equiv \dot{\Lambda} \left(\frac{\partial F}{\partial S_1} m_{ijkl}^{(0)} + \frac{\partial F}{\partial \Omega_1} m_{ijkl} + \frac{\partial F}{\partial \Omega_2} m_{ijkl}^{[2]} \right) , \tag{6.25a} $$

$$ {}^1h_{ijkl} \equiv 2\dot{\Lambda} \left(\frac{\partial F}{\partial S_2} m_{ijkl}^{(0)} + \frac{\partial F}{\partial \Omega_3} m_{ijkl} + \frac{\partial F}{\partial \Omega_4} m_{ijkl}^{[2]} \right) , \tag{6.25b} $$

$$ {}^2h_{ijkl} \equiv 3\dot{\Lambda} \left(\frac{\partial F}{\partial S_3} m_{ijkl}^{(0)} + \quad \mathbf{0} \quad + \quad \mathbf{0} \quad \right) . \tag{6.25c} $$

Without loss of generality in the case of incipient motion, the vector $\boldsymbol{v}$ can be regarded as a unit vector in the reference configuration. Therefore, only $\nu = 0, 1$ in (6.14) has to be taken into account. The number of tensor generators in the constitutive equation (6.13) is reduced from nine to six, i.e., the fourth-order tensor-valued functions (6.22a,b,c) can be simplified into:

$$ {}^0H_{ijkl} \equiv \varphi_{[0,0]} m_{ijkl}^{(0)} + \varphi_{[0,1]} m_{ijkl} , \tag{6.26a} $$

$$ {}^1H_{ijkl} \equiv \varphi_{[1,0]} m_{ijkl}^{(0)} + \varphi_{[1,1]} m_{ijkl} , \tag{6.26b} $$

$$ {}^2H_{ijkl} \equiv \varphi_{[2,0]} m_{ijkl}^{(0)} + \varphi_{[2,1]} m_{ijkl} . \tag{6.26c} $$

Furthermore, the number of irreducible invariants (6.15a,b) is reduced from ten to five,

$$S_\lambda \equiv \operatorname{tr} \boldsymbol{\sigma}^\lambda \,, \quad \lambda = 1, 2, 3 \,, \quad \Omega_1 \equiv \operatorname{tr} \boldsymbol{\sigma A} \,, \quad \Omega_3 \equiv \operatorname{tr} \boldsymbol{A \sigma}^2 \,, \quad (6.27)$$

if we regard the vector $\boldsymbol{v}$ as a unit vector.

The fourth-order tensor-valued functions (6.25a,b,c), resulting from the *creep potential hypothesis*, can be simplified into:

$$^0 h_{ijkl} \equiv \dot\Lambda \left(\frac{\partial F}{\partial S_1} m_{ijkl}^{(0)} + \frac{\partial F}{\partial \Omega_1} m_{ijkl} \right) \,, \tag{6.28a}$$

$$^1 h_{ijkl} \equiv 2\dot\Lambda \left(\frac{\partial F}{\partial S_2} m_{ijkl}^{(0)} + \frac{\partial F}{\partial \Omega_3} m_{ijkl} \right) \,, \tag{6.28b}$$

$$^2 h_{ijkl} \equiv 3\dot\Lambda \left(\frac{\partial F}{\partial S_3} m_{ijkl}^{(0)} + \quad \mathbf{0} \quad \right) \,. \tag{6.28c}$$

Comparing the fourth-rank tensors (6.26a,b,c) with the corresponding tensors (6.22a,b,c) or, alternatively, (6.29a,b,c) with (6.27a,b,c), one can see that the scalar functions $\varphi_{[2,1]}$ and $\varphi_{[2,2]}$ in (6.21c) or $\varphi_{[2,1]}$ in (6.26c) cannot be expressed through the creep potential (6.16), i.e., in the anisotropic case the creep potential hypothesis with its classical flow rule (4.14a) only furnishes restricted forms of constitutive equations even where a general creep potential $F = F(\sigma_{ij}, A_{ij})$ is assumed. Furthermore, if one considers the functions (6.26a,b,c) or alternatively (6.29a,b,c) one can see that any terms containing m_{ijkl} and $m_{ijkl}^{[2]}$ do not appear in (6.25c) or in (6.28c), i.e. the *second-order effect* in (6.24), characterized through (6.25c) or (6.28c), is not influenced by the anisotropy (6.22) of the material. Consequently, the normality rule (4.14a) of the classical flow theory of creep should be modified in the *anisotropic* case.

The results mentioned above can also be applied to *perforated materials* or *damaged materials*, if the anisotropy tensor A_{ij} in (6.22) is substituted with a *perforation tensor* (LITEWKA and SAWCZUK, 1981) or a *damage tensor* (BETTEN, 1982b; 1983b).

6.3 Modification of the Normality Rule

By taking the representation theory into account we can justify the following expansion of the flow rule (4.14a):

$$d_{ij} = \dot{\Lambda}\left(\frac{\partial F}{\partial \sigma_{ij}} + \alpha\, m_{ijkl}\frac{\partial F}{\partial A_{kl}}\right).$$

(6.29)

Assuming that the *creep potential* $F = F(\sigma_{ij}, A_{ij})$ is a scalar-valued function of the *integrity basis* (6.15a,b) and by using the *modified flow rule* (6.29), we can find a constitutive equation which is *compatible* with the representation theory of tensor functions (6.13), (6.20), (6.21a,b,c), i.e., all nine scalar-valued functions $\varphi_{[\lambda,\nu]}$, $\lambda, \nu = 0, 1, 2$, in (6.13) or (6.21a,b,c) can be expressed through the *creep potential F*:

$$\varphi_{[0,0]} \equiv \dot{\Lambda}\left(\frac{\partial F}{\partial S_1} + 3\alpha K_2\frac{\partial F}{\partial T_3}\right),$$

(6.30a)

$$\varphi_{[0,1]} \equiv \dot{\Lambda}\left(\frac{\partial F}{\partial \Omega_1} + \alpha\frac{\partial F}{\partial T_1} + 3\alpha K_2\frac{\partial F}{\partial T_3}\right),$$

(6.30b)

$$\varphi_{[0,2]} \equiv \dot{\Lambda}\left(\frac{\partial F}{\partial \Omega_2} + 2\alpha\frac{\partial F}{\partial T_2} + 3\alpha K_1\frac{\partial F}{\partial T_3}\right),$$

(6.30c)

. . . .

$$\varphi_{[1,0]} \equiv 2\dot{\Lambda}\frac{\partial F}{\partial S_2}$$

(6.30d)

$$\varphi_{[1,1]} \equiv \dot{\Lambda}\left[\frac{\partial F}{\partial \Omega_3} + (\alpha/2)\frac{\partial F}{\partial \Omega_1}\right],$$

(6.30e)

$$\varphi_{[1,2]} \equiv \dot{\Lambda}\left(\frac{\partial F}{\partial \Omega_4} + \alpha\frac{\partial F}{\partial \Omega_2}\right),$$

(6.30f)

. . . .

$$\varphi_{[2,0]} \equiv 3\dot{\Lambda}\frac{\partial F}{\partial S_3},$$

(6.30g)

$$\varphi_{[2,1]} \equiv (\alpha/2)\dot{\Lambda}\frac{\partial F}{\partial \Omega_3},$$

(6.30h)

$$\varphi_{[2,2]} \equiv \alpha\dot{\Lambda}\frac{\partial F}{\partial \Omega_4},$$

(6.30i)

where the abbreviations

$$K_1 \equiv T_1, \quad K_2 \equiv \frac{1}{2}\left(T_2 - T_1^2\right), \quad K_3 \equiv \frac{1}{6}\left(T_1^3 - 3T_1T_2 + 2T_3\right)$$

(6.31a,b,c)

have been used. In this way the *second-order effect* in (6.24) is influenced through the material tensor A because of $\alpha \neq 0$ found in (6.30h,i). This

influence is not at all possible if we use the tensor-valued function (6.25c) which results from the normality rule (4.14a) which does not contain the parameter α. Thus, *the creep potential hypothesis is compatible with the tensor function theory, if the modified flow rule (6.29) is used instead of (4.14a)*. But among the scalar functions (6.30a, ..., i) we can find additional relationships ("*conditions of compatibility*") by eliminating the plastic potential F. This can be done by closely adhering to the following procedure. First, one must find the partial derivatives $\partial F/\partial S_1$, ..., $\partial F/\partial \Omega_4$ of the creep potential F from the system of linear equations (6.30a, ..., i). Second, one must apply the $\binom{10}{2}$ equalities

$$\frac{\partial^2 F}{\partial S_1 \, \partial S_2} = \frac{\partial^2 F}{\partial S_2 \, \partial S_1} \ , \quad \cdots, \quad \frac{\partial^2 F}{\partial \Omega_3 \, \partial \Omega_4} = \frac{\partial^2 F}{\partial \Omega_4 \, \partial \Omega_3} \tag{6.32}$$

to every pair of the above mentioned ten derivatives. In this way we have eliminated the creep potential F and found 45 *conditions of compatibility* .

If the vector v is regarded as a unit vector, then it is possible to find the following identities by first taking (6.26a,b,c), (6.27) into consideration and by then using the *modified flow rule* (6.29):

$$\varphi_{[0,0]} \equiv \dot{\Lambda}\frac{\partial F}{\partial S_1} \ , \qquad \varphi_{[0,1]} \equiv \dot{\Lambda}\frac{\partial F}{\partial \Omega_1} \ , \tag{6.33a,b}$$

$$\varphi_{[1,0]} \equiv 2\dot{\Lambda}\frac{\partial F}{\partial S_2} \ , \qquad \varphi_{[1,1]} \equiv 4\frac{\varphi_{[2,1]}}{\alpha} + \alpha\varphi_{[0,1]} \ , \tag{6.33c,d}$$

$$\varphi_{[2,0]} \equiv 3\dot{\Lambda}\frac{\partial F}{\partial S_3} \ , \qquad \varphi_{[2,1]} \equiv \frac{\alpha}{2}\dot{\Lambda}\frac{\partial F}{\partial \Omega_3} \ . \tag{6.33e,f}$$

The results of (6.33a, ..., f) can be used to find the partial derivatives of the plastic potential:

$$\left.\begin{array}{lll} \dfrac{\partial F}{\partial S_1} \equiv \varphi_{[0,0]}L \ , & \dfrac{\partial F}{\partial S_2} \equiv \varphi_{[1,0]}\dfrac{L}{2} \ , & \dfrac{\partial F}{\partial S_3} \equiv \varphi_{[2,0]}\dfrac{L}{3} \ , \\[3mm] \dfrac{\partial F}{\partial \Omega_1} \equiv \varphi_{[0,1]}L \ , & \dfrac{\partial F}{\partial \Omega_3} \equiv 2\varphi_{[2,1]}\dfrac{L}{\alpha} \ . & \end{array}\right\} \tag{6.34}$$

In (6.34)

$$L \equiv 1/d\Lambda = L(S_1, S_2, S_3, \Omega_1, \Omega_3) \tag{6.35}$$

is a scalar-valued function of the integrity basis (6.27). The reader may note the analogy between (6.35) and (6.8). The creep potential F in (6.34) can be eliminated by regarding every pair of the derivatives (6.34), and by using the $\binom{5}{2}$ equalities

$$\frac{\partial^2 F}{\partial S_1 \, \partial S_2} = \frac{\partial^2 F}{\partial S_2 \, \partial S_1} \, , \quad \cdots , \quad \frac{\partial^2 F}{\partial \Omega_1 \, \partial \Omega_3} = \frac{\partial^2 F}{\partial \Omega_3 \, \partial \Omega_1} \, . \tag{6.36}$$

Then we will find, similar to (6.10), a system of ten linear equations in the partial derivatives

$$\left. \begin{array}{ll} L_{,1} \equiv \dfrac{\partial L}{\partial S_1} \, , & L_{,2} \equiv \dfrac{\partial L}{\partial S_2} \, , \qquad L_{,3} \equiv \dfrac{\partial L}{\partial S_3} \, , \\[2ex] L_{,4} \equiv \dfrac{\partial L}{\partial \Omega_1} \, , & L_{,5} \equiv \dfrac{\partial L}{\partial \Omega_3} \end{array} \right\} \tag{6.37}$$

and, using a procedure described by BETTEN (1985), a complete set of ten *sufficient and necessary "conditions of compatibility"* is obtained. In the isotropic special case these ten conditions are reduced to only one equation, which is identical to (6.12).

Finally, the special case of *incompressibility* should be considered. In such instances it is more practical to use the stress deviator $\boldsymbol{\sigma}'$ in the *integrity basis* (6.15a,b) than to use the stress tensor $\boldsymbol{\sigma}$. Furthermore, the *modified flow rule*

$$\boxed{d_{ij} = \dot{\Lambda} \left(\frac{\partial F}{\partial \sigma_{ij}} + \alpha \, m_{\{ij\}kl} \frac{\partial F}{\partial A_{kl}} \right)} \tag{6.38}$$

should be used instead of (6.29), where the *fourth-order tensor*

$$m_{\{ij\}kl} \equiv m_{ijkl} - \frac{1}{3} m_{rrkl} \delta_{ij} = m_{ijkl} - \frac{1}{3} \delta_{ij} A_{kl} \tag{6.39}$$

is *deviatoric* with respect to the free indices $\{ij\}$.

6.4 Anisotropy expressed through a Fourth-Rank Tensor

A more general case than that in (6.13) is described by BETTEN (2001c) by using a *material tensor of rank four* with index symmetries according to

$$A_{ijkl} = A_{jikl} = A_{ijlk} = A_{klij} \, . \tag{6.40}$$

Then, the creep condition (section 4.2) has the form

$$f\left(\sigma_{ij}, \, A_{ijkl} \right) = 1 \, , \tag{6.41}$$

which can be expressed as a single-valued function of the integrity basis, the elements of which are the irreducible invariants. Together with the invariants

of the single argument tensors, the set of *simultaneous* or *joint invariants* forms the *integrity basis*. The theory of invariants for several argument tensors of rank two has been developed, for instance, by RIVLIN (1970) and SPENCER (1971; 1987). Integrity bases for tensors of an order higher than two are discussed by BETTEN (1982a; 1987a; 1998).

To formulate a *creep criterion* (6.41), it is not necessary to consider the complete set of irreducible invariants. In finding the "essential invariants" we first formulate the *constitutive equation*

$$d_{ij} = f_{ij}\left(\sigma_{pq}, A_{pqrs}\right) , \qquad (6.42)$$

which is a symmetric ($f_{ij} = f_{ji}$) tensor-valued tensor function of two argument tensors. This function has to fulfill the *condition of form invariance*

$$a_{ik}a_{j\ell}f_{k\ell}\left(\sigma_{pq}, A_{pqrs}\right) \equiv f_{ij}\left(a_{pt}a_{qu}\sigma_{tu},\, a_{pt}a_{qu}a_{rv}a_{sw}A_{tuvw}\right) \qquad (6.43)$$

under the transformations of the orthogonal group ($a_{ik}a_{jk} = \delta_{ij}$).

6.4.1 Irreducible Sets of Tensor Generators and Invariants

A suitable form of the constitutive equation (6.42) is given by a linear combination

$$d_{ij} = \sum_{\lambda,\mu,\nu} \Phi_{[\lambda,\mu,\nu]} G_{ij}^{[\lambda,\mu,\nu]} \qquad (6.44)$$

of several symmetric *tensor generators*

$$G_{ij}^{[\lambda,\mu,\nu]} = \left(M_{ij}^{[\lambda,\mu,\nu]} + M_{ji}^{[\lambda,\mu,\nu]}\right)\Big/ 2 \qquad (6.45)$$

formed by matrix products of the forms

$$M_{ij}^{[\lambda,\mu,\nu]} \equiv \sigma_{ik}^{(\lambda)} A_{kjpq}^{(\mu)} \sigma_{pq}^{(\nu)} , \qquad (6.46)$$

which fulfill the condition of form invariance (6.43). Note that in (6.46) those values of λ, μ, ν that are enclosed by parentheses are exponents, whereas a square bracket gives any set λ, μ, ν the character of a label to indicate several matrix products.

In finding an irreducible set of tensor generators, we note that, according to the HAMILTON-CAYLEY *theorem*, none of the exponents λ, μ of the second-order tensor $\boldsymbol{\sigma}$ needs to be larger than two. In generalizing the HAMILTON-CAYLEY *theorem*, we find (BETTEN, 1982a; 1987a; 1988a) that a symmetric fourth-order tensor of power six and all higher powers can be

expressed in terms of lower powers, that is $\mu \leq 5$. For $\mu = 0$, we must notice that the combinations $[\lambda, 0, \nu]$ are symmetric with respect to λ, ν, and that the restriction $\lambda + \nu \leq 2$ follows. Thus we have **48** irreducible matrix products of the form (6.46), which are listed in Table 6.1 (BETTEN, 1982a; 1987a; 1988a).

Table 6.1 Matrix products (6.46)

$\mu = 0;$ $M_{ij}^{[\lambda,0,\nu]}$ with $\lambda + \nu \leq 2$		
λ	$\nu = 0$	$\nu = 1$	$\nu = 2$
0	δ_{ij}	σ_{ij}	$\sigma_{ij}^{(2)}$
1	σ_{ij}	$\sigma_{ij}^{(2)}$	
2	$\sigma_{ij}^{(2)}$		

$\mu = 1, 2, \ldots, 5;$ $M_{ij}^{[\lambda,\mu,\nu]}$		
λ	$\nu = 0$	$\nu = 1$	$\nu = 2$
0	$A_{ijrr}^{(\mu)}$	$A_{ijpq}^{(\mu)}\sigma_{pq}$	$A_{ijpq}^{(\mu)}\sigma_{pq}^{(2)}$
1	$\sigma_{ik}A_{kjrr}^{(\mu)}$	$\sigma_{ik}A_{kjpq}^{(\mu)}\sigma_{pq}^{(2)}$	$\sigma_{ik}A_{kjpq}^{(\mu)}\sigma_{pq}^{(2)}$
2	$\sigma_{ik}^{(2)}A_{kjrr}^{(\mu)}$	$\sigma_{ik}^{(2)}A_{kjpq}^{(\mu)}\sigma_{pq}$	$\sigma_{ik}^{(2)}A_{kjpq}^{(\mu)}\sigma_{pq}^{(2)}$

The coefficients $\Phi_{[\lambda,\mu,\nu]}$ in (6.44) are scalar-valued functions of the *integrity basis* associated with the representation given in (6.44). In finding this integrity basis, we notice the theorem which says that the trace of any product formed from matrices and their transposes is a polynomial invariant under the full or proper orthogonal group. Thus we form the following traces:

$$\sigma_{ji}d_{ij} = \sum_{\lambda,\mu,\nu} \Phi_{[\lambda,\mu,\nu]}\sigma_{ji}G_{ij}^{[\lambda,\mu,\nu]} \tag{6.47}$$

and

$$d_{ij}A_{jirs}\sigma_{rs} = \sum_{\lambda,\mu,\nu} \Phi_{[\lambda,\mu,\nu]}G_{ij}^{[\lambda,\mu,\nu]}A_{jirs}\sigma_{rs} , \tag{6.48}$$

from which we read the following systems of invariants:

$$\mathcal{A}_{[\lambda,\mu,\nu]} \equiv \sigma_{ij}^{(\lambda+1)}A_{jik\ell}^{(\mu)}\sigma_{\ell k}^{(\nu)} \tag{6.49}$$

and

$$\mathcal{B}_{[\lambda,\mu,\nu]} \equiv \sigma_{ij}^{(\lambda)} A_{jrk\ell}^{(\mu)} A_{rimn} \sigma_{\ell k}^{(\nu)} \sigma_{nm} , \tag{6.50}$$

respectively, if we consider the abbreviations (6.45) and (6.46). The 28 irreducible elements of the system (6.49) are listed in Table 6.2 and discussed by BETTEN, (1987c; 1988a; 2001c).

Table 6.2 Irreducible invariants of the system (6.49)

$\sigma_{ij} M_{ij}^{[\lambda,0,\nu]} = \sigma_{kk}^{(\lambda+\nu+1)}$	where	$\lambda + \nu \leq 2$	
λ	$\nu = 0$	$\nu = 1$	$\nu = 2$
0	$S_1 \equiv \mathrm{tr}\,\boldsymbol{\sigma}$	$S_2 \equiv \mathrm{tr}\,\boldsymbol{\sigma}^2$	$S_3 \equiv \mathrm{tr}\,\boldsymbol{\sigma}^3$
1	S_2	S_3	
2	S_3		
$\sigma_{ij} M_{ij}^{[\lambda,\mu,\nu]} = \sigma_{ij}^{(\lambda+1)} A_{ijk\ell}^{(\mu)} \sigma_{\ell k}^{(\nu)};$		$\mu = 1, 2, \ldots, 5$	
λ	$\nu = 0$	$\nu = 1$	$\nu = 2$
0	$\sigma_{ij} A_{ijk\ell}^{(\mu)}$	$\sigma_{ij} A_{ijk\ell}^{(\mu)} \sigma_{k\ell}$	$\sigma_{ij} A_{ijk\ell}^{(\mu)} \sigma_{k\ell}^{(2)}$
1	$\sigma_{ij}^{(2)} A_{ijk\ell}^{(\mu)}$	$\nearrow$	$\sigma_{ij}^{(2)} A_{ijk\ell}^{(\mu)} \sigma_{k\ell}^{(2)}$

Since (6.47) represents the *rate of dissipation of creep energy* of creep energy, the invariants of Table 6.2 are most important. Thus we use them to formulate the *creep conditions*

$$f\left(\sigma_{ij}^{(\lambda+1)} A_{jik\ell}^{(\mu)} \sigma_{\ell k}^{(\nu)}\right) = 1 , \tag{6.51}$$

where $\lambda = 0, 1$ and $\nu = 0, 1, 2$ for $\mu = 1, 2, \ldots, 5$. For $\mu = 0$, we have the isotropic special case with

$$A_{ijk\ell}^{(0)} = (\delta_{ik}\delta_{j\ell} + \delta_{i\ell}\delta_{jk})/2 . \tag{6.52}$$

Then the restriction $\lambda + \nu \leq 2$ must be noted (Table 6.2).

6.4.2 Special Formulations of Constitutive Equations and Creep Criteria

The special case of *transverse isotropy* is contained in (6.51). This case can be specified by a symmetric tensor of rank two, A_{ij}, as pointed out in detail

by BOEHLER and SAWCZUK (1977) or by BETTEN (1988a). We can also describe the creep behavior of such a material by using a fourth-rank tensor specified by

$$A_{ijk\ell} \equiv (A_{ik}A_{j\ell} + A_{i\ell}A_{jk})/2 \;, \tag{6.53}$$

which has the symmetry properties (6.40). Then we find the tensor power

$$A_{ijk\ell}^{(\mu)} = \left(A_{ik}^{(\mu)}A_{j\ell}^{(\mu)} + A_{i\ell}^{(\mu)}A_{jk}^{(\mu)}\right)\Big/ 2 \;. \tag{6.54}$$

Inserting this relation in (6.46), we immediately find the constitutive equation (6.13)from (6.44) and (6.45), if we select reducible elements like $\boldsymbol{\sigma}\boldsymbol{A}\boldsymbol{\sigma}$ or $\boldsymbol{A}\boldsymbol{\sigma}\boldsymbol{A}$ or $\boldsymbol{A}\boldsymbol{\sigma}^2\boldsymbol{A}$. Furthermore, substituting the special tensor (6.53) in (6.49) and (6.51), we find the *integrity basis* (6.15a,b) after omitting redundant elements. The tensor $\boldsymbol{A}$ in (6.15a,b) is a second-order tensor.

To describe the *creep-strength-differential effect* it is convenient to substitute the difference tensor

$$\overline{\sigma}_{ij} = \sigma_{ij} - B_{ij} \tag{6.55}$$

for the stress tensor $\boldsymbol{\sigma}$ in all the above equations. Then, for instance, the simultaneous invariant $\mathcal{A}_{[0,1,1]}$ from Table 6.2 takes the form

$$\mathcal{A}_{[0,1,1]} = A_{ijk\ell}\left(\sigma_{ij} - B_{ij}\right)\left(\sigma_{k\ell} - B_{k\ell}\right) \tag{6.56}$$

and a creep criterion containing this invariant only may be expressed in the simplest relation

$$A_{ijk\ell}\left(\sigma_{ij} - B_{ij}\right)\left(\sigma_{k\ell} - B_{k\ell}\right) = 1 \;. \tag{6.57}$$

In the isotropic special case characterized by

$$A_{ijk\ell} = a_1\delta_{ij}\delta_{k\ell} + a_2\left(\delta_{ik}\delta_{j\ell} + \delta_{i\ell}\delta_{jk}\right) \;,$$

and $B_{ij} = b\delta_{ij}$, the criterion in (6.57) reduces to the form

$$J_2' + c_1 J_1^2 + c_2 J_1 = c_3 \;, \tag{6.58}$$

where the constants c_1, c_2, and c_3 can be determined by experimental data (BETTEN, 1982d).

Furthermore, substituting $c_1 = -\alpha^2$, $c_2 = 2\alpha\beta$, and $c_3 = \beta$ from (6.58) we recover the well-known DRUCKER-PRAGER criterion

$$\sqrt{J_2'} + \alpha J_1 = \beta \;, \tag{6.59}$$

where the parameters α and β are determined by experimental data:

$$\alpha = \frac{1}{\sqrt{3}} \frac{\sigma_c^* - \sigma_c}{\sigma_c^* + \sigma_c} , \tag{6.60}$$

$$\beta = \frac{2}{\sqrt{3}} \frac{\sigma_c^* \sigma_c}{\sigma_c^* + \sigma_c} . \tag{6.61}$$

The symbols σ_c and σ_c^* characterize the *limiting creep stresses* (Fig 4.2) in *tension* and *compression*, respectively. Thus the parameter in (6.60) expresses the *creep-strength differential* or *C-S-D effect*.

6.4.3 Incompressibility and Volume Change

The constitutive equation (6.44) can be expressed in the form

$$d_{ij} = \sum_{\lambda,\mu,\nu} \Phi_{[\lambda,\mu,\nu]} A_{ijpqrs}^{[\mu]} \sigma_{pq}^{(\nu)} \sigma_{rs}^{(\lambda)} \tag{6.62}$$

by introducing several tensors $\boldsymbol{A}^{[\mu]}$ of rank six, the components of which can be determined from the given fourth-order tensor (6.40):

$$A_{ijpqrs}^{[\mu]} \equiv \frac{1}{4} \left(A_{irpq}^{(\mu)} \delta_{js} + A_{ispq}^{(\mu)} \delta_{jr} + \delta_{is} A_{jspq}^{(\mu)} + \delta_{is} A_{jrpq}^{(\mu)} \right) . \tag{6.63}$$

These tensors have the symmetry conditions

$$A_{ijpqrs}^{[\mu]} = A_{jipqrs}^{[\mu]} = A_{ijqprs}^{[\mu]} = A_{ijpqsr}^{[\mu]} \tag{6.64a}$$

and

$$A_{ijpqrs}^{[\mu]} = A_{rspqij}^{[\mu]} . \tag{6.64b}$$

Further symmetry conditions are not valid because the form of (6.62) is not symmetric with respect to λ and ν, except for $\mu = 0$, i.e., for the isotropic special case given by (6.52).

In order to study the magnitude of *volume change* or an *incompressible* deformation, it is convenient to decompose (6.62) into two functions, a *scalar* one and a *deviatoric* one:

$$d_{rr} = \sum_{\lambda,\mu,\nu} \Phi_{[\lambda,\mu,\nu]} \sigma_{ij}^{(\lambda)} A_{ijk\ell}^{(\mu)} \sigma_{k\ell}^{(\nu)} , \tag{6.65a}$$

$$d_{ij}' = \sum_{\lambda,\mu,\nu} \Phi_{[\lambda,\mu,\nu]} A_{\{ij\}pqrs}^{[\mu]} \sigma_{pq}^{(\nu)} \sigma_{rs}^{(\lambda)} , \tag{6.65b}$$

where the tensors

$$A^{[\mu]}_{\{ij\}pqrs} \equiv A^{[\mu]}_{ijpqrs} - \frac{1}{3}\delta_{ij}A^{(\mu)}_{pqrs} \tag{6.66}$$

are deviatoric with respect to the braced index pair $\{ij\}$, and

$$d'_{ij} = d_{ij} - d_{rr}\delta_{ij}/3$$

is the deviator of the strain-rate tensor (3.22).

   Another decomposition of (6.62) is given by

$$d_{rr} = \sum_{\mu=0}^{5} A^{(\mu)}_{ijk\ell}P^{(\mu)}_{ijk\ell} , \tag{6.67a}$$

$$d'_{ij} = \sum_{\mu=0}^{5} A^{(\mu)}_{\{ij\}pqrs}P^{(\mu)}_{pqrs} , \tag{6.67b}$$

where the fourth-rank tensors $\boldsymbol{P}^{[\mu]}$ can be presented in the following matrix product form:

$$P^{[\mu]}_{ijk\ell} = \begin{pmatrix} \delta_{k\ell} & \sigma'_{k\ell} & \sigma''_{k\ell} \end{pmatrix} \begin{bmatrix} \Psi_{(0,\mu,0)} & \Psi_{(0,\mu,1)} & \Psi_{(0,\mu,2)} \\ \Psi_{(1,\mu,0)} & \Psi_{(1,\mu,1)} & \Psi_{(1,\mu,2)} \\ \Psi_{(2,\mu,0)} & \Psi_{(2,\mu,1)} & \Psi_{(2,\mu,2)} \end{bmatrix} \begin{bmatrix} \delta_{ij} \\ \sigma'_{ij} \\ \sigma''_{ij} \end{bmatrix} , \tag{6.68}$$

i.e., we have a representation in the *traceless tensors*

$$\sigma'_{ij} \equiv \partial J'_2/\partial\sigma_{ij} = \sigma_{ij} - \sigma_{kk}\delta_{ij}/3 , \tag{6.69}$$

$$\sigma''_{ij} \equiv \partial J'_3/\partial\sigma_{ij} = \sigma'^{(2)}_{ij} - 2J'_2\delta_{ij}/3 . \tag{6.70}$$

The elements $\Psi_{[.,\mu,.]}$ in the matrix of (6.68) can be expressed by the scalar-valued functions $\Phi_{[\lambda,\mu,\nu]}$ for example,

$$\Psi_{[1,\mu,1]} \equiv \Phi_{[1,\mu,1]} + \frac{2}{3}J_1\left(\Phi_{[1,\mu,1]} + \Phi_{[2,\mu,1]} + \frac{2}{3}J_1\Phi_{[2,\mu,2]}\right) ,$$

$$\equiv \Phi_{[1,\mu,2]} + 2J_1\Phi_{[2,\mu,2]}/3 ,$$

$$\Psi_{[2,\mu,1]} \equiv \Phi_{[2,\mu,1]} + 2J_1\Phi_{[2,\mu,2]}/3 ,$$

etc. The coefficients $\Phi_{[\lambda,\mu,\nu]}$ are themselves scalar-valued functions of the integrity basis (6.49), (6.50) associated with the representation (6.44).

Using the representation (6.67a,b), we read from the rate of dissipation of creep energy $\sigma_{ij}d_{ij}$ the following 34 irreducible invariants (BETTEN, 1988a):

$$\left.\begin{array}{l} J_1, \ J_2', \ J_3', \ J_1 A_{iijj}^{(\mu)}, \ J_1 A_{iijj}^{(6)}, \ \sigma_{ij}' A_{ijkk}^{(\mu)}, \ \sigma_{ij}' A_{ijk\ell}^{(\mu)}\sigma_{k\ell}', \\[2mm] \sigma_{ij}' A_{ijk\ell}^{(\mu)}\sigma_{k\ell}'', \ \sigma_{ij}'' A_{ijkk}^{(\mu)}, \ \sigma_{ij}'' A_{ijk\ell}^{(\mu)}\sigma_{k\ell}''; \quad \mu = 1, \ 2, \ \ldots, \ 5. \end{array}\right\} \quad (6.71)$$

For practical use, it may be sufficient to consider the anisotropy by $\mu = 1$ only. Then, we have the *creep condition*

$$f\left(J_1, \ J_2', \ J_3', \ \Pi_1, \ \Pi_1', \ \Pi_2', \ \Pi_3', \ \Pi_1'', \ \Pi_2''\right) = 1 \ , \qquad (6.72)$$

where the $J_1 \equiv S_1, \ J_2', \ J_3'$ are defined by (4.9a) and (4.10a,b). The invariant $\Pi_1 = J_1 A_{iijj}$ expresses the hydrostatic pressure accompanied by anisotropy. The remaining *simultaneous invariants* are defined by

$$\left.\begin{array}{ll} \Pi_1' \equiv \sigma_{ij}' A_{ijkk} \ , & \Pi_2' \equiv \sigma_{ij}' A_{ijk\ell}\sigma_{k\ell}' \ , \\[2mm] \Pi_3' \equiv \sigma_{ij}' A_{ijk\ell}\sigma_{k\ell} \ , & \\[2mm] \Pi_1'' \equiv \sigma_{ij}'' A_{ijkk} \ , & \Pi_2'' \equiv \sigma_{ij}'' A_{ijk\ell}\sigma_{k\ell}'' \ . \end{array}\right\} \quad (6.73)$$

In the isotropic special case characterized by (6.52), the invariants Π_1 to Π_2'' in the condition (6.72) reduce to

$$\Pi_1 = 3J_1 \ , \quad \Pi_1' = 0 \ , \quad \Pi_2' = 2J_2' \ ,$$
$$\Pi_3' = 3J_3' \ , \quad \Pi_1'' = 0 \ , \quad \Pi_2'' = 2J_2'^2/3 \ ,$$

i.e., they are expressible by the invariants (4.9a) and (4.10a,b) and are therefore redundant elements in this case.

For oriented solids we can specify the fourth-rank tensor $A_{ijk\ell}$ in (6.73) by

$$A_{ijk\ell} \equiv \frac{1}{4}\left(A_{ik}\delta_{j\ell} + A_{i\ell}\delta_{jk} + \delta_{ik}A_{j\ell} + \delta_{i\ell}A_{jk}\right) \ , \qquad (6.74)$$

and the *creep condition* (6.72) reduces to the form

$$f\left(J_1, \ J_2', \ J_3', \ \sigma_{ij}' A_{ji}, \ \sigma_{ij}'^{(2)} A_{ji}\right) = 1 \ , \qquad (6.75)$$

which is an alternative representation of the yield criterion formulated by BOEHLER and SAWCZUK (1977). The results given by (6.13), (6.45), (6.51), and (6.62) are summarized in Table 6.3.

Finally, we remark that in addition to an initial anisotropy as given in (6.42) corresponding to a forming process, for instance rolling, a deformation induced anisotropy can appear, for instance, by the formation of microscopic cracks. Because of its microscopic nature, *damage* has, in general, an

Table 6.3 Tensor generators and creep criteria

	tensor generators	creep criteria
general anisotropy	$G_{ij}^{[\lambda,\mu,\nu]} = A_{ijpqrs}^{[\mu]}\sigma_{pq}^{(\nu)}\sigma_{rs}^{(\lambda)}$ $\lambda,\ \nu = 0,\ 1\,2$ $\mu = 1,\ 2,\ \ldots,\ 5$ for $\mu = 0$	$f\left(\sigma_{ji}G_{ij}^{[\lambda,\mu,\nu]}\right) = 1$ $\lambda = 0,\ 1;\quad \nu = 0,\ 1,\ 2$ $\Rightarrow \quad \lambda + \nu \leq 2$
$\nu = 0$ $\Downarrow$ oriented solids	$G_{ij}^{[\lambda,\mu]} = A_{ijrs}^{[\mu]}\sigma_{rs}^{(\lambda)}$ $\lambda,\ \mu = 0,\ 1,\ 2$	$f\left(\sigma_{ji}G_{ij}^{[\lambda,\mu]}\right) = 1$ $\lambda,\ \mu = 0,\ 1,\ 2$ but for $\mu \neq 0 \Rightarrow \lambda < 2$
$\mu = 0$ $\Downarrow$ isotropy	$G_{ij}^{[\lambda]} = \sigma_{ij}^{(\lambda)}\ ;\quad \lambda = 0,\ 1,\ 2$	$f\left(\sigma_{ji}G_{ij}^{[\lambda]}\right) = 1$

$$A_{ijpqrs}^{(\mu)} \equiv \tfrac{1}{4}\left(A_{irpq}^{(\mu)}\sigma_{js} + A_{ispq}^{(\mu)}\sigma_{jr} + \sigma_{ir}A_{jspq}^{(\mu)} + \sigma_{is}A_{jrpq}^{(\mu)}\right)$$

$$A_{ijrs}^{(\mu)} \equiv \tfrac{1}{4}\left(A_{ir}^{(\mu)}\sigma_{js} + A_{is}^{(\mu)}\sigma_{jr} + \sigma_{ir}A_{js}^{(\mu)} + \sigma_{is}A_{jr}^{(\mu)}\right)$$

anisotropic character even if the material is originally isotropic. The orientation of fissures and their length result in anisotropic macroscopic behavior. Thus, it is necessary to consider this kind of anisotropy by introducing appropriately defined *anisotropic damage tensors* into the constitutive equations. In view of polynomial representations of constitutive equations, it is convenient to use the tensor

$$D_{ij} \equiv (\delta_{ij} - \omega_{ij})^{(-1)} \equiv \psi_{ij}^{(-1)} \tag{6.76}$$

as an additional argument tensor where ω and ψ are the second-rank *damage tensor* and the *tensor of continuity*, respectively (Section 4.3.2). The undamaged state is characterized by $\omega \to 0$ or $\psi \to \delta$. Considering (6.76), the constitutive equation takes the form

$$d_{ij} = f_{ij}\left(\sigma_{pq},\ D_{pq},\ A_{pqrs}\right) \tag{6.77}$$

instead of (6.42). The representation of (6.77), that is, of a symmetric second-order tensor-valued function of two symmetric tensors of rank two and one

symmetric tensor of rank four is pointed out in detail by BETTEN (1983b), and, again, the essential invariants to formulate the creep criterion can be read from the *rate of dissipation of creep energy* $\sigma_{ji}d_{ij}$.

Based upon (6.47) one arrives at a system of invariants (6.49), which is most important to formulate creep conditions of type (6.51). However, the system (6.49) contains irreducible invariants, but this system cannot be complete, because a lot of irreducible invariants cannot be expressed through (6.49). Thus, we have to look for other methods in order to find complete sets of invariants of a single fourth-order tensor and mixed invariants. These methods should be discussed in the following three sections (6.4.4 to 6.4.6).

6.4.4 Characteristic Polynomial for a Fourth Order Tensor

In order to construct an *irreducible* set of principal invariants of a fourth-order tensor $\mathbf{A}$, the *characteristic polynomial*

$$P_n(\lambda) \equiv \det \left(A_{ijk\ell} - \lambda A_{ijk\ell}^{(0)} \right) = \sum_{\nu=0}^{n} J_\nu(A)\lambda^{n-\nu} \qquad (6.78)$$

is considered by BETTEN, (1982a; 1988a).

The *principal invariants* J_ν in (6.78) can be determined by performing the operation of alternation

$$(-1)^{n-\nu}J_\nu \equiv A_{\alpha_1[\alpha_1]}A_{\alpha_2[\alpha_2]}\cdots A_{\alpha_\nu[\alpha_\nu]} \ , \qquad (6.79)$$

where $(-1)^n J_0 \equiv 1$. The right-hand side in (6.79) is equal to the sum of all principal minors of order $\nu \leq n$, where $\nu = 1$, and $\nu = n$ lead to tr $\mathbf{A}$ and det $\mathbf{A}$, respectively.

Assuming the usual symmetry conditions (6.41), the number n in (6.78) and (6.79) is equal to 6. Thus, we have found six irreducible invariants defined in (6.79). However, this system cannot be complete because some irreducible invariants like A_{iijj}, $A_{iipq}A_{pqjj}$, $A_{ijip}A_{pjqr}A_{rsqs}$ etc. cannot be expressed through (6.79). Consequently, the *characteristic polynomial* (6.78) must be generalized. This can be achieved by using the fourth-order tensor

$$I_{ijk\ell} = \lambda\delta_{ij}\delta_{k\ell} + \mu\left(\delta_{ik}\delta_{j\ell} + \delta_{i\ell}\delta_{jk}\right) \qquad (6.80)$$

instead of the spherical tensor $\lambda A_{ijk\ell}^{(0)}$ where $A_{ijk\ell}^{(0)}$ is the zero power tensor defined in (6.52). Thus, we take into consideration the *characteristic polynomial*

$$P(\lambda, \mu) = \det\left(A_{ijk\ell} - I_{ijk\ell}\right) = 0 \ , \qquad (6.81)$$

that is, we formulate the *eigenvalue problem*

$$A_{ijk\ell}X_{k\ell} = I_{ijk\ell}X_{k\ell} \ . \tag{6.82}$$

The isotropic tensor (6.80) yield an image dyad

$$Y_{ij} = I_{ijk\ell}X_{k\ell} = \lambda X_{rr}\delta_{ij} + 2\mu X_{ij} \ , \tag{6.83}$$

which is coaxial with the dyad X.

In continuum mechanics, the relation (6.83) is known as the constitutive equation for an isotropic linear elastic solid. Such a material is characterized by the two elastic constants λ and μ, which are called the LAME *constants*. Using the notation $Y_\alpha = I_{\alpha\beta}X_\beta$, α, $\beta = 1, 2, \ldots, 6$, we see that the isotropic tensor I in (6.83) can be represented in the matrix form

$$I_{ijkl} \equiv \begin{bmatrix} 2\mu + \lambda & \lambda & \lambda & 0 & 0 & 0 \\ \lambda & 2\mu + \lambda & \lambda & 0 & 0 & 0 \\ \lambda & \lambda & 2\mu + \lambda & 0 & 0 & 0 \\ 0 & 0 & 0 & 2\mu & 0 & 0 \\ 0 & 0 & 0 & 0 & 2\mu & 0 \\ 0 & 0 & 0 & 0 & 0 & 2\mu \end{bmatrix} \tag{6.84}$$

which is quasi-diagonal of the structure $\{3, 1, 1, 1\}$. The inverse tensor of (6.80) can be found from $X_{ij} = I_{ijk\ell}^{(-1)}Y_{k\ell}$ in connection with (6.83):

$$I_{ijk\ell}^{(-1)} = \frac{1}{4\mu}\left(\delta_{ik}\delta_{j\ell} + \delta_{i\ell}\delta_{jk}\right) - \frac{\lambda}{2\mu(3\lambda + 2\mu)}\delta_{ij}\delta_{k\ell} \ . \tag{6.85}$$

To control this result, we prove

$$I_{ijpq}^{(-1)} I_{pqkl} = I_{ijpq}I_{pqkl}^{(-1)} \equiv A_{ijkl}^{(0)} \ , \tag{6.86}$$

where the zero-power tensor has the diagonal form

$$A_{ijkl}^{(0)} = \{1, 1, 1, 1, 1, 1\} \ . \tag{6.87}$$

We see that in the special case ($\lambda = 0$, $\mu = 1/2$) the isotropic tensor (6.84) tends to the unit tensor as given in (6.87). Then we find from (6.81) the simplified characteristic polynomial given in (6.78). The determinant of the form (6.84) is

$$\det(I_{ijkl}) = 32(2\mu + 3\lambda)\mu^5 \ ,$$

which tends to $\det(A^0_{ijkl}) = 1$ in the special case ($\lambda = 0$, $\mu = 1/2$).

In the following we shall calculate irreducible invariants as coefficients in the characteristic polynomial (6.81). Due to (6.40) and (6.84), the *characteristic polynomial* (6.81) can be written as

$$\begin{vmatrix} A_{1111} - \Omega & A_{1122} - \lambda & A_{1133} - \lambda & 2A_{1112} & 2A_{1123} & 2A_{1131} \\ A_{2211} - \lambda & A_{2222} - \Omega & A_{2233} - \lambda & 2A_{2212} & 2A_{2223} & 2A_{2231} \\ A_{3311} - \lambda & A_{3322} - \lambda & A_{3333} - \Omega & 2A_{3312} & 2A_{3323} & 2A_{3331} \\ A_{1211} & A_{1222} & A_{1233} & 2A_{1212} - 2\mu & 2A_{1223} & 2A_{1231} \\ A_{2311} & A_{2322} & A_{2333} & 2A_{2312} & 2A_{2323} - 2\mu & 2A_{2331} \\ A_{3111} & A_{3122} & A_{3133} & 2A_{3112} & 2A_{3123} & 2A_{3131} - 2\mu \end{vmatrix} = 0$$

<div align="right">(6.88a)</div>

or as

$$\begin{vmatrix} A_{1111} - \Omega & A_{1122} - \lambda & A_{1133} - \lambda & 2A_{1112} & 2A_{1123} & 2A_{1131} \\ & A_{2222} - \Omega & A_{2233} - \lambda & 2A_{2212} & 2A_{2223} & 2A_{2231} \\ & & A_{3333} - \Omega & 2A_{3312} & 2A_{3323} & 2A_{3331} \\ & & & 2A_{1212} - 2\mu & 2A_{1223} & 2A_{1231} \\ & & & & 2A_{2323} - 2\mu & 2A_{2331} \\ \text{symm.} & & & & & 2A_{3131} - 2\mu \end{vmatrix} = 0$$

<div align="right">(6.88b)</div>

where the abbreviation $\Omega \equiv 2\mu + \lambda$ is used. The determinant (6.88) is a polynomial of degree 3 in λ and degree 6 in μ:

$$\left. \begin{aligned} P(\lambda, \mu) &= \sum_{p,q} C_{(p,q)} \lambda^p \mu^q \ , \\ p &= 0, 1, 2, 3; \quad q = 0, 1, \ldots, 6, \quad p + q \le 6 \end{aligned} \right\} \tag{6.89}$$

with 22 scalar coefficients $C_{(p,q)}$. However, the characteristic equation $P(\lambda, \mu) = 0$ can be divided by the coefficient $C_{(0,6)}$, so that we can find no more than 21 invariants. Now the main problem is to expand the determinant (6.88) and to find out if all 21 coefficients are irreducible invariants.

To avoid the lengthy expansion of the determinant (6.88), we propose the following method. If we consider a second-order tensor, we can start from the diagonal form

$$\sigma_{ij} = \text{diag}\{\sigma_I, \sigma_{II}, \sigma_{III}\} \ . \tag{6.90}$$

Then the determinant, $\det(\sigma_{ij} - \lambda\delta_{ij})$, is identical to the characteristic polynomial

$$P_3(\lambda) = (\lambda - \sigma_I)(\lambda - \sigma_{II})(\lambda - \sigma_{III}) = \lambda^3 - J_1\lambda^2 - J_2\lambda - J_3 . \quad (6.91)$$

Similarly, we could consider the *orthotropic* case with

$$A_{1112} = A_{1123} = A_{1131} = A_{2212} = A_{2223} = A_{2231}$$
$$= A_{3312} = A_{3323} = A_{3331} = 0 .$$

Thus the dyads $\boldsymbol{X}$ and $\boldsymbol{Y}$ in $Y_{ij} = A_{ijkl}X_{kl}$ are *coaxial* and, instead the polynomial of (6.88), the following determinant is to be used:

$$\begin{vmatrix} A_I - (2\mu + \lambda) & B_I - \lambda & B_{II} - \lambda & 0 & 0 & 0 \\ B_I - \lambda & A_{II} - (2\mu + \lambda) & B_{III} - \lambda & 0 & 0 & 0 \\ B_{II} - \lambda & B_{III} - \lambda & A_{III} - (2\mu + \lambda) & 0 & 0 & 0 \\ 0 & 0 & 0 & A_{IV} - 2\mu & 0 & 0 \\ 0 & 0 & 0 & 0 & A_V - 2\mu & 0 \\ 0 & 0 & 0 & 0 & 0 & A_{VI} - 2\mu \end{vmatrix} = 0$$
$$(6.92)$$

¿From the determinant (6.92) we find the *characteristic polynomial*

$$\begin{aligned} P(\lambda, \mu) = {} & 64\mu^6 - 32I_1\mu^5 + 16I_2\mu^4 - 8I_3\mu^3 + 4I_4\mu^2 \\ & - 2I_5\mu + I_6\lambda + I_7\lambda\mu + I_8\lambda\mu^2 + I_9\lambda\mu^3 \\ & + I_{10}\lambda\mu^4 + 96\lambda\mu^5 + I_{11} , \end{aligned} \quad (6.93)$$

where the 11 invariants $I_1, \ldots, I_{11}$ are listed below:

$$\begin{aligned} I_1 &\equiv K_1 + M_1 , \\ I_2 &\equiv K_2 + M_2 + K_1 M_1 - L_1^2 + 2L_2 , \\ I_3 &\equiv D + M_3 + K_1 M_2 + M_1 \left(K_2 - L_1^2 + 2L_2 \right) , \\ I_4 &\equiv M_1 D + K_1 M_3 + M_2 \left(K_2 - L_1^2 + 2L_2 \right) , \\ I_5 &\equiv M_2 D + M_3 \left(K_2 - L_1^2 + 2L_2 \right) , \\ I_6 &\equiv M_3 \left(L_1^2 - 4L_2 - K_2 + 2N \right) , \\ I_7 &\equiv 4M_3 \left(K_1 - L_1 \right) - 2M_2 \left(L_1^2 - 4L_2 - K_2 + 2N \right) , \\ I_8 &\equiv 4M_1 \left(L_1^2 - 4L_2 - K_2 - 2N \right) - 8M_2(K_1 - L_1) - 12M_3 , \\ I_9 &\equiv 8 \left[2M_1(K_1 - L_1) - L^2 + 4L_2 + K_2 - 2N + 3M_2 \right] , \\ I_{10} &\equiv -16 \left[2(K_1 - L_1) + 3M_1 \right] , \\ I_{11} &= M_3 D . \end{aligned} \quad (6.94)$$

In the system (6.94) the following abbreviations are used:

$$K_1 \equiv A_I + A_{II} + A_{III} \ ,$$
$$M_1 \equiv A_{IV} + A_V + A_{VI} \ ,$$
$$K_2 \equiv A_I A_{II} + A_{II} A_{III} + A_{III} A_I \ ,$$
$$M_2 \equiv A_{IV} A_V + A_V A_{VI} + A_{VI} A_{IV} \ ,$$
$$K_3 \equiv A_I A_{II} A_{III} \ ,$$
$$M_3 \equiv A_{IV} A_V A_{VI} \ , \tag{6.95}$$
$$L_1 \equiv B_I + B_{II} + B_{III} \ ,$$
$$L_2 \equiv B_I B_{II} + B_{II} B_{III} + B_{III} B_I \ ,$$
$$L_3 \equiv B_I B_{II} B_{III} \ ,$$
$$N \equiv A_I B_{III} + A_{II} B_{II} + A_{III} B_I \ ,$$
$$D \equiv K_3 + 2L_3 - \left(A_I B_{III}^2 + A_{II} B_{II}^2 + A_{III} B_I^2 \right) \ .$$

We see that in the system (6.94) the invariants I_1 and I_{11} are the trace and determinant of the fourth-order tensor, respectively.

In the special case ($\lambda = 0$), only the six invariants $I_1, \ldots, I_5, I_{11}$ are relevant, and they are identical to the six invariants (6.79), if $B_I = B_{II} = B_{III} = 0$.

In the two-dimensional case (i, j, k, l = 1, 2), the *eigenvalue problem* (6.82) leads to a characteristic equation $P(\lambda, \mu) = 0$ from which we read five irreducible invariants as illustrated by BETTEN (1988a).

6.4.5 LAGRANGE Multiplier Method

In order to find the characteristic equation of a fourth-order tensor, one can utilize the LAGRANGE *multiplier method*. To do this, we start from the scalar-valued function

$$F = A_{ijkl} X_{ij} X_{k\ell} \ . \tag{6.96}$$

Since the second-order tensor X in (6.96) has three irreducible invariants

$$S_1 \equiv \mathrm{tr}\, X \ , \qquad S_2 \equiv \mathrm{tr}\, X^2 \ , \qquad S_3 \equiv \mathrm{tr}\, X^3 \tag{6.97}$$

being the elements of the *integrity basis*, we take into consideration the following three "auxiliary" conditions:

$$\left. \begin{array}{l} L = \delta_{ij}\delta_{k\ell} X_{ij} X_{k\ell} - S_1^2 = 0 \ , \\ M = \left(\delta_{ik}\delta_{j\ell} + \delta_{i\ell}\delta_{jk} \right) X_{ij} X_{k\ell} - 2S_2 = 0 \ , \\ N = \left(\delta_{jk}\delta_{p\ell} + \delta_{j\ell}\delta_{pk} \right) X_{ip} X_{ij} X_{k\ell} - 2S_3 = 0 \ . \end{array} \right\} \tag{6.98}$$

Thus, the quadratic form (6.96) of the dyad X is modified to the form

$$\Phi = F - \lambda L - \mu M - \nu N \ , \tag{6.99}$$

which is to be made stationary, that is, we require

$$\partial \Phi / \partial X_{rs} = 0_{rs} \ . \tag{6.100}$$

From (6.100), we find the system of nonlinear equations in the dyad X,

$$\left(A_{ijk\ell} - I_{ijk\ell} \right) X_{k\ell} = 3\nu X_{ij}^{(2)} \ , \tag{6.101}$$

where $I_{ijk\ell}$ are the components of the fourth-order isotropic tensor defined in (6.80). In the special case when $\nu = 0$, we find from (6.101) the *eigenvalue problem* (6.82) which yields the *characteristic equation* (6.81). Some more details concerning the system (6.101) will be investigated by BETTEN (2009). Furthermore, applications of the LAGRANGE *multiplier method* to tensors of order six will also be discussed by BETTEN (2009).

6.4.6 Combinatorial Method

In order to find *irreducible* sets of invariants for a *fourth-order material tensor*, two methods have been discussed above:

- ☐ **by way of an extended characteristic polynomial,**
- ☐ **application of a modified LAGRANGE-multiplier method.**

In the following a third one,

- ☐ **combinatorial method,**

is proposed, which is most effective and able to produce both *irreducible* and *complete* sets of invariants. As an example, let us form irreducible invariants of a fourth-order symmetric tensor

$$A_{ijk\ell} = A_{jik\ell} = A_{ij\ell k} = A_{k\ell ij} \ . \tag{6.40}$$

Since

$$\delta_{ij}\delta_{k\ell}\delta_{pq}\delta_{rs} = \delta_{ji}\delta_{k\ell}\delta_{rp}\delta_{qs} = \ldots = \delta_{sr}\delta_{k\ell}\delta_{qp}\delta_{ij}$$

represent $P_8 = \dfrac{8!}{2^4 \cdot 4!} = \mathbf{105}$ independent combinations one can form by *transvections* like

$$\left.\begin{array}{l} \delta_{ip}\delta_{jq}\delta_{kr}\delta_{\ell s}A_{ijk\ell}A_{pqrs} \equiv A_{ijk\ell}A_{ijk\ell} \equiv I_{2,4} \ , \\ \delta_{is}\delta_{jr}\delta_{kq}\delta_{\ell p}A_{ijk\ell}A_{pqrs} \equiv A_{ijk\ell}A_{\ell kji} \equiv I_{2,4} \ , \\ \delta_{ip}\delta_{\ell q}\delta_{jr}\delta_{ks}A_{ijk\ell}A_{pqrs} \equiv A_{ijk\ell}A_{i\ell jk} \equiv I_{2,5} \ , \end{array}\right\} \qquad (6.102a)$$

altogether **105** invariants. However, considering the index symmetries (6.40), this number is reduced to the following **5** different invariants of degree 2:

$$I_{2,1}, \ I_{2,2}, \ \ldots, \ I_{2,5} \ , \quad \text{where} \quad \left.\begin{array}{l} I_{2,1} \equiv A_{iij\ell}A_{jkk\ell} \ , \\ I_{2,2} \equiv A_{iijk}A_{jk\ell\ell} \ , \\ I_{2,3} \equiv A_{i\ell ij}A_{jkk\ell} \ , \\ I_{2,4} \equiv A_{ijk\ell}A_{ijk\ell} \ , \\ I_{2,5} \equiv A_{ijk\ell}A_{i\ell jk} \ . \end{array}\right\} \qquad (6.102b)$$

In 3-dimensional EUCLIDian space the *fourth-order permutation tensor* $\varepsilon_{ijk\ell}$ is a zero tensor so that the determinant

$$\varepsilon_{ijk\ell}\varepsilon_{pqrs} \equiv \begin{vmatrix} \delta_{ip} & \delta_{iq} & \delta_{ir} & \delta_{is} \\ \delta_{jp} & \delta_{jq} & \delta_{jr} & \delta_{js} \\ \delta_{kp} & \delta_{kq} & \delta_{kr} & \delta_{ks} \\ \delta_{\ell p} & \delta_{\ell q} & \delta_{\ell r} & \delta_{\ell s} \end{vmatrix} = 0 \qquad (6.103)$$

vanishes. Thus, from

$$\varepsilon_{ijk\ell}\varepsilon_{pqrs}A_{ijk\ell}A_{pqrs} = 0 \qquad (6.104)$$

we find the relation

$$8I_{2,1} = 4I_{2,2} + 4I_{2,3} + 2I_{2,4} + 2I_{2,5} \ . \qquad (6.105)$$

Consequently, the invariant $I_{2,1}$ is redundant, and there are only **4** irreducible invariants of degree 2 for a *fourth-order symmetric tensor* (6.40). Following this way by using a special developed computer program, we find more than 65 irreducible invariants of a fourth-order tensor listed in Table 6.4.

Table 6.4 Numbers of irreducible invariants of a fourth-order symmetric tensor

degree	1	**2**	3	4	5	6	
invariants	2	**4**	10	16	33	?	$\sum > 65$

The highest degree is **6**, which has to be taken into account (BETTEN, 1982a; 2001c). However, the complete set of invariants of degree **6** for a

fourth-order symmetric tensor cannot be calculated up to now because of missing computer capacities.

The combinatorial method is not restricted to the formation of invariants, but also leads to results on tensor-valued terms called *tensor generators*. For instance, the expressions

$$
\left.
\begin{aligned}
\delta_{ij}\delta_{k\ell}A_{k\ell} &\equiv A_{kk}\delta_{ij} , \quad \delta_{ik}\delta_{j\ell}A_{k\ell} \equiv A_{ij} , \\
\delta_{ip}\delta_{qr}\delta_{sj}A_{pq}A_{rs} &\equiv A_{ir}A_{rj} \equiv A^{(2)}_{ij}
\end{aligned}
\right\}
\tag{6.106}
$$

are the three irreducible tensor generators of a second-order tensor. Furthermore, the *transvections*

$$
\left.
\begin{aligned}
\delta_{ip}\delta_{qr}\delta_{sj}A_{pq}B_{rs} &\equiv A_{ir}B_{rj} , \\
\delta_{ip}\delta_{qr}\delta_{st}\delta_{uv}\delta_{wj}A_{pqrs}A_{tuvw} &\equiv A_{irrs}A_{suuj}
\end{aligned}
\right\}
\tag{6.107}
$$

are index-combinations with the two free indices ij, i.e., second-order tensor-valued terms. Our special developed computer program forms all possible index-combinations, such as (6.107), and selects all redundant elements by considering index-symmetries. Thus, we find sets of *irreducible tensor-generators*, which are complete, too. Some results are listed in Table 6.5.

Table 6.5 The numbers of irreducible invariants and tensor generators

Symmetric Argumenttensors	Irred. Invari- ants	Tensor Functions $f_{ij} = \sum_{\alpha} \varphi_\alpha\, {}^{\alpha}G_{ij}$	Tensor Generators ${}^{\alpha}G_{ij} = {}^{\alpha}G_{ji}$
X_{pq}	3	$Y_{ij} = f_{ij}(X_{pq})$	3
X_{pq}, A_{pq}	10	$f_{ij}(X_{pq}, A_{pq})$	9
X_{pq}, A_{pq}, B_{pq}	28	$f_{ij}(X_{pq}, A_{pq}, B_{pq})$	46
A_{pqrs}	> 65	$f_{ij}(A_{pqrs})$	> 108
X_{pq}, A_{pqrs}	> 156	$f_{ij}(X_{pq}, A_{pqrs})$	> 314
X_{pq}, D_{pq}, A_{pqrs}	> 512	$f_{ij}(X_{pq}, D_{pq}, A_{pqrs})$	> 884

Further mathematical considerations and possible engineering applications are discussed and illustrated, for instance, by BETTEN (1998) and BETTEN and HELISCH (1995), or by ZHENG and BETTEN (1995;1996), or ZHENG, BETTEN and SPENCER (1992). An extended survey of the theory of representations for tensor functions was provided by ZHENG (1994) and BETTEN (2001b) in the Applied Mechanics Review (AMR).

As one can see from Table 6.5, constitutive equations and anisotropic damage growth equations of the forms (4.79a,b), (4.85a,b) or (6.43) containing complete sets of *irreducible invariants* and *tensor generators* may be too complicated for practical use. Therefore, we have to look for *simplified representations* as proposed in the following.

6.4.7 Simplified Representations

As an example, we suggest the following *simplified* constitutive equation

$$d_{ij} = f_{ij}(\boldsymbol{t}, \boldsymbol{\tau}) = \frac{1}{2} \sum_{\nu,\mu=0}^{2} \Phi_{[\nu,\mu]} \left[t_{ik}^{(\nu)} \tau_{kj}^{(\mu)} + \tau_{ik}^{(\mu)} t_{kj}^{(\nu)} \right] , \qquad (6.108)$$

where the linear transformations

$$t_{ij} = D_{ijpq}\sigma_{pq} = t_{ji} , \quad D_{ijpq} := \frac{1}{2} \left(D_{ip}D_{jq} + D_{iq}D_{jp} \right) \qquad (6.109)$$

and

$$\tau_{ij} = A_{ijpq}\sigma_{pq} = \tau_{ji} \qquad (6.110)$$

have been introduced by BETTEN (1983b). We can see that the first linear transformation (6.109) considers the *anisotropic damage state*, while the second one (6.110) expresses the *initial anisotropy* of the material. The main problem now is to determine the scalar coefficients $\Phi_{[\nu,\mu]}$ in (6.108) as functions of the integrity basis and experimental data. This can be achieved by using the *interpolation method* developed by BETTEN(1984; 1987c) and applied also by BETTEN (1986a; 1989).

The tensor $\boldsymbol{t}$ defined in (6.109) is called the *pseudo-net-stress tensor* (section 7.2). This tensor is symmetric even in the anisotropic damage case. The non-symmetric property of the *actual net-stress tensor* $\hat{\boldsymbol{\sigma}}$ in (4.78) is a disadvantage, and this tensor is awkward to use in constitutive equations.

In recent years much effort has been devoted to the elaboration of *evolutional equations* such as (4.79b) or (4.85b). The results are discussed by BETTEN and MEYDANLI (1995). For the sake of simplicity, we can once again use the linear transformations (6.109) and (6.110), i.e., as in (6.108), we have to represent the tensor-valued function $\overset{\circ}{D}_{ij} = g_{ij}(\boldsymbol{t}, \tau)$ where $\overset{\circ}{D}_{ij}$ is the JAUMANN *derivative* of the tensor (4.84), (6.76).

The representation (6.108) involves nine tensor generators, where $\Phi_{[\nu,\mu]}$ are scalar-valued functions of the integrity basis associated with the representation (6.108), which can be found by forming $\operatorname{tr} \boldsymbol{t} \, \boldsymbol{d}$ and $\operatorname{tr} \boldsymbol{\tau} \, \boldsymbol{d}$. In this way we find the following invariants

$$t_{ij}^{(\nu+1)}\tau_{ji}^{(\mu)} \equiv \operatorname{tr} \boldsymbol{t}^{\nu+1}\boldsymbol{\tau}^{\mu} \tag{6.111a}$$

and

$$t_{ij}^{(\nu)}\tau_{ji}^{(\mu+1)} \equiv \operatorname{tr} \boldsymbol{t}^{\nu}\boldsymbol{\tau}^{\mu+1} \; , \tag{6.111b}$$

some of them are reducible or equivalent, which can be found by using the following Lemmas:

- □ If $\boldsymbol{G}$ is a reducible generator, then $\operatorname{tr} \boldsymbol{X}\,\boldsymbol{G}$ and $\operatorname{tr}\boldsymbol{G}\,\boldsymbol{X}$ are reducible, where $\boldsymbol{X}$ is an arbitrary tensor.
- □ The trace of a matrix product is unaltered by cyclic permutations of its factors.
- □ The trace of a matrix product is equal to the trace of the transpose of the product.
- □ The transpose of a matrix product π is the matrix product formed by writing down the transposes of the factors of π in reverse order, for instance: $\operatorname{tr} \boldsymbol{a}\,\boldsymbol{b}\,\boldsymbol{c} = \operatorname{tr} \boldsymbol{c}'\,\boldsymbol{b}'\,\boldsymbol{a}'$.

Further deliberations concerning reducibility and equivalence and consequences from the HAMILTON-CAYLEY theorem are given, for instance, by BETTEN (1987c) or by ZHENG (1994).

In selecting the redundant elements, we find from (6.111a,b) the *integrity basis*

$$\left.\begin{array}{cccccc} \operatorname{tr} \boldsymbol{t}\,, & \operatorname{tr} \boldsymbol{t}^{2}\,, & \operatorname{tr} \boldsymbol{t}^{3}\,, & \operatorname{tr} \boldsymbol{\tau}\,, & \operatorname{tr} \boldsymbol{\tau}^{2}\,, & \operatorname{tr} \boldsymbol{\tau}^{3}\,, \\[2mm] \operatorname{tr} \boldsymbol{t}\boldsymbol{\tau}\,, & \operatorname{tr} \boldsymbol{t}\boldsymbol{\tau}^{2}\,, & \operatorname{tr} \boldsymbol{t}^{2}\boldsymbol{\tau}\,, & \operatorname{tr} \boldsymbol{t}^{2}\boldsymbol{\tau}^{2}\,, \end{array}\right\} \tag{6.112}$$

associated with the representation (6.108).

We can write the constitutive equation (6.108) in a *canonical form*, like (4.81), if we introduce the following identities for *tensor generators*:

Let $\boldsymbol{X}$ and $\boldsymbol{Y}$ be two symmetric second-order tensors, i.e., $X_{ij} = X_{ji}$ and $Y_{ij} = Y_{ji}$, respectively. Then, the identities

$$\left\{\frac{1}{2}\left(\boldsymbol{X}^{\mu}\boldsymbol{Y}^{\nu} + \boldsymbol{Y}^{\nu}\boldsymbol{X}^{\mu}\right)\right\}_{ij} \equiv \eta_{ijk\ell}^{[\nu]}X_{k\ell}^{(\mu)} \equiv \xi_{ijk\ell}^{[\mu]}Y_{k\ell}^{(\nu)} \tag{6.113}$$

are valid for arbitrary values μ and ν, where the symbols $\xi_{ijk\ell}^{[\mu]}$ and $\eta_{ijk\ell}^{[\nu]}$ are μ and ν several fourth-order tensors defined by

$$\xi_{ijk\ell}^{[\mu]} \equiv \frac{1}{4}\left(X_{ik}^{(\mu)}\delta_{j\ell} + X_{i\ell}^{(\mu)}\delta_{jk} + \delta_{ik}X_{j\ell}^{(\mu)} + \delta_{i\ell}X_{jk}^{(\mu)}\right) \tag{6.114a}$$

and

$$\eta_{ijk\ell}^{[\nu]} \equiv \frac{1}{4} \left(Y_{ik}^{(\nu)} \delta_{j\ell} + Y_{i\ell}^{(\nu)} \delta_{jk} + \delta_{ik} Y_{j\ell}^{(\nu)} + \delta_{i\ell} Y_{jk}^{(\nu)} \right) , \qquad (6.114b)$$

respectively. Note that in (6.113) and (6.114a,b) those values of μ and ν which are bracketed by parentheses are exponents, while a square bracket gives any μ or ν the character of a label.

Furthermore, from (6.113) and (6.114a,b) we read the simple identities

$$\delta_{ij} \equiv \frac{1}{2} \left(\delta_{ik} \delta_{j\ell} + \delta_{i\ell} \delta_{jk} \right) \delta_{k\ell} \equiv E_{ijk\ell} \delta_{k\ell} \qquad (6.115)$$

and

$$X_{ij}^{(\mu)} \equiv E_{ijkl} X_{k\ell}^{(\mu)} \equiv \xi_{ijk\ell}^{[\mu]} \delta_{k\ell} , \qquad (6.116)$$

where E_{ijkl} is the zero power tensor of fourth-order defined by

$$E_{ijkl} = \frac{1}{2} \left(\delta_{ik} \delta_{j\ell} + \delta_{i\ell} \delta_{jk} \right) . \qquad (6.117)$$

In using the introduced algebraic relations (6.113) to (6.116), we finally find a *canonical* form

$$\boxed{ d_{ij} = {}^0 h_{ijk\ell} \delta_{k\ell} + {}^1 h_{ijk\ell} t_{k\ell} + {}^2 h_{ijk\ell} t_{k\ell}^{(2)} } \qquad (6.118)$$

of the constitutive equation (6.108) in the *pseudo-net-stress tensor* $\boldsymbol{t}$, where the fourth-order tensor-valued functions ${}^0\boldsymbol{h}$, ${}^1\boldsymbol{h}$, ${}^2\boldsymbol{h}$ are defined by

$${}^0 h_{ijk\ell} \equiv \Phi_{[0,0]} T_{ijk\ell}^{(0)} + \Phi_{[0,1]} T_{ijk\ell} + \Phi_{[0,2]} T_{ijk\ell}^{[2]} , \qquad (6.119a)$$

$${}^1 h_{ijk\ell} \equiv \Phi_{[1,0]} T_{ijk\ell}^{(0)} + \Phi_{[1,1]} T_{ijk\ell} + \Phi_{[1,2]} T_{ijk\ell}^{[2]} , \qquad (6.119b)$$

$${}^2 h_{ijk\ell} \equiv \Phi_{[2,0]} T_{ijk\ell}^{(0)} + \Phi_{[2,1]} T_{ijk\ell} + \Phi_{[2,2]} T_{ijk\ell}^{[2]} , \qquad (6.119c)$$

which can be expressed in the compact form

$${}^\lambda h_{ijk\ell} \equiv \sum_{\nu=0}^{2} \Phi_{[\lambda,\nu]} T_{ijk\ell}^{[\nu]} , \quad \lambda = 0, 1, 2 , \qquad (6.120)$$

where, by analogy of (6.114b), the symmetric tensors $\boldsymbol{T}^{[\nu]}$ of rank four are defined by

$$T_{ijk\ell}^{[\nu]} \equiv \frac{1}{4} \left(\tau_{ik}^{(\nu)} \delta_{j\ell} + \tau_{i\ell}^{(\nu)} \delta_{jk} + \delta_{ik} \tau_{j\ell}^{(\nu)} + \delta_{i\ell} \tau_{jk}^{(\nu)} \right) . \qquad (6.121)$$

For example, for $\nu = 0$ we read from (6.121) the symmetric zero power tensor of rank four $T^{[0]}_{ijk\ell} \equiv T^{(0)}_{ijk\ell} = E_{ijk\ell}$ defined by (6.117).

The result (6.120) elucidates that the anisotropy expressed by the tensors $\boldsymbol{T}^{[\nu]}$ according to (6.121) has equal influence on the contributions of orders zero, first, and second in the *pseudo-net-stresses* $t_{k\ell}$ contained in (6.118). The functions (6.119a,b,c) or (6.120) express the anisotropy of the undamaged state (6.110), while the effect of anisotropic damage is considered in (6.118) by the *pseudo-net-stress tensor* $\boldsymbol{t}$ according to (6.109) with (6.76). In the total damaged state, i.e. when $\boldsymbol{\omega} \to \boldsymbol{\delta}$ or $\boldsymbol{\psi} \to \boldsymbol{0}$, the tensors $\boldsymbol{D}$ and $\boldsymbol{t}$ are *singulär*, and the strain rates (6.118) approach infinity.

In the undamaged state ($\boldsymbol{\omega} \to \boldsymbol{0}$ or $\boldsymbol{D} \to \boldsymbol{\delta}$) the *pseudo-net-stress tensor* (6.109) is identical to CAUCHY's *stress tensor* $\boldsymbol{\sigma}$. If, furthermore, the initial state is isotropic [$\boldsymbol{A} \to \boldsymbol{E}$ according to (6.117) or $\boldsymbol{\tau} \to \boldsymbol{\sigma}$ in (6.110)], then the constitutive equation yields to the simple form (4.83) valid for isotropic materials in the secondary creep stage.

Finally, because of (6.120), one can write the constitutive equation (6.118) in the very short form

$$d_{ij} \equiv \sum_{\lambda,\nu=0}^{2} \Phi_{[\lambda,\nu]} T^{[\nu]}_{ijk\ell} t^{(\lambda)}_{k\ell} . \tag{6.122}$$

Replacing the *pseudo-net-stress tensor* $\boldsymbol{t}$ according to (6.109) in (6.118) we find the representation

$$d_{ij} = {}^{0}K_{ij} + {}^{1}K_{ijk\ell}\,\sigma_{k\ell} + {}^{2}K_{ijk\ell mn}\,\sigma_{k\ell}\,\sigma_{mn} \tag{6.123}$$

of the constitutive equation (6.108), if we define:

$$ {}^{0}K_{ij} \equiv {}^{0}h_{ijpq}\delta_{pq} , \tag{6.124a}$$

$$ {}^{1}K_{ijk\ell} \equiv {}^{1}h_{ijpq}D_{pqk\ell} , \tag{6.124b}$$

$$ {}^{2}K_{ijk\ell mn} \equiv {}^{2}h_{ijpq}D_{prk\ell}D_{rqmn} . \tag{6.124c}$$

The coeffecient tensors (6.124b,c) are decomposed into anisotropy characterized by the fourth-rank tensors (6.119b,c) and into *anisotropic damage* determined by the *fourth-rank tensor* $(D_{ijk\ell})$ defined in (6.109) in a multiplicative way. In the undamaged case [$D_{ij} \to \delta_{ij}$ according to (6.76)] the tensor $(D_{ijk\ell})$ in (6.109) is identical to the symmetric zero power tensor of fourth-order defined by (6.117), and in the total damage state ($\boldsymbol{\omega} \to \boldsymbol{\delta}$) the fourth-order tensor $\boldsymbol{D}$ in (6.109) is singular, i. e., the strain rates according to (6.108) or (6.123) approach infinity as the damage tensor $\boldsymbol{\omega}$ approaches the unit tensor $\boldsymbol{\delta}$ or as the continuity tensor $\boldsymbol{\psi}$ in (6.76) approaches the zero tensor $\boldsymbol{0}$.

7 Damage Mechanics

In sections 4.3.2 and 6.4 *constitutive equations* involving *damage* and *initial anisotropy* have been formulated in detail. This Chapter is concerned with the construction of *damage tensors* or tensors of continuity (Section 7.1).

Then, the *multiaxial state of stress* in a damaged continuum will be analyzed in detail (Section 7.2).

Finally, some *damage effective stress* concepts are proposed and discussed in Section 7.3.

7.1 Damage Tensors and Tensors of Continuity

As has been already mentioned in Chapter 4, *damage* has in general an *anisotropic* character even if the material was originally isotropic. This matter results from the microscopic nature of damage. The fissure orientation and length cause anisotropic macroscopic behavior. Therefore, damage in an isotropic or initial anisotropic material that is in a state of multiaxial stress can only be described by taking a *damage tensor* into account.

There are some different ways to construct tensors suitable for analysing the damage state in material. In the following *second-rank* and *fourth-order damage tensors* are systematically developed.

In three-dimensional space a parallelogram formed by the vectors A_i and B_i can be represented by

$$S_i = \varepsilon_{ijk} A_j B_k \qquad\qquad (7.1a)$$

or in the dual form

$$S_{ij} = \varepsilon_{ijk} S_k \quad \Leftrightarrow \quad S_i = \tfrac{1}{2}\varepsilon_{ijk} S_{jk} \, , \qquad\qquad (7.1b)$$

where ε_{ijk} is the third-order alternating tensor ($\varepsilon_{ijk} = 1$, or -1 if i, j, k are even or odd permutations of 1, 2, 3, respectively, otherwise the components ε_{ijk} are equal to zero) according to (2.5). From (7.1a,b) we immediately find

$$S_{ij} = 2! A_{[i} B_{j]} = \begin{vmatrix} A_i & A_j \\ B_i & B_j \end{vmatrix} . \tag{7.2}$$

Because of the decomposition (7.2) as an alternating product of two vectors the *bivector* S is called *simple* and has the following three nonvanishing essential components

$$S_{12} = A_1 B_2 - A_2 B_1 , \quad S_{23} = A_2 B_3 - A_3 B_2 , \tag{7.3a,b}$$
$$S_{31} = A_3 B_1 - A_1 B_3 . \tag{7.3c}$$

In rectilinear components in three-dimensional space, we see that the absolute values of the components (7.3) are the projections of the area of the parallelogram, considered above, on the coordinate planes. Thus S_{ij}, according to (7.2), represents an area vector in three-dimensional space and has an orientation fixed by (7.1a).

According to (7.1b) a surface element dS with an unit normal n_i, i.e. $dS_i = n_i dS$, is expressed by

$$dS_{ij} = \varepsilon_{ijk} dS_k \quad \Leftrightarrow \quad dS_i = \tfrac{1}{2}\varepsilon_{ijk} dS_{jk} \tag{7.4.a}$$

and

$$n_{ij} = \varepsilon_{ijk} n_k \quad \Leftrightarrow \quad n_i = \tfrac{1}{2}\varepsilon_{ijk} n_{jk} . \tag{7.4b}$$

The components of the *bivector* n are the direction cosines n_1, n_2, n_3:

$$n_{ij} = \begin{pmatrix} 0 & n_3 & -n_2 \\ -n_3 & 0 & n_1 \\ n_2 & -n_1 & 0 \end{pmatrix} . \tag{7.5}$$

The principal invariants of (7.5), defined as

$$J_1 \equiv n_{ii} , \quad -J_2 \equiv n_{i[i]} n_{j[j]} , \quad J_3 \equiv n_{i[i]} n_{j[j]} n_{k[k]} , \tag{7.6a,b,c}$$

take the following values:

$$J_1(\boldsymbol{n}) = 0 , \quad -J_2(\boldsymbol{n}) = n_1^2 + n_2^2 + n_3^2 = 1 , \quad J_3(\boldsymbol{n}) = 0 , \tag{7.7a,b,c}$$

i.e. the only nonvanishing invariant is determined by the length of the unit normal vector n_i. In (7.6a,b,c) the same notation is used as in (2.24a,b,c).
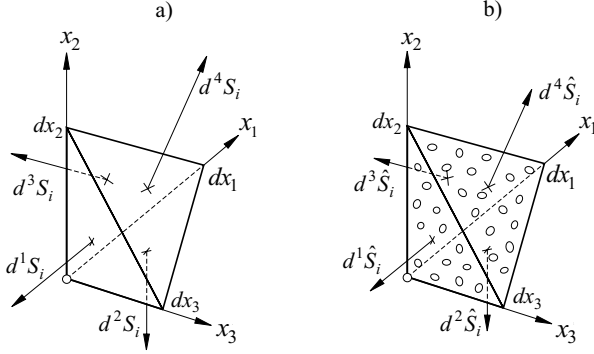
Fig. 7.1 CAUCHY's tetrahedron **a)** in an undamaged state, **b)** in a damaged state

Imagine that at a point ∘ in a continuous medium a set of rectangular coordinate axes is drawn and a differential tetrahedron is bounded by parts of the three coordinate planes through ∘ and a fourth plane not passing through ∘, as shown in Fig. 7.1a. Such a tetrahedron can be characterized by a system of *bivectors*,

$$
\begin{aligned}
d^1 S_i &= -\tfrac{1}{2}\varepsilon_{ijk}(dx_2)_j(dx_3)_k \ , \\
d^2 S_i &= -\tfrac{1}{2}\varepsilon_{ijk}(dx_3)_j(dx_1)_k \ , \\
d^3 S_i &= -\tfrac{1}{2}\varepsilon_{ijk}(dx_1)_j(dx_2)_k \ , \\
d^4 S_i &= -\tfrac{1}{2}\varepsilon_{ijk}\left[(dx_1)_j - (dx_3)_j\right]\left[(dx_2)_k - (dx_3)_k\right] \ ,
\end{aligned}
\tag{7.8}
$$

where the sum is the zero vector:

$$
\boxed{\ d^1 S_i + d^2 S_i + d^3 S_i + d^4 S_i = 0_i\ }\ .
\tag{7.9}
$$

In a damaged continuum we define a "*net cross section*" $\hat{S} \equiv \psi S$ where $\psi \le 1$ describes the "*continuity*" of the material, as mentioned in Section 4.3.1. Then, by analogy of (7.8), a tetrahedron in a *damaged continuum* (Fig. 7.1b) can be characterized by the following system of *bivectors*:

$$
\begin{aligned}
d^1 \hat{S}_i &= -\tfrac{1}{2}\alpha_{ijk}(dx_2)_j(dx_3)_k \equiv \alpha\, d^1 S_i \ , \\
d^2 \hat{S}_i &= -\tfrac{1}{2}\beta_{ijk}(dx_3)_j(dx_1)_k \equiv \beta\, d^2 S_i \ , \\
d^3 \hat{S}_i &= -\tfrac{1}{2}\gamma_{ijk}(dx_1)_j(dx_2)_k \equiv \gamma\, d^3 S_i \ , \\
d^4 \hat{S}_i &= -\tfrac{1}{2}\kappa_{ijk}\left[(dx_1)_j - (dx_3)_j\right]\left[(dx_2)_k - (dx_3)_k\right] \equiv \kappa\, d^4 S_i \ ,
\end{aligned}
\tag{7.10}
$$

where $\alpha_{ijk} \equiv \alpha\varepsilon_{ijk}$, $\beta_{ijk} \equiv \beta\varepsilon_{ijk}$, etc. are total skew-symmetric tensors of order three, which have the essential components $\alpha_{123} \equiv \alpha$, $\beta_{123} \equiv \beta$, etc., respectively.

¿From Fig. 7.1a,b we find that only

$$dS_1 = -n_1\, dS \,, \quad d^1\hat{S}_1 = \alpha\, d^1 S_1 \,, \quad d^2 S_2 = -n_2\, dS \,, \quad \text{etc.}$$

are non vanishing components of the *bivector* systems (7.8) and (7.10). Then the sum of (7.10) yields the vector

$$\Sigma_i \equiv d^1\hat{S}_i + \ldots + d^4\hat{S}_i = \begin{pmatrix} (\kappa - \alpha)n_1 \\ (\kappa - \beta)n_2 \\ (\kappa - \gamma)n_3 \end{pmatrix} dS \,, \tag{7.11}$$

which is not the zero vector, unless in the isotropic damage case ($\alpha = \beta = \gamma = \kappa$) or in the undamaged case ($\alpha = \beta = \gamma = \kappa = 1$) according to (7.9).

Furthermore, because of $d^1\hat{S}_1 \neq 0$, $d^1\hat{S}_2 = d^1\hat{S}_3 = 0$ etc., the damage state of the continuum at a point is characterized by the *bivectors*

$$\alpha_{1ij} = \begin{pmatrix} 0 & 0 & 0 \\ 0 & 0 & \alpha \\ 0 & -\alpha & 0 \end{pmatrix} \,, \quad \beta_{2ij} = \begin{pmatrix} 0 & 0 & -\beta \\ 0 & 0 & 0 \\ \beta & 0 & 0 \end{pmatrix} \,, \tag{7.12a,b}$$

$$\gamma_{3ij} = \begin{pmatrix} 0 & \gamma & 0 \\ -\gamma & 0 & 0 \\ 0 & 0 & 0 \end{pmatrix} \,. \tag{7.12c}$$

In the following we will examine if the *bivector*

$$\psi_{ij} = \alpha_{1ij} + \beta_{2ij} + \gamma_{3ij} = \begin{pmatrix} 0 & \gamma & -\beta \\ -\gamma & 0 & \alpha \\ \beta & -\alpha & 0 \end{pmatrix} \tag{7.13a}$$

$$\psi_{ij} = \alpha\varepsilon_{1ij} + \beta\varepsilon_{2ij} + \gamma\varepsilon_{3ij} \tag{7.13b}$$

could be a suitable *tensor of continuity*. Then the damage tensor ω would be of the form

$$\omega_{ij} = \delta_{(k)k}\varepsilon_{kij} - \psi_{ij} = \begin{pmatrix} 0 & 1-\gamma & -(1-\beta) \\ -(1-\gamma) & 0 & 1-\alpha \\ 1-\beta & -(1-\alpha) & 0 \end{pmatrix} \tag{7.14a}$$

(no sum on the bracketed index k) or

$$\omega_{ij} = (1-\alpha)\varepsilon_{1ij} + (1-\beta)\varepsilon_{2ij} + (1-\gamma)\varepsilon_{3ij} \ . \tag{7.14b}$$

If a tensor is symmetric or antisymmetric, respectively, in one cartesian coordinate system, it is symmetric or antisymmetric in all such systems; thus symmetry and antisymmetry are really tensor properties. Therefore, the skew-symmetric tensor (7.13a) has only three essential components in any cartesian system, for instance, α, β, γ in relation to the system x_i or α^*, β^*, γ^* with respect to the system x_i^*.

The only nonvanishing invariants of the *bivectors* (7.13) and (7.14) are determined by their lengths:

$$-J_2(\boldsymbol{\psi}) \equiv -\tfrac{1}{2}\,\mathrm{tr}\,\boldsymbol{\psi}^2 \equiv -\tfrac{1}{2}\psi_{ij}\psi_{ji} = \alpha^2 + \beta^2 + \gamma^2 \ , \tag{7.15}$$

$$-J_2(\boldsymbol{\omega}) = (1-\alpha)^2 + (1-\beta)^2 + (1-\gamma)^2 \ . \tag{7.16}$$

In the undamaged state ($\alpha = \beta = \gamma = 1$) we have

$$-J_2(\boldsymbol{\psi}) = 3 \ , \quad -J_2(\boldsymbol{\omega}) = 0 \ ,$$

and

$$\psi_{ij} \rightarrow \eta_{ij} \equiv \varepsilon_{1ij} + \varepsilon_{2ij} + \varepsilon_{3ij} = \begin{pmatrix} 0 & 1 & -1 \\ -1 & 0 & 1 \\ 1 & -1 & 0 \end{pmatrix} \ . \tag{7.17}$$

We see that the undamaged state does not yield an isotropic tensor, because the components of $\boldsymbol{\eta}$ in (7.17) transform under the change of the coordinate system.

Thus the bivector $\boldsymbol{\psi}$ defined by (7.13a,b) is not suitable to describe the state of *continuity* of a *damaged continuum*, and we have to find another tensor composed by the bivectors (7.12a,b,c). As shown below, a suitable *tensor of continuity* may be defined by

$$\boxed{\psi_{ijk} \equiv \psi_{i[jk]}} \quad \text{with} \quad \begin{cases} \psi_{1jk} \equiv \alpha_{1jk} = \alpha\varepsilon_{1jk} \\ \psi_{2jk} \equiv \beta_{2jk} = \beta\varepsilon_{2jk} \\ \psi_{3jk} \equiv \gamma_{3jk} = \gamma\varepsilon_{3jk} \end{cases} \ . \tag{7.18}$$

This tensor is skew-symmetric only with respect to the two bracketed indizes $[jk]$ and possesses the three essential components (α, β, γ), as illustrated in Fig. 7.2.
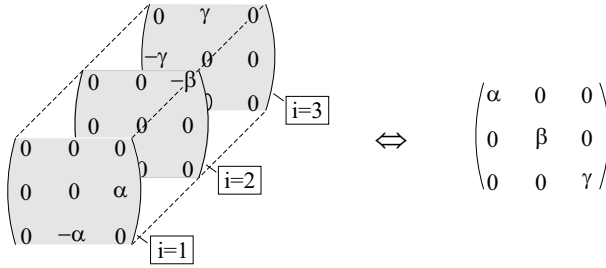
Fig. 7.2 Third-order tensor of continuity and its dual form

In the isotropic damage state ($\alpha = \beta = \gamma = \kappa$) the tensor (7.18) is total skew-symmetric, and the undamaged continuum ($\alpha = \beta = \gamma = 1$) is characterized by the third-order alternating tensor ε_{ijk}. Supplementary to (7.18) we introduce the "*damage tensor*"

$$\boxed{\omega_{ijk} \equiv \varepsilon_{ijk} - \psi_{ijk}} \quad \text{where} \quad \begin{cases} \omega_{1jk} = (1 - \alpha)\varepsilon_{1jk} \\ \omega_{2jk} = (1 - \beta)\varepsilon_{2jk} \\ \omega_{3jk} = (1 - \gamma)\varepsilon_{3jk} \end{cases} . \qquad (7.19)$$

By analogy of (7.1b) or (7.4a,b) the dual relations

$$\psi_{ijk} \equiv \psi_{i[jk]} = \varepsilon_{jkr}\psi_{ir} \quad \Leftrightarrow \quad \psi_{ir} = \tfrac{1}{2}\varepsilon_{rjk}\psi_{ijk} , \qquad (7.20)$$

$$\omega_{ijk} \equiv \omega_{i[jk]} = \varepsilon_{jkr}\omega_{ir} \quad \Leftrightarrow \quad \omega_{ir} = \tfrac{1}{2}\varepsilon_{rjk}\omega_{ijk} \qquad (7.21)$$

are valid.

Contrary to (7.13) and (7.14) the *dual tensor of continuity* ψ_{ij} according to (7.20) and the *dual damage tensor* ω_{ij} according to (7.21) have the diagonal forms

$$\boxed{\psi_{ij} = \operatorname{diag}\{\alpha,\ \beta,\ \gamma\}} \qquad (7.22)$$

and

$$\omega_{ij} = \operatorname{diag}\{(1 - \alpha),\ (1 - \beta),\ (1 - \gamma)\} , \qquad (7.23)$$

respectively. For the undamaged continuum ($\psi_{ijk} \to \varepsilon_{ijk}$) the dual tensor of continuity ψ_{ij} is equal to KRONECKER's tensor δ_{ij}, as we can see from (7.20) or immediately from (7.22). The relations (7.20) and (7.22) are illustrated in Fig. 7.2.

Especially, from Fig. 7.2 we can see the skew-symmetric character of the third order tensor of continuity indicated in (7.20) and its three essential

components α, β, γ. These values are fractions which represent the net cross-sectional elements perpendicular to the coordinate axes x_1, x_2, x_3 (Fig. 7.1b) and which can be measured in tests on specimens cut along three mutually perpendicular directions x_1, x_2, x_3.

According to (7.4a) a damaged surface element $d\hat{S}$ can be expressed in the dual form

$$d\hat{S}_{ij} = \varepsilon_{ijk}d\hat{S}_k \quad \Leftrightarrow \quad d\hat{S}_i = \tfrac{1}{2}\varepsilon_{ijk}d\hat{S}_{jk} \ , \tag{7.24}$$

and using the tensor of continuity (7.18) we find

$$d\hat{S}_{ij} = \psi_{ijk}dS_k \quad \Leftrightarrow \quad d\hat{S}_i = \tfrac{1}{2}\psi_{ijk}dS_{jk} \ . \tag{7.25}$$

Note that the bivector $d\hat{S}_{ij}$ or dS_{jk} in (7.25) must have the same indices with respect to which the tensor (7.18) is skew-symmetric. Combining (7.4a) and (7.25) we have the linear transformations

$$d\hat{S}_{ij} = \tfrac{1}{2}\psi_{ijpq}dS_{pq} \ , \quad d\hat{S}_i = \psi_{ir}dS_r \ , \tag{7.26a,b}$$

where ψ_{ir} is the tensor (7.20), (7.22), while ψ_{ijpq} is a fourth-order non-symmetric tensor defined as

$$\psi_{ijpq} \equiv \psi_{kij}\varepsilon_{kpq} \ , \tag{7.27a}$$

which, by using (7.20), can be expressed through

$$\psi_{ijpq} = (\delta_{ip}\delta_{jq} - \delta_{iq}\delta_{jp})\,\psi_{rr} - (\psi_{ip}\delta_{jq} - \psi_{iq}\delta_{jp}) - (\delta_{ip}\psi_{jq} - \delta_{iq}\psi_{jp}) \ . \tag{7.27b}$$

This tensor has the antisymmetric properties

$$\psi_{ijpq} = -\psi_{jipq} = -\psi_{ijqp} = \psi_{jiqp} \ , \tag{7.28}$$

and is symmetric only with respect to the index pairs, i.e.

$$\psi_{ijpq} = \psi_{pqij} \ . \tag{7.29}$$

More briefly, the properties of (7.28) and (7.29) can be indicated by

$$\psi_{ijpq} = \psi_{([ij][pq])} \ . \tag{7.30}$$

The essential components of the tensor (7.27) are given by

$$\psi_{ijpq} = \begin{cases} \alpha, \beta, \gamma, & \text{if } ij \text{ is an even permutation of } pq \\ -\alpha, -\beta, -\gamma, & \text{if } ij \text{ is an odd permutation of } pq, \\ 0, & \text{otherwise} \end{cases} \tag{7.31a}$$

which means

$$\psi_{2323} = \psi_{3232} \equiv \alpha \,, \quad \psi_{3131} = \psi_{1313} \equiv \beta \,,$$
$$\psi_{1212} = \psi_{2121} \equiv \gamma \,,$$
$$\psi_{3223} = \psi_{2332} \equiv -\alpha \,, \quad \psi_{1331} = \psi_{3113} \equiv -\beta \,,$$
$$\psi_{2112} = \psi_{1221} \equiv -\gamma \,. \tag{7.31b}$$

In the isotropic damage state ($\alpha = \beta = \gamma = \kappa$) the tensor (7.27) is proportional to KRONECKER's generalized delta

$$\delta_{ijpq} \equiv \varepsilon_{kij}\varepsilon_{kpq} = \begin{vmatrix} \delta_{kk} & \delta_{kp} & \delta_{kq} \\ \delta_{ik} & \delta_{ip} & \delta_{iq} \\ \delta_{jk} & \delta_{jp} & \delta_{jq} \end{vmatrix} = \delta_{ip}\delta_{jq} - \delta_{iq}\delta_{jp} \,,$$

and is identical to that one in the undamaged continuum characterized by ($\alpha = \beta = \gamma = 1$).

In order to construct the tensor of continuity (7.22) we can use the following way. In addition to Fig. 7.1 let us consider a fictitious undamaged
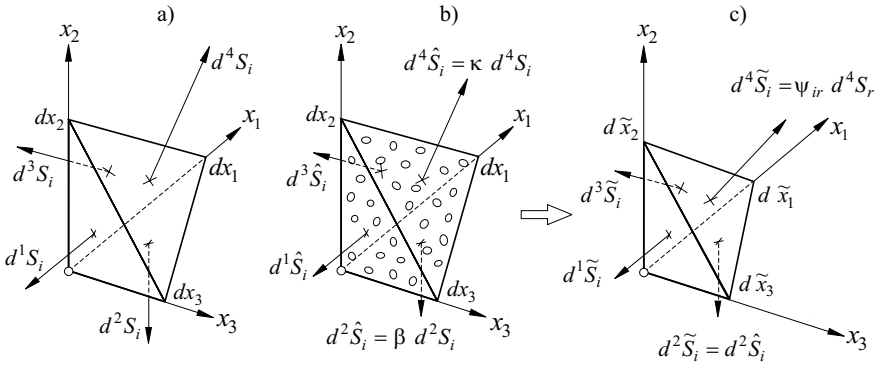
Fig. 7.3 CAUCHY's tetrahedron **a**) undamaged configuration, **b**) anisotropic damaged configuration, **c**) fictitious undamaged configuration

configuration as illustrated in Fig. 7.3c, which is, similar to (7.8) and (7.10), characterized by the following system of bivectors:

$$d^1\tilde{S}_i = -\tfrac{1}{2}\varepsilon_{ijk}(d\tilde{x}_2)_j(d\tilde{x}_3)_k \equiv d^1\hat{S}_i \,,$$
$$d^2\tilde{S}_i = -\tfrac{1}{2}\varepsilon_{ijk}(d\tilde{x}_3)_j(d\tilde{x}_1)_k \equiv d^2\hat{S}_i \,,$$
$$d^3\tilde{S}_i = -\tfrac{1}{2}\varepsilon_{ijk}(d\tilde{x}_1)_j(d\tilde{x}_2)_k \equiv d^3\hat{S}_i \,, \tag{7.32}$$
$$d^4\tilde{S}_i = -\tfrac{1}{2}\varepsilon_{ijk}\left[(d\tilde{x}_1)_j - (d\tilde{x}_3)_j\right]\left[(d\tilde{x}_2)_k - (d\tilde{x}_3)_k\right] \,,$$

where, by analogy of (7.9), the vector sum is equal to the zero vector:

$$\boxed{d^1\tilde{S}_i + d^2\tilde{S}_i + d^3\tilde{S}_i + d^4\tilde{S}_i = 0_i}\,. \tag{7.33}$$

The three area vectors $d^1\tilde{S}_i, \ldots, d^3\tilde{S}_i$ in (7.32) are identical to the corresponding vectors in (7.10) of the damaged configuration. The fourth vector $d^4\tilde{S}_i$ in (7.32), having the same magnitude as $d^4\hat{S}_i$ in (7.10), differ from the vector d^4S_i in (7.8) not only in length, but also in its direction. Therefore, the vectors $d^4\tilde{S}_i$ and d^4S_i are connected by a linear operator ψ of rank two (second order tensor):

$$\boxed{d^4\tilde{S}_i = \psi_{ir}d^4S_r}\,. \tag{7.34}$$

Comparing the three systems of bivectors (7.8), (7.10), (7.32) and using the equations (7.9), (7.33) in connection with the transformation (7.34), we find the relation:

$$\psi_{ir}\varepsilon_{rjk}\left[(dx_2)_j(dx_3)_k + (dx_3)_j(dx_1)_k + (dx_1)_j(dx_2)_k\right]$$
$$= \alpha_{ijk}(dx_2)_j(dx_3)_k + \beta_{ijk}(dx_3)_j(dx_1)_k + \gamma_{ijk}(dx_1)_j(dx_2)_k\,, \tag{7.35}$$

where the transvection $\psi_{ir}\varepsilon_{rjk}$ leads to the third-order tensor of continuity:

$$\psi_{ir}\varepsilon_{rjk} \equiv \psi_{ijk} = \psi_{i[jk]}\,, \tag{7.36}$$

which is skew-symmetric with respect to the bracketed index pair $[jk]$. The result (7.36) is contained in (7.18) and (7.20).

Because of $\alpha_{ijk} \equiv \alpha\varepsilon_{ijk}$, etc. the terms on the right-hand side of (7.35) are vectors with magnitudes

$$\left|d^1\tilde{S}_i\right| = \tfrac{1}{2}\alpha_{1jk}(dx_2)_j(dx_3)_k\,, \quad \text{etc.}$$

and with the directions of the basis vectors ${}^1e_i, {}^2e_i, {}^3e_i$ of the cartesian coordinate system. Therefore, in connection with (7.36), relation (7.35) can be written in the following form:

$$\psi_{ijk}\left[(dx_2)_j(dx_3)_k + \ldots\right] = {}^1e_i\alpha_{1jk}(dx_2)_j(dx_3)_k + \ldots\,, \tag{7.37}$$

from which we immediately read the decomposition:

$$\psi_{ijk} = {}^1e_i\alpha_{1jk} + {}^2e_i\beta_{2jk} + {}^3e_i\gamma_{3jk}\,, \tag{7.38a}$$

or because of $\alpha_{1jk} \equiv \alpha\varepsilon_{1jk}$, etc.:

$$\psi_{ijk} = \alpha^1 e_i \varepsilon_{1jk} + \beta^2 e_i \varepsilon_{2jk} + \gamma^3 e_i \varepsilon_{3jk} \; . \tag{7.38b}$$

By analogy of (7.1b) we find the dual relation from (7.36):

$$\psi_{ijk} = \psi_{i[jk]} = \varepsilon_{jkr}\psi_{ir} \quad \Leftrightarrow \quad \psi_{ir} = \tfrac{1}{2}\varepsilon_{rjk}\psi_{ijk} \; , \tag{7.39}$$

and finally the diagonal form:

$$\psi_{ir} = \tfrac{1}{2}\psi_{ipq}\varepsilon_{jpq} = \mathrm{diag}\{\alpha, \beta, \gamma\} \tag{7.40a}$$

in accordance with (7.22). Inserting the decomposition (7.38b) into (7.40a) and replacing $\delta_{1j} \equiv {}^1e_j$, etc., we see that the second rank tensor of continuity can be decomposed in terms of dyadics formed from the basis vectors:

$$\psi_{ij} = \alpha \left({}^1\boldsymbol{e} \otimes {}^1\boldsymbol{e}\right)_{ij} + \beta \left({}^2\boldsymbol{e} \otimes {}^2\boldsymbol{e}\right)_{ij} + \gamma \left({}^3\boldsymbol{e} \otimes {}^3\boldsymbol{e}\right)_{ij} \; . \tag{7.40b}$$

The relations (7.39) and (7.40a) are illustrated in Fig. 7.2. Especially, from Fig. 7.2 we can see the skew-symmetric character of a third-order tensor of continuity indicated in (7.36) and its three essential components (α, β, γ). These values are fractions which represent the net cross-sectional elements perpendicular to the coordinate axes x_1, x_2, x_3 (Fig. 7.3b) and which can be measured in tests on specimens cut along three mutually perpendicular directions x_1, x_2, x_3. Such experiments are carried out by BETTEN and his coworkers as discussed in Chapter 13.

The damage may sometimes develop *isotropically*, as observed by JOHN-SON (1960) for R.R. 59 Al alloy. In this special case ($\alpha = \beta = \gamma \equiv \psi$), the second rank tensor of continuity (7.39) is a *spherical tensor*:

$$\psi_{ijk} = \psi\varepsilon_{jkr}\delta_{ir} = \psi\varepsilon_{ijk} \quad \Leftrightarrow \quad \psi_{ir} = \tfrac{1}{2}\psi\varepsilon_{rjk}\varepsilon_{ijk} = \psi\delta_{ir} \tag{7.41}$$

and, contrary to (7.39), the third order tensor of continuity is now totally skew-symmetric ($\psi_{ijk} \equiv \psi_{[ijk]}$).

Instead of the continuity tensor ψ according to (7.39) we can use the damage tensor $\boldsymbol{\omega}$ defined by (7.19), (7.23) and characterized by the dual relation (7.21). In view of polynominal representations of constitutive equations it is convenient to use the tensor (4.84), as discussed in Section 4.3.2 in more detail.

7.2 Stresses in a Damaged Continuum

In the undamaged continuum (Fig. 7.4a) CAUCHY's formula

$$p_i = \sigma_{ji} n_j \tag{7.42}$$

is derived from equilibrium, where p_i and n_i are the components of the stress vector $\boldsymbol{p}$ and the unit vector normal $\boldsymbol{n}$, respectively. In the same way we get to the corresponding relation for a *damaged continuum*,

$$\hat{p}_i \psi(n) = \psi_{jk} \hat{\sigma}_{ki} n_j \ , \tag{7.43}$$

where ψ_{jk} are the components of the continuity tensor $\boldsymbol{\psi}$ according to (7.22).
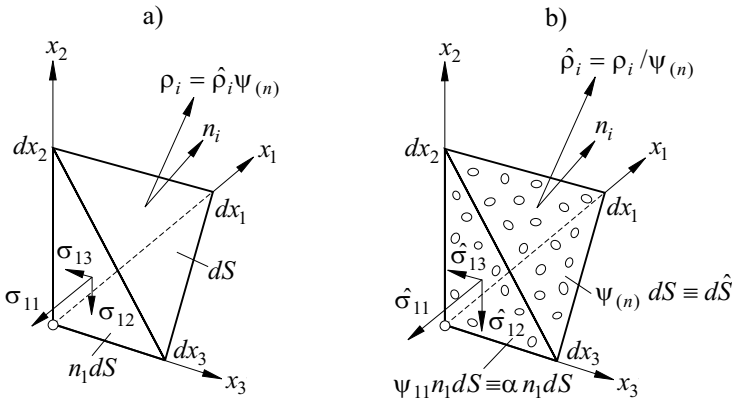
Fig. 7.4 Stress tensor regarding **a**) an undamaged, **b**) a damaged continuum

The surface elements dS and $d\hat{S}$ in Fig. 7.4 are subjected to the *same* force vector:

$$dP_i = p_i \, dS \equiv \hat{p}_i \, d\hat{S} = d\hat{P}_i \ . \tag{7.44}$$

Thus, considering (7.42) and (7.43), we finally find the actual *net-stress tensor* $\hat{\boldsymbol{\sigma}}$ as a transformation from CAUCHY's tensor:

$$\sigma_{ij} = \psi_{ir} \hat{\sigma}_{rj} = \sigma_{ji} \quad \Leftrightarrow \quad \hat{\sigma}_{ij} = \psi_{ir}^{(-1)} \sigma_{rj} \neq \hat{\sigma}_{ji} \ . \tag{7.45}$$

By suitable transvections we find $\sigma_{ij} \hat{\sigma}_{jk}^{(-1)} = \psi_{ik}$ and $\hat{\sigma}_{ij} \sigma_{jk}^{(-1)} = \psi_{ik}^{(-1)}$.

As indicated in (7.45), the actual net-stress tensor $\hat{\boldsymbol{\sigma}}$ is *non-symmetric*, unless we have isotropic damage expressed by $\psi_{ir} = \psi \delta_{ir}$.

Because of the symmetry $\sigma_{ij} = (\sigma_{ij} + \sigma_{ji})/2$ of CAUCHY's *stress tensor* $\boldsymbol{\sigma}$ we find the representations

$$\sigma_{ij} = \tfrac{1}{2} \left(\psi_{ip} \delta_{jq} + \delta_{iq} \psi_{jp} \right) \hat{\sigma}_{pq} \equiv \varphi_{ijpq} \hat{\sigma}_{pq} \ , \tag{7.46a}$$

$$\hat{\sigma}_{ij} = \tfrac{1}{2} \left(\psi_{ip}^{(-1)} \delta_{jq} + \psi_{iq}^{(-1)} \delta_{jp} \right) \sigma_{pq} \equiv \Phi_{ijpq} \sigma_{pq} \tag{7.46b}$$

from (7.45). We see that the fourth-order tensors φ and Φ defined as (7.46a,b) are only symmetric with respect to two indices:

$$\varphi_{ijpq} = \varphi_{jipq} , \qquad\qquad \Phi_{ijpq} = \Phi_{ijqp} , \tag{7.47a,b}$$

that is, the *actual net-stress tensor* $\hat{\sigma}$ is non-symmetric in the anisotropic damage case:

$$\frac{\hat{\sigma}_{12}}{\hat{\sigma}_{21}} = \frac{\beta}{\alpha} , \qquad\qquad \frac{\hat{\sigma}_{23}}{\hat{\sigma}_{32}} = \frac{\gamma}{\beta} , \qquad\qquad \frac{\hat{\sigma}_{31}}{\hat{\sigma}_{13}} = \frac{\alpha}{\gamma} . \tag{7.48}$$

This fact is a disadvantage, and it is awkward to use the actual net-stress tensor $\hat{\sigma}$ in constitutive equations with a symmetric strain rate tensor d. Therefore, we introduce a *transformed net-stress tensor* t defined by the operation

$$t_{ij} = \tfrac{1}{2} \left(\hat{\sigma}_{ik} \psi_{kj}^{(-1)} + \psi_{ki}^{(-1)} \hat{\sigma}_{jk} \right) , \tag{7.49}$$

which is *symmetric*. Inserting (7.46b) into (7.49) we have

$$\boxed{t_{ij} = C_{ijpq}^{(-1)} \sigma_{pq}} , \tag{7.50}$$

where

$$C_{ijpq}^{(-1)} = \tfrac{1}{2} \left(\psi_{ip}^{(-1)} \psi_{jq}^{(-1)} + \psi_{iq}^{(-1)} \psi_{jp}^{(-1)} \right) \tag{7.51}$$

is a symmetric fourth-order tensor

$$C_{ijpq}^{(-1)} = C_{jipq}^{(-1)} = C_{ijqp}^{(-1)} = C_{pqij}^{(-1)} , \tag{7.52}$$

which is identical to the tensor D_{ijpq} in (4.94). In the undamaged ($\psi \to \delta$) and total damaged state ($\psi \to 0$) we have

$$C_{ijpq}^{(-1)} \to E_{ijpq} \quad \Rightarrow \quad t_{ij} \to \sigma_{ij} \tag{7.53}$$

and

$$C_{ijpq}^{(-1)} \to \infty_{ijpq} \quad \Rightarrow \quad t_{ij} \to \infty_{ij} (\text{singular}) , \tag{7.54}$$

respectively, where

$$E_{ijpq} = \tfrac{1}{2} \left(\delta_{ip} \delta_{jq} + \delta_{iq} \delta_{jp} \right) \tag{7.55}$$

is the zero power tensor of rank four.

The inverse form of (7.50) is given by

$$\boxed{\sigma_{ij} = C_{ijpq}t_{pq}} \ , \tag{7.56}$$

where

$$C_{ijpq} = \tfrac{1}{2}\left(\psi_{ip}\psi_{jq} + \psi_{iq}\psi_{jp}\right) \tag{7.57}$$

is a symmetric fourth-order tensor of continuity,

$$C_{ijpq} = C_{jipq} = C_{ijqp} = C_{pqij} \ , \tag{7.58}$$

which is connected with the tensor (7.51) by the relation

$$C_{ijpq}C^{(-1)}_{pqk\ell} = C^{(-1)}_{ijpq}C_{pqk\ell} = C^{(0)}_{ijk\ell} \equiv E_{ijk\ell} \ . \tag{7.59}$$

Because of the symmetry properties (7.52) and (7.58) the fourth-order tensor of continuity (7.57) and its inversion (7.51) can be represented by 6×6 square matrices, which, because of (7.40a,b), have the diagonal forms:

$$C_{ijk\ell} = \mathrm{diag}\left\{C_{1111},\, C_{2222},\, C_{3333},\, C_{1212},\, C_{2323},\, C_{3131}\right\} \ , \tag{7.60a}$$
$$C_{ijk\ell} = \mathrm{diag}\left\{\alpha^2,\, \beta^2,\, \gamma^2,\, \tfrac{1}{2}\alpha\beta,\, \tfrac{1}{2}\beta\gamma,\, \tfrac{1}{2}\gamma\alpha\right\} \ , \tag{7.60b}$$

and

$$C^{(-1)}_{ijk\ell} = \mathrm{diag}\left\{C^{(-1)}_{1111},\, C^{(-1)}_{2222},\, C^{(-1)}_{3333},\, C^{(-1)}_{1212},\, C^{(-1)}_{2323},\, C^{(-1)}_{3131}\right\} \ , \tag{7.61a}$$
$$C^{(-1)}_{ijk\ell} = \mathrm{diag}\left\{\frac{1}{\alpha^2},\, \frac{1}{\beta^2},\, \frac{1}{\gamma^2},\, \frac{2}{\alpha\beta},\, \frac{2}{\beta\gamma},\, \frac{2}{\gamma\alpha}\right\} \ , \tag{7.61b}$$

that is, the components of the *pseudo-net stress tensor t*, according to (7.50), are given in the following manner:

$$
\begin{aligned}
&t_{11} = \frac{1}{\alpha^2}\sigma_{11} \ , &\quad &t_{12} = \frac{1}{\alpha\beta}\sigma_{12} \ , &\quad &t_{13} = \frac{1}{\alpha\gamma}\sigma_{13} \ , \\[2mm]
&t_{21} = t_{12} \ , &\quad &t_{22} = \frac{1}{\beta^2}\sigma_{22} \ , &\quad &t_{23} = \frac{1}{\beta\gamma}\sigma_{23} \ , \\[2mm]
&t_{31} = t_{13} \ , &\quad &t_{32} = t_{23} \ , &\quad &t_{33} = \frac{1}{\gamma^2}\sigma_{33} \ .
\end{aligned}
\tag{7.62}
$$

The results (7.50) and (7.56) can also be found in the following way. Using the linear transformations

$$t_{ij} = \tfrac{1}{2} \left(\delta_{ir} \psi_{js}^{(-1)} + \psi_{is}^{(-1)} \delta_{jr} \right) \hat{\sigma}_{rs} \tag{7.63}$$

and

$$\hat{\sigma}_{pq} = \tfrac{1}{2} \left(\delta_{pr} \psi_{qs} + \delta_{ps} \psi_{qr} \right) t_{rs} \ , \tag{7.64}$$

which connect a fictitious symmetric tensor t with the actual non-symmetric net stress tensor $\hat{\boldsymbol{\sigma}}$, we immediately find (7.50) by inserting (7.46b) into (7.63) and (7.56) by inserting (7.64) into (7.46a), respectively.

Because of the non-symmetric property of the actual net-stress tensor we find from (7.64) the decomposition

$$\hat{\sigma}_{pq} = \hat{\sigma}_{(pq)} + \hat{\sigma}_{[pq]} \ , \tag{7.65}$$

where the symmetric and antisymmetric parts are given by

$$\hat{\sigma}_{(pq)} = \left(t_{pr} \psi_{rq} + \psi_{pr} t_{rq} \right) / \, 2 \tag{7.66}$$

and

$$\hat{\sigma}_{[pq]} = \left(t_{pr} \psi_{rq} - \psi_{pr} t_{rq} \right) / \, 2 \ , \tag{7.67}$$

respectively. In the special case of isotropic damage ($\psi_{ij} = \psi \delta_{ij}$) we have $\hat{\sigma}_{(pq)} = \psi t_{pq}$ and $\hat{\sigma}_{[pq]} = 0_{pq}$.

An interpretation of the introduced pseudo-net stress tensor (7.49) can be given in the following way. An alternative form of CAUCHY's formula (7.42) is

$$dP_i = \sigma_{ji} \, dS_j \ , \tag{7.68}$$

where dP_i is the actual force vector (7.44), and according to (7.26b) we can write

$$dP_i = \sigma_{ji} \psi_{jr}^{(-1)} \, d\hat{S}_r \ , \tag{7.69a}$$

or inserting (7.56) we find the relation

$$dP_i = \psi_{ip} t_{pr} \, d\hat{S}_r \ , \tag{7.69b}$$

which can be multiplied by $\psi_{ki}^{(-1)}$, so that we have

$$\psi_{ki}^{(-1)} \, dP_i = t_{kr} \, d\hat{S}_r \ , \tag{7.70a}$$

or after changing the indices:

$$\psi_{ik}^{(-1)} \, dP_k \equiv d\tilde{P}_i = t_{ji} \, d\hat{S}_j \ . \tag{7.70b}$$

Comparing (7.68) and (7.70b) we see that (7.70b) can be interpreted as CAUCHY's formula for the damaged configuration, which is subjected to the pseudo-force $d\tilde{P}_i \equiv \psi_{ik}^{(-1)} \, dP_k$ instead to the actual force dP_i.

Because of the non-symmetric properties of the "net-stress tensor" $\hat{\sigma}$ and the operator φ, i.e.,

$$\hat{\sigma}_{ij} = \tfrac{1}{2} \left(\hat{\sigma}_{ij} + \hat{\sigma}_{ji} \right) + \tfrac{1}{2} \left(\hat{\sigma}_{ij} - \hat{\sigma}_{ji} \right) \tag{7.71}$$

and

$$\varphi_{ijpq} = \tfrac{1}{2} \left(\varphi_{ijpq} + \varphi_{ijqp} \right) + \tfrac{1}{2} \left(\varphi_{ijpq} - \varphi_{ijqp} \right) , \tag{7.72}$$

respectively, we find, from (7.46a), the decompositions:

$$\begin{aligned}
\sigma_{ij} = \ & \tfrac{1}{4} \left(\varphi_{ijpq} + \varphi_{ijqp} \right) \left(\hat{\sigma}_{pq} + \hat{\sigma}_{qp} \right) \\
& + \tfrac{1}{4} \left(\varphi_{ijpq} - \varphi_{ijqp} \right) \left(\hat{\sigma}_{pq} - \hat{\sigma}_{qp} \right) ,
\end{aligned} \tag{7.73a}$$

$$\begin{aligned}
\sigma_{ij} = \ & \tfrac{1}{8} \left(\psi_{ip}\delta_{jq} + \psi_{jp}\delta_{iq} + \psi_{iq}\delta_{jp} + \psi_{jq}\delta_{ip} \right) \left(\hat{\sigma}_{pq} + \hat{\sigma}_{qp} \right) \\
& + \tfrac{1}{8} \left(\psi_{ip}\delta_{jq} + \psi_{jp}\delta_{iq} - \psi_{iq}\delta_{jp} - \psi_{jq}\delta_{ip} \right) \left(\hat{\sigma}_{pq} - \hat{\sigma}_{qp} \right) .
\end{aligned} \tag{7.73b}$$

Because of (7.47a) the right-hand sides in (7.73a) and (7.73b) are symmetric with respect to the indices i and j. Furthermore, we see the symmetry with respect to the indices p and q. This fact can be seen immediately from (7.46a). In the special case of isotropic damage, i.e., $\psi_{ij} = \psi\delta_{ij}$ or $\hat{\sigma}_{pq} = \hat{\sigma}_{qp}$, the second term of the right-hand side in (7.73b) vanishes. Then, equation (7.73b) is identical to those formulated by RABOTNOV (1969).

In a similar way, from (7.46b) we find the decomposition of the "net stress tensor" $\hat{\sigma}$ into a symmetric and an antisymmetric part:

$$\hat{\sigma}_{ij} = \tfrac{1}{2} \left(\Phi_{ijpq} + \Phi_{jipq} \right) \sigma_{pq} + \tfrac{1}{2} \left(\Phi_{ijpq} - \Phi_{jipq} \right) \sigma_{pq} , \tag{7.74a}$$

$$\begin{aligned}
\hat{\sigma}_{ij} = \ & \tfrac{1}{4} \left(\psi_{ip}^{(-1)}\delta_{jq} + \psi_{iq}^{(-1)}\delta_{jp} + \psi_{jp}^{(-1)}\delta_{iq} + \psi_{jq}^{(-1)}\delta_{ip} \right) \sigma_{pq} \\
& + \tfrac{1}{4} \left(\psi_{ip}^{(-1)}\delta_{jq} + \psi_{iq}^{(-1)}\delta_{jp} - \psi_{jp}^{(-1)}\delta_{iq} - \psi_{jq}^{(-1)}\delta_{ip} \right) \sigma_{pq} .
\end{aligned} \tag{7.74b}$$

The results given above may be expressed by the damage tensor ω. For instance, from (7.27a,b) in connection with (7.19) and because of the substitution $\psi_{ij} \equiv \delta_{ij} - \omega_{ij}$ we have

$$\psi_{ijpq} = \delta_{ijpq} - \omega_{kij}\varepsilon_{kpq} \equiv \left(\varepsilon_{kij} - \omega_{kij} \right) \varepsilon_{kpq} , \tag{7.75a}$$

$$\begin{aligned}
\psi_{ijpq} = \ & \left(\delta_{ip}\delta_{jq} - \delta_{iq}\delta_{jp} \right) \left(1 - \omega_{rr} \right) + \left(\omega_{ip}\delta_{jq} - \omega_{iq}\delta_{jp} \right) \\
& + \left(\delta_{ip}\omega_{jq} - \delta_{iq}\omega_{jp} \right) .
\end{aligned} \tag{7.75b}$$

Furthermore, instead of (7.46a) and (7.73b) we find

$$\sigma_{ij} = \tfrac{1}{2} \left[\delta_{ip}\delta_{jq} + \delta_{iq}\delta_{jp} - (\omega_{ip}\delta_{jq} + \delta_{iq}\omega_{jp}) \right] \hat{\sigma}_{pq} \tag{7.76a}$$

and

$$\begin{aligned} \sigma_{ij} = {} & \tfrac{1}{2} \left(\hat{\sigma}_{ij} + \hat{\sigma}_{ji} \right) \\ & - \tfrac{1}{8} \left(\omega_{ip}\delta_{jq} + \delta_{iq}\omega_{jp} + \omega_{iq}\delta_{jp} + \delta_{ip}\omega_{jq} \right) \left(\hat{\sigma}_{pq} + \hat{\sigma}_{qp} \right) \\ & - \tfrac{1}{8} \left(\omega_{ip}\delta_{jq} + \delta_{iq}\omega_{jp} - \omega_{iq}\delta_{jp} - \delta_{ip}\omega_{jq} \right) \left(\hat{\sigma}_{pq} - \hat{\sigma}_{qp} \right) . \end{aligned} \tag{7.76b}$$

By using the inverse

$$\psi_{ir}^{(-1)} \equiv \frac{1}{2 \det(\psi)} \varepsilon_{rqp}\varepsilon_{ik\ell}\psi_{pk}\psi_{q\ell} \tag{7.77}$$

and because of the symmetry $\sigma_{ij} = (\sigma_{ij} + \sigma_{ji})/2$, we find the following relations for the net stress tensor:

$$\begin{aligned} \hat{\sigma}_{ij} = {} & \frac{1}{2 \det(\boldsymbol{\delta} - \boldsymbol{\omega})} \left[(\delta_{is}\delta_{jt} + \delta_{it}\delta_{js})(1 - \omega_{rr}) \right. \\ & \left. + (\omega_{is}\delta_{jt} + \omega_{it}\delta_{js}) + \tfrac{1}{2}\varepsilon_{ik\ell} \left(\varepsilon_{spq}\delta_{jt} + \varepsilon_{tpq}\delta_{js} \right) \omega_{pk}\omega_{q\ell} \right] \sigma_{st} , \end{aligned} \tag{7.78a}$$

$$\begin{aligned} = {} & \frac{1}{\det(\boldsymbol{\delta} - \boldsymbol{\omega})} \left[(1 - \omega_{rr})\sigma_{ij} + \omega_{ir}\sigma_{rj} \right. \\ & \left. + \tfrac{1}{2}\varepsilon_{ik\ell}\varepsilon_{spq}\omega_{pk}\omega_{q\ell}\sigma_{sj} \right] , \end{aligned} \tag{7.78b}$$

$$\begin{aligned} = {} & \frac{1}{\det(\boldsymbol{\delta} - \boldsymbol{\omega})} \left\{ \left[1 - J_1(\boldsymbol{\omega}) - J_2(\boldsymbol{\omega}) \right] \sigma_{ij} \right. \\ & \left. + \left[1 - J_1(\boldsymbol{\omega}) \right] \omega_{ir}\sigma_{rj} + \omega_{ir}^{(2)}\sigma_{rj} \right\} , \end{aligned} \tag{7.78c}$$

where

$$J_1(\boldsymbol{\omega}) \equiv \delta_{ij}\omega_{ji} , \qquad J_2(\boldsymbol{\omega}) \equiv \tfrac{1}{2} \left(\omega_{ij}\omega_{ji} - \omega_{ii}\omega_{jj} \right) \tag{7.79a,b}$$

are invariants of the damage tensor $\boldsymbol{\omega}$.

Finally, we consider CAUCHYS stress equations of equilibrium,

$$\sigma_{ji,j} = 0_i , \tag{7.80}$$

in the absence of the body forces. Then by using the transformation (7.45), we have the equilibrium equations in the net stresses:

$$\hat{\sigma}_{ri}\psi_{jr,j} + \psi_{jr}\hat{\sigma}_{ri,j} = 0_i \ . \tag{7.81}$$

The symmetry of CAUCHY's stress tensor ($\sigma_{ij} = \sigma_{ji}$) resulting from moment equilibrium yields the condition

$$\psi_{ip}\hat{\sigma}_{pj} = \psi_{jq}\hat{\sigma}_{qi} \quad \text{or} \quad \hat{\sigma}_{ij} = \psi_{iq}^{(-1)}\psi_{jp}\hat{\sigma}_{pq} \ , \tag{7.82a,b}$$

which states that the net stress tensor is non-symmetric. From (7.82b) we find the decomposition into a symmetric part and an antisymmetric one:

$$\begin{aligned}
\hat{\sigma}_{ij} = {} & \tfrac{1}{4}\left(\psi_{iq}^{(-1)}\psi_{jp} + \psi_{ip}^{(-1)}\psi_{jq}\right)(\hat{\sigma}_{pq} + \hat{\sigma}_{qp}) \\
& + \tfrac{1}{4}\left(\psi_{iq}^{(-1)}\psi_{jp} - \psi_{ip}^{(-1)}\psi_{jq}\right)(\hat{\sigma}_{pq} + \hat{\sigma}_{qp}) \ .
\end{aligned} \tag{7.83}$$

For the isotropic damage case ($\psi_{ij} = \psi\delta_{ij}$), the relation (7.83) is equal to the decomposition

$$\hat{\sigma}_{ij} = (\hat{\sigma}_{ji} + \hat{\sigma}_{ij})/2 + (\hat{\sigma}_{ji} - \hat{\sigma}_{ij})/2 \equiv \hat{\sigma}_{ji} \ , \tag{7.84}$$

i.e., the *net stress tensor* is symmetric in this special case only.

7.3 Damage Effective Stress Concepts

During the last two or three decades many scientists have devoted much effort to the stress analysis in a damaged material, and the notation *damage effective stress* has been introduced. In the following some various *damage effective stress concepts* should be reviewed.

In the case of damage being isotropic measured in terms of a single *scalar parameter* $\omega(0 \leq \omega \leq 1)$, the *effective stress tensor* $\bar{\sigma}$ is expressed in the form

$$\boxed{\bar{\boldsymbol{\sigma}} = \boldsymbol{\sigma}/(1-\omega)} \qquad \textbf{(model I)}$$

where $\boldsymbol{\sigma}$ denotes the CAUCHY *stress tensor*. This assumption leads to simple models of mechanical behavior coupling damage and is adequate in some cases, especially under conditions of proportional loading (LEMAITRE, 1984,1992) or in some materials (JOHNSON, 1960). However, many scientists (HAYHURST, 1972; LECKIE and HAYHURST, 1974; LEE, PENG and WANG, 1985; CHOW and WANG, 1987; 1988) experimentally observed that all initially isotropic or anisotropic materials under conditions of nonproportional loading and most brittle materials even though under conditions

of proportional loading develop *anisotropic damage*, for which the *damage variables* can no longer be *scalars*, but are of *tensorial nature* (LECKIE and ONAT, 1981). The damage variables are then *vectors*, *second-order* or *fourth-order tensors* (BETTEN, 2001b). ONAT (1986), ONAT and LECKIE (1988) and ADAMS et al. (1992) showed that the damage variables in isothermal mechanical behavior are irreducible tensors of even orders.

MURAKAMI and OHNO (1981) derived an *asymmetric effective stress tensor*,

$$\boldsymbol{\sigma}^* = \boldsymbol{\sigma}(\mathbf{1} - \boldsymbol{\omega})^{-1} \,,$$

where $\mathbf{1}$ denotes the second-order identity tensor and $\boldsymbol{\omega}$ is a symmetric second-order damage tensor. Only the symmetric part of $\boldsymbol{\sigma}^*$, i.e.,

$$\boxed{\bar{\boldsymbol{\sigma}} = \left[\boldsymbol{\sigma}(\mathbf{1} - \boldsymbol{\omega})^{-1} + (\mathbf{1} - \boldsymbol{\omega})^{-1}\boldsymbol{\sigma}\right]/2} \qquad \textbf{(model II)} \,,$$

has been considered by MURAKAMI (1988) in constitutive equations.

CHOW and WANG (1987) postulated an alternative model of the effective stress tensor in the damage principal coordinate system, which was applied in elasticity, plasticity and ductile fracture (CHOW and WANG, 1987; 1988; KATTAN and VOYIADJIS, 1990; VOYIADJIS and KATTAN, 1990) . It is easy to show that this model coincides with the following *tensorial* expression:

$$\boxed{\bar{\boldsymbol{\sigma}} = (\mathbf{1} - \boldsymbol{\omega})^{-1/2}\boldsymbol{\sigma}(\mathbf{1} - \boldsymbol{\omega})^{-1/2}} \qquad \textbf{(model III)} \,.$$

In particular, if $\boldsymbol{\sigma}$ and $\boldsymbol{\omega}$ are *coaxial* in their principal directions, then they are commutative, $\boldsymbol{\sigma}\boldsymbol{\omega} = \boldsymbol{\omega}\boldsymbol{\sigma}$, and both models, II and III, reduce to:

$$\boxed{\bar{\boldsymbol{\sigma}} = (\mathbf{1} - \boldsymbol{\omega})^{-1}\boldsymbol{\sigma} = \boldsymbol{\sigma}(\mathbf{1} - \boldsymbol{\omega})^{-1}} \qquad \textbf{(model IV)} \,.$$

This model is the tensorial generalization of those proposed by SIDOROFF (1981), LECKIE and HAYHURST (1974), and LEE et al. (1985) in the principal coordinate system.

In each of the above discussed **models I-IV** the effective stress tensor $\bar{\boldsymbol{\sigma}}$ depends *linear* on the CAUCHY stress tensor $\boldsymbol{\sigma}$. In general, the fourth-order tensor $\boldsymbol{M}$ as a *linear transformation* in the relation

$$\bar{\boldsymbol{\sigma}} = \boldsymbol{M}[\boldsymbol{\sigma}] \quad \text{or} \quad \bar{\sigma}_{ij} = M_{ijk\ell}\sigma_{k\ell}$$

is named the *damage effective tensor* (ZHENG and BETTEN, 1996). Originally, RABOTNOV (1968) had not considered the relation $\bar{\boldsymbol{\sigma}} = M[\boldsymbol{\sigma}]$ but

defined a symmetric *net-stress tensor* $\hat{\boldsymbol{\sigma}}$ by way of a linear transformation $\boldsymbol{\sigma} = \boldsymbol{\Omega}[\hat{\boldsymbol{\sigma}}]$ or in index notation according to (4.78), where the fourth-order tensor $\boldsymbol{\Omega}$ is assumed to be symmetric.

However, BETTEN (1982b) has pointed out in more detail that the fourth-order tensor $\boldsymbol{\Omega}$ in the linear transformation $\boldsymbol{\sigma} = \boldsymbol{\Omega}[\hat{\boldsymbol{\sigma}}]$ and consequently the *net-stress tensor* $\hat{\boldsymbol{\sigma}}$ cannot be symmetric if the damage develops *anisotropically*. Instead of $\hat{\boldsymbol{\sigma}}$, BETTEN (1983b) introduced a *transformed* net-stress tensor $\boldsymbol{t}$, called *pseudo-net-stress tensor*, as an effective stress tensor,

$$\boxed{\bar{\boldsymbol{\sigma}} = (\mathbf{1} - \boldsymbol{\omega})^{-1} \boldsymbol{\sigma} (\mathbf{1} - \boldsymbol{\omega})^{-1}} \qquad \textbf{(model V)} \; ,$$

which is *symmetric* even in cases of *anisotropic damage*. This model can be expressed in index notation according to (7.50) with (7.51), if we take the relation (4.84) into account.

Because of the broad applicability and versatility of **model V** to engineering problems (BETTEN, 1986a; 1991b; 1998), this model has been developed step by step and discussed in more detail in Section 7.2.

It must be emphasized that there is no substantive difference between **models V** and **III** since both tensors $(\mathbf{1} - \boldsymbol{\omega})$ and $(\mathbf{1} - \boldsymbol{\omega})^{1/2}$ are positive-definite second-order symmetric tensors and are phenomenological measures of the anisotropic damage state. Furthermore, it has been pointed out by ZHENG and BETTEN (1996) that the difference between **models II** and **III** is negligible, if the damage is not highly developed.

Besides the concepts of *damage effective stress* (**models I-V**) various *damage equivalence principles* play an important role in the development of continuum damage mechanics. For instance, the *strain equivalence hypothesis* (LEMAITRE, 1985; 1992; CHABOCHE, 1988; LEMAITRE and CHABOCHE, 1990; BETTEN, 2001a; 2001c; OMERSPAHIC and MATTIASSON, 2007) states that a damaged material element under the applied stress $\boldsymbol{\sigma}$ exhibits the same strain response as the undamaged one submitted to the effective stress $\bar{\boldsymbol{\sigma}}$. Unfortunately, this hypothesis leads to asymmetric effective compliance and stiffness matrices if *anisotropic damage* develops. To remove this inconsistency, SIDOROFF (1981) proposed the *complementary energy equivalence hypothesis* by replacing the equivalence for strain response with the equivalence for *complementary energy*. We particularly stress that the concept of effective stress becomes meaningful, only if either the *strain* or *complementary equivalence hypothesis* (as well as some other additional equivalence hypotheses for yield criterion function, failure criterion function, etc.) is employed.

Assume that the damage state can be characterized in terms of a set $\Re$ of scalars, vectors, and/or tensors of different orders, which operate as internal variables. The remarkable role of the effective stress tensor concept requires the most general representation for the *damage effect tensor*, or more generally, the *effective stress tensor*:

$$\bar{\sigma} = M[\sigma] \quad \text{with} \quad M = M(\Re)$$

or

$$\bar{\sigma} = \bar{\sigma}(\sigma, \Re) \ .$$

ZHENG and BETTEN (1996) postulate a generalized *damage equivalence hypothesis*. Then, the so-called *damage isotropy principle* is established that in order to coincide with the damage equivalence hypothesis, the effective stress tensor $\bar{\sigma} = \bar{\sigma}(\sigma, \Re)$ as a second-order tensor-valued function of σ and $\Re$ has to be isotropic. Particularly, this property is irrespective of the initial material symmetry (isotropy or anisotropy) and the type of damage variables. As a consequence, the damage effect tensor $M(\Re)$ is an isotropic fourth-order tensor-valued function of the damage state variables $\Re$. As *isotropic tensor functions*, the *effective stress tensor* $\bar{\sigma}(\sigma, \Re)$ and the *damage effect tensor* $M(\Re)$ can be formulated in general *invariant forms* according to the theory of *representations for tensor functions* (RIVLIN, 1970; SPENCER, 1971; WANG, 1971; BOEHLER, 1979; 1987; ZHENG, 1994; BETTEN, 1986a; 1998; 2001c; 2003a). Damage material constants are then consistently introduced to these *invariant damage models*.

8 Tensorial Generalization of Uniaxial Creep Laws to Multiaxial States of Stress

In this chapter a method is developed in order to find tensorial constitutive and evolutional equations based upon empirical uniaxial constitutive laws found in experimental investigations. For engineering applications it is very important to generalize *uniaxial* relations to *multiaxial* states of stress. This can be achieved by applying *interpolation methods for tensor functions* , as pointed out in detail in this chapter. It is illustrated that the scalar coefficients in tensorial constitutive equations can be expressed as functions of the irreducible invariants of the argument tensors and of the empirical constitutive laws found in uniaxial tests.

Some examples should be discussed. For instance, the NORTON-BAILEY creep law and a uniaxial damage relation are generalized to *tensorial constitutive equations*.

8.1 Polynomial Representation of Tensor Functions

Let
$$Y_{ij} = f_{ij}(\boldsymbol{X}) = \varphi_0 \delta_{ij} + \varphi_1 X_{ij} + \varphi_2 X_{ij}^{(2)} \tag{8.1}$$
be an isotropic tensor function where φ_0, φ_1, φ_2 are scalar-valued functions of the integrity basis, the elements of which are the irreducible invariants of the argument tensor $\boldsymbol{X}$. Furthermore, they depend on experimental data.

First, it is possible to express the scalar functions through the principal values X_I, ..., X_{III} and Y_I, ..., Y_{III} if we solve the system of linear equations
$$\left.\begin{aligned} Y_I &= \varphi_0 + \varphi_1 X_I + \varphi_2 X_I^2 \ , \\ Y_{II} &= \varphi_0 + \varphi_1 X_{II} + \varphi_2 X_{II}^2 \ , \\ Y_{III} &= \varphi_0 + \varphi_1 X_{III} + \varphi_2 X_{III}^2 \ . \end{aligned}\right\} \tag{8.2}$$
The solution can be written in the form

$$\varphi_0 = \sum_{\alpha=I}^{III} P_\alpha X_{(\alpha+I)} X_{(\alpha+II)} Y_{(\alpha)} \ , \tag{8.3a}$$

$$\varphi_1 = \sum_{\alpha=I}^{III} P_\alpha \left(X_{(\alpha+I)} + X_{(\alpha+II)} \right) Y_{(\alpha)} \ , \tag{8.3b}$$

$$\varphi_2 = \sum_{\alpha=I}^{III} P_\alpha Y_{(\alpha)} \ , \tag{8.3c}$$

where the abbreviation

$$P_\alpha := \prod_{\substack{\beta=I \\ \beta \neq \alpha}}^{III} 1 / (X_\alpha - X_\beta) \tag{8.4}$$

is introduced. A similar representation was used by SOBOTKA (1984) based upon the SYLVESTER *theorem* (SEDOV, 1966).

Because of the products P_α, the expressions (8.3a-c) can only be used if all principal values are different. Therefore, in the following an *interpolation method* is used in order to determine the scalar coefficients, even if two principal values coincide.

8.2 Interpolation Methods for Tensor Functions

In extending the LAGRANGE interpolation method to a tensor-valued function, we consider the *principal values* of the argument tensor as *interpolating points* and find the tensorial representation

$$Y_{ij} = f_{ij}(\boldsymbol{X}) = \sum_{\alpha=1}^{III} {}^\alpha L_{ij} Y_\alpha + R_{ij}(\boldsymbol{X}) \tag{8.5}$$

with the tensor polynomials

$${}^\alpha L_{ij} := P_\alpha \left(X_{ik} - X_{(\alpha+I)}\delta_{ik} \right) \left(X_{kj} - X_{(\alpha+III)}\delta_{kj} \right) \ . \tag{8.6}$$

Due to the HAMILTON-CAYLEY *theorem*, the tensor-valued remainder term R_{ij} in (8.5) is always equal to the zero tensor (BETTEN 1984; 1987b). As an alternate approach, we find, by extending the NEWTON formula, the tensorial representation

$$\begin{aligned} Y_{ij} = a_0 \delta_{ij} + a_1 \left(X_{ij} - X_I \delta_{ij} \right) \\ + a_2 \left(X_{ik} - X_I \delta_{ik} \right) \left(X_{kj} - X_{II} \delta_{kj} \right) \ , \end{aligned} \tag{8.7}$$

Further terms in (8.7) are not possible because of the HAMILTON-CAYLEY *theorem*. The coefficients in (8.7) can be found by inserting the principal values:

$$a_0 = Y_I , \qquad a_1 = (Y_I - Y_{II})/(X_I - X_{II}) , \qquad \text{(8.8a,b)}$$
$$a_2 = [a_1 - (Y_{III} - Y_I)/(X_{III} - X_I)]/(X_{II} - X_{III}) . \qquad \text{(8.8c)}$$

The interpolation formula (8.7) can be written as an isotropic tensor function (8.1) if we define

$$\varphi_0 \equiv a_0 - a_1 X_I + a_2 X_I X_{II} , \qquad \text{(8.9a)}$$
$$\varphi_I \equiv a_1 - a_2 (X_I + X_{II}) , \qquad \varphi_2 \equiv a_2 . \qquad \text{(8.9b,c)}$$

In the case of *coincident points*, we need the derivatives of the tensor function (8.1):

$$f'_{ij} := \partial Y_{ip}/\partial X_{pj} = \varphi_1 \delta_{ij} + 2\varphi_2 X_{ij} , \qquad \text{(8.10a)}$$
$$f''_{ij} := \partial f'_{iq}/X_{qj} = 2\varphi_2 \delta_{ij} . \qquad \text{(8.10b)}$$

For example, in the case of $X_I \neq X_{II} = X_{III}$, we find from (8.7) and (8.10a) the coefficients

$$a_0 = Y_I , \qquad a_1 = (Y_I - Y_{II})/(X_I - X_{II}) , \qquad \text{(8.11a,b)}$$
$$a_2 = (a_1 - f'_{II})/(X_I - X_{II}) , \qquad \text{(8.11c)}$$

if we substitute

$$Y_I = f_{II} (X_{11} \equiv X_I) ,$$
$$Y_{II} = f_{22} (X_{22} \equiv X_{II}) ,$$
$$f'_{22} (X_{22} \equiv X_{II}) \equiv f'_{II} .$$

Finally, if all principal values coincide, we calculate

$$a_0 = f_I , \qquad a_1 = f'_I , \qquad a_2 = f''_I / 2 . \qquad \text{(8.12a,b,c)}$$

However, in this special case the argument tensor is a spherical one, $X_{ij} = X_I \delta_{ij}$, and therefore the formula (8.7) reduces to the trivial result: $Y_{ij} = f_{ij} = f_I \delta_{ij}$. Note that the interpolation formula for a scalar function $y = f(x)$ approaches the TAYLOR expansion for $f(x)$ at x_0 if we make x_α, $\alpha = 1, 2, \ldots, n$, coincide at x_0. An interpolation method for tensor functions with two argument tensors can be developed in a similar way (BETTEN 1987b; 1987c).

The interpolation method for tensor functions is a very useful and powerful tool. Besides many applications in tensor algebra or tensor analysis discussed by BETTEN (1987b; 1987c), engineering applications are also very important.

In the theory of finite deformation the tensorial HENCKY measure of strain and strain rate plays a central role see FITZGERALD (1980) and BETTEN (1987b; 2001a) because it can be decomposed into a sum of an isochoric distorsion and a volume change. The problem to represent the logarithmic function

$$\boldsymbol{Y} = \ln \boldsymbol{X} \quad \text{or} \quad Y_{ij} = \{\ln \boldsymbol{X}\}_{ij} \qquad (8.13)$$

as an isotropic tensor function (8.1) is solved by determining the scalar functions $\varphi_0, \varphi_1, \varphi_2$. This can be done by using the interpolation method described before by BETTEN (1987b; 2001a).

Other examples are $\boldsymbol{Y} = \exp \boldsymbol{X}$ or $\boldsymbol{Y} = \sin \boldsymbol{X}$ etc., which can be treated in the same way. These functions play a central role, for instance, in problems concerning *vibro creep* (JAKOWLUK, 1993).

8.3 Tensoral Generalization of NORTON-BAILEY's Creep Law

The following example is concerned with the generalization of NORTON-BAILEY's *power law* (Section 4.2)

$$d/d_0 = (\sigma/\sigma_0)^n \quad \text{or} \quad d = K\sigma^n \qquad (8.14\text{a,b})$$

to multi-axial states of stress where d is the strain rate, σ the uniaxial true stress, and d_0, σ_0, n, K are constants. To solve this problem, we use an isotropic tensor function

$$d_{ij} = f_{ij}(\boldsymbol{\sigma}) = \varphi_0^* \delta_{ij} + \varphi_1^* \sigma_{ij} + \varphi_2^* \sigma_{ij}^{(2)} \qquad (8.15)$$

and determine the scalar coefficients $\varphi_0^*, \ldots, \varphi_2^*$ as functions of experimental data (K, n) in (8.14b) and of the integrity basis, the elements of which are the irreducible invariants of the CAUCHY stress tensor $\boldsymbol{\sigma}$.

Alternatively, we can represent the constitutive equation in the form

$$d_{ij} = f_{ij}(\boldsymbol{\sigma}') = \varphi_0 \delta_{ij} + \varphi_1 \sigma_{ij}' + \varphi_2 \sigma_{ij}'^{(2)} , \qquad (8.16)$$

where $\sigma_{ij}' := \sigma_{ij} - \sigma_{kk}\delta_{ij}/3$ are the cartesian components of the *stress deviator* $\boldsymbol{\sigma}'$. For the special case of incompressible behavior $(d_{kk} \equiv 0)$, we find from (8.16) the condition

$$3\varphi_0 + \varphi_2 \sigma_{kk}^{\prime(2)} = 0 \quad \Rightarrow \quad \varphi_0 = -2\varphi_2 J_2'/3 \qquad (8.17)$$

with the quadratic invariant $J_2' \equiv \sigma_{ik}' \sigma_{ki}'/2$ of the stress deviator, so that the constitutive equation (8.16) is reduced to the simple form

$$d_{ij} = \varphi_1 \sigma_{ij}' + \varphi_2 \sigma_{ij}'' \qquad (8.18)$$

containing the traceless tensors

$$\sigma_{ij}' \equiv \partial J_2'/\partial \sigma_{ij} \quad \text{and} \quad \sigma_{ij}'' \equiv \partial J_3'/\partial \sigma_{ij} \qquad (8.19\text{a,b})$$

with the cubic invariant $J_3' \equiv \sigma_{ij}' \sigma_{jk}' \sigma_{ki}'/3$ of the stress deviator. The uniaxial equivalent state of stress (index V) is characterized through the tensor variables

$$(\sigma_{ij})_V = \text{diag}\{\sigma,\, 0,\, 0\} \ , \qquad (8.20\text{a})$$
$$(\sigma_{ij}')_V = \text{diag}\{2\sigma/3,\, -\sigma/3,\, -\sigma/3\} \ , \qquad (8.20\text{b})$$
$$(d_{ij})_V = \text{diag}\{d,\, -\nu d,\, \nu d\} \ , \qquad (8.20\text{c})$$

where ν is the transverse contraction ratio.

In the following the diagonal elements in (8.20) are considered as interpolating points where two points coincide. Since the two coincident points in (8.20a) are zero, it may be more convenient to determine the coefficients $\varphi_0, \ldots, \varphi_2$ in the constitutive equation (8.16) instead of (8.15). Thus, we use the uniaxial creep law

$$d = (3/2)^n K(\sigma')^n \qquad (8.21)$$

instead of (8.14b). Because of (8.20b), i.e. $X_{II} = X_{III} \equiv -\sigma/3$, and (8.21), we find from (8.11a) the coefficient

$$a_0 = Y_1 \equiv (3/2)^n K(\sigma')^n = K\sigma^n \ . \qquad (8.22\text{a})$$

Furthermore, because of (8.20b), (8.22a), and $Y_{II} = -\nu d = -\nu K\sigma^n$, we find from (8.11b) the coefficient

$$a_1 = (1 + \nu) K\sigma^{n-1} \ . \qquad (8.22\text{b})$$

The derivative f_{II}' at the coincident points $X_{II} = X_{III}$ can be determined in the following way. From (8.21) we derive

$$f' \equiv \partial d/\partial \sigma' = n(3/2)^n (\sigma')^{n-1} = nd/\sigma' \ , \qquad (8.23\text{a})$$
$$f_{II}' = nd_{II}/\sigma_{II}' \ . \qquad (8.23\text{b})$$

From (8.20a,b) we read $\sigma' = -\sigma/3$ and $d_{II} = -\nu d_1 \equiv -\nu d = -\nu K \sigma^n$, so that (8.23b) can be written as

$$f'_{II} = 3\nu n K \sigma^{n-1} \ . \tag{8.23c}$$

Considering (8.20b) and (8.22b), we calculate from (8.11c) the coefficient

$$a_2 = (1 + \nu - 3\nu n)\, K \sigma^{n-2} \ . \tag{8.22c}$$

Inserting (8.22a,b,c) in (8.9a,b,c), we finally determine the scalar functions

$$\varphi_0 = \frac{1}{9}\left(1 - 8\nu + 6\nu n\right) K \sigma^n \ , \tag{8.24a}$$

$$\varphi_1 = \frac{2}{3}\left(1 + \nu + \tfrac{3}{2}\nu n\right) K \sigma^{n-1} \ , \tag{8.24b}$$

$$\varphi_2 = (1 + \nu - 3\nu n)\, K \sigma^{n-2} \ . \tag{8.24c}$$

Assuming the incompressibility (8.18) and neglecting tensorial nonlinearity ($\varphi_2 = 0 \Rightarrow a_2 = 0$, $\varphi_0 = 0$, and $\varphi_1 = a_1$) we find from (8.16) the simplified constitutive equation

$$d_{ij} = a_1 \sigma'_{ij} \quad \text{or} \quad d_{ij} = \frac{3}{2} K \sigma^{n-1} \sigma'_{ij} \ , \tag{8.25a,b}$$

if we use (8.22b) with $\nu = 1/2$. The result (8.25b) is identical to a constitutive equation proposed by LECKIE and HAYHURST (1977). If we insert the MISES equivalent stress $\sigma = \sqrt{3J'_2}$ into (8.25b), we can find the constitutive equation

$$d_{ij} = \frac{3}{2} K \left(3 J'_2\right)^{(n-1)/2} \sigma'_{ij} \tag{8.25c}$$

used by ODQUIST and HULT (1962).

The equivalent stress σ in (8.24a,b,c) can be determined as a function of the stress invariants if we use the *hypothesis of the equivalent dissipation rate*:

$$\dot{D} := \sigma_{ij} d_{ji} \overset{!}{=} \sigma d \ , \tag{8.26}$$

where $\dot{D}$ is called the *rate of dissipation* of creep energy. The result is

$$\sigma^3 + A\sigma^2 + B\sigma + C = 0 \ , \tag{8.27}$$

where the abbreviations

$$A \equiv -\left(1 - 8\nu + 6\nu n\right) J_1/9 \ , \tag{8.28a}$$

$$B \equiv -4\left(1 + \nu + 3\nu n/2\right) J'_2/3 \ , \tag{8.28b}$$

$$C \equiv -\left(1 + \nu - 3\nu n\right)\left(3J'_3 + 2J_1 J'_2/3\right) \tag{8.28c}$$

have been used. Thus, the scalar coefficients (8.24a,b,c) are functions of the *irreducible invariants*

$$J_1 \equiv \sigma_{kk} , \qquad J_2' \equiv \sigma_{ik}'\sigma_{ki}'/2 , \qquad J_3' \equiv \sigma_{ij}'\sigma_{jk}'\sigma_{ki}'/3 \qquad \text{(8.29a,b,c)}$$

and of *experimental data* (K, n, ν):

$$\varphi_\alpha = \varphi_\alpha \left(J_1, J_2', J_3'; K, n, \nu \right) , \qquad \alpha = 0, 1, 2 . \qquad \text{(8.30)}$$

This statement is compatible with the representation theory of tensor-valued functions (4.80) in which the coefficients φ_α are scalar-valued functions of the *integrity basis* (8.29a,b,c).

In the case of incompressible behavior ($\nu = 1/2$), the first invariant J_1 has no influence. The cubic equation (8.27) then takes the reduced form

$$\sigma^3 + B^*\sigma^2 + C^* = 0 \qquad \text{(8.27*)}$$

with the abbreviations

$$B^* \equiv - (2 + n) J_2' \quad \text{and} \quad C^* \equiv \frac{9}{2} (n - 1) J_3' \qquad \text{(8.28*b,c)}$$

depending on the irreducible invariants (8.29b,c) of the stress deviator.

Some authors (BROWN et al. 1986) are losing faith in NORTON-BAILEY's *law* since they feel that their new θ *projection concept* provides a far more comprehensive description of creep behavior for design. In this new approach, normal creep curves are envisaged as the sum of a decaying primary and an ascending tertiary stage, i.e., the *secondary stage* is merely the period of ostensibly constant rate observed when the decay in the creep rate during the primary stage is offset by the gradual acceleration caused by tertiary processes. This concept neglects the secondary component and may be valid for some special materials, e.g. $\frac{1}{2}Cr\frac{1}{2}Mo\frac{1}{4}V$, as has been discussed in detail by BROWN et al.(1986). However, an extended secondary creep stage can be observed for many materials. Thus, in spite of the discussion by BROWN et al. (1986), it is very important that NORTON-BAILEY's *law* be generalized to multi-axial states of stress. This can be achieved by applying a *tensorial interpolation method* as has been illustrated above.

8.4 Tensorial Generalization of a Creep Law including Damage

Involving the damage state in the tertiary creep stage (section 4.3.1) the uni-axial relation

$$d/d_0 = (\sigma/\sigma_0)^n D^m \quad \text{with} \quad D := 1/(1-\omega) \tag{8.31}$$

should be generalized to multi-axial states of stress where ω is the damage parameter (material deterioration) introduced by KACHANOV (1958) and also used by RABOTNOV (1969).

To generalize (8.31), we consider the tensor-valued function

$$d_{ij} = \begin{cases} f_{ij}(\boldsymbol{\sigma},\, \boldsymbol{D}) \\ \frac{1}{2} \sum\limits_{\nu,,\mu=0}^{2} \psi_{[\nu,\, \mu]} \left(\sigma_{ik}^{(\nu)} D_{kj}^{(\mu)} + D_{ik}^{(\mu)} \sigma_{kj}^{(\nu)} \right) \,, \end{cases} \tag{8.32}$$

where ν and μ are exponents of the CAUCHY stress tensor $\boldsymbol{\sigma}$ and the second-rank tensor $\boldsymbol{D}$ with the components

$$D_{ij} = (\delta_{ij} - \omega_{ij})^{(-1)}$$

given by the damage tensor $\boldsymbol{\omega}$.

Now, the main problem is to determine the scalar coefficients $\psi_{[\nu,\, \mu]}$ as functions of the integrity basis containing 10 *irreducible invariants* (BETTEN, 1987b; 1987c) and experimental data. To solve this problem, we suggest the following method which may be useful for practical applications as has been discussed by BETTEN, (1988b; 2001c) .

A representation with the same tensor generators as contained in the function (8.32) can be found by seperating the two variables $\boldsymbol{\sigma}$ and $\boldsymbol{D}$ in the following way:

$$d_{ij} = f_{ij}(\boldsymbol{\sigma},\, \boldsymbol{D}) = \frac{1}{2}(X_{ik}Y_{kj} + Y_{ik}X_{kj}) \,, \tag{8.33}$$

where the isotropic tensor functions

$$\left. \begin{array}{l} X_{ij} = X_{ij}(\boldsymbol{\sigma}) = \varphi_0^* \delta_{ij} + \varphi_1^* \sigma_{ij} + \varphi_2^* \sigma_{ij}^{(2)} \\ \varphi_\nu^* = \varphi_\nu^*(\operatorname{tr} \boldsymbol{\sigma}^\lambda) = \varphi_\nu^*(\sigma_I, \sigma_{II}, \sigma_{III}) \end{array} \right\} \,, \tag{8.34}$$

$$\left. \begin{array}{l} Y_{ij} = Y_{ij}(\boldsymbol{D}) = \Phi_0 \delta_{ij} + \Phi_1 D_{ij} + \varphi_2 D_{ij}^{(2)} \\ \Phi_\mu = \Phi_\mu(\operatorname{tr} \boldsymbol{D}^\lambda) = \Phi_\mu(D_I, D_{II}, D_{III}) \end{array} \right\} \tag{8.35}$$

($\mu, \nu = 0, 1, 2$ and $\lambda = 1, 2, 3$) are used.

Thus, we find the representation (8.32) with the scalar coefficients

$$\psi_{[\nu,\, \mu]} = \varphi_\nu^* \Phi_\mu \,, \qquad \mu, \nu = 0, 1, 2 \,, \tag{8.36}$$

where the scalars φ_ν^* are determined by BETTEN (1986a; 1986b):

$$\varphi_0^* = \varphi_0 - J_1\varphi_1/3 + J_1^2\varphi_2/9 \ , \tag{8.37a}$$

$$\varphi_1^* = \varphi_1 - 2J_1\varphi_2/3 \ , \qquad \varphi_2^* \equiv \varphi_2 \ . \tag{8.37b,c}$$

The coefficients Φ_μ can be found by solving the following system of linear equations:

$$\left.\begin{aligned} \Phi_0 + D_I\Phi_1 \ + D_I^2\Phi_2 \ &= (D_I)^{m_I} \ , \\ \Phi_0 + D_{II}\Phi_1 \ + D_{II}^2\Phi_2 \ &= (D_{II})^{m_{II}} \ , \\ \Phi_0 + D_{III}\Phi_1 + D_{III}^2\Phi_2 &= (D_{III})^{m_{III}} \ . \end{aligned}\right\} \tag{8.38}$$

The exponents $m_I, \ldots, m_{III}$ in (8.38) are determined by using the creep law (8.31) in tests on specimens cut along the mutually perpendicular directions x_1, x_2, x_3.

Because of

$$D_{ij} := (\delta_{ij} - \omega_{ij})^{(-1)} \equiv \psi_{ij}^{(-1)} \quad \text{and} \quad \psi_{ij} = \text{diag}\{\alpha,\ \beta,\ \gamma\}$$

according to (4.84) and (7.40a), respectively, the principal values in (8.38) can be expressed through

$$D_I = 1/\alpha \ , \qquad D_{II} \equiv 1/\beta \ , \qquad D_{III} \equiv 1/\gamma \ , \tag{8.39}$$

where the essential components α, β, γ are fractions that represent the net cross-sectional elements of CAUCHY's tetrahedron perpendicular to the co-ordinate axes (BETTEN, 1983a). In the case of two equal parameters, for instance $\alpha \neq \beta = \gamma$, the scalars Φ_μ, $\mu = 0, 1, 2$, in (8.38) can be determined by using the interpolation method described above in (8.1) to (8.12).

Instead of (8.34), we can use the isotropic tensor function

$$X_{ij} = X_{ij}\left(\boldsymbol{\sigma}'\right) = \varphi_0\delta_{ij} + \varphi_1\sigma_{ij}' + \varphi_2\sigma_{ij}'^{(2)} \tag{8.40}$$

and find the representation

$$d_{ij} = \frac{1}{2}\sum_{\nu,\,\mu=0}^{2}\varphi_\nu\Phi_\mu\left(\sigma_{ik}'^{(\nu)}D_{kj}^{(\mu)} + D_{ik}^{(\mu)}\sigma_{kj}'^{(\nu)}\right) \ , \tag{8.41}$$

where the scalar coefficients φ_ν are determined in the functions (8.24a,b,c) and the Φ_μ are taken from (8.38).

The scalar coefficients $\psi_{[\nu,\,\mu]} \equiv \varphi_\nu\Phi_\mu$ in the representation (8.41) must be functions of the integrity basis

$$
\left.
\begin{aligned}
&J_1 \equiv \sigma_{kk}\,, \qquad J_2' \equiv \frac{\sigma_{ij}'\sigma_{ji}'}{2}\,, \qquad J_3' \equiv \frac{\sigma_{ij}'\sigma_{jk}'\sigma_{ki}'}{3}\,, \\
&L_1 \equiv D_{kk}\,, \qquad L_2 \equiv D_{kk}^{(2)}\,, \qquad L_3 \equiv D_{kk}^{(3)}\,, \\
&\Omega_1' \equiv \sigma_{ij}' D_{ji}\,, \; \Omega_2' \equiv \sigma_{ij}'^{(2)} D_{ji}\,, \; \Omega_3' \equiv \sigma_{ij}' D_{ji}^{(2)}\,, \; \Omega_4' \equiv \sigma_{ij}'^{(2)} D_{ji}^{(2)}
\end{aligned}
\right\}
\tag{8.42}
$$

and experimental data. To show this we can start from the hypothesis (8.26) and find similarly to (8.27) the cubic equation

$$
\sigma^3 + A^*\sigma^2 + B^*\sigma + C^* = 0\,,
\tag{8.43}
$$

if we insert (8.33), (8.35) and (8.24a,b,c) into the hypothesis (8.26). In (8.43) the following abbreviations are used:

$$
\begin{aligned}
A^* \equiv -\tfrac{1}{9}\left(1 - 8\nu + 6\nu n\right)\Big[&\Phi_0 J_1 + \Phi_1\left(\Omega_1' + \tfrac{1}{3}J_1 L_1\right) \\
&+ \Phi_2\left(\Omega' + \tfrac{1}{3}J_1 L_2\right)\Big]\big/ D^m\,,
\end{aligned}
\tag{8.44a}
$$

$$
\begin{aligned}
B^* \equiv -\tfrac{2}{3}\left(1 + \nu + \tfrac{3}{2}\nu n\right)\Big[&2\Phi_0 J_2' + \Phi_1\left(\Omega_2' + \tfrac{1}{3}J_1 \Omega_1'\right) \\
&+ \Phi_2\left(\Omega_4' + \tfrac{1}{3}J_1 \Omega_3'\right)\Big]\big/ D^m\,,
\end{aligned}
\tag{8.44b}
$$

$$
\begin{aligned}
C^* \equiv -(1 + \nu - 3\nu n)\Big[&3\Phi_0\left(J_3' + \tfrac{2}{9}J_1 J_2'\right) \\
&+ \Phi_1\left(J_2'\Omega_1' + J_3' L_1 + \tfrac{1}{3}J_1\Omega_2'\right) \\
&+ \Phi_2\left(J_2'\Omega_3' + J_3' L_2 + \tfrac{1}{3}J_1\Omega_4'\right)\Big]\big/ D^m\,,
\end{aligned}
\tag{8.44c}
$$

$$
D \equiv (D_I D_{II} D_{III})^{1/3}\,, \qquad m \equiv (m_I + m_{II} + m_{III})/\,3\,.
\tag{8.44d,e}
$$

We see that the elements of the integrity basis (8.42) and experimental data are contained in (8.44a-e). Thus the coefficients $\psi_{[\nu,\,\mu]} \equiv \varphi_\nu \Phi_\mu$ in (8.41) are scalar functions of the integrity basis (8.42) and experimental data

$$
K,\; n,\; \nu;\; m_I,\; m_{II},\; m_{III};\; D_I,\; D_{II},\; D_{III}
$$

found in creep tests on specimens cut along three mutually perpendicular directions.

In the case (4.79) of damage and initial anisotropy we can use for simplification the constitutive equation

$$
d_{ij} = f_{ij}(\boldsymbol{t},\,\boldsymbol{\tau}) = \frac{1}{2}\sum_{\nu,\,\mu=0}^{2} \psi_{[\nu,\,\mu]}^* \left(t_{ik}^{(\nu)}\tau_{kj}^{(\mu)} + \tau_{ik}^{(\mu)}t_{kj}^{(\nu)}\right)\,,
\tag{8.45}
$$

where the linear transformations

$$t_{ij} = D_{ijpq}\sigma_{pq} = t_{ji} \quad \text{with} \quad D_{ijpq} := (D_{ip}D_{jq} + D_{iq}D_{jp})/2 \,, \quad (8.46)$$

$$\tau_{ij} = A_{ijpq}\sigma_{pq} = \tau_{ji} \,, \quad (8.47)$$

have been introduced in section 4.3.2 according to (4.94) and (4.95), respectively. Then the scalar functions in (8.45) can be determined in a very similar way as described above.

Further applications concerning the tensorial generalization of uniaxial relations in continuum mechanics have been considered by BETTEN (1989; 2001c). For example, the plastic behaviour of solids loaded under uni-axial stress σ may be expressed by the stress-strain-relations

$$\sigma/\sigma_F = [\tanh{(E\varepsilon/\sigma_F)^n}]^{(1/n)} \,, \quad (8.48a)$$

$$\sigma/\sigma_F = (E\varepsilon/\sigma_F) / [1 + (E\varepsilon/\sigma_F)^n]^{(1/n)} \,, \quad (8.48b)$$

proposed by BETTEN (1975b), where σ_F ist the yield stress in a uni-axial tension test, and E represents the modulus of elasticity - often called "YOUNG's modulus"(1807); however, this modulus was already used by EULER (1760). The exponent n regulates the elastic-plastic transition. For instance, an elastic-perfectly plastic behaviour is characterized by $n \to \infty$.

It has been shown by BETTEN (1975c) that independently of the parameter n the *limit carying capacity* coincides wth that for a percectly plastic body $(n \to \infty)$. Hence a new aspect of the uniqueness of the *limit load* may be formulated as we can read in the book of ZYCZKOWSKI (1981, page 210):

> *Uniqueness understood as the independence of that load of the assumed stress-strain diagram belonging to the class of asymptotically perfect plasticity. Such independence may be observed in many cases.*

For engineering applications, it is very important to generalize the relations (8.48a,b) to multiaxial states of stress. This can be achieved by using an isotropic tensor function (8.1).

Similar to (8.48a,b) we can assume the following *creep functions*

$$\kappa(t) = [\tanh{(t^n)}]^{(1/n)} \,, \quad (8.49a)$$

$$\kappa(t) = t / (1 + t^n)^{(1/n)} \,, \quad (8.49b)$$

which are compared with the creep function (11.8) of the KELVIN *solid* (Fig. 11.17) by using the following MAPLE program.

> `kappa(t)[KELVIN]:=1-exp(-G*t/eta);` $\boxed{\odot\ 8\_1.mws}$

$$\kappa(t)_{KELVIN} := 1 - e^{(-\frac{G\,t}{\eta})}$$

> `kappa(t)[tan_hyper]:=(tanh(t^n))^(1/n);`

$$\kappa(t)_{tan\_hyper} := \tanh(t^n)^{(\frac{1}{n})}$$

> `kappa(t)[root]:=t/(1+t^n)^(1/n);`

$$\kappa(t)_{root} := \frac{t}{(1+t^n)^{(\frac{1}{n})}}$$

> `alias(H=Heaviside, th=thickness):`
> `plot1:=plot({1,H(t-5),1-exp(-t)},`
> `t=0..5.001, th=1,color=black):`
> `plot2:=plot({tanh(t),(tanh(t^n))^(1/n)},`
> `t=0..5.001, th=4,color=black, style=point,`
> `symbolsize=12,symbol=cross):`
> `plot3:=plot({t/(1+t), t/(1+t^n)^(1/n)},`
> `t=0..5.001, th=2,color=black, style=point,`
> `symbolsize=12,symbol=circle):`
> `plots[display]({plot1,plot2,plot3});`
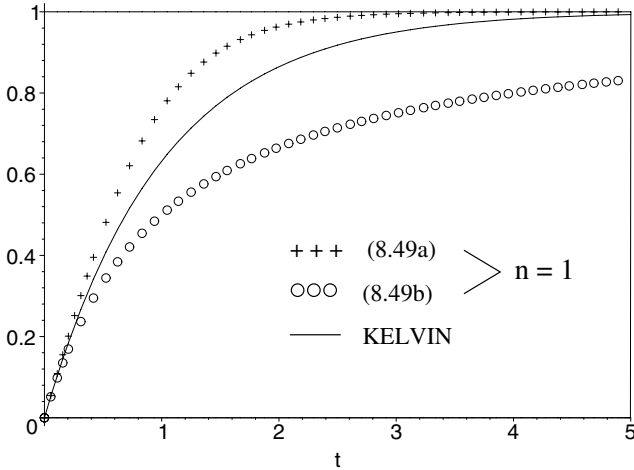
Fig. 8.1 Creep functions

Another example is the tensorial generalization of the RAMBERG-OSGOOD relation, also discussed by BETTEN (1989; 2001c) including own experiments on *aluminium alloy*.

9 Viscous Fluids

Materials are usually classified into *solids* and *fluids*, where fluids are sub-divided into *liquids* and *gases*. These divisions are not always clear because there are materials which possess both solid-like and fluid-like properties. Any *fluid* is defined as a material which deforms continously as long as a shearing stress is acting. A *solid*, on the other hand, can be in equilibrium under a shear stress. Some solids have a natural configuration to which they return if an imposed stress is removed. Such a configuration can be regarded as the reference configuration. Fluids do not possess a natural configuration, i.e., they take the shape of the surrounding boundary.

In the following we differentiate between *linear viscous fluids* and *non-linear viscous fluids* , where the latter belong to the class of *non*-NEWTON*ian fluids*.

9.1 Linear Viscous Fluids

A fluid at rest cannot sustain any shear stress, i.e., the stress state in a fluid at rest is characterized by a spherical tensor, $\boldsymbol{\sigma} \sim \boldsymbol{\delta}$, according to the constitutive equation

$$\sigma_{ij} = -p(\rho, T)\delta_{ij} \tag{9.1}$$

employed in *hydrostatics*, where the hydrostatic pressure p is related to the temperature T and the density ρ by a thermal equation of state having the form $F(p, \rho, T) = 0$. An example of an *equation of state* is the law $p = \rho RT$ of an ideal gas, where R is the special gas constant for a particular gas not to be confused with the general gas constant.

A fluid in motion ($\boldsymbol{d} \neq \boldsymbol{0}$) can sustain *viscous stress*, which can be expressed in the linear case by the linear transformation

$$\tau_{ij} = V_{ijkl}(\rho, T)d_{kl} \ . \tag{9.2}$$

This tensor is called *viscous stress tensor* or sometimes *extra stress tensor*. The cartesian components V_{ijkl} of the *viscosity tensor* $\boldsymbol{V}$ reflect the viscous

properties of the fluid. In general, one can assume that fluids are *isotropic*. Then, the viscous stress tensor is a function of only one argument tensor, namely the rate-of-deformation tensor d with components (3.22), i.e.,

$$\tau_{ij} = \tau_{ij}(d_{pq}) \ , \tag{9.3}$$

and the fourth-order viscosity tensor must be an isotropic tensor, the components of which are expressed by

$$V_{ijkl} = \xi\delta_{ij}\delta_{kl} + \eta\left(\delta_{ik}\delta_{jl} + \delta_{il}\delta_{jk}\right) \ . \tag{9.4}$$

This relation is similar to the elasticity tensor in (2.31) for isotropic linear elastic materials.

Adding (9.1) and (9.2) with (9.4), we arrive at the constitutive equation

$$\boxed{\sigma_{ij} = \left[-p(\rho, T) + \xi(\rho, T)d_{kk}\right]\delta_{ij} + 2\eta(\rho, T)d_{ij}} \tag{9.5a}$$

or

$$\tau_{ij} \equiv \sigma_{ij} + p(\rho, T)\delta_{ij} = \xi d_{kk}\delta_{ij} + 2\eta d_{ij} \ , \tag{9.5b}$$

which characterizes a NEWTON*ian fluid*.

In the special case of a *shearing flow* ($i = 1$, $j = 2$), the constitutive equation (9.5a) reduces to the simple relation $\tau = \eta\dot{\gamma}$, where $\tau = \tau_{12} \equiv \sigma_{12}$ and $\dot{\gamma} = 2d_{12}$. Thus, the parameter η in (9.5a) is the *shear viscosity*. The second parameter, ξ, in (9.5a) shall be interpreted later.

The constitutive equation (9.5a) fulfills the *principle of material frame indifference* (*objectivity*), since the rate-of-deformation tensor is an objective tensor (BETTEN, 2001a) and the right-hand side of (9.5a) is not affected by a superimposed rigid-body motion. Thus, the constitutive equation (9.5a) has the required property of being independent of any superimposed rigid-body motion. This is not true for the linear constitutive equation of an isotropic elastic material (BETTEN, 2001a).

By introducing the fourth-order spherical tensor (9.4) we have assumed that the fluid behaves *isotropic*. As a matter of fact, isotropy is a consequence of (9.2) and the requirement that the stress is not influenced by any rigid-body motion. Thus, it was not necessary to consider *isotropy* as a special assumption. However, fluids with anisotropic properties may exist, but their behavior cannot be expressed by the linear transformation (9.2).

For the sake of practical applications it may be useful to split the constitutive equation (9.5a) into a scalar and a deviatoric part. To do this, we firstly equalize the trace

$$\sigma_{kk} \equiv 3\bar{\sigma} = -3\bar{p} \tag{9.6}$$

and the trace of (9.5a) arriving at the scalar relation

$$\boxed{\bar{p} = p(\rho, T) - \left(\xi + \frac{2}{3}\eta\right) d_{kk}} \; . \tag{9.7a}$$

The deviatoric equation can be derived from the stress deviator (2.23) by taking the relations (9.5a), (9.6), and (9.7a) into account:

$$\boxed{\sigma'_{ij} = 2\eta d'_{ij}} \; , \tag{9.7b}$$

in which $d'_{ij} := d_{ij} - d_{kk}\delta_{ij}/3$ are the components of rate-of-deformation deviator $\boldsymbol{d'}$. In a similar way we arrive from (9.5b) at the following two equations

$$\bar{\tau} \equiv \frac{1}{3}\tau_{kk} = \left(\xi + \frac{2}{3}\eta\right) d_{kk} \quad \text{and} \quad \tau'_{ij} = 2\eta d'_{ij} \; . \tag{9.8a,b}$$

By analogy with the *bulk modulus*, also called *volume elasticity modulus* (BETTEN, 2001a),

$$K \equiv E_{\text{Vol}} := \sigma_{\text{Vol}}/\varepsilon_{\text{Vol}} \equiv \bar{\sigma}/\varepsilon_{kk} \; , \tag{9.9}$$

we define the *bulk viscosity* (*volume viscosity*) as the quotient from viscous volume stress τ_{Vol} and volume strain rate d_{Vol}:

$$\eta_{\text{Vol}} := \tau_{\text{Vol}}/d_{\text{Vol}} \equiv \bar{\tau}/d_{kk} \; , \tag{9.10}$$

so that we find by considering (9.8a) the result

$$\eta_{\text{Vol}} = \xi + \frac{2}{3}\eta \; . \tag{9.11}$$

Hence, the parameter ξ is immaterial since the constitutive equations (9.7a,b) and (9.8a,b) can be expressed according to

$$\boxed{\bar{p} = p(\rho, T) - \eta_{\text{Vol}} d_{kk}} \; , \qquad \boxed{\sigma'_{ij} = 2\eta d'_{ij}} \; , \tag{9.12a,b}$$

and

$$\bar{\tau} = \eta_{\text{Vol}} d_{kk} \equiv p(\rho, T) - \bar{p} \; , \qquad \tau'_{ij} = 2\eta d'_{ij} \; , \tag{9.13a,b}$$

respectively, by taking (9.11) into account. The relation (9.12a) associates the mean normal stress $\sigma_{kk}/3 = -\bar{p}$ with the *thermodynamic pressure* $p(\rho, T)$ and the *bulk viscosity* η_{Vol}, while the equation (9.12b) relates the *shear effect* of the motion with the *stress deviator*.

The *volume viscosity* η_{Vol} takes into account the molecular degrees of freedom and vanishes for one-atomic gases. Experimental investigations have shown that the volume viscosity (9.11) is very small or even negligible. Thus, in such cases it is justified in assuming the STOKES *condition*

$$\boxed{\xi + \frac{2}{3}\eta = 0}\;.\tag{9.14}$$

On this condition or in an *incompressible* NEWTON*ian fluid* ($d_{kk} = 0$) the mean pressure $\bar{p}$ in (9.7a) equals the *thermodynamic pressure* $p(\rho, T)$ at all times. For *nonlinear viscous fluids* (section 9.2), the assumption of incompressibility does not imply $\bar{p} = p$.

Assuming the STOKES condition (9.14), we immediately arrive from (9.5a) at the constitutive equation

$$\boxed{\sigma_{ij} = -p\delta_{ij} - \frac{2}{3}\eta d_{kk}\delta_{ij} + 2\eta d_{ij} \equiv -p\delta_{ij} + 2\eta d'_{ij}}\;,\tag{9.15}$$

which describes the so called STOKES *fluid*.

The importance of the *volume viscosity* (9.10), (9.11) becomes also visible when discussing the *dissipation power*

$$\dot{D} := \tau_{ij} d_{ji} = \xi d_{kk}^2 + 2\eta d_{ij} d_{ji}\;,\tag{9.16a}$$

which can be deduced from (9.5b) and represented in the form

$$\dot{D} = \eta_{\mathrm{Vol}} d_{kk}^2 + 2\eta d'_{ij} d'_{ji}\;,\tag{9.16b}$$

if we split the rate-of-deformation tensor $\boldsymbol{d}$ into the deviator (d'_{ij}) and the spherical tensor ($d_{kk}\delta_{ij}/3$). We can also express (9.16b) as

$$\dot{D} = \eta_{\mathrm{Vol}} I_1^2 + 4\eta I'_2\;,\tag{9.16c}$$

where the invariants $I_1 \equiv d_{kk}$ and $I'_2 \equiv d'_{ij} d'_{ji}/2$ have been introduced. According to (9.16b,c), the dissipation power can be decomposed into two parts characterizing the *volume change* (without change of shape) and the *distortion*, respectively.

Based upon the *second law of thermodynamics*, dissipation is required to be nonnegative. Thus, we deduce from (9.16b,c):

$$\eta_{\text{Vol}} \geq 0 \quad \text{and} \quad \eta \geq 0 , \tag{9.17a,b}$$

or, considering (9.11), we find:

$$\xi \geq -\frac{2}{3}\eta . \tag{9.17c}$$

Now, let us discuss an *extension flow* (DIN 13 342) characterized by the uniaxial stress component

$$\tau_{11} = (1 - 2\nu)\xi d_{11} + 2\eta d_{11} , \tag{9.18}$$

which results from (9.5b) by inserting $i = j = 1$, where

$$\nu := -d_{22}/d_{11} = -d_{33}/d_{11} \tag{9.19}$$

is the isotropic *transverse contraction ratio*. In contrast to the *shear viscosity* η in (9.5a,b) and the *volume viscosity* (9.10), we define an *extension viscosity* according to

$$\eta_D := \tau_{11}/d_{11} . \tag{9.20}$$

Hence, we deduce from (9.18) for a NEWTONian fluid

$$\eta_D = (1 - 2\nu)\xi + 2\eta . \tag{9.21}$$

On the other hand, we follow from (9.8b) the relation

$$\tau'_{11} = 2\eta d'_{11} , \tag{9.22}$$

so that for the extension flow

$$\tau_{ij} = \text{diag}\{\tau_{11}, 0, 0\} , \qquad d_{ij} = \text{diag}\{d_{11}, -\nu d_{11}, -\nu d_{11}\} \tag{9.23a,b}$$

with $\tau'_{11} = 2\tau_{11}/3$ and $d'_{11} = 2(1 + \nu)d_{11}/3$ the extension viscosity (9.20) yields

$$\eta_D = 2(1 + \nu)\eta . \tag{9.24}$$

This result corresponds with the similar relation of the linear theory of elasticity,

$$E = 2(1 + \nu)G , \tag{9.24*}$$

where E and G are the elasticity and the shear modulus, respectively.

For an incompressible ($\nu = 1/2$) NEWTONian fluid, we read from (9.24) the TROUTON *number* (1906)

$$N_{\mathrm{Tr}} := \eta_D/\eta = 3 \ . \tag{9.25}$$

Combining (9.21) and (9.24), the parameter ξ may be expressed as

$$\xi = \frac{2\nu}{1 - 2\nu}\eta \ , \tag{9.26}$$

so that the *volume viscosity* (9.11) becomes

$$\eta_{\mathrm{Vol}} = \frac{2}{3}\frac{1 + \nu}{1 - 2\nu}\eta \ , \tag{9.27}$$

and by eliminating the shear viscosity η from (9.24) and (9.27) we arrive at the relation

$$\eta_{\mathrm{Vol}} = \frac{1}{3(1 - 2\nu)}\eta_D \ , \tag{9.28}$$

which corresponds with the similar formula of elasticity,

$$K \equiv E_{\mathrm{Vol}} = \frac{1}{3(1 - 2\nu)}E \ , \tag{9.28*}$$

where E_{Vol} is the *volume elasticity modulus*, most called *bulk modulus*.

In a similar way, by eliminating the transvection ratio ν, we arrive from (9.27) and (9.28) at the formula

$$\eta_D = 9\eta_{\mathrm{Vol}}\eta/\left(3\eta_{\mathrm{Vol}} + \eta\right) \ , \tag{9.29}$$

which contains the TROUTON *number* (9.25) for $3\eta_{\mathrm{Vol}} \gg \eta$, while for $3\eta_{\mathrm{Vol}} \ll \eta$ th relation $\eta_D = 9\eta_{\mathrm{Vol}}$ follows.

Experimental investigations on *non*-NEWTON*ian fluids* have shown that the extension viscosity or the shear viscosity is a function of the strain rate, $\eta_D = \eta_D(d)$, or of the shear rate, $\eta = \eta(\dot\gamma)$, respectively. For example, LAUN and MÜNSTEDT (1978) have carried out experiments on the LDPE melt IUPACA at $T = 150°$C. The results are illustrated in Fig. 9.1.

We see that for small deformation rates the viscosities are approaching the TROUTON *number* (9.25):

$$\lim_{d \to 0} \eta_D(d) = 3 \lim_{\dot\gamma \to 0} \eta(\dot\gamma) \tag{9.30}$$

Further experiments on *non*-NEWTON*ian fluids* are carried out by BALL-MANN (1965), MEISSNER (1971; 1972), STEVENSON (1972), ASTARITA
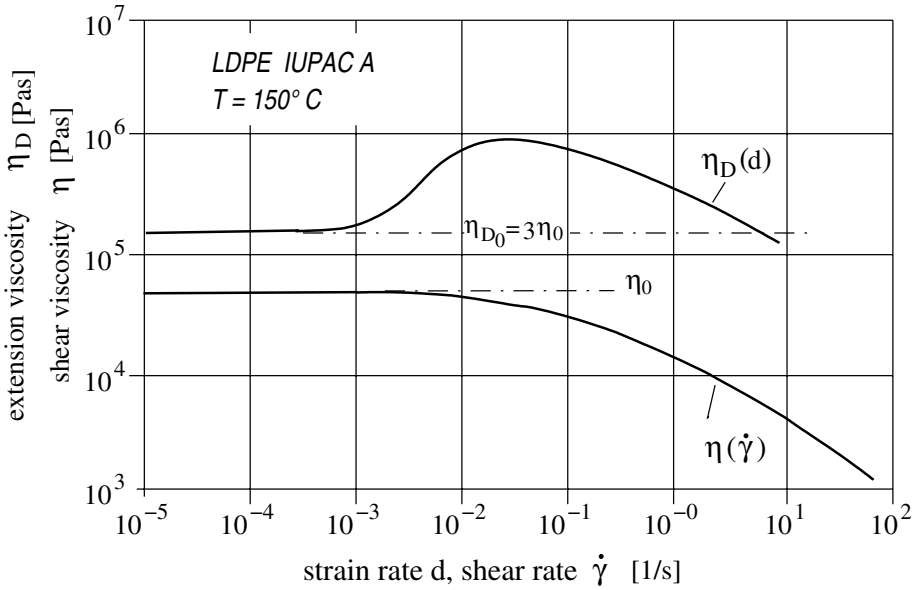
Fig. 9.1 Viscosities in strain and shear as functions of deformation rates

and MARRUCCI (1974), WALTERS (1975), BIRD et al. (1977), MIDDLE-MAN (1977), LAUN (1978), SCHOWALTER (1978), and EBERT (1980), to name just a few.

Inserting the constitutive equation (9.5a) of a NEWTON*ian fluid* into CAUCHY*'s equation of motion* (3.38) yield the NAVIER-STOKES *equations* for compressible fluids as illustrated in more detail in the following.

The partial derivative $\sigma_{ji,j} \equiv \partial\sigma_{ji}/\partial x_j$ of the constitutive equation (9.5a) can be expressed in the form

$$\frac{\partial\sigma_{ji}}{\partial x_j} = -\frac{\partial p}{\partial x_j}\delta_{ij} + \xi\frac{\partial d_{kk}}{\partial x_j}\delta_{ij} + 2\eta\frac{\partial d_{ji}}{\partial x_j}$$

or, by utilizing the *substitution rule* $A_j\delta_{ij} = A_i$, as

$$\frac{\partial\sigma_{ji}}{\partial x_j} = -\frac{\partial p}{\partial x_i} + \xi\frac{\partial d_{kk}}{\partial x_i} + 2\eta\frac{\partial d_{ji}}{\partial x_j} \ . \tag{9.31a}$$

Inserting the partial derivative of the rate-of-deformation tensor,

$$d_{ji,j} = \frac{1}{2}\left(v_{j,ij} + v_{i,jj}\right) \quad \text{and} \quad d_{kk,i} = v_{k,ki} \equiv v_{j,ij} \ ,$$

we arrive at

$$\sigma_{ji,j} = -p_{,i} + (\xi + \eta)v_{k,ki} + \eta v_{i,jj} \ . \tag{9.31b}$$

With this result we finally arrive from CAUCHY's equation of motion (3.38) at the NAVIER-STOKES-*equations* for *compressible fluids*

$$\boxed{-p_{,i} + (\xi + \eta)v_{k,ki} + \eta\, v_{i,jj} + f_i = \rho\, \dot{v}_i} \tag{9.32a}$$

or in symbolic notation

$$\boxed{-\operatorname{grad} p + (\xi + \eta)\operatorname{grad} \operatorname{div} \boldsymbol{v} + \eta\, \Delta\boldsymbol{v} + \boldsymbol{f} = \rho\, \dot{\boldsymbol{v}}} \ . \tag{9.32b}$$

Assuming the STOKES *condition* (9.14), the factor $(\xi + \eta)$ in (9.32a,b) can be substituted by $\eta/3$.

In the special case of *incompressibility* the NAVIER-STOKES-*equations* (9.32a,b) governing the motion of *viscous fluids* take the following forms:

$$\boxed{-p_{,i} + \eta\, v_{i,jj} + f_i = \rho\, \dot{v}_i} \tag{9.33a}$$

and

$$\boxed{-\operatorname{grad} p + \eta\, \Delta\boldsymbol{v} + \boldsymbol{f} = \rho\, \dot{\boldsymbol{v}}} \ . \tag{9.33b}$$

The mechanical interpretation of each term in (9.33a,b) can be obtained as follows. The first term on the left-hand side represents the pressure gradient, the second one expresses the viscous frictional force, and the third term represents the body force. Taking into account the operator (3.5), the right-hand side of (9.33a,b) can be split into two parts,

$$\rho\left(\frac{\partial v_i}{\partial t} + v_k\frac{\partial v_i}{\partial x_k}\right) \quad \text{symbolic} \quad \rho\left(\frac{\partial \boldsymbol{v}}{\partial t} + \boldsymbol{v}\cdot\nabla\boldsymbol{v}\right) \ , \tag{9.34a,b}$$

where the first term represents the *inertia force* arising because of the *local rate*, while the second one characterizes the *convective rate* of change of *linear momentum*. Note, all terms listed above are computed per unit volume of the fluid and are acting on each fluid particle. Thus, the NAVIER-STOKES-*equations* (9.33a,b) or (9.32a,b) state that the pressure gradient force, the viscous force, the body force, and the inertia force acting on a fluid particle are in balance.

9.2 Nonlinear Viscous Fluids

For *non-*NEWTON*ian fluids* we first assume a constitutive equation of the form

$$\sigma_{ij} = \sigma_{ij}(L_{pq}, \rho, T) , \tag{9.35}$$

where $L_{ij} := \partial v_i/\partial x_j \equiv v_{i,j}$ are the cartesian components of the velocity-gradient tensor $\boldsymbol{L}$. This tensor can be split, according to

$$L_{ij} = d_{ij} + w_{ij} ,$$

into the symmetric *rate-of-deformation tensor* $\boldsymbol{d}$ and the skew-symmetric *spin* or *vorticity tensor* $\boldsymbol{w}$.

Constitutive equations must be invariant under changes of frame of reference, i.e., two observers, even if in relative motion with respect to each other, observe the same stress in a loaded material. The *principle of material frame-indifference* is also called the *principle of material objectivity*. As has been pointed out in more detail by BETTEN (2001a), the spin tensor is **not** objective, while the rate-of-deformation tensor is an objective tensor. This can be proved in the following way.

Let us consider a rigid-body motion, which can be split into a time dependent *rotation*, characterized by the orthogonal tensor $\boldsymbol{Q}(t)$, and into *translation*, characterized by the time dependent vector $\boldsymbol{c}(t)$, so that this motion is described by the transformation

$$\bar{x}_i(a_p, t) = Q_{ij}(t)x_j(a_p, t) + c_i(t) . \tag{9.36}$$

Hence, by differentiating with respect to time t, we arrive at the result

$$\bar{v}_i \equiv \dot{\bar{x}}_i = Q_{ip}v_p + \dot{Q}_{ip}x_p + \dot{c}_i \neq Q_{ip}v_p , \tag{9.37}$$

from which we read that the transformation law of a vector, $\bar{v}_i = Q_{ip}v_p$, is not satisfied, i.e., the velocity vector is **not** objective.

With the result (9.37) we first find for the velocity-gradient tensor $\boldsymbol{L}$

$$\left.\begin{aligned}\bar{L}_{ij} &\equiv \partial\bar{v}_i/\partial\bar{x}_j = (\partial\bar{v}_i/\partial x_q)\,(\partial x_q/\partial\bar{x}_j)\\\bar{L}_{ij} &= \left(Q_{ip}v_{p,q} + \dot{Q}_{iq}\right)(\partial x_q/\partial\bar{x}_j) .\end{aligned}\right\} \tag{9.38}$$

By transvection with Q_{ik} and considering the orthogonal relation

$$Q_{ik}Q_{ij} = \delta_{kj} ,$$

we find from the motion (9.36) its inversion:

$$x_k = Q_{ik}(\bar{x}_i - c_i) \quad \text{or} \quad x_i = Q_{ji}(\bar{x}_j - c_j) \tag{9.39}$$

hence

$$\partial x_q / \partial \bar{x}_j = Q_{jq} , \tag{9.40}$$

so that (9.38) becomes

$$\bar{L}_{ij} \equiv \bar{v}_{i,j} = Q_{ip}Q_{jq}v_{p,q} + \dot{Q}_{iq}Q_{jq} \neq Q_{ip}Q_{jq}v_{p,q} , \tag{9.41}$$

i.e., the *velocity gradient tensor* $\boldsymbol{L}$ in (9.35) is **not** objective.

For the *rate-of-deformation tensor* $\boldsymbol{d}$, we find:

$$\begin{aligned}
\bar{d}_{ij} &= (\partial \bar{v}_i / \partial \bar{x}_j + \partial \bar{v}_j / \partial \bar{x}_i)/2 \\
&= Q_{ip}Q_{jq}d_{pq} + \left(\dot{Q}_{iq}Q_{jq} + Q_{iq}\dot{Q}_{jq} \right)\Big/ 2 ,
\end{aligned} \tag{9.42}$$

where

$$\dot{Q}_{iq}Q_{jq} + Q_{iq}\dot{Q}_{jq} = (Q_{iq}Q_{jq})\dot{} \equiv \dot{\delta}_{ij} \equiv 0_{ij} , \tag{9.43}$$

so that the *objectivity* of $\boldsymbol{d}$ is proved:

$$\boxed{\bar{d}_{ij} = Q_{ip}Q_{jq}d_{pq}} . \tag{9.44}$$

Consequently, equation (9.35) must be modified according to

$$\sigma_{ij} = \sigma_{ij}(d_{pq}, \rho, T) . \tag{9.45}$$

Furthermore, because of the principle of material objectivity, the components of the stress tensor (σ_{ij}) must be independent of superposed rigid-body motion, so that the requirement

$$\sigma_{ij} (Q_{pr}Q_{qs}d_{rs}, \rho, T) = Q_{ip}Q_{jq}\sigma_{pq} \tag{9.46}$$

is satisfied, where Q_{ij} are the cartesian components of an orthogonal tensor. A tensor-valued function with the property (9.46) is called an *isotropic tensor function* of the argumenttensor $\boldsymbol{d}$. The most general tensor polynomial function which fulfills (9.46) is of the form

$$\boxed{\sigma_{ij} = -p\delta_{ij} + \alpha d_{ij} + \beta d_{ij}^{(2)}} , \tag{9.47}$$

where p, α, and β are functions of ρ, T and the three irreducible invariants of the argumenttensor $\boldsymbol{d}$. The representation (9.47) is complete because of the

HAMILTON-CAYLEY *theorem*, which states that a tensor satisfies its own characteristic equation (BETTEN, 1987c).

Materials which obey the constitutive equation (9.47) are called REINER-RIVLIN *fluids* . They belong to the class of the *non-*NEWTON*ian fluids*.

As an example, let us consider a simple shear flow characterized by the velocity field

$$\boldsymbol{v} = (\dot{\gamma} x_2, 0, 0)^T \ , \tag{9.48}$$

for which the nonvanishing components of the rate-of-deformation tensor $\boldsymbol{d}$ are given by $d_{12} = d_{21} = \dot{\gamma}/2$, while the square $\boldsymbol{d}^2$ has the diagonal form with components $d_{11}^{(2)} = d_{22}^{(2)} = \dot{\gamma}^2/4$ and $d_{33}^{(2)} = 0$. The invariants are $I_1 = I_3 = 0$ and $I_2 = \operatorname{tr} \boldsymbol{d}^2 = \dot{\gamma}^2/2$. With these values we calculate from (9.47) the following nonvanishing stress components:

$$\sigma_{12} = \alpha \left(\dot{\gamma}^2 \right) \dot{\gamma}/2 \equiv \eta \left(\dot{\gamma}^2 \right) \dot{\gamma} \ , \tag{9.49a}$$

$$\sigma_{11} = \sigma_{22} = -p + \beta \left(\dot{\gamma}^2 \right) \dot{\gamma}^2/4 \ , \qquad \sigma_{33} = -p \ . \tag{9.49b,c}$$

We see, in contrast to a NEWTONian fluid, the shear viscosity in (9.49a) is an even function of the shear rate $\dot{\gamma}$, i.e., it is a function of the square $\dot{\gamma}^2$.

From (9.41) and (9.44) we read that the velocity gradient tensor $\boldsymbol{L}$ is **not** objective, while the rate-of-deformation tensor $\boldsymbol{d}$ fulfills the requirement of *material objectivity*, for instance. Further examples are discussed in the following.

For the *spin* or *vorticity tensor* $\boldsymbol{w}$, which is the skew-symmetric part of the velocity gradient tensor $\boldsymbol{L}$, we obtain

$$\bar{w}_{ij} = Q_{ip} Q_{jq} w_{pq} + \dot{Q}_{iq} Q_{jq} \neq Q_{ip} Q_{jq} w_{pq} \ , \tag{9.50}$$

i.e., the spin tensor is **not** objective. In arriving at the result (9.50) we have taken into consideration the relation (9.43).

Because of (3.29) the CAUCHY stress tensor is objective, i.e.,

$$\bar{\sigma}_{ij} = Q_{ip} Q_{jq} \sigma_{pq} \ . \tag{9.51}$$

Thus we find

$$\dot{\bar{\sigma}}_{ij} = Q_{ip} Q_{jq} \dot{\sigma}_{pq} + \left(\dot{Q}_{ip} Q_{jq} + Q_{ip} \dot{Q}_{jq} \right) \sigma_{pq} \neq Q_{ip} Q_{jq} \dot{\sigma}_{pq} \ , \tag{9.52}$$

hence, the material time derivative of CAUCHY's stress tensor is **not** objective. Whereas the JAUMANN *stress rate*

$$\overset{\circ}{\sigma}_{ij} = \dot{\sigma}_{ij} - w_{ik} \sigma_{kj} + \sigma_{ik} w_{kj} \tag{9.53}$$

fulfills the requirement of *objectivity*, since we arrive from

$$\overset{\circ}{\bar{\sigma}}_{ij} = \dot{\bar{\sigma}}_{ij} - \bar{w}_{ik}\bar{\sigma}_{kj} + \bar{\sigma}_{ik}\bar{w}_{kj} \tag{9.54}$$

at the relation

$$\overset{\circ}{\bar{\sigma}}_{ij} = Q_{ip}Q_{jq}\overset{\circ}{\sigma}_{pq} + \left(\dot{Q}_{ip}Q_{jq} + Q_{ip}Q_{jr}Q_{kq}\dot{Q}_{kr}\right)\sigma_{pq}, \tag{9.55}$$

where the second term on the right-hand side is equal to zero because of the orthogonal relation $Q_{kq}Q_{kr} = \delta_{qr}$ and (9.43), hence

$$\overset{\circ}{\bar{\sigma}}_{ij} = Q_{ip}Q_{jq}\overset{\circ}{\sigma}_{pq} . \tag{9.56}$$

The *convective stress rate*

$$\overset{\triangle}{\sigma}_{ij} = \overset{\circ}{\sigma}_{ij} + d_{ik}\sigma_{kj} + \sigma_{ik}d_{kj} = \dot{\sigma}_{ij} + \sigma_{ik}L_{kj} + L_{ki}\sigma_{kj} \tag{9.57}$$

is obtained by adding the objective expression $d_{ik}\sigma_{kj} + \sigma_{ik}d_{kj}$ to the JAU-MANN stress rate. Thus, the *convective stress rate* is *objective*.

By analogy of (3.8a), we define a *deformation gradient* according to $\bar{F}_{ij} := \partial\bar{x}_i/\partial a_j$ and arrive by differentiation of (9.36) and application of the chain rule at the following result

$$\bar{F}_{ij} = \frac{\partial\bar{x}_i}{\partial a_j} = \frac{\partial\bar{x}_i}{\partial x_p}\frac{\partial x_p}{\partial a_j} = Q_{ip}F_{pj}, \tag{9.58}$$

from which we can follow that the *deformation gradient* does **not** fulfill the requirement of *objectivity* (BETTEN, 2001a).

The LAGRANGE *strain tensor* (3.14) is defined as

$$\lambda_{ij} = \frac{1}{2}\left(F_{ki}F_{kj} - \delta_{ij}\right) . \tag{9.59}$$

Considering a rigid-body motion, we have the following relations

$$\left.\begin{array}{l} \bar{\lambda}_{ij} = \dfrac{1}{2}\left(\bar{F}_{ki}\bar{F}_{kj} - \bar{\delta}_{ij}\right) \\[2mm] \bar{F}_{ki} = Q_{kp}F_{pi} \\[2mm] \bar{F}_{kj} = Q_{kq}F_{qj} \\[2mm] \bar{\delta}_{ij} = Q_{ip}Q_{jq}\delta_{pq} \end{array}\right\} \quad \Rightarrow \quad \bar{\lambda}_{ij} = \frac{1}{2}\left(Q_{kp}Q_{kq}F_{pi}F_{qj} - Q_{ip}Q_{jq}\delta_{pq}\right) .$$

$$\tag{9.60}$$

Inserting the orthogonal relation $Q_{kp}Q_{kq} = \delta_{pq}$ and applying the substitution rule, one obtains from (9.60) the result

$$\bar{\lambda}_{ij} = \frac{1}{2} \left(\delta_{pq} F_{pi} F_{qj} - \delta_{ij} \right) = \frac{1}{2} \left(F_{ri} F_{rj} - \delta_{ij} \right) \equiv \lambda_{ij} \;, \tag{9.61}$$

which states that the components of the LAGRANGE strain tensor are **not** effected by a superimposed rigid-body motion, i.e., the principle of material objectivity is fulfilled.

The material time derivative of the LAGRANGE strain tensor (9.59) can be expressed by

$$\dot{\boldsymbol{\lambda}} = \boldsymbol{F}^T \boldsymbol{d} \, \boldsymbol{F} \quad \text{or by} \quad \dot{\lambda}_{ij} = F_{ip}^T d_{pq} F_{qj} = F_{pi} F_{qj} d_{pq} \;. \tag{9.62a,b}$$

Thus, a superimposed rigid-body motion yields

$$\dot{\bar{\lambda}}_{ij} = \bar{F}_{pj} \bar{F}_{qi} \bar{d}_{pq} \;. \tag{9.63}$$

Taking (9.44) and (9.58) into account, equation (9.63) can be written in the form

$$\dot{\bar{\lambda}}_{ij} = Q_{pk} F_{ki} Q_{ql} F_{lj} Q_{pr} Q_{qs} d_{rs} \;. \tag{9.64}$$

Since $\boldsymbol{Q}$ is an orthogonal tensor, we arrive from (9.64) at the relation

$$\dot{\bar{\lambda}}_{ij} = \delta_{kr} \delta_{ls} F_{ki} F_{lj} d_{rs} = F_{ri} F_{sj} d_{rs} \;. \tag{9.65}$$

Comparing (9.65) with (9.62b), we finally obtain the result

$$\boxed{\dot{\bar{\lambda}}_{ij} \equiv \dot{\lambda}_{ij}} \;, \tag{9.66}$$

stating that the *material time derivative of the* LAGRANGE *strain tensor* is objective.

The EULER *strain tensor* in (3.19) is defined as

$$\eta_{ip} = \frac{1}{2} \left(\delta_{ip} - F_{ki}^{(-1)} F_{kp}^{(-1)} \right) \;, \tag{9.67}$$

hence

$$\bar{\eta}_{ip} = \frac{1}{2} \left(\bar{\delta}_{ip} - \bar{F}_{ki}^{(-1)} \bar{F}_{kp}^{(-1)} \right) \;, \tag{9.68}$$

where

$$\bar{F}_{ij}^{(-1)} := \partial a_i / \partial \bar{x}_j = \left(\partial a_i / \partial x_p \right) \left(\partial x_p / \partial \bar{x}_j \right) = F_{ip}^{(-1)} \left(\partial x_p / \partial \bar{x}_j \right) \;. \tag{9.69}$$

From (9.36) we read

$$x_i = Q_{ij}^{(-1)} \left(\bar{x}_j - c_j \right) = Q_{ji} \left(\bar{x}_j - c_j \right) \quad \Rightarrow \quad \partial x_p / \partial \bar{x}_j = Q_{jp} = Q_{pj}^{(-1)} \;,$$

so that (9.69) reduces to the relation

$$\bar{F}_{ij}^{(-1)} = F_{ip}^{(-1)} Q_{pj}^{(-1)} \ , \tag{9.70}$$

which is the inverse form of (9.58). Note that the inverse of a matrix product π is the matrix product formed by writing down the inverses of the factors of π in reverse order, for instance

$$(\boldsymbol{ABC} \ldots \boldsymbol{Z})^{-1} = \boldsymbol{Z}^{-1} \ldots \boldsymbol{C}^{-1} \boldsymbol{B}^{-1} \boldsymbol{A}^{-1} \ . \tag{9.71}$$

This rule can also be applied to the transpose of a matrix product.

Inserting the inverse (9.70) into (9.68), we obtain

$$\bar{\eta}_{ip} = \frac{1}{2} \left(\bar{\delta}_{ip} - F_{kr}^{(-1)} Q_{ri}^{(-1)} F_{ks}^{(-1)} Q_{sp}^{(-1)} \right) \ . \tag{9.72}$$

Because $\boldsymbol{Q}$ is an *orthogonal tensor*, i.e., the inverse of $\boldsymbol{Q}$ is identical to the transpose of $\boldsymbol{Q}$, and since

$$\bar{\delta}_{ip} = Q_{ir} Q_{ps} \delta_{rs} \tag{9.73}$$

the relation (9.72) reduces to

$$\bar{\eta}_{ip} = \frac{1}{2} Q_{ir} Q_{ps} \left(\delta_{rs} - F_{kr}^{(-1)} F_{ks}^{(-1)} \right) \ . \tag{9.74}$$

Considering the definition (9.67), we can write (9.74) in the following form

$$\boxed{\bar{\eta}_{ip} = Q_{ir} Q_{ps} \eta_{rs}} \ , \tag{9.75}$$

showing that the EULERian *strain tensor* is an *objective tensor*.

The material time derivative of the EULERian strain tensor (9.67) can be expressed by

$$\dot{\boldsymbol{\eta}} = \boldsymbol{d} - \boldsymbol{\eta} \boldsymbol{L} - \boldsymbol{L}^T \boldsymbol{\eta} \quad \text{or by} \quad \dot{\eta}_{ij} = d_{ij} - \eta_{ip} L_{pj} - \eta_{jp} L_{pi} \ . \tag{9.76a,b}$$

Thus, a superimposed rigid-body motion yields

$$\dot{\bar{\eta}}_{ij} = \bar{d}_{ij} - \bar{\eta}_{ip} \bar{L}_{pj} - \bar{\eta}_{jp} \bar{L}_{pi} \ . \tag{9.77}$$

Inserting (9.41) into (9.77) and considering (9.44) and (9.75), we obtain the result

$$\boxed{\dot{\bar{\eta}}_{ij} = Q_{ik} Q_{jl} \dot{\eta}_{kl} - (Q_{ik} Q_{jl} + Q_{il} Q_{jk}) Q_{ps} \dot{Q}_{pl} \eta_{ks}} \ , \tag{9.78}$$

stating that the *material time derivative of the* EULER*ian strain tensor* is **not** an objective tensor.

The OLDROYD *time derivative* of a symmetric second rank tensor $\boldsymbol{T}$ is defined according to

$$\overset{\triangledown}{T}_{ij} := \dot{T}_{ij} + T_{ip}L_{pj} + T_{jp}L_{pi} \ . \tag{9.79}$$

Applying this derivative to the EULERian strain tensor, $T_{ij} \equiv \eta_{ij}$, and taking into account the relation (9.76b), we immediately obtain the identity

$$\boxed{\overset{\triangledown}{\eta}_{ij} \equiv d_{ij}} \ , \tag{9.80}$$

i.e., the OLDROYD *time derivative of the* EULER*ian strain tensor* can be interpreted as the rate-of-deformation tensor. Hence, the requirement of material objectivity is fulfilled.

The *second* PIOLA-KIRCHHOFF *stress tensor* (3.42) is defined as

$$\tilde{T}_{ij} = \frac{\rho_0}{\rho} F_{ip}^{(-1)} F_{jq}^{(-1)} \sigma_{pq} = \tilde{T}_{ji} \ , \tag{9.81}$$

hence

$$\bar{\tilde{T}}_{ij} = \frac{\rho_0}{\rho} \bar{F}_{ip}^{(-1)} \bar{F}_{jq}^{(-1)} \bar{\sigma}_{pq} \ . \tag{9.82}$$

Considering (9.51) and (9.69), i.e.,

$$\bar{\sigma}_{pq} = Q_{ps}Q_{qt}\sigma_{st} \quad \text{and} \quad \bar{F}_{ip}^{(-1)} = F_{ir}^{(-1)}Q_{rp}^{(-1)} = F_{ir}^{(-1)}Q_{pr} \ ,$$

respectively, we arrive at the relations

$$\bar{\tilde{T}}_{ij} = \frac{\rho_0}{\rho} F_{ir}^{(-1)} F_{jk}^{(-1)} \underbrace{Q_{pr}Q_{ps}}_{\delta_{rs}} \underbrace{Q_{qk}Q_{qt}}_{\delta_{kt}} \sigma_{st}$$

$$\bar{\tilde{T}}_{ij} = \frac{\rho_0}{\rho} \bar{F}_{ir}^{(-1)} \bar{F}_{jk}^{(-1)} \sigma_{rk} \ . \tag{9.83}$$

Comparing (9.83) with the definition (9.81), we finally obtain the result

$$\boxed{\bar{\tilde{T}}_{ij} \equiv \tilde{T}_{ij}} \ , \tag{9.84}$$

stating that, analogous to (9.66), the *second* PIOLA-KIRCHHOFF *stress tensor* is objective.

The *first* PIOLA-KIRCHHOFF *stress tensor*

$$T_{ij} = \frac{\rho_0}{\rho} F_{ik}^{(-1)} \sigma_{kj} \neq T_{ji} \tag{9.85}$$

can be expressed by the second one (9.81) according to

$$\tilde{T}_{ij} = T_{iq} F_{jq}^{(-1)} \quad \Rightarrow \quad T_{ij} = \tilde{T}_{ik} F_{jk} , \tag{9.86}$$

hence

$$\left. \begin{aligned} \bar{T}_{ij} &= \bar{\tilde{T}}_{ik} \bar{F}_{jk} \\ \bar{F}_{jk} &= Q_{jr} F_{rk} \\ \bar{\tilde{T}}_{ik} &= \tilde{T}_{ik} \end{aligned} \right\} \quad \Rightarrow \quad \bar{T}_{ij} = \underbrace{\tilde{T}_{ik} F_{rk}}_{T_{ir}} Q_{jr} ,$$

$$\boxed{\bar{T}_{ij} = T_{ir} Q_{jr}} , \tag{9.87}$$

i.e., the *first* PIOLA-KIRCHHOFF *stress tensor* is **not** objective in contrast to the second one according to (9.84).

The above discussed examples illustrate that the components of objective tensors defined in the reference configuration (*material description*) do not change, if a rigid-body motion is superimposed, for instance, the components of the LAGRANGE strain tensor:

$$\boxed{\bar{\lambda}_{ij} \equiv \lambda_{ij}} . \tag{9.61}$$

Whereas the components of objective tensors defined in the actual configuration (*spatial description*) change according to the transformation law of the tensor, if a rigid-body motion is superimposed, for instance, the components of the EULERian strain tensor:

$$\boxed{\bar{\eta}_{ij} = Q_{ip} Q_{jr} \eta_{pr}} . \tag{9.75}$$

The above discussed examples are listed in Table 9.1.

Table 9.1 Objective and non-objective tensors

tensor	material objectivity	
deformation gradient	**not** fulfilled	(9.58)
velocity gradient tensor	**not** fulfilled	(9.41)
rate-of-deformation tensor	fulfilled	(9.44)
spin tensor	**not** fulfilled	(9.50)
CAUCHY stress tensor	fulfilled	(9.51)
material time derivative of CAUCHY's stress tensor	**not** fulfilled	(9.52)
JAUMANN stress rate	fulfilled	(9.56)
convective stress rate	fulfilled	(9.57)
LAGRANGE strain tensor	fulfilled	(9.61)
material time derivative of the LAGRANGE strain tensor	fulfilled	(9.66)
EULERian strain tensor	fulfilled	(9.75)
material time derivative of the EULERian strain tensor	**not** fulfilled	(9.78)
OLDROYD time derivative of the EULERian strain tensor	fulfilled	(9.80)
first PIOLA-KIRCHHOFF stress tensor	**not** fulfilled	(9.87)
second PIOLA-KIRCHHOFF stress tensor	fulfilled	(9.84)

10 Memory Fluids

This Chapter is concerned with fluids, which exhibit the *strain history* . Such materials belong to the class of *non-*NEWTON*ian fluids*, in which the *viscous stress tensor* (9.2) or (9.3) depends not only of the actual motion, but also of the motion in the past. Hence, the notation *memory fluid* has been introduced.

Since the tensors L or d do not take *memory effects* into account, constitutive equations (9.35) or (9.45), respectively, are not suitable to describe the behavior of memory fluids. Therefore, we would like briefly concern memory fluids in the following.

10.1 MAXWELL Fluid

The MAXWELL *model* is a two-element model consisting of a linear spring element and a linear dashpot element connected in series (Section 11.3). This model can be regarded as a representative example of a memory fluid.

Based upon BOLTZMANN*'s superposition principle* (Section 11.1), we arrive at the relation

$$\tau(t) = \frac{\eta}{\lambda} \int\limits_{-\infty}^{t} \exp\left[-(t-\theta)/\lambda\right] \dot{\gamma}(\theta)\, d\theta \; , \qquad (10.1)$$

which describes the *shear flow* of the MAXWELL fluid, where η is the *shear viscosity*, $\lambda \equiv \eta/G$ a constant *relaxation time*, and $\theta < t$ a time in the past. The constant parameter $G \equiv \eta/\lambda$ is known as the elastic shear modulus.

The exponential function in (10.1) represents *weight function*, which causes that the influence of the shear rate $\dot{\gamma}(\theta)$ in the far past on the shear stress $\tau(t)$ at present time is less than that in recent history, i.e., the memory diminishes. This effect is known as *fading memory*.

The integral in (10.1) is called a *hereditary integral* since it expresses the shear stress at time t as a function of the entire shear rate history from the time $\theta = -\infty$ to the present time $\theta \equiv t$. This integral, first suggested by

VOLTERRA (1909), belongs to the class of *linear functionals* since the shear rate $\dot{\gamma}$ appears linear. Because of the substitutions $t - \theta \equiv s$ and $\eta/\lambda \equiv G$ the relation (10.1) can be written in the alternative form

$$\tau(t) = G \int_0^\infty \exp(-s/\lambda)\dot{\gamma}(t - s)\, ds \, , \qquad (10.1^*)$$

where the *kernel function*

$$K(t - \theta) = G \cdot \exp\left[-(t - \theta)/\lambda\right] \qquad (10.2)$$

describes the shear rate history dependence of shear stress and characterizes the particular fluid considered. In the case of *fading memory* the kernel function must approach zero if the past time θ tends to infinity:

$$\lim_{\theta \to -\infty} K(t - \theta) = 0 \quad \Rightarrow \quad \textit{fading memory.} \qquad (10.3)$$

Considering a special shear flow with $\dot{\gamma} = $ const. starting at time $t = 0$, we arrive from (10.1) at the simple relation

$$\tau(t) = \frac{\eta}{\lambda}\dot{\gamma} \cdot \exp(-t/\lambda) \int_0^t \exp(\theta/\lambda)\, d\theta = \eta\dot{\gamma}\left[1 - \exp(-t/\lambda)\right] \, , \quad (10.4)$$

which approaches the following limits:

$$\tau = \eta\dot{\gamma} \qquad \qquad \text{(NEWTON)} \qquad \qquad (10.5)$$

for $t \gg \lambda$ or $G \equiv \eta/\lambda \to \infty$ (rigid HOOKE's part) and

$$\tau = G\gamma \qquad \qquad \text{(HOOKE)} \qquad \qquad (10.6)$$

for $t \ll \lambda$ or $\eta \equiv G\lambda \to \infty$ (rigid NEWTON's part).

10.2 General Principle

The previous Section has been concerned with a simple shear flow. A generalization is possible by applying *tensor-valued functionals* suitable to describe the behavior of fluids involving the history dependence, i.e. memory effects.
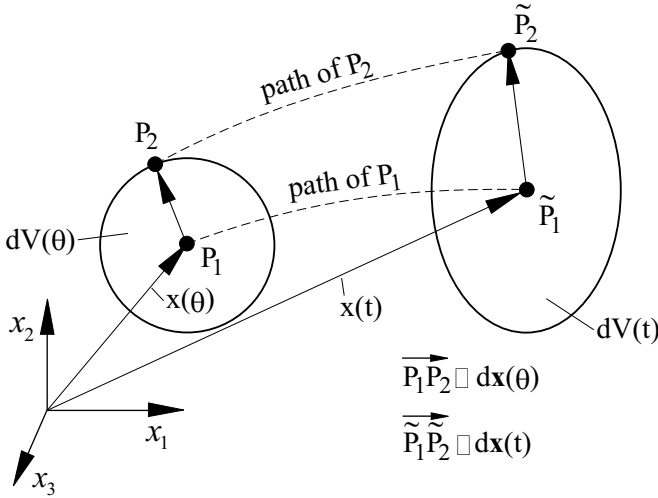
Fig. 10.1 Motion of two infinitesimal neighbouring fluid particles P_1 and P_2

Let us consider the motion of two infinitesimal neighbouring particles P_1 and P_2 from the past $\theta < t$ to the present time t, as illustrated in Fig. 10.1.

The distance vectors in the past, $d\boldsymbol{x}(\theta)$, and at the present time, $d\boldsymbol{x}(t)$, relate to the linear transformation

$$dx_i(\theta) = F_{ik}(\theta; t, \boldsymbol{x}) dx_k(t) , \qquad (10.7)$$

where $F_{ij} := \partial x_i(\theta) / \partial x_k(t)$ are the cartesian components of the *relative deformation gradient* $\boldsymbol{F}$, which reflects a line element vector at the present time back to the corresponding vector in the past.

With respect to the *principle of material frame-indifference* (*material objectivity*), we consider the square of the distance between the two particles, since the quotient $\overline{P_1 P_2}^2 / \overline{\tilde{P}_1 \tilde{P}_2}^2$ is **not** affected by any superimposed rigid-body motion. Thus, we take into consideration the relation

$$dx_i(\theta) dx_i(\theta) = F_{ij} F_{ik} dx_j(t) dx_k(t) \qquad (10.8)$$

derived from (10.7), where

$$F_{ij} F_{ik} := C_{jk}(\theta; t, \boldsymbol{x}) \quad \text{or} \quad \boldsymbol{F}^t \boldsymbol{F} := \boldsymbol{C} \qquad (10.9\text{a,b})$$

represents a symmetric second-order tensor known as the *relative right* CAUCHY-GREEN *tensor*. This tensor is a local measure of the past deformation relative to its present configuration. At the present time ($\theta = t$) the tensor $\boldsymbol{C}$ reduces to $\boldsymbol{C}(\theta = t; t, \boldsymbol{x}) = \boldsymbol{\delta}$.

The volume elements in Fig. 10.1 are related according to

$$dV(\theta) = (\det \boldsymbol{F})dV(t) , \tag{10.10}$$

i.e., $\det \boldsymbol{F}$ is identical to the JACOBIAN determinant. For incompressible flow, $dV(\theta) = dV(t)$, we have $\det \boldsymbol{F} = 1$, hence, because of (10.9), also $\det \boldsymbol{C} = 1$.

A rigid body motion is characterized by $d\boldsymbol{x}(\theta) = d\boldsymbol{x}(t)$, so that we read from (10.7) the simplification $F_{ik} = \delta_{ik}$ and then from (10.9) the trivial result $C_{jk} = \delta_{jk}$, i.e., the CAUCHY-GREEN tensor $\boldsymbol{C}$ is a spherical one in this case.

Now let us discuss a simple shear flow the motion of which is characterized by the transformation

$$\left.\begin{array}{l} x_1(\theta) = x_1(t) - \dot{\gamma}(t-\theta)x_2(t) , \\ x_2(\theta) = x_2(t) , \\ x_3(\theta) = x_3(t) . \end{array}\right\} \tag{10.11}$$

Hence the *relative deformation gradient* (10.7) yields

$$F_{ij} := \partial x_i(\theta)/\partial x_j(t) = \begin{pmatrix} 1 & -\dot{\gamma}(t-\theta) & 0 \\ 0 & 1 & 0 \\ 0 & 0 & 1 \end{pmatrix} \tag{10.12}$$

and the relative *right* CAUCHY-GREEN *tensor* (10.9) is determined as

$$C_{ij} := F_{ki}F_{kj} = \begin{pmatrix} 1 & -\dot{\gamma}(t-\theta) & 0 \\ -\dot{\gamma}(t-\theta) & 1+\dot{\gamma}^2(t-\theta)^2 & 0 \\ 0 & 0 & 1 \end{pmatrix} . \tag{10.13}$$

Because of the *steady* character of the considered flow (10.11), both $\boldsymbol{F}$ and $\boldsymbol{C}$ according to (10.12) and (10.13), respectively, depend only on the remote past $t - \theta \equiv s$ and **not** on the present time t. Furthermore, the shear flow (10.11) is assumed to be *homogen*, so that neither $\boldsymbol{F}$ nor $\boldsymbol{C}$ depend on the position vector $\boldsymbol{x}$.

The general constitutive equation involving the dependence of the deformation history is defined as

$$\sigma_{ij}(\boldsymbol{x}, t) = -p(\rho, T)\delta_{ij} + \mathop{\mathcal{F}_{ij}}_{\theta=-\infty}^{t} [\boldsymbol{C}(\theta; t, \boldsymbol{x})] , \tag{10.14}$$

where the symbol $\mathcal{F}$ characterizes a general *tensor-valued functional* of the CAUCHY-GREEN tensor $\boldsymbol{C}(\theta; t, \boldsymbol{x})$ with t and $\boldsymbol{x}$ as parameters.

As a simple equation let us consider a *linear functional*

$$\tau_{ij}(\boldsymbol{x}, t) := \sigma_{ij}(\boldsymbol{x}, t) + p\delta_{ij} = \int\limits_{-\infty}^{t} K(t - \theta) \left[C_{ij}(t - \theta) - \delta_{ij} \right] d\theta \ . \quad (10.15)$$

Assuming fluids with *fading memory*, the kernel function in (10.15) can be expressed by [1]

$$K(t - \theta) = \frac{\eta}{\lambda^2} \cdot \exp\left[-(t - \theta)/\lambda \right] \ , \quad (10.16)$$

so that we arrive from (10.15) with (10.13) at the following *viscometric functions*:

$$\tau_{12} \equiv \tau(\dot{\gamma}) = \eta\dot{\gamma} \ , \quad (10.17a)$$

$$N_1(\dot{\gamma}) := \tau_{11} - \tau_{22} = -2\eta\lambda\dot{\gamma}^2 = -2\frac{\eta^2}{G}\dot{\gamma}^2 \ , \quad (10.17b)$$

$$N_2(\dot{\gamma}) := \tau_{22} - \tau_{33} = 2\eta\lambda\dot{\gamma}^2 \ \ = -N_1(\dot{\gamma}) \ , \quad (10.17c)$$

which completely determine the behavior of simple fluids in viscometric flows. Examples for such flows are *capillar flows*, COUETTE-*flow*, and POISEUILLE-*flow*. *Viscometric flows* are discussed in more detail by BECKER and BÜRGER (1975), EBERT (1980), TRUESDELL and NOLL (1965), SCHOWALTER (1978), and RIVLIN and ERICKSEN (1955), to name just a few.

10.3 Effects of Normal Stresses

The example in the previous Section shows that the first viscometric function (10.17a) is identical to the shear stress in a NEWTONian fluid. Furthermore, from (9.5a) we calculate $\sigma_{11} = \sigma_{23} = \sigma_{33} = -p$ for a simple shear flow of a NEWTONian fluid, so that the viscometric functions N_1 and N_2 are identical to zero. However, non vanishing normal stress differences, for instance according to (10.17b,c), are essential features of *non*-NEWTON*ian fluids*.

The special normal stress functions (10.17b,c) are functions of $\dot{\gamma}^2$, i.e., they are even functions of $\dot{\gamma}$ and do not change if the shear direction is reversed.

---

[1] Note, that the factors $G \equiv \eta/\lambda$ in (10.2) and η/λ^2 in (10.16) are different, since the kernel functions in (10.1) and (10.15) have different dimensions.

The finite normal stress differences are the cause of *normal stress effects* in non-NEWTONian fluids, for instance, WEISSENBERG (1947) observed that non-NEWTONian fluids (e.g. cream, some motor oils, silicone putty etc.) climb at a rotating rod of a common kitchen mixer, whereas NEWTON fluids climb at the wall of the vessel. The normal stress effect observed by WEISSENBERG is called the WEISSENBERG *effect*.

Another well-known effect is the phenomenon of *die swell*, which can be observed when a non-NEWTONian fluid, e.g. putty, leaves a circular cylindrical tube.

A lot of other *anomalous flows* of non-NEWTONian fluids have been discussed and illustrated by WALKER (1978) and BÖHME (2000), for instance.

11 Viscoelastic Materials

Many materials exhibit both features of *elastic solids* and characteristics of *viscous fluids*. Such materials are called *viscoelastic* . One of the main features of elastic behavior is the capacity for materials to store mechanical energy when deformed by loading, and to set free this energy completely after removing the load. In viscous flow, however, mechanical energy is continuously and totally dissipated. Viscoelastic materials *store* and *dissipate* energy in varying degrees during loading/unloading cycles. Constitutive equations for viscoelastic materials include elastic deformation and viscous flow as special cases, as has already been expressed, for example, by the limits (10.5) and (10.6) of the MAXWELL body.

The behavior of polymers, e.g. PMMA (plexiglass), at moderate temperature and loading may be effectively described by a linear elastic constitutive equation. However, at elevated temperature, the same material should be considered as a viscous fluid.

Furthermore, most materials exhibit linear behavior under small stress levels, while the same material behave more and more nonlinear, when the load is increasing. In the following Sections both *linear* and *nonlinear* viscoelastic models are taken into consideration.

11.1 Linear Theory of Viscoelasticity

Linear models consist of several combinations of linear springs (HOOKE) and linear viscous dashpots (NEWTON). Such *rheological models* are suitable to describe the linear viscoelastic behavior of materials under uni-axial loading.

Based upon BOLTZMANN*'s superposition principle* , which can be utilized in the linear theory, we arrive at the tensorial *hereditary integral*

$$\varepsilon_{ij}(t) = \int\limits_{-\infty}^{t} C_{ijkl}(t-\theta)\frac{\partial \sigma_{k\ell}(\theta)}{\partial \theta}\, d\theta, \qquad (11.1)$$

describing the *multi-axial creep behavior* of linear viscoelastic materials. This integral expresses the strain tensor $\varepsilon(t)$ at the present time t as a function of the entire stress history $\sigma(\theta)$ from the beginning $\theta = -\infty$ The fourth-order *creep tensor* C depends of the particular material considered. In the special case of isotropic behavior, this tensor is a spherical one with components as

$$C_{ijk\ell} = A\delta_{ij}\delta_{k\ell} + B(\delta_{ik}\delta_{j\ell} + \delta_{i\ell}\delta_{jk}) \tag{11.2}$$

producing the following simplification:

$$\varepsilon_{ij}(t) = \delta_{ij}\int_{-\infty}^{t} A(t-\theta)\frac{\partial\sigma_{kk}(\theta)}{\partial\theta}\,d\theta + 2\int_{-\infty}^{t} B(t-\theta)\frac{\partial\sigma_{ij}(\theta)}{\partial\theta}\,d\theta\,. \tag{11.3}$$

Thus, only two scalar *creep functions* , $A(t-\theta)$ and $B(t-\theta)$, are relevant in this particular case.

Similarly, the stress *relaxation* process in a linear viscoelastic material can be described by the *hereditary integral*

$$\sigma_{ij}(t) = \int_{-\infty}^{t} R_{ijk\ell}(t-\theta)\frac{\partial\varepsilon_{k\ell}(\theta)}{\partial\theta}\,d\theta\,, \tag{11.4}$$

where $R_{ijk\ell}$ are the components of the fourth-order tensor-valued relaxation function R.

For uni-axial stress state we obtain by employing integration by parts the *creep relation*

$$E\varepsilon(t) = \sigma(t)\kappa(0) - \int_{-\infty}^{t}\sigma(\theta)\frac{\partial\kappa(t-\theta)}{\partial\theta}\,d\theta\,, \tag{11.5}$$

where E is the elastic modulus, while the *creep function* κ is defined according to

$$\frac{E\varepsilon(t)}{\sigma_0} := \kappa(t; \text{material constants})\,. \tag{11.6}$$

For example, the MAXWELL *fluid* is characterized by the *creep function*

$$\kappa = 1 + \frac{G}{\eta}t\,, \tag{11.7}$$

while the KELVIN *solid* has the following *creep function*

$$\kappa = 1 - \exp\left(-\frac{G}{\eta}t\right). \tag{11.8}$$

The shear modulus G in (11.7) and (11.8) results from HOOKE's part, whereas the shear viscosity η is descended from NEWTON's part in the viscoelastic material.

Similarly to (11.5), the uni-axial *stress relaxation* can be represented in the following way:

$$\frac{\sigma(t)}{E} = \varepsilon(t)r(0) - \int\limits_{-\infty}^{t} \varepsilon(\theta)\frac{\partial r(t-\theta)}{\partial\theta}\,d\theta\,, \tag{11.9}$$

where the *relaxation function r* is defined as

$$\frac{\sigma(t)}{E\varepsilon_0} := r(t; \text{material constants}) \tag{11.10}$$

(BETTEN, 1972). For example, the MAXWELL *fluid* is characterized by the *relaxation function*

$$r = \exp\left(-\frac{G}{\eta}t\right) \tag{11.11a}$$

whereas the KELVIN *solid* has the following *relaxation function*

$$r = 1 + \frac{\eta}{G}\delta(t)\,. \tag{11.11b}$$

In (11.11b) the DIRAC *delta function* $\delta(t)$ has been introduced (Appendix A), where $\delta(t) = 0$ for $t \neq 0$ and $\delta(t) = \infty$ for $t = 0$. Hence, the stress caused by applying a step change in strain ε_0 at time $t > 0$ has the constant value $\sigma(t > 0) = E\varepsilon_0$, i.e., the viscous stress part in (11.10) tends to infinity at time $t = 0$ and approaches immediately zero at time $t > 0$. Thus, the KELVIN *solid* does **not** relax with time.

The *hereditary integrals* in (11.1) and (11.4) or in (11.5) and (11.9) can be deduced by utilizing BOLTZMANN's *superposition principle* as shown in the following.

Consider a linear viscoelastic body loaded by several stress steps in the past as illustrated on the left side in Fig. 11.1. Then, based upon the *superposition principle* and the *creep function* (11.6), the creep response of the model will be given by the following series:

$$E\varepsilon(t) = \sigma_0\kappa(t) + \Delta\sigma_1\kappa(t-\theta_1) + \Delta\sigma_2\kappa(t-\theta_2) + \ldots =$$
$$= \sum_{i=0}^{n} \Delta\sigma_i\kappa(t-\theta_i)\,, \tag{11.12}$$
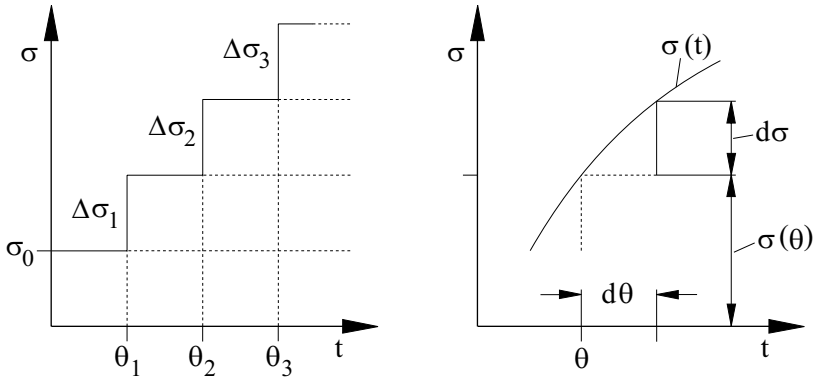
Fig. 11.1 Stepped and continuos stress history.

where θ_i denotes a time in the past at which a new stress step begins. If the steps are incremental small

$$\Delta\sigma_i \rightarrow d\sigma = (\partial\sigma(\theta)/\partial\theta)\,d\theta$$

and its number increases indefinitely, the discrete response function (11.12) yields the *hereditary integral*

$$E\varepsilon(t) = \int\limits_{-\infty}^{t} \frac{\partial\sigma(\theta)}{\partial\theta}\kappa(t-\theta)\,d\theta \quad . \tag{11.13}$$

Employing integration by parts and because of the initial value $\sigma(-\infty) = 0$ we immediately arrive from (11.13) at the *creep response* (11.5). In a similar way we obtain the *stress relaxation* according to (11.9).

Both the *creep integral* in (11.5) and the *relaxation integral* in (11.9) or the *hereditary integral* (11.13) and the corresponding integral for the relaxation process characterize the *linear viscoelastic* behavior of one particular material. Hence, there must exist a relation between the *creep function* $\kappa(t)$ and the *relaxation function* $r(t)$. In other words, it should be possible to determin the corresponding creep function from the given relaxation function, and vice versa. In order to find such a relation it is convenient to utilize the LAPLACE *transforms*

$$L\{\kappa\} \equiv \hat{\kappa}(s) = \int\limits_{0}^{\infty} \kappa(t)e^{-st}\,dt \tag{11.14a}$$

and

$$L\{r\} \equiv \hat{r}(s) = \int_0^\infty r(t)e^{-st}dt. \qquad (11.14b)$$

Then, by considering the *convolution theorem* , we arrive at the following relation (BETTEN, 1969):

$$\boxed{\hat{\kappa}(s)\hat{r}(s) = 1/s^2}. \qquad (11.15a)$$

Applying the *convolution theorem* to the left hand side of (11.15a) and because of the inverse LAPLACE transform, $L^{-1}\{1/s^2\} = t$, applied to right hand side of (11.15a), we finally obtain the result

$$\boxed{\int_0^t \kappa(t-\theta)r(\theta)d\theta = \int_0^t \kappa(\theta)r(t-\theta)d\theta = t}. \qquad (11.15b)$$

Based upon the results (11.15a,b), it is possible to determine the *creep function* $\kappa(t)$ from a given *relaxation function* $r(t)$, and vice versa, for a particular linear viscoelastic material. Two examples are listed in Table 11.1.

Table 11.1 Relation between creep and relaxation functions

MAXWELL fluid		KELVIN solid	
$r(t) = \exp\left(-\dfrac{G}{\eta}t\right)$	(11.11a)	$\kappa(t) = 1 - \exp\left(-\dfrac{G}{\eta}t\right)$	(11.8)
$\Downarrow$		$\Downarrow$	
$\hat{r}(t) = \dfrac{1}{s + G/\eta}$	(11.14b)	$\hat{\kappa}(t) = \dfrac{1}{s\left(1 + \dfrac{\eta}{G}s\right)}$	(11.14a)
$\Downarrow$		$\Downarrow$	
$\hat{\kappa}(t) = \dfrac{1}{s} + \dfrac{G}{\eta}\dfrac{1}{s^2}$	(11.15a)	$\hat{r}(t) = \dfrac{1}{s} + \dfrac{\eta}{G}$	(11.15a)
$\Downarrow$		$\Downarrow$	
$\kappa(t) = 1 + \dfrac{G}{\eta}t$	(11.7)	$r(t) = 1 + \dfrac{\eta}{G}\delta(t)$	(11.11b)

Convolution theorem. The relation (11.15a) can be obtained by utilizing the *convolution theorem* . The *convolution* of two functions, say $f_1(t)$ and $f_2(t)$, is defined according to

$$\varphi(t) := \int\limits_0^t f_1(\theta)\, f_2(t-\theta)d\theta \equiv f_1 * f_2\,.$$

Introducing the substitution $\tau = t - \theta$, the above definition can alternatively be expressed in the form

$$\varphi(t) := \int\limits_0^t f_2(\tau)\, f_1(t-\tau)d\tau \equiv f_2 * f_1\,.$$

Comparing both forms, we see that the *convolution* of two functions is *commutative*, i.e., $f_1 * f_2 = f_2 * f_1$.

Applying the LAPLACE transform to the convolution $\varphi(t)$, we arrive at the *convolution theorem* :

$$\boxed{\hat{\varphi}(s) \equiv L\{f_1 * f_2\} = L\{f_1\}\, L\{f_2\} \equiv \hat{f}_1\, \hat{f}_2}\,,$$

which states that the convolution in the original region corresponds to the usual multiplication in the transformed region (Appendix B). In other words:

The LAPLACE transform of the convolution of two functions is identical with the product of the LAPLACE transforms of these two functions.

In order to derive the relation (11.15a), we apply the convolution theorem to the integral (11.13) with $\theta = 0$ as the lower limit, i.e., we apply the convolution theorem to the following integrals:

$$E\varepsilon(t) = \int\limits_0^t \frac{\partial\sigma(\theta)}{\partial\theta}\kappa(t-\theta)d\theta \quad\text{and}\quad \frac{\sigma(t)}{E} = \int\limits_0^t \frac{\partial\varepsilon(\theta)}{\partial\theta}r(t-\theta)d\theta\,.$$

Then, because of

$$f_1(t) \equiv \partial\sigma(t)/\partial t \quad\text{and}\quad f_2(t) \equiv \kappa(t)$$

or

$$f_1(t) \equiv \partial\varepsilon(t)/\partial t \quad\text{and}\quad f_2(t) \equiv r(t)\,,$$

we obtain the following relations (Appendix B)

$$E\,\hat{\varepsilon}(s) = [s\,\hat{\sigma}(s) - \sigma(0)]\,\hat{\kappa}(s) \quad\text{and}\quad \frac{\sigma(s)}{E} = [s\,\hat{\varepsilon}(s) - \varepsilon(0)]\,\hat{r}(s),$$

which are simplified as

$$E\hat{\varepsilon}(s) = s\hat{\sigma}(s)\,\kappa(s) \quad \text{and} \quad \hat{\sigma}(s) = sE\hat{\varepsilon}(s)\hat{r}(s)\,,$$

since the initial conditions $\sigma(0)$ and $\varepsilon(0) = 0$ are valid. From these simple relations we immediately arrive at the result (11.15a).

The integrals in (11.15b) are convolutions of the functions $\kappa(t)$ and $r(t)$. Let us apply the LAPLACE transform to (11.15b). Then, by utilizing the convolution theorem and because of $L\{t\} = 1/s^2$, we arrive back at the result (11.15a).

The derivatives with respect to time t yield the following two relations

$$\int\limits_0^t \frac{\partial\kappa(t-\theta)}{\partial t}r(\theta)d\theta + \kappa(0)r(t) = 1\,,$$

$$\int\limits_0^t \frac{\partial r(t-\theta)}{\partial t}\kappa(\theta)d\theta + r(0)\kappa(t) = 1\,,$$

where the second result is a *dual* form of the first one, and vice versa. By exchanging κ for r the one expression turns into the other.

For instance, inserting the *creep function* (11.7) of the MAXWELL *fluid* into the first form and then differentiating with respect to time t, we arrive at the differential equation

$$\frac{G}{\eta}\int\limits_0^t r(\theta)d\theta + r(t) = 1 \quad \Rightarrow \quad \boxed{\frac{dr}{dt} + \frac{G}{\eta}r = 0}\,,$$

the solution of which is the *relaxation function* (11.11) of the MAXWELL fluid.

Many different problems of the linear theory of viscoelasticity have been discussed and solved in detail by CHRISTENSEN (1982), SOBOTKA (1984), KRAWIETZ (1986), TSCHOEGL (1989), and HAUPT (2000), to name just a few.

11.2 Nonlinear Theory of Viscoelasticity

Describing the mechanical behavior of a *nonlinear* viscoelastic material it is no longer possible to utilize the superposition principle. Then, the constitutive equations should be represented, in general, by *functionals* as

$$\sigma_{ij}(t) = \mathop{\mathcal{F}_{ij}}_{\substack{\theta=t \\ \theta=-\infty}} \left[\partial x_p(\theta)/\partial a_q\right], \tag{11.16}$$

where $\partial x_p/\partial a_q = F_{pq}$ are the cartesian components of the *deformation gradient tensor* $\boldsymbol{F}$. Because of *material objectivity* a supersosed rigid-body motion (11.32) or

$$\bar{x}_i = Q_{ij}(t)x_j(a_p,t) \tag{11.17}$$

should not influence the CAUCHY stress tensor. Thus, the representation (11.16) is reduced to

$$\sigma_{ij}(t) = F_{ip}F_{jq} \mathop{\mathcal{F}_{pq}}_{\substack{\theta=t \\ \theta=-\infty}} \left[C_{rs}(\theta)\right] \tag{11.18}$$

and further reductions are possible, if there are any material symmetry. The tensor $C_{ij} = F_{ki}F_{kj}$ in (11.18) is known as the *right* CAUCHY-GREEN *tensor* (10.9a,b). An example of (11.18) is the *linear functional* (10.15) employing *fading memory* .

Further representations have been proposed by TRUESDELL and NOLL (1965) or by HAUPT (2000), for instance. Nonlinear problems are also concerned in Sections 11.3.2 and 11.3.5, where the creep behavior of concrete and the relaxation behavior of glass, respectively, is investigated in more detail. Applications to several *polymers* have been discussed by GIESEKUS (1994), LUDWIG (2001), LIN (2002), DÜNGER (2005), and KOLUPAEV (2006), to name but a few.

11.3 Special Visoelastic Models

The phenomenological behavior of viscoelastic materials can be illustrated by *spring-dashpot models* consisting of several elastic springs and viscous dashpots in parallel or in series. In the following some examples should be discussed in more detail based upon the fundamental rheological models of KELVIN-VOIGT (*solid*) and MAXWELL (*fluid*).

11.3.1 Creep Spectra and Creep Functions for the Generalized KELVIN Model

The KELVIN-VOIGT model (more briefly called KELVIN *model*) consists of one linear spring (HOOKE) and one linear dashpot (NEWTON) connected in **parallel** as illustrated in Fig. 11.2.
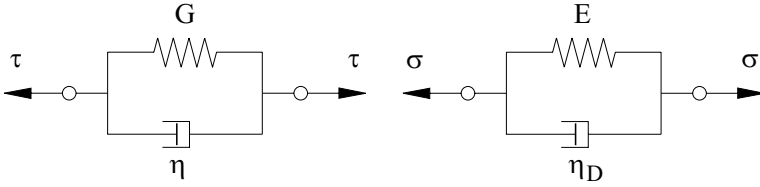
Fig. 11.2 KELVIN model loaded in shear (τ) or in tension (σ)

The KELVIN *body* may be loaded in shear (τ) or in tension (σ), where the model parameters are *shear modulus G* and *shear viscosity η* or YOUNG*'s modulus E* and *extension viscosity η_D*, respectively, according to (9.24) and (9.24*).

Since the basic elements, spring and dashpot, are connected in parallel, the total stress in the model is the sum of

$$\tau_H = G\gamma \text{ (HOOKE)} \quad \text{and} \quad \tau_N = \eta\dot{\gamma} \text{ (NEWTON)} .$$

Thus, the KELVIN model is charcterized by the following ordinary differential equation with constant coefficients:

$$\tau = G\gamma + \eta\dot{\gamma} , \tag{11.19}$$

which can be solved by introducing the integrating factor $\exp(t/\lambda)$ according to

$$\underbrace{\dot{\gamma}e^{t/\lambda} + \frac{G}{\eta}\gamma e^{t/\lambda}}_{\frac{d}{dt}(\gamma e^{t/\lambda})} = \frac{1}{\eta}\tau(t)e^{t/\lambda} \quad \Rightarrow \quad \boxed{\gamma(t) = \frac{1}{\eta}\int_{-\infty}^{t} e^{-(t-\theta)/\lambda}\,\tau(\theta)\,d\theta}$$

$$\tag{11.20}$$

The constant $\lambda \equiv \eta/G$ in (11.20) is called the *retardation time* .

The *creep function* (11.6) for the KELVIN body (11.8) can be determined by inserting the constant shear stress $\tau(t) = \tau_0$ into (11.20) and integrating from $\theta = 0$ to $\theta = t$ as stated by

$$\kappa(t) := \frac{G\gamma(t)}{\tau_0} = 1 - \exp(-t/\lambda) . \tag{11.21}$$

This result is compatible with (11.6) and (11.8), if we assume that the same *creep function κ* is valid for both loading in tension and in shear. A difference could only be between the parameters $\lambda_D = \eta_D/E$ and $\lambda = \eta/G$ due to

tension and shear, respectively. However, because of (9.24) and (9.24*) we have $\lambda_D \equiv \lambda$, i.e., the *retardation times* in tension and in shear are identical.

In the following a rheological model consisting of one HOOKE *element* and n KELVIN *elements* in series is analysed (Fig. 11.3).
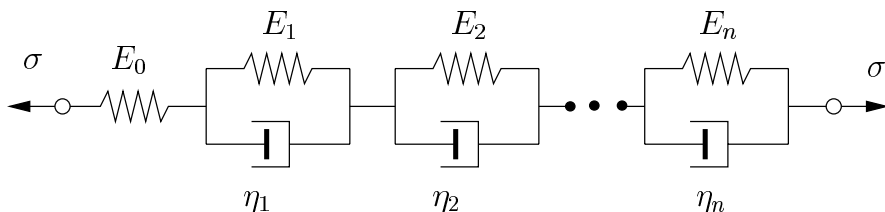
Fig. 11.3 Model with one HOOKE element and n KELVIN elements in series

The tension viscosities of the various KELVIN elements are briefly denoted by η_n instead of η_{Dn}.

The model in Fig. 11.3 contains the *standard solid model* $(n = 1)$ as as-pecial case with three parameters E_0, E_1, η_1. Due to (11.6), (11.8) or (11.21) this model is characterized by the following *creep function*

$$\frac{1}{\sigma_0}\, \varepsilon(t) := J(t) = J_0 + J_1\left[1 - \exp(-t/\lambda_1)\right] \tag{11.22a}$$

containing the three parameters

$$J_0 \equiv 1/E_0, \quad J_1 \equiv 1/E_1, \quad \text{and} \quad \lambda_1 \equiv \eta_1/E_1\,.$$

Substituting the constant loading σ_0 in (11.22a) by $\sigma_0 H(t)$, we arrive at the representations

$$\Rightarrow \quad \varepsilon(t) = \sigma_0 H(t) J(t) \tag{11.22b}$$

$$\Rightarrow \quad \varepsilon(t) = \sigma_0\left[H(t - a)J(t - a) - H(t - b)J(t - b)\right]\,, \tag{11.22c}$$

where $H(t)$ or $H(t - a)$ is the HEAVISIDE *unit step function* discussed in Appendix A in more detail. The response function (11.22c) is illustrated

in Fig. 11.4. A similar representation is shown in Fig. B.3 for the KELVIN-*model* .

$\odot$ 11_1.*mws*

```
>   alias(H=Heaviside):
>   plot1:=plot(H(t-1)-H(t-6),t=0..12,0..1):
>   plot2:=plot(H(t-1)*(0.2+0.8*(1-exp(-(t-1)/2)))
>   -H(t-6)*(0.2+0.8*(1-exp(-(t-6)/2))),t=0..12):
>   plots[display]({plot1,plot2});
```
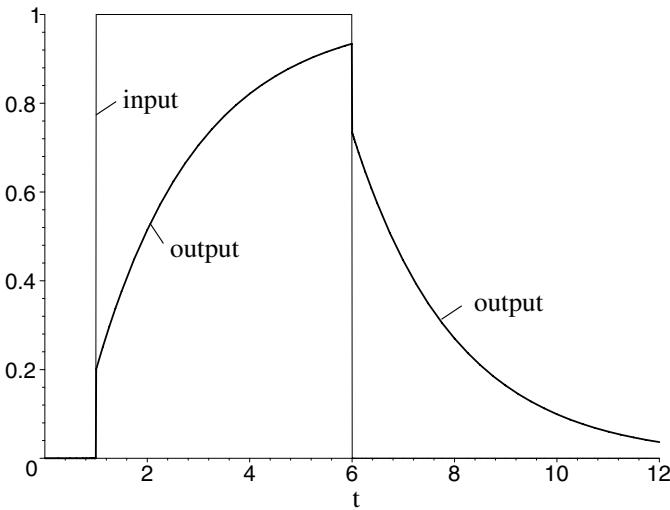

Fig. 11.4 Creep behavior of the standard solid model subjected to a constant load between $t = 1$ and $t = 6$

Supplementing the *standard solid model* by further KELVIN elements as illustrated in Fig. 11.3, we arrive from (11.22a) to the *generalized creep function* :

$$J(t) = J_0 + \sum_{k=1}^{n} J_k[1 - \exp(-t/\lambda_k)] \quad , \tag{11.23}$$

where $J_k \equiv 1/E_k$ is the reciprocal modulus, called *compliance* , while $\lambda_k \equiv \eta/E_k$ represents the corresponding *retardation time* of a KELVIN element within the series in Fig. 11.3. The values (λ_k, J_k) form a *discrete retardation spectrum* as drawn on the left side in Fig. 11.5.
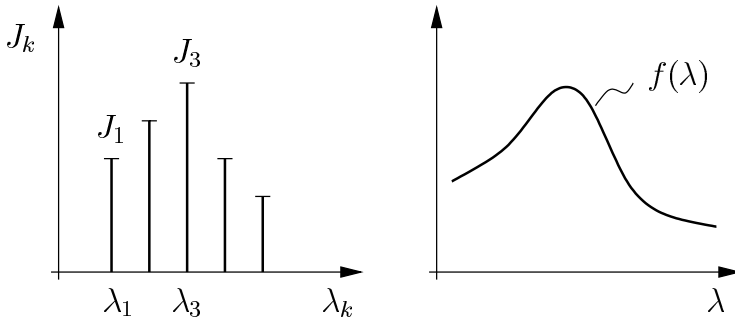
Fig. 11.5 Discrete and continous creep spectrum

The number of KELVIN elements in Fig. 11.3 may increase indefinitely ($n \rightarrow \infty$). Then the *discrete retardation spectrum* proceeds to a *continuous* $f = f(\lambda)$, as illustrated in Fig. 11.5. The *creep function* defined by

$$J(t) := \frac{1}{\sigma_0}\varepsilon(t) \tag{11.24}$$

and given in the discrete form (11.23) results for $n \rightarrow \infty$ in the integral form

$$J(t) = J_0 + \alpha \int_0^\infty f(\lambda)(1 - \exp(-t/\lambda))d\lambda, \tag{11.25}$$

where the parameter α can be determined from $J(\infty) \equiv J_\infty$ by assuming *normalized creep spectra*,

$$\int_0^\infty f(\lambda)d\lambda \equiv 1, \tag{11.26}$$

according to

$$\alpha \equiv J_\infty - J_0. \tag{11.27}$$

Hence, the creep function (11.25) is represented in the following dimensionless form

$$\boxed{K(t) := \frac{J(t) - J_0}{J_\infty - J_0} = 1 - \int_0^\infty f(\lambda)e^{-t/\lambda}d\lambda} . \tag{11.28}$$

For the sake of convenience, the integral in (11.28) is solved by utilizing a
LAPLACE *transformation* (Appendix B). Thus, we introduce the substitution

$$\frac{1}{\lambda} = \xi \quad \text{with} \quad d\lambda = -\frac{1}{\xi^2}d\xi \qquad (11.29)$$

and arrive from (11.28) at the result

$$\frac{J(t) - J_0}{J_\infty - J_0} = 1 - \int_0^\infty \frac{f(\lambda = 1/\xi)}{\xi^2}e^{-t\xi}d\xi \qquad (11.30a)$$

or

$$\frac{J(t) - J_0}{J_\infty - J_0} = 1 - L\{g(\xi)\} \quad , \qquad (11.30b)$$

where $L\{g(\xi)\}$ is the LAPLACE *transform* of the function

$$g(\xi) = \frac{1}{\xi^2}f(\lambda = 1/\xi) \, . \qquad (11.31)$$

In the following some examples should be discussed. At first we select
the POISSON *distribution*

$$f_1(\lambda) = \frac{1}{n!}\lambda^n e^{-\lambda} \quad \text{with} \quad n = 0, 1, 2, ... \qquad (11.32)$$

which is normalized in the sense of (11.26) as we can immediately see by
considering the *gamma function*

$$\Gamma(n) = \int_0^\infty \lambda^{n-1}e^{-\lambda}d\lambda \quad \text{with} \quad \Gamma(n+1) = n! \qquad (11.33)$$

If we substitute $n - 1$ for n , the POISSON *distribution* (11.32) proceeds
to the *gamma distribution* . Note, the function $\Gamma(n + 1)$ in (11.33) may be
called the *factorial function* (Appendix B) because of its connection with $n!$
Furthermore, the *gamma function* is not restricted to an *integer* n, as pointed
out in Appendix B.

The numerical evaluation of (11.30a,b) with (11.32) is carried out by the
following MAPLE computer-program.

⊙ 11.2.mws

```
>    restart:
>    alias(th=thickness,co=color):
>    macro(la=lambda,inf=infinity):
>    K:=(J(t)-J[0])/(J[inf]-J[0]);
```

$$K := \frac{J(t) - J_0}{J_\infty - J_0}$$

```
>   K:=1-int((f[1](xi)/xi^2)*exp(-t*xi),
>   xi=0..inf);
```

$$K := 1 - \int_0^\infty \frac{f_1(\xi)\, e^{(-t\,\xi)}}{\xi^2}\, d\xi$$

Example:

```
>   f[1](la,n):=(1/n!)*(la^n)*exp(-la);
```

$$f_1(\lambda,\, n) := \frac{\lambda^n\, e^{(-\lambda)}}{n!}$$

This spectrum (*POISSON* distribution) is represented in Fig. 11.6.

```
>   p[0]:=plot((1/0!)*(la^0)*exp(-la),
>   la=0..5,0..1,co=black,axes=boxed):
>   p[1]:=plot((1/1!)*(la^1)*exp(-la),
>   la=0..5,co=black):
>   p[2]:=plot((1/2!)*(la^2)*exp(-la),
>   la=0..5,co=black):
>   p[3]:=plot((1/3!)*(la^3)*exp(-la),
>   la=0..5,co=black):
>   plots[display](seq(p[k],k=0..3),th=2);
```
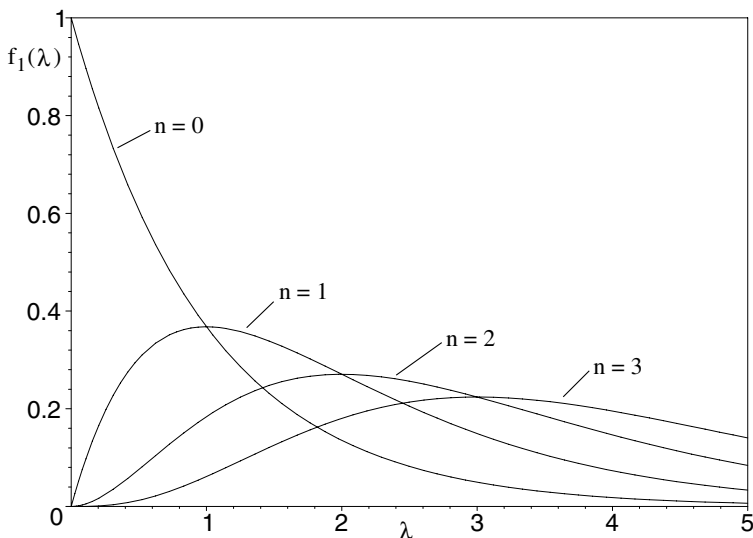

Fig. 11.6 POISSON distributions (11.32) as creep spectra

Because of

$$\frac{df_1}{d\lambda} = \frac{\lambda^{n-1}}{n!}(n - \lambda)e^{-\lambda}$$

the curves in Fig. 11.6 possess a maximum at $\lambda = n > 0$.

From the creep spectra (11.32) illustrated in Fig. 11.6 we find the *creep functions* $J(t, n)$ in dimensionless form (11.30b) as shown in Fig. 11.7.
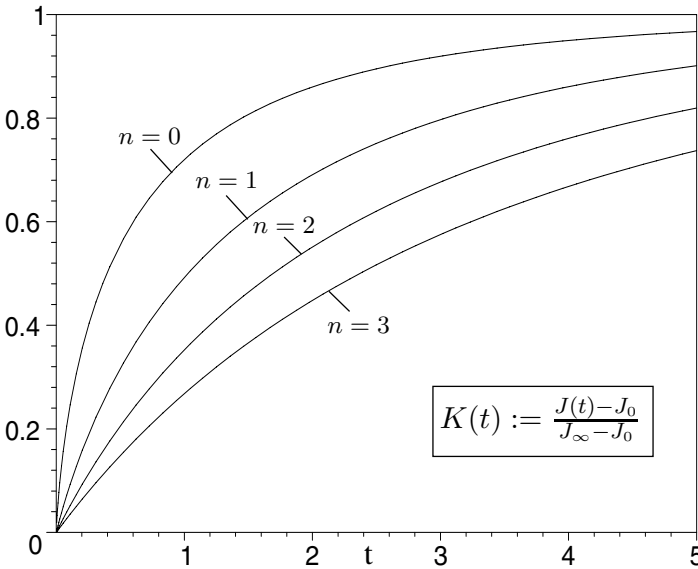
Fig. 11.7 Dimensionless creep functions (11.30) based upon the POISSON distributions (11.32) used as creep spectra

The creep functions (11.30) in Fig 11.7 have been calculated by the following Maple program including the LAPLACE transform.

⊙ $11\_3.mws$

```
>   with(inttrans):
>   g[1](xi):=subs(la=1/xi,f[1](la,n))/xi^2;
```

$$g_1(\xi) := \frac{(\frac{1}{\xi})^n\, e^{(-\frac{1}{\xi})}}{n!\,\xi^2}$$

```
>   K[n]:=1-laplace(g[1](xi),xi,t);
```

$$K_n := 1 - \frac{2\,t^{(\frac{n}{2}+1/2)}\, \mathrm{BesselK}(n+1, 2\,\sqrt{t})}{n!}$$

```
>    for i in [0,1,2,3] do
     K[i]:=subs(n=i,K[n]) od;
```

$$K_0 := 1 - \frac{2\sqrt{t}\,\mathrm{BesselK}(1,\,2\sqrt{t})}{0!}$$

$$K_1 := 1 - \frac{2\,t\,\mathrm{BesselK}(2,\,2\sqrt{t})}{1!}$$

$$K_2 := 1 - \frac{2\,t^{(3/2)}\,\mathrm{BesselK}(3,\,2\sqrt{t})}{2!}$$

$$K_3 := 1 - \frac{2\,t^2\,\mathrm{BesselK}(4,\,2\sqrt{t})}{3!}$$

```
>    plot({seq(K[k],k=0..3)},t=0..5,0..1,
     th=2,axes=boxed,co=black);
```

The second example is concerned with the MAXWELL *distribution function*

⊙ 11_4.mws

```
>    f[2](la):=(a/2/sqrt(Pi)/(la^(3/2))
     *exp(-(a^2/4/la)));
```

$$f_2(\lambda) := \frac{1}{2}\,\frac{a\,e^{(-1/4\,\frac{a^2}{\lambda})}}{\sqrt{\pi}\,\lambda^{(3/2)}} \qquad (11.34)$$

which is *normalized* in the sense of (11.26) and therefore *admissible*. This spectrum is illustrated in Fig. 11.8.
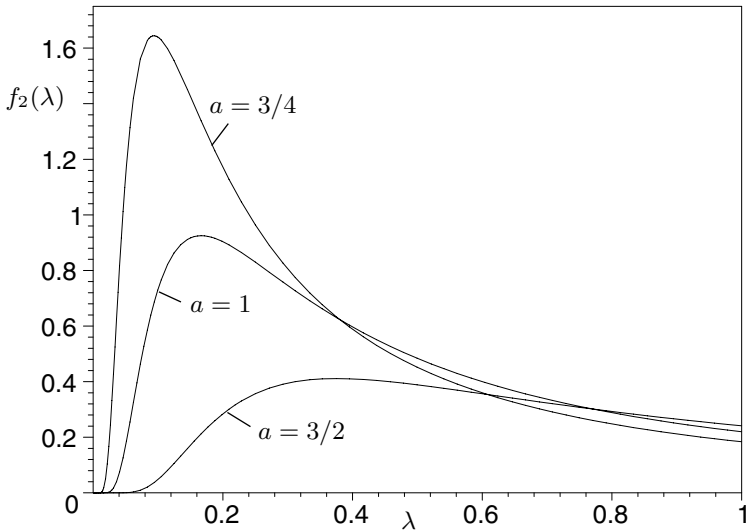
Fig. 11.8 MAXWELL distribution functions (11.34) used as creep spectra.

The distribution function (11.34) in Fig 11.8 has been calculated by the following Maple program.

```
>   p[1]:=plot(subs(a=3/2,f[2](la)),
>   la=0..1,0..1.75,co=black):
>   p[2]:=plot(subs(a=1,f[2](la)),
>   la=0..1,0..1.75,co=black,axes=boxed):
>   p[3]:=plot(subs(a=3/4,f[2](la)),
>   la=0..1,0..1.75,co=black):
>   plots[display]({seq(p[k],k=1..3)});
```

Because of

$$\frac{df_2}{d\lambda} = \frac{a}{8\sqrt{\pi}}\frac{a^2 - 6\lambda}{\lambda^{(7/2)}}e^{-a^2/4\lambda}$$

the MAXWELL distribution functions (11.34) possess a maximum at the position $\lambda = (1/6)a^2$. The associated *creep functions* $J(t,a)$ in dimensionless form (11.30b) have been calculated by the following MAPLE computer program and illustrated in Fig. 11.9.

⊙ 11_5.*mws*

```
>   K[a]:=1-laplace((a/2/sqrt(Pi)/((1/xi^(3/2)))/
>       (xi^2))*exp(-xi*a^2/(4)),xi,t);
```

$$K_a := 1 - \frac{1}{2}\frac{a}{\sqrt{t + \frac{1}{4}a^2}}$$

```
>   for i in [3/2,1,3/4]
>   do K[i]:=subs(a=i,K[a]) od;
```

$$K_{3/2} := 1 - \frac{3}{2\sqrt{4t + \frac{9}{4}}}$$

$$K_1 := 1 - \frac{1}{\sqrt{4t + 1}}$$

$$K_{3/4} := 1 - \frac{3}{4\sqrt{4t + \frac{9}{16}}}$$

```
>   plot({K[3/2],K[1],K[3/4]},t=0..5,0..1,
>   th=2,co=black,axes=boxed);
```
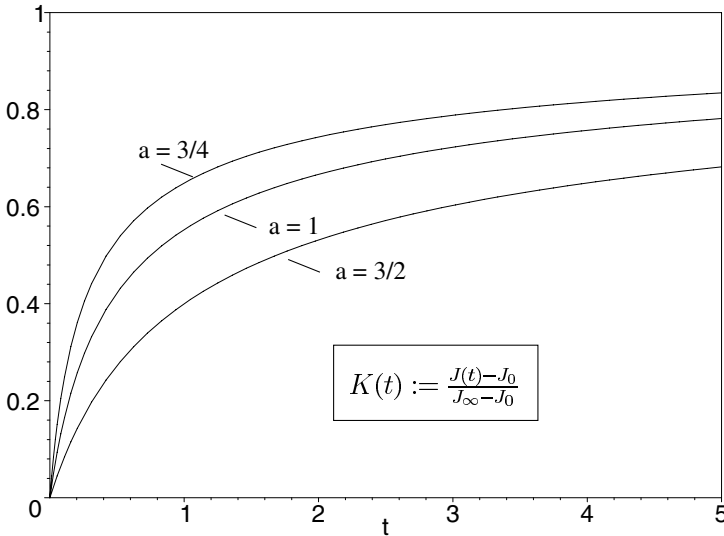
Fig. 11.9 Dimensionless creep functions (11.30) based upon the MAXWELL distrbution functions (11.34) used as creep spectra

The third example takes into consideration the *Chi-square distribution* , which is also *normalized* in the sense of (11.26) and therefore *admissible*.

$$\odot\ 11\_6.mws$$

```
>   with(Statistics):
>   X:=RandomVariable(ChiSquare(n)):
>   f[3](la,n):=PDF(X,la) assuming la>= 0;
%      # Probability Density Function (11.35)
```

$$f_3(\lambda) := \frac{\lambda^{(1/2\,n-1)}\,e^{(-1/2\,\lambda)}}{2^{(1/2\,n)}\,\Gamma(\frac{1}{2}\,n)} \tag{11.35}$$

```
>   Int(f[3],la=0..inf)=int(f[3](la,n),la=0..inf);
```

$$\int_0^\infty f_3\,d\lambda = 1$$

The *Chi-square distribution* (11.35) is a special case of the gamma distribution

$$f(\lambda) = \frac{\lambda^{(n-1}e^{-\lambda}}{\Gamma(n)}\,, \tag{11.36}$$

as we can see by comparing (11.35) with (11.36). The spectrum (11.35) is illustrated in Fig. 11.10 for several parameters n.

```
>    for i in [1,2,3,4] do f[3](la,i):=
>    subs(n=i,f[3](la,n)) od:
>    plot({seq(f[3](la,k),k=1..4)},
>    la=0..5,0..0.5,th=2,axes=boxed,co=black);
```
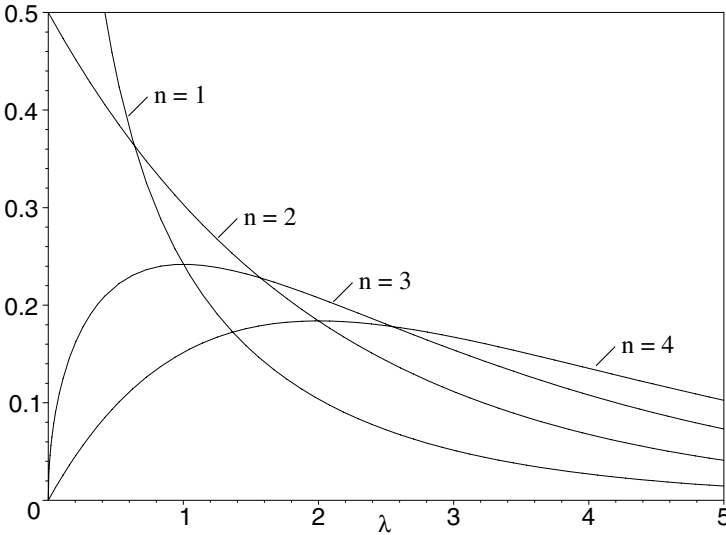

Fig. 11.10 Chi-square distributions (11.35) used as creep spectra

The curves in Fig. 11.10 with $n > 2$ possess a maximum at the position $\lambda = n - 2$.

From the *creep spectra* (11.35) illustrated in Fig. 11.10 we arrive at the *creep functions* $J(t, n)$ in dimensionless form (11.30b) illustrated in Fig. 11.11 calculated by the MAPLE program $\boxed{\odot\ 11\_6.mws}$ utilizing the LAPLACE transformation.

```
>    with(inttrans):
>    g[3](xi,n):=subs(la=1/xi,f[3](la,n))/xi^2;
```

$$g_3(\xi, n) := \frac{(\frac{1}{\xi})^{(\frac{n}{2}-1)} e^{(-\frac{1}{2\xi})}}{2^{(\frac{n}{2})} \Gamma(\frac{n}{2}) \xi^2}$$

```
>    K[n]:=1-laplace(g[3](xi,n),xi,t);
```

$$K_n := 1 - \frac{\text{BesselK}(\frac{n}{2}, \sqrt{2}\sqrt{t}) 2^{(-\frac{n}{4}+1)} t^{(\frac{n}{4})}}{\Gamma(\frac{n}{2})}$$

```
>    for i in [1,2,3,4] do K[i]:=subs(n=i,K[n]) od;
```

$$K_1 := 1 - \frac{\text{BesselK}(\frac{1}{2}, \sqrt{2}\sqrt{t})\, 2^{(3/4)}\, t^{(1/4)}}{\Gamma(\frac{1}{2})}$$

$$K_2 := 1 - \frac{\text{BesselK}(1, \sqrt{2}\sqrt{t})\, \sqrt{2}\sqrt{t}}{\Gamma(1)}$$

$$K_3 := 1 - \frac{\text{BesselK}(\frac{3}{2}, \sqrt{2}\sqrt{t})\, 2^{(1/4)}\, t^{(3/4)}}{\Gamma(\frac{3}{2})}$$

$$K_4 := 1 - \frac{\text{BesselK}(2, \sqrt{2}\sqrt{t})\, t}{\Gamma(2)}$$

```
>    plot({seq(K[n],n=1..4)},t=0..5,0..1,
>    th=2,axes=boxed,co=black);
```


$$K(t) := \frac{J(t) - J_0}{J_\infty - J_0}$$
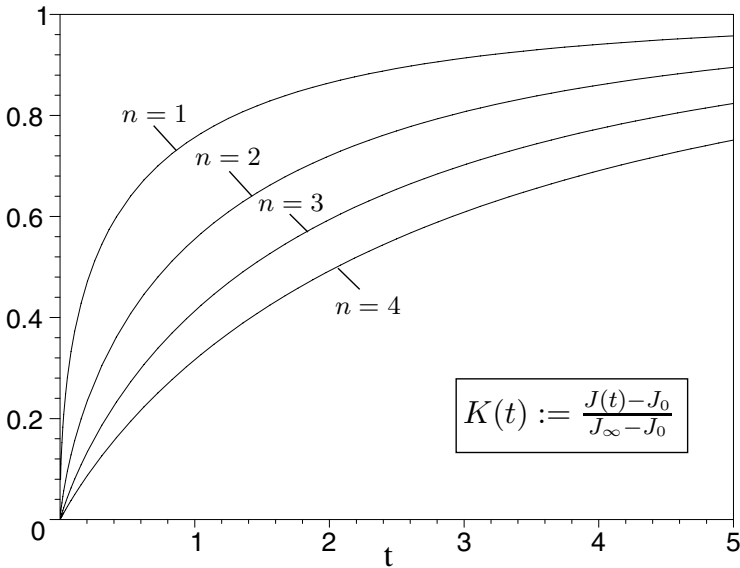
Fig. 11.11 Dimensionless creep functions (11.30) based upon the Chi-square distrbutions (11.35) used as creep functions

11.3.2 Creep Behavior due to the $\sqrt{t}$ - Law

In the previous Section 11.3.1 we started from selected *creep spectra* and cal-culated the associated *creep functions* . Conversely, we can determine creep spectra from given creep functions by using *inverse* LAPLACE *transforms* .

For example, let us concern the *creep behavior of concrete* , which can be described in many situations according to the uni-axial law

$$\varepsilon(t) := a + b\left(1 - e^{-c\sqrt{t}}\right) . \tag{11.37}$$

The three parameters $a, b,$ and c have been determined by using the MAR-QUART-LEVENBERG *algorithm* in connection with experimental data of concrete B 300 (HUMMEL et al., 1962) according to $a = 0.17, b = 1.475,$ and $c = 0.109.$ The associated creep spectrum is obtained by applying the *inverse* LAPLACE *transform* as shown in the following Maple output.

Creep function for concrete:

⊙ 11_7.*mws*

```
>   epsilon(t):=a+b*(1-exp(-c*sqrt(t)));
```

$$\varepsilon(t) := a + b\left(1 - e^{(-c\sqrt{t})}\right)$$

From this equation and considering (11.24), (11.30) we arrive at the LA-PLACE transform

```
>   L(g(xi)):=exp(-c*sqrt(t));
```

$$\mathrm{L}(g(\xi)) := e^{(-c\sqrt{t})} \quad \textit{(parabolic exponential function)} \tag{11.38}$$

```
>   with(inttrans):
>   g(xi):=invlaplace(exp(-c*sqrt(t)),t,xi);
```

$$g(\xi) := \frac{1}{2}\frac{c\,e^{(-1/4\frac{c^2}{\xi})}}{\sqrt{\pi}\,\xi^{(3/2)}} \quad \textit{(MAXWELL distribution function)} \tag{11.34}$$

Then, from (11.31) the following spectrum is obtained:

```
>   f(la):=(1/la^2)*(subs(xi=1/la,g(xi)));
```

$$f(\lambda) := \frac{1}{2}\frac{c\,e^{(-1/4\,c^2\,\lambda)}}{\lambda^2\,\sqrt{\pi}\,(1/\lambda)^{(3/2)}} \tag{11.39}$$

which is plotted for $c = 0.109$ in Fig. 11.12.

```
>   plot(subs(c=0.109,f(la)),la=0..5,0..0.10,);
```
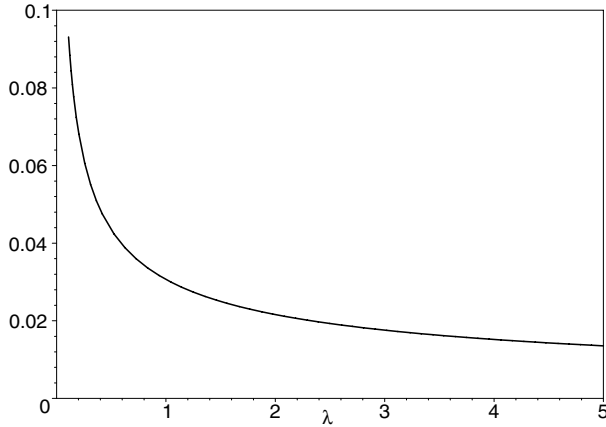
Fig. 11.12 Normalized creep spectrum (11.39) associated with the creep function (11.37)

In the next two Figures (11.13a,b) two several creep curves, ε_A and ε_B, according to (11.37) and (11.40), respectively, have been compared with experimental data, where in Fig. 11.13a the abscissa is devided *linear* in t, while in Fig. 11.13b we have chosen a $\sqrt{t}$-scale. The experiments have been carried out by HUMMEL et al. (1962) on concrete B 300.

$\odot$ $11\_8.mws$

```
>  data:=[0.0,0.17],[0.851,0.3928],[3.997,0.52],
   [7.67,0.6],[17.22,0.72],[30.69,0.858],
   [59.13,1.0],[95.64,1.1],[159.01,1.26],
   [193.21,1.31],[286.28,1.4],[334.94,1.43],
   [377.91,1.45],[900.0,1.58],[1103.56,1.65],
   [1207.56,1.64]:
>  epsilon[A](t):=a+b*(1-exp(-c*sqrt(t)));
```

$$\varepsilon_A(t) := a + b\left(1 - e^{(-c\sqrt{t})}\right) \tag{11.37}$$

```
>  epsilon[B](t):=a+b*(1-exp(-c*t));
```

$$\varepsilon_B(t) := a + b\left(1 - e^{(-ct)}\right) \tag{11.40}$$

```
>  plot1:=plot(subs(a=0.17, b=1.475,
>  c=0.109,epsilon[A](t)),t=0..1200):
>  plot2:=plot(subs(a=0.17,b=1.289,c=0.0216,
>  epsilon[B](t)),t=0..1200):
>  plot3:=plot([data],style=point,symbol=cross):
>  plots[display]({plot1,plot2,plot3});
```
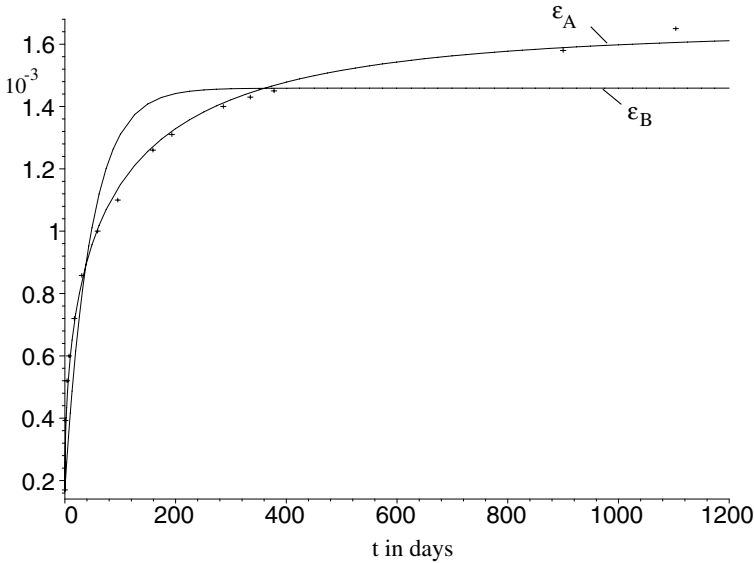
Fig. 11.13a Creep curves for concrete in comparison with experimental data

In the next Figure 11.13b the $\sqrt{t}$-scale as abscissa has been chosen.

$\odot$ 11_9.*mws*

```
>   data:=[0.0,0.17],[0.92,0.3928],[1.99,0.52],
    [2.77,0.6],[4.15,0.72],[5.54,0.858],
    [7.69,1.0],[9.78,1.1],[12.61,1.26],
    [13.90,1.31],[16.92,1.4],[18.84,1.43],
    [19.44,1.45],[30.0,1.58],[33.22,1.65],
    [34.75,1.64]:
>   epsilon[A](t):=a+b*(1-exp(-c*sqrt_t));
```

$$\varepsilon_A(t) := a + b\left(1 - e^{(-c\,sqrt\_t)}\right) \qquad (11.37^*)$$

```
>   epsilon[B](t):=a+b*(1-exp(-c*sqrt_t^2));
```

$$\varepsilon_B(t) := a + b\left(1 - e^{(-c\,sqrt\_t^2)}\right)$$

```
>   plot1:=plot(subs(a=0.17,b=1.475,c=0.109,
>       epsilon[A](t)),sqrt_t=0..40,colour=black):
>   plot2:=plot(subs(a=0.17,b=1.289,c=0.0216,
>       epsilon[B](t)),sqrt_t=0..40,colour=black):
>   plot3:=plot([data],style=point,symbol=cross):
>   plots[display]({plot1,plot2,plot3});
```
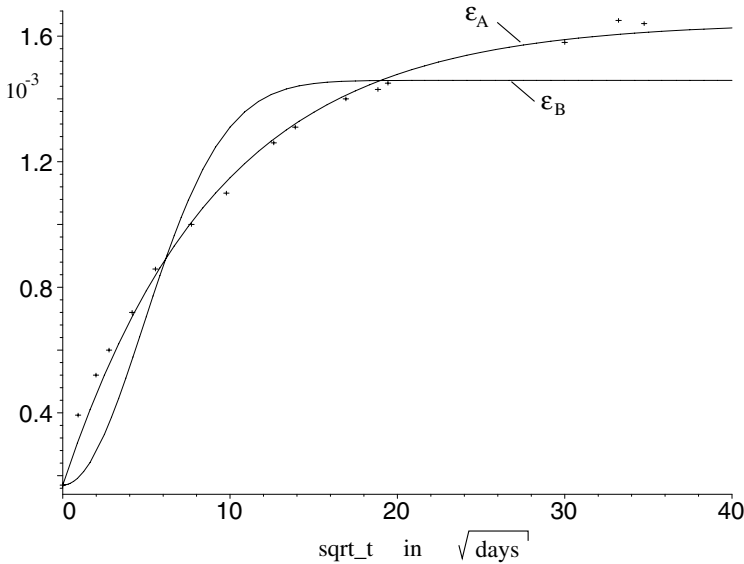
Fig. 11.13b Creep curves for concrete in comparison with experimental data

The Figures 11.13a,b illustrate that the creep curve $\varepsilon_A(t)$ according to (11.37) agrees with experimental data better than $\varepsilon_B(t)$ given by the equation (11.40). This difference becomes clearer in Fig. 11.13b than in Fig. 11.13a.

BLOK (2006) has shown that the $\sqrt{t}$-*law* according to (11.37) with only three parameters can also be successfully applied to serval polymers, e.g., *EVA copolymers* at room temperature. The use of PRONY*series* was less successful.

11.3.3 Creep as a Diffusion Process

Because of the good agreement between the $\sqrt{t}$-*law* and experimental results (Fig. 11.13a,b), we assume that creep can be interpreted as a *diffusion controlled process* (BETTEN, 1971), since the $\sqrt{t}$-*law* plays also a central role in the kinetic theory of diffusion.

The *creep strain* (4.2), i.e., the viscous part of the total strain is based upon thermal activated processes, for instance, *climbing of dislocations* (ASHBY and JONES, 1980). Besides the *dislocation creep* another creep mechanism is important: *the diffusional creep* . Diffusion of atoms can unlock dislocations from obstructions in their path. Hence, the movement of these unlocked dislocations under the applied stress results in *dislocation*

creep . This explains the *progressive*, *continuous* nature of creep as a *diffusion controlled process* .

The temperature influence on thermal activated processes can usually be expressed by an ARRHENIUS *function* . Thus, the creep behavior of solids at high temperature can be described by the law

$$\dot{\varepsilon} = A\, f(\sigma, T) \cdot \exp(-Q_k/RT)\,, \tag{11.41}$$

where A is a material constant, $Q_k[J/mol]$ is called the *activation energy for creep* , $R = 8.37\,J/(mol\,K)$ is known as the *universal gas constant* , and T denotes the *ablolute temperature* .

For many materials, in particular metals, the function $f(\sigma, T)$ in (11.41) is given by $[\sigma/E(T)]^n$ with exponents n between 4 and 8. For many metals one can observe an agreement of the *activation energy for creep* , Q_k, with the *activation energy for self-diffusion* , Q_D,

$$D = D_0 \cdot \exp(-Q_D/RT)\,. \tag{11.42}$$

Consequently, creep at temperatures in the range $0.4 \leq T/T_M \leq 0.5$ can be interpreted as a diffusion controlled process (BETTEN, 1971).

In order to describe the diffusion, we consider in the following the one dimensional differential equation

$$\boxed{\frac{\partial c}{\partial t} = D \frac{\partial^2 c}{\partial x^2}}\,, \tag{11.43}$$

where the *diffusion coefficient* D, according to (11.42), is assumed to be indepent on distance x and on concentration $c = c(x, t)$.

For integration the differential equation (11.43), it is convenient to introduce the mixed dimensionless variable

$$\boxed{\xi \equiv \frac{x}{2\sqrt{Dt}}} \quad \text{with} \quad \begin{cases} \dfrac{\partial \xi}{\partial t} = -\dfrac{x}{4\sqrt{D}\,t^{3/2}} \\[2mm] \dfrac{\partial \xi}{\partial x} = \dfrac{1}{2\sqrt{D}\,t}\,. \end{cases} \tag{11.44}$$

Hence, inserting the partial derivatives

$$\frac{\partial c}{\partial t} = \frac{\partial c}{\partial \xi}\frac{\partial \xi}{\partial t} = -\frac{x}{4\sqrt{D}t^{3/2}} = -\frac{1}{2t}\xi\frac{\partial c}{\partial \xi} \tag{11.45}$$

and

$$\frac{\partial c}{\partial x} = \frac{1}{2\sqrt{Dt}}\frac{\partial c}{\partial \xi} \quad \Rightarrow \quad \frac{\partial^2 c}{\partial x^2} = \frac{1}{4Dt}\frac{\partial^2 c}{\partial \xi^2} \tag{11.46a,b}$$

into (11.43), we arrive at the ordinary differential equation

$$\boxed{\frac{d^2 c}{d\xi^2} + 2\xi\frac{dc}{d\xi} = 0} \;, \tag{11.47}$$

which can be solved by substitution $u \equiv dc/d\xi$ and separation of the variables (u, ξ) according to

$$\frac{du}{u} = -2\xi d\xi \quad \Rightarrow \quad \ln u = -\xi^2 + b \quad \Rightarrow \quad u = Be^{-\xi^2} \;,$$

and, because of $u \equiv dc/d\xi$, we obtain by integration the concentration

$$c(x,t) - c_0 = B \int_0^\xi \exp(-\xi^{*2})d\xi^* \tag{11.48a}$$

or in the form

$$\boxed{c(x,t) - c_0 = \frac{B}{2}\sqrt{\pi}\,\mathrm{erf}(\xi)} \;. \tag{11.48b}$$

The function

$$\mathrm{erf}(\xi) = \frac{2}{\sqrt{\pi}} \int_0^\xi \exp(-\xi^{*2})d\xi^* \tag{11.49}$$

in (11.48b) is known as the GAUSS *error function* , which is implied in the MAPLE software as a standard function (Fig. 11.14) $\boxed{\odot \; 11\_10.mws}$.
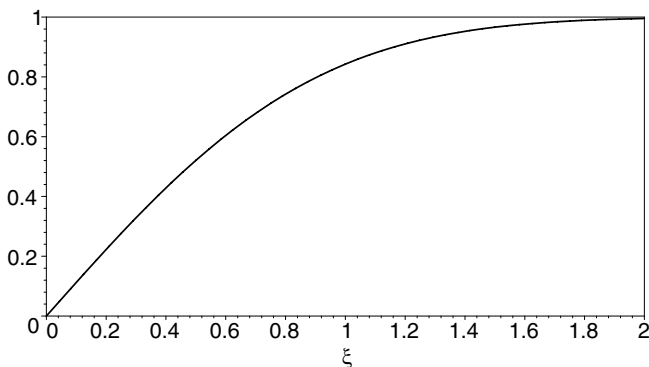
Fig. 11.14 GAUSS error function

The integration constant B in (11.48a,b) depends on boundary conditions, i.e. on the special problem considered. As an example, two specimens may by welded at a postion $x = 0$, where the left specimen, for instance, has a carbon content of a concentration c_0, while the right specimen is free of carbon at time $t = 0$. For $t > 0$ we can observe a diffussion from the left specimen to the right one (Fig. 11.15) until the concentration is balanced in both specimens to $c_0/2$.
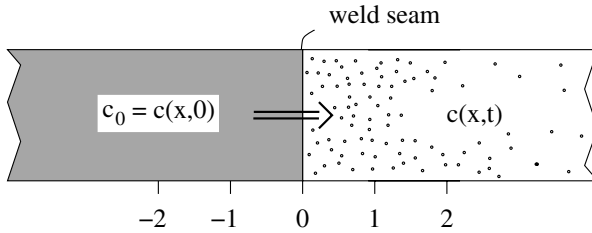
Fig. 11.15 Diffusion down a concentration gradient

For this diffusion process we arrive from (11.48b) at the *concentration*

$$ c(x,t) = \frac{1}{2}c_0 \left[1 - \operatorname{erf}\left(\frac{x}{2\sqrt{Dt}} \right) \right] \qquad (11.48c) $$

with the concentration gradient

$$ \frac{\partial c(x,t)}{\partial x} = -\frac{1}{2}\frac{c_0}{\sqrt{\pi Dt}} \exp\left(-\frac{x^2}{4Dt} \right), \qquad (11.48d) $$

which is a *normal dustribution* like (A.15). Both relations, the *concentration* (11.48c) and its *gradient* (11.48d), have been numerical evaluated with the MAPLE software and are illustrated in Fig. 11.16

$\odot$ 11_11.*mws*

```
>   c(x,t):=(c[0]/2)*(1-erf(x/2/sqrt(D*t)));
```

$$ c(x,\ t) := \frac{1}{2}\,c_0\,(1 - \operatorname{erf}(\frac{1}{2}\,\frac{x}{\sqrt{D\,t}})) $$

```
>   gradient:=diff(c(x,t),x);
```

$$ gradient := -\frac{1}{2}\,\frac{c_0\,e^{(-1/4\,\frac{x^2}{D\,t})}}{\sqrt{\pi}\,\sqrt{D\,t}} $$

```
>   alias(th=thickness,inf=infinity):
>   p[1]:=plot(subs(c[0]=1,D=1,t=0.15,{c(x,t),
     gradient}),x=-2..2,-1..1,th=3):
>   p[2]:=plot(subs(c[0]=1,D=1,t=0.8,{c(x,t),
     gradient}),x=-2..2,-1..1,th=3):
>   p[3]:=plot(subs(c[0]=1,D=1,t=inf,{c(x,t),
     gradient}),x=-2..2,-1..1,th=3):
>   p[4]:=plot(subs(c[0]=1,D=1,t=0.0001,{c(x,t),
     gradient}),x=-2..2,-1..1,th=3):
>   plots[display]({seq(p[k],k=1..4)});
```
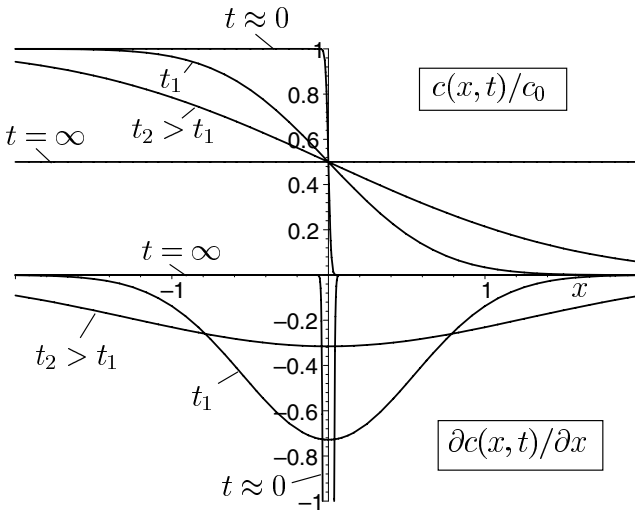

Fig. 11.16 Concentration balance and gradient

From the result (11.48b) we obtain the inverse function $\xi = \xi(c)$ and then by considering the substitution (11.44) the penetration of a concentration c, i.e., the *diffusion way* according to

$$\boxed{x = x(c,t) = 2\sqrt{D}\xi(c)\sqrt{t}}\,. \tag{11.50}$$

This result is known as the $\sqrt{t}$ -*law* for the diffusion way.

Some details about the inverse function $\xi = \xi(c)$ are discussed in the appendix B referring to (B.118b).

By analogy with (11.50) the $\sqrt{t}$ -*law* can also be applied in order to describe the *nonlinear creep behavior* of concrete (Fig. 11.13a,b) or the *stress relaxation* in glass (Section 11.3.4).

In the linear theory of viscoelasticity the viscous component is taken into account by the NEWTON term $\tau = \eta\dot{\gamma}$ in (11.19) or $\sigma_N = \eta_D\dot{\varepsilon}$, so that the response of a NEWTON dashpot loaded by a constant τ_0 or σ_0 is given by $\gamma = (\tau_0/\eta)t$ or $\varepsilon = (\sigma_0/\eta_D)t$, respectively. Utilizing the $\sqrt{t}$-*law*, i.e., substituting $\sqrt{t}$ for t, we obtain the response of the *nonlinear dashpot* according to the relations

$$\gamma = C(\tau_0/G)\sqrt{t} \quad \text{or} \quad \varepsilon = c(\sigma_0/E)\sqrt{t}\,. \qquad (11.51a,b)$$

Hence, the derivatives with respect to time t lead to:

$$\tau_0 = (2/C)G\sqrt{t}\,\dot{\gamma} \quad \text{or} \quad \sigma_0 = (2/c)E\sqrt{t}\,\dot{\varepsilon}\,. \qquad (11.52a,b)$$

If spring element and dashpot are in parallel (Fig. 11.2), we add to (11.52a,b) the HOOKE term $\tau_0 = G\gamma$ or $\sigma_0 = E\varepsilon$, repectively, and find in contrast to (11.19) the differential equation

$$\gamma + (2/C)\sqrt{t}\,\dot{\gamma} = \tau_0/G \quad \text{or} \quad \varepsilon + (2/c)\sqrt{t}\,\dot{\varepsilon} = \sigma_o/E\,. \qquad (11.53a,b)$$

The second equation (11.53b), for instance, can be solved analogous to (11.20) by introducing the integrating factor $\exp(c\sqrt{t})$ as follows:

$$\underbrace{\dot{\varepsilon}\,e^{c\sqrt{t}} + \frac{c}{2\sqrt{t}}\,\varepsilon\,e^{c\sqrt{t}}}_{\dfrac{d}{dt}(\varepsilon\,e^{c\sqrt{t}})} = \frac{\sigma_0}{E}\frac{c}{2\sqrt{t}}e^{c\sqrt{t}} \Rightarrow \boxed{\varepsilon(t) = \frac{\sigma_0}{E} + Ae^{-c\sqrt{t}}}\,. \qquad (11.54)$$

Inserting the initial condition $\varepsilon(0) = 0$ into (11.54) yields the integration constant $A = -\sigma_0/E$, so that we finally oabtain the solution

$$\boxed{\varepsilon_a(t) = \frac{\sigma_0}{E}\left[1 - \exp(-c\sqrt{t})\right]}\,. \qquad (11.55a)$$

In contrast with (11.55a) the *creep function* of the KELVIN body is, because of (11.8) and (11.21), given by the relation

$$\boxed{\varepsilon_b(t) = \frac{\sigma_0}{E}\left[1 - \exp(-t/\lambda)\right]}\,. \qquad (11.55b)$$
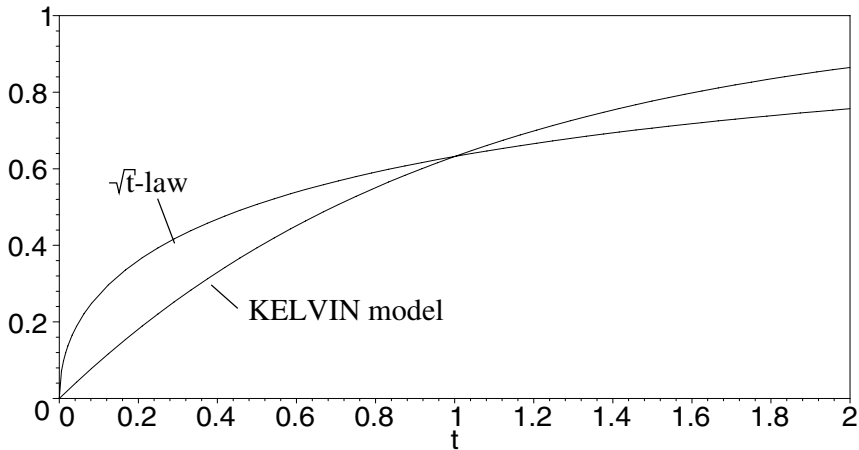
Fig. 11.17 Creep curves (11.55a,b)

Both results, (11.55a,b), are represented in Fig. 11.17 for $\sigma_0/E = 1$ and $c = 1/\lambda = 1$.

In extension of (11.55a,b) let us consider the *standard solid model* (n=1 in Fig. 11.3) and its modified model based upon the $\sqrt{t}$-*law* . We then obtain the following relations

$$
\boxed{
\begin{aligned}
\varepsilon_A(t) &= a_1 + b_1\left[1 - \exp(-c_1\sqrt{t})\right] \\
\varepsilon_B(t) &= a_2 + b_2\left[1 - \exp(-c_2 t)\right]
\end{aligned}
}
\qquad \text{(11.56a,b)}
$$

which are identical with (11.37), (11.40) and compared with experimental data in Fig. 11.13a,b.

The difference between the two creep curves (11.56a,b) in a range of $0 \le \tau \le t$, also called the *distance* of the two functions, can be expressed by the L_2-*error norm* defined as

$$
L_2 \equiv \|\varepsilon_A(t) - \varepsilon_B(t)\|_2 := \sqrt{\frac{1}{t}\int_0^t \left[\varepsilon_A(\tau) - \varepsilon_B(\tau)\right]^2 d\tau}\,. \qquad \text{(11.57)}
$$

With the experimental data of concrete (Fig. 11.13a,b) we calculate by using the MARQUART- LEVENBERG *algorithm* the following coefficients of the relations (11.56a,b):

$a_1 = 0.17$	$b_1 = 1.475$	$c_1 = 0.109$
$a_2 = 0.17$	$b_2 = 1.289$	$c_2 = 0.0216$

Hence, the error norm (11.57) on $0 \leq \tau \leq 1200$ takes the value

$$\boxed{L_2 = 0.1106}\,,$$

which is too large, i.e., the *linear standard solid model* (11.56b) is not suitable to describe the creep behavior of concrete B 300, while the modified model (11.56a) predicts a good agreement with experimental data as has been illustrated in (Fig. 11.13a,b). Further remarks on $\boxed{\odot \; 11\_12.mws}$

11.3.4 Relaxation Spectra and Relaxation Functions for the Generalized MAXWELL Model

In contrast to the KELVIN *model* (Fig. 11.2) the MAXWELL *model* consists of one linear spring (HOOKE) and one linear dashpot (NEWTON) connected in **series**. Thus, by analogy of (11.19), the MAXWELL body is characterized by the following ordinary differential equation with constant coefficients:

$$\dot{\gamma} = \dot{\tau}/G + \tau/\eta\,, \tag{11.58}$$

which can be solved by introducing the integrating factor $\exp(t/\lambda)$ according to

$$\underbrace{\dot{\tau}\,e^{t/\lambda} + \frac{G}{\eta}\tau\,e^{t/\lambda}}_{\frac{d}{dt}\left(\tau e^{t/\lambda}\right)} = G\,\dot{\gamma}\,e^{t/\lambda} \;\Rightarrow\; \boxed{\tau(t) = G \int_{-\infty}^{t} e^{-(t-\theta)/\lambda}\,\dot{\gamma}(\theta)\,d\theta}\,.$$

$$\tag{11.59}$$

The constant $\lambda \equiv \eta/G$ in (11.59) is called the *relaxation time* .

The *relaxation function* (11.10) for the MAXWELL body (11.11) can be determined by inserting the shear rate $\dot{\gamma} = 0$ into (11.58), since the MAXWELL body is assumed to be subjected by a constant shear strain γ_0 during the relaxation process. Then, (11.58) possesses the simple solution

$$r(t) := \frac{\tau(t)}{G\gamma_0} = \exp(-t/\lambda)\,, \tag{11.60}$$

if we take the initial condition $\tau(0) = G\gamma_0$ into consideration. This result is compatible with (11.10) and (11.11a), if we, in a similar way to (11.21),

assume that the same *relaxation function r* is valid for both longitudinal constant strain ε_0 and constant shear strain γ_0. A difference could only be between the parameters $\lambda_D = \eta_D/E$ and $\lambda = \eta/G$ due to longitudinal strain and shear strain, respectively. However, because of (9.24) and (9.24*) we have $\lambda_D \equiv \lambda$, i.e., the *relaxation times* in longitudinal strain and shear strain are identical.

In the following a rheological model consisting of one HOOKE *element* and n MAXWELL *elements* is analysed (Fig. 11.18).
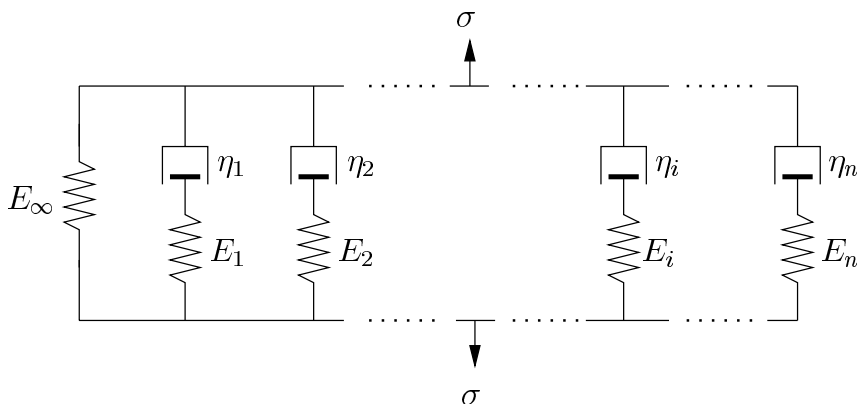
Fig. 11.18 Model with one HOOKE element and n MAXWELL elements in parallel

The model in Fig. 11.18 contains the POYNTING-THOMSON *model* $(n = 1)$ as a special case with three parameters (E_∞, E_1, η_1). Due to (11.10), (11.11) or (11.60) this model is characterized by the following *relaxation function*

$$\frac{1}{\varepsilon_0}\sigma(t) := E(t) = E_\infty + E_1 \cdot \exp(-t/\lambda_1). \qquad (11.61)$$

Supplimenting the POYNTING-THOMSON model by further MAXWELL elements as illustrated in Fig. 11.18, we arrive, by analogy with (11.23), from (11.61) to the *generalized relaxation function* :

$$\boxed{E(t) = E_\infty + \sum_{k=1}^{n} E_k \cdot \exp(-t/\lambda_k)}, \qquad (11.62)$$

where E_k are the spring constants of the several MAXWELL elements, while $\lambda_k \equiv \eta_k/E_k$ reprisent the corresponding *relaxation times* . Analogous to

the discrete creep spectrum in Fig. 11.5, the values (λ_k, E_k) form a *discrete relaxation spectrum* . The parameter E_∞ in (11.62) can be interpreted as the long-time equilibrium value of the *relaxation modulus* $E(t)$.

The number of MAXWELL elements in Fig. 11.18 may increase indefinitely $(n \to \infty)$. Then the *discrete relaxation spectrum* proceeds, by analogy with Fig. 11.5, to a continuous one, $h = h(\lambda)$. The *relaxation function* defined as

$$E(t) := \frac{1}{\varepsilon_0}\sigma(t) \tag{11.63}$$

and given in the discrete form (11.62) results for $n \to \infty$ in the integral form

$$\boxed{E(t) = E_\infty + \beta \int_0^\infty h(\lambda) \cdot \exp(-t/\lambda)d\lambda} \ , \tag{11.64}$$

where the parameter β can be determined from $E(0) \equiv E_0$ by assuming *normalized relaxation spectra* ,

$$\int_0^\infty h(\lambda)d\lambda \equiv 1 \quad , \tag{11.65}$$

according to

$$\beta = E_0 - E_\infty . \tag{11.66}$$

Hence, the relaxation function (11.64) is represented in the following dimensionless form

$$\boxed{R(t) := \frac{E(t) - E_\infty}{E_0 - E_\infty} = \int_0^\infty h(\lambda) \cdot \exp(-t/\lambda)d\lambda} . \tag{11.67}$$

For the sake of convenience, the integral in (11.67) is solved by utilizing a LAPLACE *transform* . Thus, we introduce the transformation (11.29) and arrive from (11.67) at the following result

$$\boxed{\frac{E(t) - E_\infty}{E_0 - E_\infty} = \int_0^\infty \frac{h(\lambda = 1/\xi)}{\xi^2} \exp(-t\xi)d\xi} \tag{11.68a}$$

or

$$\boxed{\frac{E(t) - E_\infty}{E_0 - E_\infty} = L\{H(\xi)\}}\,,\qquad\qquad (11.68b)$$

where $L\{H(\xi)\}$ is the LAPLACE *transform* of the function

$$H(\xi) = \frac{1}{\xi^2} h(\lambda = 1/\xi)\,. \qquad\qquad (11.69)$$

As an example, let us select the POISSON *distribution* $h(\lambda) \equiv f_1(\lambda)$ according to (11.32), which has already been used in (11.28) as a creep function and represented in Fig. 11.6. For this example, the numerical evaluation of (11.68a,b) with (11.32) for $h(\lambda)$ is carried out by the following MAPLE Computer-Program, and the results are plotted in Fig. 11.19.

$$\odot\ 11\_13.mws$$

```
>   restart:
>   with(inttrans):
>   H(xi,n):=exp(-1/xi)/n!/xi^n/xi^2;
```

$$\mathrm{H}(\xi,\, n) := \frac{e^{(-\frac{1}{\xi})}}{n!\,\xi^n\,\xi^2}$$

```
>   R[n]:=laplace(H(xi,n),xi,t);
```

$$R_n := \frac{2\, t^{(\frac{n}{2}+1/2)}\, \mathrm{BesselK}(n+1,\, 2\,\sqrt{t})}{n!}$$

```
>   for i in [0,1,2,3] do
>   R[i]:=subs(n=i,R[n]) od;
```

$$R_0 := \frac{2\,\sqrt{t}\,\mathrm{BesselK}(1,\, 2\,\sqrt{t})}{0!}$$

$$R_1 := \frac{2\,t\,\mathrm{BesselK}(2,\, 2\,\sqrt{t})}{1!}$$

$$R_2 := \frac{2\,t^{(3/2)}\,\mathrm{BesselK}(3,\, 2\,\sqrt{t})}{2!}$$

$$R_3 := \frac{2\,t^2\,\mathrm{BesselK}(4,\, 2\,\sqrt{t})}{3!}$$

```
>   alias(th=thickness,co=color):
>   plot({seq(R[n],n=0..3)},t=0..5,0..1,
>   th=2,axes=boxed,co=black);
```

$$R(t) := \frac{E(t) - E_\infty}{E_0 - E_\infty}$$

$n = 3$

2

1

0
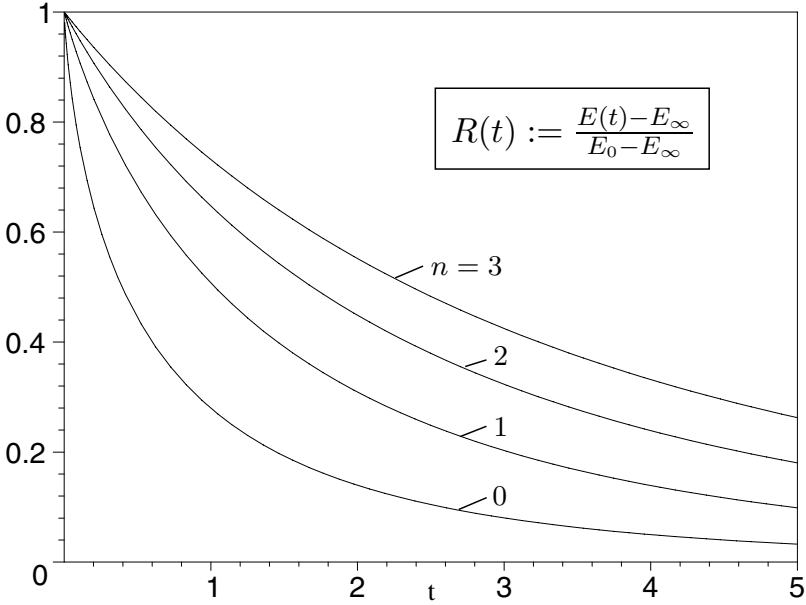
Fig. 11.19 Dimensionless relaxation functions (11.68) based upon the POISSON distributions (11.32) used as relaxation spectra

11.3.5 Relaxation Behavior due to the $\sqrt{t}-$Law

In the previous Section 11.3.4 and also in the following *stress relaxation* has been analyzed in more detail. Besides this sort of relaxation another kind, namely the *structural relaxation* , is also very important (SCHERER, 1986), which governs the time-dependent response of a fluid to a change in temperature. For instance, a liquid is held at temperature T_1 until property $p(t, T_1)$ reaches its equilibrium value $p(\infty, T_1)$, then it is suddenly cooled to T_2. The instantaneous change in p is proportional to the difference $T_2 - T_1$, followed by relaxation toward the equilibrium value $p(\infty, T_2)$.

The *stress relaxation* in glass can be described by a *modified* POYNTING-THOMSON model based upon the $\sqrt{t}$-law. Thus, by analogy with the *modified standard solid Model* (11.56a,b), we take into consideration the following two relations in comparison with relaxation experiments:

$$\boxed{\begin{array}{c} \sigma_A(t) = a_3 + b_3 \exp\left(-c_3\sqrt{t}\right) \\ \hline \sigma_B(t) = a_4 + b_4 \exp\left(-c_4 t\right) \end{array}} . \qquad (11.70\text{a,b})$$

Hence, the dimensionless relaxation functions defined as

$$R := \frac{E(t) - E_\infty}{E_0 - E_\infty} = \frac{\sigma(t) - \sigma_\infty}{\sigma_0 - \sigma_\infty} \tag{11.71}$$

are given by

$$\boxed{R_A = \exp(-c_3\sqrt{t})\ \bigg|\ R_B = \exp(-c_4 t)}. \tag{11.72a,b}$$

The first equation (11.72a) is the modified form, the second one (11.72b) refers to the MAXWELL model (Fig. 11.20).
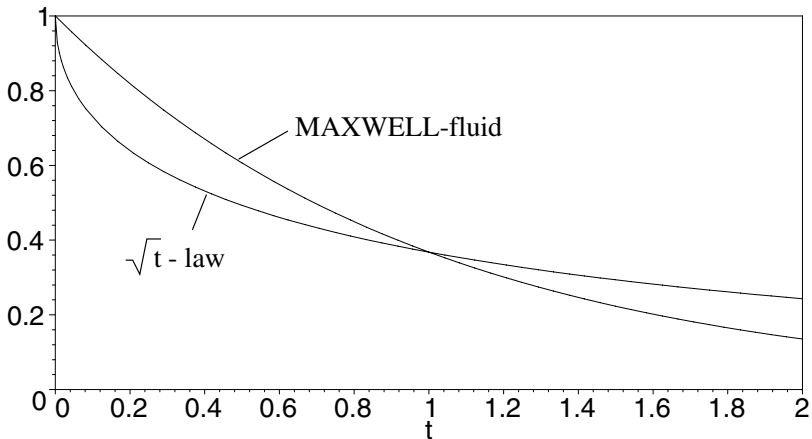
Fig. 11.20 Relaxation functions (11.72a,b)

Based upon a lot of experiments on glass, SCHERER (1986) has shown that both the stress and structural relaxation in glass can be predicted by the relation

$$\boxed{r(t) = \exp\left[-(t/\lambda)^b\right]} \tag{11.73}$$

often called KOHLRAUSCH *function* or *b-function*, which is a modified form of the MAXWELL relaxation function (11.60). The exponent b in (11.73) for a variety of glasses was found to be near the value of $b \approx 0.5$, so that the assumption of the $\sqrt{t}$-*law* is justified. However, the relation (11.73) is valid only for *stabilized glass* , i.e., the glass is held at a given temperature until its properties do no longer change with time, then the load can be applied.

In unstabilized glasses the viscosity η and other typical properties, e.g. the density, vary with time. Then, the relaxation function (11.73) should be replaced by the formula

$$r(t) = \exp\left[-\left(\int_0^t \frac{G_0 dt^*}{\eta(t^*)}\right)^b\right] \tag{11.74}$$

where, in agreement with experimental results, the exponent b can again be assumed to $b \approx 1/2$, as has been discussed in more detail by SCHERER (1986).

AIMEDIEU (2004) has investigated the nonlinear relaxation of *brain tissue* and found very good agreement between the $\sqrt{t}-law$ according to (11.70a) and his own experiments. The use of PRONY-*series* was less succesful.

11.3.6 Mechanical Hysteresis of Rheological Models

In order to discuss the *dynamic behavior* of rheological bodies, it is expedient to determine, both experimental and analytical, the hysteresis loops in $\sigma - \varepsilon-$ diagrams, which becomes significant in cyclic loading because of the *energy dissipation* . The damping capacity of a material can be investigated by taking the mechanical hysteresis effect into account.

In the following the hysteresis loop of the KELVIN body is determined assuming *harmonic loading* according to

$$\sigma(t) = \sigma_0 \cos \Omega t \tag{11.75a}$$

or in complex form

$$\sigma(t) = \sigma_0 \text{Re}\left(e^{i\Omega t}\right) , \tag{11.75b}$$

where σ_0 is the stress amplitude, and Ω is the vibration frequency. Considering (11.8) and (11.75b) we arrive from the general form (11.5) at the following response:

$$E\varepsilon(t) = \frac{\sigma_0}{\lambda} e^{-t/\lambda} \text{Re}\left\{\int_{-\infty}^t e^{i\Omega\theta} e^{\Omega/\lambda} d\theta\right\} \tag{11.76a}$$

the integration of which and seperation of real and imaginary parts yield

$$E\varepsilon(t) = \frac{1}{1 + \Omega^2 \lambda^2}\left(\sigma_0 \cos \Omega t + \Omega\lambda\sigma_0 \sin \Omega t\right). \tag{11.76b}$$

Since the loading (11.75a) is an oscillatory stress, the strain response will be an oscillation at the same frequency as the stress but lagging behind by a phase angle α, hence

$$E\varepsilon(t) = \frac{\sigma_0}{1 + \Omega^2\lambda^2}\cos(\Omega t - \alpha)\,. \tag{11.77}$$

Applying the addition theorem to (11.77) and considering (11.76b) we immediately obtain the *phase angle* as

$$\alpha = arc\tan\Omega\lambda = arc\tan\Omega\,(\eta/G)\,, \tag{11.78}$$

which is often called the *loss angle* and is influenced by the internal friction of the material. The amplitude ε_a of the response is obtained by applying the condition $\dot\varepsilon = 0$ to (11.76b), hence

$$E\varepsilon_a = \sigma_0\Big/\sqrt{1 + \Omega^2\lambda^2}\,. \tag{11.79}$$

In order to obtain the equation of the hysteresis in $\sigma-\varepsilon-$ coordinates, we insert (11.75a) into (11.75b) and find by considering (11.79) the quadratic form

$$\left(1 + \Omega^2\lambda^2\right)\varepsilon^2 - 2\varepsilon\,(\sigma/E) + (\sigma/E)^2 - \Omega^2\lambda^2\varepsilon_a^2 = 0\,, \tag{11.80}$$

which represents an ellipse. Experimental determined hysteresis of real materials can more or less deviate from the elliptical shape (BETTEN, 1969). Such deviations can be interpreted as *nonlinear effects* .

The KELVIN body satisfies the following tensorial equation

$$\sigma_{ij}' = 2\,G\,\varepsilon_{ij}' + 2\,\eta\,\dot\varepsilon_{ij}'\,, \tag{11.81}$$

where σ_{ij}' and ε_{ij}' are the stress and strain deviators, respectively.

The second term in (11.81) is the *dissipative* part of the stress deviator:

$$\left(\sigma_{ij}'\right)_d = 2\,\eta\dot\varepsilon_{ij}'\,. \tag{11.82a}$$

For the uniaxial equivalent state the tensorial form (11.82a) is simplified according to

$$\sigma_d = 2\,\eta\,(1+\nu)\,\dot\varepsilon = E\,(\eta/G)\,\dot\varepsilon \tag{11.82b}$$

with ν as the isotropic *transverse contraction ratio* .

The dynamic behavior of the KELVIN body is based upon the *linear* differential equation

$$m\ddot{x} + k\dot{x} + cx = P(t)\,, \tag{11.83}$$

where the second term represents the *dissipative force* , so that the *dissipative stress* is given by

$$\sigma_d = k\dot{x}/F = k\,(\ell/F)\,\dot\varepsilon\,, \tag{11.84}$$

hence, a comparison with (11.82b) yields:

$$\lambda = \eta/G = k/c \,. \tag{11.85}$$

The *damping factor* k in (11.83) can be expressed by LEHR*'s damping measure* D:

$$k = 2\,(c/\omega)\,D \,, \tag{11.86}$$

where ω is the *eigenfrequency* of the undamped free vibration, so that (11.85) leads to

$$\lambda = 2D/\omega \,. \tag{11.87}$$

With this expression and the nondimensional frequency ratio $\zeta \equiv \Omega/\omega$ we obtain the *elliptical hysteresis*

$$\boxed{\left(1 + 4D^2\zeta^2\right)\varepsilon^2 - 2\varepsilon\,(\sigma/E) + (\sigma/E)^2 - 4D^2\zeta^2\varepsilon_a^2 = 0} \,. \tag{11.88}$$

The *material damping* is defined as (BETTEN, 1969)

$$\vartheta = A_d/A \,, \tag{11.89}$$

where A_d is the *dissipative energy* per cycle, i.e. the area of the hysteresis loop, and A is selected as a reference value:

$$A_d = \pi/\sqrt{\gamma_1\gamma_2} \tag{11.90}$$

and

$$A = \frac{1}{2}\frac{\sigma}{E}\varepsilon_a = \frac{1}{2}\varepsilon_a^2 \,, \tag{11.91}$$

respectively.

The values γ_1 and γ_2 in (11.90) are known as the characteristic roots of the quadratic form (11.88). Thus

$$\gamma_1\gamma_2 = (1/4)D^2\zeta^2\varepsilon_a^4 \,, \tag{11.92}$$

so that the material damping defined in (11.89) with (11.90) and (11.91) is given by the simple expression (BETTEN, 1969)

$$\boxed{\vartheta = 4\pi D\zeta} \,, \tag{11.93}$$

which depends on the nondimensional frequency ratio $\zeta \equiv \Omega/\omega$.

For *damped free vibration* , BETTEN (1969) derived the material damping according to

$$\vartheta = (1 + D^2) \left[1 - \exp\left(-4\pi D \Big/ \sqrt{1 - D^2}\right)\right], \qquad (11.94)$$

which is simplified to $\vartheta \approx 4\pi D$ for small energy dissipation ($D \ll 1$) and leads to (11.93) for *resonance* $\zeta = 1$.

11.3.7 Complex Parameters of Rheological Models

Besides the mechanical hysteresis effect discussed in the previous Section *complex parameters* play also a fundamental role, when the dynamic behavior of rheological models should be investigated.

Complex modulus , *complex compliance* , and *complex viscosity* , for instance, essentially depend on the vibration frequency Ω as should be explained in the following.

Let us assume *harmonic* shear loading according to

$$\tau^*(t) = \tau_0 e^{i\Omega t} \Rightarrow \gamma^*(t) = \gamma_0 e^{i(\Omega t - \alpha)}, \qquad (11.95\text{a,b})$$

where complex values are marked by a star. The phase angle is α as has been used in (11.77).

Analogous to the usual shear modulus $G = \tau/\gamma$ of the HOOKE body we define a *complex shear modulus* as

$$\tau^*/\gamma^* := G^*(i\Omega) = G_1(\Omega) + iG_2(\Omega), \qquad (11.96)$$

which depends on the vibration frequency Ω. Considering (11.95a,b), the real and imaginary parts in (11.96) are given by

$$G_1(\Omega) = (\tau_0/\gamma_0)\cos\alpha \qquad \textit{storage modulus (elasticity)}, \qquad (11.97\text{a})$$
$$G_2(\Omega) = (\tau_0/\gamma_0)\sin\alpha \qquad \textit{loss modulus (energy dissipation)}. \quad (11.97\text{b})$$

The ratio
$$G_2(\Omega)/G_1(\Omega) = \tan\alpha(\Omega) \qquad (11.98)$$

is called *loss factor* or also known as *mechanical damping* . In contrast to (11.96) the ratio

$$\gamma^*/\tau^* := J^*(i\Omega) = J_1(\Omega) - iJ_2(\Omega) \qquad (11.99)$$

is defined as the *complex compliance* with

$$J_1(\Omega) = (\tau_0/\gamma_0)\cos\alpha \qquad \textit{storage compliance}, \qquad (11.100\text{a})$$
$$J_2(\Omega) = (\tau_0/\gamma_0)\sin\alpha \qquad \textit{loss compliance}. \qquad (11.100\text{b})$$

Analogous to the shear viscosity $\eta = \tau/\dot{\gamma}$ of a NEWTON fluid, we define, similar to (11.96), a *complex shear viscosity* as

$$\tau^*/\dot{\gamma}^* = \tau^*/(i\,\Omega\,\gamma^*) := \eta^*(i\,\Omega) = \eta_1(\Omega) - i\,\eta_2(\Omega)\,, \qquad (11.101)$$

which is a function of the vibration frequency Ω. Comparing (11.101) with (11.96), we find the relation $G^* = i\,\Omega\,\eta^*$, hence:

$$\boxed{G_1(\Omega) = \Omega\eta_2(\Omega)}\,, \qquad \boxed{G_2(\Omega) = \Omega\eta_1(\Omega)}\,. \qquad (11.102\text{a,b})$$

The real parts G_1 (*dynamic shear modulus*) and η_1 (*dynamic shear viscosity*) represent the *elastic* and *viscous* portions, respectively, in the material.

These material properties relate to the *relaxation function* of the fluid. To show that we start from the constitutive equation (11.59) represented in complex variables $(\tau^*, \dot{\gamma}^*)$ according to

$$\boxed{\tau^*(t) = G \int_0^\infty e^{-s/\lambda}\,\dot{\gamma}^*\,(t-s)\,ds}\,, \qquad (11.103)$$

where the substitution $t - \theta \equiv s$ has been introduced.

Assuming a harmonic shear strain $\gamma^* = \gamma_0 \exp(i\,\Omega\,t)$ and considering (11.101), we arrive at the relation

$$\tau^*(t) = \dot{\gamma}^*\,G \int_0^\infty e^{-(1/\lambda + i\Omega)s}ds \equiv \dot{\gamma}^*\,\eta^*(i\Omega) \qquad (11.104)$$

from which we immediately read the *complex shear viscosity*

$$\eta^*(i\Omega) = G \int_0^\infty e^{-(1/\lambda + i\Omega)s}ds = \frac{G\lambda}{1 + i\lambda\Omega} = \frac{\eta\,(1 - i\lambda\Omega)}{1 + \lambda^2\Omega^2} \qquad (11.105)$$

possessing the following real and imaginary parts:

$$\boxed{\frac{\eta_1}{\eta} = \frac{1}{1 + \lambda^2\,\Omega^2} \qquad \frac{\eta_2}{\eta} = \frac{\lambda\,\Omega}{1 + \lambda^2\,\Omega^2}}\,. \qquad (11.106\text{a,b})$$

Thus, the corresponding moduli (11.102a,b) can be expressed as

$$\boxed{\frac{G_1}{G} = \frac{\lambda^2\,\Omega^2}{1 + \lambda^2\,\Omega^2} \qquad \frac{G_2}{G} = \frac{\eta_2}{\eta}}\,. \qquad (11.107\text{a,b})$$

We see, that the sum of the real parts (11.106a) and (11.107a) is equal to one: $\eta_1/\eta + G_1/G = 1$.

Note, the integration in (11.105) can also be carried out by the LAPLACE *transform*

$$\eta^* = G\, L\{1\} = G/p \quad \text{where} \quad p \equiv 1/\lambda + i\Omega$$

is the transformed variable, also called the LAPLACE *parameter* .

The results (11.106a,b) and (11.107a,b) have been graphically reresented in Fig. 11.21.
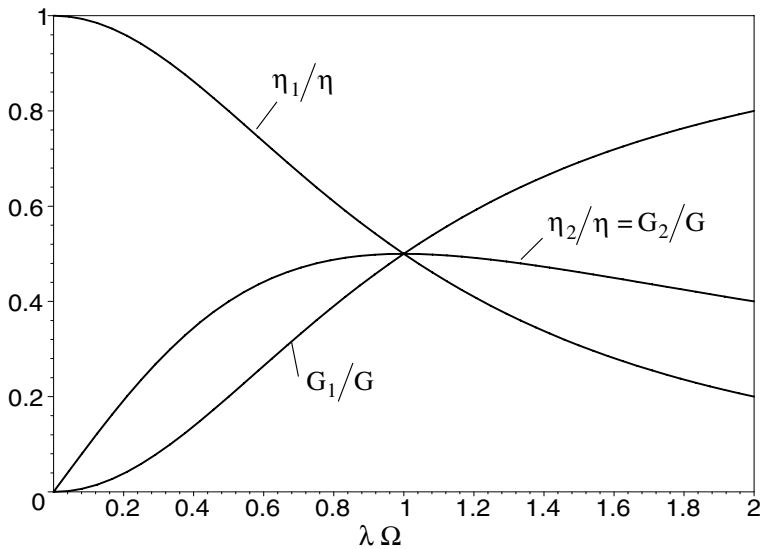
Fig. 11.21 Complex moduli of the MAXWELL body according to (11.106a,b) and (11.107a,b)

In order to find the *complex parameters* of the KELVIN *body* , let us introduce in (11.20) the substitution $t - \theta \equiv s$ and the complex variables (γ^*, τ^*). Thus, we obtain, analogous to (11.103), the following complex constitutive equation of the KELVIN body:

$$\gamma^*(t) = \frac{1}{\eta} \int_0^\infty e^{-s/\lambda}\, \tau^*\,(t-s)\, ds \qquad (11.108)$$

and inserting the *harmonic loading* (11.95a), we arrive at the *complex compliance* (11.99) according to

$$J^*(i\,\Omega) = \frac{1}{G^*} = \frac{1}{\eta} \int\limits_0^\infty e^{-(1/\lambda + i\Omega)s} ds = \frac{1}{\eta\,p}, \qquad (11.109)$$

where $p \equiv 1/\lambda + i\Omega$ denotes again the LAPLACE *parameter* .

The integral in (11.109) **formally** agrees with the corresponding integral in (11.105). The difference results from the constant $\lambda \equiv \eta/G$, which is interpreted as the *relaxation time* in (11.105) and as the *retardation time* in (11.109).

Between the *complex viscosity* (11.105) of the MAXWELL *body* and the complex compliance (11.109) of the KELVIN *body* the relation $\eta^*/\eta = G\,J^*$ is valid, if both models possess the same λ-values. Thus, because of (11.99) and (11.101) the real part $G\,J_1$ agrees with (11.106a), while the imaginary part $G\,J_2$ formally agrees with (11.106b). Further on, from $G^* = \eta\,p$ according to (11.109) we deduce $G_1/G = 1$ and $G_2/G = \lambda\,\Omega$ for the KELVIN *body* , in contrast to the relations (11.107a,b) valid for the MAXWELL body.

Experimental determined parameters can strongly disagree with the results illustrated in Fig. 11.21 for the MAXWELL body. For example, some experiments have been carried out by ASHARE (1968) on a *polymer solution* (4% Polystyrene in Chlordiphenyl at 25C) or by HAN et al. (1975) on a *polymer melt* (Polystyrene at 200C) and by MEISSNER (1975) on Polyethylene, to name just a few.

11.3.8 BURGERS Model

The BURGERS *model* consists of a MAXWELL and a KELVIN element coupled in series as shown in Fig. 11.22.
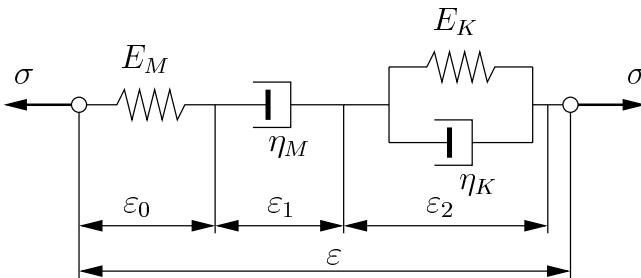
Fig. 11.22 The BURGERS model; nomenclature

The *creep behavior* of the BURGERS *model* is described in the following by considering the strain response under constant stress of piecewise con-

stant stress of the single elements connected in series (Fig. 11.22). Thus, the total strain at time t is decomposed into three parts,

$$\varepsilon(t) = \varepsilon_0 + \varepsilon_1 + \varepsilon_2 , \qquad (11.110)$$

where the first part is the strain of HOOKE's spring,

$$\varepsilon_0 = \sigma/E_M , \qquad (11.111a)$$

the second one results from NEWTON's dashpot with a strain rate according to

$$\dot{\varepsilon}_1 = \sigma/\eta_M , \qquad (11.111b)$$

and, finally, the third part is the strain in the KELVIN unit satisfying the following ordinary differential equation

$$\dot{\varepsilon}_2 + (E_K/\eta_K)\varepsilon_2 = \sigma/\eta_K . \qquad (11.111c)$$

To find the constitutive equation of the BURGERS model, i.e. the relation $\varepsilon(t) = f(\sigma)$ between the *external variables* , we have to eliminate the *internal variables* $\varepsilon_0, \varepsilon_1, \varepsilon_2$ from the equations (11.110) to (11.111c). This can be done by utilizing the LAPLACE transformation having the advantages of *simplicity* and *consistency* (Appendix B), which is applied to the set of the above equations:

$$L\{\varepsilon(t)\} \equiv \hat{\varepsilon}(s) = \hat{\varepsilon}_0(s) + \hat{\varepsilon}_1(s) + \hat{\varepsilon}_2(s) , \qquad (11.112)$$

$$\hat{\varepsilon}_0 = \hat{\sigma}(s)/E_M , \qquad (11.113a)$$

$$s\hat{\varepsilon}_1 - \varepsilon_1(0) = \hat{\sigma}(s)/\eta_M , \qquad (11.113b)$$

$$s\hat{\varepsilon}_2 - \varepsilon_2(0) + (E_K/\eta_K)\hat{\varepsilon}_2 = \hat{\sigma}(s)/\eta_K . \qquad (11.113c)$$

The transformed quantities, for example $\hat{\varepsilon}(s)$, $\hat{\sigma}(s)$ etc., are functions of the transformed variable s instead of the "actual" variable time t.

Assuming th initial values $\varepsilon_1(0^-) = \varepsilon_2(0^-) = 0$ and after that inserting the transforms (11.113a,b,c) of the internal variables into (11.112), we arrive at the following algebraic relation between the transforms of the external variables:

$$\hat{\varepsilon}(s) = \left(\frac{1}{E_M} + \frac{1}{\eta_M s} + \frac{1}{E_K + \eta_K s} \right) \hat{\sigma}(s) . \qquad (11.114)$$

If the BURGERS model is loaded by a constant stress,

$$\sigma(t) = \sigma_0 H(t) \quad \Rightarrow \quad \hat{\sigma}(s) = \sigma_0/s , \qquad (11.115)$$

we obtain from (11.114) the LAPLACE transforms

$$\frac{1}{\sigma_0}\hat{\varepsilon}(s) = \frac{1}{E_M s} + \frac{1}{\eta_M s^2} + \frac{1}{E_K}\frac{1}{s(1+\lambda_2 s)} , \qquad (11.116)$$

the inverse of which immediately furnishes the *constitutive equation* or the *creep function* of the BURGERS *model* :

$$\boxed{\frac{1}{\sigma_0}\varepsilon(t) := J(t) = J_0\left(1 + t/\lambda_1\right) + J_2\left(1 - e^{-t/\lambda_2}\right)} , \qquad (11.117)$$

where the abbreviations $J_0 \equiv 1/E_M$, $J_2 \equiv 1/E_K$ and the retardation times $\lambda_1 \equiv \eta_M/E_M$, $\lambda_2 \equiv \eta_K/E_K$ have been introduced. For $\lambda_1 \to \infty$ the BURGERS *model* tends to the *standard solid model*(11.22a). Note, forming the inverse of (11.116), we have read from a table (Appendix B) the following pairs of LAPLACE transforms:

$L^{-1}\{1/s\} = 1$	$L^{-1}\{1/s^2\} = t$	$L^{-1}\left\{\dfrac{1}{s(1+as)}\right\} = 1 - e^{-t/a}$

As an example, the creep behavior of the BURGERS *model* under piecewise constant stress, according to

$$\boxed{\varepsilon(t) = \sigma_0[H(t-a)\,J(t-a) - H(t-b)\,J(t-b)]} \qquad (11.118)$$

is illustrated in Fig. 11.23, where $H(t-a)$ is the HEAVISIDE *unit step function* discussed in Appendix A in more detail.

⊙ 11_14.mws

```
>   alias (H=Heaviside, th=thickness):
>   plot1:=plot(H(t-1)-H(t-5)-((1/2)*(H(t-6.8)-
>   H(t-7.2))),t=0..12,-1/2..2,th=2):
>   plot2:=plot(H(t-1)*(0.5+0.1*(t-1)+(1-exp(-
>   (1/2)*(t-1))))-H(t-5)*(0.5+0.1*(t-5)+(1-exp
>   (-(1/2)*(t-5))))-(1/2)*H(t-6.8)*(0.5+0.1*(t-
>   6.8)+(1-exp(-(1/2)*(t-6.8))))+(1/2)*H(t-7.2)*
>   (0.5+0.1*(t-7.2)+(1-exp(-(1/2)*(t-7.2)))),
>   t=0..12,-1/2..2,th=3):
>   plot3:=plot(H(t-1)*(0.5+0.1*(t-1)+(1-exp(-
>   (1/2)*(t-1))))-H(t-5)*(0.5+0.1*(t-5)+(1-exp(
>   -(1/2)*(t-5)))),t=6.8..12,-1/2..2,style=point,
>   symbol=cross,numpoints=5):
>   plots[display]({plot1,plot2,plot3});
```
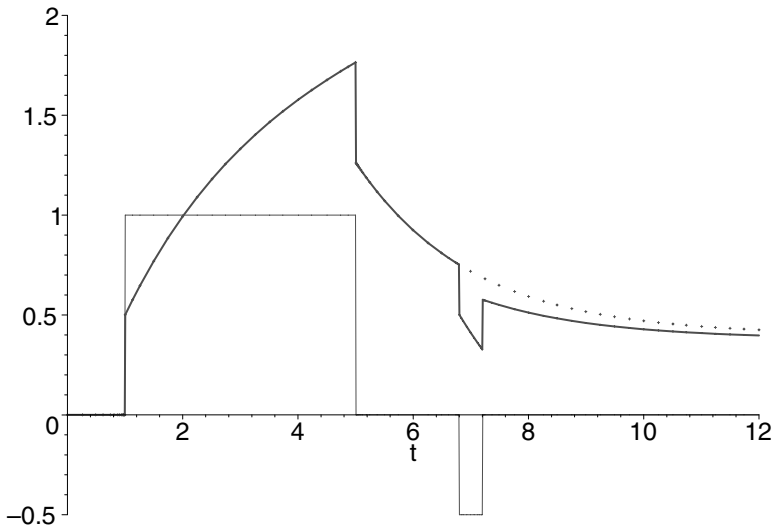
Fig. 11.23 Creep behavior and recovery of the BURGERS model subjected to constant loads between $1 \leq t \leq 5$ and $6.8 \leq t \leq 7.2$

The *relaxation function* (11.10) or (11.61) of the BURGERS *model* should be determined in the following. The LAPLACE transforms of the creep function (11.6) or (11.24) and of the relaxation function (11.10) or (11.61) are related by (11.15a):

$$\boxed{\hat{\kappa}(s)\hat{r}(s) = \hat{J}(s)\hat{E}(s) = 1/s^2}, \qquad (11.119)$$

where the LAPLACE transform $\hat{J}(s)$ of the BURGERS model is identical to the right-hand side of (11.116), which can be written in the form

$$\hat{J}(s) = \frac{s^2 + As + B}{E_M s^2 (s + E_K/\eta_K)} \qquad (11.120)$$

with the following abbreviations:

$$A \equiv \frac{E_M}{\eta_M} + \frac{E_M}{\eta_K} + \frac{E_K}{\eta_K} \quad \text{and} \quad B \equiv \frac{E_M E_K}{\eta_M \eta_K}. \qquad (11.121a,b)$$

Taking (11.120) into account, we arrive from (11.119) at the transform of the *relaxation function* :

$$\hat{E}(s) = \frac{E_M(s + E_K/\eta_K)}{s^2 + As + B} \equiv \frac{E_M(s + E_K/\eta_K)}{(s - s_1)(s - s_2)} \qquad (11.122)$$

where

$$s_{1;2} = -\frac{1}{2}A\left(1 \mp \sqrt{1 - 4B/A^2}\right) \qquad (11.123)$$

are negative and real values, which can be determined from (11.121a,b), i.e. from the four material data E_M, E_K, η_M, η_K.

Applying the *partial-fraction expansion* to (11.122), we obtain the decomposition of the LAPLACE transform

$$\hat{E}(s) = \frac{C_1}{s - s_1} + \frac{C_2}{s - s_2} \text{ with } \begin{cases} C_1 = \dfrac{E_M(s_1 + E_K/\eta_K)}{s_1 - s_2} \\[2mm] C_2 = \dfrac{E_M(s_2 + E_K/\eta_K)}{s_2 - s_1} . \end{cases} \qquad (11.124)$$

Its inverse is the *relaxation function*

$$\boxed{\frac{1}{\varepsilon_0}\sigma(t) := E(t) = C_1 e^{s_1 t} + C_2 e^{s_2 t} \text{ with } s_1 < 0,\ s_2 < 0}, \qquad (11.125)$$

since

$$L^{-1}\left\{\frac{1}{s + a}\right\} = e^{-at}. \qquad (11.126)$$

The stress at time $t = 0$ immediately follows from (11.125):

$$\sigma(0) = (C_1 + C_2)\,\varepsilon_0 \equiv E_M \varepsilon_0 \qquad (11.127)$$

in accordance with (11.111a), i.e. the stress in HOOKE's spring.

As an example, the *relaxation* (11.125) of the BURGERS *model* under piecewise constant strain, according to

$$\boxed{\sigma(t) = \varepsilon_0\left[H(t - a)\,E(t - a) - H(t - b)\,E(t - b)\right]}, \qquad (11.128)$$

is illustrated in Fig. 11.24, where $H(t - a)$ is the HEAVISIDE *unit step function* also used in (11.118).

$\odot$ 11_15.mws

```
>   alias(H=Heaviside,th=thickness):
>   epsilon(t):=epsilon[0]*[H(t-1)-H(t-5)];
```
$$\varepsilon(t) := \varepsilon_0\left[H(t - 1) - H(t - 5)\right]$$
```
>   sigma(t):=epsilon[0]*(C[1]*exp(s[1]*t)+
>   C[2]*exp(s[2]*t));
```

$$\sigma(t) := \varepsilon_0\,(C_1\,e^{(s_1\,t)} + C_2\,e^{(s_2\,t)})$$

```
>   plot1:=plot(H(t-1)*(0.4*exp(-0.4*(t-1))+
>   0.6*exp(-0.6*(t-1)))-H(t-5)*(0.4*exp(-0.4*
>   (t-5))+0.6*exp(-0.6*(t-5))),t=0..10,th=3):
>   plot2:=plot(H(t-1)-H(t-5),t=0..10,th=2):
>   plots[display]({plot1,plot2});
```
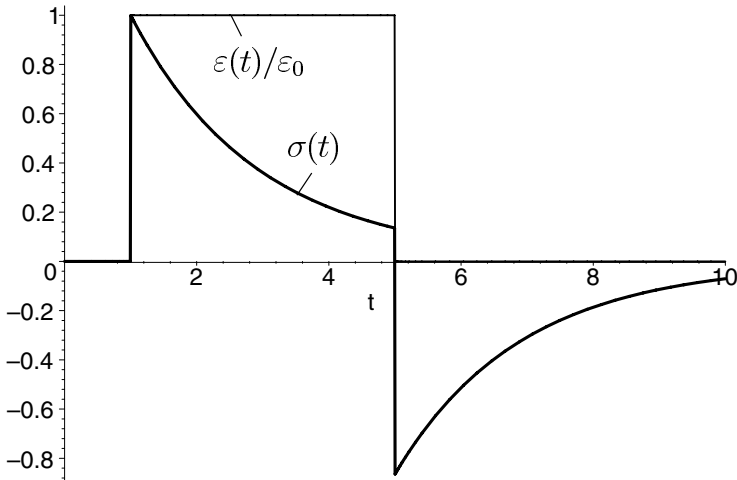

Fig. 11.24 Relaxation behavior of the BURGERS model under constant strain ε_0 between $1 \le t \le 5$

The *relaxation function* (11.125) has been deduced from (11.119). Alternatively, we can start from the relation (11.114), which can be written in the form

$$s^2\hat{\sigma}(s) + As\hat{\sigma}(s) + B\hat{\sigma}(s) = E_M s^2\hat{\varepsilon}(s) + \frac{E_M E_K}{\eta_K}\,s\,\hat{\varepsilon}(s)\,, \quad (11.129)$$

the inverse LAPLACE form of which (Appendix B) immediately yields the differential equation

$$\ddot{\sigma}(t) + A\dot{\sigma}(t) + B\sigma(t) = E_M\ddot{\varepsilon}(t) + \frac{E_M E_K}{\eta_K}\,\dot{\varepsilon}(t) \qquad (11.130)$$

of the BURGERS model, where the abbreviations A and B are defined by (11.121a,b).

Assuming a step of strain ε_0 at time $t = 0^+$, i.e.,

$$\varepsilon(t) = \varepsilon_0 H(t), \quad \dot{\varepsilon}(t) = \varepsilon_0 \delta(t), \quad \ddot{\varepsilon}(t) = \varepsilon_0 \dot{\delta}(t), \qquad (11.131\text{a,b,c})$$

then the differential equation (11.130) takes the special form

$$\ddot{\sigma}(t) + A\dot{\sigma}(t) + B\sigma(t) = \varepsilon_0 \left[E_M \dot{\delta}(t) + \frac{E_M E_K}{\eta_K} \delta(t) \right]. \qquad (11.132)$$

Applying the LAPLACE transformation to this differential equation and taking the transforms

$$L\{\delta(t)\} = 1 \quad \text{and} \quad L\{\dot{\delta}(t)\} = s \qquad (11.133)$$

into account (Appendix B), we arrive at the relation

$$s^2 \hat{\sigma}(s) + As\hat{\sigma}(s) + B\hat{\sigma}(t) = E_M \varepsilon_0 \left(s + E_K / \eta_K \right), \qquad (11.134)$$

from which we read the transform (11.122) of the *relaxation function* $E(t)$.

By analogy with the *creep behavior* of the BURGERS model represented in Fig. 11.23 the *relaxation behaviour* under piecewise constant strains ε_0 **and** α between $1 \leq t \leq 5$ **and** $6.8 \leq t \leq 7.2$, respectively, should be discussed in the following. In that case the strain $\varepsilon(t)$ can be expressed as

$$\boxed{\varepsilon(t) = \varepsilon_0 \left[H(t-a) - H(t-b) \right] + \alpha \left[H(t-c) - H(t-d) \right]},$$
$$(11.135)$$

while the *relaxation* (11.125) results in an extended form of (11.128), according to

$$\boxed{\begin{aligned} \sigma(t) = \varepsilon_0 \, [H(t-a)E(t-a) &- H(t-b)E(t-b)] + \\ \alpha \, [H(t-c)E(t-c) &- H(t-d)E(t-d)] \end{aligned}}. \qquad (11.136)$$

Assuming the parameters from Fig. 11.24, the *relaxation* (11.136) is illustrated in Fig. 11.25.

⊙ 11_16.*mws*

```
>   alias(H=Heaviside,th=thickness,co=color):
>   plot1:=plot(H(t-1)-H(t-5)+
>   0.3*(H(t-6.8)-H(t-7.2)),t=0..10,co=black):
>   plot2:=plot(H(t-1)*(0.4*exp(-0.4*(t-1))+
>   0.6*exp(-0.6*(t-1)))-H(t-5)*(0.4*
>   exp(-0.4*(t-5))+ 0.6*exp(-0.6*(t-5)))+
>   0.3*H(t-6.8)*(0.4*exp(-0.4*(t-6.8))+
>   0.6*exp(-0.6*(t-6.8)))-0.3*H(t-7.2)*
>   (0.4*exp(-0.4*(t-7.2))+ 0.6*
>   exp(-0.6*(t-7.2))),t=0..10,co=black,th=3):
```

```
>   plot3:=plot(H(t-1)*(0.4*exp(-0.4*(t-1))+
>   0.6*exp(-0.6*(t-1)))-H(t-5)*
>   (0.4*exp(-0.4*(t-5))+ 0.6*exp(-0.6*(t-5))),
>   t=6.8..10,co=black,style=point,
>   symbol=circle,symbolsize=10,numpoints=5):

>   plots[display]({plot1,plot2,plot3});
```
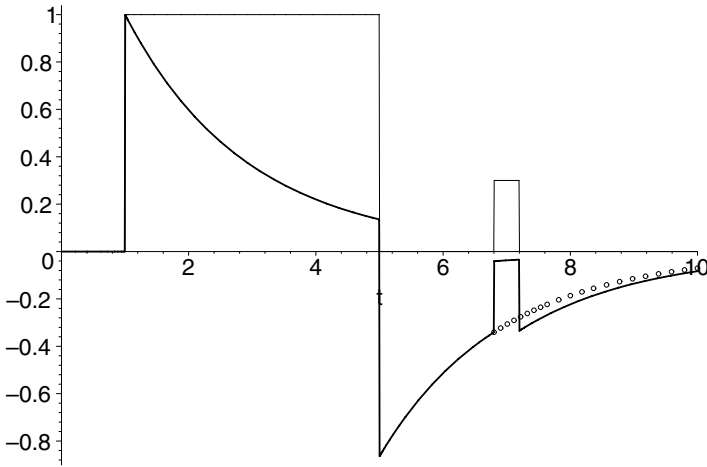

Fig. 11.25 Relaxation behavior of the BURGERS model under picewise constant strains ε_0 **and** α between $[1, 5]$ and $[6.8, 7.2]$

A general representation of the *relaxation* (11.136) resulting from the piecewise constant strains (11.135) can be seen on the CD $\boxed{\odot\ 11\_17.mws}$.

Two further worksheets, $\boxed{\odot\ 11\_18.mws}$ and $\boxed{\odot\ 11\_19.mws}$ on the CD, should be mentioned. In the first one, the two dimensionless relaxation functions (11.72a,b) have been discussed in more detail by assuming several parameters $c[3]$ and $c[4]$. In particular, optimal parameters $c[4]$ as functions of $c[3]$ have been calculated in such a way that (11.72b) leads to a best approximation to (11.72a).

The second worksheet is concerned with the comparison between PRONY-series and relaxation functions due to the $\sqrt{t}$-law including experimental data. AIMEDIEU (2004) has investigated the nonlinear relaxation of *brain tissue* and found very good agreement between (11.70a) and his own experiments. The use of PRONY-series was less successful.

12 Viscoplastic Materials

In contrast to fluids (chapter 9) *viscoplastic materials* can sustain a shear stress even at rest. They begin to flow with viscous stresses after a *yield condition* has been satisfied. Thus, viscoplastic materials are considered as *solids*. The first viscoplastic model was proposed by BINGHAM (1922). In the introduction to the Proceedings of the "First Plasticity Symposium" in Lafayette College (1924) BINGHAM writes:

> Our discussion of plasticity therefore concerns itself with the 'flow of solids'. The Greek philosopher HERAKLITUS was literally correct when he said that 'everything flows' (Panta rhei). It is therefore necessary to limit our discussion by excluding the flow of those things which we are accustomed to refer to as fluids, i.e., the pure liquids and gases. But the circle of our lives is not concerned principally with the fluids, even air and water, but with plastic materials. Our very bodies, the food we eat, and the materials which we fashion in our industries are largely plastic solids. Investigation leads us to the belief that plasticity is made up of two fundamental properties which have been made 'yield value' and 'mobility', the former being dependent upon the shearing stress required to start the deformation and the mobility being proportional to the rate of deformation after the yield value has been exceeded.

HOHENEMSER and PRAGER (1932) constructed a viscoplastic constitutive equation using the relation of stress-strain rate derived from experiments. Based upon their results, PERZYNA (1966) proposed a generalized *elastoviscoplastic* model, which considered the material stability criterion postulated by DRUCKER (1959).

In the past three decades, there has been considerable progress and significant advances made in the development of fundamental concepts of the *theory of viscoplasticity* and their application to solve practical engineering problems. A lot of results have been published by PHILLIPS and WU (1973), CHABOCHE (1977), EISENBERG and YEN (1981), BODNER and PARTOM

(1975), LIU and KREMPL (1979), KREMPL (1987), CRISTESCU and SULI-
CIU (1982), SOBOTKA (1984), SKRZYPEK (1993), SHIN (1990), BETTEN
and SHIN (1991; 1992), HAUPT (2000), LIN, BETTEN and BROCKS (2006),
to name just a few.

12.1 Linear Theory of Viscoplasticity

A linear *viscoplastic model* called BINGHAM *body* (1922) consists of a linear
viscous dashpot (NEWTON) and a solid friction element (MISES) connected
in parallel, i.e., the HOOKE element of the KELVIN model has been replaced
by the MISES element acting as a rigid body for $|\sigma_{12}| < k$ and sliding at
constant friction k with a shear rate $d_{12} \geq 0$, when $|\sigma_{12}| \geq k$. Thus, for
simple shear the viscoplastic material law is given by

$$2\eta d_{12} = \begin{cases} 0 & \text{for} \quad F < 0 \\ F\sigma_{12} & \text{for} \quad F \geq 0 \,, \end{cases} \tag{12.1}$$

where η is a material constant (*plastic viscosity*) analogous the shear viscos-
ity of a fluid. The function F in (12.1) is defined as

$$F := 1 - k\,/|\sigma_{12}| \ . \tag{12.2}$$

The friction constant k of the model is interpreted as the yield strength in
pure shear of the material considered (Fig. 12.1).
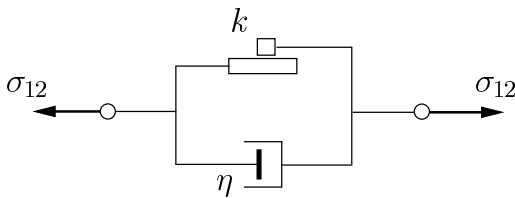
Fig. 12.1 BINGHAM model

   In generalizing the BINGHAM model (12.1) to multiaxial states of stress
we substitute the rate-of-deformation tensor d_{ij} for the shear rate d_{12} and
the stress deviator σ'_{ij} for the shear stress $\sigma_{12} \equiv \sigma'_{12}$ and furthermore the
function

$$F = 1 - \frac{k}{\sqrt{J_2'}} \tag{12.3}$$

with the quadratic deviator invariant,

$$J_2' := \sigma_{ij}'\sigma_{ji}'/2 \ , \tag{12.4}$$

for the function (12.2). Thus, we arrive at the tensorial constitutive equation

$$2\eta d_{ij} = F\sigma_{ij}' \tag{12.5}$$

valid for *isotropy*. The solution of this equation for σ_{ij}' is the viscoplastic analogy of the tensorial equation (9.7b) of a NEWTON fluid. In solving (12.5) for σ_{ij}' we first square both sides of (12.5) according to

$$4\eta^2 d_{ij}d_{ji} = F^2\sigma_{ij}'\sigma_{ji}' \tag{12.6}$$

and find by introducing the quadratic invariants (12.4) and

$$I_2' = d_{ij}d_{ji}/2 \tag{12.7}$$

the relation

$$F\sqrt{J_2'} = 2\eta\sqrt{I_2'} \tag{12.8}$$

and finally with (12.3) the following *yield function*

$$F = \frac{2\eta\sqrt{I_2'}}{k + 2\eta\sqrt{I_2'}} \quad \text{with} \quad 0 \le F \le 1 \ . \tag{12.9}$$

We see, at the onset of yielding ($d_{ij} = 0_{ij}$ or $I_2' = 0$) the yield function (12.9) is equal to zero, while it is approaching one for large rates ($d_{ij} \gg \delta_{ij}/s$). In that case the material behaves like a NEWTON fluid.

Inserting (12.9) into (12.5) we obtain the constitutive equation

$$\sigma_{ij}' = \left(2\eta + \frac{k}{\sqrt{I_2'}}\right)d_{ij} \tag{12.5*}$$

consisting of two parts: a *viscous part* (parameter η) and a *solid part* (parameter k).

The transvection of (12.5) with CAUCHY's stress tensor σ_{ij} yields

$$2\eta\sigma_{ij}d_{ji} = F\sigma_{ij}\sigma'_{ji} = F\sigma'_{ij}\sigma'_{ji} \equiv 2FJ'_2 \; . \tag{12.10}$$

Assuming the *hypothesis of the equivalent dissipation rate*

$$\dot{D} := \sigma_{ij}d_{ji} \overset{!}{=} \sigma d \tag{12.11}$$

we obtain from (12.10) the quadratic deviator invariant in the form

$$J'_2 = \eta\sigma d/F = \eta\dot{D}/F \tag{12.12}$$

and then the yield function (12.3) according to

$$F = 1 + \frac{A}{2\dot{D}} - \sqrt{\frac{A}{\dot{D}}\left(1 + \frac{A}{4\dot{D}}\right)} \quad \text{with} \quad A \equiv k^2/\eta \; . \tag{12.13}$$

In this representation the essential parameter is A, which relates the *yield strength in pure shear* k and the *shear viscosity* η, i.e., the MISES and NEWTON influence. The BINGHAM *model* approaches the following limits:

$$A \to 0 \quad \Rightarrow \quad F = 1 \qquad \text{(NEWTON \textit{fluid})},$$
$$A/4\dot{D} \gg 1 \quad \Rightarrow \quad F = 0 \qquad \text{(MISES \textit{solid})}.$$

For *anisotropic viscoplastic solids* constitutive equations are very complicated similar to that already discussed in chapter 4 or 8. Therefore, for practical use we substitute the stress deviator σ'_{ij} in the isotropic concept (12.5) by the linear transformation

$$\tau'_{ij} = \beta_{\{ij\}pq}\sigma_{pq} \quad \text{with} \quad \beta_{\{ij\}pq} := \beta_{ijpq} - \frac{1}{3}\beta_{kkpq}\delta_{ij} \tag{12.14}$$

and find the modified constitutive equation

$$\boxed{2\eta d_{ij} = F\tau'_{ij}} \quad \text{with} \quad \boxed{F = 1 - \frac{k}{\sqrt{J'_2}}} \;, \tag{12.15}$$

where, in contrast to (12.4) the invariant J'_2 is defined as

$$J'_2 := \tau'_{ij}\tau'_{ji}/2 \; . \tag{12.16}$$

The fourth-order tensor $\beta_{\{ij\}pq}$ in (12.14) is deviatoric corresponding to the free indices $\{ij\}$ and contains the anisotropic properties of the viscoplastic material (BETTEN,1981a; 1981b).

12.2 Nonlinear Theory of Viscoplasticity

In the nonlinear case the constitutive equation (12.5) may be expanded by an additional term,

$$2\eta d_{ij} = F\left(\sigma'_{ij} + \kappa\sigma''_{ij}\right),$$
(12.17)

which is quadratic in stresses and characterizes the *second-order-effect* regulated by the parameter κ. The tensor $\boldsymbol{\sigma}''$ in the second term is traceless and defined as

$$\sigma''_{ij} = \partial J'_3 / \partial\sigma_{ij} = \sigma'_{ik}\sigma'_{kj} - 2J'_2\delta_{ij}/3,$$
(12.18)

where J'_2 is the quadratic deviator invariant (12.4), while J'_3 is cubic and defined as

$$J'_3 := \sigma'_{ij}\sigma'_{jk}\sigma'_{ki}/3.$$
(12.19)

The *yield function* (12.3) is generalized according to

$$F = 1 - k\left/f\left(J'_2, J'_3\right)\right.$$
(12.20)

as a function of both deviator invariants. For example, the function $f\left(J'_2, J'_3\right)$ may be assumed in the form

$$f\left(J'_2, J'_3\right) = \sqrt{J'_2 + \alpha J'_3/\sigma_F},$$
(12.21)

where σ_F is the yield strength in uniaxial tension. The admissible range of the parameter α is

$$-3 \le \alpha \le 3/2$$
(12.22)

resulting from the *convexity* of the surface $f = \mathrm{const.}$ as has been pointed out in more detail by BETTEN (1979b).

The proposed nonlinear constitutive equation (12.17) is *compatible* with the *minimum polynomial representation* (chapter 6)

$$d_{ij} = f_{ij}(\sigma'_{pq}) = \phi_0\delta_{ij} + \phi_1\sigma'_{ij} + \phi_2\sigma'^{(2)}_{ij},$$
(12.23)

hence, by comparing (12.17) with (12.23) we arrive at the following identities:

$$\phi_0 \equiv -\frac{2}{3}J'_2\phi_2, \qquad \phi_1 \equiv \frac{F}{2\eta}, \qquad \phi_2 \equiv \kappa\phi_1.$$
(12.24a,b,c)

Because of the *incompressibility* the function ϕ_0 can be expressed by ϕ_2 according to (12.24a). The parameter κ in (12.24c) regulates the *second-order-effect* as mentioned above.

The nonlinear constitutive equation (12.17), valid for isotropy, may be modified to *anisotropy* again by introducing the linear transformation (12.14) and the corresponding quadratic tensor

$$\tau_{ij}'' = \tau_{ik}'\tau_{kj}' - 2J_2'(\boldsymbol{\tau}')\delta_{ij}/3 \; , \tag{12.25}$$

hence

$$\boxed{2\eta d_{ij} = F\left(\tau_{ij}' + \kappa\tau_{ij}''\right)} \; , \tag{12.26}$$

where the invariants (12.16) and

$$J_3' = \tau_{ij}'\tau_{jk}'\tau_{ki}'/\,3 \tag{12.27}$$

of the linear transformation (12.14) should be inserted into the *yield function* (12.20).

12.3 Viscoplastic Behavior of Metals

For example, in the following the rate-dependent deformation of an Fe-0.05 weight percent carbon steel at temperatures in excess of a homologous temperature of 0.5 should be discussed in comparison with suitable experiments.

In order to describe the tensile tests at elevated temperatures, we propose the following *viscoplastic constitutive equation*

$$\boxed{\sigma = \sigma\left(^P\varepsilon\right) = \sigma^* - (\sigma^* - \sigma_0)\exp\left(-^P\varepsilon\,/^P\varepsilon^*\right)} \; , \tag{12.28}$$

where the parameters σ^*, σ_0 and $^P\varepsilon^*$ have been determined from results of continuous isothermal tension tests, at a number of constant strain rates, performed by P.J. WRAY of the U.S. Steel Research Laboratory and pulished by ANAND (1982). The strain-rate and temperature ranges spanned by these tests were $1.4 \cdot 10^{-4}$/s to $2.3 \cdot 10^{-2}$/s and 1173 to 1573 K, respectively. In the temperature range the steel has a fcc crystal structure called *austenite*.

The three parameters determined by using the MARQUARDT-LEVEN-BERG *algorithm* and the experimental data are listed in Table 12.1 and equation (12.28) is represented in Fig. 12.2.

In order to interpret more physically the results from tensile tests at elevated temperatures ANAND (1985) and BROWN et al. (1989) have introduced

internal variables characterizing the resistance to plastic flow offered by the internal microstructural state of the material. They found also the simple phenomenological equation (12.28) sometimes called VOCE *equation* (1955).

Table 12.1 Parameters in equation (12.28)

$P_{\dot{\varepsilon}}$ [s^{-1}]	σ^* [MPa]	σ_0 [MPa]	P_{ε^*} [-]	mean error [%]
0.00014	18.63	8.42	0.0385	1.4
0.0028	29.45	11.87	0.0435	1.05
0.023	42.32	12.83	0.0444	1.96
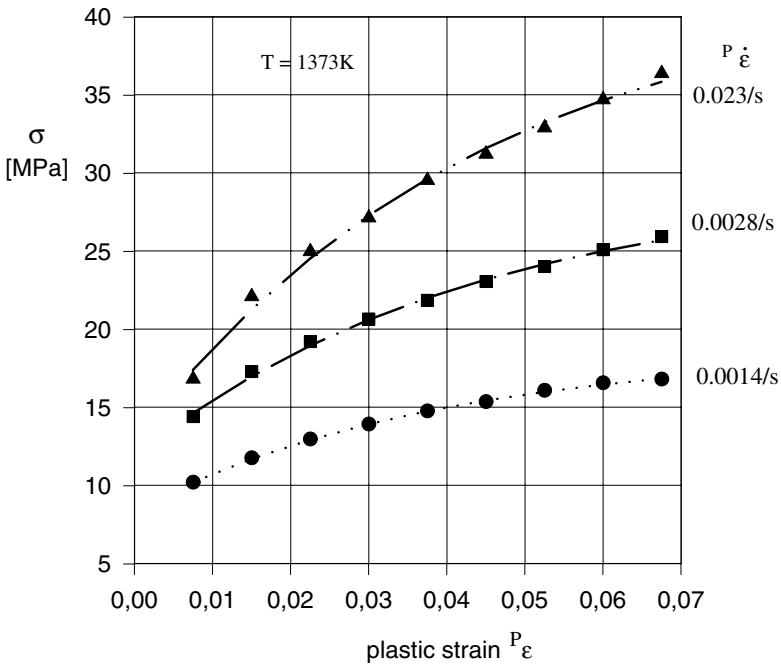
Fig. 12.2 Constitutive law (12.28) in comparison with experimental data

For engineering applications it is very important to generalize *uniaxial* constitutive relations to *multiaxial* states of stress. The method and some examples have already been discussed in chapter 8 in more detail. In the same way the uniaxial relation (12.28) may be generalized to a tensorial form. Thus, we start from the tensor-valued function

$$\boxed{\sigma'_{ij} = \varphi_1 {}^P\!\varepsilon'_{ij} + \varphi_2 {}^P\!\varepsilon''_{ij}} \,, \tag{12.29}$$

where

$${}^P\!\varepsilon''_{ij} := {}^P\!\varepsilon'^{(2)}_{ij} - \frac{1}{3}{}^P\!\varepsilon'^{(2)}_{rr}\delta_{ij} \equiv \left({}^P\!\varepsilon'^{(2)}_{ij}\right)' \tag{12.30}$$

is, similar to (12.18), a traceless tensor. The scalar-valued functions φ_1 and φ_2 in (12.29) are determined by applying the *tensorial interpolation method* introduced in chapter 8. The results are:

$$\varphi_1 = \frac{4}{9}\frac{\sigma}{{}^P\!\varepsilon}\left[1 + \frac{1}{2}\frac{{}^P\!\varepsilon}{{}^P\!\varepsilon^*}\left(1 - \frac{\sigma^*}{\sigma}\right)\right]\,, \tag{12.31a}$$

$$\varphi_2 = \frac{4}{9}\frac{\sigma}{{}^P\!\varepsilon^2}\left[1 - \frac{{}^P\!\varepsilon}{{}^P\!\varepsilon^*}\left(1 - \frac{\sigma^*}{\sigma}\right)\right]\,, \tag{12.31b}$$

where the second function φ_2 regulates the *tensorial nonlinearity* in (12.29). In the linear case ($\varphi_2 = 0$) equation (12.29) is simplified to the relation

$$\boxed{\sigma'_{ij} = \frac{2}{3}\frac{\sigma}{{}^P\!\varepsilon}{}^P\!\varepsilon'_{ij}}\,, \tag{12.32}$$

which is analogous to the plastic part ${}^P\!\varepsilon' = \Lambda^*\sigma'_{ij}$ of the HENCKY *equation* (BETTEN, 2001a).

13 Creep and Damage Experiments

As has been pointed out in more detail by AVULA (1987), "the validity of a model should not be judged by mathematical rationality alone; nor should it be judged purely by empirical validation at the cost of mathematical and scientific principles. A combination of rationality and empiricism (logic and pragmatism) should be used in the validation".

"Experimental observations and measurements are generally accepted to constitute the backbone of physical sciences and engineering because of the physical insight they offer to the scientist for formulating the theory. The concepts that are developed from observations are used as guides for the design of new experiments, which in turn are used for validation of the theory. Thus, experiments and theory have a hand-in-hand relationship" (AVULA, 1987).

However, it must be noted that experimental results can differ greatly from the reality just like a bad mathematical model (BETTEN, 1973).

In his review article KOLSKY (1978) "attempts to assess the role of experimental work in the development of the subject of solid mechanics." He is inevitably influenced to a very considerable extend by his own experience as an experimenter, and most of the examples discussed in his review article are concerned with experiments carried out by himself and his coworkers.

An excellent treatise, *Experimental Foundations of Solid Mechanics* , which is "historical in perspective and comprehensive in content", has been published by BELL (1973). If one wishes to pursue the detailed development of solid mechanics as an *interaction* between *theory* and *experiment*, then it is strongly recommended to consult BELL's authoritative and monumental work.

The development of the experimental aspects in creep mechanics has to a large extend been concerned with the measurement of the stress-strain response of real solids and various conditions of loading, or in other words, the determination of *constitutive relations* of materials under *creep conditions* and, furthermore, the development of *evolutional equations* character-

izing the *damage state* during the tertiary creep phase. In contrast with the theories of elasticity and plasticity, the essential feature of *creep* is the *time-dependence* of the stress-strain relations leading to more experimental expense and difficulties. The simplest type of *time-dependent measurement* is that of extensional creep, i.e., the dependence of the magnitude of the extensional strain as a function of *time* (and *temperature*) for which a longitudinal stress has been applied to a rod specimen. Ideally to carry out this experiment we need to apply a stress that will be kept constant with time and observe how the length of the specimen increases during the constant stress has been applied. If the load is suddenly applied to a specimen, oscillations are set up, and measurements made before these oscillations have effectively died down are difficult to interpret. Consequently, the direct measurement of creep behavior for very short times is a matter of some difficulty even if measuring apparatus is available for recording the extensional strains at very short times after the load has been applied (KOLSKY, 1972).

Further, if the strain is finite the cross section area of the specimen is less than it was in the unloaded state. Consequently, the *true stress* is greater than the *nominal (engineering) stress* , and as creep progresses the true stress continues to grow as a result of the decreasing cross section area of the tensile specimen. Various mechanisms have been proposed to compensate for this effect, for instance, one possible way proposed by ANDRADE (1914).

In his review article KOLSKY (1978) has discribed and discussed a number of experimental techniques in the field of solid mechanics.

Worldwide there are a lot of laboratories specialized to carry out different experiments under *creep conditions* , for instances, experimentally well-equipped instituts in Cachan (Paris), Grenoble (France), Jülich, Aachen (Germany), Leicester (England), Lyngby (Denmark), Kiev (Ukraine), Nagoya (Japan), Paderborn (Germany), Swansea (Walse), Teddington (England), Urbana (Illinois), Warsaw (Poland), etc., etc. Thus, one can image that not only a lot of *theoretical* and *numerical* results but also many experimental methods and data have been published.

Consequently, only a very short survey of some *experimental* ressults in *materials behavior* under *creep conditions* should be provided in the following, and a lot of excelent experimental investigations cannot be taken into account.

A large amount of experimental data has been collected on the fracture properties of a number of materials under both uniaxial and multiaxial states of stress (COCKS and LECKIE, 1987). In general, these experiments have been conducted at constant stress, or when the stress has been varied, this

has been done in a proportional manner. An exception to this are the experiments of TRAMPCZYNSKI et al. (1981) on thin-walled tubes of copper, an aluminium alloy, and a nimonic. In these experiments the axial load was kept constant while the torque experienced by the tube was cycled between two prescribed limits. COCKS and LECKIE (1987) considered the case of constant load and developed constitutive equations that can deal specifically with this situation. Further, they considered the situation of nonproportional loading. In particular, they concentrated on development *constitutive equations* for copper and an aluminium alloy, which have been extensively tested by LECKIE and HAYHURST (1974; 1977) over the temperature range $150 - 300°C$.

The aim of COCKS' and LECKIE's (1987) investigations was to try to obtain a structure for creep constitutive equations through an understanding of the *microscopic mechanisms* responsible for deformation and failure. This work extends the thermodynamic approach adopted by RICE (1971) and COCKS and PONTER (1985) to include the effects of damage, which exist either in the form of microscopic voids or as dislocation networks that aid the dislocation climb process.

The approach adopted by COCKS and LECKIE (1987) is similar in some respects to that used by LEMAITRE and CHABOCHE (1990). Their measures of damage and their kinetic relationships are, however, entirely *phenomenological* .

Over the range of stress and temperature used in the experiments of LECKIE and HAYHURST (1974; 1977) and TRAMPCZYNSKI et al. (1981), the results of their tests on copper can be explained in terms of COCKS' and LECKIE's (1987) understanding of the *void nucleation* and *growth mechanisms* .

In a polycrystalline metal subject to creep at elevated temperature, the nucleation and growth of voids to coalescence also play a major role in the failure process (TVERGAARD, 1989). In these circumstances, the voids occur primarily at the grain boundaries and the growth mechanism differs significantly from that at ductile fracture discussed by TVERGAARD (1989). In addition to dislocation creep of the grains, *grain boundary diffusion* plays a significant role.

Experimental results show that high temperature *cavitation* occurs mainly on grain boundary facets normal to the maximum principle tensile stress direction (ARGON, 1982; COCKS and ASHBY, 1982). Coalescence of these cavities leads to *micro-cracks* , and the final *intergranular creep fracture* occurs as the micro-cracks link up. In cases where *diffusion* gives the dominant

contribution to the growth of cavities, the rate of growth is often constrained by the rate of *dislocation creep* of the surrounding material, as has been noted by DYSON (1976).

A set of *constitutive relations* for creep with *grain boundary cavitation* has been proposed by TVERGAARD (1984) as an extension of the works by RICE (1981) and HUTCHINSON (1983). For the rate of growth of a single cavity both the contributions of diffusion and dislocation creep are accounted for, and furthermore, the model incorporates the creep constraint on the rate of *cavity growth* .

Further investigations concerning the *metallographical analysis* of the microstructure in polycrystalline metals and alloys have been carried out by EVANS (1984), GOODS and NIX (1978), KRAJCINOVIC (1996), LEMAITRE (1992), etc. etc., to name but a few.

The best way to provide a quick overview of some important experimental investigations in creep mechanics may be in form of a table, for instance, as proposed by BETTEN (2001b), which is devided in three parts concerning the *primary*, *secondary*, and *tertiary* creep stages.

Table 13.1: Experimental investigations in creep mechanics

References	Tests
Primary Creep	
ALTENBACH et al. (1995)	various materials, many examples
ARONS and TIEN (1980)	hot-pressed silicon nitride, 1477K, tensile stress 103 Mpa
BROWN et al.(1986)	$1/2 Cr\, 1/2 Mo\, 1/4 V$, tensile tests
BRUELLER (1991)	thermoplastic polymers under uniaxial loading and pure shear (torsion of thin walled tubes)
GOREV et al. (1979a)	titanium alloy VT9, 673K, uniaxial tension / compression, pure torsion, and thin-walled tubes
HAYMAN (1981)	creep buckling, review
HEEMANN and STEIN (1991)	rock salt, 293K, uniaxial loading

Table 13.1: Experimental investigations in creep mechanics

References	Tests
IGARI et al. (1991)	perforated plates (ASTM B435-77), 1073K and 1223K, creep strain measurement by Moire method
KOSSOWSKY et al. (1975)	hot pressed Si_3N_4, $1533K$, tensile stress 69 MPa
KOWALEWSKI (1991)	pure copper, 573K, biaxial stress, duration of primary creep
LEMAITRE and CHABOCHE (1990)	material parameters for some materials and alloys at several temperatures
LUCAS and PELLOUX (1981)	Zircaloy-2, 673K, tension and compression
NISHITANI (1978)	cellulose nitrate, 338K, uniaxial tension, biaxial compression, and various three-dimensional stress states
OHASHI et al. (1986)	316 stainless steel, 923K, tension, compression, pure torsion, and thin-walled tubes.
RABOTNOV (1969)	austenitic steel EI-257, 873K, uniaxial tension, pure torsion
SKELTON et al. (1977)	EN 25, 623K, thick-walled cylinders b/a = 1.67, internal pressure 325N/mm2
TAIRA et al. (1965)	C19, 723K, thick-walled cylinders b/a = 1.986, internal pressure 100N/mm2
Secondary Creep	
ALTENBACH et al. (1995)	various materials, many examples
BLUM and ILSCHNER (1967)	single crystal NaCl, 1010K, various tensile stresses
CHENG et al. (1968)	polycrystalline pure Ni, at several temperatures
FETT et al. (1988)	hot-pressed silicon nitride, HPSN (2.5% MgO), 1473K, bending tests

Table 13.1: Experimental investigations in creep mechanics

References	Tests
FINNIE (1966)	testing method, bending tests
GOREV et al. (1978)	aluminium alloy AK4-1T, 473K, uniaxial tension, compression, pure torsion, and thin-walled tubes
GOREV et al. (1979a)	titanium alloy OT4, 748K, thin-walled tubular specimens
IGARI et al. (1991)	perforated plates (ASTM B435-77), 1073K and 1223K, creep strain measurement by Moire method
KOWALEWSKI (1987)	austenitic steel, 873K, pure copper, 573K, thin-walled tubes
LEMAITRE and CHABOCHE (1990)	NORTON's Law parameters for some materials and alloys at several temperatures
NORMAN and DURAN (1970)	mixed crystal alloy Fe-Si, at several temperatures
OYTANA et al. (1982)	combined stresses, anisotropic behavior
PINTSCHOVIUS (1989)	ceramics (HPSN), 1473K, tension and compression
REED-HILL (1973)	activation energy (creep = self diffusion)
RUBANOV (1987)	aluminium alloy AK4-1T, 473K, thin-walled tubes
SAWCZUK and ANISIMOWICZ (1981)	prestrained materials, induced anisotropy
SÖDERQUIST (1968)	Mg-alloy, 513K, plate specimens in two perpendicular directions
TALTY and DIRKS (1978)	ceramic metals, bending tests
Tertiary Creep	
ALTENBACH et al. (1995)	various materials, many examples

Table 13.1: Experimental investigations in creep mechanics

References	Tests
BERTRAM and OLSCHEWSKI (1996)	nickel-based superalloy SRR 99, 1033K, uniaxial creep in different orientations and under different loads
CHAN et al. (1997)	clean salt from New Mexico, 298K, triaxial compression
DUFAILLY and LEMAITRE (1995)	Inconel 718, 823K, servo-hydraulic tension-compression maschine, experimental numbers of cycles to failure in the range of 1 to 102 cycles
DUNNE et al. (1990)	$2\frac{1}{4}Cr1Mo$ steel, 823K, and alloy 800H, 1073K, uni-axial creep tests
FRÈRES (1996)	notched bar specimens, 973K, X6CrNi 1811, various geometries and creep stresses
GOREV et al. (1979a)	titanium alloy OT4, 748K, thin-walled tubular specimens
GOREV et al. (1979b)	aluminium alloy AK4-1T, 473K, tension, compression, torsion, specimens taken from plates in several directions
GRATHWOHL (1984)	hot-pressed silicon nitride, 1473K, bending tests
HAYAKAWA and MURAKAMI (1997)	spheroidized graphite cast iron JIS FCD 400, a series of experiments on tubular specimens, experimental validation of a damage potential
LEMAITRE and CHABOCHE (1990)	material parameters for some materials and alloys at several high temperatures
LI and SMITH (1995)	nickel-based superalloy SRR 99, 1033K, fatigue-creep
MILES and MCLEAN (1977)	metal matrix composites, creep damage, creep rupture time

Table 13.1: Experimental investigations in creep mechanics

References	Tests
MURAKAMI et al. (1998)	spheroidized graphite cast iron JIS FCD 400, a series of experiments on tubular speciments, damage surfaces in tension-torsion stress space
NICOLINI (1999)	incoloy alloy 800HT, 1073K, tensile and compression tests
OTHMANN et al. (1993)	316 stainless steel, several elevated temperatures
QI (1998)	single crystal superalloy CMSX-6 and SRR 99, 1033K, uniaxial creep in different orientations and different loads
RIDES et al. (1989)	copper, 573K, uniaxial tensile tests
RUBANOV (1987)	aluminium alloy AK4-1T, 473K, tension, compression, torsion, specimens taken from plates in several directions
SHAMMAS (1988)	$1Cr\,Mo$, HAZ, 823K, metallographical observations, creep damage
TEOH et al. (1992)	several polymers, creep rupture experiments

Only some arbitrary selected experimental investigations under creep conditions are listed in Table 13.1. This list cannot be complete, and it is not difficult to expand it to a nearly unlimited length. Thus, many scientists may please accept my apology for the loss of completeness, if the Table is very shortened in this context.

Apart from experimental data taken from literature, the author and his coworkers have also taken results from their own experimental measurements in order to examine the validity of a mathematical model, for instance, experiments by WANIEWSKI(1984; 1985), BETTEN and WANIEWSKI (1989; 1995), BETTEN et al. (1990) and BETTEN et al. (1995), to name but a few.

In the following some of these experiments should be explained in more detail.

In order to justify the *simplified theory* based on the *mapped stress tensor* (4.11) a lot of tests were performed by BETTEN and WANIEWSKI (1989) on

thin-walled tubes (Fig. 13.1) of austenitic, chromium-nickel steel at $873K$ and of pure copper at $573K$.
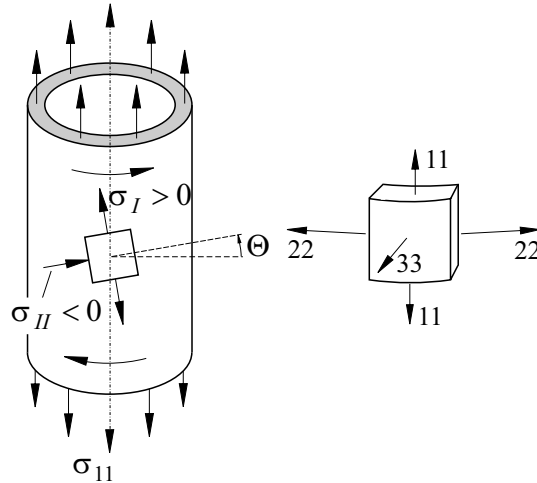
Fig. 13.1 Thin-walled tube loaded under combined tension, torsion and internal pressure

The tubes have been loaded under combined tension, torsion, and internal pressure. The anisotropy of the material is entirely involved in the fourth-rank tensor β in (4.11), the components of which are related to the experimental data. From these experiments we could illustrate that the *simplified theory* is very useful to describe the creep process under non-proportional multiaxial load paths, assuming different inclination θ between load directions and the orthonormal frame of the material.

Plastic prestrain can produce anisotropy in materials which are initial isotropic. This anisotropy strongly influences the creep behavior of such materials. Non-linear constitutive equations with two argument tensors for the secondary creep behavior have been proposed, based upon the representation theory of tensor functions. The two argument tensors in these constitutive equations are the CAUCHY *stress tensor* and the appropriately defined second-rank tensor characterizing the plastic predeformation as a function of different plastic prestrain paths. A few experimental tests have been carried out on round specimens of INCONEL 617. Firstly, the strain-induced anisotropy were produced at room temperature by several combinations of tension and torsion. After that, the specimens have been loaded uniaxially under creep conditions at $1223K$ in Helium-gas-atmosphere.

For rolled sheet-metal, the internal structure generally presents three orthogonal planes of symmetry; the macroscopic behavior is thus orthotropic. The initial orthotropy of the material is modified according to the orientation of the principal directions of the irreversible deformation with respect to the rolling direction; this is the phenomenon of *anisotropic hardening* . The multiaxial anisotropic creep behavior of rolled sheet-metals is analysed within an invariant formulation of the secondary creep constitutive equations by BETTEN et al. (1990), developed in the framework of the theory of tensor function representation. The biaxial tension method has been improved in order to determine complex stress state in specimens of orthotropic rolled sheet-metal. The shape of the specimen, for instance, the biaxial tension cruciform specimen in Fig. 13.2 has been taken into account with respect to the uniform stress distribution in the central part of the specimen.
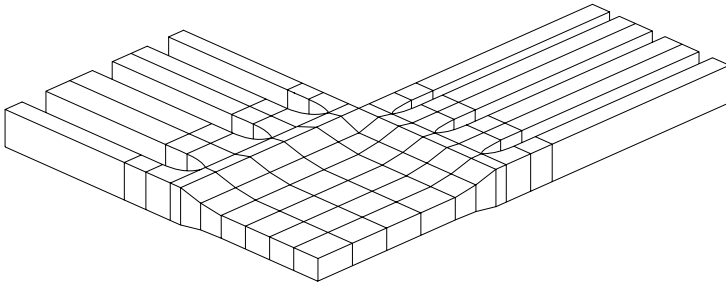
Fig. 13.2 Biaxial tension cruciform specimen

Other experiments have been carried out by BETTEN et al. (1995) in order to predict the influence of creep history, e.g. pre-damage and pre-loading, on the further creep behavior after changing the loading direction. From preloading specimens (loading direction x_1) smaller specimens were cut along in several directions $^{\theta}x_1$ and then loaded under creep conditions (Fig. 13.3).

The creep tests were performed on flat specimens of *austenitic steel* X 8 Cr Ni Mo Nb 16 16 at $953K$ and $973K$ as well as on flat specimens of *ferritic steel* 13 Cr Mo 4 4 at $803K$ and $823K$.

A continuum damage mechanics model for the *dislocation creep* response associated with the growth of parallel planar *mesocracks* in initially isotropic materials has been developed by BETTEN et al. (1998). This model describes simultaneously different damage development in tension, compression and torsion, damage-induced anisotropy, as well as different creep prop-
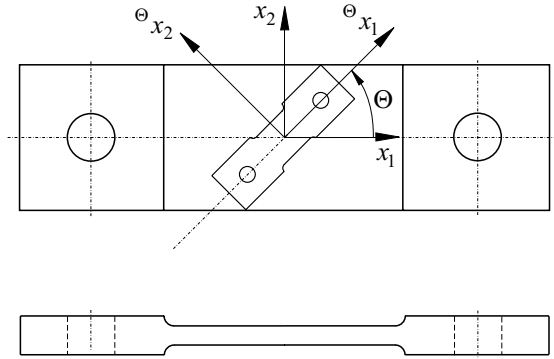
Fig. 13.3 Loading directions x_1 and $^\theta x_1$

erties in tension, compression and torsion. The proposed constitutive equation for creep and the damage growth equation contain joint invariants of the stress tensor and the second-order damage tensor constructed by BETTEN (1982b, 1983). The material parameters required in the proposed equations have been determined by BETTEN et al. (1998) based upon the following experiments:

❒ creep behavior in the *primary stage* of a tinanium alloy VT 9 at $673K$ under uniaxial tension, uniaxial compression or pure torsion,
❒ *secondary creep* behavior of aluminium alloy AK 4-1 T at temperature of $473K$ again under tension, compression and torsion,
❒ damage accumulation in two materials in the *tertiary creep* phase, i.e., again aluminium alloy AK 4-1 T at $473K$ and, furthermore, titanium alloy OT 4 at $748K$ under proportional and non-proportional loading.

The comparison of the theory with experimental results showed satisfactory agreement.

Extensive experimental research is being carried out by BETTEN, SKLEPUS and ZOLOCHEVSKY (1999) concerning the creep behavior of materials with different damage in tension and compression, namely the incorporation of the *microstructural creep* characteristics of polycrystalline materials in the damage model **and**, furthermore, the description of creep behavior of initially anisotropic materials (BETTEN, ZOLOCHEVSKA and ZOLOCHEVSKY, 1999).

Some tensile tests have recently carried out by the author and coworkers on *aluminum alloy* AA 7075 T 7351 at room temperature, as ilustrated in Fig. 13.4a,b.
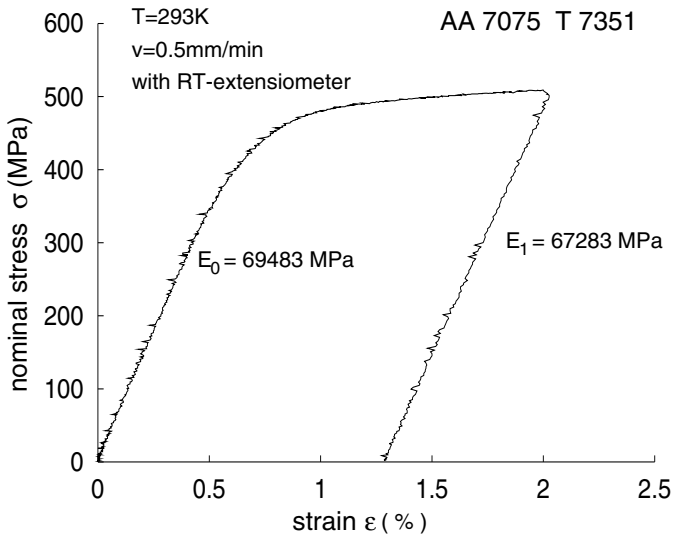
Fig. 13.4a Tensil test on aluminium alloy at room temperature
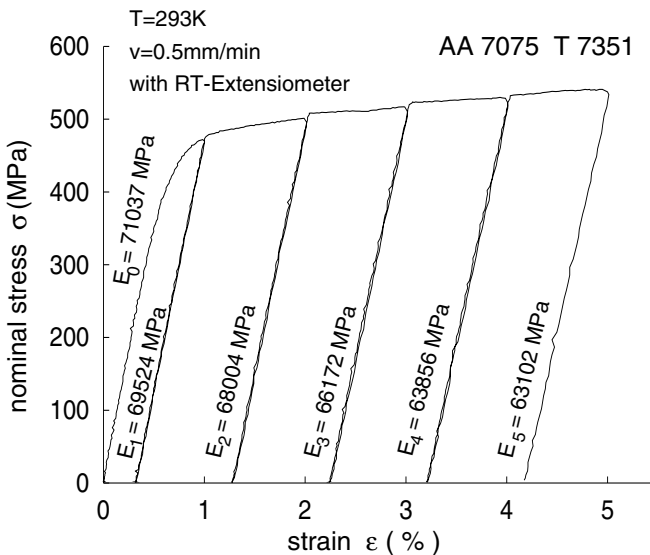
Fig. 13.4b Loading/unloading tests on aluminium alloy at room temperature

If $E_n = (1 - \omega)E_0$ is defined as the *effective elasticity modulus* of the *damaged material*, the values of the damage parameter may be derived from measurements of E_n according to $\omega = 1 - E_n/E$. The curves in Fig. 13.4c can be interpreted as the *evolution of damage* with permanent strains of loading/

unloading tests. The linear decreasing of the elasticity modulus with damage, $E_n = (1 - \omega)E_0$, is based upon the assumption of the *hypothesis of strain equivalence*, while the relation $\omega^* = 1 - (E_n/E_0)^{1/2}$ in Fig. 13.4c can be derived, if the *hypothesis of energy equivalence* is assumed (CHOW and LU (1992); SKRZYPEK and GANCZARSKI (1999); BETTEN (2001a)).
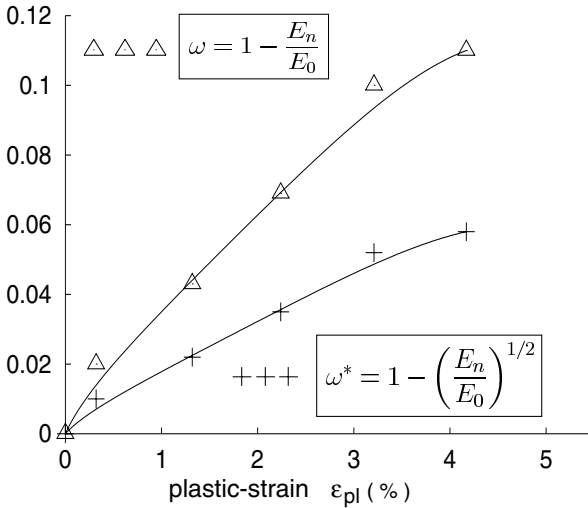
Fig. 13.4c Evolution of damage with permanent strains
of loading/unloading tests in Fig. 13.4b

Note that the symbols $\triangle \triangle \triangle$ **and** $+++$ in Fig 13.4.c indicate calculated points from the formula $\omega = 1 - E_n/E_0$ **and** $\omega^* = 1 - (E_n/E_0)^{1/2}$, respectively, where $E_i, i = 0, 1, 2, ..., n$, are experimental data taken from Fig. 13.4b. The damage parameters, ω **and** ω^*, depend on plastic-strains ε_{pl} also taken from Fig. 13.4b and listed in the following table.

n	0	1	2	3	4	5
ε_{pl} [%]	0	0.32	1.27	2.23	3.2	4.17
E_n/E_0	1	0.979	0.957	0.932	0.899	0.888
ω	0	0.021	0.043	0.068	0.0101	0.112
ω^*	0	0.011	0.022	0.035	0.052	0.058

The solid curves in Fig. 13.4c are the *best approximations* to the calculated points based upon cubic BÉZIER-*spline* (1972).

Further results concerning the *evolution of damage* in the tested aluminium alloy AA 7075 T 7351 have been achieved by the following MAPLE program.

$$\boxed{\odot\ 13\_1.mws}$$

```
>   with(CurveFitting):
>   omega[n]:=1-E[n]/E[0];
```

$$\omega_n := 1 - \frac{E_n}{E_0}$$

```
>   for i in [1,0.979,0.957,0.932,0.899,0.888]
>   do omega[i]:=1-i od;
```

$$\omega_1 := 0$$
$$\omega_{0.979} := 0.021$$
$$\omega_{0.957} := 0.043$$
$$\omega_{0.932} := 0.068$$
$$\omega_{0.899} := 0.101$$
$$\omega_{0.888} := 0.112$$

```
>   omega_star[n]:=1-(E[n]/E[0])^(1/2);
```

$$omega\_star_n := 1 - \sqrt{\frac{E_n}{E_0}}$$

```
>   for i in [1,0.979,0.957,0.932,0.899,0.888]
>   do omega_star[i]:=1-sqrt(i) od;
```

$$omega\_star_1 := 0$$
$$omega\_star_{0.979} := 0.0105557115$$
$$omega\_star_{0.957} := 0.0217362319$$
$$omega\_star_{0.932} := 0.0345985291$$
$$omega\_star_{0.899} := 0.0518438947$$
$$omega\_star_{0.888} := 0.0576624808$$

```
>   data:=[0,0], [0.32, 0.021], [1.27, 0.043],
>   [2.23,0.068], [3.2,0.101], [4.17,0.112]:

>   DATA:=[0,0], [0.32, 0.011], [1.27, 0.022],
>   [2.23,0.035], [3.2,0.052], [4.17,0.058]:
```

```
> omega[experiment](epsilon[pl]):=Spline([data],
> epsilon[pl], degree=3):
> omega_star[experiment](epsilon[pl]):=
> Spline([DATA], epsilon[pl], degree=3):

> alias(H=Heaviside, th=thickness):

> p[1]:=plot({0.12,0.12*H(epsilon[pl]-5)},
> epsilon[pl]=0..5.001):

> p[2]:=plot({omega[experiment](epsilon[pl]),
> omega_star[experiment](epsilon[pl])},
> epsilon[pl]=0..5.001, th=2,):

> p[3]:=plot([data],epsilon[pl]=0..5,
> style=point, symbol=diamond, symbolsize=30):

> p[4]:=plot([DATA],epsilon[pl]=0..5,
> style=point, symbol=cross, symbolsize=30):

> plots[display]({seq(p[k],k=1..4)});
```
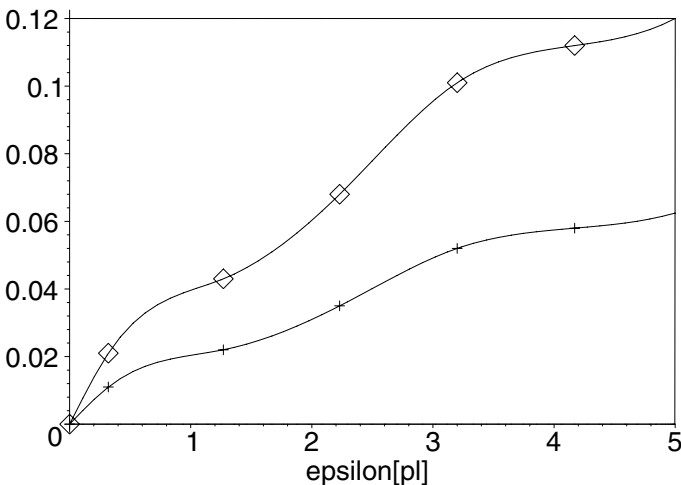

Fig. 13.5 Cubic Splines

```
> with(stats):
> fit[leastsquare[[x,y],y=a[0]+a[1]*x+a[2]*x^2,
> {a[0],a[1],a[2]}]]([[0,0.32,1.27,2.23,3.2,
> 4.17],[0,0.021,0.043,0.068,0.101,0.112]]);
```

$$y = 0.003647183500 + 0.03549888036\,x - 0.002159727141\,x^2$$

```
>   f[omega]:=subs(x=epsilon[pl], rhs(%));
>   # plastic strains in percent:
```

$$f_\omega := 0.003647183500 + 0.03549888036\, \varepsilon_{pl} - 0.002159727141\, \varepsilon_{pl}{}^2$$

```
>   fit[leastsquare[[X,Y],Y=a[0]+a[1]*X+a[2]*X^2,
>   {a[0],a[1],a[2]}]]([[0,0.32,1.27,2.23,3.2,
>   4.17],[0,0.011,0.022,0.035,0.052,0.058]]);
```

$$Y = 0.001981770866 + 0.01805435336\, X - 0.001046674668\, X^2$$

```
>   F[omega_star]:=subs(X=epsilon[pl], rhs(%));

>   # plastic strains in percent:
```

$$F_{omega\_star} :=$$
$$0.001981770866 + 0.01805435336\, \varepsilon_{pl} - 0.001046674668\, \varepsilon_{pl}{}^2$$

```
>   p[5]:=plot({0.12,0.12*H(epsilon[pl]-5)},
>   epsilon[pl]=0..5.001

>   p[6]:=plot({f[omega],F[omega_star]},
>   epsilon[pl]=0..5, 0..0.12,th=2):

>   plots[display]({seq(p[k],k=3..6)});
```
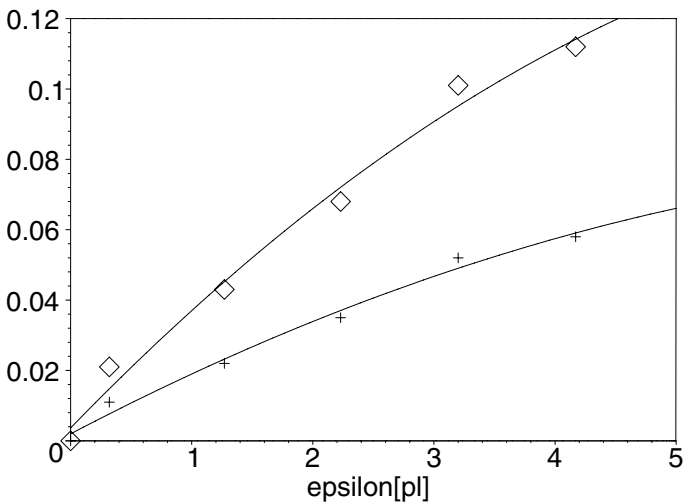

Fig. 13.6 Quadratic leastsquare curve fitting

The distance vector between the quadratic leastsquare curve f_ω and the experimental data [data] can be determined by using a "do-loop":

```
>   with(linalg):
>   for i from 1 to 6 do
>   v[i]:=subs(epsilon[pl]=data[i][1],
>   f[omega])-data[i][2]
>   od;
```

$$v_1 := 0.003647183500$$
$$v_2 := -0.00621433084$$
$$v_3 := 0.00224733765$$
$$v_4 := 0.00406957960$$
$$v_5 := -0.00587200522$$
$$v_6 := 0.0021222353$$

```
>   V:=vector([seq(v[i], i=1..6)]);
```

$$V := [0.003647183500, -0.00621433084, 0.00224733765,$$
$$0.00406957960, -0.00587200522, 0.0021222353]$$

The error norm L_2 for the distance between the quadratic leastsquare curve f_ω and the experimental data [data] is given as:

```
>   L[2][omega]:=(1/sqrt(6))*Norm(V,2)=
>   evalf((1/sqrt(6))*norm(V,2));
```

$$L_{2\omega} := \frac{1}{6}\,\sqrt{6}\,\mathrm{Norm}(V,\,2) = 0.004330438545$$

```
>   L[infinity][omega]:=((1/6)^(1/infinity))*
>   Norm(V,infinity)=((1/6)^(1/infinity))*
>   norm(V,infinity);
```

$$L_{\infty\omega} := \mathrm{Norm}(V,\,\infty) = 0.00621433084$$

```
>   L[infinity][omega]*Max(abs(v[1..6]))=
>   abs(v[2]);
```

$$L_{\infty\omega} := \mathrm{Max}(|V_{1..6}|) = 0.00621433084$$

In a similar way one can find the L_2 error norm for the distance between the quadratic leastsquare curve $F_{\omega*}$ and the experimatal data [DATA]:

```
>   for i from 1 to 6 do
>   w[i]:=subs(epsilon[pl]=DATA[i][1],
>   F[omega_star])-DATA[i][2]
>   od;
```

$$w_1 := 0.001981770866$$
$$w_2 := -0.003348015545$$
$$w_3 := 0.00122261807$$
$$w_4 := 0.00203797040$$
$$w_5 := -0.00296224698$$
$$w_6 := 0.00106790325$$

```
>  W:=vector([seq(w[i],i=1..6)]);
```

$$W := [0.001981770866, -0.003348015545, 0.00122261807,$$
$$0.00203797040, -0.00296224698, 0.00106790325]$$

```
>  L[2][omega_star]:=(1/sqrt(6))*Norm(W,2)=
>  evalf((1/sqrt(6))*norm(W,2));
```

$$L_{2\,omega\_star} := \frac{1}{6}\sqrt{6}\,\mathrm{Norm}(W,\,2) = 0.002262007467$$

```
>  L[infinity][omega_star]:=
>  ((1/6)^(1/infinity))*Norm(W,infinity)=
>  ((1/6)^(1/infinity))*norm(W,infinity);
```

$$L_{\infty\,omega\_star} := \mathrm{Norm}(W,\,\infty) = 0.003348015545$$

```
>  L[infinity][omega_star]:= Max(abs(w[1..6]))=
>  abs(w[2]);
```

$$L_{\infty\,omega\_star} := \mathrm{Max}(|w_{1..6}|) = 0.003348015545$$

The error norms show that the *quadratic leastsquare curves* are good approximations to the given experimental data.

At the beginning of the creep process ($t = 0$ in Fig. 4.1) the response of a specimen loaded by a constant uniaxial stress σ_0 can divided into an *elastic* and a *plastic* part according to (4.1).

For variable stresses σ one can assume, for instance, the stress-strain relations

$$\boxed{\varepsilon = \sigma/E + k(\sigma/E)^n} \quad \textbf{or} \quad \boxed{\varepsilon = \sigma/E + k(\sigma/\sigma_F)^n}$$

proposed by RAMBERG-OSGOOD (1943) **or** BETTEN (1989; 2001c), respectively, where E is the modulus of Elasticity, while σ_F represents the yield stress.

In Fig. 13.7a the RAMBERG-OSGOOD (1943) stress-strain curve and a modified relation are compared with the experimental results from Fig. 13.4a. One can see that the RAMBERG-OSGOOD relation does not agree
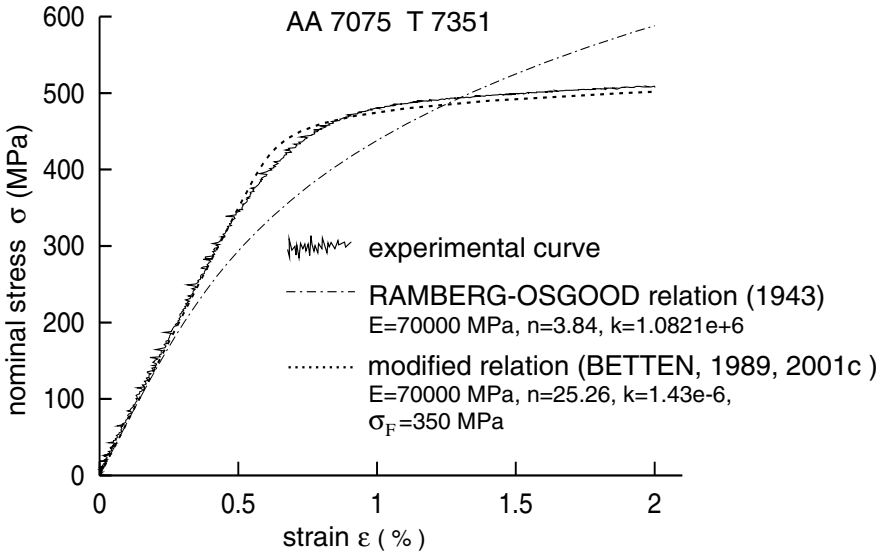
Fig. 13.7a Comparison of the RAMBERG-OSGOOD relation and a modfied relation
with the experimental curve from Fig. 13.4a

with the tension test on aluminium alloy. Thus, a modification is neces-
sary (BETTEN, 1989; 2001c). Finally, the *hardening* of aluminium alloy AA
7075 T 7351 at room temperature can be expressed by the simple formula
$\sigma = \sigma_F + k\varepsilon_{pl}^n$ as illustrated in Fig. 13.7b, where the yield stress $\sigma_F = 350$
MPa, the hardening coefficient $= 146.91 MPa$, and the hardening expo-
nent $n = 0.1758$ have been determined based upon the experimental re-
sults from Fig. 13.4a by using the *nonlinear* MARQUARDT-LEVENBERG-
algorithm with MAPLE. This algorithm has also been applied in order to
find out the parameters in Fig. 13.7a.

Instead of the MARQUARD-LEVENBERG-*algorithm* one can also effec-
tively apply the *least squares* method in order to determine the hardening
parameters, since the yield stress σ_F in the relation is known. Thus, we can
transform the nonlinear problem to a *linear regression* by conssidering the
logarithm of the hardening relation:

$$\ln(\sigma - \sigma_F) = \ln k + n \ln \varepsilon_{pl}$$
$$Y \quad = \quad K \quad + \quad nX.$$

$\varepsilon_{pl}[\%]$	0	0.32	1.27	2.23	3.2	4.17
$\sigma[MPa]$	350	472	501.2	517	530	541
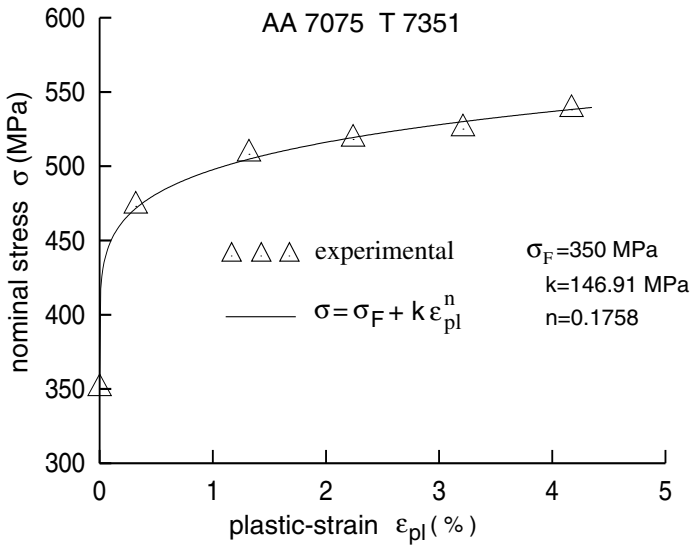
Fig. 13.7b Hardening parameters k and n for alumimium alloy at room temperature

The function **leastsquare** of the MAPLE package $stats[fit, leastsquare]$ fits a curve to the given data using the method of least squares, as shown in the following MAPLE program.

Hardening of aluminium alloy AA7075 T 7351   ⊙ 13_2.mws

```
>   data:=[0,350], [0.32, 472], [1.27, 501.2],
>   [2.23,517], [3.2, 530], [4.17,541]:
>   for i in [472, 501.2, 517, 530, 541] do
>   Y[i]:=ln(i-350.) od;
```

$$Y_{472} := 4.804021045$$
$$Y_{501.2} := 5.018603464$$
$$Y_{517} := 5.117993812$$
$$Y_{530} := 5.192956851$$
$$Y_{541} := 5.252273428$$

```
>   with(stats):
>   fit[leastsquare[[x,y], y=K+n*ln(x),
>   {K,n}]]([[0.32,1.27,2.23,3.2,4.17],
>   [4.804,5.019,5.118,5.193,5.252]]);
```

$$y = 4.991336579 + 0.1722331357 \ln(x)$$

```
>  k:=(exp(4.991336579))*MPa; n:=0.1722;
```
$$k := 147.1329469 \, MPa; \quad n := 0.1722$$

```
>  sigma(epsilon[pl]):=(350+(k/MPa)*
>  epsilon[pl]^(n))*MPa;
```
$$\sigma(\varepsilon_{pl}) := (350 + 147.1329469 \, \varepsilon_{pl}{}^{0.1722}) \, MPa$$

```
>  yield_stress:=sigma[F]=350*MPa;
```
$$yield\_stress := \sigma_F = 350 \, MPa$$

```
>  alias(H=Heaviside, th=thickness):

>  p[1]:=plot(sigma(epsilon[pl])/MPa,
>  epsilon[pl]=0..5, 350..600, th=2):

>  p[2]:=plot([data],epsilon[pl]=0..5.,
>  style=point,symbol=cross, symbolsize=30):

>  p[3]:=plot({600,600*H(epsilon[pl]-5)},
>  epsilon[pl]=0..5.001, 350..600):

>  plots[display]({seq(p[k],k=1..3)});
```
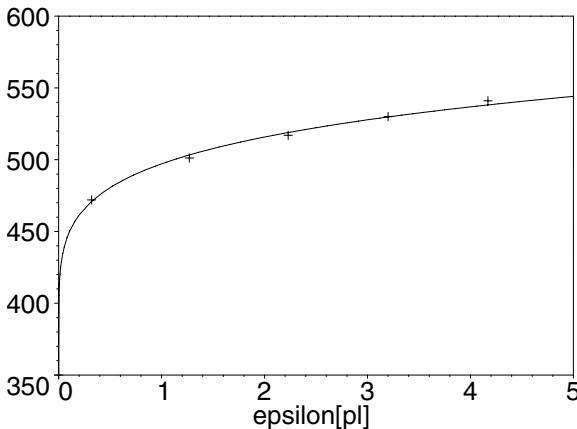

Fig. 13.8a Hardening $\sigma(\varepsilon_{p\ell})$ of aluminium alloy

distance vector between the leastsquare approximation and experimental data:

```
>   sigma[dimensionless]:=1+(k/350/MPa)*
>   epsilon[pl]^(0.1722); # plast. strains in %
```

$$\sigma_{dimensionless} := 1 + 0.4203798483\,\varepsilon_{pl}^{0.1722}$$

```
>   DATA:=[0,1],[0.32,472./350],
>   [1.27,501.2/350],[2.23,517./350],
>   [3.2, 530./350],[4.17,541./350]:

>   p[4]:=plot(sigma[dimensionless],
>   epsilon[pl]=0..5, 1..1.6,th=2):

>   p[5]:=plot([DATA],epsilon[pl]=0..5.,
>   style=point,symbol=cross, symbolsize=30):

>   p[6]:=plot({1.6,1.6*H(epsilon[pl]-5)},
>   epsilon[pl]=0..5.01,1..1.6,):
>   plots[display]({seq(p[k],k=4..6)});
```
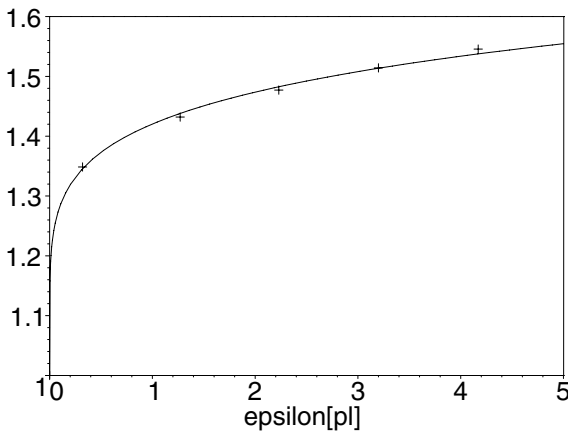

Fig. 13.8b Hardening $\sigma_{dimensionless}$ of aluminium alloy

```
>   for i from 1 to 6 do v[i]:=(subs(
>   epsilon[pl]=data[i][1],
>   sigma[dimensionless])-(1/350)*data[i][2])
>   od;
```

$$v_1 := 0.$$
$$v_2 := -0.003086811$$
$$v_3 := 0.006043146$$
$$v_4 := 0.005493447$$
$$v_5 := -0.000681338$$
$$v_6 := -0.008151349$$

```
>  with(linalg):
>  V:=vector([seq(v[i], i=1..6)]); # dist. vector
```

$V := [0., -0.003086811, 0.006043146, 0.005493447, -0.000681338,$
$-0.008151349]$

L-two error norm:

```
>  L[2]:=(1/sqrt(number_of_points))*Norm(V,2)=
>  evalf((1/sqrt(6))*norm(V,2));
```

$$L_2 := \frac{\mathrm{Norm}(V, 2)}{\sqrt{number\_of\_points}} = 0.004884238045$$

```
>  L[infinity]:=
>  (1/(number_of_points)^(1/infinity))*
>  Norm(V,infinity)=(1/(number_of_points)^(1/
>  infinity))*norm(V,infinity);
```

$$L_\infty := \mathrm{Norm}(V, \infty) = 0.008151349$$

```
>  L[infinity]:=Max(abs(v[1..6]))=abs(v[6]);
```

$$L_\infty := \mathrm{Max}(|v_{1..6}|) = 0.008151349$$

```
>  L[p]:=(1/(number_of_points)^(1/p))*Norm(V,p);
```

$$L_p := \frac{\mathrm{Norm}(V, p)}{number\_of\_points^{\left(\frac{1}{p}\right)}}$$

```
>  for i from 1 by 5 to 31 do
>  N[i]:=norm(V,i) od;
```

$$N_1 := 0.023456091$$
$$N_6 := 0.008474448012$$
$$N_{11} := 0.008187749433$$
$$N_{16} := 0.008156489928$$
$$N_{21} := 0.008152169845$$
$$N_{26} := 0.008151490898$$
$$N_{31} := 0.008151374877$$

```
>  for i from 1 by 1000 to 6001 do
>  L[i]:=(1/(6.)^(1/i))*norm(V,i) od;
```

$$L_1 := 0.003909348501$$
$$L_{1001} := 0.008136771388$$
$$L_{2001} := 0.008144053288$$
$$L_{3001} := 0.008146483659$$
$$L_{4001} := 0.008147699417$$
$$L_{5001} := 0.008148429060$$
$$L_{6001} := 0.008148915562$$

The error norms show that we have determined a suitable approximation to the given experimental data. In the following part of this MAPLE-program the above leastsquare approximation should be compared with the hardening curve in Fig. 13.5b based upon the *nonlinear MARQUARDT-LEVENBERG-algorithm:*

The relative difference between the two approaches is defined as:

```
>  rel_difference:=1-sigma[LEASTSQUARE]/
>  sigma[MARQUARDT_LEVENBERG];
```

$$rel\_difference := 1 - \frac{\sigma_{LEASTSQUARE}}{\sigma_{MARQUARDT\_LEVENBERG}}$$

```
>  alias(x=epsilon[pl]): # epsilon[pl] in [%]
>  Delta[rel](x):=1-(147.1329469*x^0.1722)/
>  (146.9071*x^0.1758);
```

$$\Delta_{rel}(x) := 1 - \frac{1.001537345}{x^{0.0036}}$$

```
>  Delta[rel][mean_value]:=(1/5)*
>  Int(abs(Delta[rel]),x=0..5)=(1/5)*int(abs
>  (Delta[rel](x)),x=0.00000000001..5);
```

$$\Delta_{rel\,mean\_value} := \frac{1}{5} \int_0^5 |\Delta_{rel}| \, dx = 0.002865461116$$

```
>  zero_of_Delta:=
>  fsolve(1.001537345-x^0.0036=0,x);
```

$$zero\_of\_Delta := 1.532211872$$

```
>  difference:=(sigma[MARQUARDT_LEVENBERG]-
>  sigma[LEASTSQUARE])/sigma[yield];
>  DELTA(x):=(146.9071*x^0.1758-
>  147.1329469*x^0.1722)/350;
```

$$difference := \frac{\sigma_{MARQUARDT\_LEVENBERG} - \sigma_{LEASTSQUARE}}{\sigma_{yield}}$$

$$\mathrm{DELTA}(x) := 0.4197345714\, x^{0.1758} - 0.4203798483\, x^{0.1722}$$

```
>  plot({0.0035,0.0035*H(x-5),abs(DELTA(x))},
>  x=0..5.001,title="difference DELTA(x)");
```
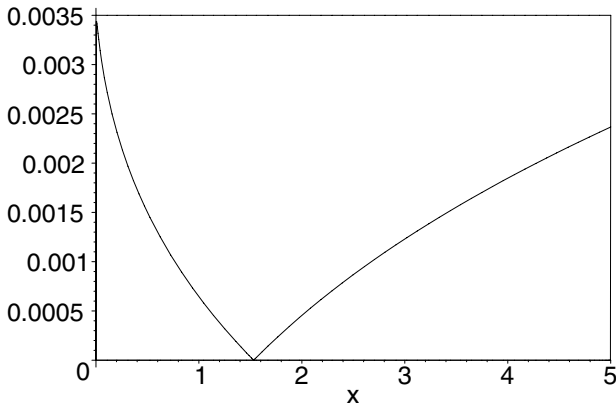

Fig. 13.9 Difference DELTA(x)

error norms:

```
>  L[p]:=
>  ((1/5)*Int((abs(DELTA))^p,x=0..5))^(1/p);
```

$$L_p := (\frac{1}{5} \int_0^5 |DELTA|^p \; dx)^{(\frac{1}{p})}$$

```
>  for i from 1 to 5 do L[i]:=((1/5)*
>  (int((-DELTA(x))^i,x=0..1.532211872) +
>  int((DELTA(x))^i,x=1.532211872..5)))^(1/i)
>  od;
```

$$L_1 := 0.001288306839$$
$$L_2 := 0.001487235818$$
$$L_3 := 0.001629074679$$
$$L_4 := 0.001741275711$$
$$L_5 := 0.001836670740$$

These error norms illustrate that in the present case the least squares method furnishes comparable approximations with the *nonlinear* MARQUARDT-LEVENBERG-*algorithm*. However, the approximations obtained in this manner are **not** the least squares approaches for the original problem, and these approximations can in some cases significantly differ from the least squares approximations to the original problem.

14 Creep Curve

As has been outlined in Chapter 13 in more detail creep tests are carried out on specimens loaded, e.g., in tension or compression, usually at constant load, inside a furnace which is maintained at a constant temperature. The extension of the specimen is measured as a function of time.

A typical *creep curve* for metals, polymers, and ceramics exsists of three parts and is schematically shown in Fig. 4.1 characterizing the three creep stages called *transient creep, steady creep,* and *accelerating creep.*

In the following MAPLE worksheet an exponential description of a *creep curve* has been represented :

$\odot$ $14\_1.mws$

Exponential Description

```
>    restart:
>    epsilon[creep](t):=A[11]*(1-exp(-A[12]*
>    sqrt(t)))+A[21]*t+A[31]*(exp(A[32]*t^n)-1);
```

$$\varepsilon_{creep}(t) := A_{11}\left(1 - e^{(-A_{12}\sqrt{t})}\right) + A_{21}\,t + A_{31}\left(e^{(A_{32}\,t^n)} - 1\right)$$

```
>    Digits:=5:
>    epsilon[c](t):=subs({A[11]=0.4,A[12]=5,
>    A[31]=0.02,A[32]=3,  n=10},%%);
```

$$\varepsilon_c(t) := 0.38 - 0.4\,e^{(-5\sqrt{t})} + A_{21}\,t + 0.02\,e^{(3\,t^{10})}$$

```
>    epsilon[c](0):=evalf(subs(t=0,%));
```

$$\varepsilon_c(0) := 0.$$

```
>    epsilon[c](1):=evalf(subs(t=1,%%));
```

$$\varepsilon_c(1) := 0.77902 + A_{21}$$

```
>    A[21]:=solve(epsilon[c](1)=1,A[21]);
```

$$A_{21} := 0.22098$$

```
>    alias(H=Heaviside,th=thickness,co=color):
>    plot1:=plot(epsilon[c](t),t=0..1,th=2):
```

```
>   plot2:=plot({epsilon[c](1),epsilon[c](1)
>   *H(t-1)}, t=0..1.001):
>   plots[display]({plot1,plot2});
```
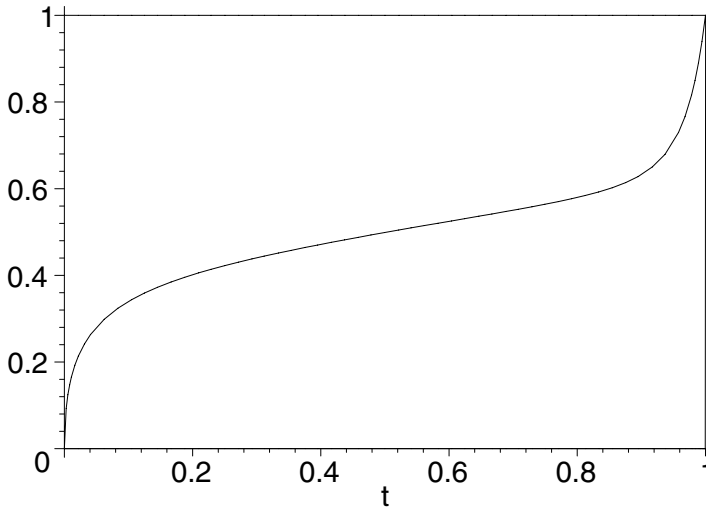

Fig. 14.1 Creep curve, exponential discription

Time Derivative

```
>   time_derivative(t):=diff(epsilon[c](t),t);
```

$$\text{time\_derivative}(t) := \frac{1.0000\, e^{(-5\,\sqrt{t})}}{\sqrt{t}} + A_{21} + 0.60\, t^9\, e^{(3\,t^{10})}$$

```
>   time_derivative(0):=infinity;
```

$$\text{time\_derivative}(0) := \infty$$

```
>   time_derivative(1):=evalf(subs({A[21]=0.22098,
>   t=1},%%));
```

$$\text{time\_derivative}(1) := 12.280$$

```
>   plot3:=plot(time_derivative(t),
>   t=0..1,0..2,th=2,co=black):
>   plot4:=plot({2,2*H(t-1)},t=0..1.001,co=black):
>   plots[display]({plot3,plot4});
```
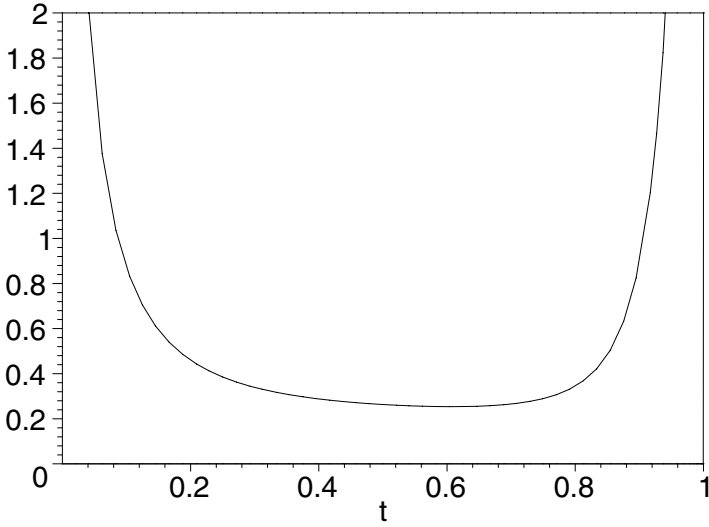
Fig. 14.2 Time derivative of a creep curve

```
>  plots[display]({plot1,plot2,plot3,plot4});
```
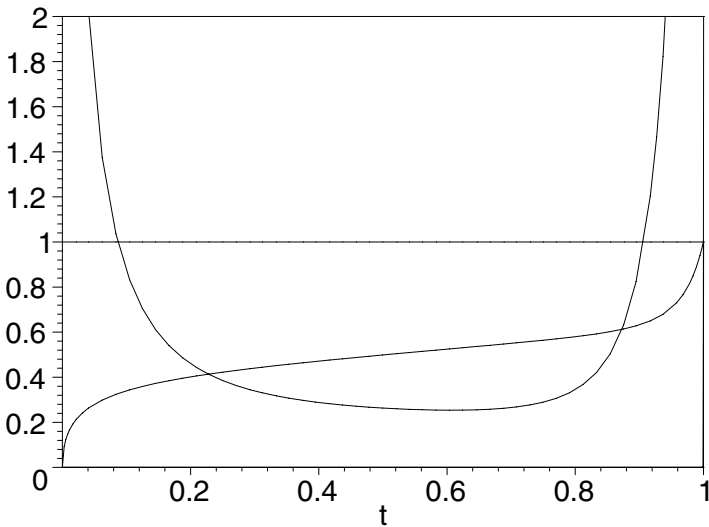

Fig. 14.3 Creep curve, exponential discription and time derivative

Creep Parameters

The creep curve exsists of three parts:

```
>   restart:
>   parameters_of_the_primary_term:=A[11], A[12];
```

$$parameters\_of\_the\_primary\_term := A_{11}, A_{12}$$

```
>   parameters_of_the_scondary_term:=A[21]=
>   K*sigma^m;    # NORTON-BAILEY
```

$$parameters\_of\_the\_scondary\_term := A_{21} = K\,\sigma^m$$

```
>   parameters_of_the_tertiary_term:=A[31],
>   A[32],n;
```

$$parameters\_of\_the\_tertiary\_term := A_{31}, A_{32}, n$$

For the *primary creep* the sqrt(t)-law has been assumed, the justification of which has been analysed in Chapter 11.

The exponent n in the tertiary term regulates the tangent of the creep curve at the creep rupture time. The creep parameters can be determined by suitable experiments, some of which are discussed in Chapter 13.

Creep Rate and Acceleration

```
>   restart: Digits:=5:
>   epsilon[creep](t):=A[11]*(1-exp(-A[12]*
>   sqrt(t)))+A[21]*t+A[31]*(exp(A[32]*t^n)-1);
```

$$\varepsilon_{creep}(t) := A_{11}\left(1 - e^{(-A_{12}\sqrt{t})}\right) + A_{21}\,t + A_{31}\left(e^{(A_{32}\,t^n)} - 1\right)$$

```
>   creep_rate(t):=diff(epsilon[creep](t),t);
```

$$\text{creep\_rate}(t) := \frac{1}{2}\frac{A_{11}\,A_{12}\,e^{(-A_{12}\sqrt{t})}}{\sqrt{t}} + A_{21} + \frac{A_{31}\,A_{32}\,t^n\,n\,e^{(A_{32}\,t^n)}}{t}$$

```
>   creep_rate(0):=infinity;
```

$$\text{creep\_rate}(0) := \infty$$

```
>   creep_rate(1):=subs(t=1,%%);
```

$$\text{creep\_rate}(1) := \frac{1}{2}A_{11}\,A_{12}\,e^{(-A_{12})} + A_{21} + A_{31}\,A_{32}\,n\,e^{A_{32}}$$

```
>   creep_rate(1):=evalf(subs({A[11]=0.4,A[12]=5,
>   A[21]=0.22098,A[31]=0.02,A[32]=3,n=10},%%));
```

$$\text{creep\_rate}(1) := 12.280$$

```
>   Creep_rate(t):=evalf(subs({A[11]=0.4,A[12]=5,
>   A[21]=0.22098,A[31]=0.02,A[32]=3,n=10},
>   creep_rate(t)));
```

$$\text{Creep\_rate}(t) := \frac{1.0000\,e^{(-5.\sqrt{t})}}{\sqrt{t}} + 0.22098 + 0.60\,t^9\,e^{(3.\,t^{10})}$$

```
>   acceleration(t):=diff(epsilon[creep](t),t$2);
```

$$\text{acceleration}(t) := -\frac{1}{4}\frac{A_{11}\,A_{12}\,e^{(-A_{12}\,\sqrt{t})}}{t^{(3/2)}}-$$

$$\frac{1}{4}\frac{A_{11}\,A_{12}{}^2\,e^{(-A_{12}\,\sqrt{t})}}{t}+\frac{A_{31}\,A_{32}\,t^n\,n^2\,e^{(A_{32}\,t^n)}}{t^2}-$$

$$\frac{A_{31}\,A_{32}\,t^n\,n\,e^{(A_{32}\,t^n)}}{t^2}+\frac{A_{31}\,A_{32}{}^2\,(t^n)^2\,n^2\,e^{(A_{32}\,t^n)}}{t^2}$$

```
>   Acceleration(t):=evalf(subs({A[11]=0.4,A[12]=5,
>   A[31]=0.02,A[32]=3,n=10},%),3);
```

$$\text{Acceleration}(t) := -\frac{0.50000\,e^{(-5.\,\sqrt{t})}}{t^{(3/2)}}-\frac{2.5000\,e^{(-5.\,\sqrt{t})}}{t}$$

$$+5.40\,t^8\,e^{(3.\,t^{10})}+18.00\,t^{18}\,e^{(3.\,t^{10})}$$

```
>   alias(H=Heaviside, th=thickness, co=color):
>   plot1:=plot({Creep_rate(t),Acceleration(t)},
>   t=0..1,-10..10,co=black,th=2):
>   plot2:=plot({10,-10,10*H(t-1),-10*H(t-1)},
>   t=0..1.001,co=black):
>   plots[display]({plot1,plot2});
```
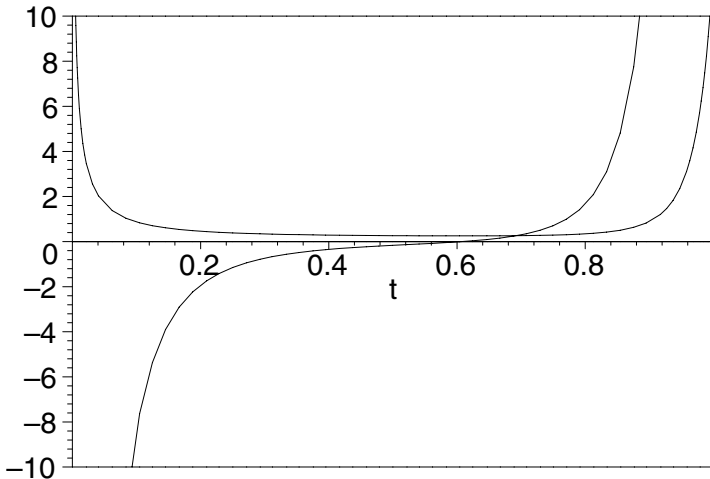

Fig. 14.4 Creep rate and acceleration

A similar worksheet has been submitted to the Maplesoft Application Center (www.maplesoft.com) as an Application Demonstration by BETTEN (2007).

Furthermore, some other worsheets have also been submitted to Maplesoft in several categories, e.g., Mathematics: Engineering-Mathematics, Differential Geometry, Linear Algebra; Engineering: Mechanics, Engineering-Mathematics.

A The HEAVISIDE and DIRAC Functions

The HEAVISIDE *unit function* , also called the *unit step function*, is defined according to

$$H(t - a) := \begin{cases} 1 \text{ for } t \geq a, \\ 0 \text{ for } t < a, \end{cases} \quad \text{or} \quad H(t - a) : \begin{cases} 1 \text{ for } t > a, \\ \frac{1}{2} \text{ for } t = a, \\ 0 \text{ for } t < a, \end{cases} \quad \text{(A.1a,b)}$$

where t is the time variable and $t = a$ denotes a time at which a step change has been occured (Fig.A.1).
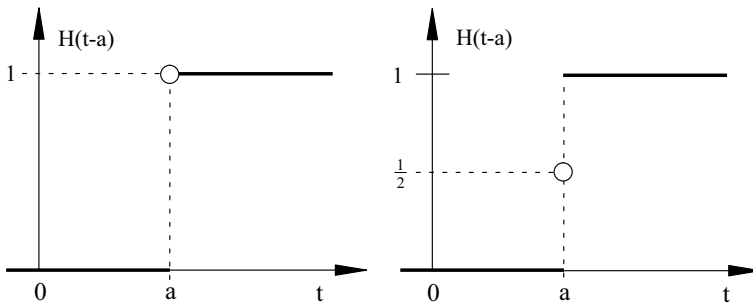
Fig. A.1 HEAVISIDE functions (A.1a,b)

A step change in shear stress from $\tau = 0$ to $\tau = \tau_0$ at $t = a$ may be expressed by

$$\tau(t) = \tau_0 H(t - a) . \quad \text{(A.2)}$$

Another step function is shown in Fig. 11.1, which can be represented as follows

$$\sigma(t) = \sigma_0 H(t) + \Delta\sigma_1 H(t - \Theta_1) + \Delta\sigma_2 H(t - \Theta_2) + \ldots \quad \text{(A.3a)}$$

$$\sigma(t) = \sigma_0 H(t) + \sum_{i=1}^{n} \Delta\sigma_i H(t - \Theta_i) , \quad \text{(A.3b)}$$

if we use the HEAVISIDE *function* $H(t - a)$ defined in (A.1).

Similarly to (A.3) and Fig.11.1 the step function

$$h(t) = H(t - a) + 2H(t - 2a) + 3H(t - 4a) \qquad \text{(A.4)}$$

is drawn in Fig. A.2.
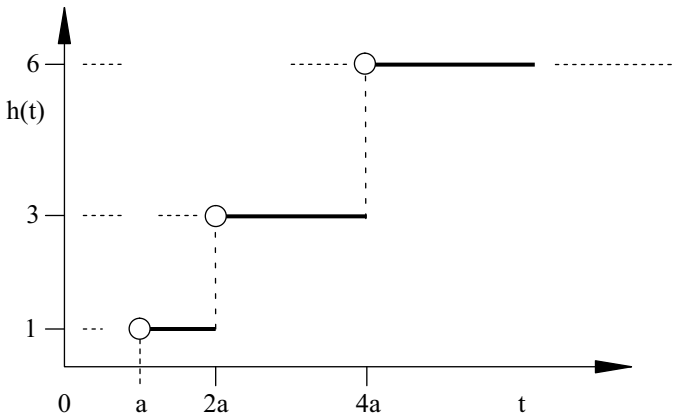
Fig. A.2 Several steps

Adding and subtracting unit step functions at times t equal to $a, 2a, 3a, ...$ we arrive at the *square wave*

$$h(t) = H(t) + 2 \sum_{n=1}^{N} (-1)^n H(t - na) \qquad \text{(A.5)}$$

illustrated in Fig. A.3.
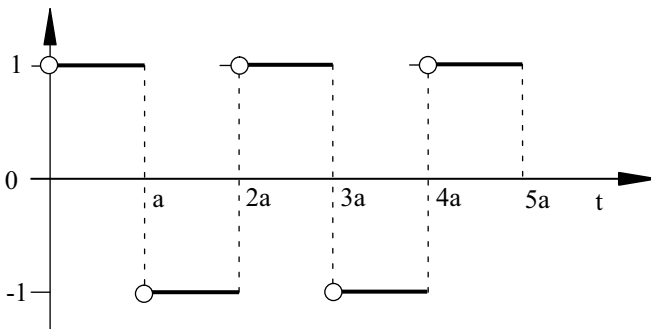
Fig. A.3 Square wave (A.5)

The *unit step function* (A.1) is defined in MAPLE under the name `Heaviside`. For example, the influence of the HEAVISIDE *function* on $sin(t)$ and $cos^2(t)$ is illustrated in Fig. A.4a.

⊙ *A_1.mws*

```
>   alias(H=Heaviside,th=thickness):
>   plot1:=plot(H(t-1),t=0..Pi,th=3):
>   plot2:=plot(sin(t)*H(t-1), t=0..Pi, th=3):
>   plot3:=plot((cos(t))^2*H(t-1),
>   t=0..Pi,th=3):
>   plots[display]({plot1,plot2,plot3});
```
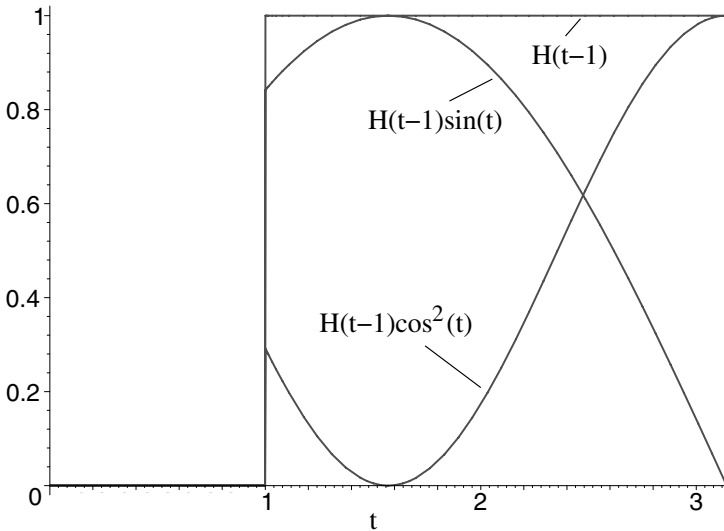

Fig. A.4a Influence of the HEAVISIDE function on $sin(t)$ and $cos^2(t)$

Another example is illustrated in Fig. A.4b, where the vertical lines have been produced by HEAVISIDE *functions*.

⊙ *A_2.mws*

```
>   alias(H=Heaviside,th=thickness):
>   plot1:=plot({-1,1,2,3,4,5}, X=0..5,-1..5,
>   scaling=constrained, color=black,th=2):
>   plot2:=plot({5*H(x-1)+5*H(x-1.001),
>   -H(x-1)-H(x-1.001), 5*H(x-2)+5*H(x-2.001),
>   2+H(x-3.5)+3*H(x-3.501),5*H(x-5)+
>   5*H(x-5),-H(x-5)-H(x-5.001)},
>   x=0..5.00001, -1..5, color=black, th=3):
>   plots[display]({plot1,plot2});
```
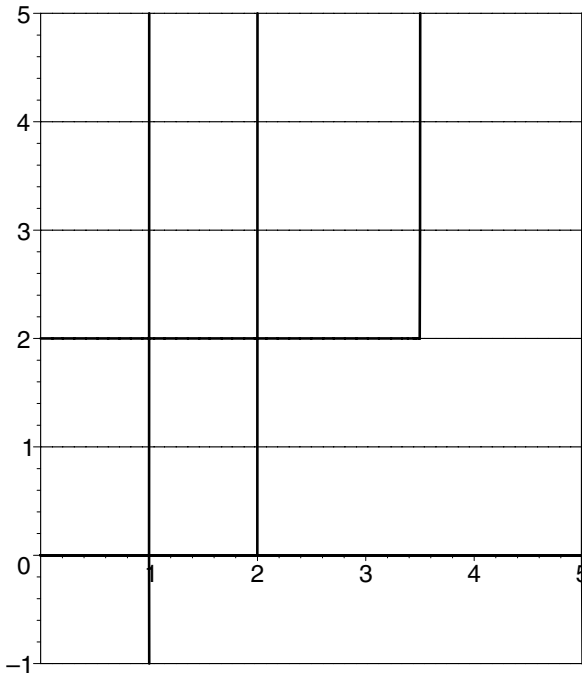
Fig. A.4b Vertical lines generated by HEAVISIDE *functions*

In some Figures, for instance in Fig. B.1, HEAVISIDE *functions* have been used in order to generate vertical lines.

Besides the HEAVISIDE *unit function* (A.1) the DIRAC *delta function*, also called the *unit impulse function*, plays a central role in creep mechanics, for instance in (11.11b), and is defined according to

$$\delta(t - a) := \begin{cases} 0 & \text{for } t \neq a, \\ \infty & \text{for } t = a. \end{cases} \tag{A.6}$$

This function has the properties

$$\int_0^\infty \delta(t - a)dt = 1 \tag{A.7}$$

and

$$\int_0^\infty \delta(t-a)\,f(t)dt = f(a) \tag{A.8}$$

for every continuous function $f(t)$ and also valid for $a = 0$.

The property (A.7) of the delta function can geometrically interpreted as illustrated in Fig. A.5.
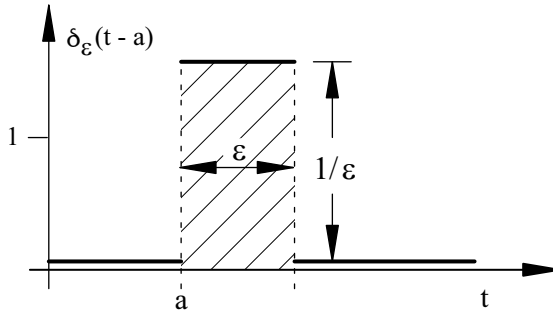
Fig. A.5 DIRAC delta function with $\varepsilon > 0$

In Fig. A.5 the *"modified"delta function*

$$\delta_\varepsilon(t-a) := \begin{cases} 1/\varepsilon & \text{for } a < t < a + \varepsilon \\ 0 & \text{for } t < a \quad \text{and} \quad t > a + \varepsilon \end{cases} \tag{A.9}$$

is represented,which tends to (A.6) as ε tends to zero, where the hatched area in Fig. A.5 is always unity. Hence, the property (A.7) is valid.

If any continuous function $f(t)$ is multiplied by the DIRAC delta function $\delta(t - a)$ the product vanishes everywhere except at $t = a$, while the value $f(a)$ is independent of t and can therefore be written outside the integral. Thus, considering (A.7), we arrive at the result (A.8), which is also applied in the *collocation method* according to

$$\boxed{\int_0^L \delta(x - x_i)R(x)dx = R(X_i) \overset{!}{=} 0} \quad, \tag{A.10}$$

where $R(x)$ is the residuum of an approximation, for instance $\Delta\Phi - g(x) = R(x) \neq 0$, and X_i is an optimal selected *collocation point*. The integral in (A.10) is setting over a domain L considered.

The collocation method can be shown to be a special case of the *weighted-residual method*

$$\int_0^L W_i(x)R(x)dx \overset{!}{=} 0 \quad , \tag{A.11}$$

where $W_i(x)$ are *weight functions* (BETTEN, 2004).

A relation between the unit step function (A.1) and the unit impulse function (A.6) is given by

$$\delta(t-a) = \frac{d}{dt}H(t-a) \equiv \dot{H}(t-a) \tag{A.12}$$

and may be deduced in the following way. The modified delta function (A.9) can be represented by the HEAVISIDE *function* (A.1) as

$$\delta_\varepsilon(t-a) = \frac{1}{\varepsilon}\left[H(t-a) - H(t-a-\varepsilon)\right] \tag{A.13a}$$

or for $a = 0$ according to

$$\delta_\varepsilon(t) = \frac{1}{\varepsilon}\left[H(t) - H(t-\varepsilon)\right]. \tag{A.13b}$$

Then, we immediately find the DIRAC *delta function* by forming the following limit

$$\delta(t) = \lim_{\varepsilon\to 0}\delta_\varepsilon(t) = \lim_{\varepsilon\to 0}\frac{H(t) - H(t-\varepsilon)}{\varepsilon} = \dot{H}(t) \tag{A.14}$$

in accordance with (A.12), that is, the DIRAC *delta function* is the derivation of the HEAVISIDE *function*. This relation is illustrated in Fig. A.6a,b by comparing Fig. A.1 with Fig. A.5.

⊙ $A\_3.mws$

```
>   with(stats):
>   with(statevalf):
>   H:=statevalf[pdf,normald[1,0.2]]:
>   delta:=statevalf[cdf,normald[1,0.2]]:
>   plot({H(t),delta(t)},t=0..2,thickness=3);
>   H:=statevalf[pdf,normald[1,0.03]]:
>   delta:=statevalf[cdf,normald[1,0.03]]:
>   plot({H(t),delta(t)},
>   t=0..2,0..2,thickness=3);
```
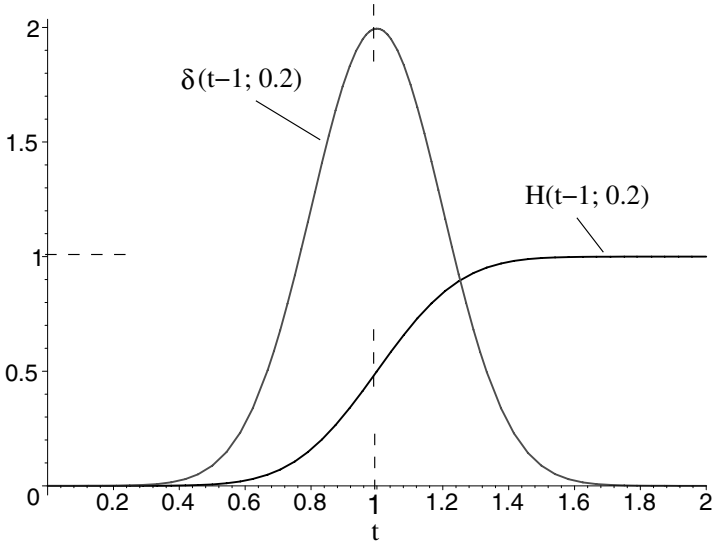
Fig. A.6a Relation between the modified Heaviside function (A.16) and the modified Dirac function (A.15); parameters: $a = 1$, $\sigma = 0.2$
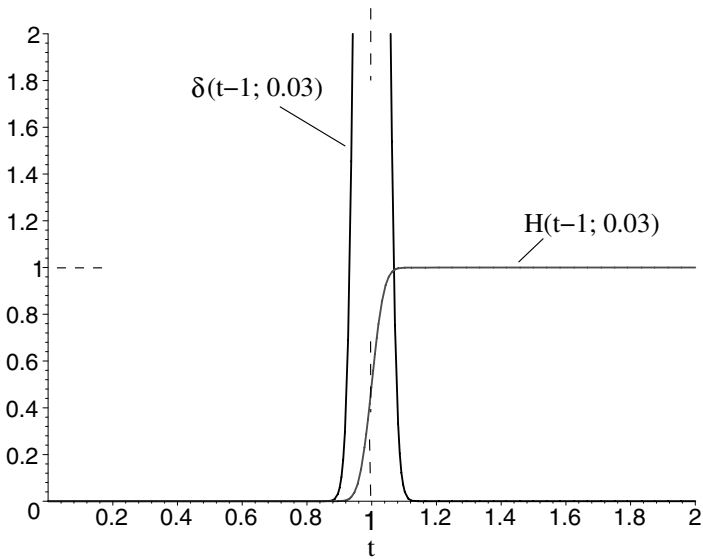
Fig. A.6b Relation between the modified Heaviside function (A.16) and the modified Dirac function (A.15); parameters: $a = 1$, $\sigma = 0.03$

As an example, the *normal distribution* (GAUSS *distribution)*

$$\delta(t - a; \sigma) := \frac{1}{\sigma\sqrt{2\pi}} \, exp \left[-\frac{1}{2} \left(\frac{t - a}{\sigma} \right)^2 \right] \quad \begin{array}{c} -\infty < t < \infty, \\ \sigma > 0 \end{array} \quad \text{(A.15)}$$

is considered in Fig. A.6 as a modified DIRAC delta function, and is, according to (A.14), the derivative of the *modified* **(continuous)** HEAVISIDE *function*

$$H(t - a; \sigma) := \frac{1}{\sigma\sqrt{2\pi}} \int\limits_{-\infty}^{t} exp \left[-\frac{1}{2} \left(\frac{x - a}{\sigma} \right)^2 \right] dx \, . \quad \text{(A.16)}$$

The parameter σ in (A.16) regulates the *continuous transition* of the HEAVISIDE function at the position $t = a$ of the step.

The GAUSS *distribution* (A.15) has the property (A.7) or

$$\int\limits_{-\infty}^{\infty} \delta(t - a; \sigma) dt = 1 \quad , \quad \text{(A.17)}$$

as can be shown by utilizing the MAPLE software, hence, it is a suitable *impulse function.*

$\odot$ A_4.mws

```
>    delta(t):=(1/sigma/sqrt(2*Pi))*
>    exp((-1/2)*((t-a)/sigma)^2);
```

$$\delta(t) := \frac{1}{2} \frac{\sqrt{2} \, e^{(-\frac{(t-a)^2}{2\sigma^2})}}{\sigma \sqrt{\pi}}$$

```
>    Int(delta,t=0..infinity)=int(subs(a=1,
>    sigma=1./10, delta(t)),t=0..infinity);
```

$$\int_0^\infty \delta \, dt = 1.000000000$$

In the following, let us discuss the *modified* **(continuous)** HEAVISIDE *function*

$$H(t - a; D) := \frac{1}{\pi} \arctan \frac{2Dt}{a^2 - t^2} \quad , \quad \text{(A.18)}$$

where the parameter $D \geq 0$ regulates the *continuous transition* at the position $t = a$ of the step, (Fig. A.7). For $D = 0$, we arrive at the "original" HEAVISIDE function (Fig. A.7).

Remark: The formula (A.18) remembers us at the *phase difference* φ between the impressed force or impressed support movement and the resulting steady-state vibration of a damped system. In that case the parameter D is the *damping factor*, while the variable t is interpreted as the *frequency ratio* Ω/ω.

```
>   y(t):=2*D*t;    x(t):=1-t^2;
```
⊙ *A_5.mws*

$$y(t) := 2\,D\,t$$

$$x(t) := 1 - t^2$$

```
>   H(t):=(1/Pi)*arctan(y(t),x(t));
```

$$H(t) := \frac{\arctan(2\,D\,t,\,1 - t^2)}{\pi}$$

```
>   plot1:=plot(subs(D=infinity,H(t)),
>   t=0..3,0..1):
>   plot2:=plot(subs(D=0.5,H(t)),t=0..3,0..1):
>   plot3:=plot(subs(D=0.1,H(t)),t=0..3,0..1):
>   plot4:=plot(subs(D=0.05,H(t)),t=0..3,0..1):
>   plot5:=plot(subs(D=0,H(t)),t=0..3,0..1):
>   plots[display]({plot1,plot2,plot3,
>   plot4,plot5});
```
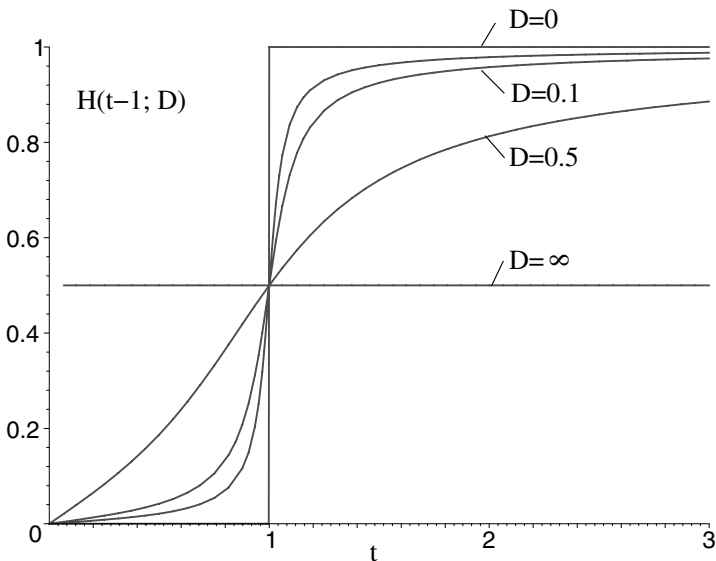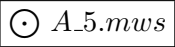

Fig. A.7 Modified HEAVISIDE function (A.18)

From (A.18) we deduce the corresponding Dirac *delta functions*:

$$\boxed{\delta(t - a; D) := \dot{H}(t - a; D) = \frac{2D}{\pi} \frac{a^2 + t^2}{(a^2 - t^2)^2 + 4D^2 t^2}}, \qquad \text{(A.19)}$$

which are graphically represented in Fig. A.8 as Maple-plot.

$$\odot \; A\_6.mws$$

```
>   delta(t):=(2*D/Pi)*(1+t^2)/
>   ((1-t^2)^2+4*(D^2)*t^2);
```

$$\delta(t) := \frac{2\,D\,(1 + t^2)}{\pi\,((1 - t^2)^2 + 4\,D^2\,t^2)}$$

```
>   plot1:=plot(subs(D=0.5,delta(t)),t=0..3):
>   plot2:=plot(subs(D=0.1,delta(t)),t=0..3):
>   plot3:=plot(subs(D=0.01,delta(t)),
>   t=0..3,0..2):
>   plots[display]({plot1,plot2,plot3});
```
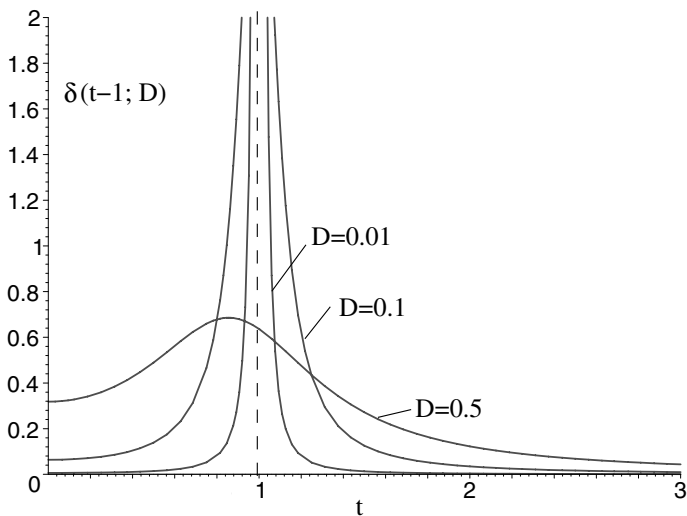

Fig. A.8 Modified Dirac delta functions (A.19)

As we can see in the Maple output (Fig. A.8), the *"modified"* Dirac *delta functions* (A.19) have the property (A.7) for all $D > 0$. For $D = 0$ the delta function (A.19) is a vertical line at $t = a = 1$ with an area identical to zero in contrast to the Gauss distribution (A.15), which satisfies the condition (A.7) also for σ identical to zero.

B The LAPLACE Transformation

The LAPLACE *transformation* is an elegant procedure, which can be used, for instance, to solve *ordinary* and *partial differential equations* or *integral equations*. It often yields results more readily than other techniques. Especially in the theory of *viscoelasticity* (Chapter 11), *operational calculus, electricity*, etc., many authors utilize this convenient tool.

The general *two-sided* LAPLACE *transformation* is defined as

$$F(s) := \int_{-\infty}^{\infty} f(t)e^{-st}dt\,, \tag{B.1}$$

where the function $f(t)$ of t is mapped into a function $F(s)$ of the transformed variable s, which may be real or complex. In the following, the lower limit of the integral in (B.1) is fixed at $t = 0$, i.e., the *one-side* (*right side*) LAPLACE *transformation*

$$L\{f(t)\} \equiv \hat{f}(s) := \int_{0}^{\infty} f(t)e^{-st}dt \tag{B.2}$$

is taken into consideration (Chapter 11).

A function $f(t)$ is transformable according to (B.2), if it is *piecewise continuous* with at most *exponential growth*, i.e.,

$$\mid f(t) \mid \le Me^{at} \quad or \quad \mid e^{-at}f(t) \mid \le M \quad with \quad M, a \in \mathbb{R}\,. \tag{B.3}$$

Then, the LAPLACE *transform* $L\{f(t)\}$ exists for all $s > a$, and the function $f(t)$ is of *exponential order* a.

Proof:

$$\mid L\{f(x)\} \mid \le \int_{0}^{\infty} \mid f(t) \mid e^{-st}dt \le M \int_{0}^{\infty} e^{-(s-a)t}dt = \frac{M}{s-a}\,. \tag{B.4}$$

Since $M/(s-a)$ has a finite value for $s > a$, the integral in (B.2) is bounded. This establishes the *absolute convergence* of the integral defining $L\{f(t)\}$. The convergence is *uniform*, if $s \geq \alpha_0 > a$, where α_0 is fixed. If s is complex, the above integral converges absolutely, provided the real part $Re(s) \geq \alpha_0 > a$.

Due to the theorem (B.3) the class of admissible functions $f(t)$, for which the LAPLACE transform (B.2) exists, is large enough for practical applications. A lot of LAPLACE transform pairs, $\hat{f}(s) \Longleftrightarrow f(t)$, is listed in a table at the end of this appendix. Further examples can be found in the MAPLE program. The exponential function $\exp(at)$ is admissible as has been shown in (B.4) for $M = 1$. Any periodic function that is piecewise continuous on its periodic is transformable. Polynomials are also admissible.

Let $f(t) = \exp(at)$ with $a = i\omega t$. Then, the LAPLACE transformation (B.2) yields

$$L\{e^{i\omega t}\} = L\{\cos \omega t + i \sin \omega t\} = \frac{1}{s - i\omega} \equiv \frac{s + i\omega}{s^2 + \omega^2}. \qquad \text{(B.5)}$$

Since the *operator* $L\{\}$ is *linear*,

$$\boxed{L\{\alpha f(t) + \beta g(t)\} = \alpha L\{f(t)\} + \beta L\{g(t)\}}, \qquad \text{(B.6)}$$

we arrive from (B.5) at the decomposition

$$L\{\cos \omega t\} + iL\{\sin \omega t\} = \frac{s}{s^2 + \omega^2} + i\frac{\omega}{s^2 + \omega^2}, \qquad \text{(B.7)}$$

hence:

$$L\{\cos \omega t\} = \frac{s}{s^2 + \omega^2} \quad \text{and} \quad L\{\sin \omega t\} = \frac{\omega}{s^2 + \omega^2} \qquad \text{(B.8a,b)}$$

for all real s and ω.

The *linearity* (B.6) immediately follows from the definiton (B.2). Differentiation of the transforms (B.8a,b) with respect to ω yields

$$L\{t \sin \omega t\} = \frac{2s\omega}{(s^2 + \omega^2)^2} \quad \text{and} \quad L\{t \cos \omega t\} = \frac{s^2 - \omega^2}{(s^2 + \omega^2)^2}. \qquad \text{(B.9a,b)}$$

Another example is $f(t) = t^p$. Introducing the substitution $st \equiv x$, we obtain the following LAPLACE transform:

$$L\{t^p\} \equiv \int_0^\infty t^p e^{-st} dt = \int_0^\infty \left(\frac{x}{s}\right)^p e^{-x} \frac{dx}{s} = \frac{1}{s^{p+1}} \int_0^\infty x^p e^{-x} dx, \qquad \text{(B.10)}$$

where the latter integral is convergent for $p > -1$ and represents the GAMMA *function* (11.33) defined as

$$\Gamma(p+1) := \int_0^\infty x^p e^{-x} dx \quad \text{with} \quad p > -1 \qquad \text{(B.11a)}$$

or

$$\Gamma(r) := \int_0^\infty x^{r-1} e^{-x} dx \quad \text{with} \quad r > 0. \qquad \text{(B.11b)}$$

Partial integration of the latter integral yields

$$\Gamma(r) := \frac{1}{r} \int_0^\infty x^r e^{-x} dx \equiv \frac{1}{r} \Gamma(r+1). \qquad \text{(B.12)}$$

The GAMMA *function* (B.11b) is drawn with MAPLE in Fig. B.1, where some integer points are marked.

$\boxed{\odot \ B\_1.mws}$

```
>    alias(H=Heaviside, th=thickness):
>    plot1:=plot({6,6*H(r-4)},r=0..4.001):
>    plot2:=plot(GAMMA(r),r=0..4,0..6,th=3):
>    plots[display]({plot1, plot2});
```
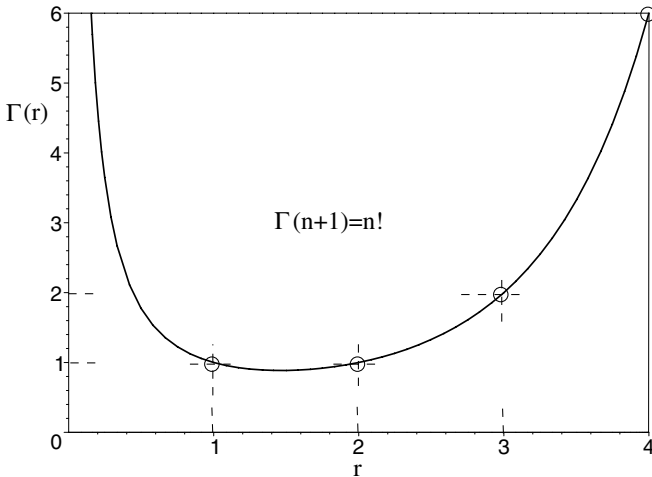

Fig. B.1 GAMMA function

For $r = 1$ we obtain from (B.11b)

$$\Gamma(1) = \int\limits_{0}^{\infty} e^{-x} dx = 1$$

and then by considering (B.12) for the following integers:

$$\Gamma(2) = 1 \cdot \Gamma(1) \equiv 1!, \quad \Gamma(3) = 2 \cdot \Gamma(2) \equiv 2!, \quad \Gamma(4) = 3 \cdot \Gamma(3) \equiv 3!,$$

and finally

$$\boxed{\Gamma(n+1) = n!} \,, \tag{B.13}$$

where $n \geq 0$ is an *integer*. Because of this connection with $n!$ the function $\Gamma(n+1)$ may be called the *factorial function*.

Comparing (B.11a) or (B.13) with (B.10), we obtain the following alternative LAPLACE *transforms*

$$\boxed{L\{t^p\} = \frac{\Gamma(p+1)}{s^{p+1}}} \quad \text{or} \quad \boxed{L\{t^n\} = \frac{n!}{s^{n+1}}} \,, \tag{B.14a,b}$$

where $s > 0$ and $p > -1$, while $n \geq 0$ is an *integer*.

For $p = -1$ the condition (B.3) is not satisfied, and for the function $f(t) = 1/t$ the LAPLACE transform $L\{1/t\}$ does not exist, since the integral (B.2) is *divergent* in that case. However, there may be *transformable functions*, which do not satisfy the criterion (B.3). Thus, the condition is *sufficient*, but **not** *necessary*.

The essential advantage and usefulness of the LAPLACE transformation is that it is necessary to know only some simple rules for solving practical problems. Therefore, the most important properties and rules of the LAPLACE *transformation* should be collected in the following.

B.1 Linearity

The *linearity* according to (B.6) of the operator $L\{\}$ immediately follows from the definition (B.2) and has been utilized in order to find the LAPLACE transforms (B.8a,b), for instance. Another example is:

$$L\{\sinh \omega t\} = \frac{1}{2} L\{e^{\omega t}\} - \frac{1}{2} L\{e^{-\omega t}\} = \frac{\omega}{s^2 - \omega^2} \,, \tag{B.15}$$

where $s > \omega$.

B.2 Inverse LAPLACE Transforms

The *inverse* LAPLACE *transform* of (B.2) is written in the form

$$\boxed{f(t) = L^{-1}\{\hat{f}(s)\}}$$ (B.16)

and is unique, if $f(t)$ satisfies the condition (B.3).

Example:

$$\hat{f}(s) = \frac{3 + 2s}{2 - 3s + s^2} = \frac{-5}{s - 1} + \frac{7}{s - 2} = L\{-5e^t + 7e^{2t}\}.$$ (B.17)

Its inverse form according to (B.16) yields

$$f(t) = -5e^t + 7e^{2t}.$$ (B.18)

Note, we have used the *partial fraction expansion* and the *linearity* (B.6) and the transform $L\{e^{\omega t}\} = 1/(s - \omega)$ in the decomposition (B.17).

B.3 Similarity Rule

The *similarity rule*

$$\boxed{L\{f(\omega t)\} = \frac{1}{\omega}\hat{f}\left(\frac{1}{\omega}s\right) \quad \text{with} \quad \omega > 0}$$ (B.19)

can be proofed by substituting $\varphi = \omega t$ in (B.2). The rule (B.19) is also valid for $\omega = 1/\alpha$.

B.4 Shift Rule

The *shift rule*

$$L\{f(t - a)\} = e^{-as}\hat{f}(s)$$ (B.20a)

or

$$L\{f(t + a)\} = e^{as}[\hat{f}(s) - \int_0^a f(t)dt]$$ (B.20b)

with $a > 0$ can be proofed by substituting $\tau = t - a$ or $\tau = t + a$, respectively, in (B.2).

B.5 Damping Rule

The *damping rule*

$$\boxed{L\{f(t)e^{-at}\} = \hat{f}(s+a)}$$
(B.21a)

immediately follows from (B.2):

$$L\{f(t)e^{-at}\} := \int\limits_0^\infty f(t)e^{-(s+a)t}dt \equiv \hat{f}(s+a)\,,$$
(B.21b)

where the parameter a is real and positiv.

B.6 LAPLACE Transforms of Derivatives

In order to utilize the LAPLACE transformation for solving ordinary differential equations we need the transform of the *derivative* $f^{(n)}(t)$, which is given by the rule

$$\boxed{\begin{aligned} L\{f^{(n)}(t)\} = s^n L\{f(t)\} - s^{n-1}f(0^+) - s^{n-2}f'(0^+) \\ -s^{n-3}f''(0^+) - \ldots - f^{(n-1)}(0^+) \end{aligned}}\,.$$
(B.22)

It is assumed that $f^{(n)}(t)$ is admissible in the sense of (B.3) and that all the lower derivatives are continuous for $t > 0$. The values at 0^+ are limits as $t \to 0$ from the right.

The *derivative rule* (B.22) can be deduced by induction in the following way.

Assuming that $f(t)$ is a continuous function which an admissible derivative $f'(t)$, integration by parts yields:

$$L\{f'(t)\} = \int\limits_0^\infty f'(t)e^{-st}dt = |f(t)e^{-st}|_0^\infty + s\int\limits_0^\infty f(t)e^{-st}dt\,,$$

where the upper limit of the first term on the right-hand side vanishes, while the lower limit is equal to $f(0^+)$. Thus, we obtain the following fundamental result:

$$\boxed{L\{f'(t)\} = sL\{f(t)\} - f(0^+)}\,.$$
(B.23)

Substituting $f(t) \equiv g'(t)$, we arrive from (B.23) at the following relations:

$$\left.\begin{array}{l} L\{g''(t)\} = s \, L \, \{g'(t)\} - g'(0^+) \\ \qquad L \, \{g'(t)\} = sL\{g(t)\} - g(0^+) \end{array}\right\} \Rightarrow$$

$$\boxed{L\{g''(t)\} = s^2 L\{g(t)\} - sg(0^+) - g'(0^+)} \qquad . \qquad (B.24)$$

Continuing this process, we finally arrive at the *derivative rule* (B.22).

As an example, let us solve the initial-value problem

$$\ddot{x} + 6\dot{x} + 5x = 0 \quad with \quad x(0) = 1 \quad and \quad \dot{x}(0) = -2. \qquad (B.25)$$

Taking into consideration (B.23) and (B.24), the differential equation (B.25) with the initial values transforms according to

$$(s^2 L\{x(t)\} - s + 2) + 6(sL\{x(t)\} - 1) + 5L\{x(t)\} = 0 \, ,$$

hence

$$L\{x(t)\} = \frac{s+4}{s^2+6s+5} = \frac{s+4}{(s+1)(s+5)} = \frac{3}{4(s+1)} + \frac{1}{4(s+5)}$$

and, similar to (B.17), the inverse transform, taken from the table of transforms, is the solution

$$x(t) = \frac{3}{4}e^{-t} + \frac{1}{4}e^{-5t} \qquad (B.26)$$

of the initial-value problem (B.25).

B.7 Differentiation of LAPLACE Transforms

The *differentiation of the transform* $\hat{f}(s)$ with respect to the transformed variable s yields

$$\boxed{\hat{f}^{(n)}(s) = \frac{d^{(n)} \hat{f}(s)}{ds^n} = (-1)^n L\{t^n f(t)\}} \qquad . \qquad (B.27)$$

This rule can be obtained as follows. The first derivative of (B.2) with respect to s is:

$$\frac{d\hat{f}(s)}{ds} = -\int_0^\infty tf(t)e^{-st}dt \equiv -L\{tf(t)\} \quad ,$$

the second one is:

$$\frac{d^2 \hat{f}(s)}{ds^2} = - \int_0^\infty t^2 f(t) e^{-st} dt \equiv +L\{t^2 f(t)\} \quad .$$

Following this way, we finally arrive at the rule (B.27).

For $f(t) = \cos \omega t$ we obtain from (B.27) by considering (B.8a) the following result

$$L\{t \cos \omega t\} = -\frac{d}{ds} L\{\cos \omega t\} = \frac{s^2 - \omega^2}{(s^2 + \omega^2)^2} \quad ,$$

which is identical to (B.9b).

Another example is $f(t) = e^{\omega t}$ with $L\{e^{\omega t}\} = 1/(s - \omega)$, hence

$$L\{t^2 e^{\omega t}\} = +\frac{d^2}{ds^2} L\{e^{\omega t}\} = \frac{2}{(s - \omega)^3} \quad .$$

Continuing this procedure, we finally obtain the following result:

$$\boxed{L\{t^n e^{\omega t}\} = \frac{n!}{(s - \omega)^{n+1}}} . \tag{B.28}$$

B.8 LAPLACE Transform of an Integral

The LAPLACE transform of an integral,

$$\boxed{L\left\{\int_0^t f(\tau) d\tau\right\} := \int_0^\infty e^{-st} \left[\int_0^t f(\tau) d\tau\right] dt = \frac{1}{s} L\{f(t)\}} , \tag{B.29}$$

can be obtained in the following way. Bearing in mind that

$$\frac{d}{dt} \int_0^t f(\tau) d\tau = f(t)$$

and integrating by parts, we arrive at

$$\int_0^\infty e^{-st} \left[\int_0^t f(\tau) d\tau\right] dt = -\frac{1}{s} e^{-st} \int_0^t f(\tau) d\tau \Big|_{t=0}^\infty + \frac{1}{s} \int_0^\infty e^{-st} f(t) dt ,$$

where the first term on the right-hand side is zero at both limits, $t = 0$ and $t = \infty$, if the integral $\int\limits_0^\infty f(\tau)d\tau$ converges. Thus, the *integration rule* (B.29) has been proofed.

As an example, we find

$$L\left\{\int\limits_0^t \sin \omega \tau d\tau\right\} = \frac{1}{s}L\{\sin \omega t\} \equiv \frac{\omega}{s(s^2 + \omega^2)}, \tag{B.30}$$

where (B.8b) has been taken into account.

B.9 Convolution Theorem

The *convolution* is of major importance, for instance, in the study of heat conduction, wave motion, plastic flow, creep, and, especially, in the theory of viscoelasticity (Section 11.1).

Based upon BOLTZMANN's *superposition principle*, the creep response of linear viscoelastic materials can be described by the *hereditary integral* (11.3) or, starting in the history at time $\Theta = 0$, by the constitutive equation

$$E\varepsilon(t) = \int\limits_0^t \frac{\partial \sigma(\Theta)}{\partial \Theta}\kappa(t - \Theta)d\Theta. \tag{B.31}$$

The integral in (B.31) can be interpreted as a *convolution integral*.

Definition: The *convolution* of two functions, say $f_1(t)$ and $f_2(t)$, is defined according to

$$\varphi(t) := \int\limits_0^t f_1(\Theta)f_2(t - \Theta)d\Theta \equiv f_1 * f_2. \tag{B.32a}$$

Introducing the substitution $\tau = t - \Theta$, the definition (B.32a) can alternatively be expressed in the form

$$\varphi(t) := \int\limits_0^t f_2(\tau)f_1(t - \tau)d\tau \equiv f_2 * f_1. \tag{B.32b}$$

Comparing both forms, we see that the *convolution* of two functions is *commutative*, i.e.,

$$\boxed{f_1 * f_2 = f_2 * f_1}\,.\tag{B.33}$$

Applying the LAPLACE transform (B.2) to the convolution integral $\varphi(t)$, we arrive at the *convolution theorem*

$$\boxed{\hat{\varphi}(s) \equiv L\{f_1 * f_2\} = L\{f_1(t)\}L\{f_2(t)\} = \hat{f}_1(s)\hat{f}_2(s)}\,,\tag{B.34}$$

which states that the convolution in the original region corresponds to the usual multiplication in the transformed region. In other words:

The LAPLACE transform of the convolution of two functions is identical with the product of the LAPLACE transforms of these two functions.

This theorem can be proofed in the following way. For

$$\hat{f}_1(s) = \int_0^\infty e^{-su} f_1(u)du \quad and \quad \hat{f}_2(s) = \int_0^\infty e^{-sv} f_2(v)dv\,,\tag{B.35a,b}$$

the right-hand side in (B.34) can be written as:

$$\hat{f}_1(s)\hat{f}_2(s) = \int_0^\infty e^{-su}\,\hat{f}_2(s)f_1(u)du = \int_0^\infty \left[\int_0^\infty f_2(v)e^{-s(u+v)}dv\right] f_1(u)du\,.\tag{B.36}$$

To make this integral applicable to a LAPLACE transformation, let us introduce a substitution

$$\left.\begin{aligned} u &= u(t,w) \\ v &= v(t,w) \end{aligned}\right\} \quad \Longleftrightarrow \quad \begin{cases} t &= t(u,v) \\ w &= w(u,v) \end{cases}\tag{B.37}$$

according to the linear form

$$\left.\begin{aligned} u &= t - w \\ v &= w \end{aligned}\right\} \quad \Longleftrightarrow \quad \begin{cases} t &= u + v \\ w &= v \end{cases}\tag{B.38}$$

where the JACOBI determinant is given by:

$$J := \begin{vmatrix} \dfrac{\partial u}{\partial t} & \dfrac{\partial v}{\partial t} \\[2ex] \dfrac{\partial u}{\partial w} & \dfrac{\partial v}{\partial w} \end{vmatrix} = 1 \quad or \quad J^{(-1)} := \begin{vmatrix} \dfrac{\partial t}{\partial u} & \dfrac{\partial w}{\partial u} \\[2ex] \dfrac{\partial t}{\partial v} & \dfrac{\partial w}{\partial v} \end{vmatrix} = 1\,.\tag{B.39}$$

Thus, the area element $dtdw$ in the mapped t-w-plane is equal to the corresponding area element $dudv$ in the u-v-plane (Fig. B.2). Then, the double integral in (B.36) can be expressed as

$$\hat{f}_1(s)\hat{f}_2(s) = \int_0^\infty \left[\int_0^t f_2(w)f_1(t-w)dw \right] e^{-st}dt \equiv L\{f_2 * f_1\} \quad \text{(B.40)}$$

in accordance with (B.34) and (B.33). The ranges of integration of the double integrals in (B.36) and (B.40) are illustrated in Fig. B.2.
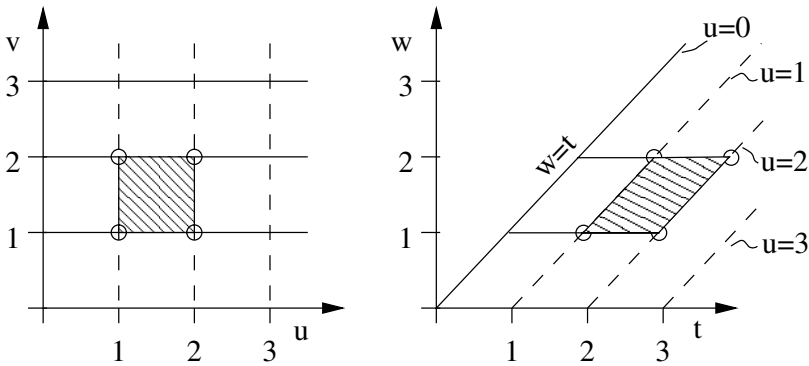
Fig. B.2 Ranges of integration in the u-v- and t-w-plane

Utilizing the *convolution theorem* (B.34) it is easy to proof the *associative* property

$$\boxed{(f_1 * f_2) * f_3 = f_1 * (f_2 * f_3)} \,, \quad \text{(B.41a)}$$

which can alternatively be expressed as

$$g * f_3 = f_1 * h \quad \text{(B.41b)}$$

by substituting

$$g \equiv f_1 * f_2 \quad and \quad h \equiv f_2 * f_3 \,. \quad \text{(B.42a,b)}$$

Applying the *convolution theorem* to the left-hand side and right-hand side of (B.41b), we obtain

$$L\{g * f_3\} = \hat{g}\hat{f}_3 = L\{f_1 * f_2\}\hat{f}_3 = (\hat{f}_1\hat{f}_2)\hat{f}_3 \quad \text{(B.43a)}$$

and

$$L\{f_1 * h\} = \hat{f}_1\hat{h} = \hat{f}_1 L\{f_2 * f_3\} = \hat{f}_1(\hat{f}_2\hat{f}_3) \,, \tag{B.43b}$$

respectively. Since the ordinary multiplication on the right-hand sides in (B.43a,b) is *associative*,

$$(\hat{f}_1\hat{f}_2)\hat{f}_3 = \hat{f}_1(\hat{f}_2\hat{f}_3) \,, \tag{B.44}$$

it follows that the convolution of three functions is *associative* according to (B.41a,b).

In a similar way, the distributive property,

$$\boxed{f_1 * (f_2 + f_3) = f_1 * f_2 + f_1 * f_3} \tag{B.45}$$

can be proofed: Substituting $k \equiv f_2 + f_3$ and considering the linearity (B.6), we obtain the following relations

$$\begin{aligned} L\{f_1 * k\} = \hat{f}_1\hat{k} = \hat{f}_1 L\{f_2 + f_3\} = \hat{f}_1(L\{f_2\} + L\{f_3\}) = \\ = \hat{f}_1(\hat{f}_2 + \hat{f}_3) = \hat{f}_1\hat{f}_2 + \hat{f}_1\hat{f}_3 \end{aligned} \tag{B.46}$$

$$L\{f_1 * (f_2 + f_3)\} = L\{f_1 * f_2\} + L\{f_1 * f_3\}$$

in accordance with (B.46).

To illustrade the *convolution theorem*, let us consider the equation of motion

$$m\ddot{x} + kx = F(t) \tag{B.47a}$$

or

$$\ddot{x} + \omega^2 x = \omega^2 f(t) \quad \text{with} \quad x(0) = \dot{x}(0) = 0 \,, \tag{B.47b}$$

where the abbreviations $\omega^2 = k/m$ and $f(t) = F(t)/k$ have been introduced. The LAPLACE *transformation*

$$\int_0^\infty (\ddot{x} + \omega^2 x)e^{-st}dt = \omega^2 \int_0^\infty f(t)e^{-st}dt \tag{B.48}$$

carried out on both sides of the equation of motion (B.47b) by taking the transform (B.24) into account yields

$$s^2 L\{x(t)\} - sx(0) - \dot{x}(0) + \omega^2 L\{x(t)\} = \omega^2 L\{f(t)\} \,.$$

Inserting the initial values $x(0) = \dot{x}(0) = 0$, we obtain

$$L\{x(t)\} = \frac{\omega^2}{s^2 + \omega^2} L\{f(t)\} \equiv L\{g(t)\}L\{f(t)\}. \tag{B.49}$$

Thus, applying the *convolution theorem* (B.34), the solution of the problem (B.47b) can be represented as (B.32a,b), i.e.:

$$x(t) = g(t) * f(t) = \int_0^t f(\Theta)g(t - \Theta)d\Theta, \tag{B.50}$$

and because of (B.8b), we finally arrive at the solution

$$\boxed{x(t) = \omega \int_0^t f(\Theta) \sin \omega(t - \Theta)d\Theta} \tag{B.51}$$

with an arbitrary forcing function $F(t) = kf(t)$ and with the assumed initial values $x(0) = 0$ and $\dot{x}(0) = 0$.

If the system is subjected to an external harmonic function of magnitude $F(t) = F_0 \sin \Omega t$, we obtain the following special solution:

$$x(t) = \omega \frac{F_0}{k} \int_0^t \sin \Omega\Theta \sin \omega(t - \Theta)d\Theta,$$

$$x(t) = \omega \frac{F_0}{k} Im \int_0^t e^{i\Omega\Theta} \sin \omega(t - \Theta)d\Theta,$$

$$F(t) = F_0 \sin \Omega t \quad \Longrightarrow \quad \boxed{x(t) = \frac{F_0/k}{1 - (\frac{\Omega}{\omega})^2} \left(\sin \Omega t - \frac{\Omega}{\omega} \sin \omega t \right)}. \tag{B.52a}$$

If the external harmonic function has a magnitude of $F(t) = F_0 \cos \Omega t$, we find in a similar way the following solution of the initial-value problem (B.47b):

$$F(t) = F_0 \cos \Omega t \quad \Longrightarrow \quad \boxed{x(t) = \frac{F_0/k}{1 - (\frac{\Omega}{\omega})^2} \left(\cos \Omega t - \cos \omega t \right)}. \tag{B.52b}$$

B.10 LAPLACE Transforms of the HEAVISIDE and DIRAC Functions

The HEAVISIDE and DIRAC *functions* (Appendix A) play a central role, for instance, in the theory of viscoelasticity (Chapter 11).
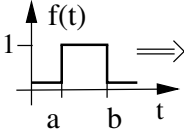
The LAPLACE *transform* of the HEAVISIDE function (A.1a) is given by

$$L\{H(t-a)\} = \frac{1}{s}e^{-as},\qquad \text{(B.53a)}$$

since

$$L\{H(t-a)\} = \int_0^\infty H(t-a)e^{-st}dt = \int_0^a 0\cdot e^{-st}dt + \int_a^\infty 1\cdot e^{-st}dt \equiv \frac{1}{s}e^{-sa}.$$

Similarly, we find the following transform

$$L\{H(t-a) - H(t-b)\} = \frac{1}{s}\left(e^{-as} - e^{-bs}\right),$$

$$\text{(B.53b)}$$

which is utilized, when the response of the KELVIN *model* subjected to the shear stress

$$\tau(t) = \tau_0\left[H(t-a) - H(t-b)\right] \qquad \text{(B.54)}$$

should be analysed. The differential equation (11.19) of the KELVIN *model* can be written as

$$\dot{\gamma} + \gamma/\lambda = \tau/\eta \quad \text{with} \quad \lambda \equiv \eta/G. \qquad \text{(B.55)}$$

Applying the LAPLACE transformation with (B.23) and taking the loading (B.54) with its transform (B.53b) into account, we arrive at the LAPLACE transform

$$L\{\gamma(t)\} = \frac{\tau_0}{G}\frac{e^{-as} - e^{-bs}}{s(1+\lambda s)}, \qquad \text{(B.56)}$$

the inverse of which is the response $\gamma = \gamma(t)$ of the KELVIN model. First let us find the inverse of the transform

$$L\{\varphi(s)\} = \frac{e^{-as}}{s(1+\lambda s)} \equiv \hat{f}_1(s)\hat{f}_2(s), \qquad \text{(B.57)}$$

where

$$\hat{f}_1(s) \equiv \frac{e^{-as}}{s} \quad and \quad \hat{f}_2(s) \equiv \frac{1}{1 + \lambda s} \tag{B.58a,b}$$

have been introduced. Because of (B.53a) and by considering (B.28) with $n = 0$ and $\omega = -1/\lambda$, the inverse forms of (B.58a,b) are given by

$$L^{-1}\{\hat{f}_1(s)\} \equiv f_1(t) = H(t - a) \tag{B.59a}$$

and

$$L^{-1}\{\hat{f}_2(s)\} \equiv f_2(t) = \frac{1}{\lambda} \, e^{-t/\lambda}. \tag{B.59b}$$

Applying the *convolution theorem* (B.34) with (B.32a) and (B.57) to (B.59a, b), we find the inverse of (B.57) according to

$$\varphi(t) = f_1 * f_2 = \int_0^t H(\Theta - a) \frac{1}{\lambda} e^{-(t-\Theta)/\lambda} d\Theta \tag{B.60a}$$

or

$$\varphi(t) = \int_a^t \frac{1}{\lambda} e^{-(t-\Theta)/\lambda} d\Theta = 1 - e^{-(t-a)/\lambda}. \tag{B.60b}$$

Thus, the solution $\gamma = \gamma(t)$ of (B.56), i.e., the creep behavior of the KELVIN *model* subjected to a step loading (B.54) can be expressed by the following *creep function*:

$$\boxed{\frac{G}{\tau_0}\gamma(t) = H(t - a)\left[1 - e^{-(t-a)/\lambda}\right] - H(t - b)\left[1 - e^{-(t-b)/\lambda}\right]} \tag{B.61}$$

This function and the HEAVISIDE function (B.54) are illustrated in Fig. B.3.

⊙ *B_2.mws*

```
>   alias(H=Heaviside, th=thickness):
>   plot1:=plot(H(t-1)-H(t-6),t=0..12,th=3):
>   plot2:=plot(H(t-1)*(1-exp(-(1/2)*(t-1))-
>   H(t-6)*(1-exp(-(1/2)*(t-6)))),t=0..12,th=3):
>   plots[display]({plot1,plot2});
```
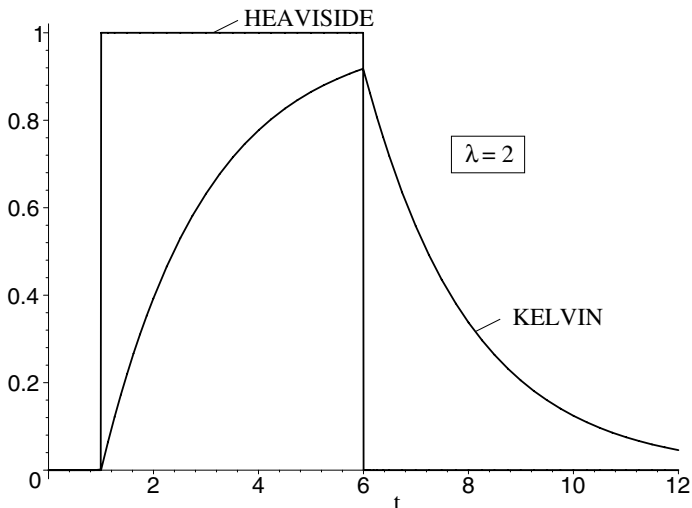
Fig. B.3 Creep behavior of a KELVIN model subjected to a constand load between
$t = 1$ and $t = 6$

The LAPLACE *transform* of the DIRAC *function* (A.6) is given by

$$\boxed{L\{\delta(t - a)\} = e^{-as}} \quad \text{and} \quad \boxed{L\{\delta(t)\} = 1} \,. \tag{B.62a,b}$$

This can be deduced as follows. The LAPLACE transform of the modified
distribution (A.9), represented in Fig. A.5, is

$$L\{\delta_\varepsilon(t - a)\} = \int_0^\infty \frac{1}{\varepsilon} e^{-st} dt = \frac{1}{\varepsilon} \int_a^{a+\varepsilon} e^{-st} dt =$$

$$= -\frac{1}{s\varepsilon} \left[e^{-s(a+\varepsilon)} - e^{-sa} \right] \,.$$

Then, by forming the limit $\varepsilon \to 0$ and applying the L'HOSPITAL rule, we
obtain:

$$L\{\delta(t - a)\} = \lim_{\varepsilon \to 0} L\{\delta_\varepsilon(t - a)\} = e^{-as}$$

in accordance with (B.62a), and for $a \to 0$ identical to (B.62b).

One can find the transform (B.62a) also in the following way. Since

$$\delta(t - a) = \dot{H}(t - a)$$

according to (A.12) and because of (B.23) together with $H(0) = 0$ and
(B.53a), we immediately arrive at the result

$$L\{\delta(t-a)\} = L\{\dot{H}(t-a)\} = sL\{H(t-a)\} \equiv e^{-as}, \qquad \text{(B.63)}$$

which agrees with (B.62a).

As an example, in which the transform (B.62b) is taken into account, let us discuss the response of an undamped vibration-system to a unit impulse at time $t = 0$. This initial-value problem is described according to the differential equation

$$\ddot{x} + \omega^2 x = \frac{F_0}{k} \omega\delta(t) \quad \text{with} \quad x(0) = 0 \text{ and } \dot{x}(0) = 0. \qquad \text{(B.64)}$$

Because of (B.24), (B.62b), and (B.8b) we obtain:

$$L\{x(t)\} = \frac{F_0}{k} \frac{\omega}{s^2 + \omega^2} \quad \Rightarrow \quad \boxed{x(t) = \frac{F_0}{k} \sin\omega t} \qquad \text{(B.65)}$$

for $t > 0$. The initial value $\dot{x}(0) = 0$ assumed in (B.64) is **not** satisfied. Because of

$$\dot{x}(t) = \frac{F_0}{k} \omega\cos\omega t \quad \rightarrow \quad \dot{x}(0) = \frac{F_0}{k}\omega,$$

the unit Dirac impuls produces a jump of magnitude $\omega F_0/k$ in the velocity $\dot{x}(0)$ at time $t = 0$. Thus, the function $x(t)$ is continuous indeed, but not differentiable at $t = 0$.

Another example is concerned with the *deflection curve* of a statically indeterminate beam rigidly clamped at both ends and loaded by a concentrated Force F as schown in Fig. B.4.
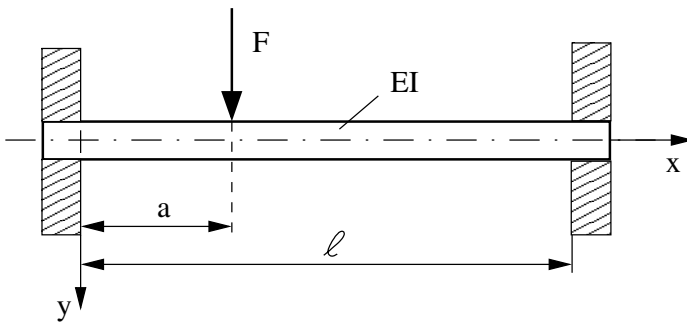
Fig. B.4 Statically interdeterminate beam

This problem can easily be solved by applying the Laplace transformation to the differential equation

$$\frac{d^4y}{dx^4} = \frac{F}{EI}\delta(x-a) \tag{B.66}$$

taking the following boundary conditions into account:

$$y(0) = 0, \quad y'(0) = 0, \quad y(\ell) = 0, \quad y'(\ell) = 0. \tag{B.67a-d}$$

Because of (B.22) and (B.62a) we obtain

$$s^4 L\{y(x)\} - s^3 y(0) - s^2 y'(0) - s y''(0) - y'''(0) = \frac{F}{EI}e^{-as},$$

and with (B.67a,b) and $y''(0) \equiv C_1$ and $y'''(0) = C_2$ we find:

$$L\{y(x)\} = \frac{C_1}{s^3} + \frac{C_2}{s^4} + \frac{F}{EI}\frac{e^{-as}}{s^4}. \tag{B.68}$$

From (B.28) we read the inverse transforms

$$L^{-1}\{1/s^3\} = \frac{x^2}{2!} \quad \text{and} \quad L^{-1}\{1/s^4\} = \frac{x^3}{3!}. \tag{B69a,b}$$

The third term on the right-hand side in (B.68) can be decomposed according to

$$\frac{\exp(-as)}{s^4} = \hat{f}_1(s)\hat{f}_2(s), \tag{B.70}$$

where the transforms

$$\hat{f}_1(s) := \frac{1}{s^3} \quad \text{and} \quad \hat{f}_2(s) := \frac{\exp(-as)}{s}, \tag{B.71a,b}$$

have been introduced. The inverse transforms can be read from (B.69a) and (B.53a), respectively,

$$f_1(x) := L^{-1}\{\hat{f}_1(s)\} = \frac{x^2}{2!} \tag{B.72a}$$

and

$$f_2(x) := L^{-1}\{\hat{f}_2(s)\} = H(x-a). \tag{B.72b}$$

Thus, utilizing the *convolution theorem* (B.34) and considering (B.32b), we arrive at the inverse transform of the product (B.70):

$$L^{-1}\{\hat{f}_1(s)\hat{f}_2(s)\} = f_1(x) * f_2(x) = \int_0^x \frac{(x-\tau)^2}{2!}H(\tau-a)d\tau$$

or

$$L^{-1}\left\{\frac{1}{s^4}\exp(-as)\right\} = \int_a^x \frac{(x-\tau)^2}{2!}\,d\tau = \frac{(x-a)^3}{3!}.$$

(B.73)

Adding the parts (B.69a,b) and (B.73) we obtain from (B.68) the *deflection curve* of the statically indeterminate beam (Fig. B.4) according to

$$y(x) = \frac{C_1}{2!}x^2 + \frac{C_2}{3!}x^3 + \frac{F}{EI}\frac{(x-a)^3}{3!}H(x-a),$$

(B.74)

where the constants C_1 and C_2 can be determined by inserting the end conditions (B.67c,d) into (B.74) as:

$$C_1 = \alpha(1-\alpha)^2\frac{F\ell}{EI} \quad \text{and} \quad C_2 = -(1+2\alpha)(1-\alpha)^2\frac{F}{EI},$$

(B.75a,b)

respectively. Thus, the final solution in dimensionless representation is given by

$$192\frac{EI}{F\ell^3}\,y(\xi) \equiv \eta(\xi;\alpha) = 96(1-\alpha)^2\left[\alpha - \tfrac{1}{3}(1+2\alpha)\xi\right]\xi^2$$
$$+32(\xi-\alpha)^3H(\xi-\alpha)$$

(B.76)

where $\xi \equiv x/\ell$ and $\alpha \equiv a/\ell$. The *deflection curve* (B.76) has a maximum at

$$\xi_{opt} = 1/(3-2\alpha) \quad \text{for} \quad \alpha \leq 1/2$$

(B.77a)

and

$$\xi_{opt} = 2\alpha/(1+2\alpha) \quad \text{for} \quad \alpha \geq 1/2$$

(B.77b)

as can be seen in Fig. B.5.

$\odot$ $B\_3.mws$

```
>   alias(H=Heaviside):
>   eta(xi):=96*((1-alpha)^2)*(alpha-(1+2*alpha)*
>   xi/3)*(xi^2)+32*((xi-alpha)^3)*H(xi-alpha);
```

$$\eta(\xi) := 96\,(1-\alpha)^2\left(\alpha - \frac{1}{3}(1+2\,\alpha)\,\xi\right)\xi^2 + 32\,(\xi-\alpha)^3\,\mathrm{H}(\xi-\alpha)$$

```
>   plot1:=plot(subs(alpha=1/4,-eta(xi)),xi=0..1):
>   plot2:=plot(subs(alpha=1/2,-eta(xi)),xi=0..1):
>   plot3:=plot(subs(alpha=2/3,-eta(xi)),xi=0..1):
>   plots[display]({plot1,plot2,plot3});
```
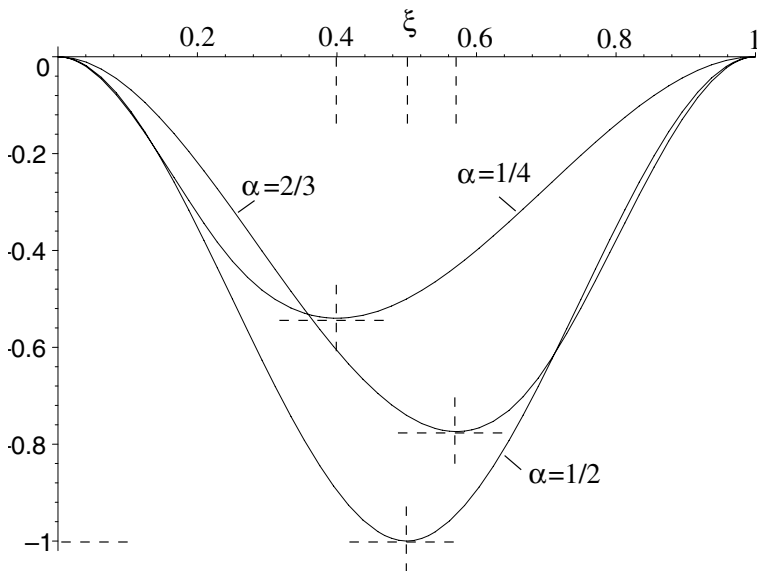
Fig. B.5 Deflection curve (B.76) of a beam clamped at both ends according to Fig. B4

B.11 LAPLACE Transformation for Integral Equations

Integral equations, for instance,

$$y(t) = f(t) + \int\limits_a^b K(\Theta, t)\, y(\Theta) d(\Theta)\,, \tag{B.78}$$

where the function $f(t)$ and the kernel function $K(\Theta, t)$ are known, while $y(t)$ is unknown, can easily be solved by utilizing the LAPLACE transformation: We differentiate the following types:

- ❑ If a and b are constant, then equation (B.78) is called a FRED-HOLM *integral equation*.
- ❑ If a is constant and $b = t$ we have a VOLTERRA *integral equation*.
- ❑ If $a = 0$ and $b = t$, the equation (B.78) is an integral equation of a *convolution type*.

The last type,

$$y(t) = f(t) + \int\limits_0^t K(t - \Theta) y(\Theta) d(\Theta)\,, \tag{B.79}$$

can be written as

$$y(t) = f(t) + K(t) * y(t), \tag{B.80}$$

since the integral in (B.79) is the *convolution* of the *kernel function* $K(t)$ and the unknown function $y(t)$ according to the definition (B.32a,b).

Applying the LAPLACE transformation to (B.80) and taking the *convolution theorem* (B.34) into account, we arrive at the transforms:

$$L\{y(t)\} = L\{f(t)\} + L\{K(t)\}L\{y(t)\}$$

or

$$L\{y(t)\} = L\{f(t)\} / \left[1 - L\{K(t)\}\right], \tag{B.81}$$

from which we find the solution by forming the inverse:

$$y(t) = L^{-1}\{\hat{y}(s)\} = L^{-1}\left\{\hat{f}(s) \middle/ \left[1 - \hat{K}(s)\right]\right\}. \tag{B.82}$$

To find the creep function (11.7) of a MAXWELL *fluid*, if the relaxation function (11.11a) is assumed to be known, then we have to solve the integral equation

$$\int_0^t \frac{\partial r(t - \Theta)}{\partial t} \kappa(\Theta)d\Theta + r(0)\kappa(t) = 1, \tag{B.83}$$

which follows from (11.15b) by differentiation with respect to time t. Inserting (11.11a), i.e., $r(t) = \exp(-t/\lambda)$, into (B.83), we obtain the integral equation of the convolution type (B.79) according to

$$\kappa(t) = 1 + \frac{1}{\lambda} \int_0^t e^{-(t-\Theta)/\lambda} \kappa(\Theta)d\Theta. \tag{B.84}$$

The Laplace transformation yields

$$\hat{\kappa}(s) = \frac{1}{2} + \frac{1}{1 + \lambda s}\kappa(s) \quad \Longrightarrow \quad \hat{\kappa}(s) = \frac{1 + \lambda s}{\lambda s^2}. \tag{B.85}$$

Using a table of transforms, we obtain the inverse of (B.85), i.e. the *creep function*

$$\boxed{\kappa(t) = 1 + t/\lambda} \tag{B.86}$$

of the MAXWELL *fluid* in accordance with (11.7).

Similar to (B.83) we arrive from (11.15b) at the *integral equation*

$$\int\limits_0^t \frac{\partial \kappa(t - \Theta)}{\partial t} r(\Theta) d(\Theta) + \kappa(0) r(t) = 1 \,, \tag{B.87}$$

which takes the form

$$\frac{1}{\lambda} \int\limits_0^t e^{-(t-\Theta)/\lambda} r(\Theta) d(\Theta) = 1 \tag{B.88}$$

for the KELVIN *creep function* (11.8). The LAPLACE transformation yields

$$\frac{1}{1 + \lambda s} \hat{r}(s) = \frac{1}{s} \quad \Longrightarrow \quad \hat{r}(s) = \frac{1}{s} + \lambda \,. \tag{B.89}$$

Using a table of transforms, we obtain the inverse of (B.89), i.e. the *relaxation function*

$$\boxed{r(t) = 1 + \lambda \delta(t)} \tag{B.90}$$

of the KELVIN *model* in accordance with (11.11b).

Another example is the integral equation

$$y(t) = 1 - e^{-t/\lambda} + \frac{1}{\lambda} \int\limits_0^t e^{-(t-\Theta)/\lambda} y(\Theta) d(\Theta) \,, \tag{B.91}$$

the LAPLACE transform of which is given by

$$\hat{y}(s) = \frac{1}{s(1 + \lambda s)} + \frac{1}{1 + \lambda s} \hat{y}(s) \;\Rightarrow\; \hat{y}(s) = \frac{1}{\lambda s^2} \,. \tag{B.92}$$

Thus, from a table of transforms we read the solution

$$\boxed{y(t) = t/\lambda} \,. \tag{B.93}$$

This solution satisfies the integral equation (B.91).

The *integral equation*

$$y(t) = \omega t + \omega \int\limits_0^t \sin \omega (t - \theta) y(\theta) d\theta \tag{B.94}$$

has the LAPLACE *transform*

$$\hat{y}(s) = \frac{\omega}{s^2} + \frac{\omega^2}{s^2 + \omega^2}\hat{y}(s) \;\Rightarrow\; \hat{y}(s) = \omega\left(\frac{1}{s^2} + \frac{\omega^2}{s^4}\right), \qquad \text{(B.95)}$$

hence the solution can be taken from a table of transforms:

$$y(t) = \omega t\left[1 + \frac{1}{6}(\omega t)^2\right]. \qquad \text{(B.96)}$$

This result has been checked by utilizing the following MAPLE program:

$$\boxed{\odot\; B\_4.mws}$$

```
>    int_eqn:=y(t)-
>    omega*int((sin(omega*(t-Theta))*y(Theta),
>    Theta=0..t))=omega*t;
```

$$int\_eqn := \mathrm{y}(t) - \omega\int_0^t \sin(\omega\,(t-\Theta))\,\mathrm{y}(\Theta)\,d\Theta = \omega\,t$$

```
>    with(inttrans):
>    laplace(int_eqn,t,s);
```

$$\text{laplace}(\mathrm{y}(t),\,t,\,s) - \frac{\omega^2\,\text{laplace}(\mathrm{y}(t),\,t,\,s)}{s^2 + \omega^2} = \frac{\omega}{s^2}$$

```
>    readlib(isolate)(%,laplace(y(t),t,s)):
>    simplify(%);
```

$$\text{laplace}(\mathrm{y}(t),\,t,\,s) = \frac{\omega\,(s^2 + \omega^2)}{s^4}$$

```
>    invlaplace(%,s,t):
>    y(t,omega):=simplify(rhs(%));
```

$$\mathrm{y}(t,\,\omega) := \frac{\omega\,t\,(6 + \omega^2\,t^2)}{6}$$

```
>    Y(Theta,omega):=subs(t=Theta, y(t,omega));
```

$$\mathrm{Y}(\Theta,\,\omega) := \frac{\omega\,\Theta\,(6 + \omega^2\,\Theta^2)}{6}$$

```
>    # check:
>    int_eqn:=simplify(y(t,omega)-
>    omega*int(sin(omega*(t-Theta))*
>    Y(Theta,omega),Theta=0..t));
```

$$int\_eqn := \omega\,t$$

```
>    # Thus, the solution (B.96) is correct.
```

Further *integral equations* are solved in the next MAPLE programs.

```
>    int_eqn:=y(t)+
>    omega*integrate((sin(omega*(t-Theta))*
>    y(Theta),Theta=0..t))=1;
```

$$int\_eqn := \mathrm{y}(t) + \omega \int_0^t \sin(\omega\,(t - \Theta))\,\mathrm{y}(\Theta)\,d\Theta = 1$$

```
>    with(inttrans):
>    laplace(int_eqn,t,s);
```

$$\mathrm{laplace}(\mathrm{y}(t),\,t,\,s) + \frac{\omega^2\,\mathrm{laplace}(\mathrm{y}(t),\,t,\,s)}{s^2 + \omega^2} = \frac{1}{s}$$

```
>    readlib(isolate)(%,laplace(y(t),t,s)):
>    simplify(%);
```

$$\mathrm{laplace}(\mathrm{y}(t),\,t,\,s) = \frac{s^2 + \omega^2}{s\,(s^2 + 2\,\omega^2)}$$

```
>    invlaplace(%,s,t):
>    y(t,omega):=simplify(rhs(%));
```

$$\mathrm{y}(t,\,\omega) := \frac{1}{2} + \frac{1}{2}\cos(\sqrt{2}\,\omega\,t)$$

```
>    Y(Theta,omega):=subs(t=Theta,y(t,omega));
```

$$\mathrm{Y}(\Theta,\,\omega) := \frac{1}{2} + \frac{1}{2}\cos(\sqrt{2}\,\omega\,\Theta)$$

```
>    # check
>    int_eqn:=y(t,omega)+
>    omega*int(sin(omega*(t-Theta))
>    *Y(Theta,omega),Theta=0..t);
```

$$int\_eqn := 1$$

$$\odot\ B\_6.mws$$

```
>   int_eqn:=
>   y(t)+omega*integrate((cos(omega*(t-Theta))
>   *y(Theta),Theta=0..t))=1;
```

$$int\_eqn := \mathrm{y}(t) + \omega \int_0^t \cos(\omega\,(t - \varTheta))\,\mathrm{y}(\varTheta)\,d\varTheta = 1$$

```
>   with(inttrans):
>   laplace(int_eqn,t,s);
```

$$\mathrm{laplace}(\mathrm{y}(t),\,t,\,s) + \frac{\omega\,\mathrm{laplace}(\mathrm{y}(t),\,t,\,s)\,s}{s^2 + \omega^2} = \frac{1}{s}$$

```
>   readlib(isolate)(%,laplace(y(t),t,s)):
>   simplify(%);
```

$$\mathrm{laplace}(\mathrm{y}(t),\,t,\,s) = \frac{s^2 + \omega^2}{s\,(s^2 + \omega^2 + \omega\,s)}$$

```
>   evalc(invlaplace(%,s,t)):
>   y(t,omega):=simplify(rhs(%));
```

$$\mathrm{y}(t,\,\omega) := 1 - \frac{2}{3}\,e^{(-\frac{\omega\,t}{2})}\,\sqrt{3}\sin(\frac{t\,\sqrt{3}\,\omega}{2})$$

```
>   Y(Theta,omega):=subs(t=Theta,%);
```

$$\mathrm{Y}(\varTheta,\,\omega) := 1 - \frac{2}{3}\,e^{(-\frac{\omega\,\varTheta}{2})}\,\sqrt{3}\sin(\frac{\varTheta\,\sqrt{3}\,\omega}{2})$$

```
>   # check:
>   int_eqn:=y(t,omega)+
>   omega*int(cos(omega*(t-Theta))*
>   Y(Theta,omega),Theta=0..t);
```

$$int\_eqn := 1$$

```
>   # Thus, the solution is correct.
>   y(t,1/2):=subs(omega=1/2,y(t,omega));
```

$$\mathrm{y}(t,\,\frac{1}{2}) := 1 - \frac{2}{3}\,e^{(-\frac{t}{4})}\,\sqrt{3}\sin(\frac{t\,\sqrt{3}}{4})$$

```
>   y(t,2):=subs(omega=2,y(t,omega));
```

$$y(t,\, 2) := 1 - \frac{2}{3}\, e^{(-t)}\, \sqrt{3}\sin(t\,\sqrt{3})$$

```
>   alias(H=Heaviside, th=thickness,c=color):
>   plot1:=plot({1,1.1,1.1*H(t-8*Pi/sqrt(3))},
>   t=0..8.001*Pi/sqrt(3),c=black):
>   plot2:=plot({y(t,1/2),y(t,2)},
>   t=0..8.001*Pi/sqrt(3),0.4..1.1001,c=black):
>   plots[display]({plot1,plot2});
```
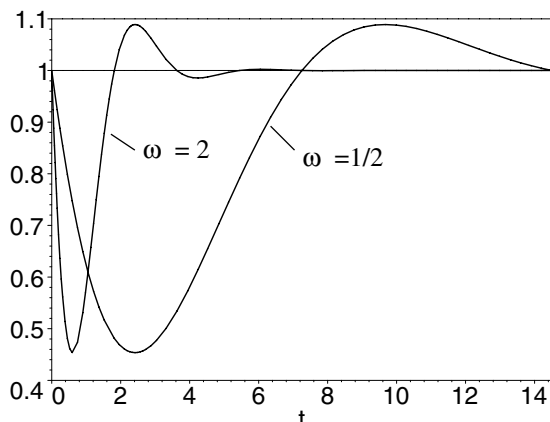

Fig. B.6 Solution of the above integral equation for $\omega = 1/2$ and $\omega = 2$

$$\boxed{\odot\ B\_7.mws}$$

```
>   VOLTERRA:=y(t)-omega*integrate((t-Theta)*
>   y(Theta),Theta=0..t)=exp(I*omega*t);
```

$$VOLTERRA := \mathrm{y}(t) - \omega \int_0^t (t - \Theta)\, \mathrm{y}(\Theta)\, d\Theta = e^{(\omega\, t\, I)}$$

```
>   VOLTERRA:=convert(%,`trig`);
```

$$VOLTERRA := \mathrm{y}(t) - \omega \int_0^t (t - \Theta)\, \mathrm{y}(\Theta)\, d\Theta = \cos(\omega\, t) + \sin(\omega\, t)\, I$$

```
>   with(inttrans):
>   laplace(VOLTERRA,t,s);
```

$$\mathrm{laplace}(\mathrm{y}(t),\, t,\, s) - \frac{\omega\, \mathrm{laplace}(\mathrm{y}(t),\, t,\, s)}{s^2} = \frac{s}{s^2 + \omega^2} + \frac{\omega\, I}{s^2 + \omega^2}$$

```
>   readlib(isolate)(%,laplace(y(t),t,s)):
```

```
>   simplify(%);
```

$$\text{laplace}(y(t),\,t,\,s) = \frac{(s+\omega\,I)\,s^2}{(s^2+\omega^2)\,(s^2-\omega)}$$

```
>   invlaplace(%,s,t):
>   y(t,omega):=simplify(rhs(%));
```

$$y(t,\,\omega) := \frac{\omega\cos(\omega\,t)+\cosh(\sqrt{\omega}\,t)+\sqrt{\omega}\sinh(\sqrt{\omega}\,t)\,I+\omega\sin(\omega\,t)\,I}{1+\omega}$$

```
>   y[re](t,omega):=(omega*cos(omega*t)+

>       cosh(sqrt(omega)*t))/(1+omega);
```

$$y_{re}(t,\,\omega) := \frac{\omega\cos(\omega\,t)+\cosh(\sqrt{\omega}\,t)}{1+\omega}$$

```
>   y[im](t,omega):=(omega*sin(omega*t)+
>   sqrt(omega)*sinh(sqrt(omega)*t))/(1+omega);
```

$$y_{im}(t,\,\omega) := \frac{\omega\sin(\omega\,t)+\sqrt{\omega}\sinh(\sqrt{\omega}\,t)}{1+\omega}$$

```
>   # check of the real part:
>   Y[re](t,omega):=subs(t=Theta,%%);
```

$$Y_{re}(t,\,\omega) := \frac{\omega\cos(\omega\,\Theta)+\cosh(\sqrt{\omega}\,\Theta)}{1+\omega}$$

```
>   VOLTERRA[re]:=simplify(y[re](t,omega)-

>       omega*int((t-Theta)*%,Theta=0..t)):
>   VOLTERRA[re]:=simplify(convert(%,'trig'));
```

$$VOLTERRA_{re} := \cos(\omega\,t)$$

```
>   # Thus the real part of the above solution
>   is correct.
>   # In a similar way one can check the
>   imiginary part.
```

$$\boxed{\odot \; B\_8.mws}$$

```
>  volterra:=y(t)-int((t-Theta)^3*y(Theta),
   Theta=0..t)=1-t+t^2-t^3;
```

$$volterra := \mathrm{y}(t) - \int_0^t (t - \Theta)^3 \, \mathrm{y}(\Theta) \, d\Theta = 1 - t + t^2 - t^3$$

```
>  with(inttrans):
>  laplace(volterra,t,s);
```

$$\mathrm{laplace}(\mathrm{y}(t),\, t,\, s) - \frac{6 \, \mathrm{laplace}(\mathrm{y}(t),\, t,\, s)}{s^4} = \frac{1}{s} - \frac{1}{s^2} + \frac{2}{s^3} - \frac{6}{s^4}$$

```
>  simplify(readlib(isolate)
>  (%,laplace(y(t),t,s)));
```

$$\mathrm{laplace}(\mathrm{y}(t),\, t,\, s) = \frac{s^3 - s^2 + 2\,s - 6}{s^4 - 6}$$

```
>  Digits:=4;
>  evalf(invlaplace(%%,s,t));
```

$$Digits := 4$$

$$\mathrm{y}(t) = 0.9082 \cosh(1.565\,t) + 0.0918 \cos(1.565\,t)$$
$$- 1.102 \sinh(1.565\,t) + 0.4631 \sin(1.565\,t)$$

```
>  0.9082=convert(0.9082,'rational'):
>  0.0918=convert(0.0918,'rational'):
>  1.102=convert(1.102,'rational'):
>  0.4631=convert(0.4631,'rational'):
>  1.565=convert(1.565,'rational'):

>  macro(a=36/23):
>  Y(t):=(10/11)*cosh(a*t)+(9/98)*cos(a*t)-
>      (54/49)*sinh(a*t)+(19/41)*sin(a*t);
```

$$\mathrm{Y}(t) := \frac{10}{11} \cosh(\frac{36\,t}{23}) + \frac{9}{98} \cos(\frac{36\,t}{23}) - \frac{54}{49} \sinh(\frac{36\,t}{23}) + \frac{19}{41} \sin(\frac{36\,t}{23})$$

```
>  Y[i](Theta):=subs(t=Theta,%);
```

$$Y_i(\Theta) := \frac{10}{11} \cosh(\frac{36\,\Theta}{23}) + \frac{9}{98} \cos(\frac{36\,\Theta}{23}) - \frac{54}{49} \sinh(\frac{36\,\Theta}{23})$$
$$+ \frac{19}{41} \sin(\frac{36\,\Theta}{23})$$

```
>  volterra:=Y(t)-int((t-Theta)^3*Y[i](Theta),
>  Theta=0..t):DELTA(t):=1-t+t^2-t^3-%:
```

```
>   error_norm:=
>   L[2]=evalf(sqrt(int(%^2,t=0..1)),15);
```

$$error\_norm := L_2 = 0.00142880337743571$$

For **Digits:=10** the *error-norm* is given by $L_2 = 0.2246731\,10^{-6}$ as shown on the CD-ROM $\boxed{\odot \; B\_9.mws}$.

$$\boxed{\odot \; B\_10.mws}$$

```
>   ABEL:=int((1/sqrt(t-Theta))*y(Theta),
>   Theta=0..t)=T;
```

$$ABEL := \int_0^t \frac{y(\Theta)}{\sqrt{t-\Theta}}\, d\Theta = T$$

This is a singular *integral equation*. For the special case of the tautochrone the right hand side T is independent of t.

```
>   with (inttrans):
>   laplace(ABEL,t,s);
```

$$\text{laplace}\left(\int_0^t \frac{y(\Theta)}{\sqrt{t-\Theta}}\, d\Theta,\, t,\, s\right) = \frac{T}{s}$$

appliction of the convolution theorem:

```
>   laplace(1/sqrt(t),t,s)*laplace(y(t),t,s)=
>   laplace(T,t,s);
```

$$\frac{\sqrt{\pi}\,\text{laplace}(y(t),\, t,\, s)}{\sqrt{s}} = \frac{T}{s}$$

```
>   readlib(isolate)(%,laplace(y(t),t,s));
```

$$\text{laplace}(y(t),\, t,\, s) = \frac{T}{\sqrt{s}\,\sqrt{\pi}}$$

```
>   invlaplace(%,s,t);
```

$$y(t) = \frac{T}{\pi\,\sqrt{t}}$$

check:

```
>   ABEL:=Int(T/Pi/sqrt(Theta)/sqrt(t-Theta),
>   Theta=0..t)=int(T/Pi/sqrt(Theta)/
>   sqrt(t-Theta),Theta=0..t);
```

$$ABEL := \int_0^t \frac{T}{\pi\,\sqrt{\Theta}\,\sqrt{t-\Theta}}\,d\Theta = T$$

Thus, the solution is correct.

Further results are listed in the following Table:

T	const.	at	at^2	$at^{3/2}$	$a\sqrt{t}$	$\ln(at)$
$y(t)$	$\dfrac{T}{\pi\sqrt{t}}$	$\dfrac{2\,a}{\pi}\sqrt{t}$	$\dfrac{8\,a}{3\pi}t^{3/2}$	$\dfrac{3\,a}{4}t$	$\dfrac{a}{2}$	$\dfrac{1}{\pi\sqrt{t}}\ln(4at)$

The last result in the table is explained in more detail in the following MAPLE-program.

⊙ B_11.mws

```
>   abel:=int((1/sqrt(t-Theta))*y(Theta),
Theta=0..t)=ln(a*t);
```

$$abel := \int_0^t \frac{y(\Theta)}{\sqrt{t-\Theta}}\,d\Theta = \ln(a\,t)$$

This is a singular *integral equation*.

```
>   with (inttrans):
>   laplace(abel,t,s);
```

$$\text{laplace}\left(\int_0^t \frac{y(\Theta)}{\sqrt{t-\Theta}}\,d\Theta,\, t,\, s\right) = -\frac{\gamma + \ln(s)}{s} + \frac{\ln(a)}{s}$$

appliction of the convolution theorem:

```
>   laplace(1/sqrt(t),t,s)*laplace(y(t),t,s)=
```

```
>       laplace(ln(a*t),t,s);
```

$$\frac{\sqrt{\pi}\,\text{laplace}(y(t),\, t,\, s)}{\sqrt{s}} = -\frac{\gamma + \ln(s)}{s} + \frac{\ln(a)}{s}$$

```
>   readlib(isolate)(%,laplace(y(t),t,s));
```

$$\text{laplace}(y(t),\, t,\, s) = \frac{\left(-\dfrac{\gamma + \ln(s)}{s} + \dfrac{\ln(a)}{s}\right)\sqrt{s}}{\sqrt{\pi}}$$

```
>   invlaplace(%,s,t);
```

$$y(t) = \frac{\dfrac{2\ln(2)}{\sqrt{\pi}\,\sqrt{t}} + \dfrac{\ln(t)}{\sqrt{\pi}\,\sqrt{t}} + \dfrac{\ln(a)}{\sqrt{t}\,\sqrt{\pi}}}{\sqrt{\pi}}$$

```
>   simplify(%);
```

$$y(t) = \frac{2\ln(2) + \ln(t) + \ln(a)}{\pi\sqrt{t}}$$

```
>   y(t):=ln(4*a*t)/Pi/sqrt(t);
```

$$y(t) := \frac{\ln(4\,a\,t)}{\pi\sqrt{t}}$$

```
>   # check:
>   Int(ln(4*a*Theta)/Pi/sqrt(Theta)/
>   sqrt(t-Theta),Theta=0..t)=
>   simplify(int(ln(4*a*Theta)/Pi/sqrt(Theta)/
>   sqrt(t-Theta),Theta=0..t));
```

$$\int_0^t \frac{\ln(4\,a\,\Theta)}{\pi\,\sqrt{\Theta}\,\sqrt{t-\Theta}}\,d\Theta = \ln(t) + \ln(a)$$

```
>   # Thus, the solution is correct.
```

$$\boxed{\odot\ B\_12.mws}$$

```
>   integro_diff_eqn:=
>   diff(y(t),t)+int(cos(omega*(t-Theta))*
>   y(Theta),Theta=0..t)=sin(omega*t);
```

$$integro\_diff\_eqn := \left(\tfrac{d}{dt}\,y(t)\right) + \int_0^t \cos(\omega\,(t-\Theta))\,y(\Theta)\,d\Theta = \sin(\omega\,t)$$

```
>   # initial value y(0)
>   with(inttrans):
>   laplace(integro_diff_eqn,t,s);
```

$$s\,\text{laplace}(y(t),\,t,\,s) - y(0) + \frac{\text{laplace}(y(t),\,t,\,s)\,s}{s^2 + \omega^2} = \frac{\omega}{s^2 + \omega^2}$$

```
>   simplify(readlib(isolate)
>   (%,laplace(y(t),t,s)));
```

$$\text{laplace}(y(t),\,t,\,s) = \frac{\omega + y(0)\,s^2 + y(0)\,\omega^2}{s\,(s^2 + \omega^2 + 1)}$$

```
>   invlaplace(%,s,t);
```

$$y(t) = \frac{(y(0) - \omega)\cosh(\sqrt{-\omega^2 - 1}\,t) + \omega\,(1 + y(0)\,\omega)}{\omega^2 + 1}$$

```
>   # example: y(0)=1, omega = 4
>   subs (y(0)=1, omega=4,%);
```

$$y(t) = -\frac{3}{17}\cosh(\sqrt{-17}\,t) + \frac{20}{17}$$

```
>   simplify(%);
```

$$y(t) = -\frac{3}{17}\cos(\sqrt{17}\,t) + \frac{20}{17}$$

```
>   # check:
>
>   Diff(y(t),t)+Int(cos(4*(t-Theta))*(20/17-(3/17)*
>   cos(sqrt(17)*Theta)),Theta=0..t)=(3/sqrt(17))*
>   sin(sqrt(17)*t)+int(cos(4*(t-Theta))*
>   (20/17-(3/17)*cos(sqrt(17)*Theta)),Theta=0..t):
>   Delta:=rhs(%)-sin(4*t);
```

$$\Delta := 8\sin(t)\cos(t)^3 - 4\sin(t)\cos(t) - \sin(4\,t)$$

```
>   Delta:=simplify(%);
```

$$\Delta := 0$$

```
>   # Thus, the solution is correct.
```

B.12 Periodic Functions

A function $f(x)$ is said to be *periodic* if $f(x + L) = f(x)$ for all $x \in \mathbb{R}$, where L is a nonzero constant. Any number L with this property is a period of the function $f(x)$. For instance, $\sin x$ has the periods $2\pi, -2\pi, 4\pi, ...$

In the following we take into consideration a *periodic function* with a period $T > 0$ and defined as

$$f(t) = \begin{cases} f(t + nT), & \text{where } t > 0 \quad \text{and} \quad n \in \mathbb{N} \\ 0 & \text{for} \quad t < 0. \end{cases} \qquad (B.97)$$

Its LAPLACE *transform* can be calculated by the fundamental formula

$$L\{f(t)\} = \frac{1}{1 - \exp(-sT)} \int\limits_0^T f(t)\exp(-st)\,dt \;, \qquad (B.98)$$

which can be deduced in the following way.

We represent the LAPLACE transformation (B.2) as an *infinite series* according to

$$L\{f(t)\} = \int\limits_{0}^{\infty} f(t)e^{-st}dt =$$

$$= \int\limits_{0}^{T} f(t)e^{-st}dt + \int\limits_{T}^{2T} f(t)e^{-st}dt + ... \int\limits_{nT}^{(n+1)T} f(t)e^{-st}dt + ...$$

$$L\{f(t)\} = \sum_{n=0}^{\infty} \int\limits_{nT}^{(n+1)T} f(t)e^{-st}dt .$$

(B.99)

Substituting $t \equiv \tau + nT$ yields

$$L\{f(t)\} = \sum_{n=0}^{\infty} \int\limits_{0}^{T} f(t + nT)e^{-s(\tau+nT)}d\tau =$$

$$= \sum_{n=0}^{\infty} e^{-snT} \int\limits_{0}^{T} f(\tau + nT)e^{-s\tau}d\tau ,$$

(B.100)

where the *geometric series* converges to:

$$\sum_{n=0}^{\infty} e^{-snT} = \lim_{n\to\infty} \frac{1 - \exp(-snT)}{1 - \exp(-sT)} = \frac{1}{1 - exp(-sT)}$$

(B.101)

since $|\exp(-sT)| < 1$, and because $f(\tau + nT) = f(\tau)$ by periodicity (B.97), we finally obtain from (B.100) the formula (B.98).

As an example, let us consider the *periodic function*

$$f(t) = H(t) + 2\sum_{n=1}^{\infty} (-1)^n H(t - na)$$

(B.102)

illustrated in Fig. B.7.

```
>   alias(H=Heaviside,th=thickness):
>   f:=H(t)+2*sum(((-1)^n)*H(t-n*a),
>   n=1..infinity);
```

⊙ *B_13.mws*

$$f := H(t) + 2\left(\sum_{n=1}^{\infty} (-1)^n H(t - n\,a)\right)$$

```
>   assume(a>0):
>   f[1]:=H(t)+2*sum(((-1)^n)*H(t-n*a),n=1..5):
>   plot(subs(a=1,f[1]),t=0..5,th=3,scaling=
>   constrained,style=point,numpoints=10000);
```
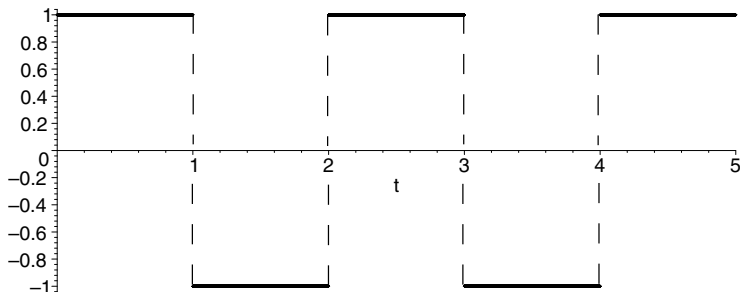

Fig. B.7 Periodic function (B.102) with $a = 1$

The function (B.102) has a period of $T = 2a$. Thus, we have to insert into the formula (B.98) only the following part of the periodic function(B.102),

$$f(t) = H(t) - 2H(t - a) + H(t - 2a),\qquad\text{(B.103)}$$

which represents (B.102) within the first period $0 \leq t < 2a$. The result is given by

$$L\{f(t)\} = \frac{1}{s}\frac{1 - \exp(-as)}{1 + \exp(-as)} \equiv \frac{1}{s}\tanh\left(\frac{as}{2}\right),\qquad\text{(B.104)}$$

which has been calculated by using the following MAPLE programm.

⊙ $B\_14.mws$

```
>   LAPLACE(f(t)):=(1/(1-exp(-s*T)))*Int(f(t)*
>   exp(-s*t),t=0..T);
```

$$\text{LAPLACE}(f(t)) := \frac{\displaystyle\int_0^T f(t)\, e^{(-st)}\, dt}{1 - e^{(-sT)}}\qquad\text{(B.98)}$$

```
>   alias(H=Heaviside):
>   f:=H(t)-2*H(t-a)+H(t-2*a);
```

$$f := \mathrm{H}(t) - 2\,\mathrm{H}(t-a) + \mathrm{H}(t-2\,a) \tag{B.103}$$

```
>   LAPLACE:=simplify((1/(1-exp(-2*a*s))))*
>   int(f*exp(-s*t),t=0..2*a));
```

$$LAPLACE := -\frac{-e^{(-a\,s)} + 2\,\mathrm{H}(a)\,e^{(-a\,s)} - 2\,\mathrm{H}(a) + 1}{s\,(e^{(-a\,s)} + 1)}$$

```
>   LAPLACE:=subs(H(a)=1,%);
```

$$LAPLACE := -\frac{e^{(-a\,s)} - 1}{s\,(e^{(-a\,s)} + 1)} \tag{B.104}$$

```
>
```

Alternatitively, we can find the LAPLACE transform (B.104) in the following way.

Because of the LAPLACE transform (B.53a) and taking the *linearity rule* (B.6) into account, we immediately arrive at the LAPLACE transform

$$L\{f(t)\} = \frac{1}{s}\left[1 + 2\sum_{n=1}^{\infty}(-1)^n \exp(-nas)\right] \tag{B.105}$$

of the periodic function (B.102), where the *infinite series* can be expressed as

$$\sum_{n=1}^{\infty}(-1)^n \exp(-nas) = \sum_{n=0}^{\infty}(-1)^n \exp(-nas) - 1. \tag{B.106}$$

The first term on the right-hand side in (B.106) is a *geometric series*, which converges to the limit

$$\lim_{n\to\infty}\frac{1 - (-1)^n \exp(-nas)}{1 + \exp(-as)} = \frac{1}{1 + \exp(-as)}. \tag{B.107}$$

Hence, the LAPLACE transform (B.105) yields the result (B.104).

Another example is $f(t) = \sin(\omega t)$ with a period of $T = 2\pi/\omega$. The formula (B.98) immediately furnishes the LAPLACE transform (B.8b).

B.13 Application to Partial Differential Equations

The LAPLACE transformation is also suitable to solve *partial differential equations*.

In *creep mechanics* the *diffusion equation*

$$\frac{\partial c}{\partial t} = D\frac{\partial^2 c}{\partial x^2} \quad \text{with} \quad t \geq 0 \text{ and } x \geq 0 \tag{B.108}$$

plays an important role, since creep of metals, for instance, at temperatures in the range $0.4 \leq T/T_M \leq 0.5$ can be interpreted as a *diffusion controlled process* (BETTEN, 1971).The diffusion coefficient D in (B.108) according to (11.42) is assumed to be independent on distance x and on concentration $c = c(x,t)$. The usual integration method has been discussed in section 11.3.3 in more detail. In the following the LAPLACE transformation should be applied to the *diffusion equation* (B.108).

Because of (B.23) the LAPLACE transform of the left-hand side in (B.108) is given by

$$L\{\partial c(x,t)/\partial t\} = sL\{c(x,t)\} - c(x,0)\,. \tag{B.109}$$

In contrast to this, we find:

$$L\{\partial c(x,t)/\partial x\} = \frac{\partial}{\partial x}L\{c(x,t)\} = \frac{\partial}{\partial x}\hat{c}(x,s)\,, \tag{B.110}$$

$$L\{\partial^2 c(x,t)/\partial x^2\} = \frac{\partial}{\partial x}L\{\partial c(x,t)/\partial x\} = \frac{\partial^2}{\partial x^2}\hat{c}(x,s)\,. \tag{B.111}$$

Note that the LAPLACE operator $L\{...\}$ in (B.109) to (B.111) is taken with respect to the transformed variable t:

$$L\{c(x,t)\} = \hat{c}(x,s) := \int\limits_0^\infty c(x,t)\exp(-st)dt. \tag{B.112}$$

We call $\hat{c}(x,s)$ the *time transform* of $c(x,t)$. Thus, the LAPLACE transformation in (B.110) and (B.111) is assumed to be interchangeable with the partial derivative $\partial/\partial x$ with respect to the non-transformed spatial variable x.

Assuming the conditions

$$c(x,0) = 0 \quad \text{and} \quad c(0,t) = c_0 \tag{B.113a,b}$$

we arrive from the *partial differential* equation (B.108) by considering the LAPLACE transforms (B.109), (B.111) and (B.112) at the *ordinary differential equation*

$$D\frac{\partial^2 \hat{c}(x,s)}{\partial x^2} - s\hat{c}(x,s) = 0\,, \tag{B.114}$$

where $s > 0$ and $D > 0$ are constant. Its solution is given by

$$\hat{c}(x, s) = A \exp(-x\sqrt{s/D}) + B \exp(x\sqrt{s/D}) \,. \tag{B.115}$$

Since the growth of $\hat{c}(x, s)$ is restricted, the second constant B in (B.115) must be equal to zero, while the first constant A follows from the condition (B.113b) to

$$A = \hat{c}(0, s) = L\{c_0\} = c_0/s \,, \tag{B.116}$$

hence

$$\hat{c}(x, s) = c_0 \frac{1}{s} \exp(-x\sqrt{s/D}) \,. \tag{B.117}$$

From a table of transforms or using the MAPLE software we find the inverse of (B.117), i.e. the solution

$$c(x, t) = c_0 \operatorname{erfc}\left(\frac{x}{2\sqrt{Dt}}\right) \equiv c_0 \operatorname{erfc}(\xi) \,, \tag{B.118a}$$

where the mixed dimensionless variable ξ has already been introduced in (11.44). Instead of the *complementary error function* $\operatorname{erfc}(\xi)$ in (B.118a) one can use the GAUSS *error function* $\operatorname{erf}(\xi)$. Hence, the solution (B.118a) can be written as

$$\boxed{c(\xi, t) = c_0\,[1 - \operatorname{erf}(\xi)] \quad \text{with} \quad \xi \equiv \frac{x}{2\sqrt{Dt}}} \tag{B.118b}$$

in accordance with (11.48a,b).

Some details about the *best approximation* to the *error function* $\operatorname{erf}(\xi)$ on $[0, r]$ by $\tanh(a\xi)$ and the corresponding *inverse function* are explained in the following MAPLE program.

$$\odot\ B\_15.mws$$

Best approximation to the error function erf(xi) on [0, r] by tanh(a*xi) and the corresponding inverse function:

```
>   approximant:=tanh(a*xi);
```
$$approximant := \tanh(a\,\xi)$$

This function is suitable because it is similar to erf(xi). Furthermore, the inverse can easily be determined:

```
>   inverse:=(1/a)*arctanh(xi);
```
$$inverse := \frac{\operatorname{arctanh}(\xi)}{a}$$

Note that the *Area Tangent,* artanh(...), is indicated as arctanh(...) in MAPLE. The *best approximation* by the *hyperbolic tangent* is guaranteed by an *optimal parameter* a which minimizes the L-two error norm:

```
>   L[2][r]:=sqrt((1/r)*int((erf(xi)-
>   tanh(a*xi))^2,xi=0..r))=minimum;
```

$$L_{2r} := \sqrt{\frac{1}{r} \int_0^r (\mathrm{erf}(\xi) - \tanh(a\,\xi))^2 \, d\xi} = minimum$$

Thus, the derivative of the integral with respect to the parameter a should be equal to zero.

```
>   derivative[r]:=
>   diff(int((erf(xi)-tanh(a*xi))^2, xi=0..r),a);
```

$$derivative_r := \int_0^r -2\,(\mathrm{erf}(\xi) - \tanh(a\,\xi))\,(1 - \tanh(a\,\xi)^2)\,\xi \, d\xi$$

Depending on the range [0, r] considered, we obtain the following optimal parameters:

```
>   for r in [1,2,3,4,5,infinity] do
>   a[optimal][r]:= fsolve(int(xi*(erf(xi)-
>   tanh(a_*xi))*(1-(tanh(a_*xi))^2),
>   xi=0..r)=0,a_) od;
```

$$a_{optimal_1} := 1.172868316$$

$$a_{optimal_2} := 1.201270935$$

$$a_{optimal_3} := 1.202760580$$

$$a_{optimal_4} := 1.202782281$$

$$a_{optimal_5} := 1.202782515$$

$$a_{optimal_\infty} := 1.202782517$$

The corresponding L-two error norms are given as:

```
>   for r in [1,2,3,4,5,infinity] do
>   L[2][r]:=evalf(sqrt((1/r)*int((erf(xi)-
>   tanh(a[optimal][r]*xi))^2,xi=0..r)))
>   od;
```

$$L_{21} := 0.008219954058$$

$$L_{22} := 0.01428838030$$

$$L_{23} := 0.01216051374$$

$$L_{24} := 0.01053649880$$

$$L_{25} := 0.009424169402$$

$$L_{2\infty} := 0.$$

Depending on the range [0, r] we obtain the following inverse functions:

```
>   for r in [1,2,3,4,5,infinity] do
>   inverse[r]:=(1/a[optimal][r])*arctanh(xi)
>   od;
```

$$inverse_1 := 0.8526106353 \, \text{arctanh}(\xi)$$

$$inverse_2 := 0.8324516734 \, \text{arctanh}(\xi)$$

$$inverse_3 := 0.8314206640 \, \text{arctanh}(\xi)$$

$$inverse_4 := 0.8314056632 \, \text{arctanh}(\xi)$$

$$inverse_5 := 0.8314055014 \, \text{arctanh}(\xi)$$

$$inverse_\infty := 0.8314055001 \, \text{arctanh}(\xi)$$

In the following some examples should be plotted:

```
>   alias(H=Heaviside,th=thickness,
>   con=constrained):
>   plot({1,H(xi-2),erf(xi),tanh(a[optimal][2]*
>       xi)},xi=0..2.001,color=black);
```
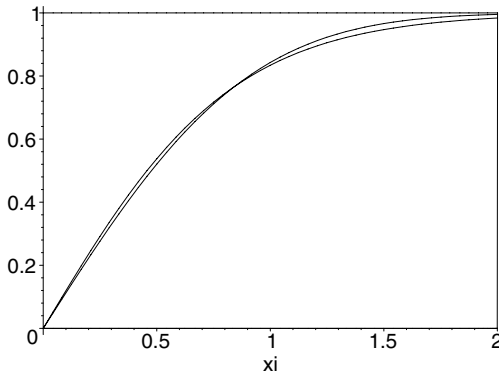

Fig. B.8 Error function and approximant on $[0, 2]$

```
>   Delta(xi):=erf(xi)-tanh(a[optimal][2]*xi);
```

$$\Delta(\xi) := \text{erf}(\xi) - \tanh(1.201270935\,\xi)$$

```
>   for i from 1 to 3 do
>   zero[i-1]:=fsolve(Delta(xi)=0,
>   xi,(i-1)/2..i/2) od;
```

$zero_0 := 0.$

$zero_1 := 0.8439158081$

$zero_2 := \text{fsolve}(\text{erf}(\xi) - \tanh(1.201270935\,\xi) = 0,\ \xi,\ 1..\dfrac{3}{2})$

```
>   plot1:=
>   plot({-0.02,0.02,0.02*H(xi-5),-0.02*H(xi-5)},
>   xi=0..5.001,color=black):
>   plot2:=
>       plot(erf(xi)-tanh(a[optimal][5]*xi),
>       xi=0..5,color=black,th=3):
>   plots[display]({plot1,plot2});
```
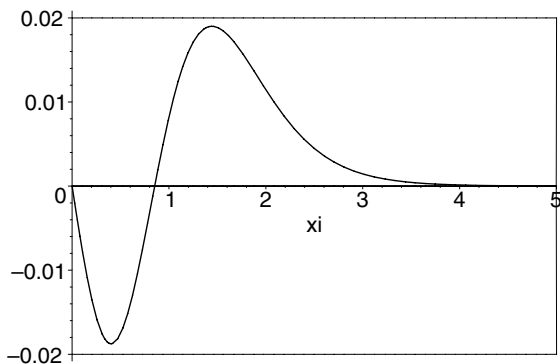

Fig. B.9 Deviation between $\text{erf}(\xi)$ and $\tanh(a,\xi)$ on $[0,5]$

```
>   L[2][5]:=sqrt((1/5)*Int((Delta)^2,xi=0..5))=
>   evalf(sqrt((1/5)*int((erf(xi)-
>   tanh(a[optimal][5]*xi))^2,xi=0..5)));
```

$$L_{25} := \frac{1}{5}\,\sqrt{5}\,\sqrt{\int_0^5 \Delta^2\,d\xi} = 0.009424169402$$

The following Figures illustrate the erro function erf(xi) and some inverse approximations (1/a)*arctanh(xi):

```
>   plot1:=plot({1,xi,H(xi-1)},xi=0..1.001,
>   scaling=con,color=black):
```

```
>   plot2:=plot({erf(xi),(1/a[optimal][1])*
>   arctanh(xi)},xi=0..1,0..1,color=black,th=2):
>   plots[display]({plot1,plot2});
```
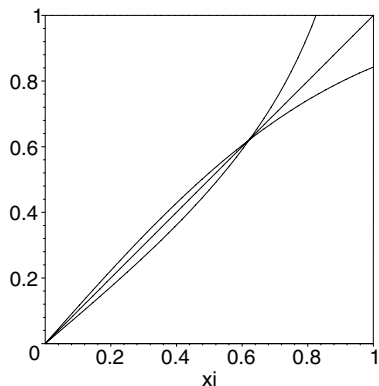

Fig. B.10a erf(ξ) and $(1/a)$ arctanh(ξ) on $[0, 1]$

```
>   plot1:=plot({1,2,xi,2*H(xi-2),2*H(xi-1),
>   -2*H(xi-1.002)},xi=0..2.001,scaling=con):
>   plot2:=plot({erf(xi),(1/a[optimal][2])*
>   arctanh(xi)},xi=0..2,0..2,th=2):
>   plots[display]({plot1,plot2});
```
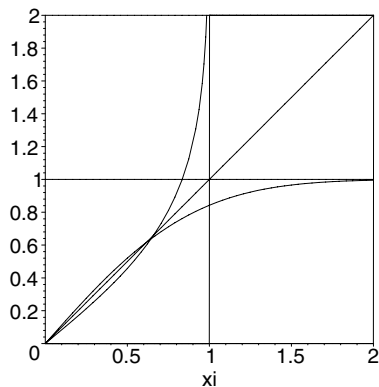

Fig. B.10b erf(ξ) and $(1/a)$ arctanh(ξ) on $[0, 2]$

```
>   plot1:=plot({1,5,xi,5*H(xi-5),
>   5*H(xi-1),-5*H(xi-1.002)},
>   xi=0..5.001,scaling=con,color=black):
>   plot2:=plot({erf(xi),
>   (1/a[optimal][5])*arctanh(xi)},
>   xi=0..5,0..5,color=black,th=2):
>   plots[display]({plot1,plot2});
```
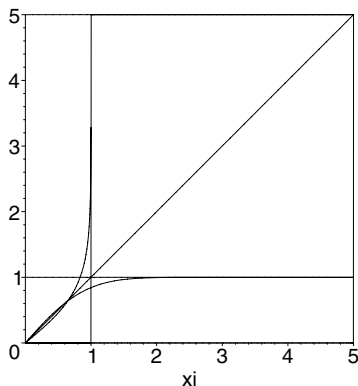

Fig. B.10c erf(ξ) and $(1/a)$ arctanh(ξ) on $[0, 5]$

The results show that the approximant $\tanh(a\xi)$ furnishes a suitable approximation to the error function erf(xi). In view of the inverse $(1/a)\tanh(\xi)$ and the approximant $\tanh(a\xi)$ the influence of the range $[0, r]$ on the parameter a is less important.

In the following tables some pairs of LAPLACE transforms are listed. Additional examples can be found in many textbooks, for instance in the books of AMELING (1984), BRONSTEIN et al.(2000; 2004), DOETSCH (1971-73), to name just a few. Furthermore, it is very convenient to use modern *computer algebra systems*, for instance MATHEMATICA or MAPLE, which are powerful tools indispensable in modern pure and applied scientific research and education.

Table B.1: LAPLACE transform pairs

$f(t)$ for $t > 0$	$L\{f(t)\} \equiv \hat{f}(s) = \int\limits_0^\infty f(t)e^{-st}dt$
a	a/s
at	a/s^2
$(1/2!)t^2$	$1/s^3$
$(1/3!)t^3$	$1/s^4$
$(1/n!)t^n$	$\dfrac{1}{s^{n+1}};$ $(n \geq 0, \text{integer})$
$t^{n-1}\exp(at)$	$\dfrac{(n-1)!}{(s-a)^n};$ $(n \geq 1, \text{integer})$
t^n	$\dfrac{n!}{s^{n+1}};$ $(n \geq 0, \text{integer})$
t^p	$\dfrac{\Gamma(p+1)}{s^{p+1}};$ $(p > -1)$
$\delta(t)$ DIRAC	1
$\delta(t-a)$	$\exp(-as)$
$\exp(at)$	$\dfrac{1}{s-a}$
$\dfrac{1}{\lambda}\exp(-t/\lambda)$	$\dfrac{1}{1+\lambda s}$
$1 - \exp(-t/\lambda)$	$\dfrac{1}{s(1+\lambda s)}$
$t\exp(at)$	$\dfrac{1}{(s-a)^2}$
$\dfrac{1}{a^2}t\exp(-t/a)$	$\dfrac{1}{(1+as)^2}$

Table B.1: LAPLACE transform pairs

$f(t)$ for $t > 0$	$L\{f(t)\} \equiv \hat{f}(s) = \int\limits_0^\infty f(t)e^{-st}dt$
$\dfrac{\exp(at) - \exp(bt)}{a - b}$	$\dfrac{1}{(s-a)(s-b)}$
$\dfrac{a\exp(at) - b\exp(bt)}{a - b}$	$\dfrac{s}{(s-a)(s-b)}$
$(1 + at)\exp(at)$	$\dfrac{s}{(s-a)^2}$
$\dfrac{1}{2}t^2\exp(at)$	$\dfrac{1}{(s-a)^3}$
$\left(t + \dfrac{1}{2}at^2\right)\exp(at)$	$\dfrac{s}{(s-a)^3}$
$\exp(i\omega t)$	$\dfrac{1}{s - i\omega} \equiv \dfrac{s + i\omega}{s^2 + \omega^2}$
$\sin\omega t$	$\dfrac{\omega}{s^2 + \omega^2}$
$\cos\omega t$	$\dfrac{s}{s^2 + \omega^2}$
$\sin^2\omega t$	$\dfrac{2\omega^2}{s(s^2 + 4\omega^2)}$
$\cos^2\omega t$	$\dfrac{s^2 + 2\omega^2}{s(s^2 + 4\omega^2)}$
$\sin(\omega t + \varphi)$	$\dfrac{s\sin\varphi + \omega\cos\varphi}{s^2 + \omega^2}$
$\cos(\omega t + \varphi)$	$\dfrac{s\cos\varphi - \omega\sin\varphi}{s^2 + \omega^2}$
$\exp(\alpha t)\sin\omega t$	$\dfrac{\omega}{(s-\alpha)^2 + \omega^2}$
$\exp\alpha t\cos\omega t$	$\dfrac{s - \alpha}{(s-\alpha)^2 + \omega^2}$

Table B.1: LAPLACE transform pairs
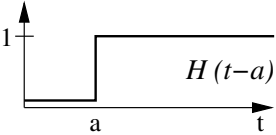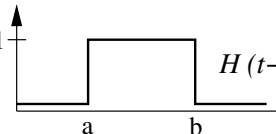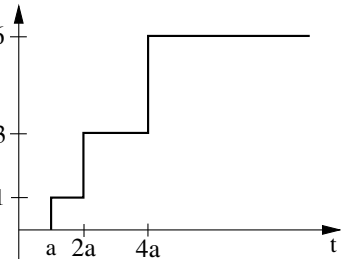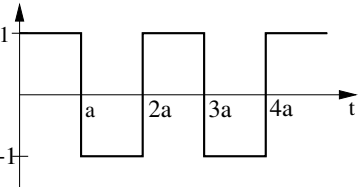
$f(t)$ for $t > 0$	$L\{f(t)\} \equiv \hat{f}(s) = \int\limits_{0}^{\infty} f(t)e^{-st}dt$
$\sinh \omega t$	$\dfrac{\omega}{s^2 - \omega^2}$
$\cosh \omega t$	$\dfrac{s}{s^2 - \omega^2}$
$\sinh^2 \omega t$	$\dfrac{2\omega^2}{s(s^2 - 4\omega^2)}$
$\cosh^2 \omega t$	$\dfrac{s^2 - 2\omega^2}{s(s^2 - 4\omega^2)}$
$\exp(\alpha t) \sinh \omega t$	$\dfrac{\omega}{(s - \alpha)^2 - \omega^2}$
$\exp(\alpha t) \cosh \omega t$	$\dfrac{s - \alpha}{(s - \alpha)^2 - \omega^2}$
$\dfrac{t}{2} \sin \omega t$	$\dfrac{\omega s}{(s^2 + \omega^2)^2}$
$t \cos \omega t$	$\dfrac{s^2 - \omega^2}{(s^2 + \omega^2)^2}$
$\dfrac{t}{2} \sinh \omega t$	$\dfrac{\omega s}{(s^2 - \omega^2)^2}$
$t \cosh \omega t$	$\dfrac{s^2 + \omega^2}{(s^2 - \omega^2)^2}$
$\dfrac{t^2 \sinh \omega t}{2\omega}$	$\dfrac{3s^2 + \omega^2}{(s^2 - \omega^2)^3}$
$\dfrac{1}{2}t^2 \cosh \omega t$	$\dfrac{s^3 + 3\omega^2 s}{(s^2 - \omega^2)^3}$
$\dfrac{1}{\sqrt{\pi t}}$	$\dfrac{1}{\sqrt{s}}$
$2\sqrt{\dfrac{t}{\pi}}$	$\dfrac{1}{s\sqrt{s}}$

Table B.1: LAPLACE transform pairs

$f(t)$ for $t > 0$	$L\{f(t)\} \equiv \hat{f}(s) = \int\limits_0^\infty f(t)e^{-st}dt$
$\dfrac{4}{3}t\sqrt{\dfrac{t}{\pi}}$	$\dfrac{1}{s^2\sqrt{s}}$
$\dfrac{\exp(-at)}{\sqrt{\pi t}}$	$\dfrac{1}{\sqrt{s+a}}$
$\dfrac{\mathrm{erf}\sqrt{at}}{\sqrt{a}}$	$\dfrac{1}{s\sqrt{s+a}}$
$\dfrac{t^{\nu-1}}{\Gamma(\nu)}\exp(-at)$	$\dfrac{1}{(s+a)^\nu}$
$\dfrac{a}{2\sqrt{\pi t^3}}\exp(-\dfrac{a^2}{4t})$	$\exp(-a)\sqrt{s}$
$\dfrac{\exp(-\dfrac{a^2}{4t})}{\sqrt{\pi t}}$	$\dfrac{\exp(-a\sqrt{s})}{\sqrt{s}}$
$\mathrm{erf}\left(\dfrac{x}{2\sqrt{Dt}}\right)$	$\dfrac{1}{s}\left[1-\exp(-x\sqrt{s/D})\right]$
$\mathrm{erfc}\left(\dfrac{x}{2\sqrt{Dt}}\right)$	$\dfrac{1}{s}\exp\left(-x\sqrt{s/D}\right)$
$\dfrac{1-\exp(at)}{t}$	$\ln\dfrac{s-a}{s}$
$\dfrac{\exp(bt)-\exp(at)}{t}$	$\ln\dfrac{s+a}{s-a}$
$a+b\left[1-\exp(-ct)\right]$	$\dfrac{a}{s}+b\left(\dfrac{1}{s}-\dfrac{1}{s+c}\right)$
$a+b\left[1-\exp(-c\sqrt{t})\right]$	$\dfrac{a}{s}+\dfrac{1}{2}\dfrac{bc\sqrt{\pi}\exp\left(\dfrac{c^2}{4s}\right)\mathrm{erfc}\left(\dfrac{c}{2\sqrt{s}}\right)}{s^{3/2}}$
$\mathrm{erf}(t)$	$\dfrac{\exp(s^2/4)\,\mathrm{erfc}(s/2)}{s}$

Table B.2: LAPLACE transfrom of HEAVISIDE functions

HEAVISIDE $H(t)$	$1/s$
$H(t{-}a)$	$\dfrac{1}{s}\exp(-as)$
$H(t{-}a) - H(t{-}b)$	$\dfrac{1}{s}\left[\exp(-as) - \exp(-bs)\right]$
$H(t-a) + 2H(t-2a) + 3H(t-4a)$ 	$\dfrac{1}{s}\left[\exp(-as) + 2\exp(-2as)\right.$ $\left. +\,3\exp(-4as)\right]$
$H(t) + 2\displaystyle\sum_{n=1}^{N}(-1)^n H(t-na)$ 	(geometrical series) $\dfrac{1}{s}\left[1 + 2\displaystyle\sum_{n=1}^{N}(-1)^n \exp(-nas)\right]$ for $N \to \infty$ $\Downarrow$ $\dfrac{1}{s}\cdot\dfrac{1 - \exp(-as)}{1 + \exp(-as)}$

Table B.2: LAPLACE transfrom of HEAVISIDE functions
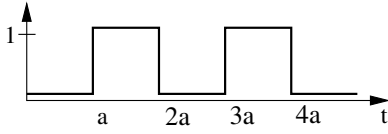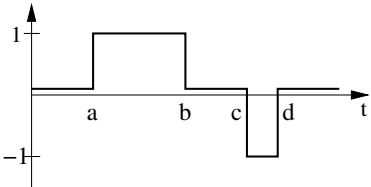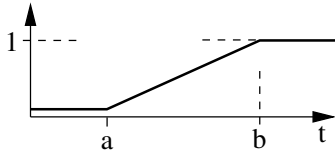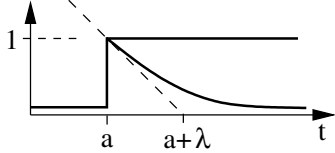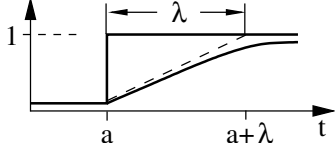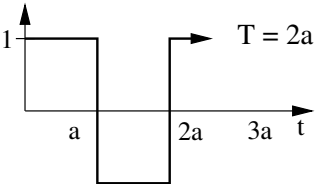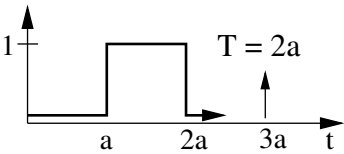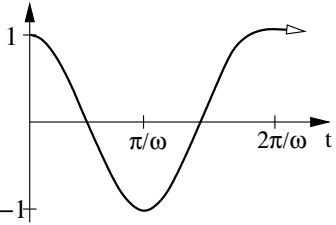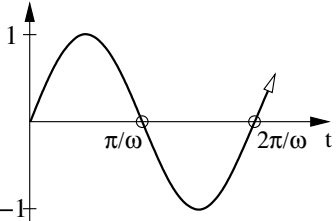
HEAVISIDE $H(t)$	$1/s$
$H(t) - \sum_{n=0}^{N}(-1)^n H(t - na)$ a 2a 3a 4a t	$\dfrac{1}{s}\left[1 - \sum_{n=0}^{N}(-1)^n \exp(-nas)\right]$ for $N \to \infty$ $\Downarrow$ $\dfrac{1}{s(1 + \exp(as))}$
$H(t-a)-H(t-b)-H(t-c)+H(t-d)$ 	$\dfrac{1}{s}\left[\exp(-as) - \exp(-bs)\right.$ $\left. - \exp(-cs) + \exp(-ds)\right]$
$(t - a)H(t - a) - (t - b)H(t - b)$ 	$\dfrac{1}{s^2}\left[\exp(-as) - \exp(-bs)\right]$
$\exp\left[-(t - a)/\lambda\right] H(t - a)$ 	$\dfrac{\lambda}{1 + \lambda s}\exp(-as)$
$\{1 - \exp\left[-(t - a)/\lambda\right]\} H(t - a)$ 	$\dfrac{1}{s(1 + \lambda s)}\exp(-as)$

Table B.3: LAPLACE transfrom of periodic functions

$f(t) = f(t + nT) \quad n \in I\!N$	$\dfrac{1}{1 - e^{(-sT)}} \displaystyle\int_0^T f(t)e^{(-st)}dt$
$H(t) - 2H(t - a) + 2H(t - 2a)$	$\dfrac{1}{s} \cdot \dfrac{1 - \exp(-as)}{1 + \exp(-as)} \equiv \tanh\left(\dfrac{as}{2}\right)$
$H(t - a) - 2H(t - 2a)$	$\dfrac{1}{s\,[1 + \exp(as)]}$
$\cos \omega t; \quad T = 2\pi/\omega$	$\dfrac{s}{s^2 + \omega^2}$
$\sin \omega t; \quad T = 2\pi/\omega$	$\dfrac{\omega}{s^2 + \omega^2}$

References

ADAMS, B., BOEHLER, J., GUIDI, M. and ONAT, E. (1992). Group theory and representation of microstructure, and Mechanical behavior of polycrystals, *J. Mech. Phys. Solids* **40**: 723–747.

AIMEDIEU, P. (2004). *Contributation à la biomécanique de tissues mous intrácraniens*, PhD Thesis of Université de Picardie Jules Vernes, Faculte de medicine, Amiens Cedex, France.

AL-GADHIB, A., BALUCH, M., SHAALAN, A. and KHAN, A. (2000). Damage Model for Monotonic and Fatigue Response of High Strength Concrete, *Int. Journal of Damage Mechnics* **9**: 57–78.

ALTENBACH, H., ALTENBACH, J. and SCHIESSE, P. (1990). Konzept der Schädigungsmechanik und ihre Anwendung bei der werkstoffmechanischen Bauteilanalyse, *Tech Mech* **11**: 81–93.

ALTENBACH, H., MORACHKOVSKY, O., NAUMENKO, K. and SYCHOV A. (1997). Geometrically nonlinear bending of thin-walled shells and plates under creep damage conditions, *Arch Appl Mech* **67**: 339–352.

ALTENBACH, J., ALTENBACH, H. and NAUMENKO, K. (1997). Lebensdauerabschätzung dünnwandiger Flächentragwerke auf der Grundlage phenomenologischer Materialmodelle für Kriechen und Schädigung, *Tech Mech* **12**: 353–364.

ALTENBACH, J., ALTENBACH, H. and ZOLOCHEVSKY, A. (1995). *Erweiterte Deformationsmodelle und Versagenskriterien der Werkstoffmechanik*, Deutscher Verlag für Grundstoffindustrie, Stuttgart.

AMELING, W. (1984). *Laplace Transformation*, 3. edn, Vieweg-Verlag, Braunschweig / Wiesbaden.

ANAND, L. (1982). Constitutive Equations for the Rate-Dependent Deformation of Metals at Elevated Temperatures, *Transactions of the ASME* **104**: 12–17.

ANAND, L. (1985). Constitutive Equations for Hot-Working of Metals, *Intern. J. of Plasticity* **1**: 213–231.

ANDRADE, E. (1910). The viscous flow in metals and allied phenomena, *Proc. R. Soc. London* **A 84**: 1–12.

ANDRADE, E. (1914). Flow of Metals under large constant Stress, *Proc. Roy. Soc.* **A 90**: 329–342.

ARGON, A. (1982). Mechanism and mechanics of fracture in creeping alloys, *in* B. WILSHIRE and D. OWEN (eds), *Recent Advantages in Creep and Fracture of Engineering Materials and Structures*, Pinerage Press, Swansea, pp. 1–52.

ARONS, R. and TIEN, J. (1980). Creep and strain recovery in hot-pressed silicon nitride, *J. of Materials Science* **15**: 2046–2058.

ASHARE, E. (1968). Rheological properties of narrow distribution polystyrene solutions, *Trans. Soc. Rheol.* **12**: 535–557.

ASHBY, M. and JONES, D. (1980). *Engineering Materials 1*, Pergamon Press, Oxford/New York/.../ Toronto. reprinted 1989.

ASTARITA, G. and MARRUCCI, G. (1974). *Principles of Non-Newtonian Fluid Mechanics*, McGraw-Hill Book Company, Berkshire.

ASTRARITA, G. (1979). Why do we search for constitutive equations? Presented at the Golden Jubilee Meeting of the Society of Rheology, Boston, MA.

AVULA, X. (1987). Mathematical Modelling, *Encyclopedia of Physical Science and Technology* **7**: 719–728.

BAILEY, R. (1935). The utilization of creep test data in engineering design, *Proceeding, Inst. Mech. Eng.* **131**: 131–349.

BALLMANN, R. (1965). Extensional Flow of Polystyrene Melt, *Rheologia Acta* **4**: 137–140.

BASAR, Y. and WEICHERT, D. (2000). *Nonlinear Continuum Mechanics of Solids*, Springer-Verlag, Berlin/Heidelberg.

BECKER, E. and BÜRGER, W. (1975). *Kontinuumsmechanik, Leitfäden der angewandten Mathematik und Mechanik*, Vol. 20, Teubner Studienbücher, Stuttgart.

BELL, J. (1973). The experimental Foundations of Solid Mechanics, *in* S. FLÜGGE (ed.), *Encyclopedia of Physics*, Vol. VIa/1, Springer Verlag, Berlin / New York.

BERTRAM, A. (2005). *Elasticity and Plasticity of Large Deformations*, Springer-Verlag, Berlin/Heidlberg/New York.

BERTRAM, A. and OLSCHEWSKI, J. (1996). Anisotropic creep modeling of the single crystal superalloy SRR 99, *J. Comp. Math. Sci.* **5**: 12–16.

BESSELING, J. (1962). Investigation of transient creep in thick-walled tubes under axially symmetric loading, *IUTAM Colloquium on Creep in Structures, Stanford University 1960*, Springer, Berlin, pp. 174–194.

BETTEN, J. (1969). *Mathematische Modelle in der Werkstoffkunde*. Vorlesung an der RWTH Aachen seit SS 1969.

BETTEN, J. (1971). *Lösung von Festigkeitsproblemen unter Berücksichtigung des Kriechens*. Habilitationsschrift, RWTH Aachen 1971.

BETTEN, J. (1972). Zur Ermittlung der mechanischen Hysterese rheologischer Körper, *Zeitschrift für Naturforschung* **27a**: 718–719.

BETTEN, J. (1973). Die Traglasttheorie der Statik als mathematisches Modell, *Schweizerische Bauzeitung* **91**: 6–9. Habilitationsvortrag am 30.11.1971.

BETTEN, J. (1974). Tensorrechnung für Ingenieure II. Vorlesung an der RWTH-Aachen seit SS1974.

BETTEN, J. (1975a). Beitrag zum isotropen kompressiblen plastischen Fliessen, *Arch. Eisenhüttenwes.* **46**: 317–323.

BETTEN, J. (1975b). Bemerkungen zum Versuch von Hohenemser, *Z. Angew. Math. Mech.* **55**: 149–158.

BETTEN, J. (1975c). Zum Traglastverfahren bei nichtlinearem Stoffgesetz, *Ing.-Archiv* **44**: 199–207.

BETTEN, J. (1975d). Zur Verallgemeinerung der Invariantentheorie in der Kriechmechanik, *Rheol. Acta* **14**: 715–720.

BETTEN, J. (1976a). Ein Beitrag zur Invariantentheorie in der Plastomechanik anisitroper Werkstoffe, *ZAMM* **56**: 557–559.

BETTEN, J. (1976b). Plastische Anisotropie und Bauschinger-Effekt; allgemeine Formulierung und Vergleich mit experimentell ermittelten Fließortkurven, *Acta Mechanica* **25**: 75–94.

BETTEN, J. (1977). Plastische Stoffgleichungen inkompressibler anisotroper Werkstoffe, *Z. angew. Math. Mech. (ZAMM)* **57**: 671–673.

BETTEN, J. (1979a). Theory of Invariants in Creep Mechanics of Anisotropic Materials, *in* J. P. BOEHLER (ed.), *Euromech Colloquium 115 on "Mechanical Behaviour of Anisotropic Solids"*, Grenoble, pp. 65–80.

BETTEN, J. (1979b). Über die Konvexität von Fliesskörpern isotroper und anisotroper Stoffe, *Acta Mechanica* **32**: 233–247.

BETTEN, J. (1980). Zur Kriechaufweitung zylindrischer Hochdruckbehälter, *Rheol. Acta* **19**: 517–524. Vorgetragen auf der Jahrestagung d. Deutschen Rheologischen Gesellschaft in Aachen, März 1979.

BETTEN, J. (1981a). Creep theory of anisotropic solids, *J. Rheol.* **25**: 565–581. Presented at the Golden Jubilee Meeting of the Society of Rheology, Boston, MA, 1979.

BETTEN, J. (1981b). Representation of constitutive equations in creep mechanics of isotropic and anisotropic materials, pp. 179–201. In: Ponter ARS, Hayhurst DR (ed), Creep in Structures, Berlin, Heidelberg, New York: Springer-Verlag. Presented at the third IUATM Syposium on Creep in Structures in Leicester, UK, Sept. 1980.

BETTEN, J. (1982a). Integrity basis for a second-order and a fourth-order tensor, *Int. J. Math. Math. Sci.* **5**: 87–96.

BETTEN, J. (1982b). Net-stress analysis in creep mechanics, *Ing.-Archiv* **52**: 405–419. Presented at the second Symposium on Inelastic Solids and Structures in Bad Honnef, Germany, 24.09.1981.

BETTEN, J. (1982c). On the Creep Behaviour of an Elastic-Plastic Thick-Walled Circular Cylindrical Tube subjected to internal Pressure, *in* O. MAHRENHOLTZ and A. SAWCZUK (eds), *Mechanics of inelastic Media and Structures*, Polish Academy of Sciences, Warszawa, Poznan, pp. 51–72. Presented at the international Symposium on Mechanics of Inelastic Media and Structures in Warschau, September 1978.

BETTEN, J. (1982d). Pressure-Dependent Yield Behaviour of Isotropic and Anisotropic Materials, *in* P. VERMEER and H. LUGER (eds), *Deformation and Failure of Granular Materials*, A.A. Balkema, Rotterdam, pp. 81–89. Presented at the IUTAM Symposium in Delft, Sept. 1982.

BETTEN, J. (1983a). Damage tensors and tensors of continuity in stress analysis, *Z. Naturforschung* **38a**: 1383–1390.

BETTEN, J. (1983b). Damage tensors in continuum mechanics, *Journal de Mécanique théorique et appliqué* **2**: 13–32. Presented at Euromech Colloquium 147 on Damage Mechanics, Paris- VI, Cachan, 1981.

BETTEN, J. (1984). Interpolation Methods for Tensor Functions, *in* X. J. R. AVULA (ed.), *Mathematical Modelling in Science and Technology*, Pergamon Press, New York, pp. 52–57. Presented at the fourth Int. Conf. on Mathematical Modeling in Zürich, August 1983.

BETTEN, J. (1985). The classical plastic potential theory in comparison with the tensor function theory, *Eng. Fracture Mech.* **21**: 641–652. Presented at the Int. Symposium Plasticity Today, Udine, June 1983.

BETTEN, J. (1986a). Applications of tensor functions to the formulation of constitutive equations involving damage and initial anisotropy, *Eng. Fracture Mech.* **25**: 573–584. Presented at the IUTAM Symposium on Mechanics of Damage and Fatigue, Haifa and Tel Aviv, Israel, July 1985.

BETTEN, J. (1986b). Beitrag zur tensoriellen Verallgemeinerung einachsiger Stoffgesetze, *Z. Angew. Math. Mech.* **66**: 577–581.

BETTEN, J. (1987a). Irreducible invariants of fourth-order tensors, *in* X. J. R. AVULA (ed.), *Mathematical Modelling in Science and Technology*, Pergamon Journals Limited, Exeter, pp. 29–33. Presented at the fith Int. Conf. on Mathem. Modelling in Berkely, USA, July 1985.

BETTEN, J. (1987b). Tensor functions involving second-order and fourth-order argument tensors, *in* J. P. BOEHLER (ed.), *Applications of Tensor Functions in Solid Mechanics*, Springer-Verlag, Berlin. CISM-Course in Udine, July 1984.

BETTEN, J. (1987c). *Tensorrechnung für Ingenieure*, Teubner-Verlag, Stuttgart.

BETTEN, J. (1988a). Applications of Tensor Functions to the Formulation of Yield Criteria for Anisotropic Materials, *Int. J. of Plasicity* **4**: 29–46.

BETTEN, J. (1988b). Mathematical modelling of materials behaviour, *in* X. J. R. AVULA (ed.), *Mathematical Modelling in Science and Technology*, Pergamon Press, Oxford,

pp. 702–708. Presented at the sixth Int. Conf. on Mathem. Modelling in St Louis, Missouri, USA, August 1987.

BETTEN, J. (1989). Generalization of nonlinear material laws found in experiments to multiaxial states of stress, *Eur. J. Mech. A/Solids* **8**: 325–339. Presented at Euromech Colloquium 244 on Experimental Analysis of Nonlinear Problems in Solid Mechanics, Poznan, Poland 1988.

BETTEN, J. (1990). Recent Advances in Mathematical Modelling of Materials Behavior, *in* E. RODIN and X. AVULA (eds), *Mathematical and Computer Modelling*, Pergamon Press, Oxford, pp. 37–51. Presented as a plenary lecture at the seventh Int. Conf. on Mathem. Modelling in Chicago, Illinois, USA, August 1989.

BETTEN, J. (1991a). Applications of tensor functions in creep mechanics, *in* M. ZYCZKOWSKI (ed.), *Creep in Structures*, Springer-Verlag, Berlin/Heidelberg/New York, pp. 3–22. Presented as a "general lecture" on the IUTAM-Symposium in Cracow/Poland, Sept. 1990.

BETTEN, J. (1991b). Recent advances in applications of tensor functions in solid mechanics, *Adv. Mechanics (Uspechi Mechaniki)* **14**: 79–109.

BETTEN, J. (1992). Applications of tensor functions in continuum damage mechanics, *Int. J. Damage Mechanics* **1**: 47–59.

BETTEN, J. (1998). Anwendungen von Tensorfunktionen in der Kontinuumsmechanik anisotroper Materialien, *ZAMM* **78**: 507–521. Hauptvortrag auf der 75. GAMM-Tagung in Regensburg, 24-27, März 1997.

BETTEN, J. (2001a). *Kontinuumsmechanik*, 2. Aufl., Springer-Verlag, Berlin, Heidelberg, New York.

BETTEN, J. (2001b). Mathematical modelling of materials behaviour under creep conditions, *Appl. Mech. Rev. (AMR)* **54**(2): 107–132.

BETTEN, J. (2001c). Recent Advances in Applications of Tensor Functions in Continuum Mechanics, *in* E. GIESSEN V.D. and T. WU (eds), *Advances in Applied Mechanics*, Vol. 37, pp. 277–363.

BETTEN, J. (2003a). Applications of Tensor Functions in Damage Mechanics, *in* J. SKRZYPEK and A. GANCZARSKI (eds), *Anisotropic Behaviour of Damaged Materials*, Springer-Verlag, Berlin/Heidelberg/New York.

BETTEN, J. (2003b). *Finite Elemente für Ingenieure 1*, zweite Aufl., Springer-Verlag, Berlin / Heidelberg / New York.

BETTEN, J. (2004). *Finite Elemente für Ingenieure 2*, zweite Aufl., Springer-Verlag, Berlin / Heidelberg / New York.

BETTEN, J. (2007). Creep Curve, *Maplesoft Appliction Center, Category Engineering Mechanics* . Waterloo, Ontario, Canada.

BETTEN, J. (2009). Zum Eigenwertproblem für Tensoren vierter Stufe, *ZAMM* . In Vorbereitung.

BETTEN, J., BORRMANN, M. and BUTTERS, T. (1989). Materialgleichungen zur Beschreibung des primären Kriechverhaltens innendruckbeanspruchter Zylinderschalen aus isotropem Werkstoff, *Ing. Archiv (Arch. Appl. Mech.)* **60**: 99–109.

BETTEN, J., BREITBACH, G. and WANIEWSKI, M. (1990). Multiaxial Anisotropic Creep Behaviour of Rolled Sheet-Metals, *Z. Angew. Math. Mech. (ZAMM)* **70**: 371–379.

BETTEN, J. and BUTTERS, T. (1990). Rotationssymmetrisches Kriechbeulen dünnwandiger Kreiszylinderschalen im primären Kriechbereich, *Forschung. Ingenieur.* **56**: 84–89.

BETTEN, J., EL-MAGD, E., MEYDANLI, S. and PALMEN, P. (1995). Anisotropic damage growth under multi-axial stress (theory and experiments), *Arch. Appl. Mech.* **65**: 110–120 and 121–132.

BETTEN, J. and HELISCH, W. (1995). Integrity basis for a fourth-rank tensor, *in* D. PARKER and A. ENGLAND (eds), *IUTAM Symposium on Anisotropy, Inhomogeneity and Nonlinearity in Solid Mechanics*, Kluwer Academic Publishers, Netherlands, pp. 37–42.

BETTEN, J. and MEYDANLI, S. (1995). Untersuchung des anisotropen Kriechverhaltens vorgeschädigter austenitischer Stähle, *ZAMM* **75**: 181–182. DFG-Report Be766/12-2.

BETTEN, J. and SHIN, C. (1991). Inelastisches Verhalten rotierender Scheiben unter Berück-sichtigung der werkstoffbedingten Anisotropie und der tensoriellen Nichtlinearität, *Forschung im Ingenieurwesen* **7**: 137–147.

BETTEN, J. and SHIN, C. (1992). Inelastic Analysis of Plastic Compressible Materials Using the Viscoplastic Model, *Intern. J. Plasticity* **9**.

BETTEN, J., SKLEPUS, S. and ZOLOCHEVSKY, A. (1998). A creep damage model for initially isotropic materials with different properties in tension and compression, *Engineering Fracture Mechanics* **59**: 623–641.

BETTEN, J., SKLEPUS, S. and ZOLOCHEVSKY, A. (1999). A Microcrack Describtion of Creep Damage in Crystalline Solids With Different Behaviour in Tension and Compression, *Int. J. of Damage Mech* **8**: 197–232.

BETTEN, J. and WANIEWSKI, M. (1989). Multiaxial creep behaviour of anisotropic materials, *Arch. Mech.* **41**: 679–695. Presented at the Fourth Polish-German Symposium on Mechanics of Inelastic Solids and Structures, Mogilany, Poland, 1987.

BETTEN, J. and WANIEWSKI, M. (1995). Tensorielle Stoffgleichungen zur Beschreibung des anisotropen Kriechverhaltens isotroper Stoffe nach plastischer Verformung, *Z. Angew. Math. Mech. (ZAMM)* **75**: 831–845.

BETTEN, J., ZOLOCHEVSKA, L. and ZOLOCHEVSKY, A. (1999). Modelling of elastic deformation for initially anisotropic materials sustaining damage, *Tech. Mechanik* **19**: 211–222.

BEZIER, P. (1972). *Numerical Control*, Mathematics and Appications, London/New York/Toronto.

BHATNAGAR, N. and ARYA, V. (1974). Large strain creep analysis of thick-walled cylinders, *Int. J. Non-Linear Mechanics* **9**: 127–140.

BIRD, R., ARMSTRONG, R. and HASSAGER, O. (1977). *Dynamics of Polymeric Liquids*, Vol. 1: Fluid Mechanics, John Wiley & Sons, New York/ ... / Toronto.

BLOK, A. (2006). *Vergleich rheologischer Modelle zum Kriechverhalten eines EVA-Copolymers*, Presentation on the occation of doctorial examination, RWTH-Aachen University.

BLUM, W. and ILSCHNER, B. (1967). *Phys. Stat. Sol.* **20**: 629.

BODNER, S. and HASHIN, Z. (1986). *Mechanics of Damage and Fatigue*, Pergamon Press, New York, Toronto.

BODNER, S. and PARTOM, Y. (1975). Constitutive Equations for Elastic-Viscoplastic Strain-Hardening Materials, *J. Appl. Mech.* **42**: 385–389.

BOEHLER, J. (1979). A simple derivation of representations for non-polynomial constitutive equations in some cases of anisotropy, *ZAMM* **59**: 157–167.

BOEHLER, J. (1987). *Applications of Tensor Functions in Solid Mechanics*, Springer-Verlag, Wien, New York.

BOEHLER, J. and SAWCZUK, A. (1976). Application of representation theorems to describe yielding of transversely isotropic solids, *Mech. Res. Comm.* **3**: 277–283.

BOEHLER, R. and SAWCZUK, A. (1977). On yielding of oriented solids, *Acta Mechanica* **27**: 185–206.

BÖHME, G. (2000). *Strömungsmechanik nicht-newtonscher Fluide*, 2. Aufl., Teubner-Verlag, Stuttgart.

BRONSTEIN, I., SEMENDJAJEW, K. and MUSIOL, G. (2000). *Taschenbuch der Mathematik*, Verlag Harri Deutsch, Frankfurt.

BRONSTEIN, I., SEMENDJAJEW, K., MUSIOL, G. and MUEHLIG, H. (2004). *Handbook of Mathematics*, Springer-Verlag, Berlin, Heidelberg, New York.

BROWN, S., EVANS, R. and WILSHIRE, B. (1986). Exponential descriptions of normal creep curves, *Scripta Metallurgica* **20**: 855–860.

BROWN, S., KIM, K. and ANAND, L. (1989). An Internal Variable Constitutive Model for Hot-Working of Metals, *Intern. J. of Plasticity* **5**: 95–130.

BRUELLER, O. (1991). Some new Aspects of the Nonlinear Characterization of Creep and Stress Relaxation of Polymers, *in* M. ZYCZKOWSKI (ed.), *Creep in Structures*, Springer-Verlag, Berlin, pp. 55–62.

BUCHTER, H. (1967). *Apparate und Armaturen der Chemischen Hochdrucktechnik*, Springer-Verlag, Berlin.

CHABOCHE, J. (1974). Une Loi Differentielle d'Endommagement de Fatigue avec Cumulation non Lineaire, *Revue Francaise de Mecanique* pp. 50–51. English trans In Annales de l'IBTP 39.

CHABOCHE, J. (1977). Viscoplastic Constitutive Equations for the Description of Cyclic and Anisotropic Behaviour of Metals, *Bullet. De L'Academie Polonaise des Sciences* **25**: 33–43.

CHABOCHE, J. (1981). Continuous damage mechanics: A tool to describe phenomena before crack initiation, *Nucl Eng Des* **64**: 233–247.

CHABOCHE, J. (1984). Anisotropic creep damage in the framework of continuum damage mechanics, *Nucl. Eng. Des.* **79**: 304–319.

CHABOCHE, J. (1988). Continuum damage mechanics - Part I: General concepts, Part II: Damage growth, crack initiation, and crack growth, *J. Appl. Mech.* **55**: 59–71.

CHABOCHE, J. (1993). Development of continuum damage mechanics for elastic solids sustaining anisotropic and unilateral damage, *Int J Damage Mech* **2**: 311–329.

CHABOCHE, J. (1999). *Creep and Damage in Materials and Structures*, Springer-Verlag, Wien/New York, chapter Thermodynamically founded CDM Models for Creep and other Conditions, pp. 209–283. CISM-Course 399.

CHABOCHE, J., LESNE, P. and MOIRE, J. (1995). Continuum damage mechanics, anisotropy and damage deactivation for brittle materials like concrete and ceramic composites, *Int J Damage Mech* **4**: 5–22.

CHAN, K., BODNER, S., FOSSUM, A. and MUNSON, D. (1997). A Damage Mechanics Treatment of Creep Failure in Rock Salt, *Int. J. of Damage Mech.* **6**: 121–152.

CHEN, X. and CHOW, C. (1995). On damage strain energy release rate Y, *Int J Damage Mech* **4**: 251–263.

CHENG, C., KARIM, A., LANGDORN, T. and DORN, J. (1968). *Trans Met. Soc. AIME* **242**: 584.

CHOW, C. and LU, T. (1992). An analytical and experimental study of mixed-mode ductile fracture under nonproportional loading, *Int J Damage mech* **1**: 191–236.

CHOW, C. and WANG, J. (1987). An anisotropic theory of elasticity for continuum damage mechanics, *Int. J. Fracture* **33**: 3–16.

CHOW, C. and WANG, J. (1988). Ductile fracture characterization with an anisotropic continuum damage theory, *Eng. Fracture Mech.* **30**: 547–563.

CHRISTENSEN, R. (1982). *Theory of Viscoelasticity*, second edn, Academic Press, New York/ London/ Toronto.

CHRZANOWSKI, M. (1973). The Description of Metallic Creep in the Light of Damage Hypothesis and Strain Hardening, *Diss. Hab., Politechnika Krakowska, Krakow* .

CHRZANOWSKI, M. (1976). Use of the damage concept in describing creep-fatigue interaction under prescribed stress, *Int. J. Mech. Sci.* **18**: 69–73.

COCKS, A. and ASHBY, M. (1982). On creep fracture by void growth, *Prog. Materials Science* **27**: 189–244.

COCKS, A. and LECKIE, F. (1987). Creep Constitutive Equations for Damaged Materials, *in* T. WU and J. HUTCHINSON (eds), *Advances in Applied Mechanics*, Vol. 25, pp. 239–294.

COCKS, A. and PONTER, A. (1985). Constitutive equations for the plastic deformation of solids, *Leicester Univ. Eng. Dep. Rep.* **85**: 1–2.

COFFIN, L. (1954). A study of the effects of cyclic thermal stresses in a ductile metal, *Trans ASME* **76**: 931.

CRISTESCU, N. and SULICIU, I. (1982). *Viscoplasticity*, Martinus Nijhoff Publishers, The Hague/ Boston/ London.

DAVIS, E. (1960). Relaxation of a cylinder on a rigid shaft, *Journal of Applied Mechanics* **27**(3): 41–44.

DAVISON, L. and KIPP, M. (1978). Calculation of spall damage accumulation in ductile metals, *in* K. KAWATA and SHIRATORI (eds), *Proc IUTAM Symp High Velocity Deformation of Solids, Tokyo, Japan 1977*, Springer-Verlag, New York, pp. 163–175.

DAVISON, L., STEVENS, L. and KIPP, M. (1977). Theory of spall damage accumulation in ductile metals, *J Mech Phys Solids* **25**: 11–28.

DOETSCH, G. (1971). *Handbuch der Laplace Transformation 1-3*, Birkhäuser Verlag, Basel.

DRAGON, A. (1985). Plasticity and ductile fracture damage, *Eng Fracture Mech* **21**: 875–892.

DRUCKER, D. (1959). A Definition of Stable Inelastic Material, *J. Appl. Mech.* **26**: 101–106.

DUBEY, R. and HILLER, M. (1972). Yield Criteria and the Bauschinger-Effect for a Plastic Solid, *Journal of Basic Engineering, Transactions of the ASME* pp. 228–230.

DUFAILLY, J. and LEMAITRE, J. (1995). Modeling very low cycle fatigue, *Int. J. Damage Mech.* **4**: 153–170.

DÜNGER, U. (2005). *Untersuchungen zum dynamischen Verhalten von offenzelligen fluidgefüllten Schaumstoffen*, Dissertation, Universität Karlsruhe (TH).

DUNNE, F. and HAYHURST, D. (1994). Efficient cycle jumping techniques for the modelling of materials and structures under cyclic mechanical and thermal loadings, *Eur J Mech A/Solids* **13**: 639–660.

DUNNE, F., OTHMAN, A., HALL, F. and HAYHURST, D. (1990). Representation of Uni-Axial Creep Curves Using continuum Damage Mechanics, *Int. J. Mech. Sci.* **32**: 945–957.

DYSON, B. (1976). Constraints on diffusional cavity growth rates, *Metal Science* **10**: 349–353.

EBERT, F. (1980). *Strömung nicht-newtonscher Medien*, Vieweg-Verlag, Braunschweig / Wiesbaden.

EDWARD, G. and ASHBY, M. (1979). Intergranular fracture during power-law creep, *Acta Metall* **27**: 1505–1518.

EINSTEIN, A. (1916). Die Grundlagen der allgemeinen Relativitätstheorie, *Annalen der Physik, 4. Folge* **49**: 769–822.

EISENBERG, M. and YEN, C. (1981). A Theory of Multiaxial Anisotropic Viscoplasticity, *J. Appl. Mech.* **48**: 276–284.

ENGELN-MÜLLGES, G. and REUTER, F. (1993). *Numerik-Algorithmen mit Fortan 77-Programmen*, Wissenschaftsverlag, Mannheim. 7. völlig neu bearbeitete und erweiterte Auflage.

EVANS, H. (1984). *Mechanisms of Creep Rupture*, Elsevier, London.

FAIRBAIRN, J. and MACKIE, W. (1972). The creep of thick-walled tubes subjected to internal pressure, *IUTAM Symposium on Creep in Structures, Gothenburg 1970*, Springer, Berlin, pp. 189–202.

FETT, T., KELLER, K. and MUNZ, D. (1988). An analysis of the creep of hot-pressed silicon nitride in bending, *J. of Materials Science* **23**: 467–474.

FINNIE, I. (1966). Method of predicting creep tension and compression from bending tests, *J. of the American Ceramic Society* **49**: 218–220.

FITZGERALD, J. (1980). A tensorial Hencky measure of strain and strain rate for finite deformations, *J. Appl. Phys.* **51**: 5111–5115.

FOUX, A. (1964). An experimental Investigation of the Poynting Effect, *in* M. REINER and D. ABIR (eds), *Second-order Effects in Elasticity, Plasticity and Fluid Dynamics*, Pergamon Press, Oxford/London/New York/Paris, pp. 228–251.

FRÈRES, P. (1996). *Enstehung und Wachstum von Mikrorissen in gekerbten Stäben unter Hochtemperatur-Kriechbeanspruchung*, Dissertation RWTH-Aachen.

GANCZARSKI, A. and SKRZYPEK, J. (1997). Optimal design of rotationally symmetric disks in thermo-damage coupling conditions, *Tech Mech* **17**: 365–378.

GANCZARSKI, A. and SKRZYPEK, P. (1995). Concept of thermo-damage coupling in continuum damage mechanics, *in* R. HETNARSKI and N. NODA (eds), *First Int Symp Thermal Stresses 1995, Hamamatsu, Japan, Act City, June 5-7, 1995*, pp. 83–86.

GIESEKUS, H. (1994). *Phänomenologische Rheologie*, Springer-Verlag, Berlin/Heidelberg.

GITTUS, J. (1978). *Irradiation Effects in Crystalline Solids*, Applied Science Publ., London.

GOEL, R. (1975). On the creep rupture of a tube and a spere, *J. Appl. Mech. Trans. ASME* **43**: 625–629.

GOODS, S. and NIX, W. (1978). The kinetics of cavity growth and creep fracture in silver containing implanted grain boundary cavities, *Acta Metallurgica* **26**: 739–752.

GOREV, B., RUBANOV, V. and SOSNIN, O. (1978). *in* G. PISARENKO (ed.), *Strength of materials and Structural Members under Multiaxial Loading*, Naukova Dumka, Kiev, pp. 223–231.

GOREV, B., RUBANOV, V. and SOSNIN, O. (1979a). *J. Appl. Mech. and Techn. Phys.* **4**: 121–128.

GOREV, B., RUBANOV, V. and SOSNIN, O. (1979b). *Strength of Materials* **7**: 62–67.

GRABACKI, J. (1994). Constitutive equations for some damaged materials, *Eur J Mech A/Solids* **13**: 51–71.

GRADY, D. (1982). Local inertial effects in dynamic fragmentation, *J Mech Phys Solids* **53**: 322–325.

GRATHWOHL, G. (1984). Regimes of creep and slow crack growth in high-temperature rupture of hot-pressed silicon nitride, *Deformation of Ceramics II*, Plenum Publishing Corporation, pp. 573–586.

GROSS, D. and SEELIG, T. (2001). *Bruchmechanik*, 3 edn, Springer-Verlag, Berlin / Heidelberg / New York.

HAN, C., KIM, K., SISKOVIIC, N. and HUANG, C. (1975). An appraisal of rheological models as applied to polymer melt flow, *Rheol. Acta.* **14**: 533–549.

HAUPT, P. (2000). *Continuum Mechanics and Theory of Materials*, Springer-Verlag, Berlin/Heidelberg/New York.

HAYAKAWA, K. and MURAKAMI, S. (1997). Thermodynamical Modeling of Elastic-Plastic Damage and Experimental Validation of Damage Potential, *Int. J. of Damage Mech.* **6**: 381–390.

HAYAKAWA, K. and MURAKAMI, S. (1998). *Damage Mechanics in Engineering Materials*, Elsevier, chapter Space of damage conjugate force and damage potential of elastic-plastic damage materials, pp. 27–44.

HAYHURST, D. (1972). Creep rupture under multiaxial states of stress, *J. Mech. Phys. Solids* **20**: 381–390.

HAYHURST, D., DIMMER, P. and MORRISON C.J. (1984). Development of continuum damage in the creep rupture of notched bars, *Phil Trans R Soc London A* **311**: 103.

HAYHURST, D. and LECKIE, F. (1973). The effect of creep constitutive and damage relationships upon rupture time of solid circular torsion bar, *Mech Phys Solids* **21**: 431–446.

HAYHURST, D., TRAMPCZYNSKI, W. and LECKIE, F. (1980). Creep rupture and nonproportional loading, *Acta Metall* **28**: 1171–1183.

HAYMAN, B. (1980). Creep buckling - a general view of the phenomena, pp. 289–307. 3. IUTAM-Symposium.

HAYMAN, B. (1981). Creep Buckling - A General View of The Phenomena, *in* A. PONTER and D. HAYHURST (eds), *Creep in Structures*, Springer-Verlag, Berlin, pp. 289–307.

HECKER, F. (1967). Die Wirkung des Bauschinger-Effekts bei großen Torsions-Formänderungen, *Dissertation, Techn. Hochschule Hannover* .

HEEMANN, U. and STEIN, E. (1991). Transient Creep in Rock Salt Structures, *in* M. ZYCZKOWSKI (ed.), *Creep in Structures*, Springer-Verlag, Berlin, pp. 91–98.

HELLE, S. and TVERGAARD, V. (1998). Intergranular fracture under creep-fatigue interaction, *Int J Damge Mech* **7**: 3–23.

HENCKY, H. (1925). Die Bewegungsgleichungen beim nichtstationären Flieen elastischer Massen, *Z. angew. Math. Mech.* **5**: 144–146.

HILL, R. (1950). *The Mathematical Theory of Plasticity*, Clarendon Press, Oxford.

HOHENEMSER, K. and PRAGER, W. (1932). Über die Ansätze der Mechanik isotroper Kontinua, *Z. Ang. Math. Mech. (ZAMM)* **12**: 216–226.

HULT, J. (1974). Creep in continua and structures, *in* F. ZEMAN, J. L. AND ZIEGLER (ed.), *Topics in applied continuum mechanics*, Springer, Wien, pp. 137–155.

HUMMEL, A., WESCHE, K. and BRAND, W. (1962). Versuche über das Kriechen unbewehrten Betons, *Deutscher Ausschuss für Stahlbeton* **Heft 146**. Verlag Wilhelm Ernst & Sohn, Berlin.

HUTCHINSON, J. (1983). Constitutive behaviour and crack tip fields for materials undergoing creep-constained grain boundary cavitation, *Acta Metall* **31**: 1079–1088.

IGARI, T., SETOGUCHI, K. and NOMURA, S. (1991). Prediction of Macroscopie and Load Creep Behavior of Perforated Plates, *in* M. ZYCZKOWSKI (ed.), *Creep in Structures*, Springer-Verlag, Berlin, pp. 579–586.

ILSCHNER, B. (1973). *Hochtemperatur-Plastizität*, Springer-Verlag, Berlin.

ILSCHNER, B. and SINGER, R. (2002). *Werkstoffwissenschaften und Fertigungstechnik*, 3. edn, Springer- Verlag, Berlin / Heidelberg / New York.

JAKOWLUK, A. (1993). *Process of Creep and Fatigue in Materials*, Wydawnictwa Naukowo-Techniczne, Warszawa. In Polish.

JAKOWLUK, A. and MIELESZKO, E. (1983). Method of optimizing the description of primary creep, *Bulletin of the Polish Academy of Sciences, Appl. Mech.* **31**.

JAKOWLUK, A. and MIELESZKO, E. (1985). On the assumption of the creep potential existence, *Bulletin of the Polish Academy of Sciences, Appl. Mech.* **33**: 429–437.

JOHNSON, A. (1960). Complex-stress creep of metals, *Metallurg. Rev.* **5**: 447–506.

JOHNSON, J. (1981). Dynamic fracture and spallation in ductile solids, *J Mech Phys Solids* **53**: 2812–2825.

KACHANOV, L. (1986). *Introduction to Continuum Damage Mechanics*, Martinus Nijhoff Publishers, Dordrecht.

KACHANOV, L. (1958). On the time failure under creep conditions, *Izv. Akad. Nauk USSR Otd. Tekh. Nauk* **8**: 26–31. In Russian.

KATTAN, P. and VOYIADJIS, G. (1990). A coupled theory of damage mechanics and finite strain elasto-plasticity - I: Damage and elastic deformations, *Int. J. Eng. Sci.* **28**: 421–435.

KAVIANY, M. (1995). *Principles of Heat Transfer in Porous Media*, Springer-Verlag, New-York.

KOLSKY, H. (1972). Some recent experimental investigations in stress-wave propagation and fracture, *in* G. HERRMANN and N. PERRONE (eds), *Dynamic Response of Structures*, Pergamon, Oxford, pp. 327–343.

KOLSKY, H. (1978). The Role of Experiment in the Development of Solid Mechanics - Some examples, *in* CHIA-SHUN YIH (ed.), *Advances in Applied Mechanics*, Academic Press, New York / San Francisco / London, pp. 309–368.

KOLUPAEV, V. (2006). *Dreidimensionales Kriechverhalten von Bauteilen aus unverstärkten Thermoplasten*, Dissertation, Martin-Luther Universität Halle-Wittenberg.

KOSSOWSKY, R., MILLER, D. and DIAZ, E. (1975). Tensile and creep strength of hot-pressed Si3N4, *J. of Materials Science* **10**: 983–997.

KOWALEWSKI, Z. (1987). The surface of constant dissipation energy rate under creep and its experimental determination, *Arch. Mech.* **39**: 445–454.

KOWALEWSKI, Z. (1991). The Influence of Deformation History on Creep in Pure Copper, *in* M. ZYCZKOWSKI (ed.), *Creep in Structures*, Springer-Verlag, Berlin, pp. 115–122.

KRAJCINOVIC, D. (1983). Constitutive equations for damaging materials, *J. Appl. Mech.* **50**: 355–360.

KRAJCINOVIC, D. (1984). Continuum damage mechanics, *ASME Appl. Mech. Rev.* **37**: 1–6.

KRAJCINOVIC, D. (1996). *Damage Mechanics*, Elsevier, North-Holland, Amsterdam / NewYork / Tokyo.

KRAJCINOVIC, D. and FONSEKA, G. (1981). The continuous damage theory of brittle materials, *J Appl Mech* **48**: 809–815.

KRAJCINOVIC, D. and LEMAITRE, J. (1987). *Continuum Damage Mechanics*, Springer-Verlag, Wien, New York.

KRAWIETZ, A. (1986). *Materialtheorie*, Springer-Verlag, Berlin/ ... /Tokyo.

KREMPL, E. (1987). Viscoplasticity, Some Comments on Equilibrium Stress and Drag Stress, *Acta Mechanica* **69**: 25–42.

LADEVEZE, P. (1990). A damage approach for composite structures theory and identification, *in* A. VAUTRIN and H. SOL (eds), *Mechanical Identification of Composites*, Elsevier, pp. 44–57.

LAMÉ, G. (1852). *Lecons sur la théorie mathématique de l' élasticite des corps solides*, Paris.

LAUN, H. (1978). Description of the non-linear shear behaviour of a low density polyethylene melt by means of an experimentally determined strain dependent memory function, *Rheologica Acta* **17**: 1–15.

LAUN, H. and MÜNSTEDT, M. (1978). Elongational behaviour of a low density polyehylene melt, *Rheol. Acta* **17**: 415–425.

LECKIE, F. and HAYHURST, D. (1974). Creep rupture of structures, *Proc. R. Soc. London A* **340**: 323–347.

LECKIE, F. and HAYHURST, D. (1977). Constitutive equations for creep rupture, *Acta Metallurg.* **25**: 1059–1070.

LECKIE, F. and ONAT, E. (1981). *Physical Nonlinearities in Structural Analysis*, Springer-Verlag, Berlin.

LECKIE, F. and PONTER, A. (1974). On the state variable description of creeping materials, *Ing.-Archiv.* **43**: 158–167.

LEE, H., PENG, K. and WANG, J. (1985). An anisotropic damage criterion for deformation instability and its application to forming limit analysis of metal plates, *Eng. Fracture Mech.* **21**: 1031–1054.

LEHMANN, T. (1960). Einige Betrachtungen zur Beschreibung von Vorgängen in der klassischen Kontinuumsmechanik, *Ingenieur-Archiv* **29**: 316–330.

LEHMANN, T. (1962). Einige ergänzende Bemerkungen zur Beschreibung von Vorgängen in der klassischen Kontinuumsmechanik, *Ingenieur-Archiv* **31**: 371–384.

LEHMANN, T. (1972). Einige Bemerkungen zu einer allgemeinen Klasse von Stoffgesetzen für große elasto-plastische Formänderungen, *Ingenieur-Archiv* **41**: 297–310.

LEIGH, D. (1968). *Nonlinear Continuum Mechanics*, Mc Graw-Hill Book Company, New York.

LEMAITRE, J. (1985). A continuum damage mechanics model for ductile fracture, *ASME J Eng Mat Tech* **107**: 83–89.

LEMAITRE, J. (1992). *A Course on Damage Mechanics*, Springer-Verlag, Berlin, Heidelberg, New-York. (second edition 1996).

LEMAITRE, J. (1996). *A course on damage mechanics*, Springer-Verlag, Berlin, Heidelberg, New-York.

LEMAITRE, J. and CHABOCHE, J. (1975). A nonlinear model of creep fatigue damage cumulation and interaction, *in* J. HULT (ed.), *Proc IUTAM Symp Mechanics of Visco-Elastic Media and Bodies, Gothenburg, Sweden*, Springer-Verlag, pp. 291–301.

LEMAITRE, J. and CHABOCHE, J. (1990). *Mechanics of solid materials*, Cambridge University Press.

LI, S. and SMITH, D. (1995). High temperature fatigue-creep behaviour of single crystal SRR99 nickle base superalloys, *Fracture Engng. Mater. Struct.* **18**: Part I: 617–629, Part II: 631–643.

LIN, R. (2002). *Viscoelastic and Elastic-viscoelastic-elastoplastic Constitutive Characterization of Polymers at Finite Strains: Theoretical and Numerical Aspects*, Dissertation, UniBW Hamburg.

LIN, R., BETTEN, J. and BROCKS, W. (2006). Modeling of finite strain viscoplasticity based on logarithmic corotational description, *Arch. Appl. Mech* **75**: 693–708.

LIS, Z. (1992). Creep damage of solids under non-proportional loading, *ZAMM* **72**: T164–T166.

LITEWKA, A. (1985). Effective material constants for orthotropically damaged elastic solids, *Arch Mech* **37**: 631–642.

LITEWKA, A. (1989). Creep rupture of metals under multi-axial state of stress, *Arch Mech* **41**: 3–23.

LITEWKA, A. and HULT, J. (1989). One parameter cdm model for creep rupture prediction, *Eur J Mech A / Solids* **8**: 185–200.

LITEWKA, A. and MORZÝNSKA, J. (1989). Theoretical and experimental study of fracture for a damaged solid, *Res. Mechanica* **27**: 259–272.

LITEWKA, A. and SAWCZUK, A. (1981). A yield criterion for perforated sheets, *Ingenieur-Archiv* **50**: 393–400.

LIU, M. and KREMPL, E. (1979). A Uniaxial Viscoplastic Model based on Total Strain and Overstress, *J. Mech. Phys. Solids* **27**: 377–391.

LUBAHN, J. and FELGAR, R. (1961). *Placticity and Creep of Metals*, John Wiley & Sons, New York.

LUCAS, G. and PELLOUX, R. (1981). Texture and stress state dependent creep in Zircaloy-2, *Met. Trans.* **12A**: 1321–1331.

LUDWIG, R. (2001). *Tensorielle Verallgemeinerung eines Stoffmodels für Elastomere*, Dissertation, RWTH-Aachen University.

LUDWIK, P. (1909). *Elemente der Technologischen Mechanik*, Springer, Berlin.

MACVEAN, D. (1968). Die Elementararbeit in einem Kontinuum und die Zuordnung von Spannungs- und Verzerrungstensoren, *Z. angew. Math. Phys. (ZAMP)* **19**: 157–185.

MANG, H. and HOFSTETTER, G. (2000). *Festigkeitslehre*, Springer-Verlag, Wien / New York.

MANSON, S. (1979). Some useful concepts for the designer in treating cumulative damage at elevated temperature. ECM 3, *Cambridge* **1**: 13–45.

MARIGO, J. (1985). Modelling of brittle and fatigue damage for elastic material by growth of microvoids, *Eng Fracture Mech* **21**: 861–874.

MARIOTT, D. (1972). A review of reference stress methods for estimating creep deformation, *IUTAM Symposium on Creep in Structures, Gothenburg 1970*, Springer-Verlag, Berlin/Heidelberg/New York, pp. 137–152.

MATZENMILLER, A. and SACKMANN, J. (1994). On Damage Induced Anisotropy for Fiber Composites, *Int J Damage Mech* **3**: 71–86.

MEISSNER, J. (1971). Dehnungsverhalten von Polyäthylen-Schmelzen, *Rheologica-Acta* **10**: 230–241.

MEISSNER, J. (1972). Modification of the Weissenberg Rheogoniometer for Measurement of Transient Rheological Properties of Molten Polyethylene under Shear-Comparison with Tensile Data, *Journal of Applied Polymere Science* **16**: 2877–2899.

MEISSNER, J. (1975). Basis parameters melt rheology processing and end-use properties of free similar low density polyethylene samples, *Pure and Applied Chemistry* **42**: 551–612.

MICHAL, A. (1927). Funktionals of r-dimensional manifolds admitting continuous groups of point transformations, *Trans. Am. Math. Soc.* **29**: 612–646.

MICHAL, A. (1947). *Matrix and Tensor Calculus*, John Wiley, New York.

MIDDLEMAN, S. (1977). *Fundamentals of Polymere Processing*, McGraw-Hill Book Company, New York/ ... / Toronto.

MISES, V. (1928). Mechanik der plastischen Formänderung von Kristallen, *Z. angew. Math. Mech. (ZAMM)* **8**: 161–185.

MONKMAN, F. and GRANT, N. (1956). An empirical relationship between rupture life and minimum creep rate in creep-rupture tests, *Proc. ASTM* **56**: 593–620.

MOU, Y. and HAN, R. (1996). Damage evolution in ductile materials, *Int J Damage Mech* **5**: 241–258.

MURAKAMI, S. (1983). Notion of continuum damage mechanics and its application to anisotropic creep damage theory, *J. Eng. Mat. Tech.* **105**: 99–105.

MURAKAMI, S. (1987). Progress of continuum damage mechanics, *JSME Int. J. Ser. A* **30**: 701–710.

MURAKAMI, S. (1988). Mechanical modeling of material damage, *Trans. ASME, J. Appl. Mech.* **55**: 280–286.

MURAKAMI, S., HAYAKAWA, K. and LIU, Y. (1998). Damage evolution and damage surface of elastic-plastic-damage materials under multiaxial loading, *Int. J. Damage Mech.* **7**: 103–128.

MURAKAMI, S. and KAMIYA, K. (1997). Constitutive and damage evolution equations of elastic-brittle materials based on irreversible thermodynamics, *Int. J. Solids Struct.* **39**: 473–486.

MURAKAMI, S. and MIZUNO, M. (1992). A constitutive equation of creep, swelling and damage under neutron irradiation applicable to multiaxial and variable states of stress, *Int J Solids Struct* **29**: 2319–2328.

MURAKAMI, S. and OHNO, N. (1981). *Creep in Structures 1980*, Springer-Verlag, Berlin, Heidelberg, New York, chapter A continuum theory of creep and creep damage, pp. 422–444. (ed: Ponter, A.R.S Hayhurst, D.R).

MURAKAMI, S., SANOMURA, Y. and SAITOH, R. (1986). Formulation of cross-hardening in creep and its effect on the creep damage process of copper, *J. Eng. Mat. Tech.* **108**: 167–173.

MURAKAMI, S. and SAWCZUK, A. (1979). On description of rate-independent behaviour for prestrained solids, *Archives of Mechanics* **31**: 251–264.

MURAKAMI, S. and SAWCZUK, A. (1981). A unified approach to constitutive equations of inelasticity based on tensor function representations, *Nucl. Eng. Des.* **65**: 33–47.

MURAKAMI, S. and TANAKA, E. (1976). On the creep buckling of circular shells, *Int. J. Mech. Sci.* **18**: 185–194.

MURZEWSKI, J. (1992). Brittle and ductile damage of stochastically homogeneous solids, *Int J Damage Mech* **1**: 276–289.

NAJAR, J. (1994). Brittle residual strain and continuum damage at variable uniaxial loading, *Int J Damage Mech* **3**: 260–277.

NAUMENKO, K. (1996). *Modellierung und Berechnung der Langzeitfestigkeit dünnwandiger Flächentragwerke unter Einbeziehung von Werkstoffkriechen und Schädigung*, Otto-von-Guericke Universität Magdeburg. Preprint MBI-96-2, April 1996.

NAUMENKO, K. and ALTENBACH, H. (2007). *Modeling of Creep for Structural Analysis*, Springer-Verlag, Berlin/Heidelberg.

NEEDLEMAN, A., TVERGAARD, V. and GIESSEN, E. (1995). Evolution of void shape and size in creeping solids, *Int J Damage Mech* **4**: 134–152.

NEMES, J., EFTTIS, J. and RANDLES, P. (1990). Viscoplastic constitutive modeling of high strain-rate deformation, material damage and spall fracture, *Trans ASME* **57**: 282–291.

NICOLINI, G. (1999). *Mikrostruktur und Zeitstandverhalten teilchengehärteter Hochtemperaturwerkstoffe*, Dissertation, RWTH-Aachen.

NISHITANI, T. (1978). Mechanical behaviour of nonlinear viscoelastic celluloid under superimposed hydrostatic pressure, *Trans. ASME. J. Pressure Vessel Technol.* **100**: 271–276.

NORMAN, E. and DURAN, S. (1970). *Acta Metall.* **19**: 723.

NORTON, F. (1929). *Creep of high Temperatures*, Mc Graw Hill, New York.

OBRECHT, H. (1977). Creep buckling and postbuckling of circular cylindrical shells under axial compression, *Int. J. Solids Struct.* **13**: 337–355.

ODQUIST, F. (1966). *Mathematical Theory of Creep and Creep Rupture*, University Press, Oxford.

ODQUIST, F. and HULT, J. (1962). *Kriechfestigkeit metallischer Werkstoffe*, Springer Berlin.

OHASHI, Y., KAWAI, M. and MOMOSE, T. (1986). *J. Engng. Mater. Technol.* **108**: 68–74.

OMERSPAHIC, E. and MATTIASSON, K. (2007). Oriented Damage in Ductile Sheets: Constitutive Modeling and Numerical Integration, *Int. J. Damage Mechanics* **16**: 35–56.

ONAT, E. (1986). Representation of mechanical behavior in the presence of internal damage, *Eng. Fracture Mech.* **25**: 605–614. Presented at the IUTAM Symposium on Mechanics of Damage and Fatigue, Haifa and Tel Aviv, Israel, 1985.

ONAT, E. and LECKIE, F. (1988). Representation of mechanical behavior in the presence of changing internal structure, *Trans. ASME, J. Appl. Mech.* **55**: 1–10.

OTHMANN, A., HAYHURST, D. and DYSON, B. (1993). Skeletal point stresses in circumferentially notched tension bars undergoing tertiary creep modelled with physically based constitutive equations, *Proc. R. Soc. London* **441**: 343–358.

OYTANA, C., DELOBELLE and MERMET, A. (1982). Constitutive equations study in biaxial experiments, *J. Eng. mat. Tech.* **104**: 1–11.

PANTELAKIS, S. (1983). *Kriechverhalten metallischer Werkstoffe bei zeitveränderlicher Spannung*, PhD thesis, RWTH-Aachen.

PENNY, R. and MARIOTT, D. (1971). *Design for Creep*, Mc Graw-Hill, London.

PERZYNA, P. (1966). Fundamental Problems in Viscoplasticity, *Advances in Appl. Mech.*, Academic Press, New York.

PERZYNA, P. (1986). Internal state variable description of dynamic fracture of ductile solids, *Int J Solids Struct* **22**: 797–818.

PHILLIPS, A. and WU, H. (1973). A Theory of Viscoplasticity, *Int. J. Solids Structures* **9**: 15–30.

QI, W. (1998). *Modellierung der Kriechschädigung einkristalliner Superlegierungen im Hochtemperaturbereich*, Vol. 230, Fortschritt-Berichte VDI 18: Mechanik / Bruchmechanik, Düsseldorf.

QI, W. and BERTRAM, A. (1997). Anisotropic creep damage modeling of single crystal superalloys, *Tech Mech* **17**: 313–332.

RABOTNOV, Y. (1968). Creep rupture, *in* M. HETENYI AND H. VINCENTI (ed.), *Appl. Mech. Conf.*, Stanford University, Palo Alto, pp. 342–349.

RABOTNOV, Y. (1969). *Creep Problems in Structural Members*, North-Holland, Amsterdam/London.

REED-HILL, R. (1973). *Physical metallurgy principles*, D. van Nostrand Company, New York.

REICHARDT, H. (1968). Vorlesung über Vektor- und Tensorrechnung, *in* K. H. GRELL (ed.), *Hochschulbücher für Mathematik*, Vol. 34, VEB, Berlin.

RICE, J. (1970). On the structure of stress-strain relations for time-dependent plastic deformations in metals, *Trans. ASME J. Appl. Mech.* **37**: 728–737.

RICE, J. (1971). Inelastic constitutive relations for solids, *J. Mech. Phys. Solids* **19**: 433–455.

RICE, J. (1981). Constraints on the diffusive cavitation of isolated grain boundary facets in creeping polycrystals, *Acta Metall.* **29**: 675–681.

RICHTER, H. (1949). Verzerrungstensor, Verzerrungsdeviator und Spannungstensor bei endlichen Formänderungen, *Z. angew. Math. Mech.* **29**: 65–75.

RIDES, M., COCKS, A. and HAYHURST, D. (1989). The elastic response of damaged materials, *J. Appl. Mech.* **56**: 493–498.

RIEDEL, H. (1987). *Fracture at High Temperatures*, Springer-Verlag, Berlin.

RIMROTT, F. (1959). Versagenszeit beim Kriechen, *Ingenieur-Archiv* **27**: 169–178.

RIMROTT, F., MILLS, E. and MARIN, J. (1960). Prediction of creep failure time for pressure vessels, *Journal of Applied Mechanics* **27**(6): 303–308.

RIVLIN, R. (1955). Further remarks on the stress-deformation relations for isotropic materials, *J. Rat. Mech. Anal.* **4**: 681–702.

RIVLIN, R. (1970). *Non-Linear Continuum Theories in Mechanics and Physics and their Applications*, Centro Internazionale Mathematico Estivo (C.I.M.E.), Edizione Cremonense, Roma.

RIVLIN, R. and ERICKSEN, J. (1955). Stress-deformation relations for isotropic materials, *J. Rational Mech. Anal.* **4**: 323–425.

RUBANOV, V. (1987). *Experimental Foundation of the Constitutive Equations of Creep for Materials with Different Behaviour in Tension and Compression*, Ph. D. Thesis, Institute of Hydrodynamics, Novosibirsk.

SAANOUNI, K., FORSTER, C. and BEN HATIRA, F. (1994). On the anelastic flow with damage, *Int J Damage Mech* **3**: 140–169.

SAWCZUK, A. and ANISIMOWICZ, M. (1981). Tensor Functions Approach to Creep Laws after Prestrain, *in* A. PONTER and D. HAYHURST (eds), *Creep in Structures*, Springer-Verlag, Berlin / Heidelberg / New York, pp. 220–232.

SAYIR, M. (1970). Zur Fließbedingung der Plastizitätstheorie, *Ing.-Archiv* **39**: 414–432.

SCHERER, G. (1986). *Relaxation in Glass and Composites*, John Wiley & Sohn, New York/ ... / Singapore.

SCHOWALTER, W. (1978). *Mechanics of Non-Newtonian Fluids*, Pergamon Press, Oxford/ ... / Frankfurt.

SEDOV, L. (1966). *Foundations of the Non-Linear Mechnics of Continua*, Pergamon Press, Oxford.

SETH, B. (1972). Creep transition in cylinders, *International Centre for Mechanical Sciences Courses and Lectures No. 149, Udine 1972*, Springer, Wien.

SHAMMAS, M. (1988). Metallographic Methods for Predicting the Remament Life of Ferritic Coarse-Grained Weld Heat Affected Zones Subject to Creep Cavitation, *Int. Conf. on Life Assessment* . VGB, KEMA, EPRI, Essen, Arnheim, Palo Alto.

SHIN, C. (1990). *Inelastisches Verhalten anisotroper Werkstoffe*, Dissertation, RWTH Aachen.

SIDOROFF, F. (1981). Description of anisotropic damage application to elasticity, *IUTAM Colloquium on Physical Nonlinearities in Structural Analysis*, Springer-Verlag, Berlin, pp. 237–244.

SKELTON, W., SALIM, A. and PATTON, R. (1977). The creep of thick-walled 2 1/2 % NiCrMo cylinders under internal pressure at $350°C$: Development of a testing machine and prliminary results., *Proc. Inst. Mech. Eng.* **192**: 73–98.

SKOCZEN, B. (1996). Generalization of the Coffin equations with respect to the effect of large mean plastic strain, *J Eng Mat Tech, ASME* pp. 387–393.

SKRZYPEK, J. (1999). *Creep and Damage in Materials and Structures*, Springer-Verlag, Wien/New York, chapter Material Damage Models for Creep Failure Analysis and Design of Structures, pp. 97–166.

SKRZYPEK, J. (1993). *Plasticity and Creep*, CRC-Press, Boca Raton / Ann Arbor / London / Tokyo.

SKRZYPEK, J. and GANCZARSKI, A. (1998). Modeling of damage effect on heat transfer in time-dependent non-homogeneous solids, *J Thermal Stresses* **21**: 205–231.

SKRZYPEK, J. and GANCZARSKI, A. (1999). *Modeling of Material Damage and Failure of Structures-Theory and Applications*, Springer-Verlag, Berlin, Heidelberg, New York.

SKRZYPEK, J. and GANCZARSKI, A. (2003). *Anisotropic Behaviour of Damaged Materials*, (Eds.), Springer-Verlag, Berlin, Heidelberg, New York.

SOBOTKA, Z. (1984). *Rheology of Materials and Engineering Structures*, Vydala Academia vêd, Praha.

SÖDERQUIST, B. (1968). *Acta Polytech. Scand., Series (f)* **53**: 1–36.

SOKOLNIKOFF, I. (1964). *Tensor Analysis, Theory and Applications to the Geometry and Mechanics of Continua*, John Wiley, New York/London/Sydney. Second Edition.

SPENCER, A. (1971). Theory of Invariants, *in* A. ERINGEN (ed.), *Continuum Physics*, Academic Press, New York and London, pp. 239–353.

SPENCER, A. (1987). Polynomial invariants and tensor functions, *in* J. BOEHLER (ed.), *Applications of Tensor Functions in Solid Mechanics*, Springer-Verlag, Wien, New York, pp. 141–201.

STEVENSON, J. (1972). Elongational Flow of Polymer Melts, *A. I. Ch. E. Journal* **18**: 540–547.

STIGH, U. (1985). *Material Damage and Constitutive Properties*, chalmers University of Technology, Göteborg, Sweden.

SWIFT, H. (1947). Length Changes in Metals under Torsional Overstrain, *Engineering* **163**: 253–257.

SZABÓ, I. (1964). *Höhere Technische Mechanik*, 4. aufl. edn, Springer, Berlin.

TAIRA, S., KOTERAZAWA, R. and OHTANI, R. (1965). Creep of thick-walled cylinders under internal pressure at elevated temperature, *in* T. NISHIHARA (ed.), *Proc. 8th Japan Congr. testing materials*, Soc. Mat. Sci., Kyoto, pp. 53–60.

TALTY, R. and DIRKS, R. (1978). Determination of tensile and conpressive creep behaviour of ceramic materials from bend tests, *J. of Materials Science* **13**: 580–586.

TEOH, S., CHERRY, B. and KAUSCH, H. (1992). Creep Rupture Modelling of Poymers, *Int. J. of Damage Mech.* **1**: 245–256.

TETELMAN, A. and McEVILY, A. (1970). *Fracture of Structural Materials*, John Wiley.

TIMOSHENKO, S. (1934). *Theory of Elasticity*, Mc Graw-Hill Book Company, London.

TRAMPCZYNSKI, W., HAUHURST, D. and LECKIE, F. (1981). Creep rupture of copper and aluminium under non-proportional loading, *J. Mech. Phys. Solids* **29**: 353–374.

TROOST, A., BETTEN, J. and EL-MAGD, E. (1973). Einschnürvorgang eines Zugstabes unter konstanter Last bei Raumtemperatur, *Materialprüfung* **15**: 113–116.

TRUESDELL, C. (1964). Second-order Effects in the Mechanics of Materials, *in* M. REINER and D. ABIR (eds), *Second-order Effects in Elasticity, Plasticity and Fluid Dynamics*, Pergamon Press, Oxford/London/New York/Paris, pp. 1–47.

TRUESDELL, C. (1977). *A First Course in Rational Continuum Mechanics*, Vol. 1: General Concepts, Academic Press, New York.

TRUESDELL, C. and NOLL, W. (1965). The non-linear field theories of mechanics. In: Handbuch der Physik, Vol III/3 (ed Flügge S), Berlin, Heidelberg, New York: Springer Verlag.

TRUESDELL, C. and TOUPIN, R. (1960). The classical field theories, *in* S. FLGGE (ed.), *Handbuch der Physik*, Vol. III/1, Springer, Berlin, pp. 226–793.

TSCHOEGL, N. (1989). *The Phenomenological Theory of Linear Viscoelastic Behavior*, Springer-Verlag, Berlin/ ... / Tokyo.

TURNER, L. (1909). The stresses in a thick hollow cylinder subjected to internal pressure, *Trans. Camb. Phil. Soc.* **21**: 377–396.

TVERGAARD, V. (1984). Constitutive Relations for Creep in Polycrystals with Grain Boundary Cavitation, *Acta Metall* **32**: 1977–1990.

TVERGAARD, V. (1988). Material failure by void coalescence in localized shear bands, *DCAMM Report , Tech Univ of Denmark, Lyngby* **221**: 1–26.

TVERGAARD, V. (1989). Material Failure by Void Growth to Coalescence, *in* J. HUTCHINSON and T. WU (eds), *Advances in Applied Mechanics*, Vol. 27, pp. 83–151.

VOCE, E. (1955). A practical strain-Hardening function, *Metallurgia* **51**: 219–226.

VOYIADJIS, G. and KATTAN, P. (1990). A coupled theory of damage mechanics and finite strain elasto-plasticity - II: Damage and finite strain plasticity, *Int. J. Eng. Sci.* **28**: 505–524.

VOYIADJIS, G. and KATTAN, P. (1992). A plasticity-damage theory for large deformation of solids, Part I: Theoretical formulation, *Int J Eng Sci* **30**: 1089–1108.

VOYIADJIS, G. and VENSON, A. (1995). Experimental damage investigation of a SiC - Ti aluminium metal matrix composite, *Int J Damage Mech* **4**: 338–361.

WALKER, J. (1978). The Amateur Scientist, Serious fun with Polyox, Silly Putty, Slime and other non-Newtonian fluids, *Sci. Am.* **239**: 142–149.

WALTERS, K. (1975). *Rheometry*, Chapman and Hall, London.

WANG, C.-C. (1971). Representations for isotropic functions, *Arch. Rational Mech. Anal.* **43**: 392–395.

WANG, J. (1992). Low cycle fatigue and cycle dependant creep with continuum damage mechanics, *Int J Damage Mech* **1**: 237–244.

WANIEWSKI, M. (1984). The influence of direction and value of lplastic prestrain on steady-state creep rate using the combined isotropic-kinematic hardening rule, *Rozpr. Inz.* **23**: 4.

WANIEWSKI, M. (1985). A simple law of steady-state creep for material with anisotropy induced by plastic prestraining, *Ing.-Archiv* **55**: 368–375.

WEISSENBERG, K. (1947). A Continuum Theory of Rheological Phenomena, *Nature* **159**: 310–311.

ZHENG, Q.-S. (1994). Theory of representation for tensor functions - a unified invariant approach to constitutive equations, *Appl. Mech. Rev. (AMR)* **47**: 545–587.

ZHENG, Q.-S. and BETTEN, J. (1995). On the tensor function representation of 2nd-order and 4th-order tensors: Part I, *Z. Angew. Math. Mech.* **75**: 269–281.

ZHENG, Q.-S. and BETTEN, J. (1996). On damage effective stress and equivalence hypothesis, *Int. J. Damage Mech.* **5**: 219–240.

ZHENG, Q.-S., BETTEN, J. and SPENCER, A. (1992). The formulation of constitutive equations for fibre-reinforced composites in plane problems: Part I, *Arch. Appl. Mech.* **62**: 530–543.

ZYCZKOWSKI, M. (1981). *Combined Loadings in the Theory of Plasticity*, PWN-Polish Scientific Publishers, Warszawa.

ZYCZKOWSKI, M. (1988). Optimal structural design under creep conditions, *Appl. Mech. Rev.* **41**: 453–461.

ZYCZKOWSKI, M. (1996). Optimal structural design under creep conditions, *Appl. Mech. Rev.* **49**: 433–446.

ZYCZKOWSKI, M. and SKRZYPEK, J. (1972). Stationary creep and creep rupture of a thick-walled tube under combined loadings, *IUTAM Symposium on Creep in Structures, Gothenburg 1970*, Springer, Berlin, pp. 315–329.

Index